

DECLARATION

Co-ordination Chemistry of Novel Tripodal Ligands Designed to Host Anions

STATEMENT 1

This thesis has been submitted as partial fulfillment of the requirements for the degree of Ph.D.

Fawaz Ahmed Saad

STATEMENT 2

This thesis is the work of the author and has not been submitted for publication in any form.

Signature: _____

Date: _____



A thesis submitted to Cardiff University in accordance with the requirements for the degree of Doctor of Philosophy in the Faculty of Science, School of Chemistry, Cardiff University.

2011

UMI Number: U585501

All rights reserved

INFORMATION TO ALL USERS

The quality of this reproduction is dependent upon the quality of the copy submitted.

In the unlikely event that the author did not send a complete manuscript and there are missing pages, these will be noted. Also, if material had to be removed, a note will indicate the deletion.



UMI U585501

Published by ProQuest LLC 2013. Copyright in the Dissertation held by the Author.
Microform Edition © ProQuest LLC.

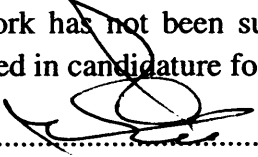
All rights reserved. This work is protected against
unauthorized copying under Title 17, United States Code.



ProQuest LLC
789 East Eisenhower Parkway
P.O. Box 1346
Ann Arbor, MI 48106-1346

DECLARATION

This work has not been submitted in substance for any degree and is not being concurrently submitted in candidature for any degree.

Signed.......... (Candidate)

Date.....9/9/2011.....

STATEMENT 1

This thesis is being submitted in partial fulfilment of the requirements for the degree of PhD.

Signed.......... (candidate)

Date.....9/9/2011.....

STATEMENT 2

This thesis is the result of my own work investigations except where otherwise stated. Other sources are acknowledged reference. References are appended to each chapter.

Signed.......... (Candidate)

Date.....9/9/2011.....

STATEMENT 3

I hereby give consent for this thesis, if accepted, to be available for photocopying and for inter-library loan, and for the title and summary to be made available to outside organisations.

Signed.......... (Candidate)

Date.....9/9/2011.....

ACKNOWLEDGMENTS

I am extremely grateful to my supervisor Dr. Angelo Amoroso for his supervision of this work and for his continuous advice, help and encouragement throughout the project. This research project would not have been possible without his support.

These thanks are also extended to include Dr. Simon Pope, Dr. Paul Newman and Dr. Ben Ward, who were also available for help and advice. Big thanks should go to Dr. Abdulrazaq Alsudany who provided inspiration and encouragement.

Special thanks are given to Dr. James Knight for always being so generous with his time and knowledge. Honestly, I can't imagine how the last three years would be without his support and valuable help.

Any acknowledgment would not be complete without thanking Dr. Niek Burma for his help in calculating the stability constant, Dr. Rob Jenkins and Robin Hicks for invaluable technical assistance. For their help and assistance in obtaining the crystallographic data, thanks must go to Dr. Benson Kariuki and Dr. James Knight. I am also indebted to the colleagues in the Inorganic Chemistry department specially people in 1.124 and 1.125 for their general assistance in many ways.

The financial support of Umm Al-Qura University, Saudi Arabia, for this work is highly appreciated.

Lastly, I wish to express my sincere love and gratitude to my beloved parents (Ahmed) & (Maryam), wife (Basmah), daughter (Reem) and son (Rayyan) for their patience, support, understanding & endless love, through the duration of my study.

In the name of Allah, Most Gracious, Most Merciful

"My Lord! Increase me in knowledge"

The holy Qur'an (114)

Summary

The development of novel ligands for the complexation of transition metal ions in inorganic chemistry is a rapidly developing field of study. The broad objective of this work is to design novel tripodal transition metal based receptors of (TPA) frame work which can act as hosts for small molecules (guests) e.g. fluoride and succinate. In addition, investigation into the co-ordination chemistry of those receptors with first row transition metals were explored using variety of characterizing techniques such as: Infrared Spectroscopy (IR), Electronic transitions (UV-Vis), Mass Spectrometry (MS), Nuclear Magnetic Resonance (NMR), Cyclic voltammetry (CV) and Single Crystal Diffractometer (X-Ray).

Mono, Bis and Tris thiourea tripodal ligands have been synthesised and their co-ordination chemistry has been investigated (chapter 2, 3 and 4) as well as the binding studies of the bithiourea (chapter 3) to bind: fluoride and succinate using ^1H NMR titration technique.

The co-ordination chemistry of TPPA with some first row transition metals has been studied and it was expected to show high affinity for seven coordination sphere and indeed it has shown strong preference for mono capped octahedral geometry (chapter 5).

Contents

Abbreviations

Chapter 1: Introduction and Background Theory.....	1
INTRODUCTION.....	2-3
Physical techniques.....	4
Electronic transitions (UV-Vis).....	4-5
Ligand spectra.....	5
Charge transfer transitions.....	6
d-d transitions.....	6-9
Crystallography X-Ray.....	10
Single Crystal X-ray structure analysis.....	11-13
Cyclic Voltammetry.....	14-16
Shape Mapping.....	17-19
Ligands classes.....	20
Tripodal tetradentate triamine ligands.....	21
Tris(2-pyridylmethyl)amine (TPA).....	22-24
Guest- Host molecules.....	25
Characterising supramolecular systems.....	26-27
Thermodynamic information.....	27
Solvent effects.....	28-29
Cation binding.....	29-31
Anion binding.....	32-37
Aim of this work.....	37
References.....	38-41

Chapter 2: A novel Monothiourea Tripodal Ligand; Structural, spectroscopic and electrochemical properties of Copper (II), Zinc (II) and Cadmium (II).....

Chapter 2: A novel Monothiourea Tripodal Ligand; Structural, spectroscopic and electrochemical properties of Copper (II), Zinc (II) and Cadmium (II).....	42
INTRODUCTION.....	43-46
EXPERIMENTAL.....	47
General.....	47
Preparations.....	47
Synthesis of (L ¹).....	47-48
General procedure for the synthesis of metal complexes.....	48-49
RESULTS AND DISCUSSION.....	50-52
Ligand Synthesis(L ¹).....	50-52
Synthesis of complexes.....	52-54
Spectroscopic properties of complexes.....	54
Vibrational Spectroscopy.....	54-55
¹ H and ¹³ C NMR of Cd complex.....	55
Electronic absorption spectra.....	56-58
Electrochemical studies of Cu ^{II}	59-60
Crystallographic studies.....	61-62
Crystal structure of [Cu ^{II} (L ¹)](ClO ₄) ₂ .H ₂ O.CH ₃ CN (2.1).....	62-64
Crystal structure of [Zn ^{II} (L ¹)](ClO ₄) ₂ .H ₂ O (2.2.1).....	65-67
Crystal structure of [Cd ^{II} (L ¹)(ClO ₄)(CH ₃ CN)](ClO ₄) (2.3).....	67-79
CONCLUSIONS.....	70
REFERENCES.....	71-73

Chapter 3: Co-ordination Behaviour of a Novel Bisthiourea Tripodal Ligand; Structural, Spectroscopic and Electrochemical Properties of a series of Transition Metal Complexes with Binding Studies.....74

INTRODUCTION.....	75-76
EXPERIMENTAL.....	77
General.....	77
Synthesis of (L ²).....	77
General procedure for the synthesis of metal complexes.....	78-79
RESULTS AND DISCUSSION.....	80
Ligand Synthesis (L ²).....	80-82
Synthesis of Complexes.....	82
Spectroscopic Properties of Complexes.....	83
Vibrational Spectroscopy.....	83
¹ H and ¹³ C NMR of Zn and Cd Complexes.....	83-84
Electronic Absorption Spectra.....	85-87
Electrochemical Studies.....	87-90
Crystallographic Studies.....	91-92
Crystal structure of L ²	93-94
Crystal structure of [Mn ^{II} (L ²)(ClO ₄)][ClO ₄].2(H ₂ O) (3.1).....	94-97
Crystal structure of [Co ^{II} (L ²)] [ClO ₄] ₂ (3.2).....	98-100
Crystal structure of [Ni ^{II} (L ²)(ClO ₄)(CH ₃ CN)] [ClO ₄].0.5(CH ₃ COCH ₃).0.5(H ₂ O) (3.3).....	101-103
Crystal structure of [Cu ^{II} (L ²)] [ClO ₄] ₂ (3.4).....	104-106
Crystal structure of [Zn ^{II} (L ²)] [ClO ₄] ₂ .2(CH ₃ CN) (3.5).....	107-109
Crystal structure of [Cd ^{II} (L ²)(ClO ₄)] [ClO ₄].CH ₃ CN (3.6).....	110-112
Crystal structure of [Mn ^{II} (L ²)(CH ₃ O)] [ClO ₄] ₂ (3.7).....	113-117
Binding studies.....	118-121
EXPERIMENTAL.....	122
RESULTS AND DISCUSSION.....	123-127
Titration of [ZnL ²] ²⁺ and [CdL ²] ²⁺ with fluoride.....	128
Titration of [ZnL ²] ²⁺ and [CdL ²] ²⁺ with succinate.....	128-133
CONCLUSIONS.....	134-136
REFERENCES.....	137-140

Chapter 4: A Tristhiourea Tripodal Framework: Co-ordination behaviour, Structural, spectroscopic and electrochemical properties of a series of transition metal complexes.....141

INTRODUCTION.....	142-145
EXPERIMENTA.....	145
General.....	145
Synthesis of (L ³).....	145-146
General procedure for the synthesis of metal complexes.....	146-147
RESULTS AND DISCUSSION.....	148
Ligand Synthesis (L ³).....	148-150
Synthesis of complexes.....	150
Spectroscopic properties of complexes.....	151
Vibrational spectroscopy.....	151
¹ H NMR of Zn and Cd complexes.....	151-152
Electronic absorption spectra.....	153-155
Electrochemical studies.....	156-158
Crystallographic studies.....	159-160
Crystal structure of [Mn ^{II} (L ³)] [ClO ₄] ₂ .CH ₃ CN (4.1).....	161-164
Crystal structure of [Ni ^{II} (L ³)(CH ₃ CN)] [ClO ₄] ₂ .3.5(CH ₃ CN).0.5(H ₂ O) (4.3).....	164-166
Crystal structure of [Zn ^{II} (L ³)] [ClO ₄] ₂ .CH ₃ CN.CHCl ₃ (4.5).....	167-169
Crystal structure of [Zn ^{II} (L ³)] [ClO ₄] ₂ .1.5(CH ₃ CN).0.5(H ₂ O) (4.5.1).....	170-172
Crystal structure of [Cd ^{II} (L ³)] [ClO ₄] ₂ .0.5(H ₂ O) (4.6).....	173-175

Addition of dihydrophosphate to Cd ^{II} -L ³	176
REFERENCES.....	177-178

Chapter 5: Co-ordination behaviour of TPPA Tripodal Ligand: Spectroscopic, Electrochemical properties and Structural Exploration of some Transition Metal Complexes.....179

INTRODUCTION.....	180-182
Seven co-ordinate geometry.....	182-183
Pentagonal Bipyramid.....	184
Capped Octahedron.....	184-185
Capped Trigonal Prism.....	185-186
Trigonal base – Tetragonal base.....	187
EXPERIMENTAL.....	188
General.....	188
Synthesis of (L ⁴).....	188
General Procedure for the Synthesis of Metal Complexes.....	188-190
RESULTS AND DISCUSSION.....	191
Ligand synthesis (L ⁴).....	191
Synthesis of ligand and complexes.....	192
Spectroscopic properties of complexes.....	192
Vibrational spectroscopy.....	192-193
¹ H NMR of Zn and Cd complexes.....	193-194
Electronic absorption spectra.....	195-196
Electrochemical studies.....	197-198
Crystallographic studies.....	199-200
Crystal structure of [Mn ^{II} (L ⁴)](ClO ₄)[Br].CH ₃ CN (5.1).....	201-202
Crystal structure of [Fe ^{II} (L ⁴)](ClO ₄)[Br].CH ₃ CN (5.2).....	202-203
Crystal structure of [Co ^{II} (L ⁴)](Br) ₂ .0.5(H ₂ O).2(CH ₃ CN) (5.3).....	204-205
Crystal structure of [Ni ^{II} (L ⁴)](ClO ₄) _{1.67} [Br] _{0.33} .0.67(H ₂ O) (5.4).....	205-206
Crystal structure of [Zn ^{II} (L ⁴)](ClO ₄) ₂ .2(CH ₃ CN) (5.5).....	207-208
Crystal structure of [Zn ^{II} (L ⁴)Cl ₂] (5.6).....	208-210
Crystal structure of [Zn ^{II} (L ⁴)](ZnI ₄) _{0.5} [I] (5.7).....	211
Crystal structure of [Cd ^{II} (L ⁴)](ClO ₄) ₂ .Na(ClO ₄).H ₂ O (5.8).....	212-213
Structural Analysis.....	214
CONCLUSIONS.....	216
REFERENCES.....	217-218

Appendix 1: Attempted work.....219

INTRODUCTION.....	220
EXPERIMENTS AND DISCUSSION.....	221
Cleaving of L ²	221
Bromination of methyle groups.....	222-223
Growing metal complex crystals of L ¹ , L ² and L ³	224-225
Preparation of bis phenyl urea tripodal ligand.....	226-227
Preparation of tris benzoyl urea tripodal ligand.....	228-229
Preparation of 1,3-(dibenzoylthiourea) pyridine.....	230-231
Converting bithiourea tripodal ligand into urea using oxone.....	232-233
REFERENCES.....	234

Appendix 2: Publications.....235

Appendix 3: Crystals data.....236-310

Abbreviations

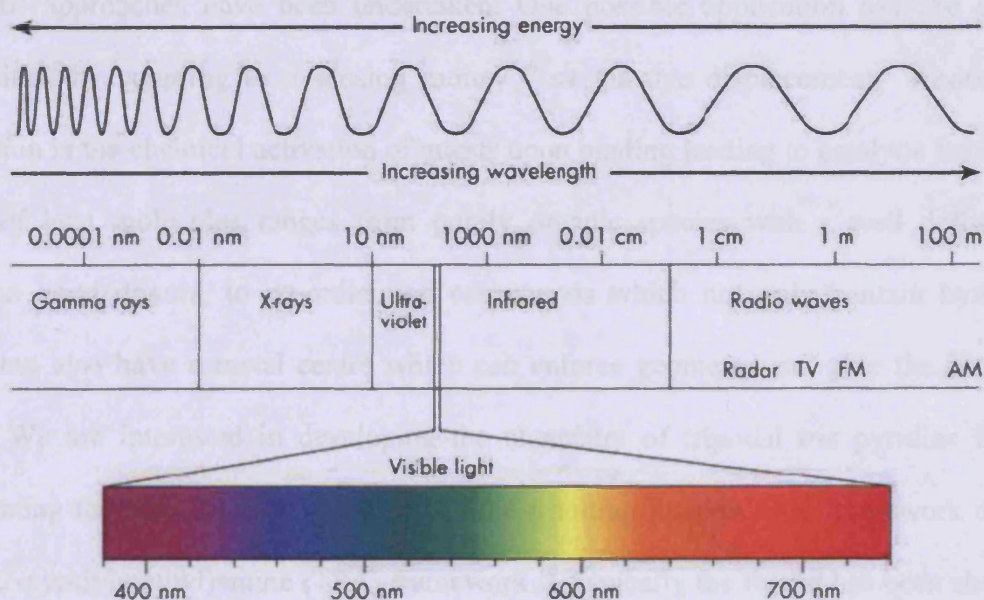
TPA	Tris(2-pyridylmethyl)amine
MAPA	Mono(6-amino-2-pyridylmethyl)(2-pyridylmethyl)amine
MPPA	Mono(6-pivaloylamino)(2-pyridylmethyl)amine
BAPA	Bis(6-amino-2-pyridylmethyl)(2-pyridylmethyl)amine
BPPA	Bis(6-pivaloylamino)(2-pyridylmethyl)amine
TAPA	Tris(6-amino-2-pyridylmethyl)amine
TPPA	Tris(6-pivaloylamino)(2-pyridylmethyl)amine
TREN	Tris(2-aminoethyl)amine
EDTA	Ethylene diamine tetra acetic acid
CV	Cyclic Voltammetry
UV-Vis	Ultraviolet-visible
NMR	Nuclear Magnetic Resonance
Eq	Equivalent
MeCN	Acetonitrile
Å	Angstrom
Ar	Aromatic
Br	Broad
¹³ C	Carbon 13 isotope
J	Coupling constant
Δ	Crystal field splitting
°C	Degrees centigrade
CD ₃ CN	Deuterated acetonitrile
CDCl ₃	Deuterated chloroform
D ₂ O	Deuterated water
DCM	Dichloromethane
DMSO	Dimethylsulfoxide
EtOH	Ethanol
D	Doublet
eV	Electron volt
ESMS	Electrospray ionisation mass spectrometry
CFSE	Crystal field stabilisation energy
□	Extinction coefficient
G	Grams
Hz	Hertz
HRMS	High resolution mass spectrometry
Hr	Hour
IR	Infrared
kJ	Kilojoule
L	Litre/ligand
MS	Mass spectrometry
<i>m/z</i>	Mass/charge ratio
MHz	Mega hertz
M	Metal/Molar concentration

Me	Methyl
Mg	Milligram
mL	Millilitre
Mmol	Millimole
Mol	Mole
Mw	Molecular weight
m	Multiplet
DMF	N,N-dimethylformamide
Δ	NMR chemical shift
NMR	Nuclear magnetic resonance
Asu	Asymmetric unit
Oh	Octahedron
MCO	Mono Capped Octahedron
MCTP	Mono Capped Trigonal Prism
ppm	Parts per million
Ph	Phenyl
KBr	Potassium bromide
^1H	Proton
Py	Pyridine
cm^{-1}	Reciprocal centimetres/wavenumber
RT	Room temperature
S	Singlet
Td	Tetrahedron
THF	Tetrahydrofuran
T	Triplet
UV	Ultraviolet
Vis	Visible
λ_{max}	Wavelength of the band at maximum absorption
tBu	tertiary butyl
TBP	Trigonal Bipyramidal
V	Volt
mV	Millivolt

Introduction

While I am writing my thesis I can't really help but think of all the things I have learned in the past few years and how much I have grown. It's amazing to look back and see how far I've come. I've learned so much about myself and the world around me. I've met so many great people and they've helped me so much. I'm really excited about the future and all the possibilities that are out there. I'm going to keep working hard and trying to be the best I can be. I'm going to keep learning and growing and I'm going to keep making a difference in the world. I'm going to keep being a good person and I'm going to keep being a good friend. I'm going to keep being a good student and I'm going to keep being a good citizen. I'm going to keep being a good person and I'm going to keep being a good friend. I'm going to keep being a good student and I'm going to keep being a good citizen.

Chapter 1: Introduction and Background Theory



Introduction

While I am writing my thesis I am certainly breathing taking in dioxygen from the atmosphere and using it for the essential process of respiration through its interaction with the iron atoms present in haemoglobin. Co-ordination chemistry becomes an important field of inorganic chemistry, especially its role in biological aspects. Sodium, potassium, magnesium, calcium, vanadium, chromium, molybdenum, manganese, iron, cobalt, nickel, copper and zinc are essential for plants, animals and are present in the human body. It has been said that life is organic, life is inorganic too.

There is much interest in the design of host molecules for anionic species.¹⁻³ Anion receptors based on metal centres are a well established class of anion binding compound. The design of new molecules that can specifically host a given guest remains a significant challenge and numerous approaches have been undertaken. One possible application may be in analytical applications by coupling to a sensing moiety⁴⁻⁶ or via dye displacement.⁷ Another potential application is the chemical activation of guests upon binding leading to catalytic behaviour.⁸ The design of host molecules ranges from purely organic species with a well defined array of hydrogen bond donors, to co-ordination compounds which not only contain hydrogen bond donors but also have a metal centre which can enforce geometry and give the host a positive charge. We are interested in developing the chemistry of tripodal tris pyridine ligands⁹ and investigating the co-ordination chemistry of the resulting ligands. One framework of interest is the tris(2-pyridylmethyl)amine (TPA) framework.¹⁰ Typically the ligand has been shown to have a strong preference for five co-ordinate trigonal bipyramidal geometries with the three pyridyl donors taking equatorial positions and the axial donors being the bridge-head nitrogen donor and one additional monodentate ligand. The 6-position of the three pyridine rings in TPA may be systematically substituted with a variety of derivatives. Such derivatives have been extensively

Chapter 1: Introduction and Background Theory

studied, with much attention being given to the tris (6-amino-2-pyridylmethyl) amine (TAPA), its bis and mono functionalised analogues (BAPA and MAPA)^{11, 12} and the alkylated derivatives of these ligands¹³ as well as the analogous tertiary butyl amides (TPPA, BPPA and MPPA).¹⁴ In the trigonal bipyramidal metal complexes of these ligands, it was shown that strong H-bonding can exist between the NH groups in the 6 position and a monodentate guest ligand co-ordinating to the vacant axial position of the metal. In fact, even in octahedral Fe(III) complexes, similar hydrogen bonding has still been observed.¹⁵ This hydrogen bonding has been found to greatly modify the stability of the guest-host complex and also modify the reactivity of the guest.^{12, 13, 16-}
²¹ Also, it may modify the redox behaviour of the metal centre.²¹⁻²³

A co-ordination compound (complex) is the product of a Lewis acid-base reaction in which a central atom surrounded by neutral molecules possessing lone pairs of electrons or anions (ligands) forming co-ordination covalent bonds. Such compounds could be characterised using different methods such as: Mass spectrometry, Infrared spectroscopy, Nuclear magnetic resonance spectroscopy, UV-Vis spectroscopy, Elemental analysis and perhaps the most important method “X-ray crystallography” where a solid state of the molecular structure is provided.

In this first chapter, some of those physical techniques will be discussed as well as the topic of shape mapping. In addition, the history of tris(2-pyridylmethyl)amine (TPA) is reviewed. The idea of guest-host molecules will be highlighted as well, to give the reader an overview regarding supramolecular chemistry; its definition, classifications, interactions methods and some real examples of cation and anion binding into some common guests.

Physical Techniques

Electronic transitions (UV-Vis)

Ultraviolet and visible radiation (UV= 200-400 nm, visible = 400-700 nm) interacts with matter which causes electronic transitions (promotion of electrons from the ground state to higher energy state).²⁴ Those transitions are controlled by selection rules. For example, d-d transitions are weak because of one or more of the following rules are not applied:

1- Spin rule: only one electron is involved in any transition; transitions are allowed when there is no change in the spin multiplicity (i.e. $\Delta S=0$) of the ground and excited states.

e.g. Ti^{3+} , d^1 octahedral, $\epsilon \sim 10\text{M}^{-1}\text{cm}^{-1}$ (spin allowed).

e.g. Mn^{2+} , d^5 high spin Oh, $\epsilon \ll 1\text{M}^{-1}\text{cm}^{-1}$ (spin forbidden).

2- Laporte rule: in a centrosymmetric system allowed transitions are only between orbitals of different symmetry, i.e. $u \rightarrow g$, $g \rightarrow u$.²⁵ $\Delta l = \pm 1$ rule: only transitions that involve a change in the orbital angular momentum quantum number (l) of 1 are allowed, but transitions within the same sub-level are forbidden, i.e. $s \rightarrow p$, $p \rightarrow d$ allowed; $d \rightarrow d$, $f \rightarrow f$ forbidden.

Fully allowed electronic transitions such as the $\pi \rightarrow \pi^*$ transitions of aromatic organic compounds have molar extinction coefficients of 10^4 - $10^6 \text{ l.cm}^{-1}.\text{mol}^{-1}$. At the other extreme, Laporte and spin forbidden d-d transitions in centrosymmetric molecules, such as the crystal field spectra of octahedral manganese (+2) species may have intensities of the order of 10^{-2} - $10^{-3} \text{ l.cm}^{-1}.\text{mol}^{-1}$.

Molar extinction coefficients for various types of complexes are given in Table.1.²⁶

Chapter 1: Introduction and Background Theory

Table 1: Molar extinction coefficients for various types of complex²⁵

Molar Extinction Coefficients (l.cm ⁻¹ .mol ⁻¹)	Type of Transition	Type of Complex	Example
10 ⁻³ -1	Spin forbidden Laporte forbidden	Many octahedral and tetrahedral complexes of d ⁵ ions	[Mn(H ₂ O) ₆] ⁺²
1-10	Spin forbidden Laporte forbidden	Tetrahedral complexes of d ⁵ ions with intensity stealing	[MnBr ₄] ⁻²
	Spin allowed Laporte forbidden	Ionic six coordinate molecules	[Ni(H ₂ O) ₆] ⁺²
10-10 ²	Spin forbidden Laporte forbidden	Certain of the more covalent tetrahedral complexes of the d ⁵ ions	[FeBr ₄] ⁻ 3rd row transition metal complexes
	Spin allowed Laporte forbidden	Six coordinate molecules with intensity stealing complexes with organic ligands	[PdCl ₄] ⁻²
10 ² -10 ³	Spin allowed Laporte forbidden	Tetrahedral complexes , certain six coordinate molecules of low symmetry,	[NiCl ₄] ⁻² , (2-picoline) ₂ Co(NO ₃) ₂
	Spin allowed Laporte allowed	many square complexes particularly with organic ligands Some MLCT bands in molecules with unsaturated ligands, some forbidden charge transfer bands	-
10 ² -10 ⁴	Spin allowed Laporte forbidden	Asymmetric complexes with covalent ligands	acac, soft ligands P, As
10 ³ -10 ⁶	Spin allowed Laporte allowed	Many charge transfer absorptions. Electronically allowed transitions in organic species	-

For co-ordination compounds there are three main types of electronic transition which can be considered:

- Ligand spectra:** Transitions involving electrons between orbitals on the ligand ($\pi-\pi^*$, $n-\pi^*$). Typical, unless a ligand has an extended π system, these transitions occur at high energy and are more intense than other transitions observed for co-ordination compounds.

2. **Charge transfer transitions:** Transitions involving movement of electrons from L to M, M to L. Many inorganic species show charge-transfer absorption and are called charge-transfer complexes. These involve a temporary movement of an e^- from $M \rightarrow L$ or $L \rightarrow M$. These transitions are much more intense compared with the forbidden d-d transitions as they are spin allowed and Laporte allowed; the molar extinction coefficient for charge-transfer absorptions are large (10^2 - 10^4 L mol⁻¹ cm⁻¹). Examples include MnO_4^- (LMCT) and $[Ru(bipy)_3]^{2+}$ (MLCT).²⁷ Typically, these transitions occur at intermediate energy, between those of the $\pi \rightarrow \pi^*$ ligand transitions. In addition, they also are of an intermediate intensity. In general, their energy may be related to the ease of oxidation/reduction of the metal centre.

3. **d-d transitions:** Transitions of electrons within the d orbitals, or within f orbitals (d-d, f-f). In order to discuss d-d transitions, a crystal field theory should be clarified. A representation of the d orbitals is shown in (Fig.1). In the absence of any ligands around the metal, the energies of all five d-orbitals of a transition metal are degenerate. The presence of ligands will result in an increase in the energy levels of all these orbitals. This will result in the removal of the degeneracy, because some ligands and orbitals will interact more strongly than others. The most common geometry encountered in transition metal chemistry is based on octahedral symmetry with the six ligands lying along the x, y, and z axes. In this arrangement the greatest interaction will be between the ligands and the metal $d_{x^2-y^2}$ and d_z^2 orbitals since these orbitals have their maximum electron density along the x, y, and z axes. The d_{xy} , d_{xz} , and d_{yz} orbitals have their electron density maxima lying between the axes and so interaction between these orbitals and the ligands will be less. The presence of six octahedrally coordinated ligands therefore results in two sets of orbitals, one triply degenerate t_{2g}

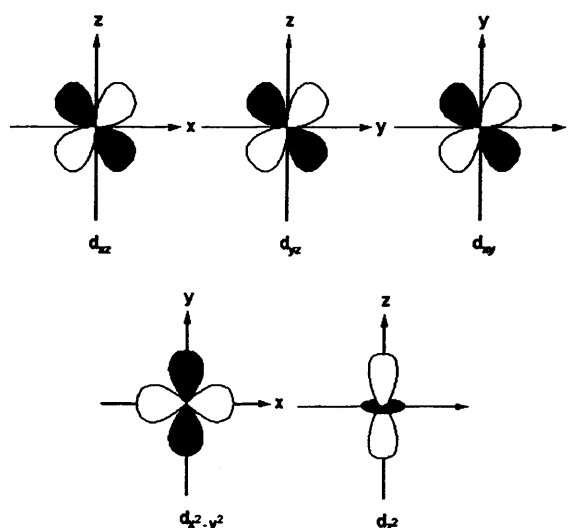


Figure 1: The shape of the d-orbitals.

orbitals will interact more strongly than others. The most common geometry encountered in transition metal chemistry is based on octahedral symmetry with the six ligands lying along the x, y, and z axes. In this arrangement the greatest interaction will be between the ligands and the metal $d_{x^2-y^2}$ and d_z^2 orbitals since these orbitals have their maximum electron density along the x, y, and z axes. The d_{xy} , d_{xz} , and d_{yz} orbitals have their electron density maxima lying between the axes and so interaction between these orbitals and the ligands will be less. The presence of six octahedrally coordinated ligands therefore results in two sets of orbitals, one triply degenerate t_{2g}

and the other doubly degenerate e_g . The sets of orbitals are separated by an energy gap labelled as Δ_o . The t_{2g} orbitals are stabilised by $2/5 \Delta_o$ and the e_g orbitals destabilised by $3/5 \Delta_o$. This splitting of the orbital energy levels is referred to as crystal field splitting. By multiplying the number of electrons in each orbital and its relative energy, expressed as Δ_o , the CFSE is obtained. There are many factors affecting Δ_o such as the nature of the ligand and the strength of both σ and π bonding. Although the octahedral arrangement of six ligands around a metal centre is the most prevalent for transition metal complexes, tetrahedral and square planar geometries are also fairly common. The splitting diagram and energy level for some common geometries are shown in (Fig. 2).

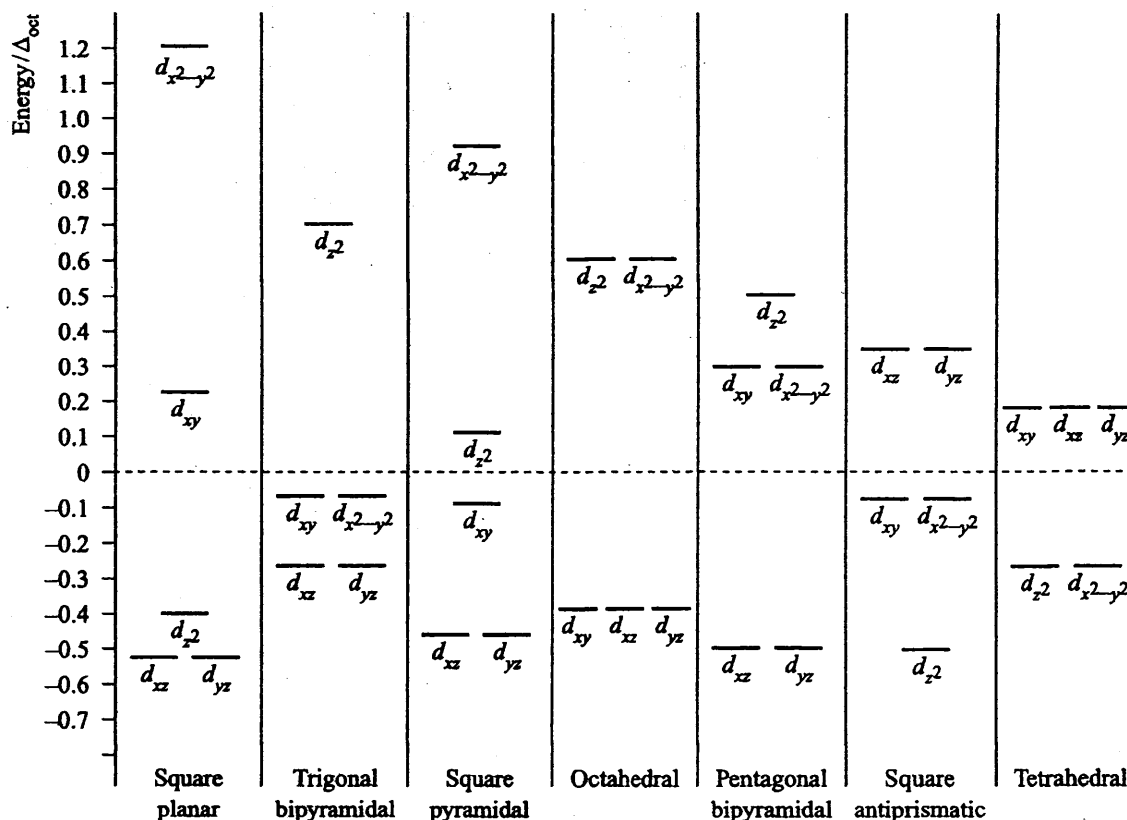


Figure 2: Crystal field splitting diagram for some common fields; splitting are given with respect to Δ_{oct} .²⁸

Initially, one might think that the number of observed d-d transitions directly relates to the splitting of the d-orbitals in the applied ligand field.

While this is true for a d^1 configuration, multi electron systems are not so simplistic and a group theoretical approach is required to readily determine the number of different transitions that can be expected for the different electronic configurations in the different ligand field geometries.

However, the situation is slightly simplified by hole formalism which allow us to inter-relate the various electron configurations such that we can relate d^4 , d^6 and d^9 to d^1 and we can relate d^3 , d^7 and d^8 to d^2 . For example, the expected spectra for O_h and T_d complexes may be summarised by two Orgel diagrams (Fig. 3 and 4). They are useful for showing the energy levels of both high spin octahedral and tetrahedral transition metal ions. They only show the spin-allowed transitions.

For complexes with D ground terms only one electronic transition is expected and the transition energy corresponds directly to D. Hence, the following high spin configurations are dealt with: d^1 , d^4 , d^6 and d^9 .

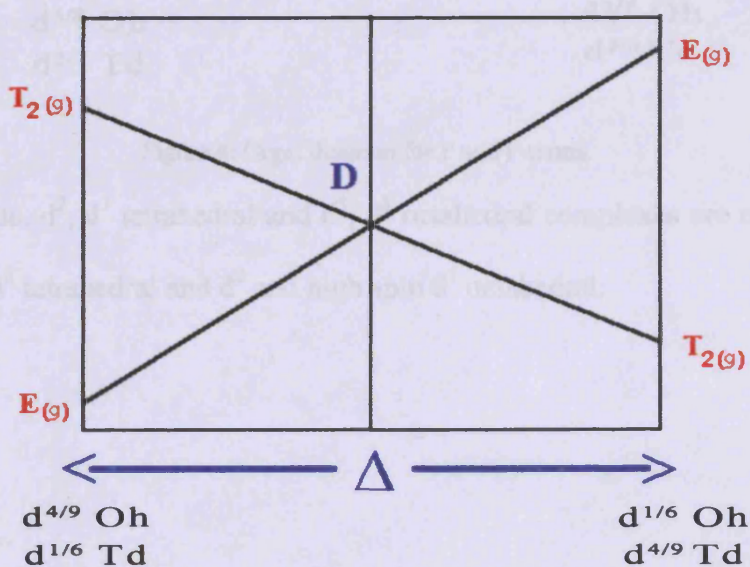


Figure 3: Orgel diagram for D term.

On the left hand side d^1 , d^6 tetrahedral and d^4 , d^9 octahedral complexes are covered and on the right hand side d^4 , d^9 tetrahedral and d^1 , d^6 octahedral.

Crystallography (X-ray)

For complexes with F ground terms, three electronic transitions are expected. The following configurations are dealt with: d^2 , d^3 , high spin d^7 and d^8 .

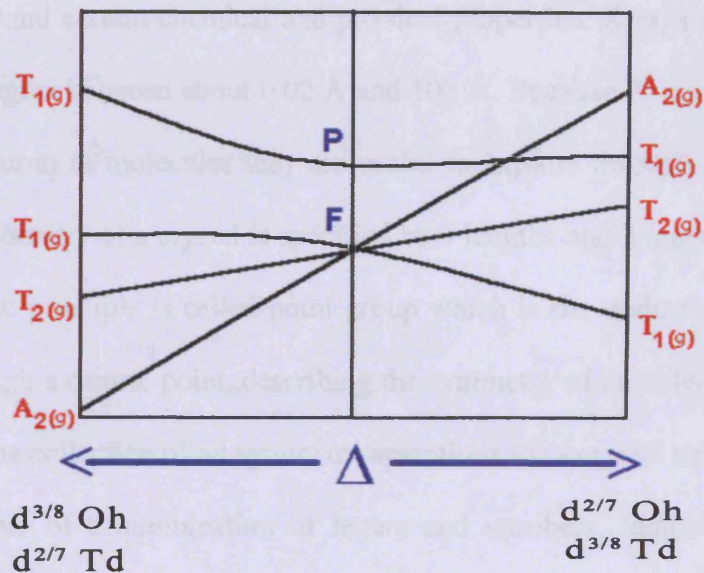


Figure 4: Orgel diagram for P and F terms.

On the left hand side, d^2 , d^7 tetrahedral and d^3 , d^8 octahedral complexes are covered and on the right hand side d^3 , d^8 tetrahedral and d^2 and high spin d^7 octahedral.

Complex	Ground State	Excited States
d^2 Td	A_2	T_2 , T_1 , A_1
d^3 Oh	T_2	T_1 , T_2 , A_1 , A_2
d^7 Td	T_2	T_1 , T_2 , A_1 , A_2
d^8 Oh	T_2	T_1 , T_2 , A_1 , A_2

Crystallography (X-Ray)

The main purpose of crystallography is to determine the atomic structure of crystalline solids giving information about the location and type of atoms, bond distances, local environment and absolute configuration. Although the crystal structure represents compounds in the solid state and tell us little about compounds in solution.²⁹ Knowing the structure is extremely important when trying to understand certain chemical and physical properties. X-rays are electromagnetic radiation with wavelengths between about 0.02 Å and 100 Å. Because X-rays have wavelengths similar to the size of atom in molecules they are useful to explore through diffraction patterns within crystals. The geometry of a crystal is specified by 3 lengths and 3 angles which define the unit cell. Another basic principle is called point group which is the collection of all symmetry elements passing through a central point, describing the symmetry of an individual object. There are 32 point groups. The collection of all symmetry operations for a crystal structure is known by space group. It consists of a combination of letters and numbers, indicating the symmetry present. There are 230 space groups.³⁰ A unique part of the structure which may have one molecule or more or a fraction of a unit cell is called the asymmetric unit. Operation of symmetry except for pure translation generates the unit cell, and then operation of translation symmetry generates the complete crystal structure. Space groups and crystals are divided into 7 crystal systems according to their point groups (Table 2).²⁹

Crystal system	Unit cell edges	Unit cell angles
Cubic	$a = b = c$	$\alpha = \beta = \gamma = 90^\circ$
Hexagonal	$a = b \neq c$	$\alpha = \beta = 90^\circ, \gamma = 120^\circ$
Rhombohedral	$a = b = c$	$\alpha = \beta = \gamma \neq 90 \text{ or } 120^\circ$
Tetragonal	$a = b \neq c$	$\alpha = \beta = \gamma = 90^\circ$
Orthorhombic	$a \neq b \neq c$	$\alpha = \beta = \gamma = 90^\circ$
Monoclinic	$a \neq b \neq c$	$\alpha = \gamma = 90^\circ, \beta \neq 90 \text{ or } 120^\circ$
Triclinic	$a \neq b \neq c$	$\alpha \neq \beta \neq \gamma \neq 90 \text{ or } 120^\circ$

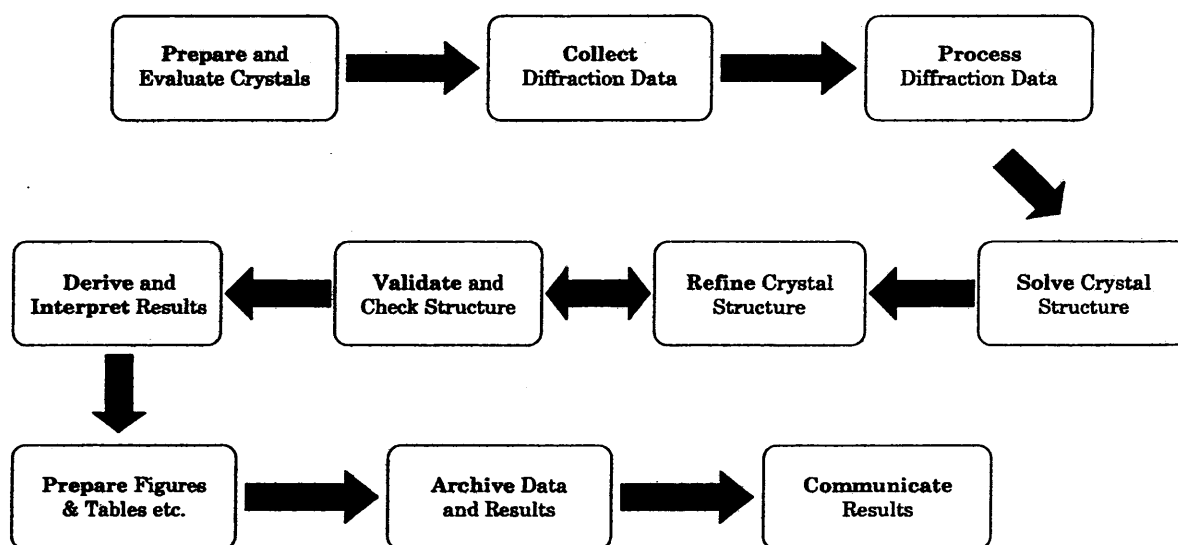
Table 2: seven crystal systems

Single Crystal X-ray Structure Analysis

The over-all process of structure analysis is outlined in the diagram below. The principal operations are:

1- Crystal Growth, Selection and Mounting: For most analyses, only one crystal is used, so it is important that it should be of excellent quality and representative of the whole sample. The crystal is the primary source of information for the analysis, and all else is influenced by its quality. This is the last chance that the analyst has to experimentally influence the analysis. Crystals can be delicate, so should always be handled with care. Effort spent in choosing a good crystal will almost certainly be repaid later.

Diagram of a Typical Crystal Structure Analysis



2- Crystal Characterisation and Data Collection: Modern instruments are supplied with excellent software able to determine the unit cell and some measures of crystal quality from very short experiments. Even so, the cautious analyst will look at the diffraction image carefully, and verify that the proposed unit cell does indeed predict all the diffraction spots. However, even if only low quality crystals, cracked, split, twinned, or otherwise flawed, are available, it may be

possible to use them to obtain an indicative analysis, which although un-publishable, would be adequate to settle some chemical issue. This also is largely automatic with modern machines.

The diffraction pattern is the first step in data collections

processes which tells us:

a) Geometry of diffraction pattern (positions of spots, directions of diffracted beams) is related to unit cell (lattice) (Fig. 5).

b) Symmetry of diffraction pattern is related to symmetry of crystal structure (space group).

c) Intensities: of diffraction pattern are related to the nature and positions of atoms within the asymmetric unit.

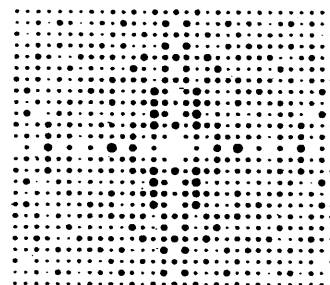


Figure 5: Example of a diffraction pattern

3- *Space Group Determination*: Again, modern software gets the best true answer more often than not, but most analysts will come across marginal cases where insight and experience will help resolve ambiguous or ill-determined situations.

4- *Phasing the Diffraction Data*: Because diffraction is an interference phenomenon the emergent beams have both an amplitude and phase. The amplitude is quite easily measured. The phase is effectively un-measurable except with considerable effort, if both the amplitude and phase are known, the continuous electron density throughout the crystals could be computed. Between 1930 and 1960 phases could only be derived indirectly by proposing structural models, and back calculating the structure factors. The Patterson method, particularly for structures with a single "heavy" atom, was the most successful procedure. However, from the 1950's onwards, techniques were developed for estimating the probable values for the phase angles directly from the measured intensities Direct Methods. These techniques have matured into programs which can usually yield recognisable solutions for structures containing up to several hundred atoms in the unit cell. These programs are the key to modern structure analysis.

Chapter 1: Introduction and Background Theory

5- *Refinement*: Direct Methods gives approximate phases, which can be used in a Fourier synthesis to yield an approximate atomic structure. Further Fourier syntheses may improve the model, but eventually the atomic coordinates are refined by the method of Least Squares. This is an iterative process in which the atomic coordinates are adjusted to minimize the difference between the observed-structure amplitudes and ones computed from the model. Refinement can be extremely trivial and almost automatic, but in a large percentage of cases there are small (or large) problems which will require careful attention and experience.³¹

6- *Validation, Evaluation, Publication and Archiving*: Eventually the model is evaluated in order to assess the probability that it is correct. Two kinds of validation are generally involved. One simply looks at various mathematical properties of the model, and is suitable for detecting gross problems. The other is more subjective, and involves assessing the chemical/physical features of the model. A validated structure ought to be published, or failing that, at least archived in a public place for the benefit of crystallographers. The International Union of Crystallography has devised a file syntax to help with publication and archiving - the "cif" format.³² For small organic and organometallic materials, the most common archive is the Cambridge Structural Database (CSD)³³ which is well established together with good tools for accessing it. Access to the CSD is by subscription. Recently a "public domain" archive has been formed, the Crystallographic Open Database (COD).³⁴

Cyclic Voltammetry

Early contributions to cyclic voltammetry were made by investigators including Randles.³⁵ Electrochemical studies of the complexes formed were undertaken using the cyclic voltammetry (CV) technique which is the study of the electron transfer and transport properties of electrolysis reactions. The setup consists of a three-electrode system: the working, reference and counter electrodes. The potential of the working electrode is controlled against the reference electrode (Ag/AgCl). The current flows between the working electrode and the counter electrode (Pt). The basics of CV involve immersing a working electrode (Pt) in an unstirred solution of the compound to be studied, cycling the potential and measuring the resulting change in current. The potential is normally swept as shown in the graph (Fig. 6), which illustrates two cycles each consisting of a forward and a backward scan.

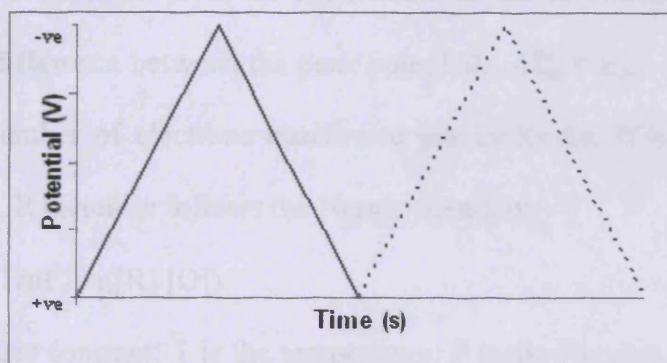


Figure 6: Cyclic voltammogram potential sweep

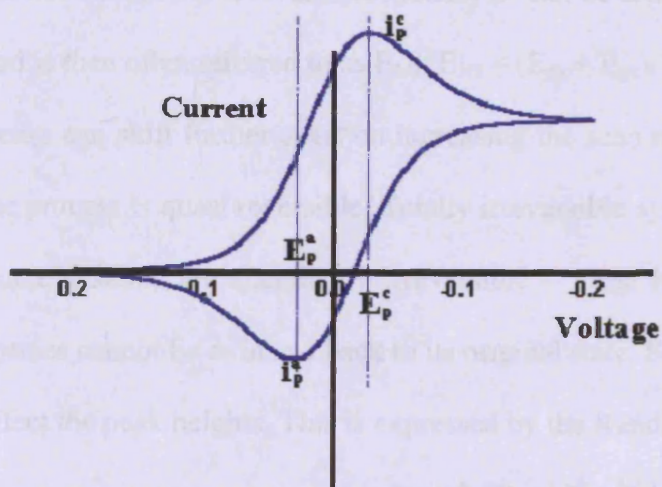


Figure 7: Typical CV experiment

(Fig. 7) shows a typical cyclic voltammogram. The current depends on the movement of the redox species to the surface of the electrode and the electron transfer reaction. The rate constant for the reduction electron transfer process is exponentially dependent on the applied potential. As the species close to the

electrode is reduced, there is less and less reducible species in the vicinity of the electrode.

Chapter 1: Introduction and Background Theory

Eventually the rate depends on the diffusion of reducible species – a slow process. This explains why, for the forward scan, there is a peak with a maximum current. On the reverse scan, there is a large amount of reduced species close to the electrode surface. This is then oxidised back to the starting material, provided the reduction is reversible. For reversible redox processes, therefore, the peaks are often a mirror of each other. A typical cyclic voltammogram is shown. E_{pa} and E_{pc} are the potential values at the maxima. i_{pa} and i_{pc} are the peak heights, or the respective currents for the oxidation and reduction processes. Reversibility is an important concept in CV. For a reaction to be considered to be reversible, the redox system needs to be able to maintain concentrations of the reduced and oxidised forms, and form an equilibrium at the electrode surface³⁶. For a truly reversible process, the difference between the peak potentials, $\Delta E_p = E_{pc} - E_{pa}$, is equal to $59/n$ mV, where n is the number of electrons transferred per molecule. If a process is reversible, it is said to be Nernstian. It therefore follows the Nernst equation:

$$E = E^\circ - (RT/nF) \ln([R]/[O])$$

E° is the formal reduction potential; R is the gas constant; T is the temperature; F is the Faraday constant; $[R]$ is the concentration of the reduced form; and $[O]$ is the concentration of the oxidised form. For a reversible system, E° can be estimated as the average of the peak potentials, and is then often referred to as $E_{1/2}$: $E_{1/2} = (E_{pa} + E_{pc})/2$

Peaks can shift further apart on increasing the scan rate of the potential sweep. This means that the process is quasi reversible. Totally irreversible systems have peaks that do not overlap at all. Some systems are chemically irreversible – these have no return peak at all, as the reduced species cannot be oxidised back to its original state. For reversible systems, the scan rate can also affect the peak heights. This is expressed by the Randles-Sevcik equation:³⁷

$$i_p = (2.69 \times 10^5) n^{3/2} A D_o^{1/2} \nu^{1/2} C_o$$

The current is given as amps; A is the electrode area (cm^2); D_o is the diffusion coefficient (cm^2/sec); ν is the scan rate (V/sec); and C_o is the bulk concentration (moles/cm^3). It can be seen

Chapter 1: Introduction and Background Theory

from the equation that the current is proportional to the square root of the scan rate. Quasi reversible systems do not have this relationship. For a completely reversible system, the values of i_{pc} and i_{pa} should be identical. It can therefore be written that: $i_{pa}/i_{pc} = 1$.

Shape Mapping

For a coordination chemist, the geometry around a metal is important; donor atoms take different positions around the metal to reduce electronic repulsion, if possible. By looking to any given structure in 3 dimensions you cannot be certain of predicting the geometry of the structure! By using the programme SHAPE v1.1b, it is easy to confidently calculate the most fitting description of the geometry of a given crystal structure. This programme uses the concept of continuous shape measures (CShM), which provide quantitative parameters and can be used to calculate the deviation of geometries from the ideal shapes.³⁸ First, a reference shape needs to be found. The search requires optimization with respect to size, orientation in space and pairing of vertices of the reference and example structures. A comparison is therefore made using the formula:

$$SP(R) = (\sum_{k=1}^N q_k^2) / N * 100$$

SP(R) is the shape measure, q_k is the distances between the ideal and actual positions, and N is the normalisation factor, making the results size independent.³⁹ The equation gives a result between 0 (no deviation) and 100, allowing a gauge of the structural distortion.

Scatter plots have been constructed for shapes with the same number of vertices. These shape maps, along with the results from the computer programme, give an indication of the distortion pathway that the shape is most likely to undergo. The shape map for 5-coordinate geometries is included in (Fig. 8). By using the values given for trigonal bipyramidal and square planar geometry, the most likely distortion pathway the crystal structure follows

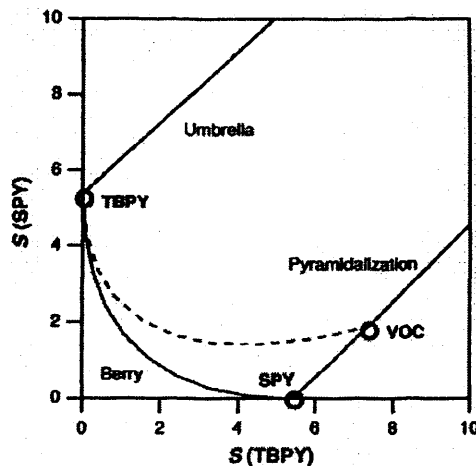


Figure 8: Shape map for 5-coordinate geometries

can be derived by where on the shape map the geometry lies. The Berry distortion can be seen as the minimum distortion pathway – the route between ideal trigonal bipyramidal (TBPY) and square planar (SPY) geometries. The dotted line shows the transition from trigonal bipyramidal to vacant octahedral (VOC) geometries: the pseudo-Berry path. Umbrella and pyramidalization pathways are also marked. These are illustrated in (Fig. 9). Using the values of $SP(R)$ generated from the programme for trigonal bipyramidal and square planar, the position of the tested geometry can be found on the scatter plot. This gives an indication of the distortion pathway followed.

Another, more shape simple, shape determining method is the Reedijk parameter.⁴⁰ This considers the degree of TBPY and SPY geometries in the complex

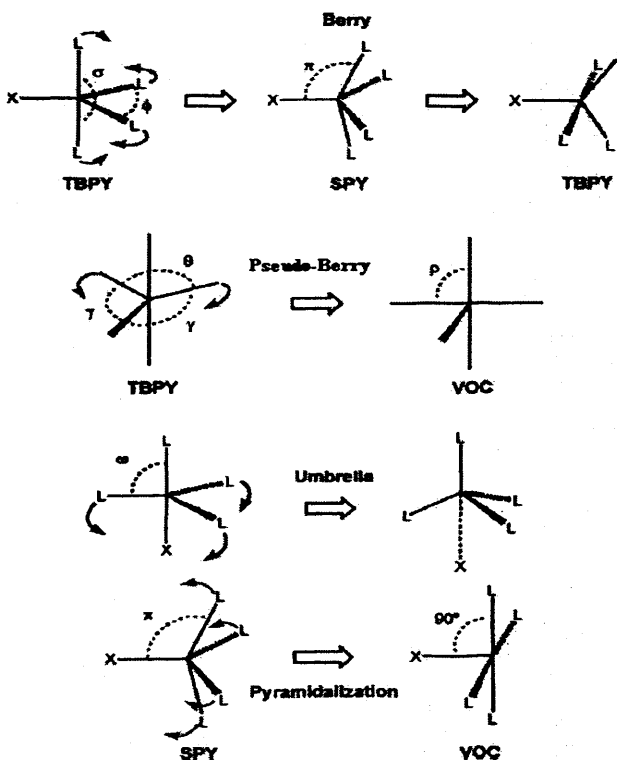


Figure 9: Distortion pathways 5-coordinate geometries

Chapter 1: Introduction and Background Theory

and the two largest angles: σ and Φ . The parameter is then calculated via the equation:

$\tau = (\sigma - \Phi)/60$. A value of 1 denotes trigonal bipyramidal and 0 denotes square pyramidal. The

parameter therefore gauges roughly where the geometry is along the Berry distortion pathway.

Unfortunately, this approach does not consider the vacant octahedral geometry and the angle π .

The approach therefore does not account for the Pseudo-Berry or Umbrella distortion pathways.

While useful, this method clearly has some limitations.

Ligands classes

Monodentate ligand is a ligand which forms only one bond with the central atom. Bidentate ligand has two points at which it can attach to the central atom. Bidentate ligands are often referred to as chelating ligands. Hexadentate ligand has 6 lone pairs of electrons, all of which can form co-ordinate bonds with the same metal ion. The best example is EDTA. Macrocyclic ligands are polydentate ligands containing donor atoms either incorporated in or, less commonly, attached to a cyclic backbone. As usually defined, macrocyclic ligands contain at least three donor atoms and the macrocyclic rings typically consist of a minimum of nine atoms.⁴¹ Although the number of possible complex ions and compounds formed in aqueous solution is very large, there are two generalizations which allow the prediction of the most likely complexes to form a complicated mixture of metal ions and ligands.

1. *Chelate Effect*: Chelate ligands form more stable complexes than analogous monodentate ligands e.g. ethylene diamine and ammonia.

2. *Macrocyclic Effect*: Macrocyclic ligands form more stable complexes than chelate ligands.⁴²

Stability follows the order Macrocyclic > Chelate > Monodentate because of the strength of the interaction between such ligands and metals because of thermodynamic consideration, entropy and enthalpy which are related to the stability constant and the change in free energy by this equation: $\Delta G^\circ = -RT \ln K = \Delta H^\circ - T\Delta S^\circ$.⁴³

Tripodal Tetradentate Triamine ligands

Tripodal tetradentate triamine ligands contain a tertiary N atom bonded to three arms, each of which contains an N-donor atom, via at least one methylene group on each arm, and generally bind to a single transition metal or lanthanide ion using all four N-donor atoms. Tetradentate tripodal ligands have the general structure depicted in (Fig. 10) and consist of a central

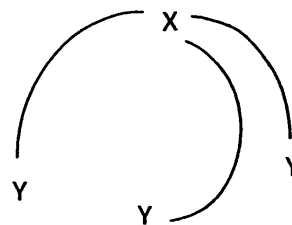
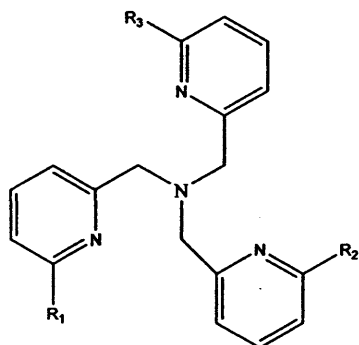


Figure 10: General structure of a tetradentate tripodal ligand

donor atom X attached to three arms, each of which also contains at least one methylene group and a donor atom Y. A large number of such ligands contain identical sets or combinations of the donor atoms N, S, O and P. The ligands can differ both in the lengths of the arms and in the nature of the N donor atoms on each arm and there are at least 54 such ligands (not including their alkylated and substituted derivatives) known, the majority of these ligands have been prepared only in the last 20 years and much of their coordination chemistry remains to be explored in detail. As is the case with many organic ligands, most tripodal tetraamine ligands are known by an abbreviation, usually of three or four letters, nominally derived from the full name of the ligand. While this is convenient, this is an unsatisfactory situation and ideally a systematic abbreviation system should be developed.¹⁰

Tris(2-pyridylmethyl)amine (TPA)



TPA was first prepared by Anderegg and Wenk in 1967 from the reaction of 2-(aminomethyl) pyridine with two equivalents of 2-(chloromethyl) pyridine in aqueous solution.⁴⁴ Derivatives of TPA substituted on either the pyridine rings or at a methylene carbon can be prepared by adaptation of this method and use of the

appropriately substituted starting materials. Particular interest has centred on the synthesis of TPA derivatives having substituents at the 6-positions of the pyridyl rings. TPA is one of the most studied tripodal tetradentate amine ligands with complexes of all first row metals except Ti having been reported, along with most second and third row metals, as well as the majority of lanthanide ions.¹⁰ Tables 3 and 4 show the known 6-substituted TPA derivatives and structurally characterized complexes.

Chapter 1: Introduction and Background Theory

Table 3: Known 6-substituted TPA derivatives

R1	R2	R3	References
F	F	F	45
Br	Br	Br	46
NH ₂	NH ₂	NH ₂	47
NH-CH ₂ -CMe ₃	NH-CH ₂ -CMe ₃	NH-CH ₂ -CMe ₃	48
NH-C(O)-CMe ₃	NH-C(O)-CMe ₃	NH-C(O)-CMe ₃	14
COOH	COOH	COOH	49
C(O)Net ₂	C(O)NEt ₂	C(O)NEt ₂	49
CH ₂ OH	CH ₂ OH	CH ₂ OH	50
(4-H ₂ OCH ₂ CH ₂ OMe)C ₆ H ₄	(4-H ₂ OCH ₂ CH ₂ OMe)C ₆ H ₄	(4-H ₂ OCH ₂ CH ₂ OMe)C ₆ H ₄	46
C ₆ H ₅	C ₆ H ₅	C ₆ H ₅	51
Me	Me	Me	52
Br	Br	Cl	46
Me	Me	C ₆ H ₅	53
Me	Me	CH ₂ OH	54
NH ₂	NH ₂	H	55
3,5-Me ₂ C ₆ H ₃	3,5-Me ₂ C ₆ H ₃	H	56
NH-CH ₂ -CMe ₃	NH-CH ₂ -CMe ₃	H	57
NH-C(O)-(2-C ₁₀ H ₇)	NH-C(O)-(2-C ₁₀ H ₇)	H	58
CH ₂ OH	CH ₂ OH	H	50
NH-C(O)-CMe ₃	NH-C(O)-CMe ₃	H	59
Br	Br	H	46
C ₆ H ₅	C ₆ H ₅	H	60
Me	Me	H	52
NH ₂	H	H	61
C ₆ H ₄ (2-NH-SO ₂ -(4-MeC ₆ H ₄))	H	H	62
2,5-(HO) ₂ C ₆ H ₃	H	H	63
2,5-(O-(2-C ₅ H ₉ O)) ₂ C ₆ H ₃	H	H	63
2,5-(MeO) ₂ C ₆ H ₃	H	H	63
2-HOC ₆ H ₄	H	H	53
2-DC ₆ H ₄	H	H	53
3-(OMe)C ₆ H ₄	H	H	53
3-MeC ₆ H ₄	H	H	53
3-ClC ₆ H ₄	H	H	53
3-F ₃ CC ₆ H ₄	H	H	53
3-O ₂ NC ₆ H ₄	H	H	53
4-OMeC ₆ H ₄	H	H	64
NH-CH ₂ CMe ₃	H	H	57
NH-C(O)CMe ₃	H	H	57
CH ₂ Cl	H	H	50
CHO	H	H	50
CH ₂ OH	H	H	50
(4-OCH ₂ OCH ₂ CH ₂ OMe)C ₆ H ₄	H	H	46
Cl	H	H	46
Br	H	H	46
4-(benzo-18-crown-6)	H	H	46
C ₆ H ₅	H	H	60
Me	H	H	65

Chapter 1: Introduction and Background Theory

Table 4: Structurally characterised $[M(\text{TPA})X]^{n+}$ complexes

M	X	References
Cu^{2+}	CN^-	66
Cu^{2+}	Cl^-	67
Cu^{2+}	Cl^-	68
Cu^{2+}	MeCN	69
Cu^+	MeCN	69
Co^{2+}	Cl^-	70
Cu^{2+}	F^-	71
Co^{2+}	Cl^-	72
Zn^{2+}	Cl^-	73
Zn^{2+}	$\text{C}_6\text{H}_5\text{COO}^-$	73
Cu^{2+}	$\text{C}_6\text{H}_5\text{C}(\text{O})\text{COO}^-$	74
Cu^{2+}	OH_2	75
Hg^{2+}	Cl^-	76
Co^{2+}	MeCN	77
Cu^{2+}	ONO^-	78
Zn^{2+}	$(\text{p-NO}_2\text{C}_6\text{H}_4\text{O})_2\text{PO}_2^-$	79
Cu^{2+}	CN^-	80
Fe^{2+}	$2,4,6\text{-Me}_3\text{C}_6\text{H}_2\text{S}^-$	81
Cu^{2+}	NO_2^-	78
Zn^{2+}	Cl^-	82
Zn^{2+}	I^-	83
Cu^{2+}	Br^-	82
Cu^+	Cl^-	84
Fe^{2+}	Cl^-	85
Ru^{2+}	Cl^- , DMSO, PF_6^-	86

Guest-Host Molecules

The field of supramolecular chemistry has been defined as ‘chemistry beyond the molecule’ investigating new molecular systems in which the most important feature is that the components are held together by intermolecular forces not by covalent bonds.⁸⁷ In 1894 Emil Fischer described guest-host molecules by the ‘lock and key’ principle.⁸⁸ In another words the size, shape and position of the binding sites within the active site should be ideal for specific substrate recognition. There are a number of interactions that hold molecules together to be supramolecular compounds:

- 1- Electrostatics (ion-ion, ion-dipole and dipole-dipole): attraction between opposite charges.
- 2- Hydrogen bonding: directional nature and precision.
- 3- π - π stacking interactions: occur in aromatic rings (face-to-face or edge-to-face).
- 4- Dispersion forces (Van der Waals forces): dipoles in the electron clouds interact favourably.
- 5- Hydrophobic effects.

These forces can be used individually, but more often than not, all are used to maximize the selectivity of the receptor and increase the strength of the complex formed.⁸⁹ The strengths of many of the non-covalent interactions are generally much weaker ranging 2 kJmol⁻¹ for dispersion forces, through to 20 kJmol⁻¹ for a hydrogen bond to 250 kJmol⁻¹ for an ion-ion interaction, while the bond energy of a typical single covalent bond is around 340 kJmol⁻¹.

Characterising supramolecular systems

The accurate characterization of supramolecular complexes involves the use of:

1- *Crystallography*: a crystal structure is the most convincing evidence of the guest-host complex. It shows the binding sites, it also gives information about the interaction that hold the guest in place, however as I have already said before it is only valid for the solid state and for more about solution phase, alternative methods are used.

2- *NMR titration*: where the NMR spectrum of a solution of the host in deuterated solvent is measured and then the guest is added to this solution in small aliquots. The NMR resonances of the host are monitored, and if binding occurs, the guest perturbs their electronic environments. Protons which form specific hydrogen bonds to the guest, or are located in parts of the receptor with close guest contact are more strongly affected. Structural information about the super molecule can therefore be obtained. This technique is not limited to ^1H NMR, and titration experiments may be performed by monitoring any nmr active nucleus in the host or the guest provided that the electronic environment of the nucleus is perturbed on binding. Complexation is a dynamic exchange between the bound and unbound forms of the host, and the nmr response therefore provides an insight into the binding kinetics. If the binding is kinetically fast compared to the frequency separation of free and complexed host NMR resonances (i.e. complex lifetime $< 10^{-2}$ - 10^{-3} s), then the host's NMR resonances are observed as an average peak. On the addition of increasing quantities of guest, this time averaged peak shifts continuously until the receptor is saturated. A titration curve having a distinctive shape can then be extracted. Initially, the host is strongly perturbed by the addition of small amounts of guest, but at higher concentrations, it becomes saturated by the guest, and is not further perturbed. If however, binding is kinetically slow compared to the nmr timescale, then a time averaged nmr peak is not observed on guest addition. Instead, the resonances for free host gradually diminish in intensity, whilst resonances for the host-guest complex (at different chemical shifts) grow. Quantitative

information can also be obtained. For any exchange process, such as complexation, the kinetics can be varied by changing the temperature. If a solution exhibiting slow exchange is heated, the two individual peaks gradually broaden and merge. Eventually, a point intermediate between fast and slow exchange is reached at which a single broad peak is observed. This is referred to as coalescence. Other techniques for investigating host-guest interactions operate on different timescales. In UV-Vis spectroscopy, for example the lifetime is typically 10^{-15} s, and as this rate is faster than a diffusion-controlled process, all recognition events investigated by this method exhibit slow exchange.

3- *UV-Vis spectroscopy*: it can be used to monitor the other receptor properties in order to study the effect of guest molecules. It is especially effective for investigating π -electron systems or transition metals as their spectra can be strongly perturbed on complex formation.

4- *Mass spectrometry*: it is being used to ascertain the mass of host-guest complexes, but the ionization method must be mild, otherwise the complex will be broken into its constituent pieces.

5- *Electrochemistry*: it is used with redox active groups such as: ferrocene and cobaltocenium which allow the detection of anions and cations as we shall see later.

Thermodynamic Information

Titration experiments can provide thermodynamic data. NMR experiments will be taken as an example. If the binding is kinetically slow, the relative concentrations of host and complex can be obtained from integration of the proton resonances. For a 1:1 complex, this allows direct calculation of the binding constant K_1 , as all three concentrations (host, guest and complex) are known. If the binding is kinetically fast, the titration curve contains all the necessary information. The 'sharpness' of curve reflects the affinity of the host for the guest. Computer programs such as: HypNMR⁹⁰ and WinEQNMR⁹¹ are routinely used to find the binding constant from this data. Performing titration experiments at different temperatures yields different binding constants, and this data can be used to yield values for ΔH and ΔS .

Solvent effects

In supramolecular chemistry there are competing interactions from potential guests and surrounding solvent molecules. Solvent molecules greatly outnumber the amounts of the host and guest present and therefore can have a very pronounced effect upon the dynamics and energetics of association. When in solution, host and guest species are surrounded by solvent molecules which interact with them. In order for binding to occur, many of these interactions must be broken, which has both enthalpic and entropic consequences. This desolvation process is shown in a simplified way in (Fig. 11). Enthalpically, energy must be expended to break the solvent–host and solvent–guest bonds. The removal of solvent molecules from the host and the guest leads to the solvent molecules having more freedom in the solution, which increases the entropy and also leads to the formation of solvent-solvent bonds. The choice of solvent can have significant consequences on the binding of a guest.



Figure 11: Host–guest binding equilibrium showing the desolvation of both species required prior to the binding occurring. The final complex is still solvated but overall there are more free solvent molecules present, hence increasing the entropy of the system.

Solvent effects can be understood by the way in which the individual molecules can interact with the host and the guest. Polar solvents are able to interact with host molecules via electrostatic interactions. Such solvents are particularly able to inhibit binding of charged species, as the solvent dipole can interact strongly with a charged centre, thus making the solvent–host or solvent–guest interactions harder to break. Other solvents are able to disrupt the binding by means of electron-pair or hydrogen bond donation and acceptance. Many solvents display both of these properties, for example, dimethylsulfoxide (DMSO) acts as both an electron-pair donor

and hydrogen bond acceptor by virtue of oxygen and sulfur lone pairs. The vast majority of supramolecular interactions are electrostatic in nature, meaning that polar solvents often act to reduce the observed binding. For this reason it is usual for any studies to be carried out in the least polar solvent possible to reduce the competition for the host. The conditions used can help to moderate the binding process, for example, if the binding is too strong to be conveniently measured, more polar solvents can be employed to reduce the binding constant.⁹² This makes comparisons of different systems very difficult.

Cation binding

Cations play an essential role in biological processes, large quantities of sodium, potassium, magnesium and calcium ions in particular are all critical to life and exist in body. Complexes of platinum have been shown to coordinate to DNA and hindering the growth of tumor cells.⁹³ Cations also play important roles in the environment where build-up of toxic heavy metals, such as lead, mercury and cadmium which could be separated. It is of critical importance to be able to isolate these ions from the environment.^{87, 94} The discovery of dibenzo[18]crown-6 (Fig. 12), by Charles J. Pedersen was a key step in the development of the discipline of supramolecular chemistry.⁹⁵ After that Lehn and co-workers prepared a range of bicyclic systems named cryptands (Fig. 13).

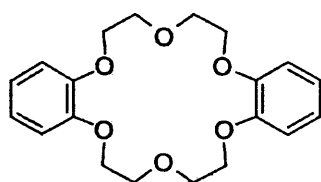


Figure 12: The first crown ether was made in 1960.

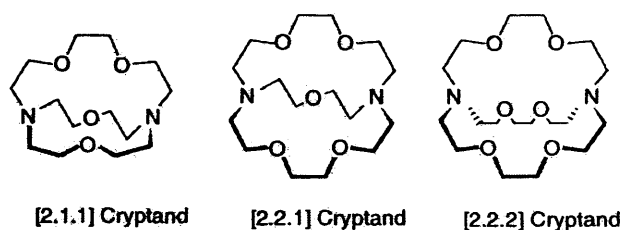


Figure 13: cryptands contain four, five and six oxygen atoms, respectively.

Chapter 1: Introduction and Background Theory

There is an optimal spatial fit between crown ethers and particular cations. It is true that [18]crown-6 is selective for K^+ , whereas the larger [21]crown-7 has a higher affinity for Rb^+ and Cs^+ than K^+ .⁹⁶ The cavity size of the [2.2.2] cryptand is similar to the cavity size of [18]crown-6 and is also a good host for K^+ . Due to the three-dimensional nature of the host, the cryptand encapsulates the metal ion and shields it from the outside environment. The binding constant of the [2.2.2]cryptand for K^+ is 10^4 times larger than [18]crown-6. The smaller [2.2.1]cryptand, is selective for Na^+ . Due to their lower flexibility and greater degree of preorganisation, cryptands display peak selectivity, in which binding constants are at a maximum for a particular metal ion. This is in contrast to the crown ethers, since they often bind a number of metal ions equally well. Spherands are the most preorganised of the macrocyclic ligands and are very rigid (Fig. 14), the fact that inter-oxygen repulsions present in the free host are ameliorated when the metal ion is inserted into the spherand cavity.

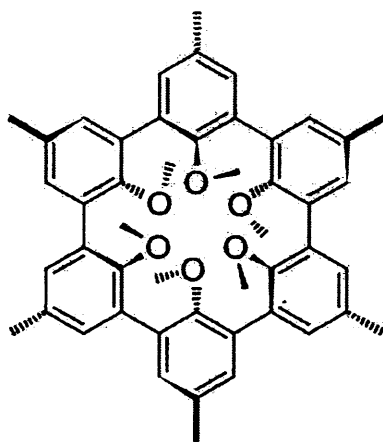


Figure 14: spherand-6 is one of the best-known examples.

To date, there have been many derivatives of spherands prepared and these include hybrids of spherands with crown ethers, podands and cryptands, form hemispherands, and cryptaspherands (Fig. 15).

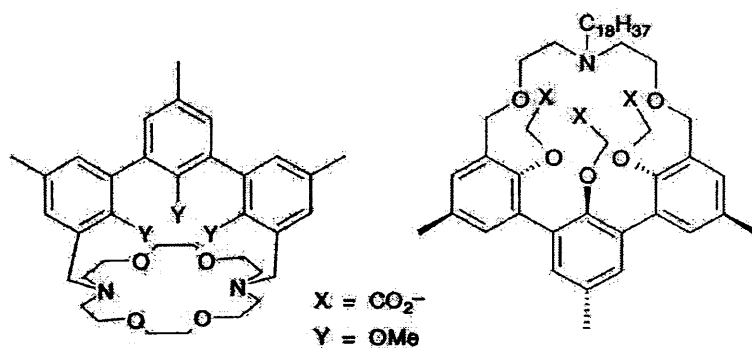


Figure 15: Examples of spherands's derivatives.

Another kind of cation receptors is the Calixarenes (Fig. 16).

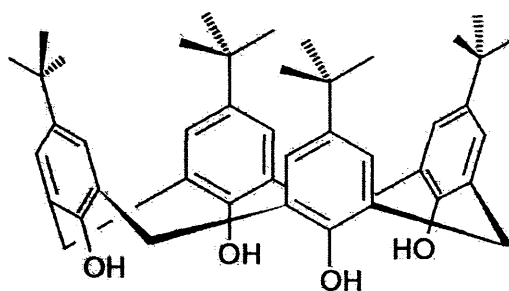


Figure 16: p-t-butylcalix[4]arene.

The calixarene framework is very versatile and many derivatives have been prepared by functionalizing the groups on the 'upper' and 'lower' rims (the upper, or wide rim is where the t-butyl substituents are located, while the hydroxyl groups are on the lower or narrow rim). By selectively changing the framework, chemists have been able to design hosts capable of binding cations, anions, neutral species or simultaneously combining different guests.⁹⁷

Anion binding

Anions play essential roles in many processes:

- Chemically: anions act as catalysts and bases. The use of a receptor to bind an anion can alter its reactivity. Anion receptors may also assist in the separation of complex chemical mixtures.
- Environmentally: anions can pose severe pollution problems. Per technetate anions are a toxic radioactive by-product of the nuclear power industry. Selective binding, extraction and sensing of such anions are, therefore, important goals.
- Biologically: 70% of all enzyme substrates are negatively charged (PO_4^{-3} and SO_4^{-2}).
- Medically: anions play key roles in many diseases (cystic fibrosis).

Anion binding was relatively slow to develop, even though one of the earliest anion receptors can be traced back to the work of Simmons and Park in 1968 on the katapinands (Fig. 17).

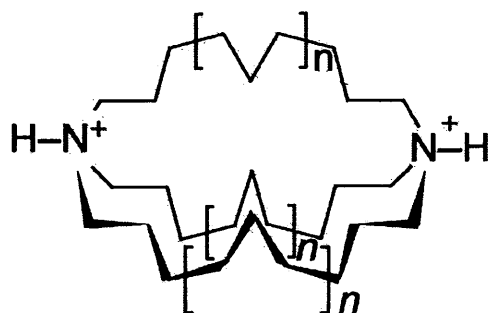


Figure 17: katapinands; $n=1$ or 2 .

The design of cation and anion hosts uses the same criteria, arising from the preorganised placement of complementary binding sites. However, there are some properties of anions that make the task a little more challenging, as follows:

1- Anions come in many shapes and sizes. Anions are generally larger than cations and therefore larger hosts are required to bind them. The smallest anion, F^- has a radius approximately comparable to the radius of K^+ . Generally, cations are spherical (except for molecular cations, such as ammonium ions), but anions are found in various shapes, for example, spherical

Chapter 1: Introduction and Background Theory

(halides), linear SCN^- , planar NO_3^- , tetrahedral ClO_4^- , HPO_4^{2-} and octahedral PF_6^- . Biologically important anions, such as nucleotides and many proteins, have much more complex shapes.

2- Anions have high free energies of solvation compared to cations of similar size and hence hosts for anions experience more competition from the surrounding medium.

3- Generally, most anions exist in a narrow pH window. This can be problematic for hosts that contain, for example, polyammonium functionalities within the receptor, as the host may not be fully protonated in the pH range where the anion is deprotonated.

4- Many anions are generally co-ordinatively saturated and they only bind via weak interactions, such as hydrogen bonding and Van der Waals interactions.⁹⁸

Most anions are Lewis-basic. The Lewis acid-base interaction is both strong and directional. The Lewis-basic nature also means that they are good hydrogen bond acceptors. Anions are also polarisable and therefore Van der Waals interactions play a significant role in binding, particularly when the anion has been encapsulated within the cavity of a host system and exhibits a high degree of surface-area contact. As with cations, the solvent medium drastically influences the host-guest affinity. Markedly higher binding affinity in charged systems is observed in non-polar solvents^{99,100} e.g. chloroform, than in highly polar solvents, such as dimethylsulfoxide or water, in which a lot of competition between the anion and the solvent is observed. Unfortunately, however, the chemist is controlled by the solubility of his designed receptor.^{101,102} The most obvious way to bind anions is to design a host that contains a positive electrostatic charge as electrostatic interactions are often the first interactions between the substrate and the host. Early work showed that electrostatic interactions to a tetrahedral tertiary ammonium cryptand (Fig. 18) resulted in a very effective host for iodide.¹⁰³

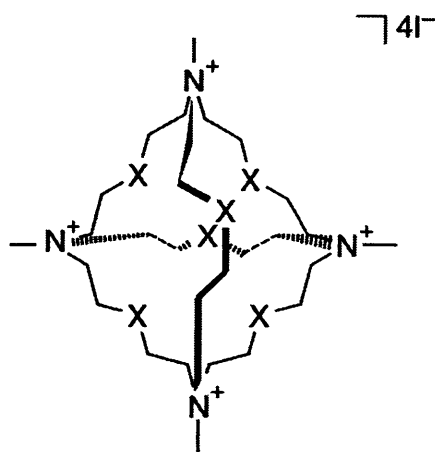


Figure 18: ammonium cryptand effective host for iodide

However, the most common class of anion binding host is a combination of electrostatic interactions and hydrogen bonding (Fig. 19).

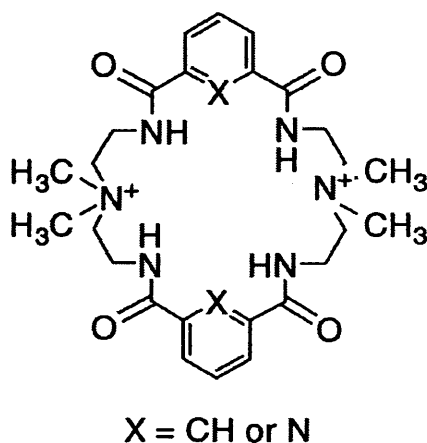


Figure 19: High affinity compound for binding anions

The anions might be bound by using neutral receptors too, which has been suggested that they could potentially exhibit greater selectivity as a class of receptors.¹⁰⁴ Typically, neutral anion receptors incorporate strong multiple hydrogen bond-donor groups such as ureas. For example, the urea group in (Fig. 20) acts as both a binding site and also as the backbone of the dipodal system. The receptor also utilizes two amide functionalities that are also excellent hydrogen bond donors. The four hydrogen bond-donor NH groups can interact with oxo- anions, such as benzoate, as shown below. This receptor was designed such that all of the hydrogen bonding sites are pointing into the molecular cleft, and are complementary to benzoate.

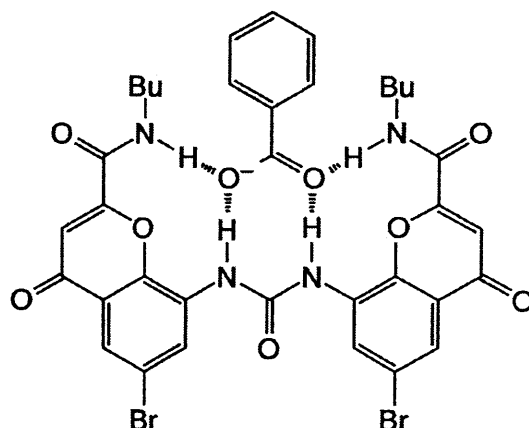


Figure 20: Binding of benzoate by neutral anion receptor

Metals play an important role in anion binding. Anion receptors based on metal centre can be classified into two broad categories: 1- those in which the metal plays a structural role (Fig. 21) which shows two thiourea derived terpyridyl ligands are held together in a well-defined way by a relatively inert (low-spin d^6) ruthenium(+2) centre. The host binds long dicarboxylates, particularly pimelate.^{1, 105, 106}

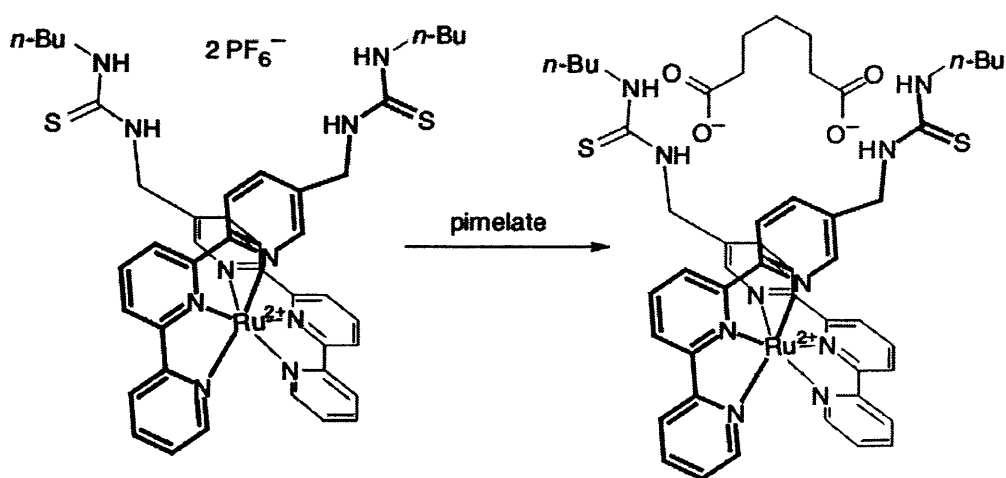


Figure 21: Use of an inert Ru^{2+} centre to organize an anion chelate ligand.

Labile coordination compounds are not true anion hosts in the conventional sense. Instead, they fall into the category of self-assembly and are frequently templated by anions, cations or both. A good example of this is shown in Fig. 22.

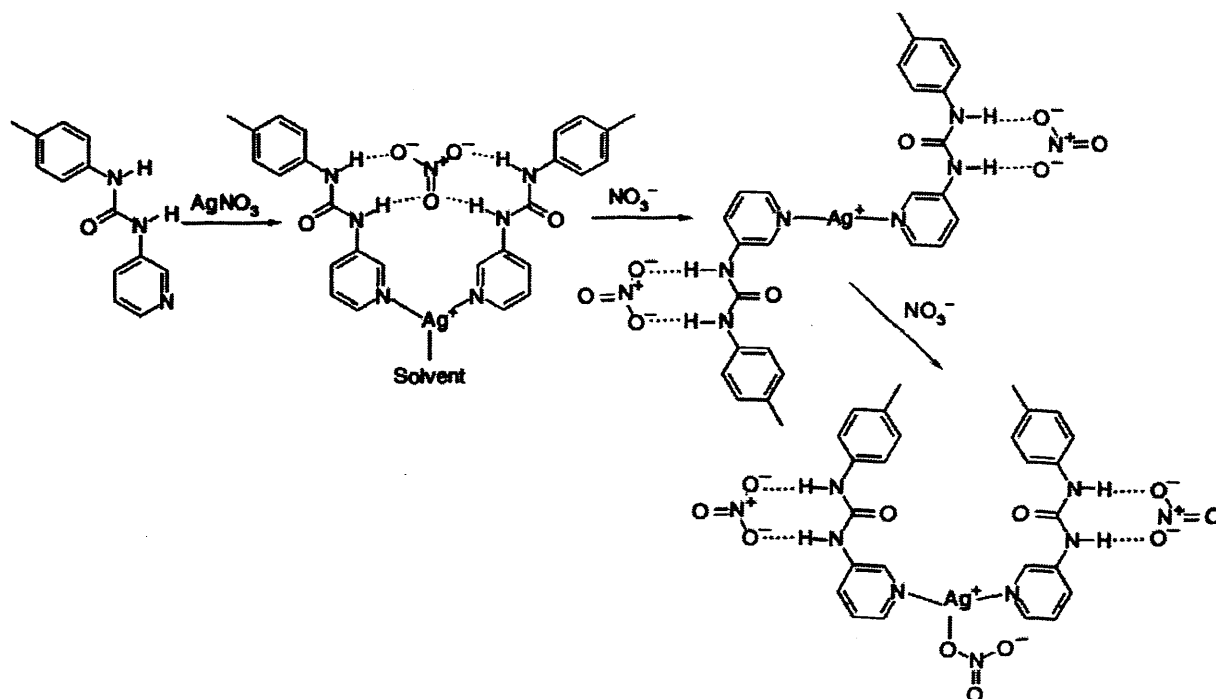


Figure 22: Use Self-assembly of a labile nitrate-binding Ag(I) complex and its evolution in the presence of excess nitrate.

In the presence of the labile Ag⁺ cation and nitrate anion, the complex self-assembles. The labile nature of the complex may be demonstrated by addition of excess nitrate which results initially in conversion to a dinitrate complex, in which each urea group binds a single anion and, ultimately, binding of nitrate at the Ag⁺ centre itself.¹⁰⁷

2-Anion receptors containing redox-active groups, such as ferrocene or cobaltocenium, that allow the detection of anions and cations via electrochemical means, are a popular area of research.¹⁰⁸ Ferrocene and cationic cobaltocenium moieties have been incorporated into many acyclic, macrocyclic and calix[4]arene frameworks. These receptors contain either amide or amine functionalities that are able to form hydrogen bonds to the anions, or typical cation-binding groups such as bipyridine. Three interesting examples are the cyclophane organometallic receptor, tripodal receptor and the molecular cleft (Fig. 23) respectively. Receptor 1 binds bromide in acetonitrile via electrostatic interactions only, whereas the receptors 2 and 3 utilise amide functionalities attached to the cyclopentadienyl rings on the cobaltocenium bind dihydrogen phosphate over chloride in acetonitrile.¹⁰⁹

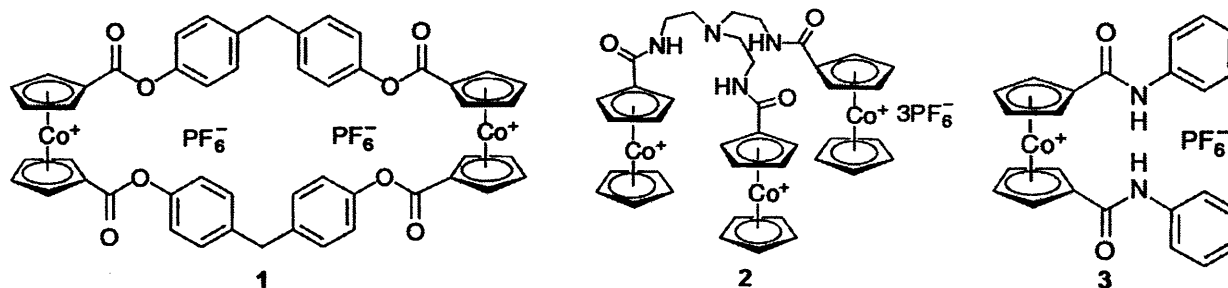


Figure 23: The cyclophane organometallic receptor, tripodal receptor and the molecular cleft

Aim of this work

The aim of this project is to synthesise novel host molecules based upon tripodal metal complexes bearing additional H-bonding moieties designed to bind anions such as halides and amino acids (Fig. 24). The character of the host may be modified by:

- The nature of the metal centre.
- The coordination number/geometry of the metal centre.
- The nature of the H-bonding units (e.g. amides and thioureas).
- The number of H-bonding units and their geometrical arrangements.

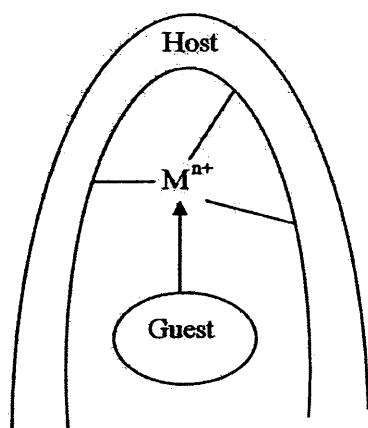


Figure 24: The general structure of the achieved Guest-Host molecule

Additionally, studying the binding of guests into the prepared host was of interest. Such studies were carried out by $^1\text{H-NMR}$ titration. Origin programme and HypNMR software were used to calculate the stability constant.⁹⁰

References

1. J. W. Steed, *Chem. Soc. Rev.*, 2009, **38**, 506-519.
2. P. D. Beer and P. A. Gale, *Angew. Chem. Int. Ed.*, 2001, **40**, 486-516.
3. F. P. Schmidtchen and M. Berger, *Chem. Rev.*, 1997, **97**, 1609-1646.
4. S. V. Eliseeva and J.-C. G. Bünzli, *Chem. soc. Rev.*, 2010, **39**, 189-227.
5. C. P. Montgomery, B. S. Murray, E. J. New, R. Pal and D. Parker, *Acc. Chem. Res.*, 2009, **42**, 925-937.
6. R. Martinez-Manez and F. Sancenon, *Chem. Rev.*, 2003, **103**, 4419-4476.
7. S. L. Wiskur, H. Ait-Haddou, J. J. Lavigne and E. V. Anslyn, *Acc. Chem. Res.*, 2001, **34**, 963-972.
8. A. S. Borovik, *Acc. Chem. Res.*, 2004, **38**, 54-61.
9. J. C. Knight, S. Alvarez, A. J. Amoroso, P. G. Edwards and N. Singh, *Dalton Trans.*, 2010, **39**, 3870-3883.
10. A. G. Blackman, *Polyhedron*, 2005, **24**, 1-39.
11. S. Yamaguchi, A. Wada, Y. Funahashi, S. Nagatomo, T. Kitagawa, K. Jitsukawa and H. Masuda, *Eur. J. Inorg. Chem.*, 2003, 4378-4386.
12. A. Wada, Y. Honda, S. Yamaguchi, S. Nagatomo, T. Kitagawa, K. Jitsukawa and H. Masuda, *Inorg. Chem.*, 2004, **43**, 5725-5735.
13. J. C. M. Rivas, R. Prabakaran, R. T. M. d. Rosales, L. Metteau and S. Parsons, *Dalton Trans.*, 2004, 2800-2807.
14. M. Harata, K. Jitsukawa, H. Masuda and H. Einaga, *Chem. Lett.*, 1995, 61-62.
15. S. Ogo, R. Yamahara, M. Roach, T. Suenobu, M. Aki, T. Ogura, T. Kitagawa, H. Masuda, S. Fukuzumi and Y. Watanabe, *Inorg. Chem.*, 2002, **41**, 5513-5520.
16. D. Natale and J. C. Mareque-Rivas, *Chem. Commun.*, 2008, 425-437.
17. S. Yamaguchi, I. Tokairin, Y. Wakita, Y. Funahashi, K. Jitsukawa and H. Masuda, *Chem. Lett.*, 2003, **32**, 403-406.
18. S. Yamaguchi, T. Takahashi, A. Wada, Y. Funahashi, T. Ozawa, K. Jitsukawa and H. Masuda, *Chem. Lett.*, 2007, 842-844.
19. K. Jitsukawa, Y. Oka, S. Yamaguchi and H. Masuda, *Inorg. Chem.*, 2004, **43**, 8119-8129.
20. J. C. M. Rivas, E. Salvagni and S. Parsons, *Dalton Trans.*, 2004, 4185-4192.
21. J. C. M. Rivas, R. T. M. d. Rosales and S. Parsons, *Dalton Trans.*, 2003, **11**, 2156 - 2163.
22. A. S. Borovik, *Acc. Chem. Res.*, 2004, **38**, 54-61.
23. J. C. M. Rivas, S. L. Hinchley, L. Metteau and S. Parsons, *Dalton Trans.*, 2006, 2316-2325.
24. R. J. Anderson, D. J. Bendell and P. W. Groundwater, *Organic Spectroscopic Analysis*, 2004.
25. A. B. P. Lever, *Inorganic Electronic Spectroscopy*, Elsevier Science & Technology, 1968.
26. A. B. P. Lever, *Inorganic Electronic Spectroscopy (Studies in Physical and Theoretical Chemistry)*, Elsevier Science Ltd, 1984.
27. A. K. Brisdon, *Inorganic Spectroscopic Methods*, Oxford Chemistry Primers, 2003.
28. C. E. Housecroft and A. G. Sharpe, *Inorganic Chemistry*, 2008.
29. W. Clegg, *Crystal Structure Determination*, Oxford Chemistry Primers, 1998.
30. *International Tables for Crystallography Volume A: Space-group symmetry*, Kluwer Academic Publishers 2002.
31. D. Watkin, in *The 12th BCA/CCG*, 2008.
32. S. R. Hall and B. McMahon, *International Tables for Crystallography*, <http://www.iucr.org/resources/cif/software/trip>.

Chapter 1: Introduction and Background Theory

33. D. O. Kennard, The Cambridge Structural Database, <http://www.ccdc.cam.ac.uk>.
34. S. Grazulis, D. Chateigner, R. T. Downs, A. F. T. Yokochi, M. Quiros, L. Lutterotti, E. Manakova, J. Butkus, P. Moeck and A. Le Bail, *J. App. Cryst.*, 2009, **42**, 726-729.
35. J. E. B. Randles, *Trans. Faraday Soc.*, 1952, **48**, 828 - 832.
36. G. Mabbott and G. A., *J. Chem. Ed.*, 1983, **60**, 697-702.
37. P. Kissinger and W. Heineman, *J. Chem. Ed.*, 1983, **60**, 702-707.
38. Santiago Alvarez, David Avnir, M. L. I and a. M. Pinsky, *New J. Chem.*, 2002, **26**, 996-1009
39. S. Alvarez, P. Alemany, D. Casanova, J. Cirera, M. Llunell and D. Avnir, *Coord. Chem. Rev.*, 2005, **249**, 1693-1708.
40. A. W. Addison, T. N. Rao, J. Reedijk, J. v. Rijn and G. C. Verschoor, *J. Chem. Soc., Dalton Trans.*, 1984, 1349 - 1356.
41. L.F.Lindoy, *The chemistry of Mmacrocyclic ligand complexes*, Cambridge Texts in Chemistry and Biochemistry, 1999.
42. M. J. Winter, *The d-block chemistry*, Oxford Chemistry Primers, 1994.
43. R. D. Hancock, *J. Chem. Ed.*, 1992, **69**, 615-621.
44. G. Anderegg and F. Wenk, *Helv. Chim. Acta*, 1967, **50**, 2330.
45. A. Machkour, D. Mandon, M. Lachkar and R. Welter, *Inorg. Chem.*, 2004, **43**, 1545.
46. C.-L. Chuang, O. d. Santos, X. Xu and J. W. Canary, *Inorg. Chem.*, 1997, **36**, 1967.
47. K. Jitsukawa, M. Harata, H. Arai, H. Sakurai and H. Masuda, *Inorg. Chim. Acta*, 2001, **324**, 108.
48. S. Ogo, S. Wada, Y. Watanabe, M. Iwase, A. Wada, M. Harata, K. Jitsukawa, H. Masuda, H. Einaga and A. Chem., *Int. Ed. Engl.*, 1998, **37**, 2102.
49. Y. Bretonniere, M. Mazzanti, J. Pecaut, F. A. Dunand and A. E. Merbach, *Chem. Commun.*, 2001, 621.
50. Z. He, P. J. Chaimungkalanont, D. C. Craig and S. B. Colbran, *J. Chem. Soc., Dalton Trans.*, 2000, 1419.
51. C.-L. Chuang, K. Lim, Q. Chen, J. Zubieta and J. W. Canary, *Inorg. Chem.*, 1995, **34**, 2562.
52. M. M. D. Mota, J. Rodgers and S. M. Nelson, *J. Chem. Soc.*, 1969, A, 2036.
53. M. P. Jensen, S. J. Lange, M. P. Mehn, E. L. Que and L. Q. Jr., *J. Am. Chem. Soc.*, 2003, **125**, 2113.
54. H. Hayashi, K. Uozumi, S. Fujinami, S. Nagatomo, K. Shiren, H. Furutachi, M. Suzuki, A. Uehara and T. Kitagawa, *Chem. Lett.*, 2002, 416.
55. J. C. Mareque-Rivas, R. Prabaharan and R. T. M. d. Rosales, *Chem. Commun.*, 2004, 76.
56. M. M. Makowska-Grzyska, E. Szajna, C. Shipley, A. M. Arif, M. H. Mitchell, J. A. Halfen and L. M. Berreau, *Inorg. Chem.*, 2003, **42**, 7472.
57. K. Jitsukawa, Y. Oka, H. Einaga and H. Masuda, *Tetrahedron Lett.*, 2001, **42**, 3467.
58. T. Kojima, K.-I. Hayashi and Y. Matsuda, *Chem. Lett.*, 2000, 1008.
59. M. Harata, K. Hasegawa, K. Jitsukawa, H. Masuda and H. Einaga, *Bull. Chem. Soc. Jpn.*, 1998, **71**, 1031.
60. C.-L. Chuang, K. Lim and J. W. Canary, *Supramol. Chem.*, 1995, **5**, 39.
61. J. C. M. Rivas, E. Salvagni, R. T. M. d. Rosales and S. Parsons, *Dalton Trans.*, 2003, 3339.
62. M. P. Jensen, M. P. Mehn, L. Q. Jr. and A. Chem., *Int. Ed. Engl.*, 2003, **42**, 4357.
63. Z. He, S. B. Colbran and D. C. Craig, *Chem. Eur. J.*, 2003, **9**, 116.
64. D. Mandon, A. Nopper, T. Litrol and S. Goetz, *Inorg. Chem.*, 2001, **40**, 4803.
65. F. Højland, H. Toftlund, S. Yde-Andersen and S. A., *Acta Chem. Scand.*, 1983, **37**, 251.

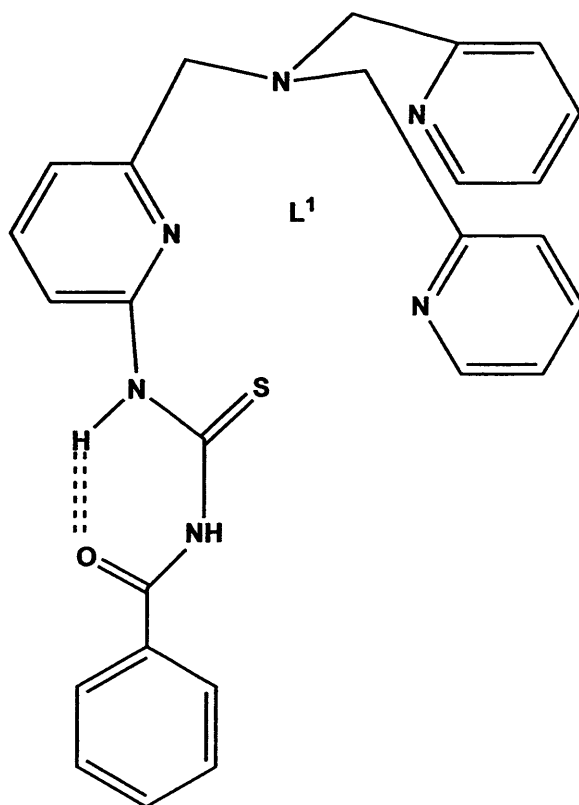
Chapter 1: Introduction and Background Theory

66. D. M. Corsi, N. N. Murthy, V. G. Young and K. D. Karlin, *Inorg. Chem.*, 1999, **38**, 848-858.
67. K. D. Karlin, J. C. Hayes, S. Juen, J. P. Hutchinson and J. Zubieta, *Inorg. Chem.*, 1982, **21**, 4106.
68. S. Yan, C. Li, P. Cheng, D. Liao, Z. Jiang, G. Wang, X. Yao and H. Wang, *J. Chem. Cryst.*, 1999, **29**, 1085.
69. B. S. Lim and R. H. Holm, *Inorg. Chem.*, 1998, **37**, 4898.
70. M. Nieger, G. Hilt and E. Steckhan, *Private communication to Cambridge Crystallographic Database (Refcode IGUZUF)*, 2002.
71. R. R. Jacobson, Z. T. r, K. D. Karlin and J. Zubieta, *Inorg. Chem.*, 1991, 2035.
72. T. M. Kooistra, K. F. W. Hekking, Q. Knijnenburg, B. d. Bruin, P. H. M. Budzelaar, R. d. Gelder, J. M. M. Smits and A. W. Gal, *Eur. J. Inorg. Chem.*, 2003, 648.
73. H. Adams, N. A. Bailey, D. E. Fenton and Q.-Y. He, *J. Chem. Soc., Dalton Trans.*, 1997, 1533.
74. H. Zheng and L. Q. Jr., *Inorg. Chim. Acta* 1997, **263**, 301.
75. H. Nagao, N. Komeda, M. Mukaida, M. Suzuki and K. Tanaka, *Inorg. Chem.*, 1996, **35**, 6809.
76. D. C. Bebout, D. E. Ehmman, J. C. Trinidad, K. K. Crahan, M. E. Kastner and D. Parrish, *Inorg. Chem.*, 1997, **36**, 4257.
77. A. Nanthakumar, S. Fox, N. N. Murthy and K. D. Karlin, *J. Am. Chem. Soc.*, 1997, **119**, 3898.
78. N. Komeda, H. Nagao, Y. Kushi, G. Adachi, M. Suzuki, A. Uehara and K. Tanaka, *Bull. Chem. Soc. Jpn.*, 1995, **68**, 581.
79. M. Ito, K. Fujita, F. Chitose, T. Takeuchi, K. Yoshida and Y.-S. Takita, *Chem. Lett.*, 2002, 594.
80. R. J. Parker, L. Spiccia, B. Moubaraki, K. S. Murray, B. W. Skelton, A. H. White and 922., *Inorg. Chim. Acta* 2000, **922**, 300-302.
81. Y. Zang and L. Q. Jr., *Inorg. Chem.*, 1995, **34**, 1030.
82. C. S. Allen, C.-L. Chuang, M. Cornebise, J. W. Canary and 29., *Inorg. Chim. Acta* 1995, **239**, 29.
83. C. Duboc, T. Phoeung, D. Jouvenot, A. G. Blackman, L. F. McClintock, J. Pécaut, M.-N. Collomb and A. Deronzier, *Polyhedron*, 2007, **26**, 5243-5249.
84. W.T.Eckenhoff and T.Pintauer, *Inorg. Chem.*, 2007, **46**, 5844.
85. M. Kim, Y.-U. Kim and J. Han, *Polyhedron*, 2007, **26**, 4003.
86. M.Yamaguchi, H.Kousaka, S.Izawa, Y.Ichii, T.Kumano, D.Masui and T.Yamagishi, *Inorg. Chem.*, 2006, **45**, 8342.
87. P. D. Beer, P. A. Gale and D. K. Smith, *Supramolecular Chemistry*, 1999.
88. F. Cramer, *Pharm. Acta Helv.*, 1995, **69**, 193-203.
89. K. Muller-Dethlefs and P. Hobza, *Chem. Rev.*, 1999, **100**, 143-168.
90. C. Frassinetti, L. Alderighi, P. Gans, A. Sabatini, A. Vacca and S. Ghelli, *Anal Bioanal Chem* 2003, **376**, 1041-1052
91. M. J. Hynes, *J. Chem. Soc. Dalton Trans.*, 1993, 311-312.
92. D. B. Smithrud, E. M. Sanford, I. Chao, S. B. Ferguson, D. R. Carcanague, J. D. Evanseck, K. N. Houk and F. Diederich, *Pure Appl. Chem.*, 1990, **62**, 2227-2236.
93. P. C. Wilkins and R. G. Wilkins, *Inorganic Chemistry in Biology* 1997.
94. T. D. J. a. C. J. W. James H. Hartley, *J. Chem. Soc., Perkin Trans.*, 2000, **1**, 3155-3184.
95. C. J. Pedersen, *Angew. Chem., Int. Ed. Engl.*, 1988, **27**, 1021-1027.
96. J. W. Steed, *Coord. Chem. Rev.*, 2001, **215**, 171-221.
97. C. D. Gutsche, *The Royal Society of Chemistry, Cambridge, UK*, 1989.

Chapter 1: Introduction and Background Theory

98. G. W. Gokel, *Advances in Supramolecular Chemistry*, 1997.
99. T. Tuntulani, S. Poompradub, P. Thavornnyutikarn, N. Jaiboon, V. Ruangpornvisuti, N. Chaichit, Z. Asfari and J. Vicens, *Tetrahedron Lett.*, 2001, **42**, 5541-5544.
100. E. Kleinpeter and A. Holzberger, *Tetrahedron*, 2006, **62**, 10237-10247.
101. X. Hou and K. Kobiro, *Tetrahedron*, 2005, **61**, 5866-5875.
102. M. Rehm, M. Frank and J. Schatz, *Tetrahedron Lett.*, 2009, **50**, 93-96.
103. K. Bowman-James, *Acc. Chem. Res.*, 2005, **38**, 671-678.
104. M. M. G. A. a. D. N. Reinhoudt, *J. Chem. Soc., Chem. Commun.*, 1998, 443-448.
105. B. Linton and A. D. Hamilton, *Chem. Rev.*, 1997, **97**, 1669-1680.
106. M. S. Goodman, V. Jubian and A. D. Hamilton, *Tetrahedron Letters*, 1995, **36**, 2551-2554.
107. D. R. Turner, B. Smith, E. C. Spencer, A. E. Goeta, I. R. Evans, D. A. Tocher, J. A. K. Howard and J. W. Steed, *New J. Chem.*, 2005, **29**, 90-98.
108. P. D. Beer and E. J. Hayes, *Coord. Chem. Rev.*, 2003, **240**, 167-189.
109. P. D. Beer and S. R. Bayly, *Top. Curr. Chem.*, 2005, **255**, 125-162.

Chapter 2: A Novel Monothiourea Tripodal Ligand; Structural, Spectroscopic and Electrochemical properties of Copper (II), Zinc (II) and Cadmium (II) Complexes



Introduction

There has been much interest over the last 20 years in investigating the co-ordination chemistry of tetradentate tripodal TPA ligands. These ligands contain a tertiary N atom bonded to three arms, each arm contains an N-donor atom connected via at least one methylene group, and generally bind to a single transition metal or lanthanide ion using all four N-donor atoms.¹ Tris(2-pyridylmethyl)amine (TPA) frame work, was prepared by Andregg and Wenk in 1967 and is perhaps the second most well studied tripodal tetraamine ligands frame work after tris(2-aminoethyl)amine (TREN).² Many TPA derivatives having substituents at the 6-positions of the pyridyl rings have been synthesised and extensively studied with respect to their transition metal complexes.³⁻⁹

Tripodal tetradentate amine ligands and their metal complexes provide interesting topics in the field of coordination chemistry as a result of the increasing need to model the active sites in the biologically important molecules.¹⁰⁻³⁸ A variety of tripodal amines were synthesized with a tertiary amine nitrogen that is connected via methylene groups to three aliphatic or aromatic arms including heterocyclic rings (pyridyl, quinoline, imidazolyl, benzimidazolyl, pyrazolyl) (Fig. 1).^{10-13, 17, 22-24, 29, 30, 37-45}

The main method for the synthesis of tripyridyl tripodal ligands is alkylation of either ammonia or a primary (2-pyridyl)alkylamine with an appropriate pyridine precursor. For example, TPA was prepared by the reaction of 2-(aminomethyl)pyridine with two equivalents of 2-(chloromethyl) pyridine.^{2, 46} Similarly tris(2-quinolylmethyl)amine (TMQA) was prepared via the alkylation of the primary amine with 3-chloromethylisoquinoline hydrochloride⁴¹ while the synthesis of tris[2-(1-pyrazolyl)ethyl]amine (TRPYN) involved the reaction of tris(2-chloroethyl)amine hydrochloride with four equivalents of pyrazole in distilled DMF.³⁹ Likewise, the compound tris(3,5-dimethyl -pyrazolyl- methyl)amine (MeTPyA) was obtained by reacting

Chapter 2: A novel Monothiourea Tripodal Ligand; Structural, Spectroscopic and Electrochemical properties of Copper (II), Zinc (II) and Cadmium (II) Complexes

tris(chloromethyl) amine with 3,5-dimethylpyrazolate refluxing in anhydrous THF.⁴² In addition, tris(2-benzimidazolymethyl)amine (NTB) was synthesised by reacting either nitrilotriacetonitrile or nitrilotriacetic acid with o-phenylenediamine at 190-210°C.⁴³

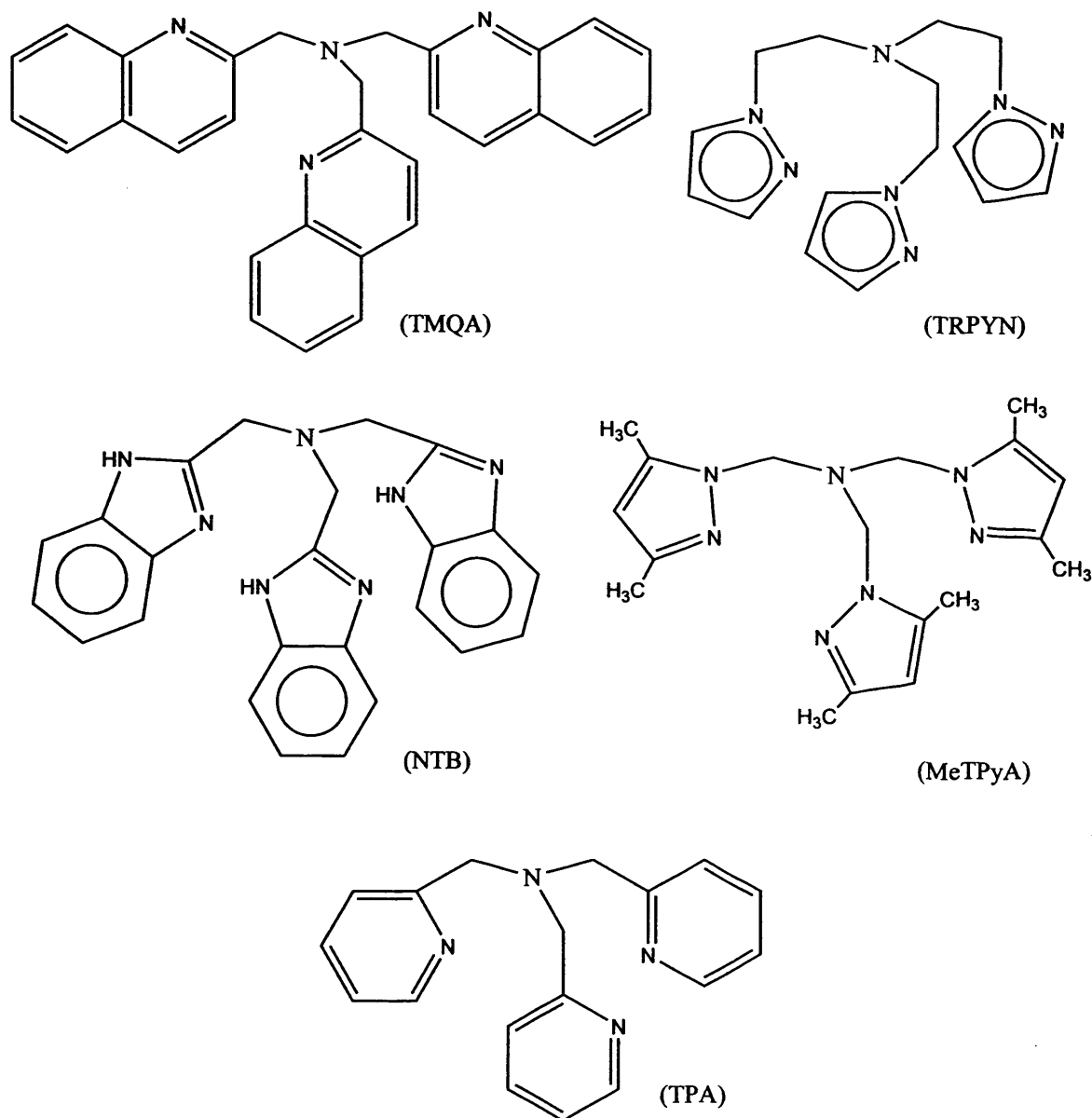


Figure 1: Some examples of known tripodal amines

These ligands, including TPA, were originally employed to enforce a non-planar coordination around the metal centres. There is a need to investigate novel complexes of tripodal ligands that

Chapter 2: A novel Monothiourea Tripodal Ligand; Structural, Spectroscopic and Electrochemical properties of Copper (II), Zinc (II) and Cadmium (II) Complexes

have the ability firstly, to bind transition metals and secondly, to get in ditopic binding (lock and key principle) explained in the previous chapter. Additionally, it is of a great interest from a structural point of view to synthesise such ligands as they work as hosts for various guests such as transition metals and may also be able to bind another guest e.g. anions, cations or neutral molecules. One arm functionalised species with a TPA frame work have been synthesised and studied during the last 20 years. For example, Rivas and co-workers have investigated the mono amide t-butyl substituent of TPA which provides a good ligand platform for mimicking several key active site features of peptidases and amidases including co-ordination of the amide carbonyl group. They have also explored the validity of the covalent attachment of a pivaloylamido group adjacent to a metal ligating pyridine nitrogen as a useful strategy to induce hydrogen bonding to another metal-bound ligand (Fig. 2).⁴⁷

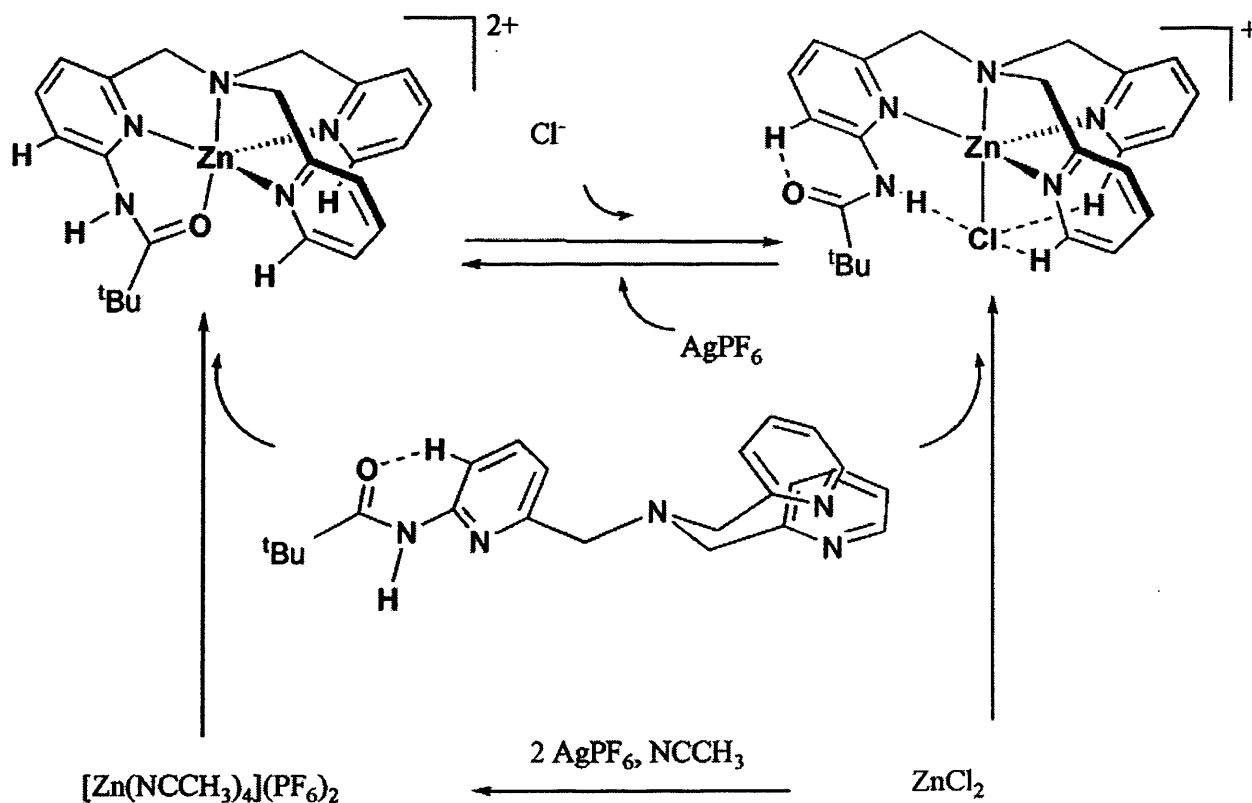


Figure 2: A one arm species (from a free ligand to guest-host molecule supported by hydrogen bonding).

Chapter 2: A novel Monothiourea Tripodal Ligand; Structural, Spectroscopic and Electrochemical properties of Copper (II), Zinc (II) and Cadmium (II) Complexes

A search of the Cambridge Crystallographic Database Centre (CCDC) revealed there were 25 examples of those one arm TPA based ligands (Fig. 3) in 2011.⁴⁸⁻⁵⁰

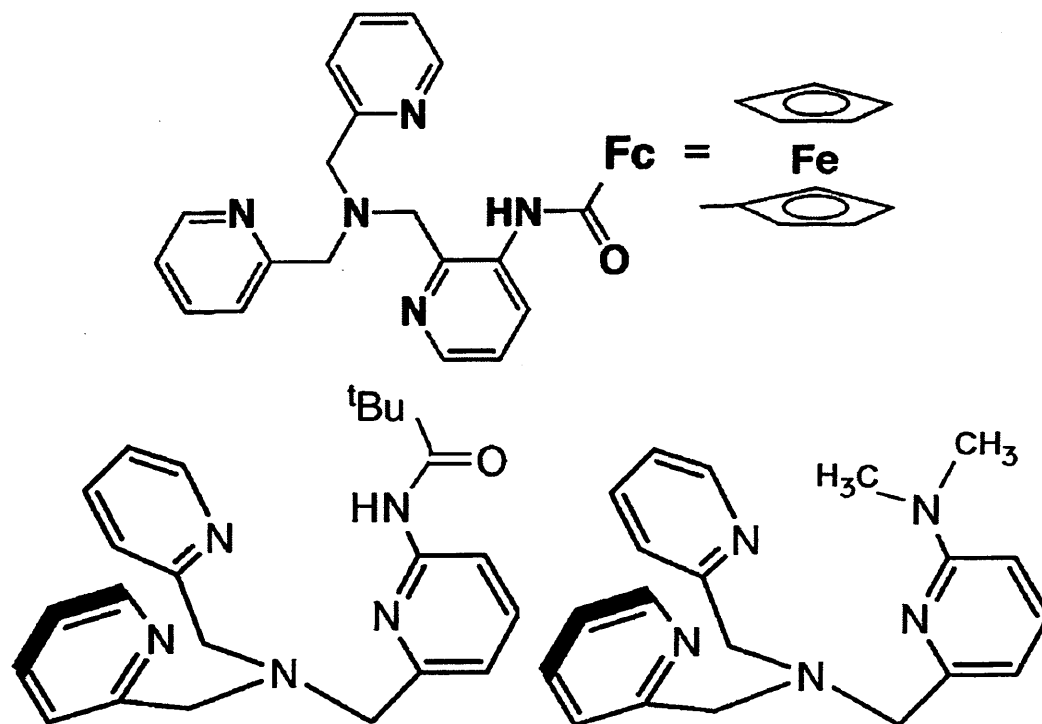


Figure 3: Some of one arm TPA based ligands.

Those ligands have been used to investigate the co-ordination chemistry of transition metals. It also offers the possibility of investigating the effect of hydrogen bonding environments.⁵⁰⁻⁵³

In this chapter, we will illustrate the preparation and characterization of a novel monothiourea tripodal ligand which is designed to be able to co-ordinate transition metals and to explore the ability of this ligand to bind the counter ion through hydrogen bond. Copper, zinc and cadmium complexes have been fully characterised.

Experimental

General

NMR spectra were measured on a Bruker AM-400 or Bruker Av-500 or Bruker AC-250 Plus FT-NMR spectrometer. For infrared spectra, each compound was pressed into a disk with an excess of dried KBr and measured on a Jasco FT-IR spectrophotometer. Electrospray ionisation mass spectrometry (ESMS) were measured on a Waters LCT Premier XE (oa-TOF) mass spectrometer. UV-VIS absorption spectra were run in HPLC grade acetonitrile (Fisher) and measured on a Jasco V-570 spectrophotometer from 230 to 1,100 nm (optical path length 1.0 cm). Elemental analyses were carried out by the Warwick Analytical Service, University of Warwick.

Preparations

Mono(6-amino-2-pyridylmethyl)(2-pyridylmethyl)amine (MAPA) was prepared as reported by Rivas *et al.*⁵⁴ and Yamaguchi *et. al.*⁵⁵

Synthesis of L¹

MAPA (0.955g, 3.131mmol) was dissolved in EtOH 50 mL and benzoylisothiocyanate (0.421 mL, 3.131 mmol) was added dropwise. The mixture was heated up to 40°C with stirring for 40 min then allowed to cool to RT. The solvent was removed under reduced pressure to yield a brown oil which then treated with mixture of ether and acetone to produce a white solid of L¹, (0.447g, 0.955mmol) 30%. ¹H NMR δH (250 MHz; CDCl₃): 3.84 (2H, s); 3.89 (4H, s); 7.14 (2H, t, Ar, J= 4.9Hz); 7.42 (1H, d, Ar, J=7.5Hz); 7.50-7.76 (8H, m, Ar); 7.90 (2H, d, Ar, J =7.5Hz); 8.52 (2H, d, Ar, J= 4.1Hz); 8.67 (1H, d, Ar, J= 8.1Hz); 9.06 (1H, s, NH); 13.05 (1H, s, NH). ¹³C

Chapter 2: A novel Monothiourea Tripodal Ligand; Structural, Spectroscopic and Electrochemical properties of Copper (II), Zinc (II) and Cadmium (II) Complexes

δ_C (62.5 MHz; $CDCl_3$): 59.3, 60.1, 114.0, 120.5, 121.9, 122.9, 127.4, 129.1, 131.6, 133.6, 136.4, 138.0, 149.0, 150.4, 158.6, 159.2, 166.3, 176.7. Accurate ESMS (m/z): 491.1625 (30) $[L^1 + Na]^+$, 469.1805 (10) $[L^1 + H]^+$. [calculated 469.58]. $C_{26}H_{24}N_6O_1S_1$. IR KBr/ cm^{-1} : $\nu = 3431br$, 1671s, 1540s, 1455s, 1330s, 1085s, 624s. UV/Vis [λ_{max} , nm (ϵM , $M^{-1}cm^{-1}$)] in CH_3CN : 268 (62,300), 310 (33,500).

General Procedure for the Synthesis of Metal Complexes

Ligand L^1 (1 equivalent, typically 0.42 mmol) was dissolved in hot acetonitrile (typically 3 mL). To this stirring solution, the metal perchlorate salt (1 equivalent) dissolved in acetonitrile (ca. 2 mL) was added dropwise. Recrystallisation of the compounds typically involved the diffusion of diethyl ether into acetonitrile in the case of copper and cadmium. Slow evaporation of a solution was used in the case of zinc. All solutions of complexes were filtered through celite before setting up a recrystallisation.

WARNING: Perchlorate salts of metal complexes are potentially explosive. Care should be taken while handling such complexes.

$[Cu^{II}(L^1)][ClO_4]_2 \cdot CH_3CN \cdot H_2O$ (2.1): green plate crystals (45% yield). Found: C, 42.33; H, 3.51; N, 12.26 %. $CuC_{26}H_{24}N_6O_1S_1(ClO_4)_2(CH_3CN)(H_2O)$ requires C, 42.63; H, 3.70; N, 12.43%; ESMS m/z (%): 530.0974 (100) $[Cu(L^1) - H]^+$, [calculated 530.0950]. IR (KBr pellet/ cm^{-1}): 3416(br), 1609(s), 1539(s), 1433(s), 1261(s), 1088(s), 625(s). UV/Vis [λ_{max} , nm (ϵM , $M^{-1}cm^{-1}$)] in CH_3CN : 255 (13100), 268 (10960), 326 (8690), 353 (5460), 631 (95), 822 (140), 950 (115).

Chapter 2: A novel Monothiourea Tripodal Ligand; Structural, Spectroscopic and Electrochemical properties of Copper (II), Zinc (II) and Cadmium (II) Complexes

[Zn^{II}(L¹)](ClO₄)₂ (2.2): colourless solid (10% yield). ESMS *m/z* (%): 515.1200 (50), [Zn(L^{*}) - H]⁺, [calculated 515.1174]; 531.0948 (100) [Zn(L¹) - H]⁺, [calculated 531.0945]. ¹H NMR (250 MHz; CD₃CN): 4.32 (2H, s); 4.33 (4H, s); 7.40 (1H, d, Ar, J= 7.8Hz); 7.55 (1H, d, Ar, J= 7.3Hz); 7.62-8.23 (12H, m, Ar); 8.72 (2H, d, Ar, J= 4.7Hz). IR (KBr pellet/cm⁻¹) for solid: 3446(br), 1616(s), 1550(s), 1262(s), 1090(s), 621(s).

[Zn^{II}(L^{*})](ClO₄)₂.H₂O (2.2.1): L^{*} = C₂₆H₂₄N₆O₂. colourless needle crystals. ESMS *m/z* (%): 515.1200 (50), [Zn(L^{*}) - H]⁺, [calculated 515.1174]; 531.0948 (100) [Zn(L¹) - H]⁺, [calculated 515.0945]. IR (KBr pellet/cm⁻¹) for solid: 3502(br), 1612(s), 1558(s), 1441(s), 1267(s), 1088(s), 622(s).

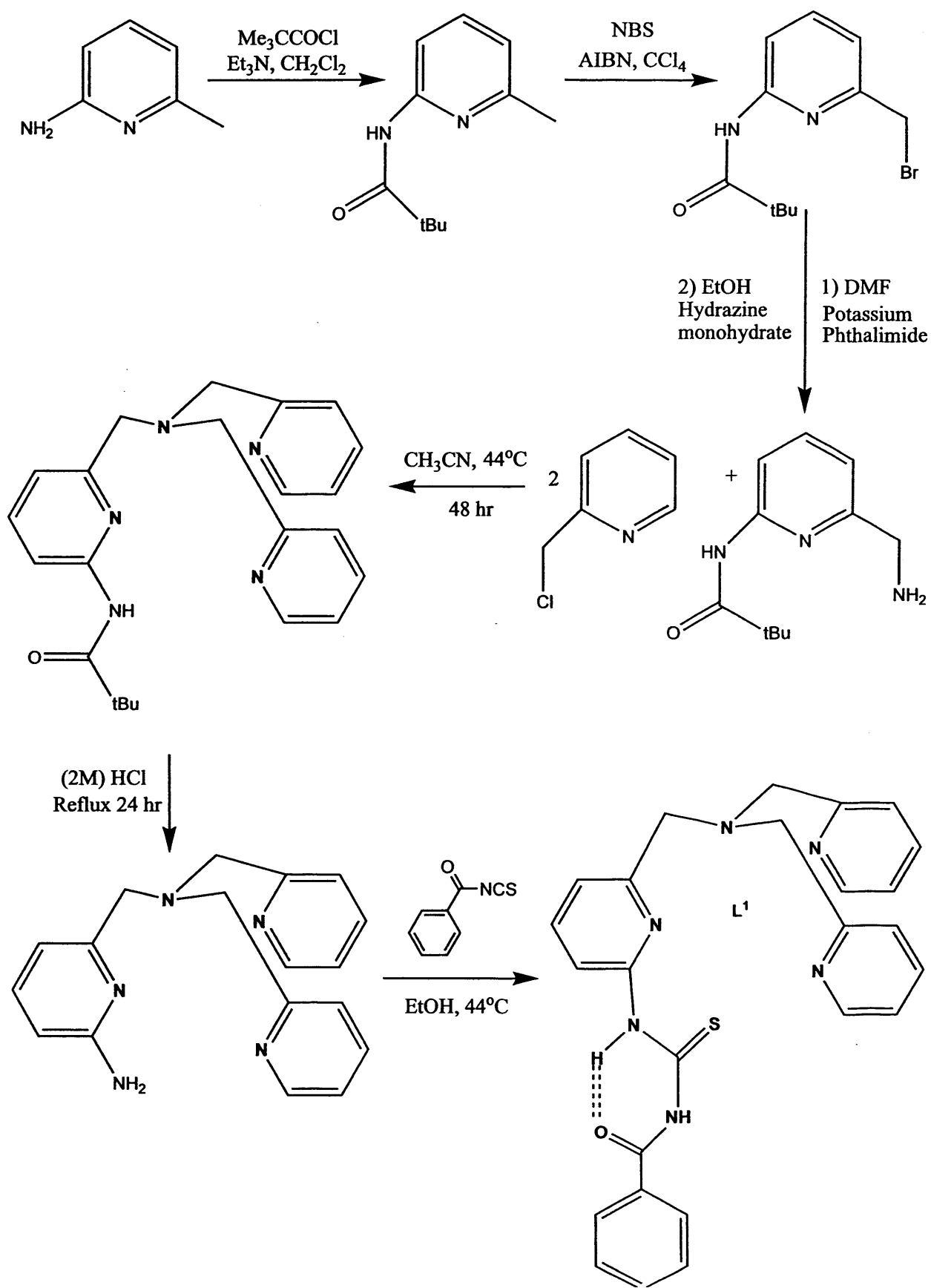
[Cd^{II}(L¹)(ClO₄)(CH₃CN)](ClO₄) (2.3): white needle crystals (30% yield). Found: C, 40.56; H, 3.12; N, 11.68%. CdC₂₆H₂₄N₆O₁Si(ClO₄)₂(CH₃CN) requires C, 40.92; H, 3.31; N, 11.93%; ESMS *m/z* (%): 577.0677 (100), [Cd(L¹) - H]⁺, [calculated 577.0884]. ¹H NMR (250 MHz; DMSO): 3.99 (2H, s); 4.06 (4H, s); 6.52 (1H, d, Ar, J= 6.9Hz); 7.46-8.71 (15H, m, Ar). ¹³C δ_C (62.5 MHz; DMSO): 56.5, 66.4, 119.3, 124.3, 124.4, 126.9, 128.5, 128.8, 133.3, 136.9, 139.7, 149.0, 154.1, 168.9, 171.3, 183.4, 191.7, 222.6. IR (KBr pellet/cm⁻¹): 3436(br), 1605(s), 1527(s), 1438(s), 1261(s), 1094(s), 622(s). UV/Vis [λ_{max}, nm (εM, M⁻¹cm⁻¹)] in CH₃CN: 260 (18,190), 289 (17,570).

Results and Discussion

Ligand Synthesis (L¹)

The precursor compounds mono(6-pivaloylamino)(2-pyridylmethyl)amine (MPPA) and mono(6-amino-2-pyridylmethyl)(2-pyridylmethyl)amine (MAPA) were synthesised as described by Rivas *et al.*⁵⁴ and Yamaguchi *et. al.*⁵⁵ respectively. L¹ was prepared in reasonable yield by the reaction of a primary amine with isothiocyanate as described by Sukeri *et. al.*⁵⁶ This synthesis involved the reaction of MAPA in EtOH with one equivalent of benzoyl isothiocyanate to yield an oily crude in 40 min which was difficult to transform into solid by using any solvent (chloroform, water, dichloromethane, acetone, acetonitrile, ether, dimethylsulfoxide, dimethylformamide). However, washing with 50% ether/acetone led to a white solid, stable in air and not hygroscopic, of L¹ (30%). The ligand may be anticipated as having a steric preference for trigonal bipyramidal complexes as the pyridyl nitrogens may take equatorial positions with the central nitrogen acting as an axial donor. The fifth co-ordination site may be occupied by the sulphur atom or a solvent donor. The synthetic route to L¹ is shown in scheme 1.1.

Chapter 2: A novel Monothiourea Tripodal Ligand; Structural, Spectroscopic and Electrochemical properties of Copper (II), Zinc (II) and Cadmium (II) Complexes



Scheme 1.1: Synthetic route to L^1 .

Chapter 2: A novel Monothiourea Tripodal Ligand; Structural, Spectroscopic and Electrochemical properties of Copper (II), Zinc (II) and Cadmium (II) Complexes

A comparison between L^1 and the tripodal monoamide ligand (MPPA), shows that while they are similar in many respects, L^1 may potentially be pentadentate and in addition, the spatial positioning of the different hydrogen bond donors is very different (Fig. 4).^{54, 55, 57}

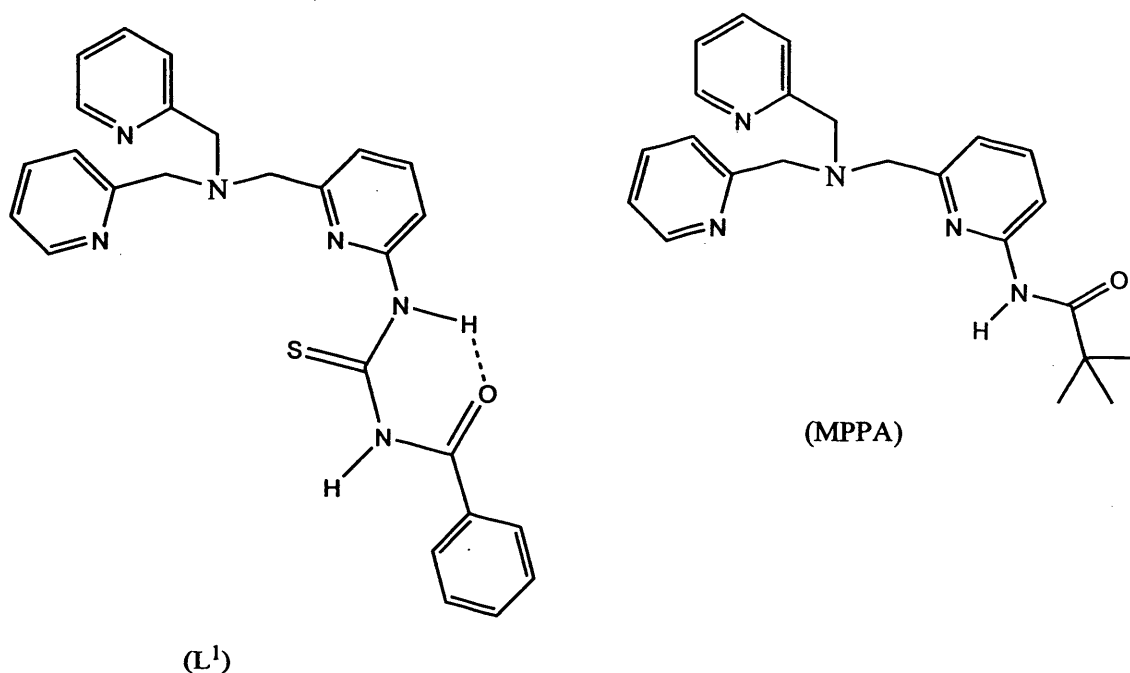


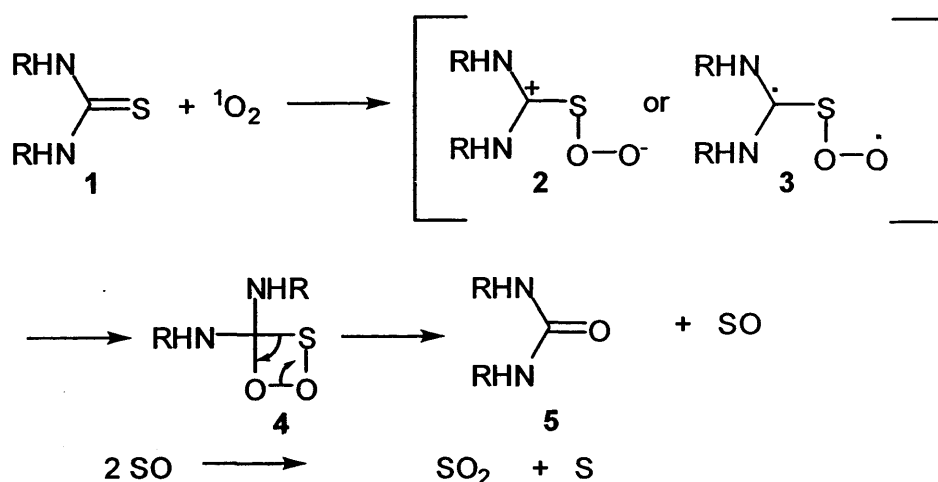
Figure 4: The thiourea derivative L^1 (left) has a longer arm than the MPPA ligand (right). In the case of MPPA, the t Bu group makes it more soluble in organic solvents than L^1 and this is the reason behind warming up L^1 in acetonitrile in order to have it fully dissolved.

Synthesis of Complexes

The ligand was dissolved in the minimum amount (typically 3 mL) of hot acetonitrile. The dropwise addition of an aqueous solution containing the relevant metal perchlorate salt yielded a clear green solution in the case of Cu^{II} and a clear colourless solution in the case of Zn^{II} and Cd^{II} . Copper and cadmium compounds were recrystallised via the diffusion of diethyl ether into acetonitrile solutions resulting in crystals suitable for single-crystal X-ray diffraction. The yields from these reactions were 45 and 30% respectively. The crystalline samples of Cu^{II} and Cd^{II} were subsequently used for all spectroscopic measurements. A zinc crystal was grown using the slow evaporation method. However, only few crystals of Zn^{II} complex were grown which was

Chapter 2: A novel Monothiourea Tripodal Ligand; Structural, Spectroscopic and Electrochemical properties of Copper (II), Zinc (II) and Cadmium (II) Complexes

just enough to get the crystallographic data, where IR, MS and ^1H NMR were taken for solid materials. ^{13}C NMR could not be obtained due to the compounds poor solubility and there were no enough sample for UV-Vis. Zn^{II} complex of L^1 is also insoluble in CHCl_3 , CH_3COCH_3 , H_2O , CHCl_2 and DMSO and shows an interesting behaviour in solution, when left standing for a long time (approximately a month) open to air. Oxidation of thiourea to urea is observed which is confirmed by ESMS and the crystal structure determination. To eliminate the possibility that the urea ligand was not originally present when the thiourea compound was made, the IR spectrum of the isothiocyanate was obtained and it did not show any trace of the isocyanate analogue. In addition, close inspection of IR and MS data did not suggest the presence of any urea species in the thiourea ligand or the initial zinc thiourea complex. Currently, it would appear that the urea species is slowly formed on standing in air. The mechanism of this conversion from sulfur to oxygen has been investigated by Rao *et.al.*. The oxidation of thioureas to the corresponding ureas took place by the use of singlet oxygen (the diamagnetic form of molecular oxygen). Singlet oxygen is less stable and chemically different than the normal triplet oxygen. Thioureas (**1**) can be oxidized by singlet oxygen to produce the corresponding ureas (**5**) as shown in Scheme 1.2.⁵⁸ It is believed that either zwitterionic (**2**) or diradical peroxide (**3**) was formed as an intermediate. Intermediate **2** was formed via nucleophilic attack of the C=S bond at the oxygen, while, **3** was formed via radicals formation due to the homolytic fission of both C=S and O=O double bonds. Cyclization of either **2** or **3** would give 1,2,3-dioxathietane (**4**) but no solid evidence for the formation of **4** yet. Ring opening of **4** would give ureas **5** with elimination of sulfur monoxide (Scheme 1.2). Two moles of sulfur monoxide should give a mole of sulfur dioxide and one mole of sulfur.



Scheme 1.2: Oxidation of thioureas (1) to the corresponding ureas (5) using singlet oxygen.

Spectroscopic Properties of Complexes

Vibrational Spectroscopy

According to the literature, the amide carbonyl stretch comes at $\sim(1620-1670)$ cm^{-1} . Similarly, a carbonyl stretch of L^1 is observed at 1671 cm^{-1} (Table 1). Even though the carbonyl is not directly coordinating to any metal, it appears to be at lower energy when the ligand co-ordinates to a metal perhaps due to the formation of a stronger intramolecular hydrogen bond within the thiourea arm. A strong peak at 1331 cm^{-1} , assigned to the $\nu(\text{C}=\text{S})$ also shifted to lower energy between 1261 cm^{-1} upon co-ordination of sulfur atom to the metal which reduces the bond order and thus weakens the $\text{C}=\text{S}$ bond. It is worth noting that the ESMS of Zn^{II} complex **2.2** and **2.2.1** have confirmed the presence of mixture of thiourea and urea species. However, the IR spectra of **2.2** and **2.2.1** seems to be identical. By leaving a ZnL^1 (**2.2**) acetonitrile solution to evaporate slowly over a month open to air, the IR spectra did not change and the $\text{C}=\text{S}$ stretch is still present, indicating that if the complex does oxidise on standing, it does so very slowly, with the bulk of the sample remaining as the thiourea. The shift of the pyridine ring vibration at around 1600 cm^{-1} and 1450 cm^{-1} in all complexes indicates

Chapter 2: A novel Monothiourea Tripodal Ligand; Structural, Spectroscopic and Electrochemical properties of Copper (II), Zinc (II) and Cadmium (II) Complexes

co-ordination from the pyridine ring nitrogens. All compounds reveal two characteristic unsplit infrared active bands at $\sim 1,100\text{ cm}^{-1}$ and $\sim 622\text{ cm}^{-1}$ indicative of ionic perchlorate (Td symmetry).^{59,60} All of these features are consistent with the X-ray diffraction data for all complexes.

Table 1: IR Stretching Frequencies of L¹ and complexes. IR spectra measured as KBr discs

Compound	$\nu(\text{C}=\text{O})$	$\nu(\text{C}=\text{S})$	$\nu(\text{O}-\text{H})$	$\nu(\text{C}=\text{N}), \nu(\text{C}=\text{C})$	$\nu(\text{Cl}-\text{O})$
L ¹	1671(s)	1330(s)	3431(br)	1540(s), 1455(s)	-
2.1	1609(s)	1261(s)	3416(br)	1539(s), 1433(s)	1088(s), 625(s)
2.2	1616(s)	1262(s)	3446(br)	1558(s), 1450(s)	1090(s), 621(s)
2.2.1	1612(s)	1267(s)	3502 (br)	1558(s), 1441(s)	1088(s), 622(s)
2.3	1605(s)	1261(s)	3436(br)	1527(s), 1438(s)	1094(s), 622(s)

¹H and ¹³C NMR of L¹, Zn and Cd Complexes

Despite considerable effort to obtain the ¹³C NMR spectrum for ZnL¹ complex, all attempts failed due to the poor solubility of the sample, as the complex precipitate out from CD₃CN and is insoluble in acetone-d⁶, CDCl₃, D₂O and DMSO. Similarly, the cadmium complex of L¹ is insoluble in acetone-d⁶, CDCl₃ and D₂O. However, it shows partial solubility in DMSO-d⁶ solutions. As a result of this, the ¹H and ¹³C NMR data are of poor quality for CdL¹ in comparison to the free ligand spectra which is highly soluble in deuterated chloroform. The ¹H NMR of CdL¹ in CD₃CN is even worse which consists of broad unexplainable peaks. Additionally, it is clear from the ¹H NMR spectra for the ZnL complex that the NH proton easily exchanges with the deuterated solvent which cause the NH protons signals to disappear.

Electronic Absorption Spectra

The electronic spectra of L^1 and the complexes 1.1 and 1.3 have been measured and the data are presented in Table 2. Unfortunately, the sample is not enough to run UV-Vis for Zn complex. The electronic absorption spectra for L^1 and both Cu^{II} and Cd^{II} complexes possess two strong peaks between ~ 260 nm and ~ 280 nm characteristic of intra-ligand pyridyl $\pi-\pi^*$ transitions.

Table 2: Electronic spectral assignments for L^1 , 2.1 and 2.3

Compound ^a	$\pi-\pi^*$ transitions / λ (nm)	MLCT / λ (nm)	d-d transitions / λ (nm)	Δ (cm^{-1}) ^b	B (cm^{-1}) ^b	β
L^1	268(62,300), 310(33,500)	-	-	-	-	-
2.1	255 (13,100), 280 (8,500)	326 (8,700), 353(5,460)	631(95), 822 (140), 950 (115)	10,530	-	-
2.3	260(18,200), 289(17,570)	-	-	-	-	-

^aPerformed in CH_3CN solution at room temperature; Numbers in parentheses indicate molar absorption coefficients ϵ ($M^{-1}cm^{-1}$). ^b values calculated by assuming an octahedral geometry.

The copper compound, 2.1, features an N_4S_1 chromophore surrounding the Cu^{II} centre and exhibits D_{3h} symmetry in the solid state forming a trigonal bipyramidal geometry. According to crystal field theory (CFT), the trigonal bipyramidal geometry is not Jahn-Teller active as the odd electron is in a non degenerate orbital (Fig. 5). There are two transitions that would occur in such geometry: $d_{xz}, d_{yz} \rightarrow d_z^2$ at higher energy and $d_{xy}, d_{x^2-y^2} \rightarrow d_z^2$.

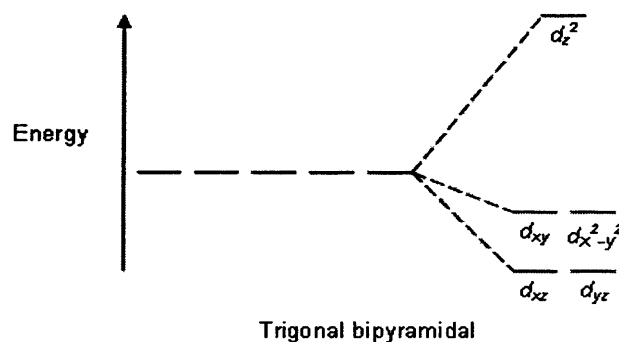


Figure 5: Crystal field splitting of Trigonal bipyramidal geometry.

Chapter 2: A novel Monothiourea Tripodal Ligand; Structural, Spectroscopic and Electrochemical properties of Copper (II), Zinc (II) and Cadmium (II) Complexes

Thus two peaks observed for **2.1** ($15,850$ and $12,160\text{ cm}^{-1}$) (Fig. 6) and these transitions may be labelled as ($d_{xz}, d_{yz} \rightarrow d_z^2$) and ($d_{xy}, d_{x^2-y^2} \rightarrow d_z^2$) respectively. Additionally, the slight shoulder at 1000 nm suggest that perhaps in solution the compound has a different structure to that in the solid state.

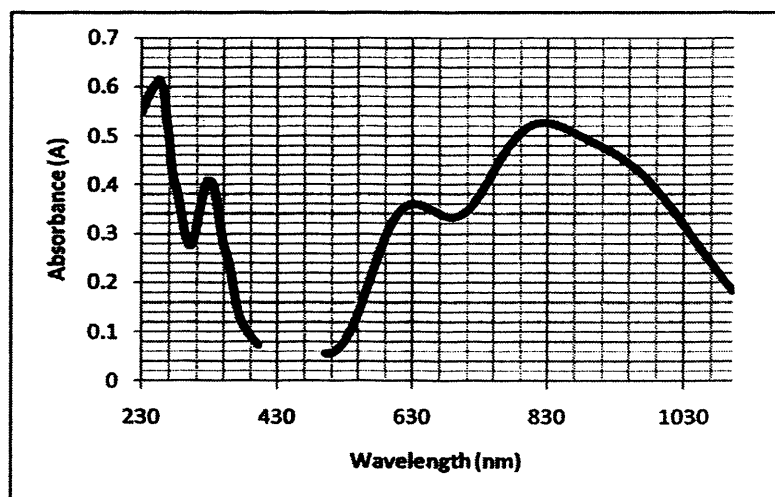


Figure 6: The electronic spectrum of Cu^{II} compound, **1.1**.

However, this spectral pattern is typical of a five co-ordinate copper (II) complex with a trigonal bipyramidal based geometry.^{61, 62} While the bands of $15,850$ and $12,160\text{ cm}^{-1}$ are tentatively assigned to ${}^2A_1' \rightarrow {}^2E''$ and the symmetry allowed ${}^2A_1' \rightarrow {}^2E'$ transitions respectively in D_{3h} symmetry,⁶³ the little shoulder at $\sim 1000\text{ nm}$ does suggest a lower symmetry. In (Fig. 7) are the qualitative energy diagrams for Cu^{2+} ion in ligand fields of D_{3h} (TBP), C_{4v} (SP) and intermediate C_{2v} symmetry bearing in mind the only difference between D_{3h} and C_{3v} is the energy difference change, depending on nature of axial ligand. However, it is difficult to suggest the nature of the species in solution, as additional ligands may be binding to the metal centre.

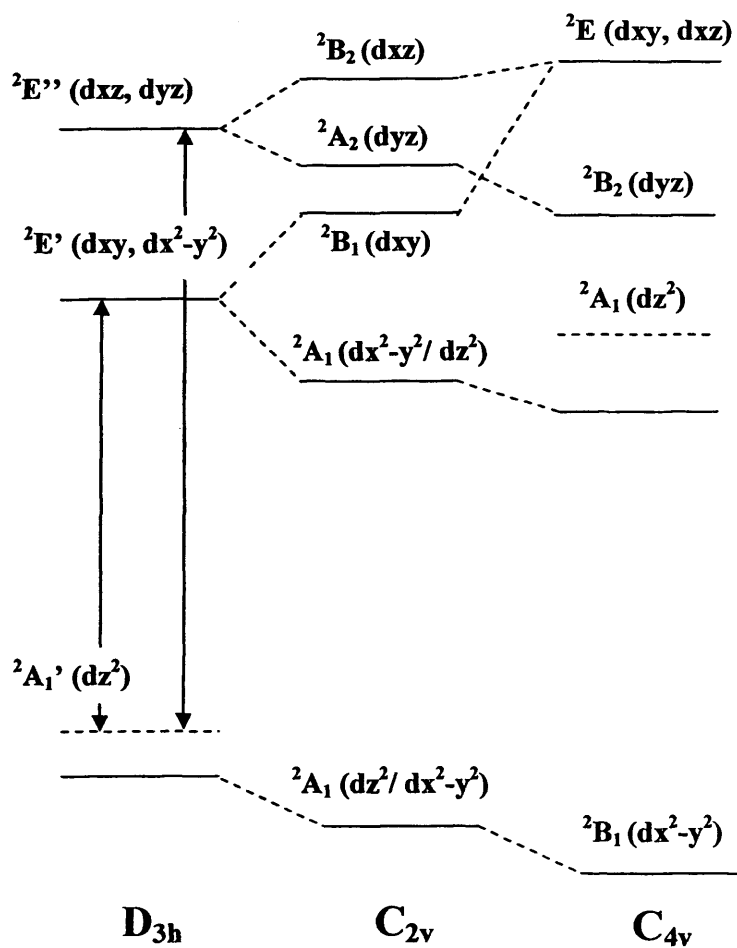


Figure 7: Term diagrams for copper (II) ion in the ligand fields of D_{3h} (TBP), C_{4v} (SP) and intermediate C_{2v} symmetry.⁶³

Electrochemical Studies

The cyclic voltammetry experiments were carried out with an PARSTAT 2273 (Advanced Electrochemical System from Princeton Applied Research) in conjunction with General Purpose Electrochemical System software (GPES version 4.7 for Windows) in a specially designed three-electrode glass cell with a Teflon-coated cell cap. A Bioanalytical platinum working electrode (model no. MF2013) with a 1.6 mm disk was used for all experiments. The counter electrode was a platinum wire and the reference electrode a non-aqueous Ag/AgNO₃ electrode. To regain electrochemical sensitivity and reproducibility the working electrode was polished, with 600 grid emery paper, to a mirror surface and then ultrasonicated. Prior to each experiment, the electrode was washed with high performance liquid chromatography (HPLC) grade CH₃CN and dried in air for about 15 min. A 0.1 M [Bu₄N][PF₆] solution in CH₃CN was used as supporting electrolyte. In all cases, ferrocene was used as an internal reference. Solutions were degassed with nitrogen and a nitrogen atmosphere was maintained over the solution during the experiment.

The voltammogram of Cu^{II} compound, **2.1** (Fig. 8), reveals a reversible Cu^{III} redox couple centred at -0.40V.

Table 3: Electrochemical parameters for the redox process exhibited by complex **2.1** in acetonitrile solution (supporting electrolyte: [Bu₄N][PF₆] (0.1 mol dm⁻³); T = 20 °C). Measured at 0.1 Vs⁻¹.

Compound	E_p/V (ΔE , mV) ^{a,b}
2.1	-0.66(95), -0.40(73)

^a The potential at which reversible process occur is calculated as the average of the oxidative and reductive peak potentials ($E_p^{ox} + E_p^{red}$)/2. ^b For irreversible processes, the anodic or cathodic peak potentials are given. Potentials are given in volts *versus* Ferrocenium/Ferrocene.

In the Cu^{II} complex, **2.1**, there are two processes one of which could be ascribed as a ligand based process and the second might be reduction of the metal centre observed. No oxidation of either Cu^{II} to Cu^{III} or the ligand was apparent. Reversal of the potential scan, results in a

reversible $\text{Cu}^{\text{II}}\text{-Cu}^{\text{I}}$ couple, with E value of -0.40 V ($\Delta E = 73$ mV) which is in an agreement with typical one-electron redox process of copper.⁶⁴ The separation between anodic and cathodic waves for this complex is similar to that observed for ferrocene indicating uncompensated resistance in the cell. Another redox couple is observed at -0.66 V and is most likely a ligand based process, however the anodic and cathodic peak potential differences ($\Delta E = 95$ mV) is slightly larger than expected for a fully reversible one-electron process, even when compared with ferrocene. However, the ligand itself does not reveal such behaviour. Similar case has been reported by Zhang *et al.* for the dinuclear compound $[\text{Cu}_2(\text{L})(\text{py})_2(\text{H}_2\text{O})_2]$ (L=1,3-di[o-(o-vanillideneimino)phenoxo]-2-propanol, the potential of two couples is similar to what is observed for **2.1** ($E = -0.55\text{V}$ and -0.84V versus ferrocene).⁶⁵

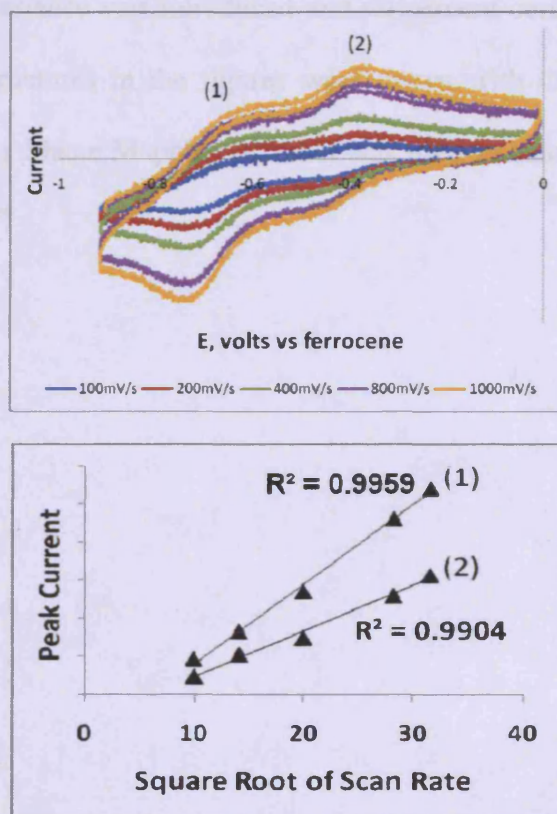


Figure 8: cyclic voltammograms of 1.1.

Crystallographic Studies

All single crystal X-ray data was collected at 150 K on a Bruker/Nonius Kappa CCD diffractometer using graphite monochromated Mo-K α radiation ($\lambda = 0.71073 \text{ \AA}$), equipped with an Oxford Cryostream cooling apparatus. Crystal parameters and details of the data collection, solution and refinement are presented in Table 4. The data was corrected for Lorentz and polarization effects and for absorption using SORTAV.⁶⁶ Structure solution was achieved by direct methods (Sir-92 program system)⁶⁷ and refined by full-matrix least-squares on F2 (SHELXL-97)⁶⁸ with all non hydrogen atoms assigned anisotropic displacement parameters. Hydrogen atoms attached to carbon atoms were placed in idealised positions and allowed to ride on the relevant carbon atom. In the final cycles of refinement, a weighting scheme that gave a relatively flat analysis of variance was introduced and refinement continued until convergence was reached. Molecular structures in the figures were drawn with ORTEP-3.0 for Windows (version 2.02).⁶⁹ Continuous Shape Mapping (CShM) was used to calculate the deviation from the idealised polyhedron.⁷⁰⁻⁷⁶

Chapter 2: A novel Monothiourea Tripodal Ligand; Structural, Spectroscopic and Electrochemical properties of Copper (II), Zinc (II) and Cadmium (II) Complexes

Table 4: Crystal Structure Data for 2.1, 2.2.1 and 2.3

Chemical formula	CuC ₂₈ H ₂₉ N ₇ O ₁₀ Cl ₂ S	ZnC ₂₆ H ₂₆ N ₆ O ₁₁ Cl ₂	CdC ₂₈ H ₂₇ N ₇ O ₉ Cl ₂ S
Colour/shape	green/ plate	colourless/needle	white/ needle
Geometry	Trigonal bipyramid	Trigonal bipyramid	Capped trigonal prism
Mw, (g/mol)	790.08	734.8	820.93
Crystal system	Triclinic	Monoclinic	Monoclinic
Space group	P-1	P2 ₁ /c	C2/c
T(K)	150(2)	150(2)	150(2)
a (Å)	10.0397(9)	18.9883(10)	32.3620(5)
b (Å)	12.7362(9)	9.7711(6)	13.3540(2)
c (Å)	13.7012(10)	18.2005(11)	15.8960(3)
α (Å)	96.995(5)	90	90
β (Å)	90.820(4)	118.765(3)	113.2920(10)
γ (Å)	110.356(4)	90	90
V (Å) ³	1627.3(2)	2960.2(3)	6309.78(18)
Z	2	4	8
Observed Reflections	7349	6166	7212
Unique Reflections	4686	3996	5135
_refine_ls_goodness_of_fit_ref	1.068	1.030	1.040
R _{int}	0.0469	0.0398	0.035
R ₁ [I>2σ(I)]	0.0879	0.0684	0.0482
wR ₂ (all data)	0.23	0.1632	0.1228

Crystal Structure of [Cu^{II}(L¹)](ClO₄)₂.H₂O.CH₃CN (2.1)

The copper compound crystallises in the triclinic space group P-1 and contains a single complex within the asu (Fig. 9). A closer look at the co-ordination sphere of Cu^{II} shows a trigonal bipyramidal geometry (as $S(TP) = 1.47$) (Fig. 10; Table 5) which consists of N1, N2, N5, N6 and S1. The four nitrogen bonds range between 2.006(5) Å and 2.086(5) Å and the sulfur bond is significantly longer at 2.2612(17) Å (Table 6). A related compound [Cu^{II}(TPA)₂S₂](ClO₄)₂[Et₂O], also exhibits a trigonal bipyramidal co-ordination environment and contains very similar bond lengths and angles which likewise range between 2.048(6) Å and 2.096(2) Å likewise, Cu^{II}-S is also similar at 2.280(2).⁷⁷ An intramolecular hydrogen bond is observed between the hydrogen of the amide and the oxygen of the carbonyl (O₁...H_{3a}) at 1.815 Å (Table 7). According to structures on the CCDC, there are 57 crystal structures of Cu^{II} with

Chapter 2: A novel Monothiourea Tripodal Ligand; Structural, Spectroscopic and Electrochemical properties of Copper (II), Zinc (II) and Cadmium (II) Complexes

TPA based ligands, all of which are five coordinate except one structure where copper has an approximately octahedral geometry.^{77, 78} A molecular packing diagram of **2.1** shows head to head π - π stacking interaction at 3.959 Å (Fig.11) and it is a long bond in comparison to normal π - π stacking interactions in the literature which range between 2.7-3.4 Å.⁷⁹

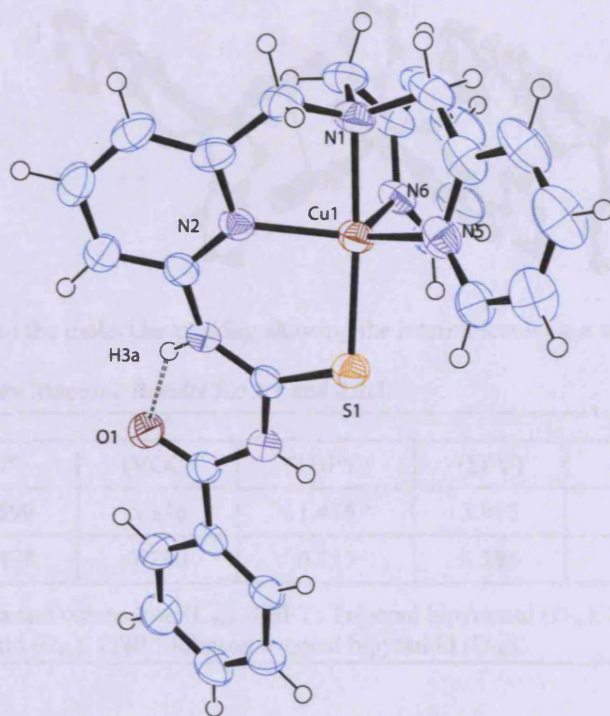


Figure 9: Perspective view of the asymmetric unit of **2.1**. Displacement ellipsoids are shown at the 50% probability level. H atoms are represented by circles of arbitrary size.

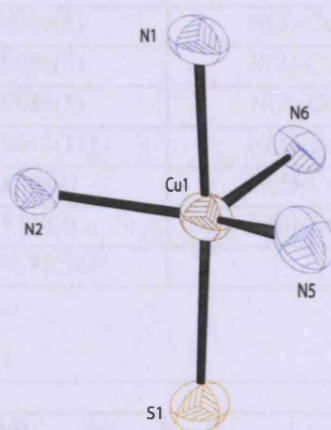


Figure 10: A view of the core geometry of **2.1** of covalent bond radius less than 3 Å.

Chapter 2: A novel Monothiourea Tripodal Ligand; Structural, Spectroscopic and Electrochemical properties of Copper (II), Zinc (II) and Cadmium (II) Complexes

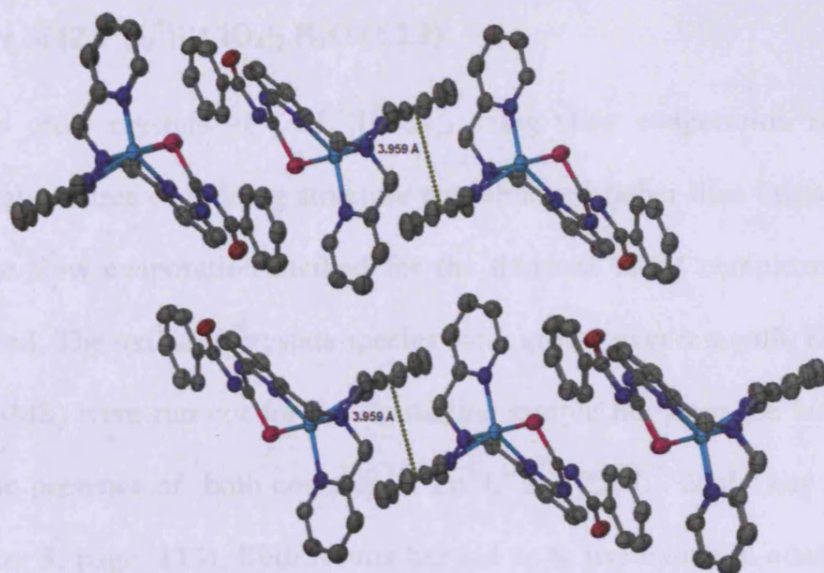


Figure 11: A view of the molecular packing showing the intermolecular π - π stacking interactions.

Table 5: Continuous symmetry Mapping Results for 2.1 and 2.2.1

Structure	(PP)	(VOC)	(TBPY)	(SPY)	(JSPY)	(JTBP)
2.1	33.699	5.346	1.476	3.915	5.346	3.437
2.2.1	33.498	7.230	0.855	5.195	7.230	3.199

PP: Pentagon (D_{5h}), VOC: Vacant octahedron (C_{4v}), TBPY: Trigonal bipyramid (D_{3h}), SPY: Square pyramid (C_{4v}), JSPY: Johnson square pyramid (C_{4v}), JTBP: Johnson trigonal bipyramid (D_{3h}).

Table 6: Relevant Bond lengths (\AA) and Angles ($^\circ$) for $[\text{Cu}^{\text{II}}(\text{L}^1)]_2[\text{ClO}_4]_2[\text{CH}_3\text{CN}][\text{H}_2\text{O}]$

Cu(1)-N(1)	2.015(5)	N(2)-Cu(1)-N(1)	82.4(2)
Cu(1)-N(2)	2.006(5)	N(2)-Cu(1)-N(5)	129.3(2)
Cu(1)-N(5)	2.036(5)	N(2)-Cu(1)-N(6)	110.8(2)
Cu(1)-N(6)	2.086(5)	N(2)-Cu(1)-S(1)	94.20(14)
Cu(1)-S(1)	2.2612(17)	N(5)-Cu(1)-N(6)	114.6(2)
N(1)-Cu(1)-N(5)	82.8(2)	N(5)-Cu(1)-S(1)	96.52(16)
N(1)-Cu(1)-N(6)	81.8(2)	N(6)-Cu(1)-S(1)	102.95(14)
N(1)-Cu(1)-S(1)	174.95(16)		

Table 7: H-bonding geometry (\AA , $^\circ$) for 2.1

D-H...A	D-H	H...A	D...A	D-H...A
N3-H3A ...O1	0.88	1.815	2.561	141.25

Crystal Structure of $[Zn^{II}(L^*)][ClO_4]_2 \cdot H_2O$ (2.2.1)

In an attempt to grow crystals of $[ZnL^1][ClO_4]_2$ using slow evaporation recrystallization method, suprisingly, a urea containing structure was obtained rather than thiourea. It appears that by using the slow evaporation method for the thiourea metal complexes an oxidized species is produced. The oxidized crystals species were grown over a month. High resolution mass spectra (ESMS) were run not for the crystalline sample but from the bulk sample and has confirmed the presence of both complexes: $Zn^{II}L^1$ and $Zn^{II}L^*$. MnL^2 has shown similar behaviour (chapter 3; page: 113). Both results has led us to use oxone in attempt to convert thiourea into urea species (Appendix 1; page: 232).

The zinc compound crystallises in the monoclinic space group $P2_1/c$ and contains one complex within the asu. The Zn^{II} cation lies at the centre of a slightly distorted trigonal bipyramid geometry as confirmed by shape mapping analysis (Table 5) similar to the analagous Cu^{II} complex. There are three equatorial nitrogen donors (N2, N5 and N6) which are located on the pyridyl groups with the bridge-head nitrogen N1, and an oxygen donor occupying axial position (Fig. 12, 13). The co-ordinative bond lengths of the equatorial nitrogen donors are almost identical and vary from 2.014(4) Å to 2.070(4) Å whereas the bridge-head nitrogen is longer at 2.181(4) Å while the bond length of the oxygen donor O1 is quite short at 2.013(3) Å in comparision to other Zn^{II} -N (TPA) species but longer in comparison to the oxygen donor in given examples.^{80, 81} Among 20 Zn^{II} (TPA) framework structures on the CCDC, there are 17 five coordinate structures whereas the rest are octahedral. A similar compound, $[Zn^{II}(TPA)phosphate\ di\text{-}nitrobenzene]$, reported by Ito *et al*, which has an identical donor set environment has bond lengths ranging from 2.059(4) Å to 2.075(3) Å for the pyridyl nitrogens bond length, the bridge-head nitrogen of this example is 2.201(4) Å, and the axial oxygen bond length is short at 1.962(3) Å.⁸¹ It is worth noting that

Chapter 2: A novel Monothiourea Tripodal Ligand; Structural, Spectroscopic and Electrochemical properties of Copper (II), Zinc (II) and Cadmium (II) Complexes

the angle of $O1-Zn1-N2= 87.87^\circ(14)$ is more acute than the analogous copper (II) thiourea species **2.1** which has $S1-Cu1-N2= 94.20^\circ(14)$, this is due perhaps to the larger size (and hence long M-S bond length) of the sulfur atom in comparison to the oxygen atom (Table 9).

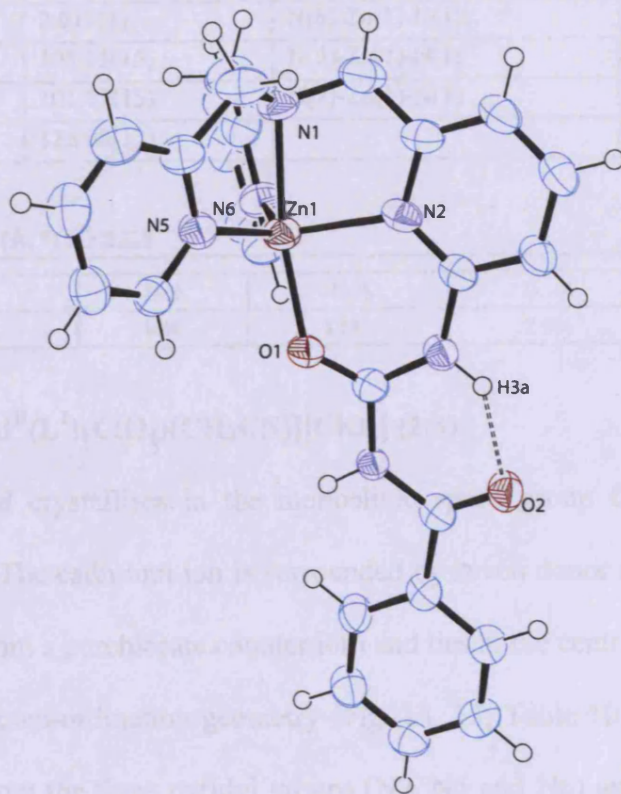


Figure 12: Perspective view of the asymmetric unit of **2.2.1**. Displacement ellipsoids are shown at the 50% probability level. H atoms are represented by circles of arbitrary size.

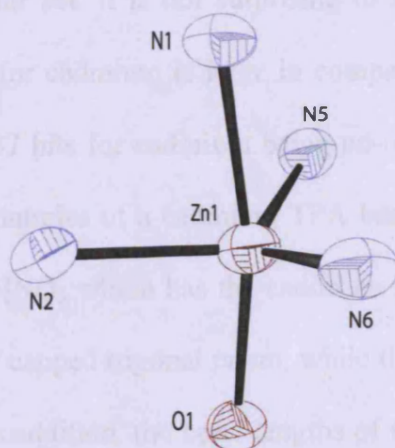


Figure 13: A view of the core geometry of **2.2.1** of covalent bond radius less than 3 Å.

Chapter 2: A novel Monothiourea Tripodal Ligand; Structural, Spectroscopic and Electrochemical properties of Copper (II), Zinc (II) and Cadmium (II) Complexes

Table 8: Relevant Bond lengths (Å) and Angles (°) for $[Zn^{II}(L^*)].2[ClO_4][H_2O]$

Zn(1)-N(1)	2.181(4)	O(1)-Zn(1)-N(2)	87.87(14)
Zn(1)-N(2)	2.070(4)	N(6)-Zn(1)-N(2)	111.34(16)
Zn(1)-N(5)	2.048(4)	N(5)-Zn(1)-N(2)	116.69(16)
Zn(1)-N(6)	2.014(4)	O(1)-Zn(1)-N(1)	168.86(15)
Zn(1)-O(1)	2.013(3)	N(6)-Zn(1)-N(1)	81.69(16)
O(1)-Zn(1)-N(6)	105.15(15)	N(5)-Zn(1)-N(1)	80.66(15)
O(1)-Zn(1)-N(5)	101.77(15)	N(2)-Zn(1)-N(1)	81.39(15)
N(6)-Zn(1)-N(5)	125.05(17)		

Table 9: H-bonding geometry (Å, °) for 2.2.1

D-H...A	D-H	H...A	D...A	D-H...A
N3-H3A...O2	0.88	1.882	2.606	138.45

Crystal Structure of $[Cd^{II}(L^1)(ClO_4)(CH_3CN)][ClO_4]$ (2.3)

The cadmium compound crystallises in the monoclinic space group $C2/c$ and contains one complex within the asu. The cadmium ion is surrounded by seven donor atoms (five N atoms, a S atom and an O atom from a perchlorate counter ion) and lies at the centre of a slightly distorted capped trigonal prismatic co-ordination geometry (Fig. 14, 15; Table 10). Four of the nitrogen donor atoms originate from the three pyridyl groups (N2, N5 and N6) and the bridging N1, the last nitrogen, N7, comes from acetonitrile. This is the first example of a complex where Cd is surrounded by this particular donor set. It is not surprising to have Cd^{2+} surrounded by seven donors since the atomic radius for cadmium is large in comparison to other transition metals. According to CCDC there are 687 hits for cadmium being co-ordinated by seven donor atoms. However, there are only three examples of a cadmium TPA based complex, one of them is the compound $[Cd(TPA)(H_2O)(NO_3)]NO_3$ which has the cadmium surrounded by seven atoms (N4 and O3) with similar geometry of capped trigonal prism, while the other two are surrounded by 6 and 8 co-ordination sphere.^{7, 82} In addition, the bond lengths of the related octahedral compound $[Cd^{II}(4'-(2-Pyridyl)-2,2':6',2''-terpyridin)(SCN)_4]$ reported by Gou *et al*, range between 2.326(4) Å and 2.484(5) Å, the Cd^{II} -S bond length is almost identical at 2.5877(16). In both

examples, the co-ordinative bond lengths of nitrogen donors N1, N2, N5 and N6 are statistically similar (Table 11).^{7, 83} Intramolecular hydrogen bonding exists between N3-H3a-O1 (1.887 Å) which is identical to copper and zinc analogues but shorter than the normal hydrogen bond length (~2 Å) due to the formation of a favourable six membered ring (Table 1⁷).

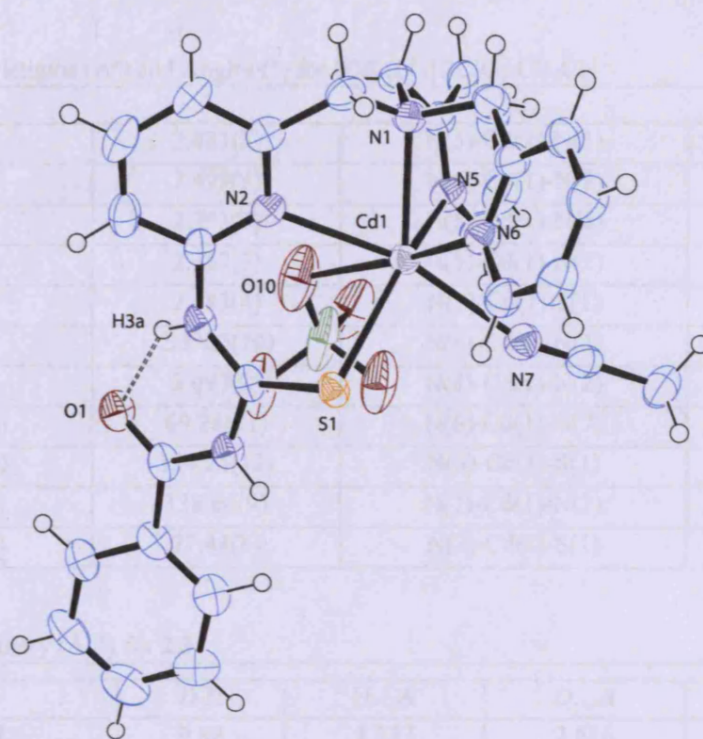


Figure 14: Perspective view of the asymmetric unit of 2.3. Displacement ellipsoids are shown at the 50% probability level. H atoms are represented by circles of arbitrary size.

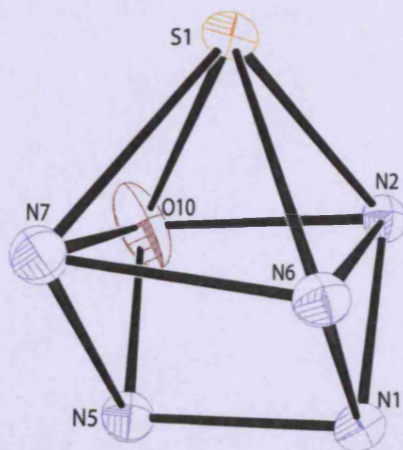


Figure 15: A view of the core geometry of 2.3 of covalent bond radius less than 3 Å.

Chapter 2: A novel Monothiourea Tripodal Ligand; Structural, Spectroscopic and Electrochemical properties of Copper (II), Zinc (II) and Cadmium (II) Complexes

Table 10: Continuous Symmetry Mapping Results for 2.3

Structure	(HP)	(HPY)	(PBPY)	(OCF)	(TPRS)	(JPBP)	(JETPY)
2.3	36.549	19.089	7.225	2.804	1.352	13.043	20.564

HP: Heptagon (D7h), HPY: Hexagonal pyramid (C6v), PBPY: Pentagonal bipyramid (D5h), OCF: Capped octahedron (C3v), TPRS: Capped trigonal prism (C2v), JPBP: Johnson pentagonal bipyramid J13 (D5h), JETPY: Johnson elongated triangular pyramid J7 (C3v).

Table 11: Relevant Bond lengths (Å) and Angles (°) for [Cd^{II}(L¹)]₂ClO₄·CH₃CN

N(1)-Cd(1)	2.431(3)	N(5)-Cd(1)-N(1)	71.93(12)
N(2)-Cd(1)	2.499(3)	N(5)-Cd(1)-N(2)	110.30(11)
N(5)-Cd(1)	2.293(3)	N(5)-Cd(1)-N(6)	114.79(12)
N(6)-Cd(1)	2.357(3)	N(5)-Cd(1)-N(7)	82.57(12)
N(7)-Cd(1)	2.483(4)	N(5)-Cd(1)-S(1)	145.18(9)
S(1)-Cd(1)	2.5962(10)	N(6)-Cd(1)-N(1)	69.80(11)
O(10)-Cd(1)	3.097(3)	N(6)-Cd(1)-N(2)	102.71(11)
N(1)-Cd(1)-N(2)	69.28(11)	N(6)-Cd(1)-N(7)	78.09(12)
N(1)-Cd(1)-N(7)	124.24(12)	N(6)-Cd(1)-S(1)	95.29(9)
N(1)-Cd(1)-S(1)	138.66(9)	N(7)-Cd(1)-N(2)	164.68(11)
N(2)-Cd(1)-S(1)	77.44(8)	N(7)-Cd(1)-S(1)	87.24(9)

Table 12: H-bonding geometry (Å, °) for 2.3

D-H...A	D-H	H...A	D...A	D-H...A
N3-H3A ...O1	0.88	1.887	2.616	139.13

Conclusion

Cu^{II} and Cd^{II} complexes with mono thiourea tripodal ligand have been synthesised and fully characterised. The redox-behaviour of copper species has also been probed via cyclic voltammetry and shows two redox processes. Air may act as an oxidising agent which causes the conversion of the thiourea in ZnL^1 into a urea group ZnL^* . The structure of the oxidized species ZnL^* has been obtained as well as the accurate mass. Continuous shape mapping results have confirmed a strong preference for trigonal bipyramidal for Cu and Zn complexes since the ligand is set up to bind through four nitrogens and one sulfur, whereas in Cd complex and since the cadmium is larger metal, it chose to be seven co-ordinate and favoure a capped trigonal prism. All complexes of L^1 has shown a strong short hydrogen bond between the C=O and N-H to form six member ring in the co-ordinated arm. The co-ordination geometry is typical for all complexes since metals are surrounded by five donor atoms and this is typical of TPA complexes.

References

1. A. G. Blackman, *Polyhedron*, 2005, **24**, 1-39.
2. G. Anderegg and F. Wenk, *Helv. Chim. Acta*, 1967, **50**, 2330.
3. J. C. M. Rivas, E. Salvagni, R. T. M. d. Rosales and S. Parsons, *Dalton Trans.*, 2003, 3339.
4. C.-L. Chuang, O. d. Santos, X. Xu and J. W. Canary, *Inorg. Chem.*, 1997, **36**, 1967.
5. K. Jitsukawa, Y. Oka, H. Einaga and H. Masuda, *Tetrahedron Lett.*, 2001, **42**, 3467-3469.
6. C.-L. Chuang, K. Lim and J. W. Canary, *Supramol. Chem.*, 1995, **5**, 39.
7. C. S. Allen, C.-L. Chuang, M. Cornebise and J. W. Canary, *Inorg. Chim. Acta*, 1995, **239**, 29-37.
8. S. Yan, C. Li, P. Cheng, D. Liao, Z. Jiang, G. Wang, X. Yao and H. Wang, *J. Chem. Cryst.*, 1999, **29**, 1085.
9. G. Anderegg, E. Hubmann, N. G. Podder and F. Wenk, *Helv. Chim. Acta*, 1977, **60**, 123.
10. M. Schatz, M. Becker, F. Thaler, F. Hampel, S. Schindler, R. R. Jacobson, Z. Tyeklar, N. N. Murthy, P. Ghosh, Q. Chen, J. Zubieta and K. D. Karlin, *Inorg. Chem.*, 2001, **40**, 2321.
11. S. Fox, A. Nanthakumar, M. Wikstrom, K. D. Karlin and N. J. Blackburn, *J. Am. Chem. Soc.*, 1996, **118**, 24-34.
12. N. Wei, N. N. Murthy and K. D. Karlin, *Inorg. Chem.*, 1994, **33**, 6093-6100.
13. K. D. Karlin, J. C. Hayes, S. Juen, J. P. Hutchinson and J. Zubieta, *Inorg. Chem.*, 1982, **21**, 4106-4108.
14. F. Thaler, C. D. Hubbard, F. W. Heinemann, R. van Eldik, S. Schindler, I. Fabian, A. M. Dittler-Klingemann, F. E. Hahn and C. Orvig, *Inorg. Chem.*, 1998, **37**, 4022-4029.
15. J. Dietrich, F. W. Heinemann, A. Schrodtr and S. Schindler, *Inorg. Chim. Acta*, 1999, **288**, 206-209.
16. N. N. Murthy and K. D. Karlin, *J. Chem. Soc., Chem. Commun.*, 1993, 1236 - 1238.
17. U. Mukhopadhyay, I. Bernal, S. S. Massoud and F. A. Mautner, *Inorg. Chim. Acta*, 2004, **357**, 3673-3682.
18. S. S. Massoud, *J. Inorg. Biochem.*, 1994, **55**, 183-191.
19. K. D. Karlin and Z. Tyeklar, *Bioinorganic Chemistry of Copper* Chapman & Hall, New York, 1993.
20. S. S. Massoud, F. A. Mautner, M. A. M. Abu-Youssef and N. M. Shuaib, *Polyhedron*, 1999, **18**, 2061-2067.
21. S. S. Massoud and R. M. Milburn, *J. Inorg. Biochem.*, 1990, **39**, 337-349.
22. K. D. Karlin, J. C. Hayes, J. P. Hutchinson, J. R. Hyde and J. Zubieta, *Inorg. Chim. Acta*, 1982, **64**, L219-L220.
23. K. N. Raymond and J. L. Shafer, *Inorg. Chem.*, 1971, **10**, 1799-1803.
24. M. Di Vaira and P. Orioli, *Inorg. Chem.*, 1967, **6**, 955-957.
25. A. M. Dittler-Klingemann and F. E. Hahn, *Inorg. Chem.*, 1996, **35**, 1996-1999.
26. A. M. Dittler-Klingemann, C. Orvig, F. E. Hahn, F. Thaler, C. D. Hubbard, R. van Eldik, S. Schindler and I. Fabian, *Inorg. Chem.*, 1996, **35**, 7798-7803.
27. S. Schindler, *Eur. J. Inorg. Chem.*, 2000, 2311-2326.
28. M. M. Ibrahim, K. Ichikawa and M. Shiro, *Inorg. Chim. Acta*, 2003, **353**, 187-196.
29. Y. Kawamura, Y. Tsukahara, S. Nasu, S. Morimoto, A. Fuyuhiko and S. Kaizaki, *Inorg. Chim. Acta*, 2004, **357**, 2437-2440.

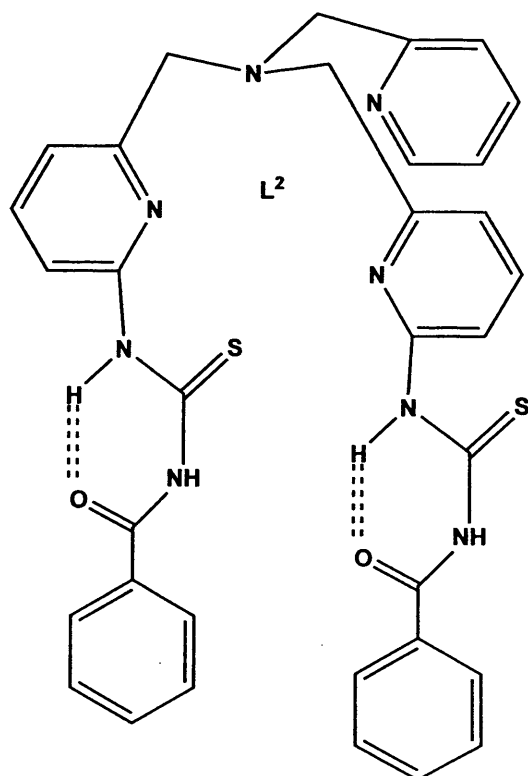
Chapter 2: A novel Monothiourea Tripodal Ligand; Structural, Spectroscopic and Electrochemical properties of Copper (II), Zinc (II) and Cadmium (II) Complexes

30. G. S. Matouzenko, A. Bousseksou, S. Lecocq, P. J. van Koningsbruggen, M. Perrin, O. Kahn and A. Collet, *Inorg. Chem.*, 1997, **36**, 2975-2981.
31. F. Tafesse, S. S. Massoud and R. M. Milburn, *Inorg. Chem.*, 1985, **24**, 2591-2593.
32. F. Tafesse, S. S. Massoud and R. M. Milburn, *Inorg. Chem.*, 1993, **32**, 1864-1865.
33. J. Chin, *J. Acc. Chem. Res.*, 1991, **24**, 145-152.
34. R. L. Fanshawe, A. G. Blackman and C. R. Clark, *Inorg. Chim. Acta*, 2003, **342**, 114-124.
35. R. Wijesekera, P. Hendry and A. Sargeson, *Aust. J. Chem.*, 1992, **45**, 1187-1190.
36. R. Hettich and H.-J. Schneider, *J. Am. Chem. Soc.*, 1997, **119**, 5638-5647.
37. K. D. Karlin, J. C. Hayes, Y. Gultneh, R. W. Cruse, J. W. McKown, J. P. Hutchinson and J. Zubieta, *J. Am. Chem. Soc.*, 1984, **106**, 2121-2128.
38. Z. Tyeklar, R. R. Jacobson, N. Wei, N. N. Murthy, J. Zubieta and K. D. Karlin, *J. Am. Chem. Soc.*, 1993, **115**, 2677-2689.
39. T. N. Sorrell and D. L. Jameson, *Inorg. Chem.*, 1982, **21**, 1014-1019.
40. P. Halasyamani, M. J. Willis, C. L. Stern and K. R. Poeppelmeier, *Inorg. Chim. Acta*, 1995, **240**, 109-115.
41. J. Xu, C.-I. Chuang and J. W. Canary, *Inorg. Chim. Acta*, 1997, **256**, 125-128.
42. F. Mani and G. Scapacci, *Inorg. Chim. Acta*, 1980, **38**, 151-155.
43. L. K. Thompson, B. S. Ramaswamy and E. A. Seymour, *Can. J. Chem.*, 1977, 878-888.
44. C. J. Davies, G. A. Solan and J. Fawcett, *Polyhedron*, 2004, **23**, 3105-3114.
45. Y. Zhang, P. H. M. Budzelaar, J. M. M. Smits, R. d. Gelder, P. R. Hageman and A. W. Gal, *Polyhedron*, 2003, 648-655.
46. J. W. Canary, Y. Wang, R. R. Jr, L. Q. Jr and H. Miyake, *Inorg. Synth.*, 1998, **32**, 70-75.
47. J. C. M. Rivas, E. Salvagni and S. Parsons, *Dalton Trans.*, 2004, 4185-4192.
48. D. Maiti, A. A. Narducci Sarjeant and K. D. Karlin, *J. Am. Chem. Soc.*, 2007, **129**, 6720-6721.
49. D. Cati and H. Stoeckli-Evans, *Private communication to the Cambridge Crystallographic Database*, 2004.
50. J. C. M. Rivas, E. Salvagni, R. T. M. de Rosales and S. Parsons, *Dalton Trans.*, 2003, 3339-3349.
51. J. C. M. Rivas, R. Prabakaran, R. T. M. d. Rosales, L. Metteau and S. Parsons, *Dalton Trans.*, 2004, 2800-2807.
52. T. Kojima, D. Noguchi, T. Nakayama, Y. Inagaki, Y. Shiota, K. Yoshizawa, K. Ohkubo and S. Fukuzumi, *Inorg. Chem.*, 2008, **47**, 886-895.
53. D. Maiti, A. A. Narducci Sarjeant and K. D. Karlin, *Inorg. Chem.*, 2008, **47**, 8736-8747.
54. J. C. M. Rivas, R. T. M. d. Rosales and S. Parsons, *Dalton Trans.*, 2003, **11**, 2156 - 2163.
55. S. Yamaguchi, A. Wada, Y. Funahashi, S. Nagatomo, T. Kitagawa, K. Jitsukawa and H. Masuda, *Eur. J. Inorg. Chem.*, 2003, 4378-4386.
56. M. S. M. Yusof, S. K. C. Soh, N. Ngah and B. M. Yamin, *Acta Cryst.*, 2006, **E62**, 1446-1448.
57. S. Yamaguchi, A. Wada, S. Nagatomo, y. T. Kitagawa, y. K. Jitsukawa and H. Masuda, *The Chem. Soc. Japan*, 2004, 1556.
58. V. J. Rao, K. Muthuramu and V. Ramamurthy, *J. Org. Chem.*, 1982, **47**, 127-131.
59. M. G. B. Drew, J. Nelson, F. Esho, V. McKee and S. M. Nelson, *J. Chem. Soc., Dalton Trans.*, 1982, 1837 - 1843.
60. P. Dapporto, G. De Munno, A. Sega and C. Mealli, *Inorg. Chim. Acta*, 1984, **83**, 171-176.

Chapter 2: A novel Monothiourea Tripodal Ligand; Structural, Spectroscopic and Electrochemical properties of Copper (II), Zinc (II) and Cadmium (II) Complexes

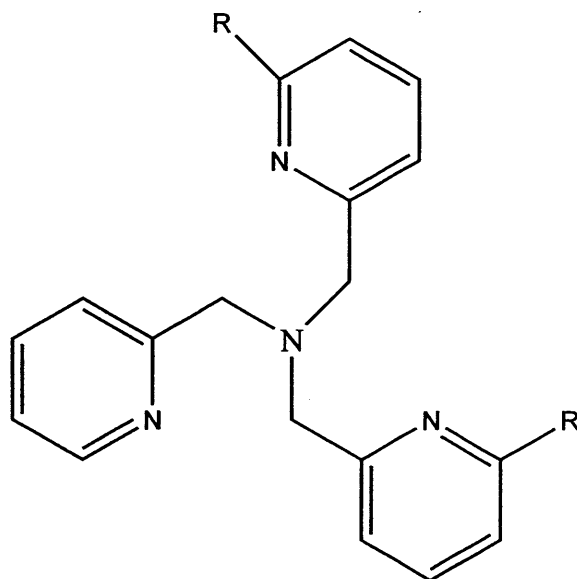
61. B. J. Hathaway, in *Comprehensive Coordination Chemistry*, Pergamon press, Oxford, 1987.
62. C. Su, W. Lu, T. Hui, T. Chang, S. Wang and F. Liao, *Polyhedron*, 1993, **12**, 2249.
63. D. Reinen and M. Atanasov, *Chem. Phys.*, 1989, **136**, 27-46.
64. P. Bindu, M. R. P. Kurup and T. R. Satyakeerty, *Polyhedron*, 1998, **18**, 321-331.
65. W. Zhang, S. Liu, C. Ma and D. Jiang, *Polyhedron*, 1999, **17**, 3835-3839.
66. R. Blessing, *Acta Cryst. Section A*, 1995, **51**, 33-38.
67. A. Altomare, G. Cascarano, C. Giacovazzo and A. Guagliardi, *J. App. Cryst.*, 1993, **26**, 343-350.
68. G. M. Sheldrick, *Acta Cryst.*, 2008, **A46**, 112.
69. L. Farrugia, *J. App. Cryst.*, 1997, **30**, 565.
70. S. Alvarez, P. Alemany, D. Casanova, J. Cirera, M. Llunell and D. Avnir, *Coord. Chem. Rev.*, 2005, **249**, 1693-1708.
71. S. Álvarez, D. Avnir, M. Llunell and M. Pinsky, *New J. Chem.*, 2002, **26**, 996-1009.
72. S. Alvarez, P. Alemany, D. Casanova, J. Cirera, M. Llunell and D. Avnir, *Coord. Chem. Rev.*, 2005, **249**, 1693-1708.
73. S. Alvarez, P. Alemany and D. Avnir, *Chem. soc. Rev.*, 2005, **34**, 313-326.
74. S. Alvarez, D. Avnir, M. Pinsky and M. Llunell, *Cryst. Engineer.*, 2001, **4**, 179-200.
75. M. Pinsky and D. Avnir, *Inorg. Chem.*, 1998, **37**, 5575-5582.
76. M. Pinsky, K. B. Lipkowitz and D. Avnir, *J. Math. Chem.*, 2001, **1**, 109-120.
77. M. E. Helton, P. Chen, P. P. Paul, Z. Tyeklar, R. D. Sommer, L. N. Zakharov, A. L. Rheingold, E. I. Solomon and K. D. Karlin, *J. Am. Chem. Soc.*, 2003, **125**, 1160-1161.
78. R. R. Jacobson, Z. T. r, K. D. Karlin and J. Zubieta, *Inorg. Chem.* , 1991, 2035.
79. E. V. Anslyn and D. A. Dougherty, *Modern physical organic chemistry*, University Science Books, 2004.
80. H. Adams, N. A. Bailey, D. E. Fenton and Q.-Y. He, *Dalton Trans.*, 1997, 1533-1540.
81. M. Ito, K. Fujita, F. Chitose, T. Takeuchi, K. Yoshida and Y.-S. Takita, *Chem. Lett.* , 2002, 594.
82. D. C. Bebout, S. W. Stokes and R. J. Butcher, *Inorg. Chem.*, 1999, **38**, 1126-1133.
83. L. Gou, Q.-R. Wu, H.-M. Hu, T. Qin, G.-L. Xue, M.-L. Yang and Z.-X. Tang, *Polyhedron*, 2008, **27**, 1517-1526.

Chapter 3: Co-ordination Behaviour of a Novel Bisthiourea Tripodal Ligand; Structural, Spectroscopic and Electrochemical properties of a series of Transition Metal Complexes with Binding Studies



Introduction

Transition metal complexes of tris(2-pyridylmethyl)amine (TPA) ligands and their derivatives have been much studied in the last 20 years. TPA derivatives having two difunctionalised moieties at the 6-positions of the two pyridine rings are well known. According to, Cambridge Crystallographic Data Centre (CCDC), there are 41 example of TPA based complexes having two derivatives of different functional groups such as amide, amine, halide and phenyl.¹⁻⁸ Some of these ligands are shown in (Fig. 1).



R= NH₂, ^tBuCONH, F, Br, Ph, C(CH₃)₂CONH, CH₂OH, ^tBuCH₂NH,

Figure 1: Examples of difunctionalised ligands of TPA.

Here in this chapter an investigation into the preparation of the TPA ligand difunctionalised with benzoylthiourea groups is explored. The synthesis of this new ligand may lead to different chemistry to previous BAPA based structures and may be more like Anslyn's guanidinium substituted TPA framework,⁹ with the H bonding groups being further removed from the metal centre. In addition, though this molecule contains the thiourea moiety, it is expected that each

Chapter 3: Co-ordination Behaviour of a Novel Bisthiourea Tripodal Ligand; Structural, Spectroscopic and Electrochemical properties of a series of Transition Metal Complexes with Binding Studies

benzoyl thiourea will cyclise through intramolecular hydrogen bonding, leaving only one NH available for intermolecular H bonding, but with the sulfur atoms potentially available for co-ordination to the metal centre (Fig. 2). Thus we have conducted an investigation into the basic co-ordination chemistry of the ligand with a variety of metal ions. Of particular interest is the variation of the binding modes with the covalent radii of the metal centre along with the stereochemical preferences of the different d electron configurations. Additionally, binding studies of small molecules (fluoride and succinate) into this ligand with its zinc and cadmium complexes are also investigated via ^1H NMR titration technique.

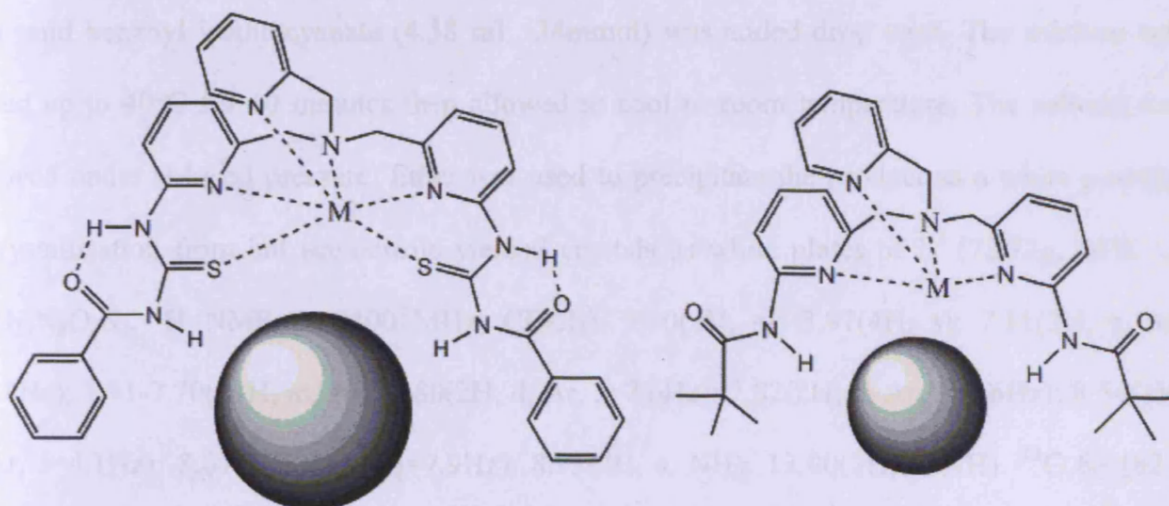


Figure 2: The thiourea derivative L^2 (left) with potentially a larger guest cavity than the BAPA ligand (right). In the case of L^2 , not only is the cavity larger but the guest is more remote to the metal centre.

Experimental

General

NMR, mass spectrometry, UV-Vis and elemental analyses were carried out as explained in the previous chapter.

Synthesis of L²

Bis(6-amino-2-pyridylmethyl)(2-pyridylmethyl)amine (BAPA) was synthesised as literature procedures reported by Harata *et.al.*¹⁰ (5.453g, 17mmol) of BAPA was dissolved in EtOH (50 mL) and benzoyl isothiocyanate (4.58 mL, 34mmol) was added drop wise. The mixture was heated up to 40°C for 10 minutes then allowed to cool to room temperature. The solvent was removed under reduced pressure. Ether was used to precipitate the product as a white powder. Recrystallisation from hot acetonitrile yielded crystals as white plates of L² (7.272g, 66%) of C₃₄H₃₀N₈O₂S₂. ¹H NMR δ_H (400 MHz; CDCl₃): 3.90(2H, s); 3.97(4H, s); 7.11(2H, t, Ar, J=5.8Hz); 7.41-7.70(11H, m, Ar); 7.80(2H, d, Ar, J=7.6Hz); 7.82(2H, d, Ar, J=7.6Hz); 8.54(1H, d, Ar, J=4.1Hz); 8.64(2H, d, Ar, J=7.9Hz); 8.93(2H, s, NH); 13.00(2H, s, NH). ¹³C δ_C (62.5 MHz; CDCl₃): 59.4, 60.3, 114.1, 120.8, 120.7, 122.1, 123.2, 127.5, 129.2, 131.7, 133.7, 136.6, 136.7, 138.2, 149.0, 150.5, 166.3, 176.7. Accurate ESMS (*m/z*): 645.1859 (100) [L² - H]⁺, 646.1887 (30) [L²]⁺. [calculated 646.1933]. IR KBr/cm⁻¹: 3318(br), 3049(br), 1673(s), 1594(s), 1454(s), 1331(s), 756(s). UV/Vis [λ_{max}, nm (εM, M⁻¹cm⁻¹)] in CH₃CN: 266(50,300), 309(28,600).

General Procedure for the synthesis of metal complexes

Perchlorate salts were used as sources for transition metals. Thus extra care should be taken when using such explosive metal salts. Ligand L^2 (1 equivalent, typically 0.1 mmol) was dissolved in the minimum amount of mixture of acetonitrile and acetone (typically 3 mL). The solutions were warmed to ca. 60°C to ensure that the ligand fully dissolved. To this stirring solution, the metal perchlorate salt (1 equivalent) dissolved in acetonitrile (ca. 2 mL) was added dropwise. Recrystallisation of the compounds typically involved the diffusion of diethyl ether into acetonitrile solutions which were filtered through Celite.

[Mn^{II}(L²).ClO₄][ClO₄].2H₂O (3.1): yellow block crystals (44% yield).

MnC₃₄H₃₀N₈O₂S₂(ClO₄)₂(H₂O)₂ requires C, 43.63; H, 3.66; N, 11.98%; ESMS m/z (%): 709.11 (100), 711.11 (75), 713.11 (50); IR (KBr pellet, cm⁻¹): 3424(br), 1602(s), 1541(m), 1458(s), 1260(s), 1086(s), 706s, 621(s); UV/Vis [λ_{max} , nm (ϵ M, M⁻¹cm⁻¹)] in CH₃CN: 256(17,300), 314(10,600).

[Co^{II}(L²)](ClO₄)₂ (3.2): brown-green needle crystals (59 % yield). Found: C, 45.08; H, 3.47; N, 12.38. CoC₃₄H₃₀N₈O₂S₂(ClO₄)₂ requires C, 45.18; H, 3.34; N, 12.40%; ESMS m/z (%): 730.1117 (100), 704.1196 (40), [Co(L²) - H]⁺, [calculated 704.1186]; IR (KBr pellet, cm⁻¹): 3437(br), 1613(s), 3069(m), 1551(m), 1439(s), 1258(s), 726(s), 1091(s), 622(s). UV/Vis [λ_{max} , nm (ϵ M, M⁻¹cm⁻¹)] in CH₃CN: 280(33,200), 351(7,400), 400(3,100), 507(80), 568(55).

[Ni^{II}(L²).CH₃CN](ClO₄)₂.0.5(CH₃COCH₃).0.5(H₂O) (3.3): brown needle crystals (94% yield).

Found: C, 45.85; H, 4.02; N, 12.95. NiC_{37.5}H₃₇N₉O₁₁S₂Cl₂ requires C, 45.79; H, 3.79; N, 12.81%; ESMS m/z (%): 703.1216 (100), [Ni(L²) - 1H]⁺, [calculated 703.1208]; IR (KBr pellet, cm⁻¹): 3432(br), 1610(s), 3069(m), 1566(s), 1456(s), 1262(s), 709(s), 1090(s), 621(s). UV/Vis [λ_{max} , nm (ϵ M, M⁻¹cm⁻¹)] in CH₃CN: 323(15,800), 385(1,500), 549(17), 849(15), 940(16).

Chapter 3: Co-ordination Behaviour of a Novel Bisthiourea Tripodal Ligand; Structural, Spectroscopic and Electrochemical properties of a series of Transition Metal Complexes with Binding Studies

[Cu^{II}(L²)](ClO₄)₂ (3.4): green block crystals (88% yield). Found: C, 44.75; H, 3.37; N, 12.34. CuC₃₄H₃₀N₈O₂S₂(ClO₄)₂ requires C, 44.98; H, 3.33; N, 12.35%; ESMS m/z (%): 708.1176 (100), [Cu(L¹) - H]⁺, [calculated 708.1151]; IR (KBr pellet, cm⁻¹): 3449(br), 1609(s), 3069(m), 1546(s), 1490(s), 1260(s), 726(s), 1090(s), 623(s). UV/Vis [λ_{max} , nm (ϵ M, M⁻¹cm⁻¹)] in CH₃CN: 315 (17,000), 623(131), 793(96).

[Zn^{II}(L²)](ClO₄)₂.CH₃CN (3.5): colourless rectangle crystals (85% yield). Found: C, 45.41; H, 3.45; N, 13.30. Zn₂C₇₀H₆₃N₁₇O₂₀S₄Cl₄ requires C, 45.12; H, 3.40; N, 13.01 %; ESMS m/z (%): 709.1146 (100) [Zn(L²) - H]⁺, [calculated 709.1146], 546.1091 (40) [Zn(L²) - (C₈H₅S₁O₁)]⁺, [calculated 546.1054]; ¹H NMR (400 MHz; CD₃CN): 4.35(2H, s); 4.36(4H, s); 7.58-7.80(12H, m, Ar); 8.04 (2H, d, Ar, J=7.9 Hz); 8.04(2H, d, Ar, J=7.9Hz); 8.19(1H, t, Ar, J=7.6Hz); 8.23(2H, t, Ar, J=8.4Hz); 8.63(1H, d, Ar, J=8.7Hz); 10.26(2H, s, NH); 13.58(2H, s, NH). ¹³C NMR: (62.5 MHz; CD₃CN): 56.1, 56.2, 122.3, 123.8, 125.0, 125.6, 128.7, 129.0, 130.9, 134.5, 141.9, 143.8, 148.2, 150.5, 154.3, 154.4, 169.4, 179.4; IR (KBr pellet, cm⁻¹): 3394(br), 1612(s), 3069(m), 1556(s), 1442(s), 1257(s), 726(s), 1092(s), 622(s). UV/Vis [λ_{max} , nm (ϵ M, M⁻¹cm⁻¹)] in CH₃CN: 260(29,200), 321(10,500).

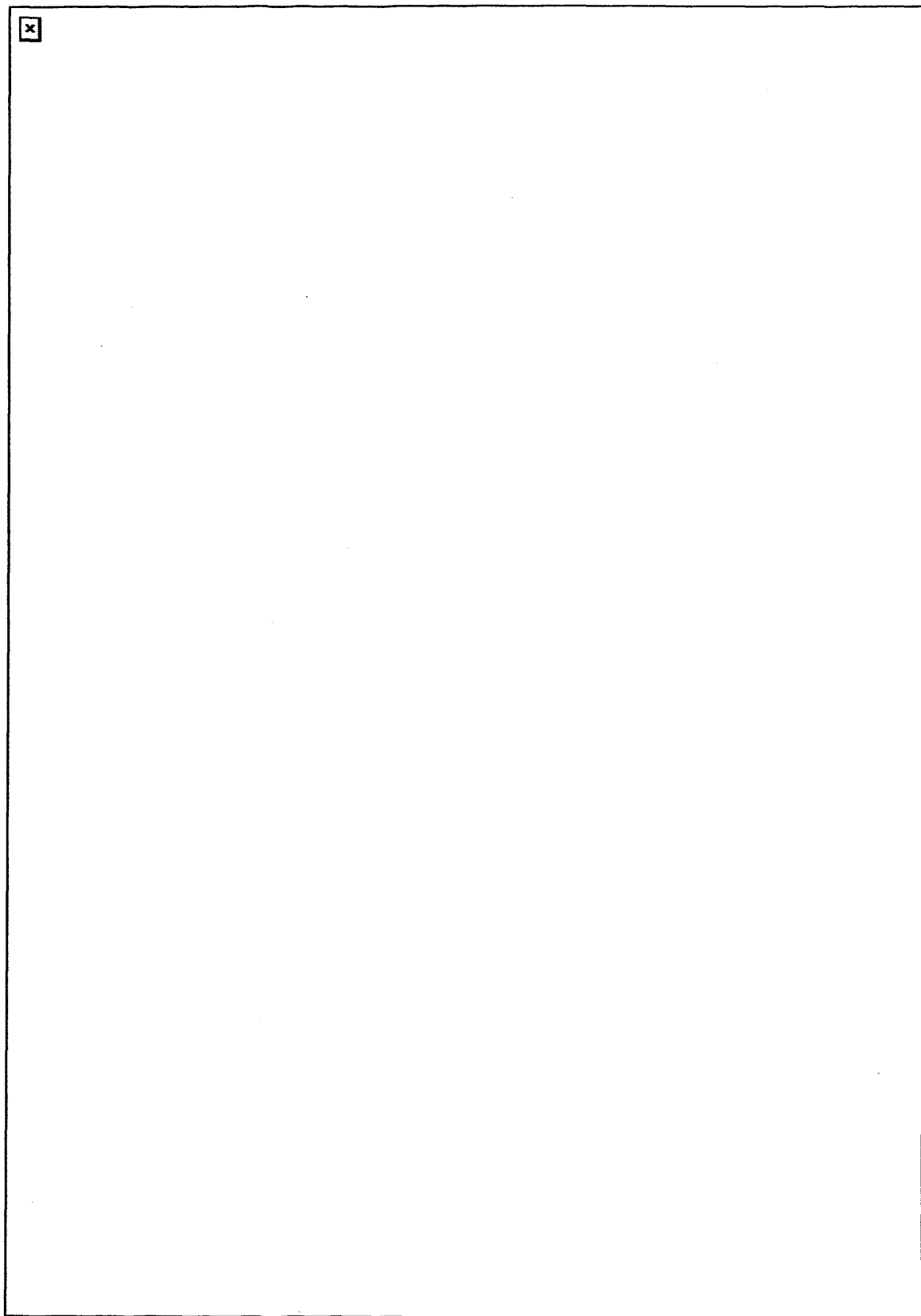
[Cd^{II}(L²).ClO₄](ClO₄).CH₃CN (3.6): colourless block crystals (82% yield). Found: C, 43.56; H, 3.31; N, 12.59. CdC₃₄H₃₀N₈O₂S₂(ClO₄)₂(CH₃CN) requires C, 43.24; H, 3.32; N, 12.61%; ESMS m/z (%): 759.0936 (100), [Cd(L¹) - H]⁺, [calculated 759.0888]; ¹H NMR (400 MHz; CD₃CN): 4.16(4H, s); 4.25(2H, s); 7.38(2H, d, Ar, J=7.4Hz); 7.49(2H, d, Ar, J=7.5Hz); 7.48-8.14(15H, m, Ar); 8.70(1H, d, Ar, J=5.0Hz); 10.36(2H, s, NH); 13.72(2H, s, NH). ¹³C NMR: (62.5 MHz; CD₃CN): 56.6, 56.7, 120.9, 123.6, 125.1, 125.2, 128.5, 128.7, 130.5, 134.2, 140.3, 142.2, 148.3, 150.2, 153.2, 153.4, 169.3, 179.3; IR (KBr pellet, cm⁻¹): 3439(br), 3069(m), 1609(s), 1541(s), 1438(s), 1261(s), 704(m), 1098(s), 620(s); UV/Vis [λ_{max} , nm (ϵ M, M⁻¹cm⁻¹)] in CH₃CN: 260(27,800), 321 (9,900).

Results and Discussion

Ligand Synthesis (L²)

The procedure to synthesise the ligand is outlined in Scheme 1. The amino groups of the BAPA ligand were converted into thiourea groups via the dropwise addition of 2 equivalents of benzoyl-isothiocyanate in ethanol with continuous stirring and gentle heating to approximately 50°C.¹¹ Following this addition, after 10 minutes the reaction mixture changed from a clear yellow solution to a creamy suspension. The product was isolated as a white precipitate. It is worth noting that after initial unsuccessful reactions using chloroform as a solvent because there were no reaction progress, it was found that conducting the reaction in ethanol resolved this issue. The ligand L² is thought to be suitable for anion binding especially, when a transition metal occupies a centre of the receptor consequently, the complex becomes more rigid and orientated to host a guest of interest. The presence of an intra-molecular hydrogen bond between the carbonyl oxygen atom and the amine nitrogen atom makes the second hydrogen point towards the cavity and available to bind a guest (Fig. 3), which of course needs to be suitable in terms of: shape, geometry and size as explained in the first chapter.

Chapter 3: Co-ordination Behaviour of a Novel Bisthiourea Tripodal Ligand; Structural, Spectroscopic and Electrochemical properties of a series of Transition Metal Complexes with Binding Studies



Scheme 1: Synthetic route to L²

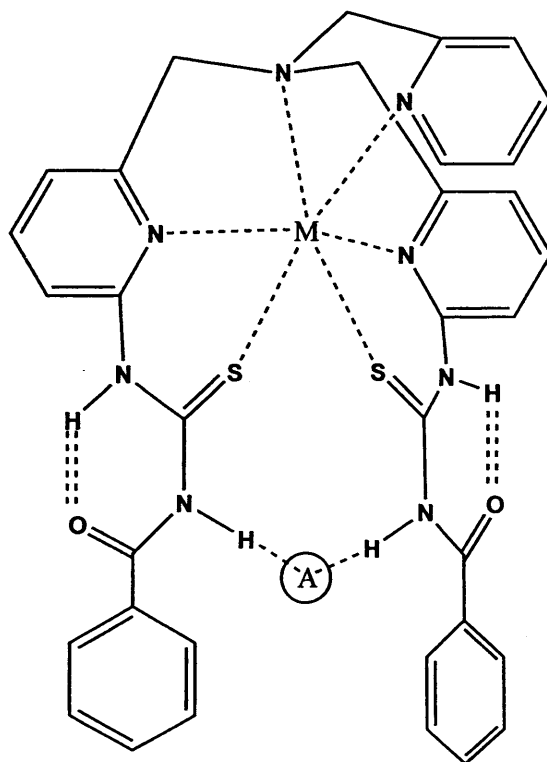


Figure 3: Expected tripodal arrangements of L^2 when hosting anion.

Synthesis of Complexes

Ligand L^2 (1 equivalent, typically 0.1 mmol) was dissolved in the minimum amount of acetonitrile and acetone (typically 3 mL). The solutions were warmed to *ca.* 60°C to ensure that the ligand fully dissolved. To this stirring solution, the metal perchlorate salt (1 equivalent) dissolved in acetonitrile (*ca.* 2 mL) was added dropwise. Crystallisation of the compounds typically involved the diffusion of diethyl ether into acetonitrile solutions which had been filtered through Celite. The yields from these reactions were moderate to high (60-95%). This crystalline material was then subsequently used for all spectroscopic measurements.

Spectroscopic Properties of Complexes

Vibrational Spectroscopy

The amide carbonyl stretch for L^2 appears at 1673 cm^{-1} , typical for an amido group and it is red-shifted in all its complexes (Table 1). A strong peak at 1331 cm^{-1} , assigned to the $\nu(\text{C}=\text{S})$ is also shifted to lower energy between $1257\text{-}1262\text{ cm}^{-1}$ indicating the co-ordination of the sulfur groups which reduces the bond order and thus weakens the $\text{C}=\text{S}$ bond. The shift of the pyridine ring vibration at around 1550 cm^{-1} and 1450 cm^{-1} in all complexes indicates co-ordination from the pyridine ring nitrogens. All compounds reveal two characteristic unsplit infrared active bands at $\sim 1,100\text{ cm}^{-1}$ and $\sim 623\text{ cm}^{-1}$ indicative of ionic perchlorate (T_d symmetry).^{12,13} All of these features are consistent with the X-ray diffraction data for all complexes.

Table 1: IR Stretching Frequencies of L^2 and complexes. IR spectra measured as KBr discs

Co	$\nu(\text{C}=\text{O})$	$\nu(\text{C}=\text{S})$	$\nu(\text{O}-\text{H})$	aromatic $\nu(\text{C}-\text{H})$	$\nu(\text{C}=\text{N})$ and $\nu(\text{C}=\text{C})$	(C-H)	$\nu(\text{Cl}-\text{O})$
L^2	1673(s)	1331(s)	3318(br)	3049(m)	1594(s), 1454(s)	756(s)	-
3.1	1602(s)	1260(s)	3424(br)	-	1541(m), 1458(s)	706(s)	1086(s), 621(s)
3.2	1613(s)	1258(s)	3437(br)	3069(m)	1551(m), 1439(s)	726(s)	1091(s), 622(s)
3.3	1610(s)	1262(s)	3432(br)	-	1566(s), 1456(s)	709(s)	1090(s), 621(s)
3.4	1609(s)	1260(s)	3449(br)	-	1546(s), 1490(s)	726(s)	1090(m), 623(s)
3.5	1612(s)	1257(s)	3394(br)	-	1556(s), 1442(s)	726(s)	1092(s), 622(s)
3.6	1609(s)	1261(s)	3439(br)	-	1541(s), 1438(s)	704(m)	1098(s), 620(s)

^1H and ^{13}C NMR of Zn and Cd Complexes

The ^1H NMR spectra of the zinc and cadmium complexes of L^2 are both highly comparable to their ligand, the slight differences arising in the respective chemical shifts. All protons in the zinc and cadmium complexes are more deshielded in comparison to the free ligand L^2 . This is as expected since there is a greater decrease in electron density around the protons when compared to the protons in the free ligand because of the coordination of nitrogen and sulfur

Chapter 3: Co-ordination Behaviour of a Novel Bisthiourea Tripodal Ligand; Structural, Spectroscopic and Electrochemical properties of a series of Transition Metal Complexes with Binding Studies

donors to the metal centre. Due to the presence of three different aromatic rings, it becomes very difficult to assign the protons range between 7.5 and 8.5 ppm. The two singlets of methylene groups are extremely important when it comes to the binding studies because they are in a clear window in the spectrum and may be easily assigned. Typically, they are shifted to higher frequency when the guest is bound into the cavity and it is a very clear area to follow the addition of a specific guest.

The ^{13}C NMR spectra of L^2 have been shown in (Fig. 4) with its Cd^{II} and Zn^{II} complexes. It is clear that the spectra of Zn^{II} and Cd^{II} are very similar. Such comparison can not be made for L^2 due to the use of different solvent. All ^{13}C NMR spectra reveal the expected eighteen carbon atoms.

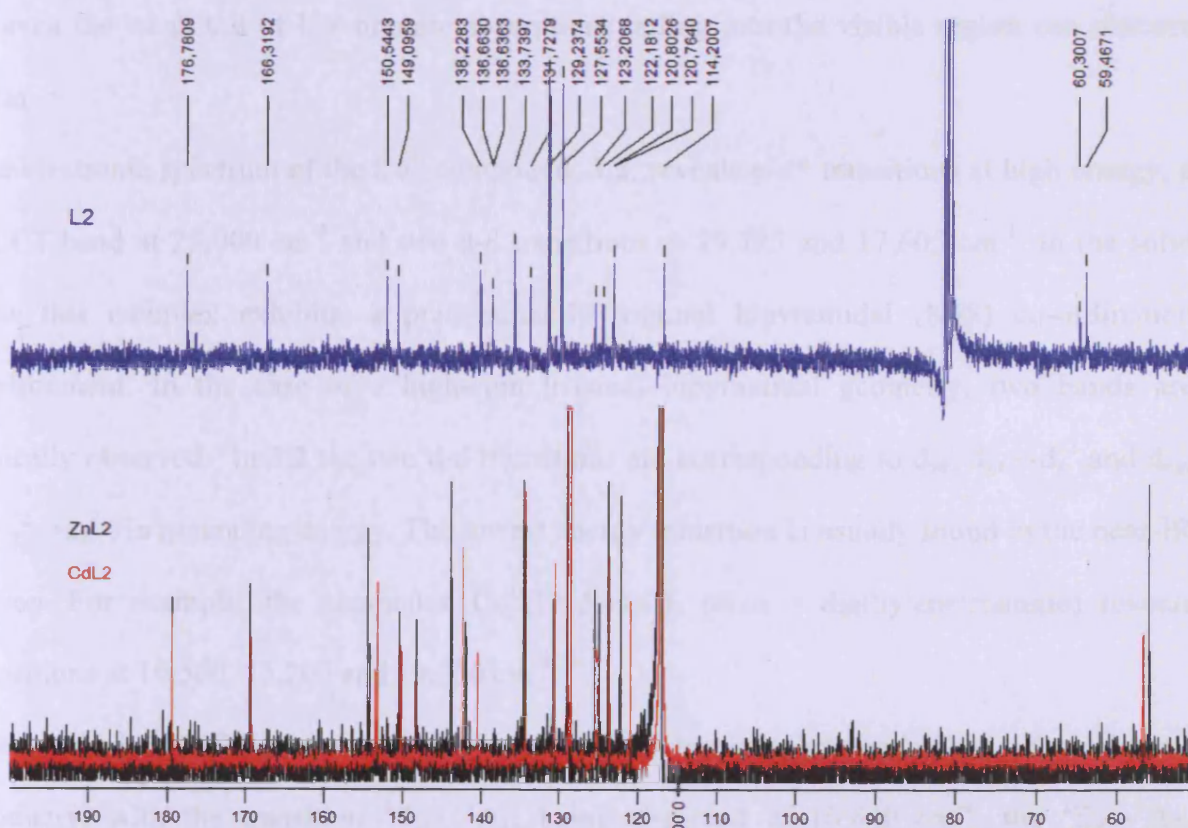


Figure 4: Superimposed ^{13}C NMR spectra of the free ligand L^2 (blue), zinc (black) and cadmium (red) complexes.

Electronic Absorption Spectroscopy

The electronic spectra of L^2 and its complexes have been obtained and the data are presented in (Table 2). The free ligand shows typical $\pi-\pi^*$ transitions at high energy (~ 265 and 310 nm). Similarly, the d^{10} metals, Zn^{2+} and Cd^{2+} , form complexes which also have absorptions at similar energies, though the extinction coefficients of these absorptions are now significantly decreased.

The manganese complex, **3.1**, did not reveal any indication of a d-d transition even in highly concentrated solutions (20 mg/ 5 mL). The molar extinction coefficients for the spin-forbidden d-d transitions of an octahedral Mn^{II} complex are typically in the range 10^{-2} - 10^{-1} $dm^3 mol^{-1} cm^{-1}$. The identification of the d-d bands of a Mn^{II} complex is usually not possible as even the weak tail of UV organic absorptions tailing into the visible region can obscure them.

The electronic spectrum of the Co^{II} compound, **3.2**, reveals $\pi-\pi^*$ transitions at high energy, a MLCT band at $25,000\text{ cm}^{-1}$ and two d-d transitions at $19,725$ and $17,605\text{ cm}^{-1}$. In the solid state this complex exhibits, a predominantly trigonal bipyramidal (N4S) co-ordination environment. In the case of a high-spin trigonal bipyramidal geometry, two bands are typically observed. In **3.2** the two d-d transitions are corresponding to $d_{xz}, d_{yz} \rightarrow d_z^2$ and $d_{xy}, d_x^2-y^2 \rightarrow d_z^2$, in ascending energy. The lowest energy transition is usually found in the near-IR region. For example, the compound $Co^{II}(Et_4dien)Cl_2$ (dien = diethylenetriamine) reveals transitions at $10,500$, $15,200$ and $19,200\text{ cm}^{-1}$.¹⁴

The octahedral $Ni(II)$ compound, **3.3**, gives an electronic spectrum typical of octahedral geometry, with the transition ${}^3T_{2g} \leftarrow {}^3A_{2g}$ being observed at $10,640\text{ cm}^{-1}$, the ${}^1E_g \leftarrow {}^3A_{2g}$ transition at $11,765\text{ cm}^{-1}$ and ${}^3T_{1g}(F) \leftarrow {}^3A_{2g}$ occurring at $18,180\text{ cm}^{-1}$. The final spin allowed

Chapter 3: Co-ordination Behaviour of a Novel Bisthiourea Tripodal Ligand; Structural, Spectroscopic and Electrochemical properties of a series of Transition Metal Complexes with Binding Studies

transition, ${}^3T_{1g}(P) \leftarrow {}^3A_{2g}$, was obscured by a MLCT band at $\sim 26,315 \text{ cm}^{-1}$. Using these assignments yields $\Delta = 10,640 \text{ cm}^{-1}$, $B = 575.8 \text{ cm}^{-1}$ and $\beta = 0.553$. These values are in good agreement with the related mononuclear compound $[\text{Ni}^{\text{II}}(\text{TPA})(\text{NCS})_2] \cdot \text{H}_2\text{O}$ which has a similar absorption profile, containing bands at 11,390, 17,540 and $26,900 \text{ cm}^{-1}$.¹⁵ The Dq and B values for this example were 1,139 and 666 cm^{-1} respectively, from which the nephelauxetic parameter can be calculated as 0.616. Therefore, the co-ordinative bonding in **3.3** evidently has slightly more covalent character which reflects the incorporation of a 'soft' sulfur donor atom within the inner co-ordination sphere.

The electronic spectrum of the five-coordinate Cu^{II} complex, **3.4**, reveals two d-d transitions in the visible region at 12,790 and $16,285 \text{ cm}^{-1}$ (Fig. 5). Both square planar and trigonal bipyramidal Cu^{II} complexes typically present similar absorption patterns with two bands at comparable wavelength. This is the case for the essentially regular trigonal bipyramidal structure $\text{Cu}^{\text{II}}(\text{NH}_3)_2\text{Ag}(\text{SCN})_3$ which exhibits transitions at 12,800 and $14,500 \text{ cm}^{-1}$.¹⁶ Therefore, this is in good agreement with the continuous shape mapping calculations based on the solid state structure of **3.4** which indicate a slightly distorted trigonal bipyramid, albeit with some square planar character.

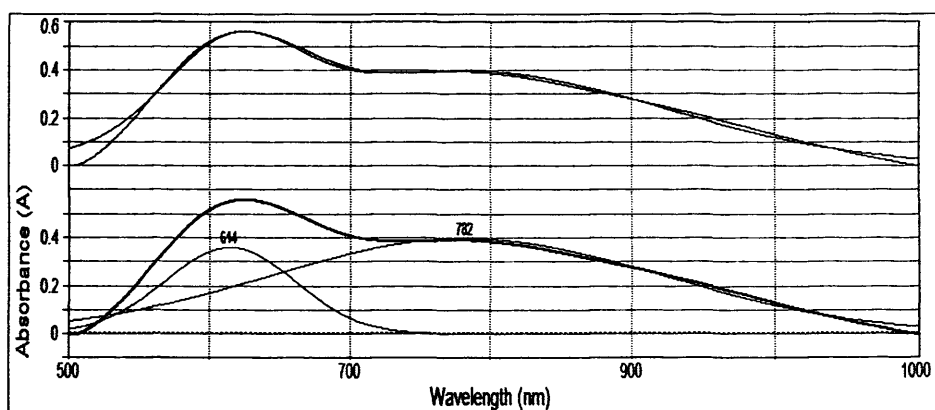


Figure 5: Deconvolution of the electronic spectrum of the Cu^{II} compound, **3.4**. The lower graph contains a trace revealing the individual component peaks, while the upper graph has a trace which reflects the sum curve of these peaks. Both the upper and lower graphs also contain a trace of the raw input data.

Chapter 3: Co-ordination Behaviour of a Novel Bisthiourea Tripodal Ligand; Structural, Spectroscopic and Electrochemical properties of a series of Transition Metal Complexes with Binding Studies

Table 2: Electronic spectral assignments for the ligand and complexes

Compound	π - π^* transitions / λ (nm)	MLCT / λ	d-d transitions / λ (nm)	Δ (cm^{-1}) ^b	B (cm^{-1}) ^b	β
L²	265(50,300),310(28,600)	-	-	-	-	-
3.1	256(17,300),314(10,600)	-	-	-	-	-
3.2	280(33,200), 351(7400)	400(3,100)	507(80), 568 (55)	-	-	-
3.3	323(15,800)	385(1,500)	549(17),849(15), 940(16)	10,640	575.8	0.55
3.4	315(17,000)	-	623(130), 793 (96)	-	-	-
3.5	260(29,200), 321(10,500)	-	-	-	-	-
3.6	260(27,800), 321(9,900)	-	-	-	-	-

Performed in CH₃CN solution at room temperature; Numbers in parentheses indicate molar absorption coefficients ϵ ($\text{M}^{-1}\text{cm}^{-1}$). ^bvalues calculated by assuming an octahedral geometry

Electrochemical Studies

The cyclic voltammogram of the manganese compound, **3.1**, reveals two irreversible reductions in the cathodic region at -1.95 V and -1.70 V referenced against ferrocenium/ferrocene (Fc^+/Fc).

Discrete mononuclear complexes of manganese in a heptacoordinated environment are quite rare, thus only limited comparisons can be drawn. The seven co-ordinate manganese(II) complex

of $\text{N,N,N}'\text{-tris(2-pyridylmethyl)-N}'\text{-(2-salicylideneethyl)ethane-1,2-diamine}$ and

$\text{Mn}^{\text{II}}(\text{pyrdoxTPA})_2$ reveal anodic wave processes at +0.56 V and +0.64 V (*vs* SCE) that is 0.10 V and 0.18 V (*vs* Fc^+/Fc), respectively (Fig. 6).^{17,18} These features have been attributed to the

$\text{Mn}(\text{II/III})$ redox couple. For each of these complexes, no other metal-based redox processes were reported within the bounds of scan window. Interestingly, the voltammogram of compound

3.1 reveals no wave processes in the anodic region and thus no indication of the $\text{Mn}(\text{II/III})$ redox

couple. Without performing more extensive experiments it is difficult to ascribe the cathodic processes as either metal or ligand-based reductions.

Chapter 3: Co-ordination Behaviour of a Novel Bisthiourea Tripodal Ligand; Structural, Spectroscopic and Electrochemical properties of a series of Transition Metal Complexes with Binding Studies

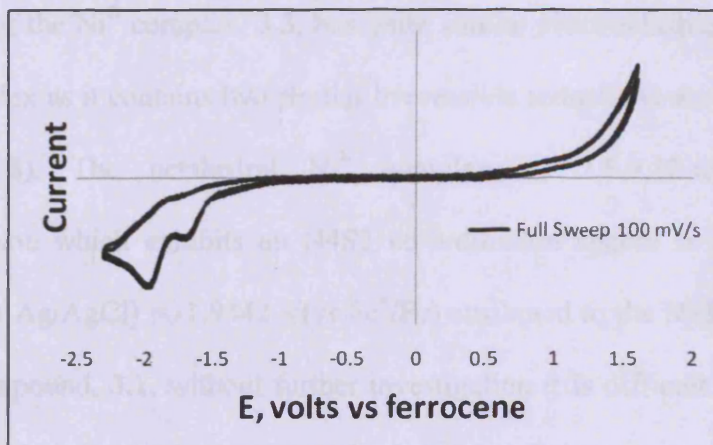


Figure 6: Electro chemistry for 3.1.

The cobalt complex, **3.2**, undergoes a wave process at +0.362 V (vs Fc^+/Fc). Inspection of this isolated feature reveals a linear proportional relationship between i_{pc} and $v^{1/2}$ in the interval 100 – 1000 mVs^{-1} which confirms an ideal diffusion controlled response adhering to the Randles-Sevcik equation.¹⁹ Furthermore, the ratio of i_{pa} to i_{pc} is close to unity, which also supports the reversibility of this process. This feature is most likely attributable to the Co(II/III) redox couple. The mononuclear five co-ordinate complex, $[\text{Co}^{\text{II}}(\text{SMe}_2\text{N}_4(\text{tren}))]^+$, which has a similar co-ordination sphere exhibits a wave process at +0.270 V (vs SCE) (-0.19 V vs Fc^+/Fc) which was also attributed to this process (Fig. 7).²⁰

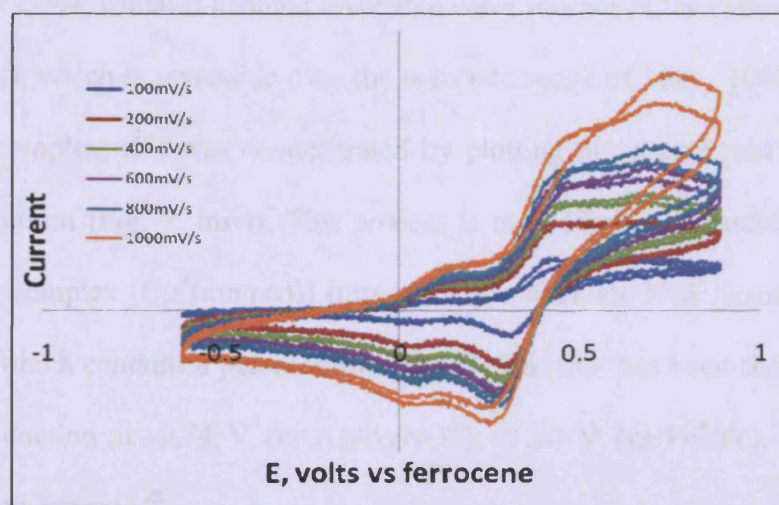


Figure 7: Electrochemistry for 3.2.

Chapter 3: Co-ordination Behaviour of a Novel Bisthiourea Tripodal Ligand; Structural, Spectroscopic and Electrochemical properties of a series of Transition Metal Complexes with Binding Studies

The voltammogram of the Ni^{II} complex, **3.3**, has quite similar electrochemical behaviour to the analogous Mn^{II} complex as it contains two similar irreversible reductions at -1.78 V and -1.37 V (vs Fc⁺/Fc) (Fig. 8). The octahedral Ni^{II} complex of 2,5,9,12-tetramethyl-1,4,8,11-tetraazacyclotetradecane which exhibits an N4S2 co-ordination sphere is reported to have a process at -1.44 V (vs Ag/AgCl) = -1.9442 V (vs Fc⁺/Fc) attributed to the Ni(II/I) redox couple.²¹ As with the Mn^{II} compound, **3.1**, without further investigation it is difficult to assign the exact origins of this feature, but the similar behaviour in the two complexes seems to suggest that the molecular orbital involved is primarily ligand based in nature.

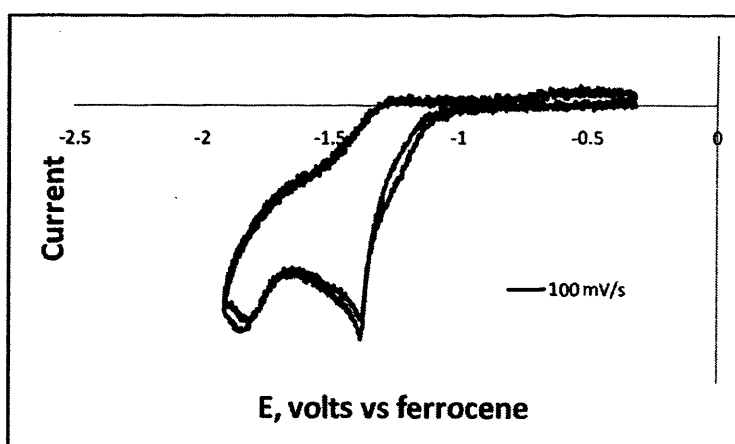


Figure 8: small window of electro chemistry for **3.3**.

The copper complex, **3.4**, contains a single reversible wave process at the cathodic potential of -0.349 V (vs Fc⁺/Fc), which is reversible over the scan rate range of 100 – 1000 mVs⁻¹ (Fig. 9). As with the Co^{II} complex, this was demonstrated by plotting the square root of the scan rate against the peak current (Fig. 9; inset). This process is most likely attributable to the Cu(II/I) redox couple. The complex [Cu^{II}(mmpcd)] (mmpcd = pentadentate N4S ligand with appended pyrazolyl groups) which contains a pentacoordinating N4S ligand has been shown to undergo a quasi-reversible reduction at -0.74 V (vs Ag/AgNO₃); -1.20 V (vs Fc⁺/Fc), which has been attributed to the same process.²²

Chapter 3: Co-ordination Behaviour of a Novel Bisthiourea Tripodal Ligand; Structural, Spectroscopic and Electrochemical properties of a series of Transition Metal Complexes with Binding Studies

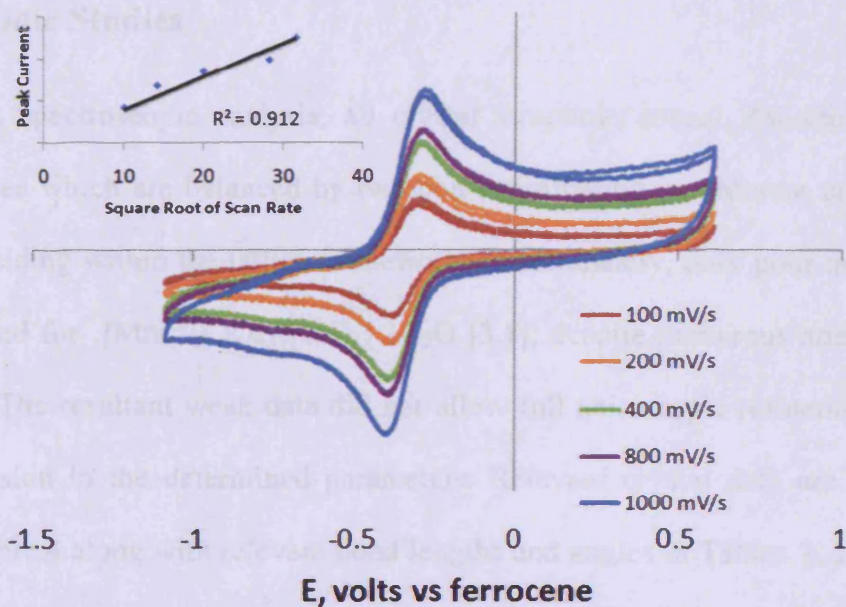


Figure 9: Isolation of the Cu(II/I) redox couple for 3.4.

Table 3: Electrochemical parameters for the redox processes exhibited by complexes 3.1, 3.2, 3.3, and 3.4 in acetonitrile solution (supporting electrolyte: $[\text{Bu}_4\text{N}][\text{PF}_6]$ (0.1 mol dm^{-3}); $T = 20 \text{ }^\circ\text{C}$). Measured at 0.1 Vs^{-1} .

Compound	E_p/V (ΔE , mV) ^{a,b}
3.1	-1.70, -1.95
3.2	+0.362(79)
3.3	-1.37, -1.78
3.4	-0.349(90)

^athe potentials at which reversible processes occur are calculated as the average of the oxidative and reductive peak potentials ($E_p^{\text{ox}} + E_p^{\text{red}}/2$). ^bFor irreversible processes, the anodic or cathodic peak potentials are given. Potentials are given in volts *versus* Ferrocenium/Ferrocene.

Crystallographic Studies

Consistent with spectroscopic analysis, all crystal structures reveal discrete mononuclear dicationic species which are balanced by two non-coordinating perchlorate counterions per formula unit residing within the lattice framework. Unfortunately, only poor quality crystals could be obtained for $[\text{MnL}^2(\text{ClO}_4)][\text{ClO}_4] \cdot 2\text{H}_2\text{O}$ [3.1], despite numerous attempts to grow better crystals. The resultant weak data did not allow full anisotropic refinement leading to the lower precision in the determined parameters. Relevant crystal data are given for all structures in Table 4 along with relevant bond lengths and angles in Tables 7, 10, 13, 15, 17, 19 and 22.

Table 4: Crystal Structure Data for L², 3.1, 3.2, 3.3, 3.4, 3.5 and 3.6

compound	Chemical formula	Colour/shape	Mw, g/mol	Crystal system	Space group	T(K)	a, Å	b, Å	c, Å	α, deg	β, deg	γ, deg	V, Å ³	Z	Observed Reflections	Unique Reflections	R _{int}	R ₁ [I>2σ(I)]	wR ₂ (all data)
L ²	C ₂₄ H ₃₀ N ₄ O ₂ S ₂	white/ plate	646.78	Triclinic	P-1	150(2)	5.7870(10)	15.603(2)	17.042(4)	97.285(5)	96.425(6)	91.148(7)	1515.9(5)	2	2516	1394	0.1388	0.0916	0.1978
3.1	MnC ₃₄ H ₃₂ N ₄ O ₁₂ Cl ₂ S ₂	yellow/ block	936.65	Monoclinic	P2 ₁ /n	150(2)	14.846(3)	11.049(3)	23.882(6)	90	97.313(9)	90	3885.6(16)	4	2818	2541	0.0838	0.2481	0.5138
3.2	CoC ₃₄ H ₃₀ N ₄ O ₁₀ Cl ₂ S ₂	dark brown/ block	904.61	Monoclinic	P2 ₁ /n	150(2)	14.0690(6)	11.8060(4)	22.1260(9)	90	90.400(10)	90	3675.0(2)	4	7889	4307	0.1589	0.0782	0.1912
3.3	NiC ₃₇ H ₃₇ N ₉ O ₁₁ Cl ₂ S ₂	brown/ needle	983.49	Monoclinic	P2 ₁ /n	150(2)	12.6653(6)	18.0877(9)	18.8600(10)	90	96.484(3)	90	4292.9(4)	4	4431	3687	0.0624	0.0939	0.186
3.4	CuC ₃₄ H ₃₀ N ₄ O ₁₀ Cl ₂ S ₂	green/block	909.22	Monoclinic	P2 ₁ /n	150(2)	13.9290(3)	11.8320(2)	22.3070(5)	90	91.2240(10)	90	3675.53(13)	4	8371	5895	0.1136	0.0538	0.1302
3.5	2(C ₁₂ H ₃₀ N ₄ O ₂ S ₂ Zn), C ₂ H ₃ N ₄ (ClO ₄)	colourless/ rectangle	1863.23	Monoclinic	P2 ₁ /c	150(2)	10.4666(10)	42.1309(4)	17.5050(2)	90	91.2101(4)	90	7717.41(14)	4	17709	9711	0.1463	0.0800	0.2425
3.6	CdC ₃₆ H ₃₃ N ₉ O ₁₀ Cl ₂ S ₂	colourless/ block	999.13	Monoclinic	P2 ₁ /n	293(2)	16.4240(3)	10.8230(2)	22.9750(6)	90	97.7600(10)	90	4046.57(15)	4	9235	4804	0.1183	0.0598	0.1465

Crystal Structure of L^2

The bisthiourea ligand crystallises in the triclinic space group P-1. There are two intramolecular hydrogen bonds (Fig. 10) which help establish the molecular conformation of L^2 . Specifically, these interactions occur between the carbonyl oxygen atoms and the amine nitrogen atoms immediately adjacent to the pyridyl groups in the 2-position. These form two six-membered rings which can be observed in each complex discussed herein. Hydrogen bond lengths are 1.901 Å and 1.913 Å and surprisingly, all literature examples of 1-Benzoyl-3-(6-methylpyridin-2-yl)thiourea don't appear to have this intramolecular hydrogen bond shown in (Fig. 10). A comparison of the bond lengths of donor atoms in L^2 and similar ligands are given in (Table 5) and indicating that all bond lengths are typical of organic compounds. Those bonds in general will become shorter when bound to any transition metal due to the co-ordination into the metal centre as we shall see later.

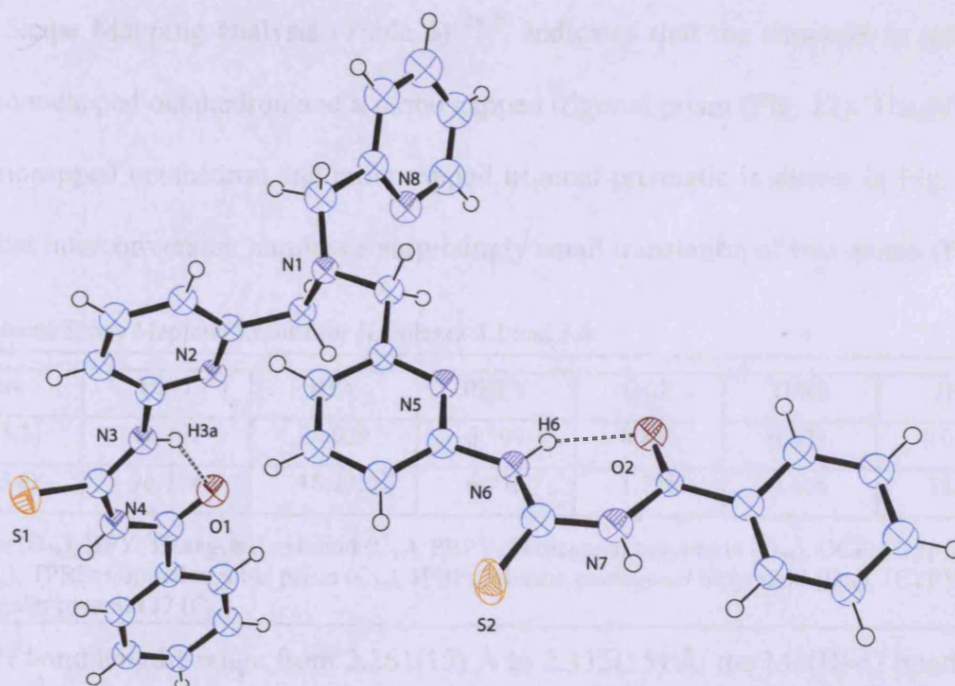


Figure 10: The asymmetric unit of L^2 . Displacement ellipsoids are shown at 50% probability. H atoms are of arbitrary size.

Chapter 3: Co-ordination Behaviour of a Novel Bisthiourea Tripodal Ligand; Structural, Spectroscopic and Electrochemical properties of a series of Transition Metal Complexes with Binding Studies

Table 5: Average bond lengths (°A) of L² in comparison to TPA and other ligand.

Bond/Compound	L ²	TPA	1-Benzoyl-3-(6-methylpyridin-2-yl)thiourea
C-N(Bridge)	1.458	1.437	-
C-N(Pyridyl)	1.333	1.343	1.335
C=O	1.236	-	1.205
C=S	1.672	-	1.661

Refcodes for the structures used are listed in reference²³

Crystal Structure of [Mn^{II}(L²)(ClO₄)] [ClO₄].2(H₂O) (3.1)

Crystallographic data for this complex are listed in Tables 4 and 7. The manganese compound crystallises in the monoclinic space group P2₁/n and contains one complex within the asymmetric unit (asu). The Mn^{II} ion is seven co-ordinate and is surrounded by three types of donor atoms: four nitrogen donors (N1, N2, N5 and N8), two sulfur donors (S1 and S2) and a single oxygen donor (O3) located on a perchlorate counterion within the lattice framework. This complex is unique amongst the first row transition metals of complexes in that the metal ion is situated at the centre of a slightly distorted capped trigonal prismatic co-ordination geometry. Continuous Shape Mapping analysis (Table 6)²⁴⁻²⁹ indicates that the structure is intermediate between a monocapped octahedron and a mono capped trigonal prism (Fig. 12). The relationship between monocapped octahedron and monocapped trigonal prismatic is shown in Fig. 13 which also shows that interconversion requires a surprisingly small translation of two atoms (Fig. 13).³⁰

Table 6: Continuous Shape Mapping Results for complexes 3.1 and 3.6.

Structure	HP-7	HPY	PBPY	OCF	TPRS	JPBP
L ² _Mn (3.1)	35.142	20.029	6.509	0.831	0.671	10.339
L ² _Cd (3.6)	36.154	18.225	6.776	1.726	0.606	11.475

HP-7: Heptagon (D_{7h}), HPY: Hexagonal pyramid (C_{6v}), PBPY: Pentagonal bipyramid (D_{5h}), OCF: Capped octahedron (C_{3v}), TPRS: Capped trigonal prism (C_{2v}), JPBP: Johnson pentagonal bipyramid (D_{5h}), JETPY: Johnson elongated triangular pyramid J7 (C_{3v}).

The Mn(II)-N bond lengths range from 2.261(15) Å to 2.335(15) Å, the Mn(II)-O bond length is longer at 2.508(17) Å. This is the first example of a complex in which a Mn(II) cation is surrounded by this particular donor set, however the co-ordinative bond lengths are typical. The

Chapter 3: Co-ordination Behaviour of a Novel Bisthiourea Tripodal Ligand; Structural, Spectroscopic and Electrochemical properties of a series of Transition Metal Complexes with Binding Studies

nitrogen donors N1, N2, N5 and N8 display very similar values to those in several other manganese complexes involving similar TPA frameworks. For example, the compound [Mn(tpa)(η^1 -NO₃)(η^2 -NO₃)] exhibits co-ordinating pyridine groups with distances ranging from 2.262(1) Å to 2.319(1) Å (while Mn(II)-O bond distances range from 2.171(2) Å to 3.175(1) Å).³¹ The Mn-S bond lengths in 3.1 are typically longer, 2.527(16) Å and 2.560(12) Å but are very similar to the value found in [Mn(bis(4-N-ethyl thiosemicarbazone)-2,6-diacetylpyridine)(H₂O)₂][CH₃COO]₂, reported by Pedrido *et al.*, at 2.6285(10) Å.³² Finally, a water molecule can be observed hydrogen bonding between the two pendant benzoyl thiourea groups. Both benzoyl thiourea groups cyclise through hydrogen bonding (N6-H6 \cdots O2 and N3-H3a \cdots O1) and the remaining NH groups hydrogen bond to the water molecule (N4-H4a \cdots O11 and N7-H7 \cdots O11) (Table 8).



Chapter 3: Co-ordination Behaviour of a Novel Bisthiourea Tripodal Ligand; Structural, Spectroscopic and Electrochemical properties of a series of Transition Metal Complexes with Binding Studies

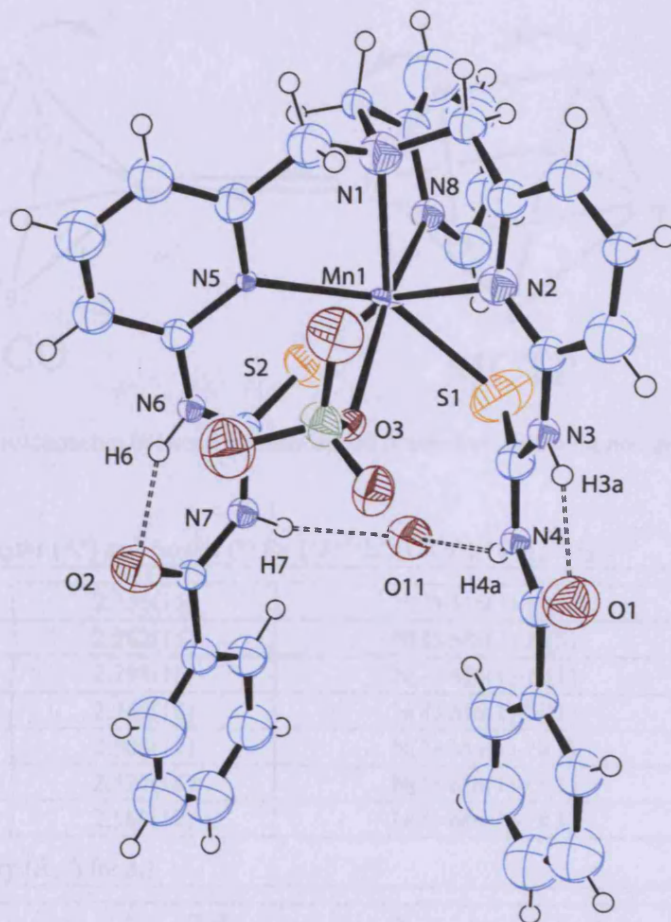


Figure 11: The asymmetric unit of **3.1**. Displacement ellipsoids are shown at 50% probability. H atoms are of arbitrary size. H-bonds are represented by dashed lines.

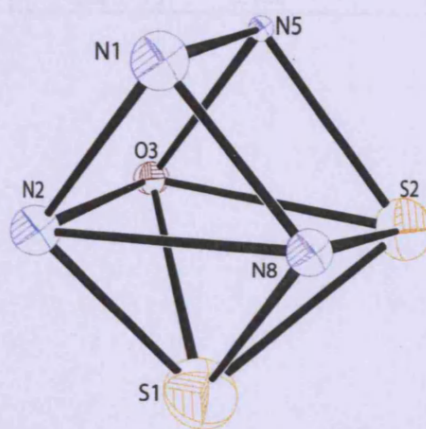


Figure 12: A view of the core geometry of **3.1** of covalent bond radius less than 3 Å.

Chapter 3: Co-ordination Behaviour of a Novel Bisthiourea Tripodal Ligand; Structural, Spectroscopic and Electrochemical properties of a series of Transition Metal Complexes with Binding Studies

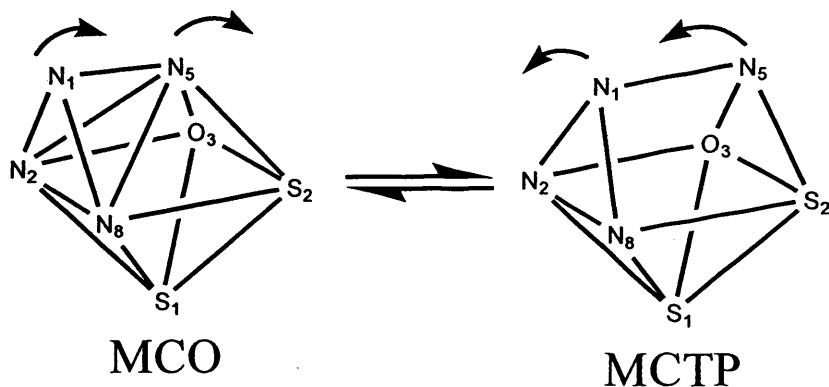


Figure 13: Structural relationship between a monocapped octahedron and a monocapped trigonal prism.

Table 7: Relevant Bond lengths (Å) and Angles (°) for $[\text{Mn}^{\text{II}}(\text{L}^2)(\text{ClO}_4)][\text{ClO}_4] \cdot 2\text{H}_2\text{O}$

N(1)-Mn(1)	2.335(15)	N(2)-Mn(1)-N(5)	117.7(6)
N(2)-Mn(1)	2.262(15)	N(8)-Mn(1)-N(5)	116.5(6)
N(5)-Mn(1)	2.298(16)	N(2)-Mn(1)-N(1)	74.9(5)
N(8)-Mn(1)	2.269(16)	N(8)-Mn(1)-N(1)	72.3(6)
O(3)-Mn(1)	2.508(17)	N(5)-Mn(1)-N(1)	75.2(5)
S(1)-Mn(1)	2.527(16)	N(2)-Mn(1)-O(3)	79.6(6)
S(2)-Mn(1)	2.560(12)	N(8)-Mn(1)-O(3)	166.3(6)

Table 8: H-bonding geometry (Å, °) for 3.1

D-H...A	D-H	H...A	D...A	D-H...A
N3-H3A ...O1	0.88	1.924	2.618	134.63
N4-H4A ...O11	0.88	2.313	3.115	151.61
N6-H6...O2	0.88	1.907	2.648	140.88
N7-H7...O11	0.88	2.160	2.977	154.04

Crystal Structure of $[\text{Co}^{\text{II}}(\text{L}^2)][\text{ClO}_4]_2$ (3.2)

The cobalt compound crystallises in the monoclinic space group $P2_1/n$ and contains one complex within the asu (Fig. 14). In an identical fashion to the analogous Cu^{II} (3.4) and Zn^{II} (3.5) complexes, the Co^{II} ion is co-ordinated by four N-donors and one S donor (Fig. 15) in what is best described as a trigonal bipyramidal co-ordination geometry, with $S(\text{TBPY})$, $S(\text{SPY})$ and $S(\text{JTBP})$ values of 2.300, 4.982 and 3.685 respectively (Table 9).

Table 9: Continuous Shape Mapping Results for 3.2, 3.4 and 3.5.

Structure	(PP)	(VOC)	(TBPY)	(SPY)	(JSPY)	(JTBP)
L^2_{Co} (3.2)	33.308	7.072	2.300	4.982	7.072	3.685
L^2_{Cu} (3.4)	32.959	5.574	1.749	3.914	5.574	3.906
L^2_{Zn} (3.5)	32.380	6.592	2.454	4.595	6.592	3.754

PP: Pentagon (D_{5h}), VOC: Vacant octahedron (C_{4v}), TBPY: Trigonal bipyramid (D_{3h}), SPY: Square pyramid (C_{4v}), JSPY: Johnson square pyramid (C_{4v}), JTBP: Johnson trigonal bipyramid (D_{3h}).

The co-ordinative pyridyl nitrogens (N2, N5 and N8) occupy the equatorial positions and their bond lengths range from 2.051(4) Å to 2.086(4) Å whereas the axial positions are occupied by N1 and S1 are 2.147(4) Å and 2.3170(14) Å respectively; Table 10). This feature is identical to those observed for other Co(II) trigonal bipyramidal complexes. For example, the four nitrogen donors in the compound $[\text{Co}(\text{TPA})\text{Cl}][\text{ClO}_4]$, range between 2.046(6) and 2.184(6) Å.³³ Similarly, the four nitrogen donor bond lengths in $[(\text{F}_8\text{TPP})\text{Fe}^{\text{III}}-(\text{O}^{2-})-\text{Co}(\text{TMPA})]^+$ are 2.176(6) Å for bridge-head nitrogen and 2.064(5) Å for the pyridyl donors.³⁴ The Co(II)-S bond length is quite typical when compared to complexes with similar donors sets; for instance the complex [1,5-bis(2-pyridylmethyl)-1,5-diazacyclooctane $\text{Co}(\text{S}-\text{C}_6\text{H}_4\text{-p-CH}_3)[\text{BPh}_4]$ has a Co(II)-S bond length of 2.2670(12) Å.³⁵ The cationic character of the complex is balanced by two perchlorate counterions, one of which is involved in the H-bonding interaction N7-H7...O8. Other hydrogen bond interactions can be observed between the two arms i.e. N4-H4a...O2. Finally, as is the case

Chapter 3: Co-ordination Behaviour of a Novel Bisthiourea Tripodal Ligand; Structural, Spectroscopic and Electrochemical properties of a series of Transition Metal Complexes with Binding Studies

in all the structures of this ligand, each arm is involved in intramolecular hydrogen bonding forming a six-membered ring. (Fig. 16; Table 11).

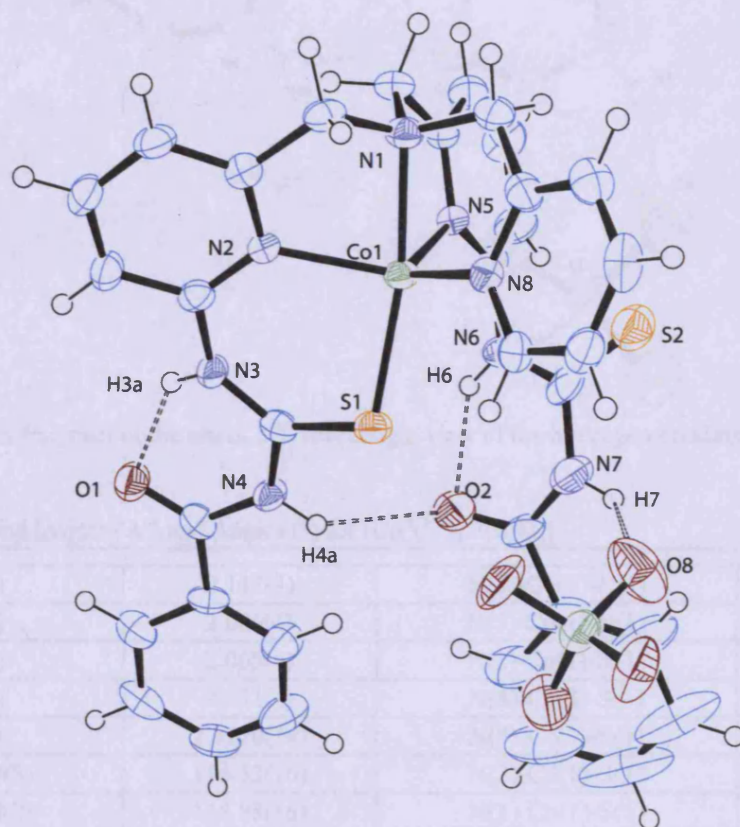


Figure 14: The asymmetric unit of **3.2**. Displacement ellipsoids are shown at 50% probability. H atoms are of arbitrary size. H-bonds are represented by dashed lines.

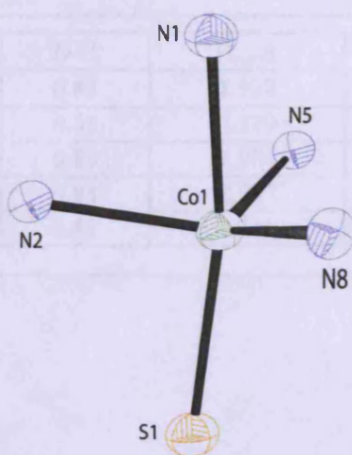


Figure 15: A view of the core geometry of **3.2**.

Chapter 3: Co-ordination Behaviour of a Novel Bisthiourea Tripodal Ligand; Structural, Spectroscopic and Electrochemical properties of a series of Transition Metal Complexes with Binding Studies

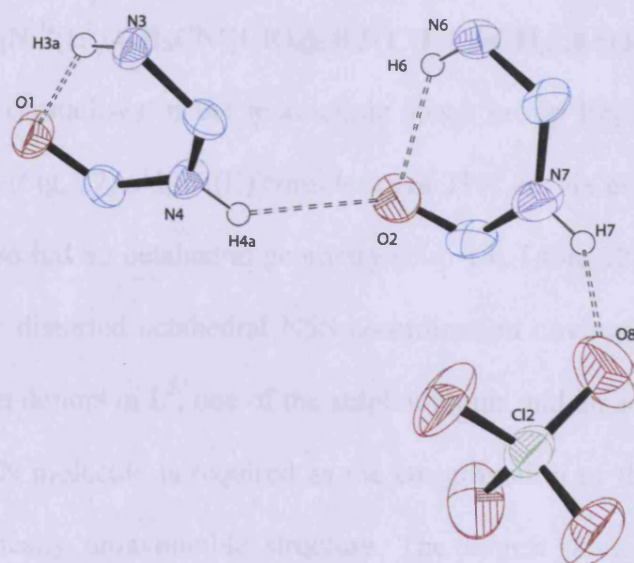


Figure 16: A fragment of the asu of 3.2, revealing a view of the hydrogen bonding interactions.

Table 10: Relevant Bond lengths (Å) and Angles (°) for $[\text{Co}^{\text{II}}(\text{L}^2)]_2[\text{ClO}_4]$

N(1)-Co(1)	2.147(4)	N(8)-Co(1)-N(1)	78.33(16)
N(2)-Co(1)	2.086(4)	N(5)-Co(1)-N(1)	78.39(15)
N(5)-Co(1)	2.065(4)	N(2)-Co(1)-N(1)	78.67(15)
N(8)-Co(1)	2.051(4)	N(8)-Co(1)-S(1)	99.42(12)
S(1)-Co(1)	2.3170(14)	N(5)-Co(1)-S(1)	114.08(12)
N(8)-Co(1)-N(5)	116.53(16)	N(2)-Co(1)-S(1)	91.04(12)
N(8)-Co(1)-N(2)	118.88(16)	N(1)-Co(1)-S(1)	166.45(11)
N(5)-Co(1)-N(2)	112.89(15)		

Table 11: H-bonding geometry (Å, °) for 3.2

D-H...A	D-H	H...A	D...A	D-H...A
N3-H3A ...O1	0.88	1.928	2.636	136.32
N4-H4A ...O2	0.88	2.379	3.115	141.34
N6-H6...O2	0.88	1.984	2.667	133.47
N6-H6...O3	0.88	2.507	3.023	118.09
N7-H7...O8	0.88	2.318	3.058	141.74

Chapter 3: Co-ordination Behaviour of a Novel Bisthiourea Tripodal Ligand; Structural, Spectroscopic and Electrochemical properties of a series of Transition Metal Complexes with Binding Studies

Crystal Structure of $[\text{Ni}^{\text{II}}(\text{L}^2)\cdot\text{CH}_3\text{CN}][\text{ClO}_4]_2\cdot 0.5(\text{CH}_3\text{COCH}_3)\cdot 0.5(\text{H}_2\text{O})$ (3.3)

The nickel compound crystallises in the monoclinic space group $P2_1/n$ and contains a single complex within the asu (Fig. 17). All Ni(II) complexes of TPA are six co-ordinate, and typical of Ni(II), this complex also has an octahedral geometry (Fig. 18; Table 12). The Ni^{II} cation lies at the centre of a slightly distorted octahedral N5S co-ordination environment. The donor atoms consist of the 4 nitrogen donors in L^2 , one of the sulphur atoms and an additional CH_3CN donor. Presumably, the CH_3CN molecule is required as the co-ordination of the second sulphur atom would result in a sterically unfavourable structure. The largest deviations to the octahedral geometry can be seen in the angles N8-Ni1-N2 [157.47(16) Å] and N1-Ni1-N2 [75.9(2) Å] where significant distortions from the classical 180° and 90° angles, respectively, can be observed (Table 13).

Table 12: Continuous Shape Mapping Results for complex 3.3.

Structure	(HP-6)	(PPY-6)	(OC-6)	(TPR-6)	(JPPY-6)
$\text{L}^2\text{-Ni}$ (3.3)	29.789	23.186	1.600	13.283	26.645

HP: Hexagon (D_{6h}), PPY: Pentagonal pyramid (C_{5v}), OC: Octahedron (O_h), TP: Trigonal Pyramidal (D_{3h}), JPPY: Johnson's pentagonal pyramid J2 (C_{5v}).

The $\text{Ni}^{\text{II}}\text{-N}$ co-ordinative bond lengths range from 2.050(4) Å to 2.237(4) Å, and the $\text{Ni}^{\text{II}}\text{-S}$ bond length is significantly longer at 2.345(3) Å. These values are quite similar compared to those of related compounds. For instance, the compound, $[\text{Ni}^{\text{II}}(\text{TPA})(\text{NCS})_2]$ reported by Randeniya and Norman exhibits co-ordinative bond lengths which range between 2.04(5) Å and 2.122(4) Å.³⁶ Two perchlorate counterions also reside within the asu, one of which is involved in H-bonding with nitrogen atoms N4 and N7 (Fig. 19; Table 14).

Chapter 3: Co-ordination Behaviour of a Novel Bisthiourea Tripodal Ligand; Structural, Spectroscopic and Electrochemical properties of a series of Transition Metal Complexes with Binding Studies

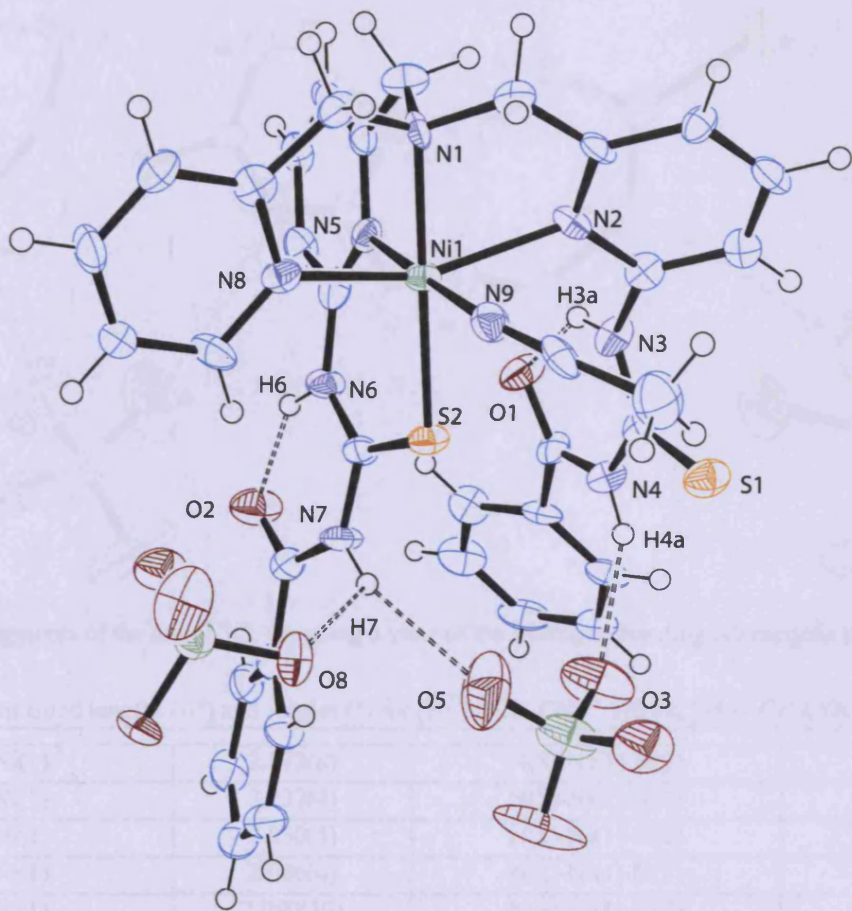


Figure 17: The asymmetric unit of 3.3. Displacement ellipsoids are shown at 50% probability. H atoms are of arbitrary size.

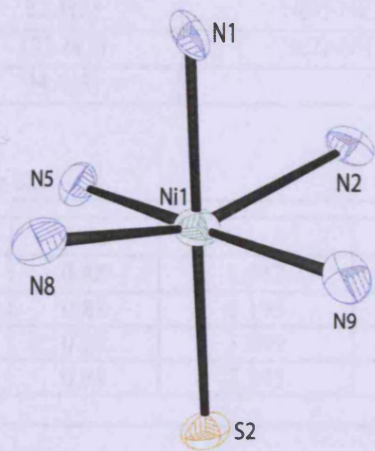


Figure 18: A view of the core geometry of 3.3.

Chapter 3: Co-ordination Behaviour of a Novel Bisthiourea Tripodal Ligand; Structural, Spectroscopic and Electrochemical properties of a series of Transition Metal Complexes with Binding Studies

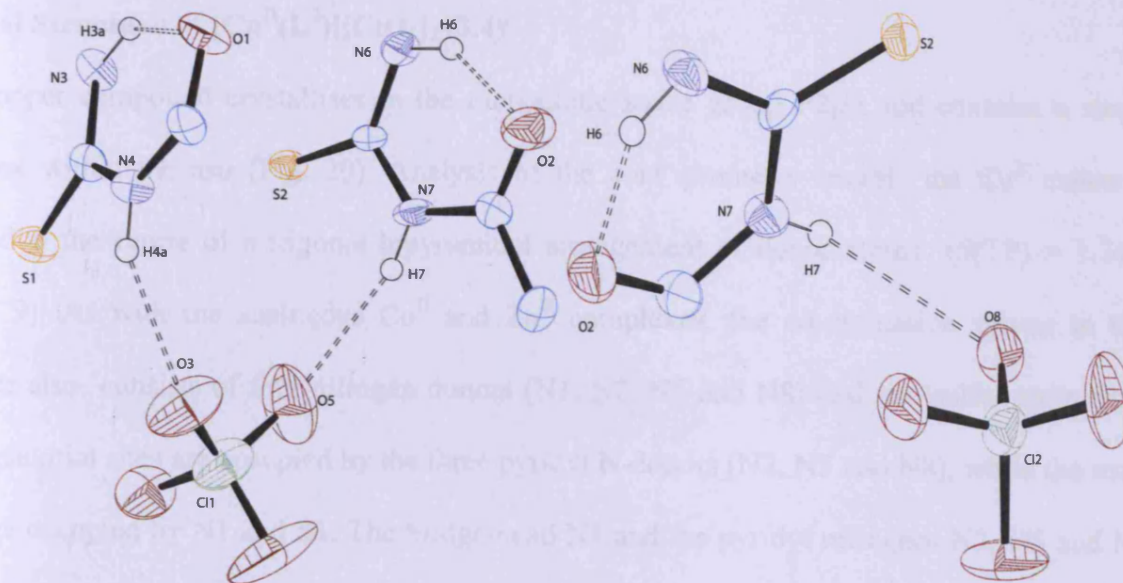


Figure 19: fragments of the asu of **3.3**, revealing a view of the hydrogen bonding interactions (dashed lines).

Table 13: Relevant Bond lengths (Å) and Angles (°) for $[\text{Ni}^{\text{II}}\text{L}^2 \cdot \text{CH}_3\text{CN}]^{2+} \cdot 2[\text{ClO}_4^-] \cdot \text{H}_2\text{O} \cdot \text{CH}_3\text{COCH}_3$

N(1)-Ni(1)	2.072(8)	N(8)-Ni(1)-N(9)	94.0(3)
N(2)-Ni(1)	2.237(4)	N(5)-Ni(1)-N(2)	95.07(14)
N(5)-Ni(1)	2.050(4)	N(1)-Ni(1)-N(2)	75.9(2)
N(8)-Ni(1)	2.086(4)	N(8)-Ni(1)-N(2)	157.47(16)
N(9)-Ni(1)	2.090(10)	N(9)-Ni(1)-N(2)	82.7(3)
S(2)-Ni(1)	2.345(3)	N(5)-Ni(1)-S(2)	94.15(13)
N(5)-Ni(1)-N(1)	85.9(3)	N(1)-Ni(1)-S(2)	179.8(3)
N(5)-Ni(1)-N(8)	88.44(15)	N(8)-Ni(1)-S(2)	98.01(13)
N(1)-Ni(1)-N(8)	82.1(2)	N(9)-Ni(1)-S(2)	85.6(2)
N(5)-Ni(1)-N(9)	177.6(3)	N(2)-Ni(1)-S(2)	103.90(13)
N(1)-Ni(1)-N(9)	94.4(3)		

Table 14: H-bonding geometry (Å, °) for **3.3**

D-H...A	D-H	H...A	D...A	D-H...A
N3-H3A ... O1	0.88	1.912	2.618	136.08
N4-H4A ... O3	0.88	2.195	3.014	154.78
N6-H6...O2	0.88	1.809	2.570	143.44
N7-H7...O5	0.88	2.343	3.171	156.93

Crystal Structure of [Cu^{II}(L²)](ClO₄)₂ (3.4)

The copper compound crystallises in the monoclinic space group P2₁/n and contains a single complex within the asu (Fig. 20). Analysis of the core geometry reveals the Cu^{II} cation is situated at the centre of a trigonal bipyramidal arrangement of donor atoms ($S(TP) = 1.749$) (Table 9). As with the analogous Co^{II} and Zn^{II} complexes, the co-ordination sphere in this instance also consists of four nitrogen donors (N1, N2, N5 and N8) and one sulfur atom (S1). The equatorial sites are occupied by the three pyridyl N-donors (N2, N5 and N8), while the axial sites are occupied by N1 and S1. The bridge-head N1 and the pyridyl nitrogens N2, N5 and N8 are typical with bond lengths ranging from 2.018(3) Å to 2.148(3) Å. The sulphur bond is significantly longer at 2.2605(9) Å (Table 15). A related compound [Cu^{II}(TPA)₂S₂](ClO₄)₂[Et₂O], also exhibits a trigonal bipyramidal co-ordination environment and contains very similar bond lengths and angles ranging between 2.048(6) Å and 2.280(2) Å.³⁷ There is an intermolecular H-bonding interaction between one of the two perchlorate counterions and the nitrogen atom N7 (Fig. 22; Table 16). In addition, there are intra-molecular hydrogen bonds within each of the two thiourea arms (N3-H3a[⋯]O1), (N6-H6[⋯]O2) and between the two arms (N4-H4a[⋯]O2).

Chapter 3: Co-ordination Behaviour of a Novel Bisthiourea Tripodal Ligand; Structural, Spectroscopic and Electrochemical properties of a series of Transition Metal Complexes with Binding Studies

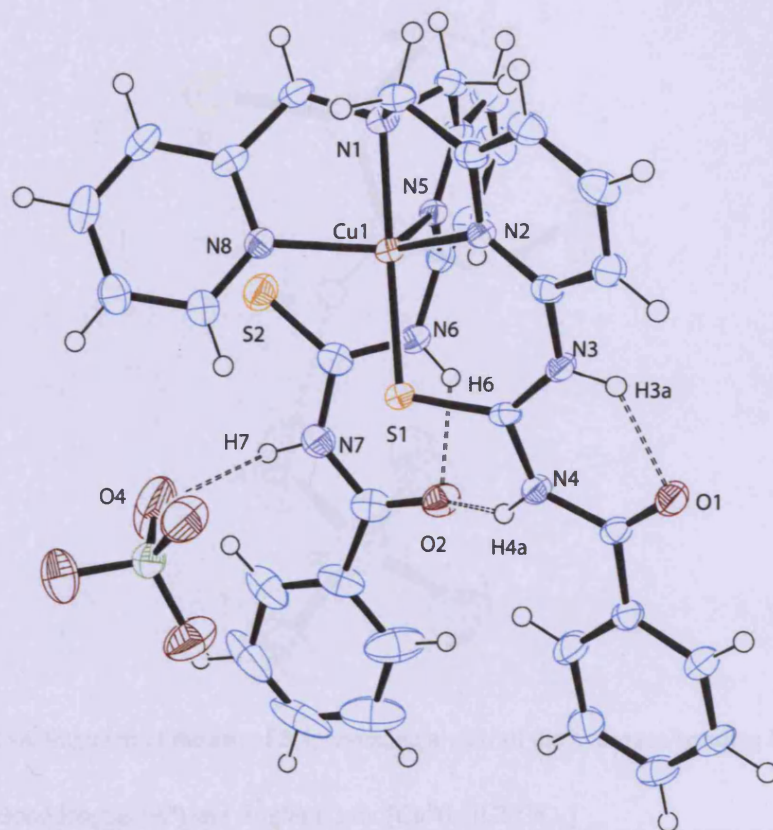


Figure 20: The asymmetric unit of **3.4** and the core geometry. Displacement ellipsoids are shown at 50% probability. H atoms are of arbitrary size.

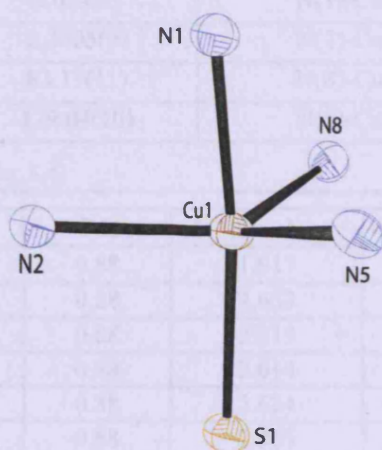


Figure 21: A view of the core geometry of **3.4**.

Chapter 3: Co-ordination Behaviour of a Novel Bisthiourea Tripodal Ligand; Structural, Spectroscopic and Electrochemical properties of a series of Transition Metal Complexes with Binding Studies

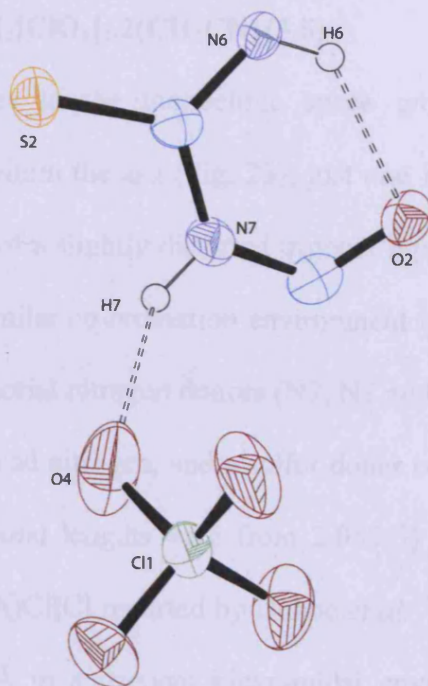


Figure 22: A fragment of the asu of 3.4, revealing a view of the hydrogen bonding interaction.

Table 15: Relevant Bond lengths (Å) and Angles (°) for $[\text{Cu}^{\text{II}}(\text{L}^2)] \cdot 2[\text{ClO}_4]$

N(1)-Cu(1)	2.018(3)	N(1)-Cu(1)-N(5)	80.11(10)
N(2)-Cu(1)	2.030(2)	N(2)-Cu(1)-N(5)	113.57(10)
N(5)-Cu(1)	2.148(3)	N(8)-Cu(1)-N(5)	111.11(10)
N(8)-Cu(1)	2.034(3)	N(1)-Cu(1)-S(1)	172.88(8)
S(1)-Cu(1)	2.2605(9)	N(2)-Cu(1)-S(1)	92.79(8)
N(1)-Cu(1)-N(8)	83.17(11)	N(8)-Cu(1)-S(1)	97.24(8)
N(2)-Cu(1)-N(8)	129.04(10)	N(5)-Cu(1)-S(1)	106.23(7)

Table 16: H-bonding geometry (Å, °) for 3.4

D-H...A	D-H	H...A	D...A	D-H...A
N3-H3A ...O1	0.88	1.917	2.620	135.75
N3-H3A ...O10	0.88	2.653	3.173	118.88
N4-H4A...O2	0.88	2.311	3.084	146.67
N6-H6...O2	0.88	2.014	2.686	132.24
N6-H6...O7	0.88	2.624	3.141	118.50
N7-H7...O4	0.88	2.365	3.083	138.93

Crystal Structure of $[\text{Zn}^{\text{II}}(\text{L}^2)]_2[\text{ClO}_4]_2 \cdot 2(\text{CH}_3\text{CN})$ (3.5)

The zinc compound crystallises in the monoclinic space group $P2_1/c$ and contains two structurally similar complexes within the asu (Fig. 23); just one is discussed. In both instances the Zn^{II} cation lies at the centre of a slightly distorted trigonal bipyramid geometry ($S(\text{TBPY}) = 2.454$; Table 9) and reveals a similar co-ordination environment to the analogous Co^{II} and Cu^{II} complexes. There are three equatorial nitrogen donors (N2, N3 and N4) which are located on the pyridyl groups with the bridge-head nitrogen, and a sulfur donor occupying axial positions (Fig. 24). The $\text{Zn}^{\text{II}}\text{-N}$ co-ordinative bond lengths vary from 2.058(5) Å to 2.181(5) Å (Table 17) similar to the compound $[\text{Zn}(\text{TPA})\text{Cl}]\text{Cl}$ reported by Duboc *et al.*³⁸ where the Zn-N bonds range from 2.062(2) Å to 2.2744(8) Å in a trigonal bipyramidal environment. The axial position occupied by S2 has a longer bond at 2.3716(15) but is similar to $[\text{Zn}(\text{mmpcd})\text{ClO}_4]$ which has a Zn(II)-S bond length of 2.294(1) Å.^{22, 39} Hydrogen bond interactions are again observed as intra-molecular (Fig. 25; Table 18), within each of the two thiourea arms (N5-H5a...O1) and N7-H7...O2) and an intermolecular bound to the perchlorate counter ion (N5-H5a...O7).

Chapter 3: Co-ordination Behaviour of a Novel Bisthiourea Tripodal Ligand; Structural, Spectroscopic and Electrochemical properties of a series of Transition Metal Complexes with Binding Studies

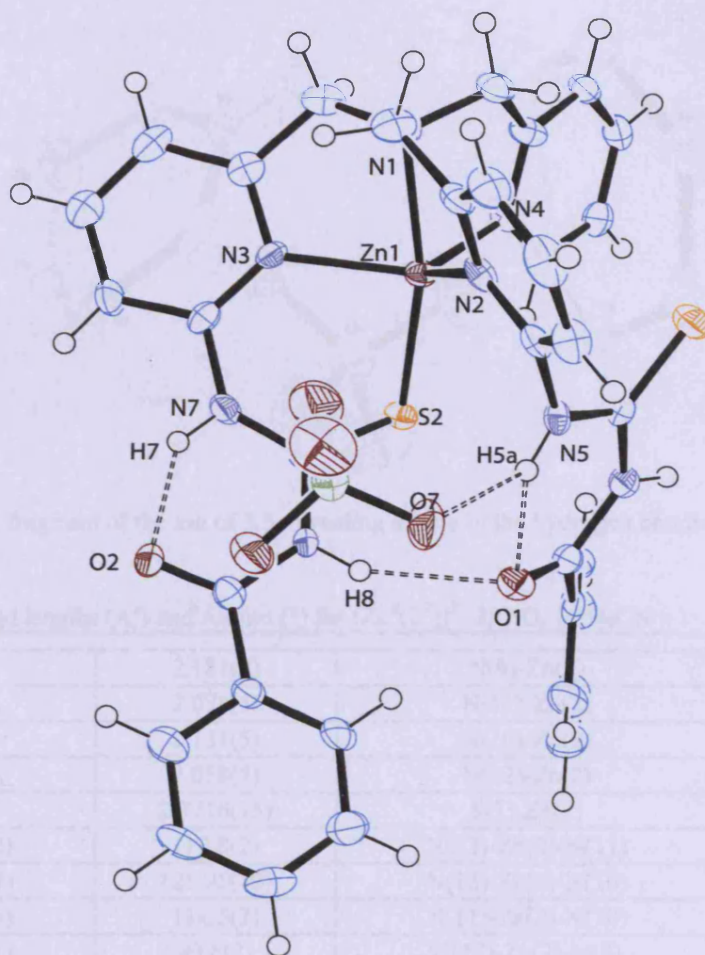


Figure 23: A fragment of 3.5. Displacement ellipsoids are shown at 50% probability. H atoms are of arbitrary size.



Figure 24: A view of the core geometry of 3.5.

Chapter 3: Co-ordination Behaviour of a Novel Bisthiourea Tripodal Ligand; Structural, Spectroscopic and Electrochemical properties of a series of Transition Metal Complexes with Binding Studies

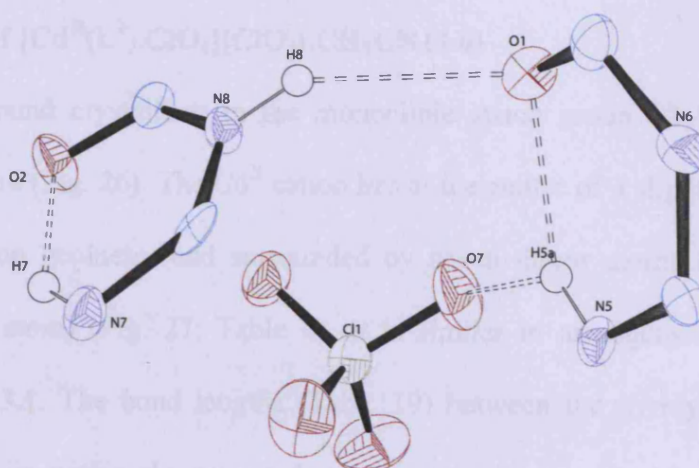


Figure 25: A fragment of the asu of 3.5, revealing a view of the hydrogen bonding interactions

Table 17: Relevant Bond lengths (Å) and Angles (°) for $[\text{Zn}^{\text{II}}(\text{L}^2)]^{2+} \cdot 2[\text{ClO}_4^-] \cdot \text{CH}_3\text{CN}$

N(1)-Zn(1)	2.181(5)	N(9)-Zn(2)	2.163(5)
N(2)-Zn(1)	2.078(5)	N(11)-Zn(2)	2.066(5)
N(3)-Zn(1)	2.131(5)	N(10)-Zn(2)	2.134(5)
N(4)-Zn(1)	2.058(5)	N(12)-Zn(2)	2.054(5)
S(2)-Zn(1)	2.3716(15)	S(3)-Zn(2)	2.3653(17)
N(4)-Zn(1)-N(2)	113.8(2)	N(12)-Zn(2)-N(11)	111.5(2)
N(4)-Zn(1)-N(3)	121.05(19)	N(12)-Zn(2)-N(10)	122.8(2)
N(2)-Zn(1)-N(3)	114.5(2)	N(11)-Zn(2)-N(10)	115.0(2)
N(4)-Zn(1)-N(1)	80.6(2)	N(12)-Zn(2)-N(9)	79.3(2)
N(2)-Zn(1)-N(1)	79.3(2)	N(11)-Zn(2)-N(9)	79.8(2)
N(3)-Zn(1)-N(1)	77.16(19)	N(10)-Zn(2)-N(9)	78.1(2)
N(4)-Zn(1)-S(2)	99.70(14)	N(12)-Zn(2)-S(3)	99.24(16)
N(2)-Zn(1)-S(2)	114.35(14)	N(11)-Zn(2)-S(3)	115.22(15)
N(3)-Zn(1)-S(2)	89.42(13)	N(10)-Zn(2)-S(3)	89.58(15)
N(1)-Zn(1)-S(2)	164.19(15)	N(9)-Zn(2)-S(3)	163.92(15)

Table 18: H-bonding geometry (Å, °) for 3.5.

D-H...A	D-H	H...A	D...A	D-H...A
N5-H5A ...O1	0.88	2.01	2.688	133
N5-H5A ...O7	0.88	2.33	2.981	130
N7-H7...O2	0.88	1.85	2.588	141
N8-H8...O1	0.88	2.26	3.040	148
N13-H13A...O3	0.88	1.91	2.625	138
N14-H14A...O4	0.88	2.23	3.013	148
N15-H15...O4	0.88	1.96	2.636	133
N15-H15...O9	0.88	2.32	2.951	129
N16-H16...O14	0.88	2.10	2.954	162

Crystal Structure of $[\text{Cd}^{\text{II}}(\text{L}^2)\cdot\text{ClO}_4][\text{ClO}_4]\cdot\text{CH}_3\text{CN}$ (3.6)

The cadmium compound crystallises in the monoclinic space group $P2_1/n$ and contains one complex within the asu (Fig. 26). The Cd^{II} cation lies at the centre of a slightly distorted trigonal prismatic co-ordination geometry and surrounded by seven donor atoms (four N atoms, two sulphurs and one O atom) (Fig. 27; Table 6). It is similar in arrangement to the analogous manganese complex 3.1. The bond lengths (Table 19) between the pyridyl N-donors and the central Cd(II) cation lie within the expected ranges on comparison to similar complexes, for example the compound synthesised by Tarulli *et al.* which comprises of three pyridyl-units arranged around a cadmium centre. This example has (pyridyl)-N-Cd(II) bond lengths which vary from 2.354(4) Å to 2.402(4) Å. A further similarity is the Cd(II)-S bond lengths of 2.6041(14) Å and 2.7875(15) Å.⁴⁰ The compound $[\text{Cd}(\text{TMPA})_2](\text{ClO}_4)_2$ toluene (TMPA= tris[(2-pyridyl)methyl]amine) reported by Bebout *et al.* shows similar bond length of the bridging N1 ranging between 2.281(7) Å and 2.576(11) Å.⁴¹ In the structure, one perchlorate counter ion is hydrogen bonded in the ligand cavity via two NH groups (Table 20) and again intramolecular hydrogen bonding occurs within the thiourea units forming six membered ring (Fig. 28) and causing sulphurs to be pointed towards the cadmium ion.

Chapter 3: Co-ordination Behaviour of a Novel Bisthiourea Tripodal Ligand; Structural, Spectroscopic and Electrochemical properties of a series of Transition Metal Complexes with Binding Studies

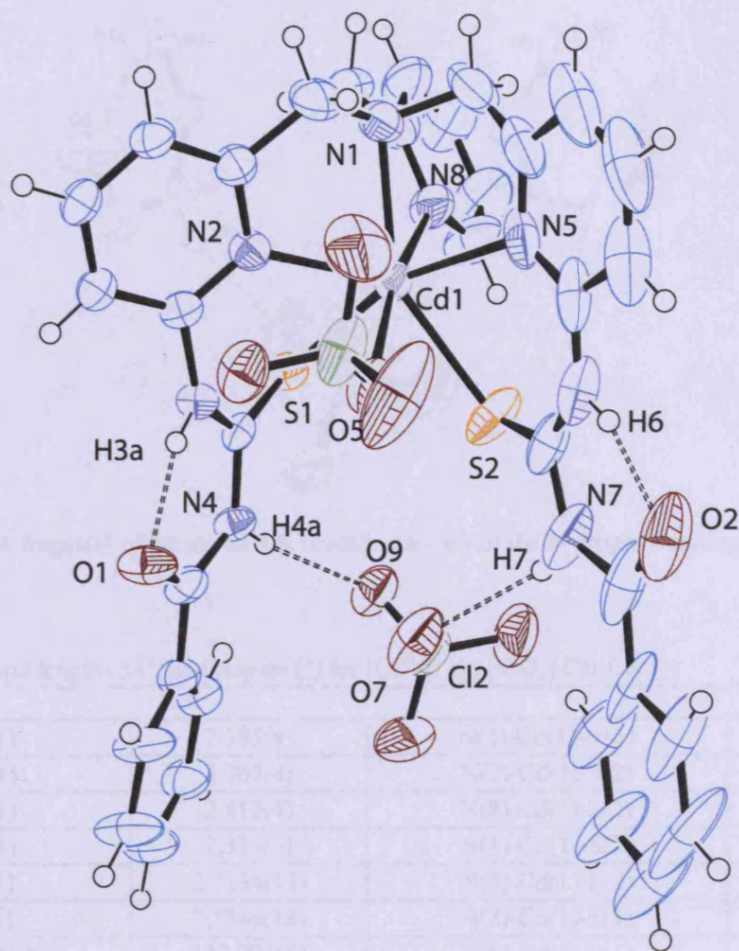


Figure 26: The asymmetric unit of 3.6. Displacement ellipsoids are shown at 50% probability. H atoms are of arbitrary size.

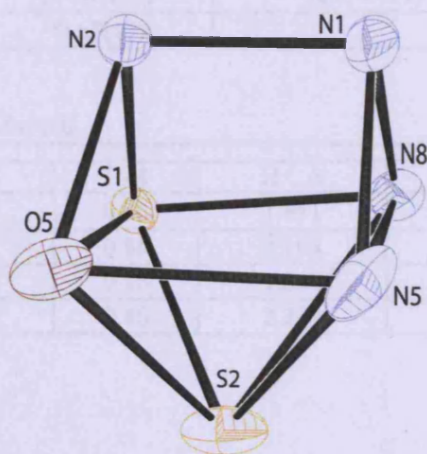


Figure 27: A view of the core geometry of 3.6 of covalent bond radius less than 3 Å.

Chapter 3: Co-ordination Behaviour of a Novel Bisthiourea Tripodal Ligand; Structural, Spectroscopic and Electrochemical properties of a series of Transition Metal Complexes with Binding Studies

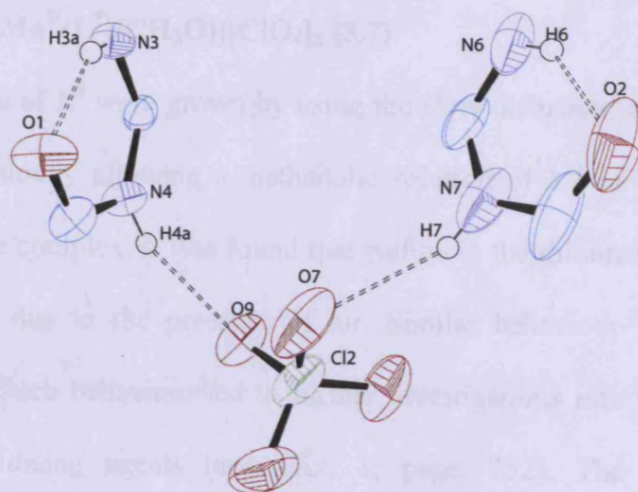


Figure 28: A fragment of the asu of 3.5, revealing a view of the hydrogen bonding interactions

Table 19: Relevant Bond lengths (Å) and Angles (°) for $[Cd^{II}(L^2)] \cdot 2[ClO_4] \cdot CH_3CN$

N(1)-Cd(1)	2.385(4)	N(1)-Cd(1)-N(5)	74.18(18)
N(2)-Cd(1)	2.367(4)	N(2)-Cd(1)-S(2)	138.59(11)
N(5)-Cd(1)	2.412(4)	N(8)-Cd(1)-S(2)	94.93(12)
N(8)-Cd(1)	2.377(5)	N(1)-Cd(1)-S(2)	148.18(11)
S(1)-Cd(1)	2.7134(13)	N(5)-Cd(1)-S(2)	81.08(14)
S(2)-Cd(1)	2.5746(14)	N(2)-Cd(1)-S(1)	78.54(9)
N(2)-Cd(1)-N(8)	117.77(15)	N(8)-Cd(1)-S(1)	82.94(11)
N(2)-Cd(1)-N(1)	71.48(14)	N(1)-Cd(1)-S(1)	122.62(13)
N(8)-Cd(1)-N(1)	70.37(17)	N(5)-Cd(1)-S(1)	162.38(14)
N(2)-Cd(1)-N(5)	114.61(14)	S(2)-Cd(1)-S(1)	81.33(4)
N(8)-Cd(1)-N(5)	99.68(17)		

Table 20: H-bonding geometry (Å, °) for 3.6

D-H...A	D-H	H...A	D...A	D-H...A
N3-H3A ...O1	0.86	1.841	2.560	139.95
N4-H4A ...O9	0.86	2.196	3.018	159.69
N6-H6...O2	0.86	1.856	2.597	143.28
N7-H7...O7	0.86	2.320	3.092	149.52

Crystal Structure of $[\text{Mn}^{\text{II}}(\text{L}^*)(\text{CH}_3\text{O})][\text{ClO}_4]_2$ (3.7)

All previous six crystals of L^2 were grown by using the slow diffusion of ether into solution of acetonitrile. However, slowly allowing a methanolic solution of 3.1 to evaporate result in an interesting change to the complex. It was found that sulfurs in the thiourea arm were oxidised to give ureas most likely due to the presence of air. Similar behaviour is observed for ZnL^1 (chapter: 2; page: 15). Such behaviour led to further investigations into the preparation of the urea ligands using oxidising agents (appendix: 1; page: 232). The manganese structure crystallizes from CH_3OH in the monoclinic space group P2_1 . Crystal data details are listed in (Table 21) and significant bond lengths and angles are compiled in (Table 22). The structure, core geometry and hydrogen bonds interactions are presented in (Fig 29,30 and 31) respectively. The geometry of 3.7, exhibits different arrangement in comparison to the analogous 3.1, it can best be described as a pentagonal bipyramid (Table 24) because the N1, N2, N5, O2, O3 donor set are suitable for the formation of a pentagonal plane but with sulphur, as in 3.1, the long M-S bonds are too big to form a pentagon and therefore, the donors come out of the plane (Diagram 1).

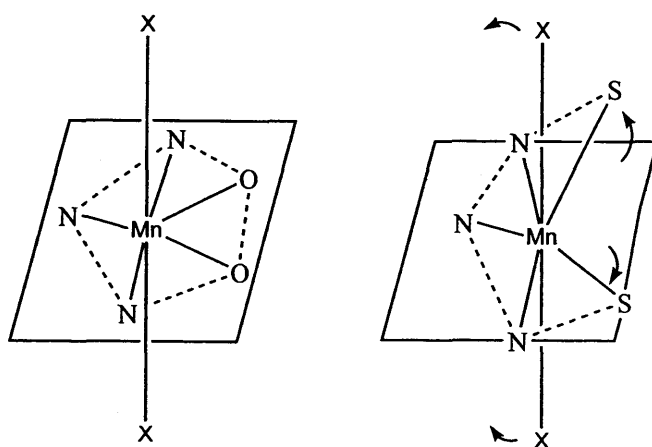


Diagram 1: A comparison between the geometry of 3.1 (left) and 3.7 (right).

Chapter 3: Co-ordination Behaviour of a Novel Bisthiourea Tripodal Ligand; Structural, Spectroscopic and Electrochemical properties of a series of Transition Metal Complexes with Binding Studies

The manganese is surrounded by two types of donor atoms (N and O). It is not unusual for Mn to be surrounded by 4N and 3O and there are 74 published structures of this particular donor set according to the CCDC, 21 of them are approximately pentagonal bipyramidal. The hepta-coordinated compound [Mn(H₃tris(6-hydroxymethyl-2-pyridylmethyl) amine)]Cl₂ published by Guisado-barrios *et al.* reveals similar Mn-N bond length range between 2.269(4) Å and 2.251(4) Å, another similarity comes from Mn-O bond length at 2.251(4) Å.⁴² Hydrogen bond interaction involves two NH of ureas in both arms which hold the perchlorate nicely in the cavity, hydrogen bond lengths and angles are presented in (Table 23).

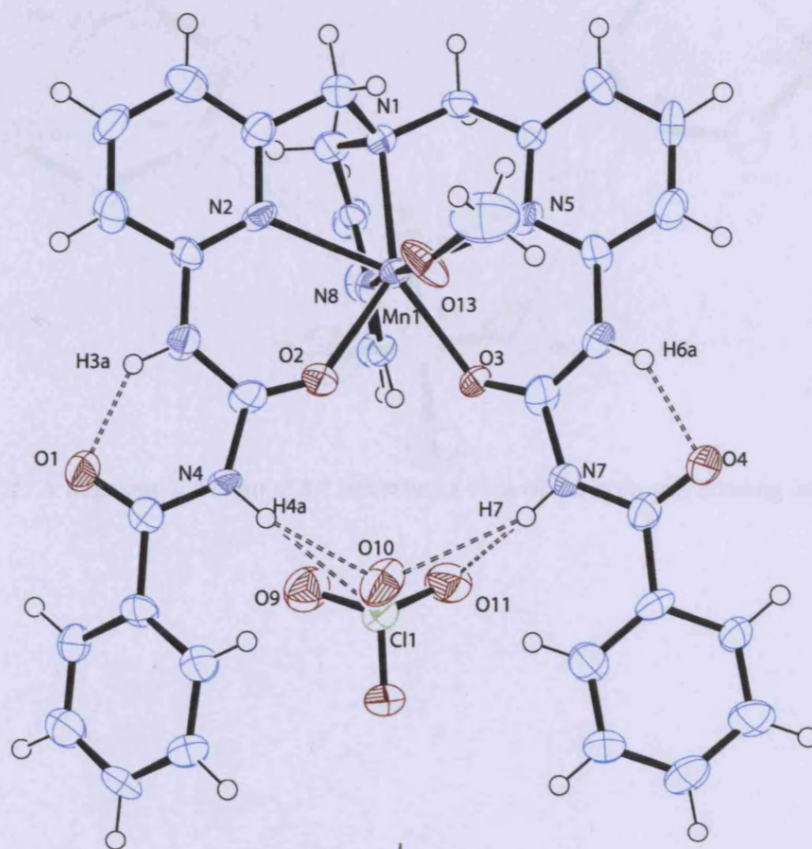


Figure 29: The asymmetric unit of 3.7. Displacement ellipsoids are shown at 50% probability. H atoms are of arbitrary size.

Chapter 3: Co-ordination Behaviour of a Novel Bisthiourea Tripodal Ligand; Structural, Spectroscopic and Electrochemical properties of a series of Transition Metal Complexes with Binding Studies

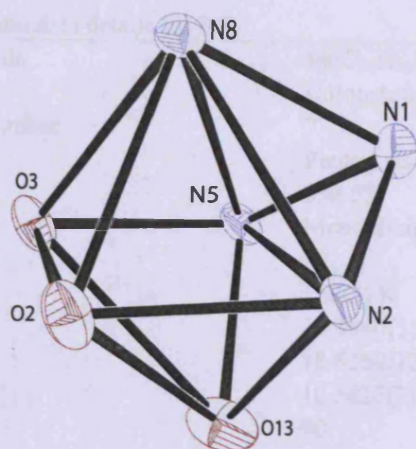


Figure 30: A view of the core geometry of 3.7 of covalent bond radius less than 3 Å.

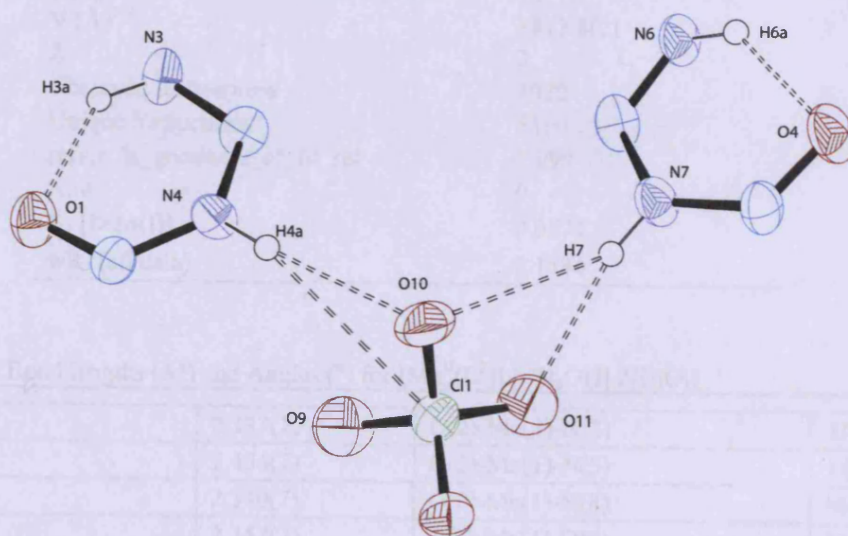


Figure 31: A fragment of the asu of 3.7, revealing a view of the hydrogen bonding interaction.

Chapter 3: Co-ordination Behaviour of a Novel Bisthiourea Tripodal Ligand; Structural, Spectroscopic and Electrochemical properties of a series of Transition Metal Complexes with Binding Studies

Table 21: crystal data details for 3.7

Chemical formula	MnC ₃₅ H ₃₃ N ₈ Cl ₂ O ₁₃
Colour/shape	Colourless/ plate
Coordination number	7
Geometry	Pentagonal bipyramid
Mw, (g/mol)	899.53
Crystal system	Monoclinic
Space group	P2 ₁
T(K)	150(2) K
a (Å)	10.3840(5)
b (Å)	18.6250(12)
c (Å)	10.5820(7)
α (Å)	90
β (Å)	113.785(3)
γ (Å)	90
V (Å) ³	1872.8(2)
Z	2
Observed Reflections	4020
Unique Reflections	5390
refine_ls_goodness_of_fit_ref	1.099
Rint	0
R ₁ [I>2σ(I)]	0.0874
wR ₂ (all data)	0.1594

Table 22: Relevant Bond lengths (Å) and Angles (°) for [Mn^{II}(L²)]·[CH₃OH]·2[ClO₄]

Mn(1)-N(1)	2.333(7)	O(2)-Mn(1)-N(2)	73.8(2)
Mn(1)-N(2)	2.454(7)	O(2)-Mn(1)-N(5)	144.3(2)
Mn(1)-N(5)	2.340(7)	O(2)-Mn(1)-N(8)	96.8(3)
Mn(1)-N(8)	2.247(7)	O(2)-Mn(1)-O(3)	75.2(2)
Mn(1)-O(2)	2.184(6)	O(2)-Mn(1)-O(13)	82.8(2)
Mn(1)-O(3)	2.228(6)	O(3)-Mn(1)-N(1)	138.7(2)
Mn(1)-O(13)	2.212(7)	O(3)-Mn(1)-N(2)	149.0(2)
N(1)-Mn(1)-N(2)	70.8(2)	O(3)-Mn(1)-N(5)	75.0(2)
N(1)-Mn(1)-N(5)	73.8(2)	O(3)-Mn(1)-N(8)	85.0(2)
N(5)-Mn(1)-N(2)	133.5(3)	O(13)-Mn(1)-N(1)	107.4(3)
N(8)-Mn(1)-N(1)	74.4(3)	O(13)-Mn(1)-N(2)	83.6(3)
N(8)-Mn(1)-N(2)	98.6(2)	O(13)-Mn(1)-N(5)	79.3(2)
N(8)-Mn(1)-N(5)	99.8(2)	O(13)-Mn(1)-N(8)	177.5(3)
O(2)-Mn(1)-N(1)	141.6(2)	O(13)-Mn(1)-O(3)	92.5(3)

Chapter 3: Co-ordination Behaviour of a Novel Bisthiourea Tripodal Ligand; Structural, Spectroscopic and Electrochemical properties of a series of Transition Metal Complexes with Binding Studies

Table 23: H-bonding geometry (Å, °) for 3.7

D-H...A	D-H	H...A	D...A	D-H...A
N3-H3A ...O1	0.88	1.876	2.60	138.25
N4-H4A ...O10	0.88	2.168	3.012	160.49
N6-H6A...O4	0.88	1.928	2.617	133.95
N7-H7...O11	0.88	2.303	3.086	148.28
N7-H7...O4	0.88	2.596	3.389	150.43
N7-H7...Cl1	0.88	2.989	3.856	169.21

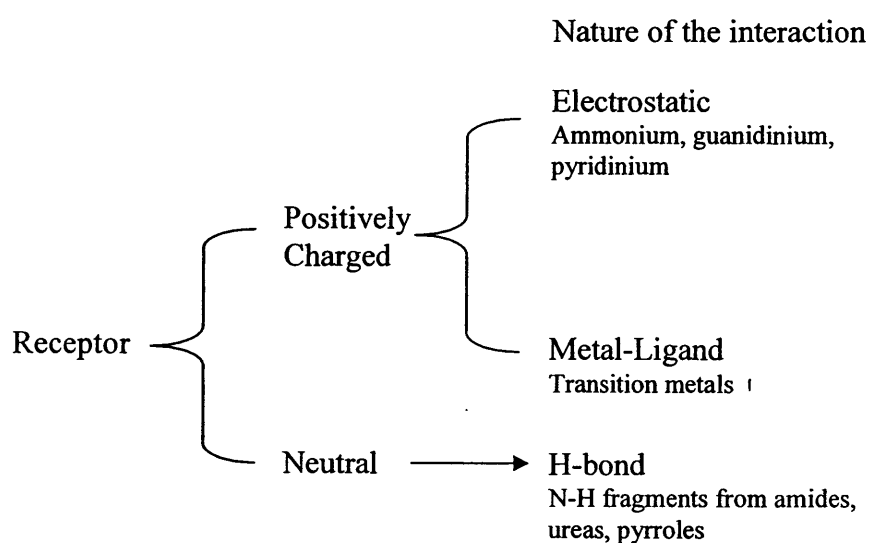
Table 24: Continuous Shape Mapping Results for complex 3.7.

Structure	HP-7	HPY	PBPY	OCF	TPRS	JPBP	JETPY
L ² _Mn	32.448	20.976	2.209	3.639	2.435	5.377	19.880

HP-7: Heptagon (D_{7h}), HPY: Hexagonal pyramid (C_{6v}), PBPY: Pentagonal bipyramid (D_{5h}), OCF: Capped octahedron (C_{3v}), TPRS: Capped trigonal prism (C_{2v}), JPBP: Johnson pentagonal bipyramid (D_{5h}), JETPY: Johnson elongated triangular pyramid J7 (C_{3v}).

Binding studies

Anions play key roles in chemical and biological processes. It is of great importance to detect anionic pollutants such as phosphates and nitrates in ground and waste water. Consequently, it is highly desirable to obtain anion binders which would be characterized by high binding constants and selectivity to perhaps extract these anions.⁴³ This demand has fueled research in the field of anion sensing during the last 20 years, which has resulted in numerous publications which have been reviewed.⁴⁴⁻⁵⁰ These anion receptors vary considerably and can be organometallic, organic-metallocene, porphyrin or just organic frameworks. Receptors may be positively charged, or they may be neutral. In that case, they should interact with the anion through hydrogen bonding and should contain H-bond donor groups, essentially NH fragments from amides⁵¹⁻⁵⁵, urea^{54, 56-60} and thioureas.⁶¹⁻⁶³ The classification of anion receptors on the basis of the nature of the interaction is summarised in (Scheme 1).⁶⁴



Scheme 1. Electrical state of anion receptors and nature of the receptor–anion interaction.

Chapter 3: Co-ordination Behaviour of a Novel Bisthiourea Tripodal Ligand; Structural, Spectroscopic and Electrochemical properties of a series of Transition Metal Complexes with Binding Studies

However, the use of transition metal ions to assemble hydrogen bonding anion receptors has received much less attention. The use of metal complexes may potentially allow not only electrostatic interactions but also hydrogen bonding interactions when co-ordination about a metal centre will template the formation of a cavity capable of anion binding. In addition, changing the co-ordinated metal may change the binding ability of the ligand potentially making a one ligand selective for different anions depending on the cation present. Thus, the often simple act of co-ordination can result in the formation of highly organised and complex systems. The formation of a C_3 anion binding cavity with units capable of acting as hydrogen bond donors to anions with C_3 symmetry is the main class of metal assembled anion receptors. These cavities have been shown to bind a large range of different anions and can discriminate between ions.⁶⁵⁻⁶⁷

When building artificial metal based receptors for tetrahedral anions such as SO_4^{2-} , ClO_4^- or PO_4^{3-} , as with the design of any supramolecular host system, consideration should be given to the size and shape of the targeted anion and that has been taken into consideration when L^2 and L^3 were first prepared. Molecules containing N-H fragments behave as H-bond donors toward anions and are widely used as receptors for recognition and sensing purposes in less polar solvents such as $CHCl_3$, CH_3CN and DMSO to avoid the competition for the anion by the solvent such as H_2O provided that it ensures solubility of the host as well as the guest. As this is a hot topic of chemistry, it has been considered widely by researchers and there are numerous examples of metal or non-metal based receptor that can selectively bind halide⁶⁸⁻⁷¹, amino acids^{72, 73} and oxyanions.^{9, 45} For example, Beer and his group have developed a calixarene (Fig. 32) that bound F^- with an association constant of $1330 M^{-1}$ compared with $172 M^{-1}$ for Cl^- . Since this bis-calix[4]arene is comprised of the lower rim of one calixarene

Chapter 3: Co-ordination Behaviour of a Novel Bisthiourea Tripodal Ligand; Structural, Spectroscopic and Electrochemical properties of a series of Transition Metal Complexes with Binding Studies

covalently linked to the upper rim of another calixarene by two amide groups, the cavity was too small for chloride, phosphate and sulphate but was a very good match for F^- .⁷⁴

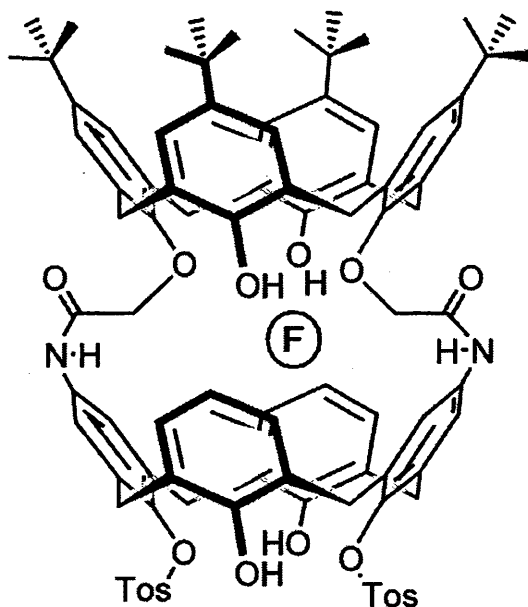
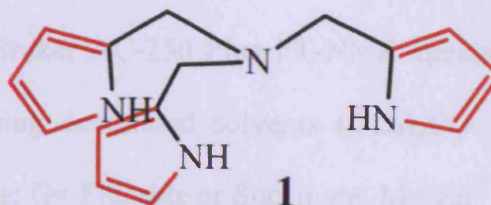


Figure 32: a bis-calx[4]arene selectively bound fluoride.

Stability constant, binding constant and association constant are synonymous for one concept which can be obtained by various methods. One method is via an 1H NMR titration, analysing the data by the HypNMR or WinEQ programmes as explained in chapter 1.^{75, 76} Another example is made by Yin and co-workers and it shows great affinity for fluoride and phosphate of 187 and 240 M^{-1} respectively. While it shows weaker interaction with Cl^- and $H_2SO_4^-$ (Table 25).⁷⁷

Chapter 3: Co-ordination Behaviour of a Novel Bisthiourea Tripodal Ligand; Structural, Spectroscopic and Electrochemical properties of a series of Transition Metal Complexes with Binding Studies

Table 25: Association constants (K_a) of **1** with anions in DMSO.



Anions	K_a (M^{-1})
F^-	187
$H_2PO_4^-$	240
Cl^-	29
HSO_4^-	< 10

It should also be noted, that of all anions, it is typically F^- which displays the strongest guest-host binding; a feature no doubt caused by the strength of the X-H...F hydrogen bond. As such we might expect relatively strong binding of F^- with our host, L^2 .

The ligand L^2 has two arms bearing thiourea groups. Thus, it is possible for this host to bind anions in a 1:1 or perhaps 2:1 fashion, depending on the size of guest, its shape and its solubility. The reaction can be monitored through the variation of the chemical shift of CH_2 protons (methylene groups). Fluoride and succinate was selected due to the diversity in size, shape and electric charge and was expected to be suitable to bind into L^2 , ZnL^2 and CdL^2 .

Experimental

¹H NMR spectra were measured on a Bruker AC-250 Plus FT-NMR spectrometer. All the titration experiments were recorded using deuterated solvents (CD₃)₂CO for (L²-G) and CD₃CN for (ML²-G) in room temperature; G= Fluoride or Succinate; M= Zn^{II} or Cd^{II}.

- 1- In an NMR tube was added 1 mL of (CD₃)₂CO or CD₃CN containing 0.01 mmol of host.
- 2- A stock solution was made of 1 mL of (CD₃)₂CO or CD₃CN contains 0.01 mmol of host with 0.08 mmol of Bu₄N⁺F⁻ or (Bu₄N⁺)₂ succinate⁻².
- 3- 0.05 mL of guest solution was added each time and the H¹ NMR were measured. Each addition of 0.05 mL by micropipette contains 0.004 mmol of guest. Overall, after 20 additions the final ratio of host to guest will be 1:8. Note that the concentration of host remains constant at all times.
- 4- By following the variation of the chemical shift of some protons (methylene groups), a graph can be plotted between concentration of guest against chemical shift (Fig. 33).
- 5- Calculating the stability constant using WinEQNMR, HypNMR or Origin programmes.^{75, 76, 78}

Results and Discussion

It is always recommended in such studies to use less polar solvents such as CDCl_3 , due to the competitive hydrogen bonding polar solvents would provide. However, the solubility of reactants is the main point here. In the ^1H NMR spectrum of L^2 and ML^2 , there are two well-resolved signals due to 2 CH_2 and 1 CH_2 protons and both are affected in a similar manner (i.e. downfield shifted) in the ^1H NMR titration with anions (Fig. 33). The change in chemical shifts of the methylene protons was used to determine the association constants (K_a) in presence of anions such as fluoride and succinate (as a tetrabutyl ammonium salt) at various concentrations but constant temperature (25°C). In a typical titration, a 1 mL solution of (fluoride or succinate) anion (concentration range from 0.0038 to 0.04 M; i.e. 0.05 mL at a time) was added to a 1 mL of the receptor solution (L^2 or ML^2) (0.01 M). Acetone- d_6 was used in the case of L^2 , whereas CD_3CN in the case of ML^2 ($\text{M} = \text{Zn}$ or Cd). On each addition the mixture was allowed to equilibrate and the NMR spectrum was recorded. Significant changes in the chemical shift of the methylene protons are found in the NMR titration of receptor (L^2) with fluoride and succinate anions (Fig. 36 and 38). The association constants (K) were calculated by plotting the changes in chemical shift as a function of the concentration of added anions (Fig. 37 and 39) using the Origin program and a routine written by Niek Buurma.⁷⁸ In all titrations, the concentration of the receptor was kept constant.

Chapter 3: Co-ordination Behaviour of a Novel Bisthiourea Tripodal Ligand; Structural, Spectroscopic and Electrochemical properties of a series of Transition Metal Complexes with Binding Studies

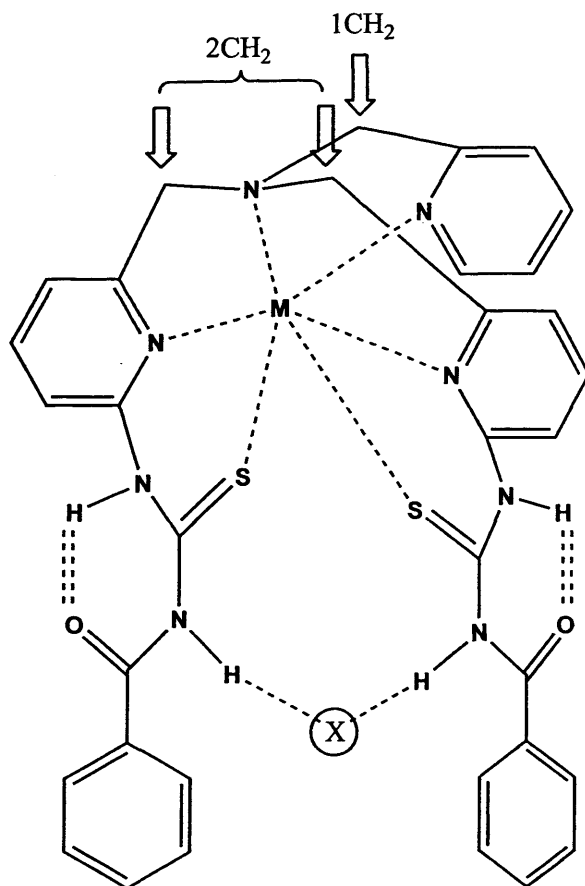


Figure 33: Expected confirmation of guest-host interaction, M= Zn or Cd, X= F⁻ or Succinate²⁻

The titration curve of fluoride and succinate with L² are different and suggests a stronger binding for succinate (Fig. 34 and 35) and this has been confirmed when calculating the binding constant using Origin programme⁷⁸, this model is written by Niek Buurma, both the succinate and fluoride data sets have been analysed globally, i.e. both the titration curves in each graph were used during the data analysis. The model used assumes identical binding sites. It has been suggested that the fluoride is bound in as 2:1 fashion as well as the succinate. The binding constants are ($K_a = 4,265 \text{ M}^{-1}$) for L²F and relatively higher for L²succinate ($K_a = 16,190 \text{ M}^{-1}$), this explains the colour change from light yellow into dark yellow for L²succinate solution when 2 eq is reached, interestingly no colour change was observed in L² with fluoride titration.

Chapter 3: Co-ordination Behaviour of a Novel Bisthiourea Tripodal Ligand; Structural, Spectroscopic and Electrochemical properties of a series of Transition Metal Complexes with Binding Studies

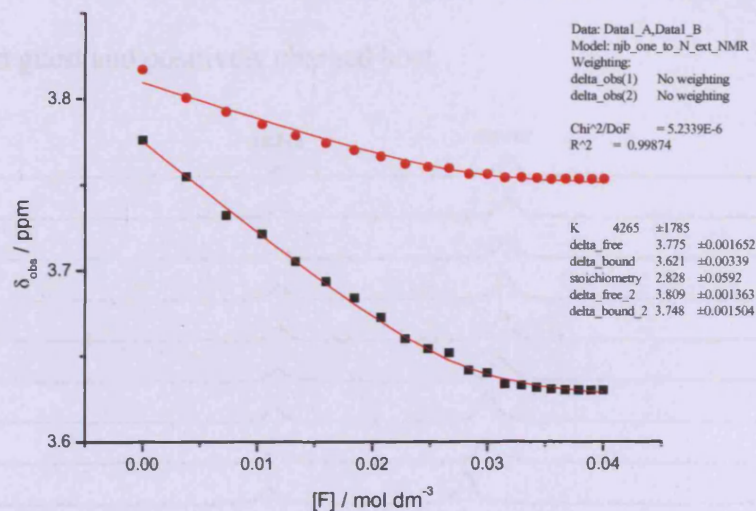


Figure 34: Fluoride titration into L².

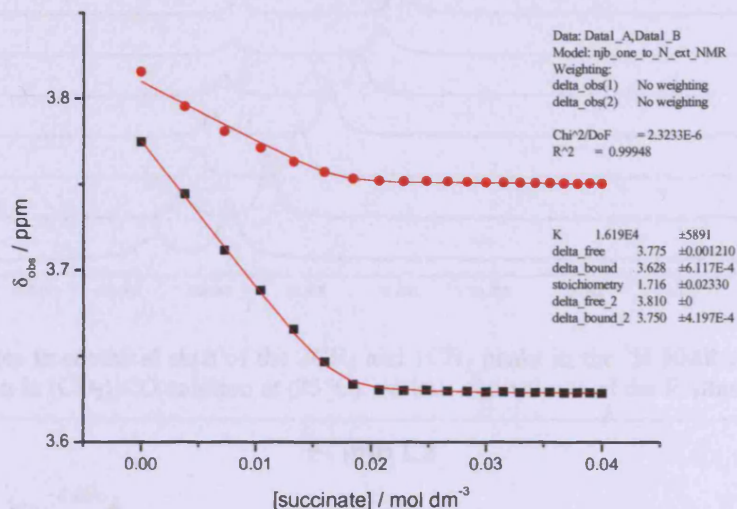


Figure 35: Succinate titration into L².

It is worth noting, in the fluoride titration of L² (Fig. 36) signals vary until 4 equivalents of F⁻ is reached, whereas in succinate titration (Fig. 37) 2 equivalents are enough for the reaction to be completed and this indicates a stronger binding for succinate. However, it is expected that a metal based receptor will have much higher binding constants due to the prearrangement of the anion binding site upon cation co-ordination. In addition, there will be an electrostatic interaction

Chapter 3: Co-ordination Behaviour of a Novel Bisthiourea Tripodal Ligand; Structural, Spectroscopic and Electrochemical properties of a series of Transition Metal Complexes with Binding Studies

between the guest and the host. Therefore we expect the interaction to be stronger between negatively charged guest and positively charged host.

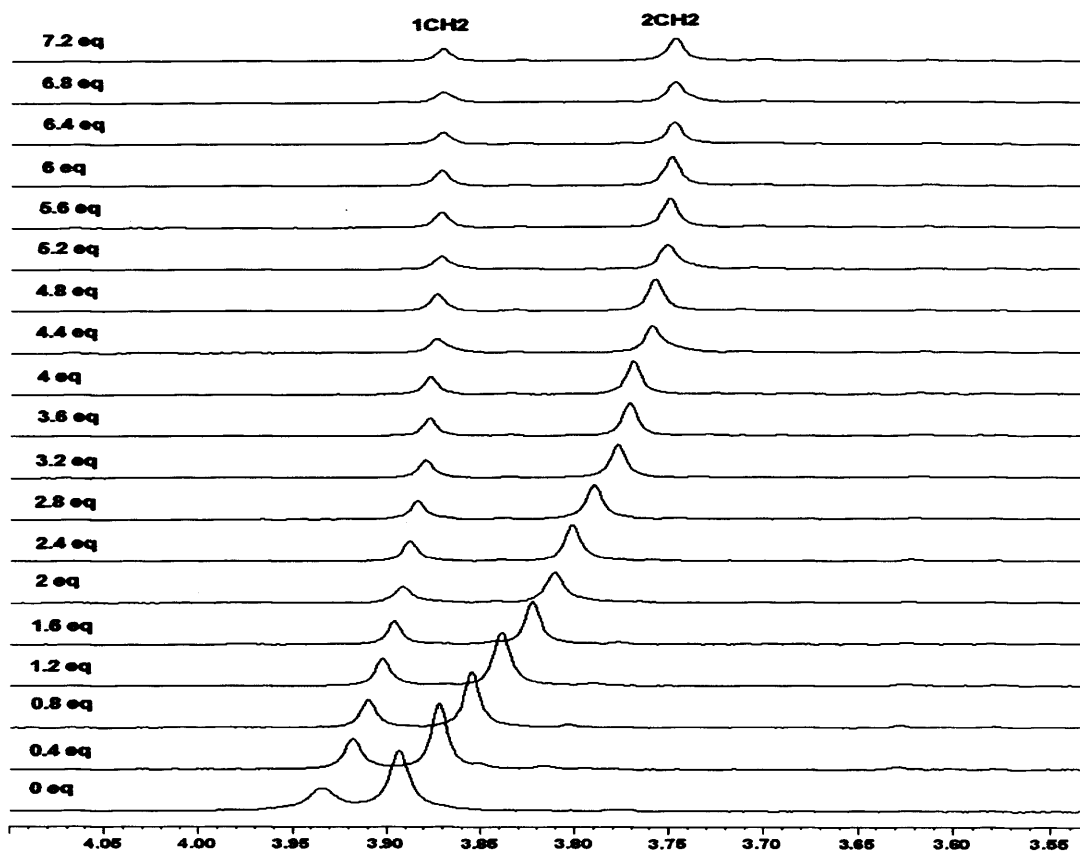


Figure 36: The changes in chemical shift of the 2CH₂ and 1CH₂ peaks in the ¹H NMR titration of receptor L² with the fluoride anion in (CD₃)₂CO solution at (25°C). various equivalents of the F⁻ illustrated on the graph.

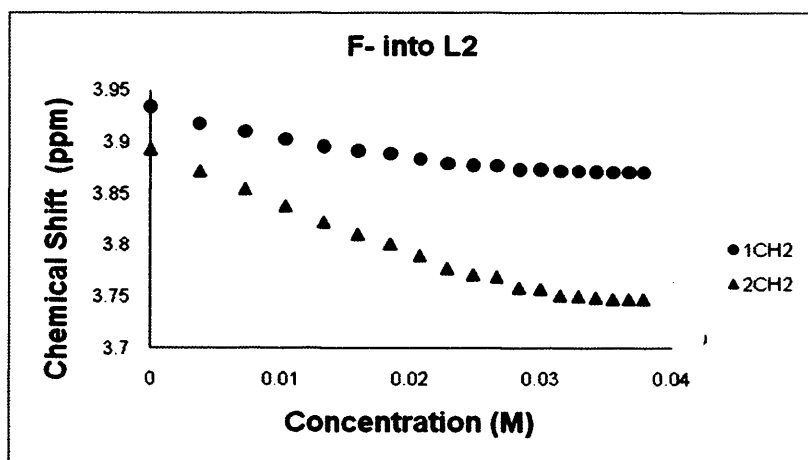


Figure 37: ¹H NMR titration curves of the receptor L² (0.01 mM) and the guest F⁻ (0.04 mM) (as tetrabutylammonium salts) done in (CD₃)₂CO at (25°C). Small aliquots of anion solutions of (0.05 mL) were added to the NMR tube without changing the overall concentration of the receptor.

Chapter 3: Co-ordination Behaviour of a Novel Bisthiourea Tripodal Ligand; Structural, Spectroscopic and Electrochemical properties of a series of Transition Metal Complexes with Binding Studies

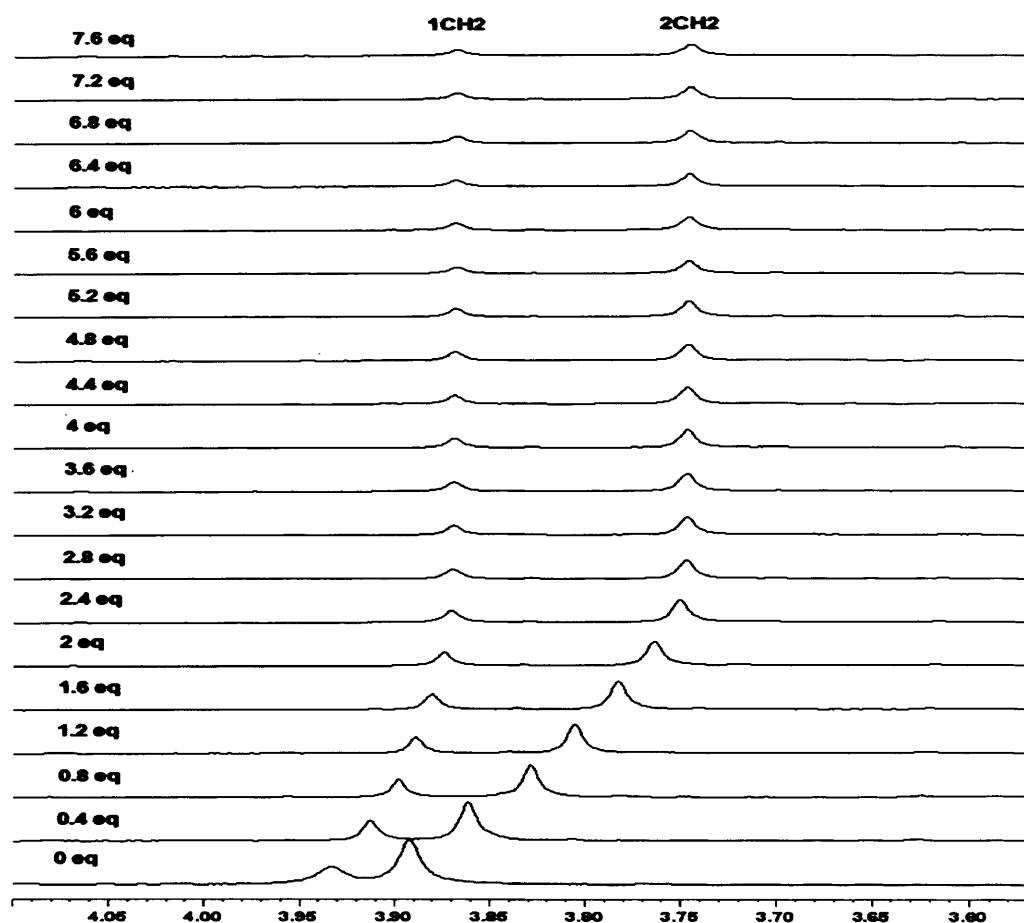


Figure 38: The changes in chemical shift of the 2CH₂ and 1CH₂ peaks in the ¹H NMR titration of receptor L² with the succinate anion in (CD₃)₂CO solution at (25°C). various equivalents of the succinate⁻² illustrated on the graph.

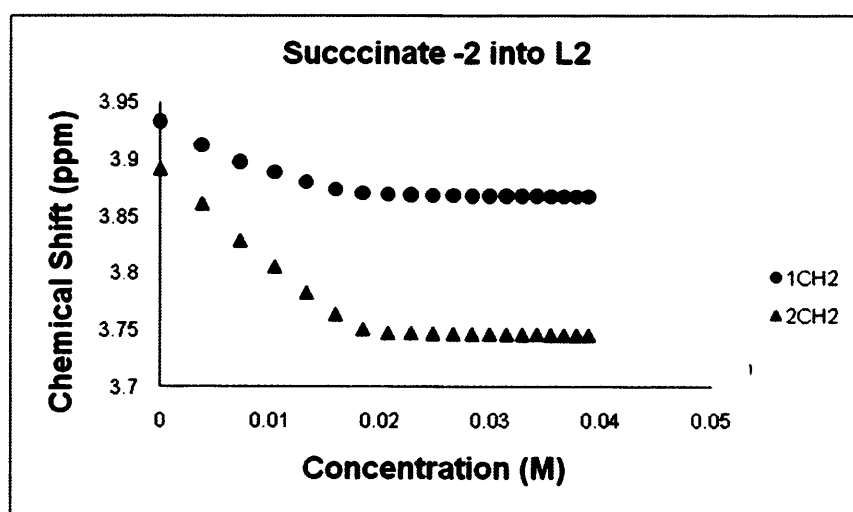


Figure 39: ¹H NMR titration curves of the receptor L² (0.01 mM) and the guest succinate⁻² (0.04 mM) (as tetrabutylammonium salts) done in (CD₃)₂CO at (25°C). Small aliquots of anion solutions of (0.05 mL) were added to the NMR tube without changing the overall concentration of the receptor.

Chapter 3: Co-ordination Behaviour of a Novel Bisthiourea Tripodal Ligand; Structural, Spectroscopic and Electrochemical properties of a series of Transition Metal Complexes with Binding Studies

Interestingly, for Zn and Cd L^2 complexes, different behaviour is observed in the 1H NMR spectra as more than 2 peaks are observed for the two methylene groups, indicating different species present in solution such as 1:1 and 2:1 guest- host species in the case of fluoride but surly, not the free ligand. Thus the process of slow exchange is observed in all (ML^2 -guest) titration (Fig. 40, 42, 44 and 46) indicating a strong binding between anion and the metal based receptor.

Titration of $[ZnL^2]^{2+}$ with F^-

When fluoride is titrated into $[ZnL^2]^{2+}$, the two closely spaced methylene signals in the 1H NMR initially start to move away from each other (Fig. 40). However, by the time that 1.2 equivalent of F^- have been added, 3 peaks start to emerge. After this point two broadened peaks are observed, however now the more intense peak is observed at low ppm, where as initially it was at high ppm. By the time that 5.2 eq are added a new pair of signals are observed at much lower ppm. (3.3-3.6 ppm).

Titration of $[CdL^2]^{2+}$ with F^-

This compound shows even more complex behaviour. Again the parent host gives 1H NMR spectrum with both methylene signals having very similar shifts. Initially, the addition of F^- causes similar changes to the spectrum as in the zinc case, albeit the changes occur more rapidly. However, upon addition of 3.2 eq the set of peaks at low ppm start to appear and the set of peaks at low ppm bcome more prominent (Fig. 45).

Titration of $[ZnL^2]^{2+}$ and $[CdL^2]^{2+}$ with succinate

interestingly, for both compounds ZnL^2 -succinate and CdL^2 -succinate (Fig. 42 and 46) a solid species was observed in the NMR tube after the second eddition of 0.8 equivalents which confirm the presence of a new species in the solution, this solid was dissolved back into solution after the addition of more equivalents of succinate (2.4 eq) for both experiments, this indicates

Chapter 3: Co-ordination Behaviour of a Novel Bisthiourea Tripodal Ligand; Structural, Spectroscopic and Electrochemical properties of a series of Transition Metal Complexes with Binding Studies

another species present in the solution. Clearly this data cannot be interpreted by using the Origin program, as the products are not in fast exchange.

A further investigation in the future should be carried out for these systems of ML^2-G . At higher temperature we may observe fast exchange behaviour in the 1H NMR thus allowing us to determine binding constants at the higher temperature. Alternatively, we might try an approach utilising dye displacement⁹ allowing us to determine binding constants by UV-Vis spectroscopy.

Chapter 3: Co-ordination Behaviour of a Novel Bisthiourea Tripodal Ligand; Structural, Spectroscopic and Electrochemical properties of a series of Transition Metal Complexes with Binding Studies

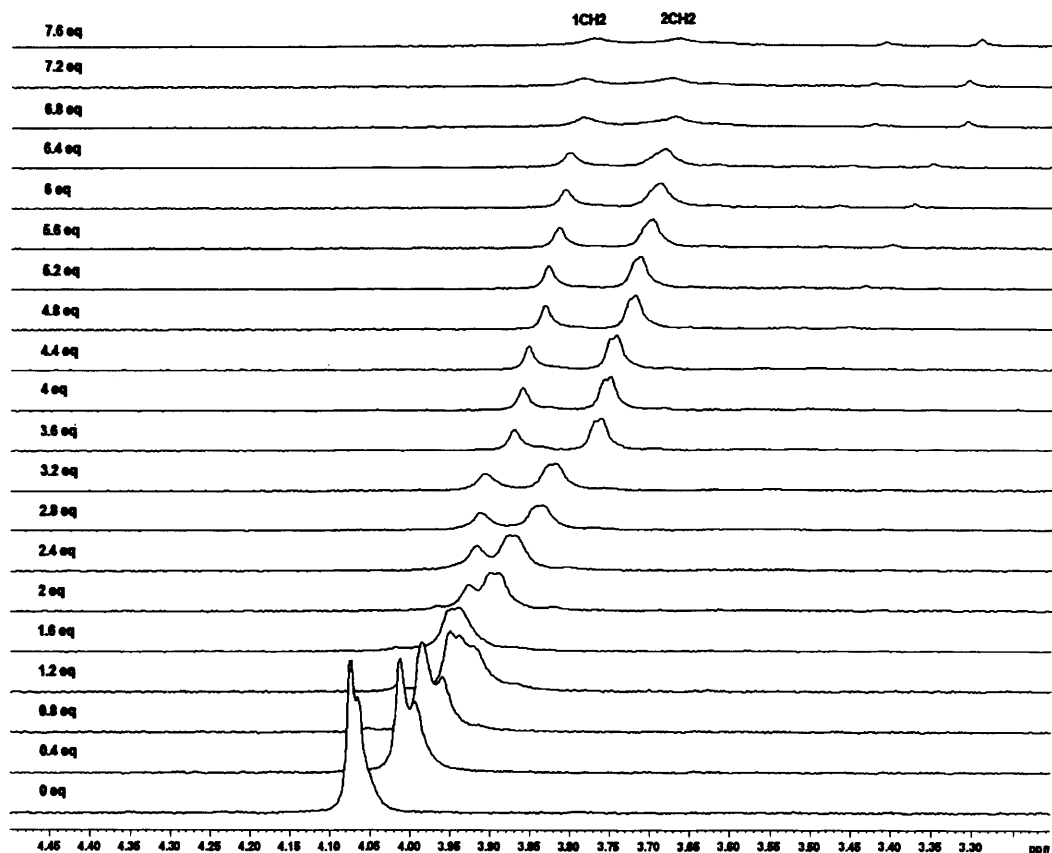


Figure 40: The changes in chemical shift of the 2CH₂ and 1CH₂ peaks in the ¹H NMR titration of receptor ZnL² with the fluoride anion in CD₃CN solution at (25°C). various equivalents of the F⁻ illustrated on the graph.

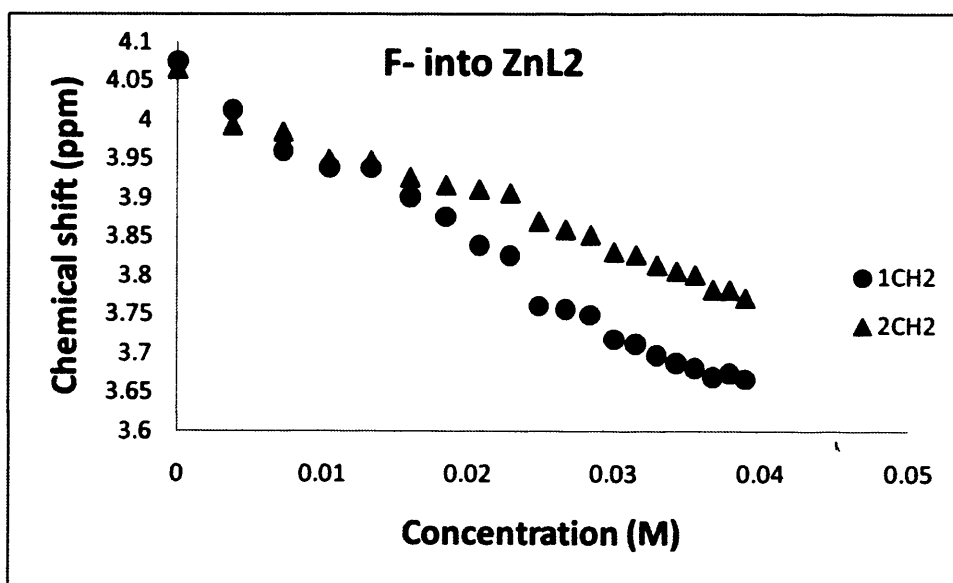


Figure 41: ¹H NMR titration curves of the receptor ZnL² (0.01 mM) and the guest F⁻ (0.04 mM) (as tetrabutylammonium salts) done in CD₃CN at (25°C). Small aliquots of anion solutions of (0.05 mL) were added to the NMR tube without changing the overall concentration of the receptor.

Chapter 3: Co-ordination Behaviour of a Novel Bisthiourea Tripodal Ligand; Structural, Spectroscopic and Electrochemical properties of a series of Transition Metal Complexes with Binding Studies

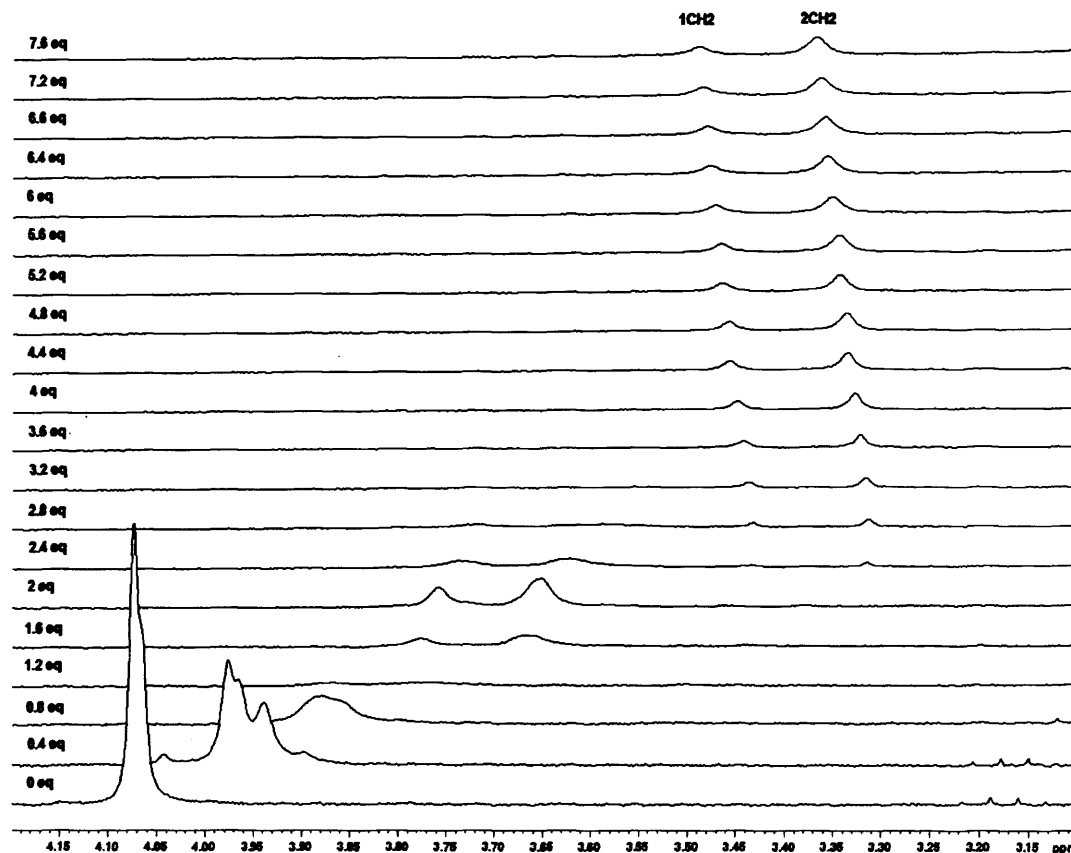


Figure 42: The changes in chemical shift of the 2CH₂ and 1CH₂ peaks in the ¹H NMR titration of receptor ZnL² with the succinate anion in CD₃CN solution at (25°C). various equivalents of the succinate⁻² illustrated on the graph.

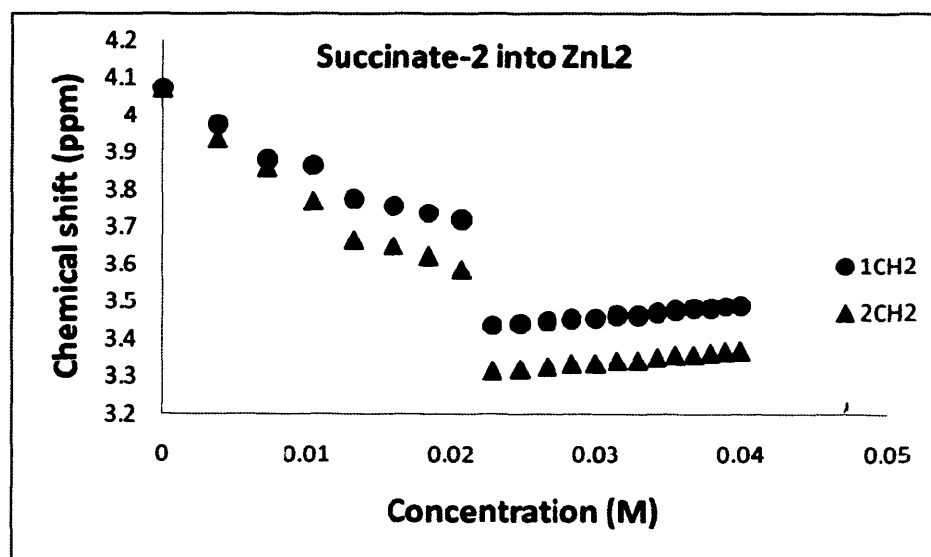


Figure 43: ¹H NMR titration curves of the receptor ZnL² (0.01 mM) and the guest succinate⁻² (0.04 mM) (as tetrabutylammonium salts) done in CD₃CN at (25°C). Small aliquots of anion solutions of (0.05 mL) were added to the NMR tube without changing the overall concentration of the receptor.

Chapter 3: Co-ordination Behaviour of a Novel Bisthiourea Tripodal Ligand; Structural, Spectroscopic and Electrochemical properties of a series of Transition Metal Complexes with Binding Studies

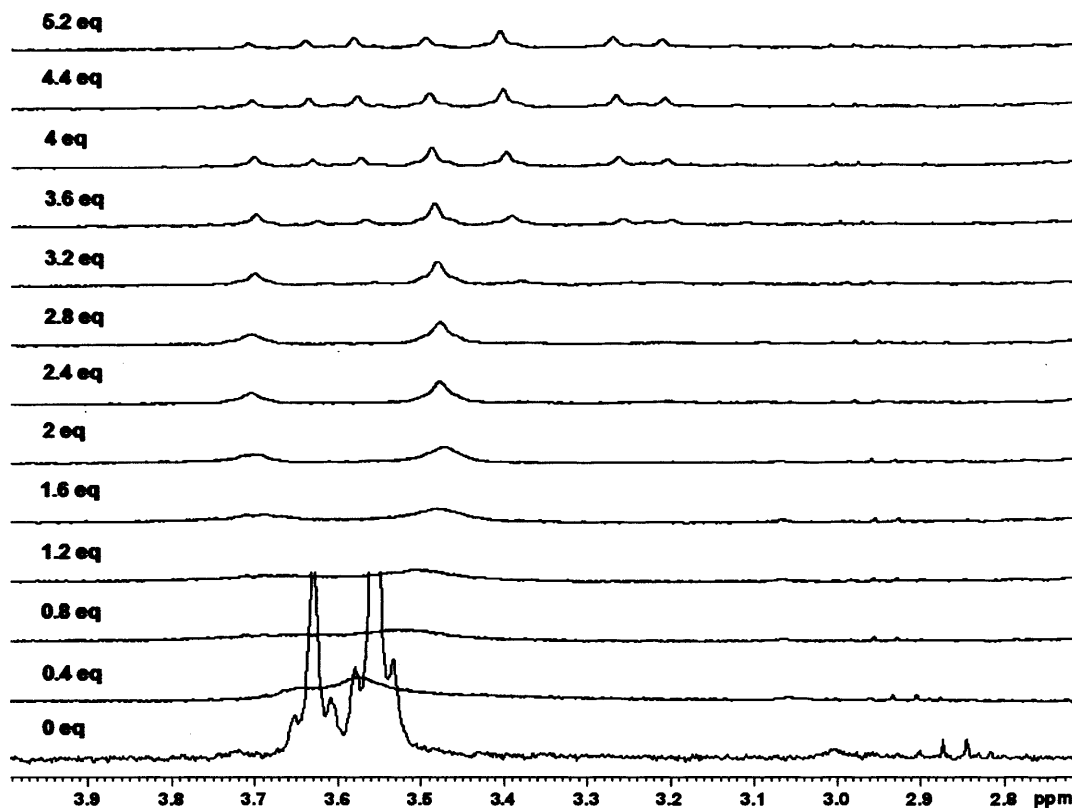


Figure 44: The changes in chemical shift of the 2CH₂ and 1CH₂ peaks in the ¹H NMR titration of receptor CdL² with the fluoride anion in CD₃CN solution at (25°C). various equivalents of the F⁻ illustrated on the graph.

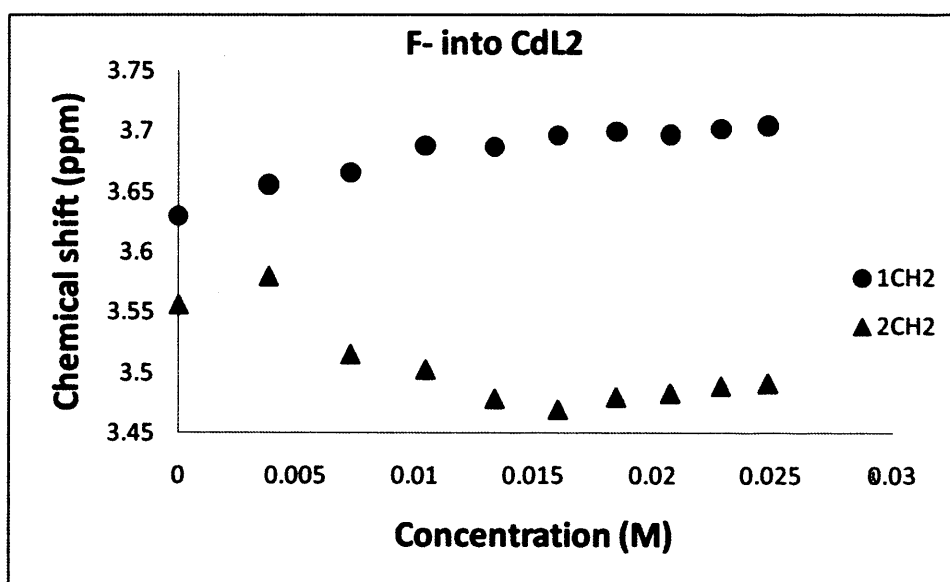


Figure 45: ¹H NMR titration curves of the receptor CdL² (0.01 mM) and the guest F⁻ (0.04 mM) (as tetrabutylammonium salts) done in CD₃CN at (25°C). Small aliquots of anion solutions of (0.05 mL) were added to the NMR tube without changing the overall concentration of the receptor.

Chapter 3: Co-ordination Behaviour of a Novel Bisthiourea Tripodal Ligand; Structural, Spectroscopic and Electrochemical properties of a series of Transition Metal Complexes with Binding Studies

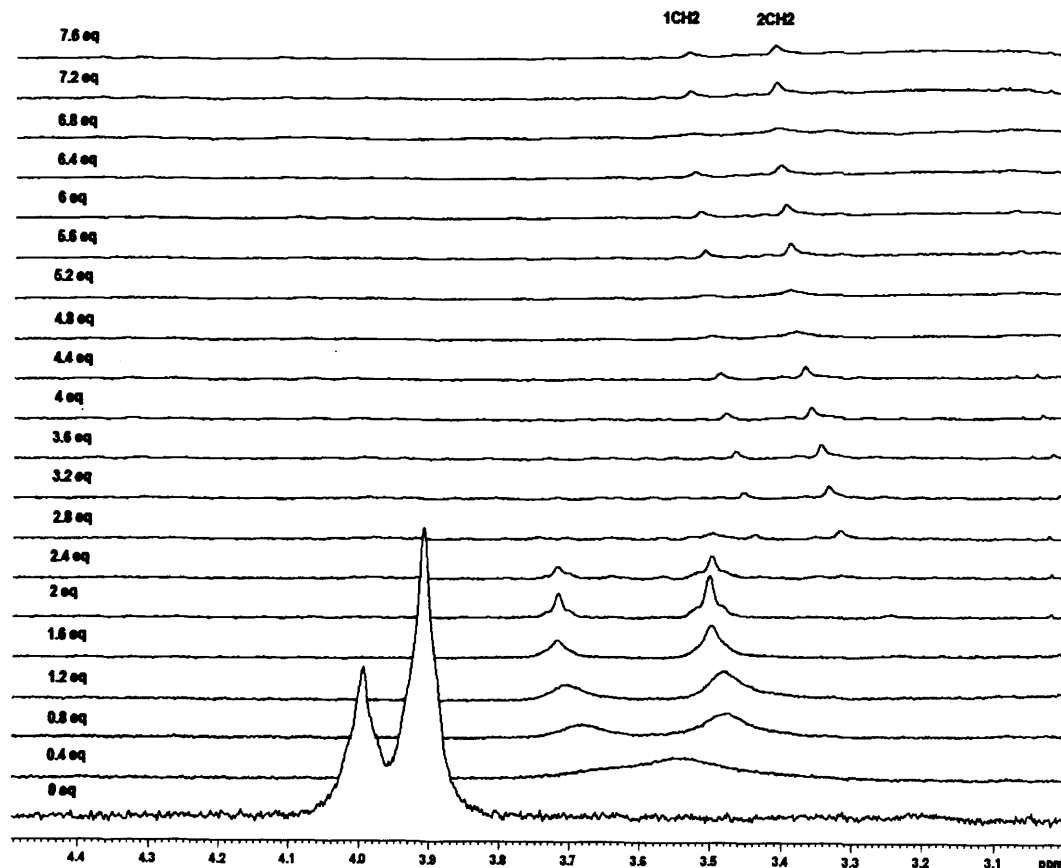


Figure 46: The changes in chemical shift of the 2CH₂ and 1CH₂ peaks in the ¹H NMR titration of receptor CdL² with the succinate anion in CD₃CN solution at (25°C). various equivalents of the succinate⁻² illustrated on the graph.

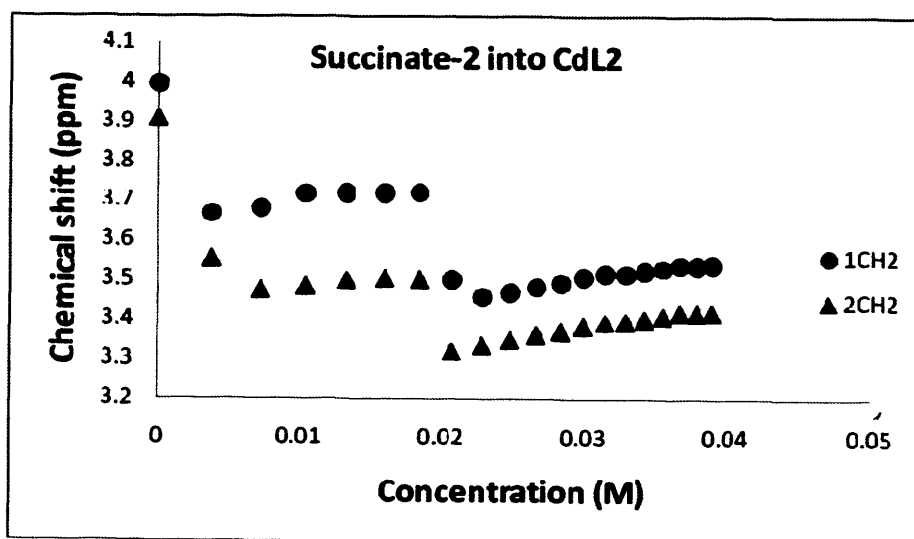


Figure 47: ¹H NMR titration curves of the receptor CdL² (0.01 mM) and the guest succinate⁻² (0.04 mM) (as tetrabutylammonium salts) done in CD₃CN at (25°C). Small aliquots of anion solutions of (0.05 mL) were added to the NMR tube without changing the overall concentration of the receptor.

Conclusion

The co-ordination chemistry of tris(2-pyridylmethyl)amine (TPA) ligand has been studied extensively, especially with first row transition metals.⁷⁹ While the ligand has a strong geometrical preference for trigonal bipyramidal complexes, other geometries may be adopted to suit the electronic preference of the metal. In conclusion, TPA derivatives having two benzoylthiourea moieties at the 6-positions of the two pyridine rings of TPA and their Mn(II), Co(II), Ni(II), Cu(II), Zn(II) and Cd(II) complexes were synthesized and characterized by spectroscopic methods, X-ray crystallography and electrochemical measurements. A useful comparison between TPA metal complexes based on structures in CCDC database and with those of L^2 is shown in Table 26. General conclusions are:

- a) All complexes display typical M-N bond lengths when compared to previously reported M(TPA) complexes.
- b) While most TPA complexes of Mn(II) are 6 co-ordinate, the seven co-ordinate structure observed with L^2 is not unusual.
- c) The five co-ordinate, TBP, geometry observed for Zn(II) and Cu(II) complexes of L^2 is typical of that observed with TPA ligands. A TBP geometry was also observed for Co(II), while it is less common it is not unusual.
- d) Typical of Ni(II), the metal resists the predisposition of the ligand to TBP geometries and instead forms an octahedral species.
- e) There is limited structural data for Cd(II) complexes. However, the larger size of the metal ions means that the metal will readily form complexes with high co-ordination numbers. (A search of the CDS shows approximately ~7% of all the Cd containing structures have a 7 co-ordinate centre).

Chapter 3: Co-ordination Behaviour of a Novel Bisthiourea Tripodal Ligand; Structural, Spectroscopic and Electrochemical properties of a series of Transition Metal Complexes with Binding Studies

f) The five co-ordinate structures of Co(II), Cu(II) and Zn(II), and the six co-ordinate Ni(II) complex, all have only one sulphur atom co-ordinated to the metal centre. This results in two thiourea groups coming close together, with hydrogen bonded occurring between the two arms.

g) The large metal ions, Mn(II) and Cd(II) form seven co-ordinate species with both sulphur atoms co-ordinated. This appears to cause the two thiourea arms to spread out, creating a central cavity below the metal ion where a counter-ion (perchlorate) or water molecule can reside and hydrogen bond with the thiourea arms (Fig. 48).

The titration of F⁻ and succinate to L² has shown stronger binding constant for succinate. However, they both bound in 2:1 fashion. Whereas the situation becomes not very encouraging in the presence of Zn²⁺ and Cd²⁺ due to slow exchange behaviour.

Future work will focus on the ability of L² to bind anions and how its preorganisation (by co-ordinating to cations of varying size and charge) affects its ability to act as a host for different guests especially when UV-Vis technique is used.

Table 26: Co-ordination numbers of TPA with first row transition metals and comparison in M-N bond lengths between L² and other TPA complexes.

M(II)	# hits ^a	TPA frame work				L ²	Bond length Å					
		% with Coordination number					N1-Bridge head		M-Pyridyl Bond lengths			
		5	6	7	8	Coord. #	TPA ^a	L ²	TPA ^a	L ² (N2)	L ² (N3)	L ² (N4)
Mn	22	0	81.8	13.6	4.5	7	2.341	2.335(15)	2.296	2.262(15)	2.298(16)	2.269(16)
Co	17	47	53	0	0	5	2.182	2.147(4)	2.104	2.086(4)	2.065(4)	2.051(4)
Ni	14	0	100	0	0	6	2.102	2.072(8)	2.078	2.237(4)	2.050(4)	2.086(4)
Cu	42	97.6	2.4	0	0	5	2.040	2.018(3)	2.066	2.030(2)	2.148(3)	2.034(3)
Zn	16	87.5	12.5	0	0	5	2.233	2.181(5)	2.083	2.078(5)	2.131(5)	2.058(5)
Cd	3	0	33.3	33.3	33.3	7	2.49	2.386(4)	2.42	2.365(4)	2.409(4)	2.378(5)

^a Refcodes for the structures used are listed in reference.⁸⁰

Chapter 3: Co-ordination Behaviour of a Novel Bisthiourea Tripodal Ligand; Structural, Spectroscopic and Electrochemical properties of a series of Transition Metal Complexes with Binding Studies

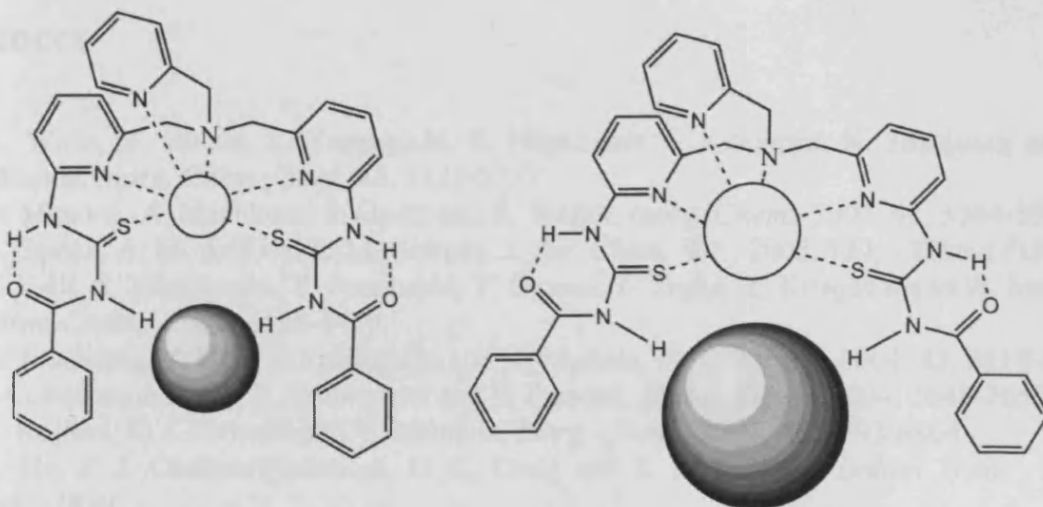


Figure 48: Effect of varying metal ion size on the guest cavity.

11. D. G. B. Dwyer, J. Nelson, F. Effen, V. McKee and S. M. Nelson, *J. Chem. Soc., Dalton Trans.*, 1982, 1337-1343.
12. Pappalardo, G., De Marco, A., Sica, and C. Nocelli, *Inorg. Chim. Acta*, 1974, 21, 167-176.
13. Z. J. Wang and H. B. Gray, *J. Am. Chem. Soc.*, 1966, 88, 1594-1599.
14. S.-Y. Ha, H.-D. Kim, W. Gu, H.-P. Yoo, P. Chang, D.-J. Lim, Z.-H. Jung and P.-W. Ewh, *J. Mol. Struct.*, 2003, 646, 131-142.
15. K. G. Blake, A. A. G. Tomlinson, B. J. Hathway and P. F. Dilling, *J. Chem. Soc.*, 1962, 21.
16. D. Hirsch, J.-J. Over, C. Makritz and H. Liebman, *Inorg. Chim. Acta*, 1971, 49, 139-144.
17. F. G. H. M. G. Maria Reyes, P. Maria Lopez, M. P. C. Garcia de Sosa, Y. Y. Tong and A. J. Lopez de Haro, *Inorg. Chim. Acta*, 1991, 245, 27-34.
18. J. P. D. P. Mendes, *Coord. Chem. Rev.*, 1988, 94, 17.
19. J. M. Garcia, J. Suarez, J. K. Forder, J. Schwenter, S. C. Shost, D. Barnhart, W. Kaminsky, S. Gopal and J. A. Kovacs, *Inorg. Chim. Acta*, 1991, 179, 277-277.
20. K.-Y. Cho, S. H. Cho and I. H. Seo, *Polymer*, 1991, 32, 1812-1821.
21. S. Bhattacharya, S. B. Khatkar, S. K. Dutta, S. K. Palit and M. Choudhury, *Inorg. Chim. Acta*, 1996, 245, 1864-1873.
22. M. Garcia, P. Alcaraz, M. Lopez and M. Prieto, *Acta Cryst. B*, 1985, 11, 985-990.
23. M. Garcia, P. Alcaraz and V. Lopez, *J. Chem. Soc. Chem. Commun.*, 1985, 11, 1975.
24. M. Garcia, P. Alcaraz, D. Casuyaya, J. Garcia, M. Lopez, *Inorg. Chim. Acta*, 1985, 85, 1693-1703.
25. P. Alcaraz, M. Garcia, M. Lopez and M. Prieto, *Coord. Chem. Rev.*, 1991, 107, 171-180.
26. M. Garcia and D. Casuyaya, *Inorg. Chim. Acta*, 1993, 197, 1515-1522.

References

1. A. Wada, Y. Honda, S. Yamaguchi, S. Nagatomo, T. Kitagawa, K. Jitsukawa and H. Masuda, *Inorg. Chem.*, 2004, **43**, 5725-5735.
2. D. Mandon, A. Machkour, S. Goetz and R. Welter, *Inorg. Chem.*, 2002, **41**, 5364-5372.
3. E. Szajna, A. M. Arif and L. M. Berreau, *J. Am. Chem. Soc.*, 2005, **127**, 17186-17187.
4. T. Fujii, S. Yamaguchi, Y. Funahashi, T. Ozawa, T. Tosha, T. Kitagawa and H. Masuda, *Chem. Comm.*, 2006, 4428-4430.
5. K. Jitsukawa, Y. Oka, S. Yamaguchi and H. Masuda, *Inorg. Chem.*, 2004, **43**, 8119-8129.
6. J. C. Mareque-Rivas, R. Prabakaran and S. Parsons, *Dalton Trans.*, 2004, 1648-1655.
7. T. Kojima, K.-i. Hayashi and Y. Matsuda, *Inorg. Chem.*, 2004, **43**, 6793-6804.
8. Z. He, P. J. Chaimungkalanont, D. C. Craig and S. B. Colbran, *Dalton Trans.*, 2000, 1419-1429.
9. S. L. Tobey and E. V. Anslyn, *Org. Lett.*, 2003, **5**, 2029-2031.
10. M. Harata, K. Hasegawa, K. Jitsukawa, H. Masuda and H. Einaga, *Bull. Chem. Soc. Jpn.*, 1998, **71**, 1031.
11. M. S. M. Yusof, S. K. C. Soh, N. Ngah and B. M. Yamin, *Acta Cryst.*, 2006, **E62**, 1446-1448.
12. M. G. B. Drew, J. Nelson, F. Esho, V. McKee and S. M. Nelson, *J. Chem. Soc., Dalton Trans.*, 1982, 1837 - 1843.
13. P. Dapporto, G. De Munno, A. Segal and C. Mealli, *Inorg. Chim. Acta*, 1984, **83**, 171-176.
14. Z. Dori and H. B. Gray, *J. Am. Chem. Soc.*, 1966, **88**, 1394-1398.
15. J.-Y. Xu, H.-D. Bian, W. Gu, S.-P. Yan, P. Cheng, D.-Z. Liao, Z.-H. Jiang and P.-W. Shen, *J. Mol. Struct.*, 2003, **646**, 237-242.
16. R. C. Slade, A. A. G. Tomlinson, B. J. Hathaway and D. E. Billing, *J. Chem. Soc.*, 1968, 61.
17. O. Horner, J.-J. Girerd, C. Philouze and L. Tchertanov, *Inorg. Chim. Acta*, 1999, **290**, 139-144.
18. P. Gili, M. G. Martín Reyes, P. Martín Zarza, M. F. C. Guedes da Silva, Y. Y. Tong and A. J. L. Pombeiro, *Inorg. Chim. Acta*, 1997, **255**, 279-288.
19. J. E. B. Randles, *Trans. Faraday Soc.*, 1948, **44**, 327.
20. L. M. Brines, J. Shearer, J. K. Fender, D. Schweitzer, S. C. Shoner, D. Barnhart, W. Kaminsky, S. Lovell and J. A. Kovacs, *Inorg. Chem.*, 2007, **46**, 9267-9277.
21. K.-Y. Choi, S. N. Choi and I.-H. Suh, *Polyhedron*, 1998, **17**, 1415-1422.
22. S. Bhattacharyya, S. B. Kumar, S. K. Dutta, E. R. T. Tiekink and M. Chaudhury, *Inorg. Chem.*, 1996, **35**, 1967-1973.
23. *Refcodes for the structures used are: AHEZES, AHEZIW, AHEZOC, CASDUW, CUBDIN, ELUZO, FESPIC, GOWCEA, INOYUF, JISWEO, KOFFAM, KOFFAM01, NIGHAM, OHEDEK, TERLAE, UJAQAX, VISCAC, DOKTIH, MELTUT, WEFTAD.*
24. S. Alvarez, D. Avnir, M. Llunell and M. Pinsky, *New J. Chem.*, 2002, **26**, 996-1009.
25. S. Alvarez, P. Alemany and D. Avnir, *Chem. Soc. Rev.*, 2005, **34**, 313-326.
26. S. Alvarez, P. Alemany, D. Casanova, J. Cirera, M. Llunell and D. Avnir, *Coord. Chem. Rev.*, 2005, **249**, 1693-1708.
27. S. Alvarez, D. Avnir, M. Pinsky and M. Llunell, *Cryst. Engineer.*, 2001, **4**, 179-200.
28. M. Pinsky and D. Avnir, *Inorg. Chem.*, 1998, **37**, 5575-5582.

Chapter 3: Co-ordination Behaviour of a Novel Bisthiourea Tripodal Ligand; Structural, Spectroscopic and Electrochemical properties of a series of Transition Metal Complexes with Binding Studies

29. M. Pinsky, K. B. Lipkowitz and D. Avnir, *J. Math. Chem.*, 2001, **1**, 109-120.
30. A. J. Amoroso, P. G. Edwards, S. T. Howard, B. M. Kariuki, J. C. Knight, L. Ooi, K. M. A. Malik, L. Stratford and A.-R. H. Al-Sudani, *Dalton Trans.*, 2009, 8356.
31. S. M. Baldeau, C. H. Slinn, B. Krebs and A. Rompel, *Inorg. Chim. Acta*, 2004, **357**, 3295-3303.
32. R. Pedrido, A. M. González-Noya, M. J. Romero, M. Martínez-Calvo, M. V. López, E. Gómez-Fórneas, G. Zaragoza and M. R. Bermejo, *Dalton Trans.*, 2008, 6776 - 6787.
33. S. S. Massoud, K. T. Broussard, F. A. Mautner, R. Vicente, M. K. Saha and I. Bernal, *Inorg. Chim. Acta*, 2008, **361**, 123-131.
34. E. E. ChufÄjn, C. N. Verani, S. C. Puiu, E. Rentschler, U. Schatzschneider, C. Incarvito, A. L. Rheingold and K. D. Karlin, *Inorg. Chem.*, 2007, **46**, 3017-3026.
35. D. C. Fox, A. T. Fiedler, H. L. Halfen, T. C. Brunold and J. A. Halfen, *J. Am. Chem. Soc.*, 2004, **126**, 7627-7638.
36. S. R. Randeniya and R. E. Norman, *Acta Cryst.*, 2009, **E65**, m771.
37. M. E. Helton, P. Chen, P. P. Paul, Z. Tyeklar, R. D. Sommer, L. N. Zakharov, A. L. Rheingold, E. I. Solomon and K. D. Karlin, *J. Am. Chem. Soc.*, 2003, **125**, 1160-1161.
38. C. Duboc, T. Phoeung, D. Jouvenot, A. G. Blackman, L. F. McClintock, J. Pécaut, M.-N. Collomb and A. Deronzier, *Polyhedron*, 2007, **26**, 5243-5249.
39. H. Luhmann, Z. Rejai, K. Moller, P. Leisner, M.-E. Ordolff, C. Nather and W. Bensch, *Z. Anorg. Allg. Chem.*, 2008, **634**, 1687.
40. S. H. Tarulli, O. V. Quinzani, E. J. Baran and O. E. Piro, *J. Inorg. Gen. Chem.*, 2002, **628**, 751.
41. D. C. Bebout, S. W. Stokes and R. J. Butcher, *Inorg. Chem.*, 1999, **38**, 1126-1133.
42. G. Guisado-Barrios, Y. Li, A. M. Z. Slawin, D. T. Richens, I. A. Gass, P. R. Murray, L. J. Yellowlees and E. K. Brechin, *Dalton Trans.*, 2008, 551-558.
43. M. Renic, N. Basaric and K. Mlinaric-Majerski, *Tetrahedron Lett.*, 2007, **48**, 7873-7877.
44. C. R. Bondy and S. J. Loeb, *Coord. Chem. Rev.*, 2003, **240**, 77-99.
45. E. A. Katayev, Y. A. Ustynyuk and J. L. Sessler, *Coord. Chem. Rev.*, 2006, **250**, 3004-3037.
46. P. D. Beer and S. R. Bayly, *Top. Curr. Chem.*, 2005, **255**, 125-162.
47. P. D. Beer and J. Cadman, *Coord. Chem. Rev.*, 2000, **205**, 131-155.
48. P. D. Beer and P. A. Gale, *Angew. Chem. Int. Ed.*, 2001, **40**, 486-516.
49. P. D. Beer and P. Schmitt, *Curr. Opin. in Chem. Bio.*, 1997, **1**, 475-482.
50. V. Amendola, D. Esteban-Gómez, L. Fabbrizzi and M. Licchelli, *Acc. Chem. Res.*, 2006, **39**, 343-353.
51. I. Ravikumar, P. S. Lakshminarayanan and P. Ghosh, *Inorganica Chimica Acta*, **363**, 2886-2895.
52. J. Cookson, M. S. Vickers, R. L. Paul, A. R. Cowley and P. D. Beer, *Inorganica Chimica Acta*, 2008, **361**, 1689-1698.
53. G. W. Lee, N. Singh, H. J. Jung and D. O. Jang, *Tetrahedron Lett.*, 2009, **50**, 807-810.
54. J. Cookson, M. S. Vickers, R. L. Paul, A. R. Cowley and P. D. Beer, *Inorg. Chim. Acta*, 2008, **361**, 1689-1698.
55. I. Ravikumar, P. S. Lakshminarayanan and P. Ghosh, *Inorg. Chim. Acta*, 2010, **363**, 2886-2895.
56. P. R. Edwards, J. R. Hiscock and P. A. Gale, *Tetrahedron Lett.*, 2009, **50**, 4922-4924.
57. T. Zielinski, P. Dydio and J. Jurczak, *Tetrahedron*, 2008, **64**, 568-574.

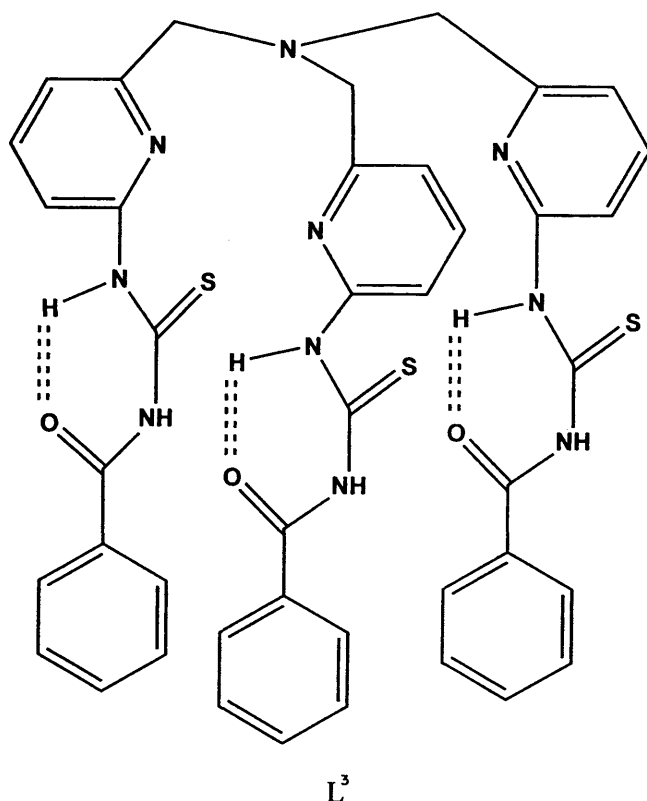
Chapter 3: Co-ordination Behaviour of a Novel Bisthiourea Tripodal Ligand; Structural, Spectroscopic and Electrochemical properties of a series of Transition Metal Complexes with Binding Studies

58. K. Lang, P. Curínová, M. Dudic, P. Prosková, I. Stibor, V. St'astný and P. Lhoták, *Tetrahedron Letters*, 2005, **46**, 4469-4472.
59. A. Fan, H. Kah Hong, S. Valiyaveetil and J. J. Vittal, *Journal of Supramolecular Chemistry*, 2002, **2**, 247-254.
60. A. Fan, H. K. Hong, S. Valiyaveetil and J. J. Vittal, *J. Supramol. Chem.*, 2002, **2**, 247-254.
61. K. Ghosh and S. Adhikari, *Tetrahedron Lett.*, 2006, **47**, 8165-8169.
62. S.-i. Kondo and M. Sato, *Tetrahedron*, 2006, **62**, 4844-4850.
63. S.-i. Kondo, M. Nagamine, S. Karasawa, M. Ishihara, M. Unno and Y. Yano, *Tetrahedron*, 2011, **67**, 943-950.
64. V. Amendola, M. Bonizzoni, D. Esteban-Gómez, L. Fabbrizzi, M. Licchelli, F. Sancenón and A. Taglietti, *Coord. Chem. Rev.*, 2006, **250**, 1451-1470.
65. K. H. Lee and J.-I. Hong, *Tetrahedron Lett.*, 2000, **41**, 6083-6087.
66. J. Shao, Y. Qiao, H. Lin and H. Lin, *Spectrochimica Acta Part A: Molecular and Biomolecular Spectroscopy*, 2009, **71**, 1736-1740.
67. A. Fan, H. Kah Hong, S. Valiyaveetil and J. J. Vittal, *Journal of Supramolecular Chemistry*, **2**, 247-254.
68. Y. Zhao, Z. Lin, S. Ou, C. Duan, H. Liao and Z. Bai, *Inorg. Chem. Comm.*, 2006, **9**, 802-805.
69. D. Saravanakumar, N. Sengottuvelan, M. Kandaswamy, P. G. Aravindan and D. Velmurugan, *Tetrahedron Letters*, 2005, **46**, 7255-7258.
70. S. Devaraj, D. Saravanakumar and M. Kandaswamy, *Sensors and Actuators B: Chemical*, 2009, **136**, 13-19.
71. F. Wang, J. Wu, X. Zhuang, W. Zhang, W. Liu, P. Wang and S. Wu, *Sensors and Actuators B: Chemical*, 2010, **146**, 260-265.
72. M. S. Han and D. H. Kim, *Tetrahedron*, 2004, **60**, 11251-11257.
73. H.-L. Kwong, W.-L. Wong, C.-S. Lee, C.-T. Yeung and P.-F. Teng, *Inorganic Chemistry Communications*, 2009, **12**, 815-818.
74. P. D. Beer, P. A. Gale and D. Hesk, *Tetrahedron Letters*, 1995, **36**, 767-770.
75. C. Frassinetti, L. Alderighi, P. Gans, A. Sabatini, A. Vacca and S. Ghelli, *Anal Bioanal Chem* 2003, **376**, 1041-1052
76. M. J. Hynes, *J. Chem. Soc. Dalton Trans.*, 1993, 311-312.
77. Z. Yin, Y. Zhang, J. He and J.-P. Cheng, *Tetrahedron*, 2006, **62**, 765-770.
78. Originlab company, <http://www.originlab.com/>.
79. A. G. Blackman, *Polyhedron*, 2005, **24**, 1-39.
80. Refcodes for the structures used are, for Mn(II): EXOCAV, EXOCID, GIVTIO, GIVTOU, HADVEO, MIKKEX, MIKKIB, NAPYEJ, NIJWIN, NIJWOT, OHEDIO, PIFVUV, PIFWAC, PIFWEG, QIVHEJ, QIVROD, QIVRUJ, SAFTEZ, WASLAE, WOHNAL, XESVOH, YAYLEP. For Co(II): LIWRAL, MOLCIA, OHEDUA, QALZOT, QAMBAI, RECPEV, REMREH, REMRIL, RITWOH, RITWUN, RUKZOM, SATYIW, SICLEW, UMIPUB, UMIRAJ, XESVIB, KUCCOB. For Ni(II): AJIREQ, CICTUD, CICXIV, COHNUJ, FAFNEG, HODWOM, LEYSEO, POXGEP, ROPCEE, TOXXEJ, VILQOW, XESVEX, XEXHEN, XIJXUJ. For Cu(II): BEJPOW, BIXMEA, BIXMUQ, BIXPIH, BUBCIK, COHNIX, EBAWIN, EHIDII, EHIDOO, EHIDUU, EHIFEG, EHIFIK, EXEPUS, GECRAH, GIHWOK, HEQWEF, HEQXAC, KIWKEG, KIWKIK, MADZIB, MOQKAE, MUHNOS, NOCQOL, POGYOA, RABFUV, RARYEP, SAHBIM, SIXLUH, SIZCAG, SOQJIS, TARMEF, UKACIS, VACJAL, WEGHOF, XEMDOI, XUSPUW,

Chapter 3: Co-ordination Behaviour of a Novel Bisthiourea Tripodal Ligand; Structural, Spectroscopic and Electrochemical properties of a series of Transition Metal Complexes with Binding Studies

YANNOR, YAVVOG, YIWKUL, ZEMXUK, ZIFDUN, ZUBZIF. For Zn(II): CIWVAG, NABCAU, NABDOJ, NABKIK, PEMBIS, PEMBOY, SINWES, SINWIN, SINWOC, SINWUI, UMIQOW, WUCGOQ, ZERBIH, ZUBZAX, ZUBZEB, ZUDHAH. For Cd(II): VIQLOW, ZUBZOL, ZUBZUR.

Chapter 4: Co-ordination Behaviour of a Novel Tristhiourea Tripodal Ligand; Structural, Spectroscopic and Electrochemical properties of a series of Transition Metal Complexes



Introduction

The use of molecular sensors is a unique method for the detection of species. Anions play an important role in a wide range of chemical and biological processes. Designing and synthesising anion receptors are of high importance in host-guest chemistry due to their significance in developing chemical sensors and membranes for selective transport and separation of anions.¹⁻⁶ In particular, the synthesis of colorimetric anion sensors is of great importance because visual detection can offer qualitative and quantitative information.⁷⁻¹¹ Efforts have been made to develop hydrogen-bonding donors (receptors) containing imine⁹, amide¹²⁻¹⁴, urea^{10, 15, 16}, thiourea^{17, 18} and of transition metal based receptors.¹⁹⁻²² Urea and thiourea groups are powerful hydrogen bond donors which showed selective anion recognition through hydrogen bonding.^{23, 24} C_{3v} symmetrical systems seem to create a suitable cavity for anions so long as those receptors have hydrogen bond donors able to bind the guest of interest. For example, the tripodal tren-based amide receptors have been shown to host fluoride, chloride but not bromide or iodide, however the stability constant varies depending on the position of the nitro group (Fig. 1).

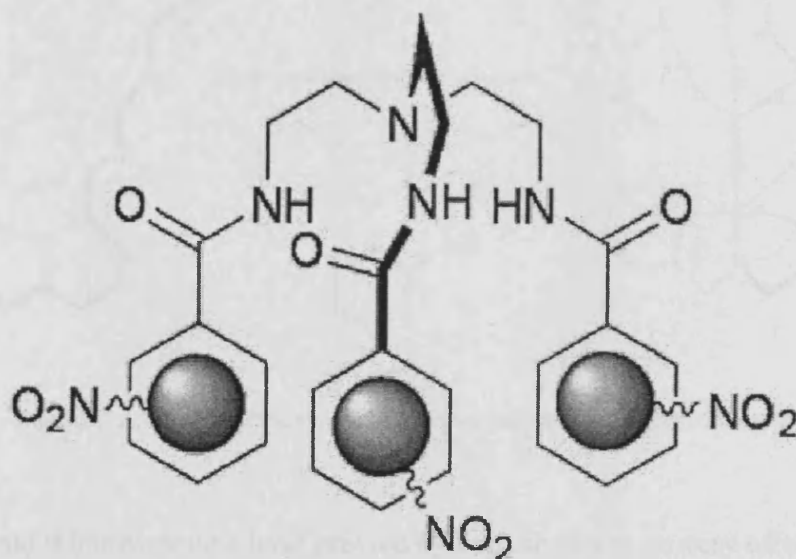


Figure 1: Tren based tripodal C_3 receptor system.

Chapter 4: Co-ordination Behaviour of a Novel Trithiourea Tripodal Ligand; Structural, Spectroscopic and Electrochemical properties of a series of Transition Metal Complexes

This ligand shows exclusive binding toward only fluoride in the halide series when the nitro is placed in the ortho position, though the ligand shows binding toward fluoride as well as chloride when the nitro is being in the para position. On the other hand, meta-nitro does not show selectivity among fluoride and chloride in solution state studies. Solution state binding of halides in the above cases indicate the participation of amide $-NH$ and aryl- CH protons in the anion binding process. The solid-state structural study of *para*-isomer, shows that two of the three amide functional groups present in the ligand are in strong intramolecular hydrogen-bonding interactions which create a C_{3v} symmetric cleft which could be suitable for encapsulation of an anionic guest.²⁵

In another example, TPA ligand framework has been substituted in 6 position with guanidinium groups and used as a host molecule for phosphate ions which makes effective chromogenic chemosensor for inorganic phosphate.⁷ Anslyn and co-workers demonstrated the colorimetric detection of phosphate anion (Fig. 2).

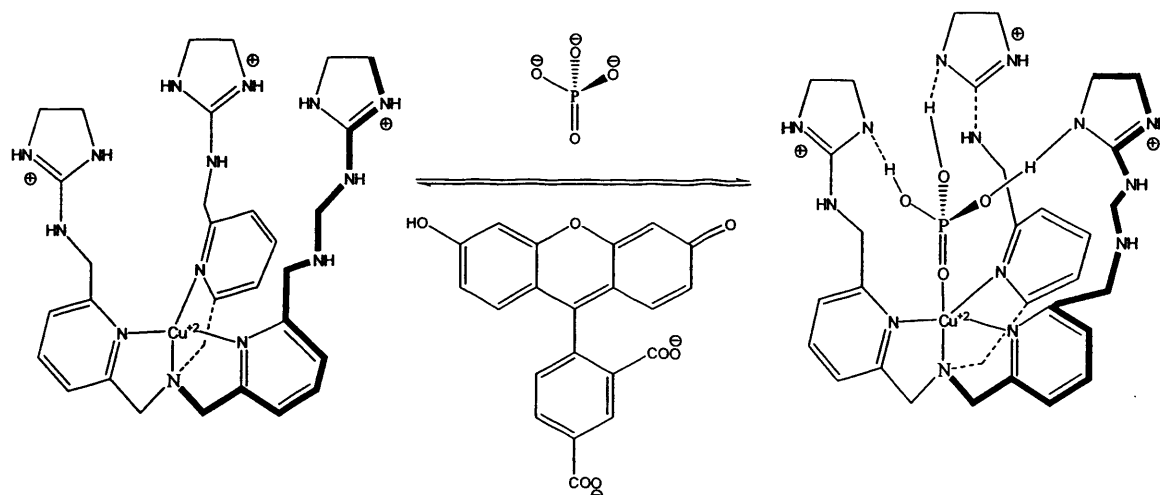


Figure 2: A C_3 symmetric synthetic receptor indicator displacement assay.

While the urea and thiourea groups have previously been shown to be very effective in hydrogen bonding to anions,²⁶⁻²⁹ this modification of TPA has not been reported.

Chapter 4: Co-ordination Behaviour of a Novel Trithiourea Tripodal Ligand; Structural, Spectroscopic and Electrochemical properties of a series of Transition Metal Complexes

In addition, as we have already seen in previous chapters, new TPA metal based receptors have shown promising results towards binding small molecules.

The aim of this chapter was to design a C_{3v} symmetrical new tripodal ligand which could be used to form a transition metal complex. This complex, in turn, was hoped to be used as a molecular sensor which is set up to bind tetrahedral anions such as: perchlorate and phosphate as there will be three N-H groups available to bind via hydrogen bonds to three oxygens in the anion (Fig. 3).

Tripodal ligands were focused on due to prevalent success as molecular sensors in previous literature. They are easily tuneable, meaning that a whole series can be synthesised and tested for trends. The flexible arms also allow the ligand to wrap itself around the guest species – maximising interactions.

In this chapter, we wish to report the investigation, characterization and electrochemistry and crystal structures of trithiourea tripodal metal complexes as well as their ability to bind tetrahedral anion such as phosphate using ^{31}P NMR technique.

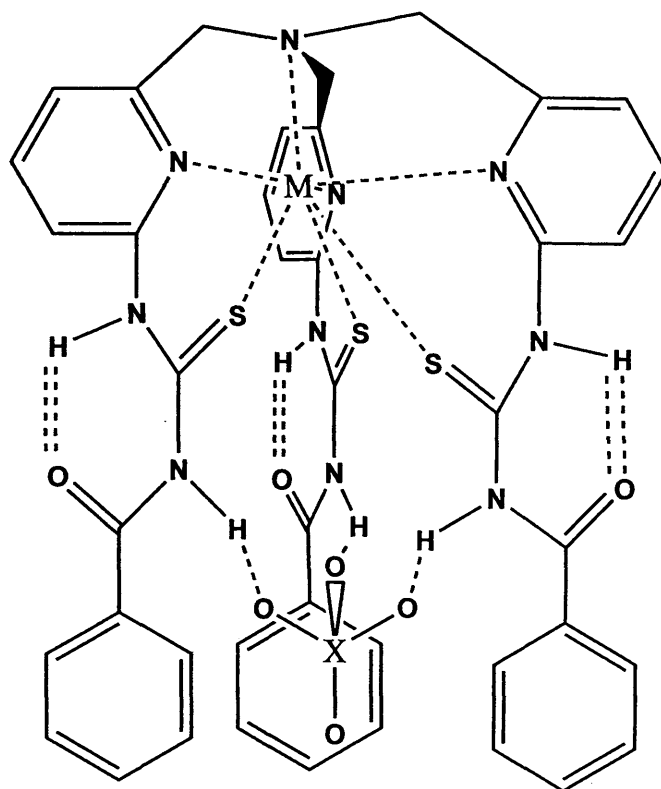


Figure 3: Expected metallo-receptor of L^3 binding tetrahedral anion.

Experimental

General

The details regarding the collection of experimental data are the same as those reported in the preceding chapters.

Synthesis of L^3

Tris(6-amino-2-pyridylmethyl)amine (TAPA), was prepared as reported by Harata *et al.* and Jitsukawa *et al.*^{30,31} TAPA (3.40 g, 10.139 mmol) was dissolved in EtOH (200 mL) and benzoyl isothiocyanate (4.9 mL, 30.4194 mmol) was added drop wise. The mixture was heated to 40°C for 30 minutes then allowed to cool to room temperature. The solvent was removed under reduced pressure.³² Ether was used to precipitate the product L^3 as a brown solid (3.147 g, 37 %). $C_{42}H_{36}N_{10}O_3S_3$ (Fig. 2). 1H NMR δ H (400 MHz; $CDCl_3$): 3.80(6H, s); 7.39-7.43(9H, m, Ar); 7.53(3H, m, Ar); 7.69(3H, t, Ar, $J=7.8$ Hz); 7.77(6H, d, Ar, $J=6.6$ Hz); 8.61(3H, d, Ar, $J=4.1$ Hz);

Chapter 4: Co-ordination Behaviour of a Novel Tristhiourea Tripodal Ligand; Structural, Spectroscopic and Electrochemical properties of a series of Transition Metal Complexes

8.87(3H, s, NH); 12.96(3H, s, NH). ^{13}C δC (62.5 MHz; CDCl_3): 59.6, 114.1, 120.8, 127.5, 129.1, 131.6, 133.6, 138.1, 150.3, 150.4, 166.2, 176.7. Accurate ESMS (m/z): 825.2249 (100) [$\text{L}^3 + \text{H}$] $^+$. [Calculated 825.2212]. IR KBr/ cm^{-1} : $\nu = 3414\text{br}$, 3053br, 1674s, 1598s, 1454s, 1331s, 755s. UV/Vis [λ_{max} , nm (ϵM , $\text{M}^{-1}\text{cm}^{-1}$)] in THF: 268 (106,600), 288 (94,200) 310 (58,100).

General Procedure for the synthesis of metal complexes

Ligand L^3 (1 equivalent, typically 0.077 mmol) was dissolved in the minimum amount of CHCl_3 or THF (typically 3 mL). The solutions were warmed to ca. 60°C to ensure that the ligand fully dissolved. To this stirring solution, the metal perchlorate salt (1 equivalent) dissolved in acetonitrile (ca. 2 mL) was added dropwise. Recrystallisation of the compounds typically involved the diffusion of diethyl ether into mixture of acetonitrile and THF or CHCl_3 solutions which were first filtered through Celite.

[Mn^{II}(L^3)] [ClO_4] $_2 \cdot \text{CH}_3\text{CN}$ (4.1): colourless plate crystals (37% yield). Found: C, 47.36; H, 3.551; N, 13.86 %. $\text{MnC}_{42}\text{H}_{36}\text{N}_{10}\text{O}_3\text{S}_3(\text{CH}_3\text{CN})(\text{ClO}_4)_2$ requires C, 47.22; H, 3.51; N, 13.77%; ESMS m/z (%): 878.14 (100) [$\text{Mn}(\text{L}^3) - \text{H}$] $^+$; IR (KBr pellet, cm^{-1}): 3432(br), 1608(s), 1532(m), 1455(s), 1262(s), 1086(s), 706(s), 622(s).

[Co^{II}(L^3)] [ClO_4] $_2$ (4.2): dark red glassy solid (40% yield). ESMS m/z (%): 882.13 (60), [$\text{Co}(\text{L}^3) - \text{H}$] $^+$; IR (KBr pellet, cm^{-1}): 3419(br), 1613(s), 1539(m), 1447(m), 1263(s), 710(s), 1087(s), 626(s). UV/Vis [λ_{max} , nm (ϵM , $\text{M}^{-1}\text{cm}^{-1}$)] in CH_3CN : 260 (20500), 290 (14300), 310 (18000), 350 (6600), 500 (100), 630 (50), 960 (2).

[Ni^{II}(L^3)(CH_3CN)] [ClO_4] $_2 \cdot 3.5(\text{CH}_3\text{CN}) \cdot 0.5(\text{H}_2\text{O})$ (4.3): green needle crystals (69% yield). Found: C, 48.12; H, 4.20; N, 15.99. $\text{NiC}_{51}\text{H}_{50.50}\text{N}_{14.50}\text{O}_{11.50}\text{Cl}_2\text{S}_3$ requires C, 48.05; H, 3.99; N, 15.94 %; ESMS m/z (%): 881.14 (90), [$\text{Ni}(\text{L}^3) - \text{H}$] $^+$; IR (KBr pellet, cm^{-1}): 3464(br), 1616(s), 1539(m), 1488(s), 1261(s), 707(s), 1082(s), 622(s). UV/Vis [λ_{max} , nm (ϵM , $\text{M}^{-1}\text{cm}^{-1}$)]

Chapter 4: Co-ordination Behaviour of a Novel Tristhiourea Tripodal Ligand; Structural, Spectroscopic and Electrochemical properties of a series of Transition Metal Complexes

¹)] in CH₃CN: 260 (43950), 280 (36435), 320 (265000), 395 (2000), 560 (15), 795 (10), 850 (10), 1046 (16).

[Cu^{II}(L³)] [ClO₄]₂ (4.4): green glassy solid (62% yield). ESMS m/z (%): 886.13 (100), [Cu(L³) - H]⁺; IR (KBr pellet, cm⁻¹): 3448(br), 1610(s), 1523(m), 1480(s), 1261(s), 709(s), 1088(s), 621(s). UV/Vis [λ_{\max} , nm (ϵ M, M⁻¹cm⁻¹)] in CH₃CN: 242 (35700), 262 (40825), 287 (31580), 311 (27535), 430 (900), 621 (60), 975 (10).

[Zn^{II}(L³)] [ClO₄]₂.CH₃CN.CHCl₃ (4.5): colourless needle crystals (24% yield). Found: C, 43.29; H, 3.17; N, 12.13%. ZnC₄₂H₃₆N₁₀O₃S₃(CHCl₃)(CH₃CN)(ClO₄)₂ requires C, 43.37; H, 3.23; N, 12.37%; ESMS m/z (%): 887.14 (100) [Zn(L³) - H]⁺; ¹H NMR (400 MHz; CD₃CN): 4.41(6H, s); 7.49(6H, t, Ar, J=7.8Hz); 7.59(3H, d, Ar, J=7.8Hz); 7.69(6H, t, Ar, J=8.0Hz); 7.78(6H, d, Ar, J=7.5Hz); 8.23(3H, d, Ar, J=7.9Hz); 10.23(3H, s, NH); 13.39(3H, s, NH). ¹³C NMR (62.5 MHz; CD₃CN): 56.7, 123.2, 124.5, 129.5, 129.7, 131.7, 135.0, 144.5, 151.5, 155.0, 170.0, 180.7. IR (KBr pellet, cm⁻¹): 3437(br), 1623(s), 1522(s), 1447(s), 1261(s), 711(s), 1094(s), 622(s).

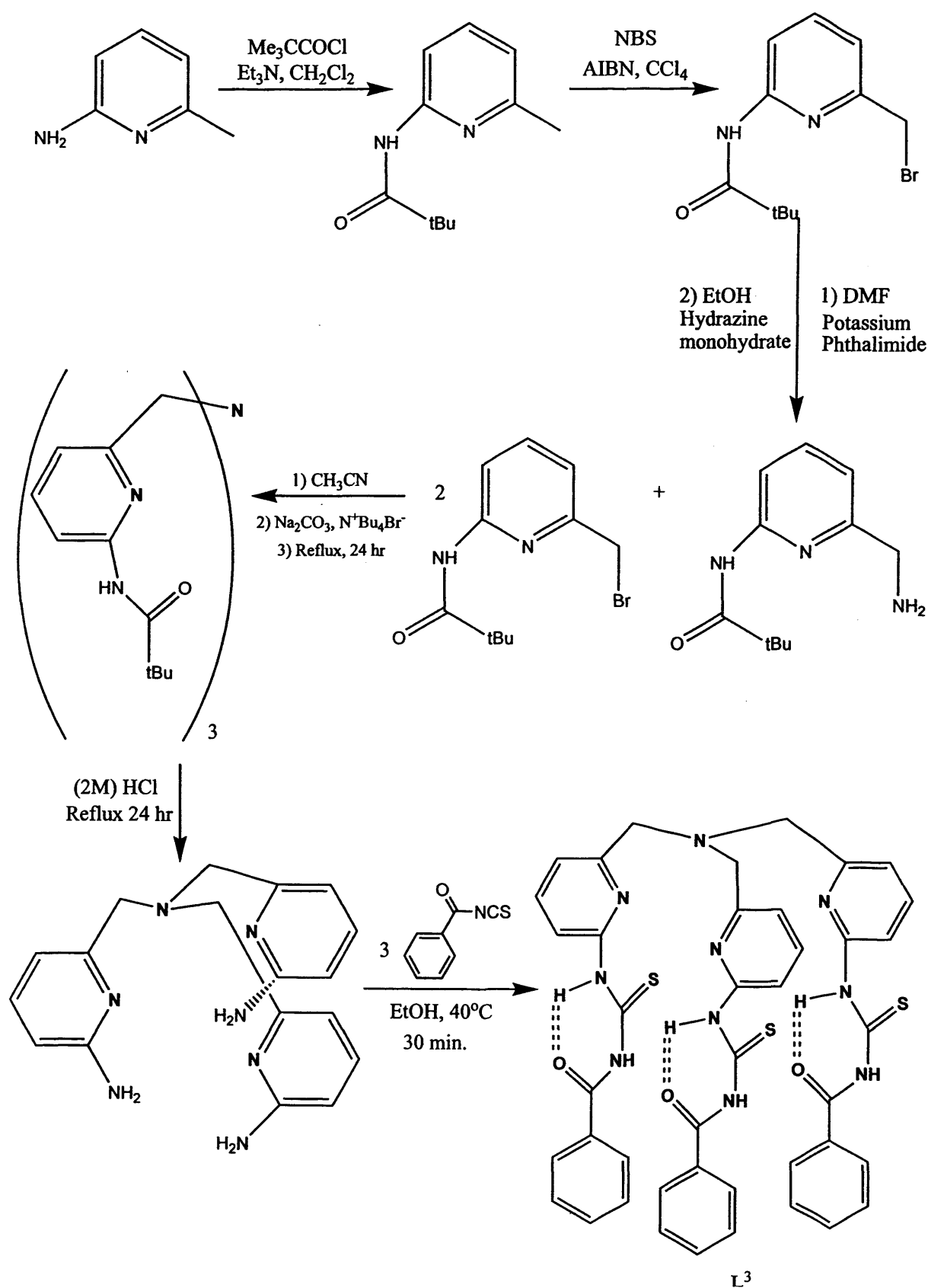
[Cd^{II}(L³)] [ClO₄]₂.0.5H₂O (4.6): colourless plate crystals (7% yield). Found: C, 43.81; H, 3.17; N, 12.02 %. CdC₄₂H₃₇N₁₀O_{11.50}Cl₂S₃ requires C, 44.04; H, 3.25; N, 12.22 %; ESMS m/z (%): 937.12 (30), [Cd(L¹) - H]⁺, 469.05 (20), [Cd(L¹) / 2]⁺; ¹H NMR (500 MHz; CD₃CN): 4.20(6H, s); 7.38(3H, d, Ar, J=7.5Hz); 7.51(3H, d, Ar, J=7.5Hz); 7.57(3H, t, Ar, J=7.6Hz); 7.58(3H, t, Ar, J=7.5Hz); 7.76(3H, t, Ar, J=7.5Hz); 7.92(3H, d, Ar, J=7.9Hz); 7.94(3H, d, Ar, J=7.9Hz); 8.12(3H, t, Ar, J=7.8Hz) 10.27(3H, s, NH); 13.60(3H, s, NH). ¹³C NMR (78 MHz; CD₃CN): 57.9, 122.3, 124.9, 129.6, 129.9, 131.9, 135.3, 143.3, 151.2, 154.0, 170.5, 181.1. IR (KBr pellet, cm⁻¹): 3450(br), 1601(s), 1522(s), 1451(s), 1263(s), 706(m), 1107(s), 620(s).

Results and Discussion

Ligand Synthesis (L^3)

The amino groups of the TAPA ligand were converted into thiourea groups via the dropwise addition of 3 equivalents of benzoyl-isothiocyanate in ethanol with continuous stirring and gentle heating up to 40°C for 30min.³² Following this addition, the reaction mixture changed from a clear yellow solution to a brown suspension. After great effort using different solvents such as acetone, CH_3CN , and $CHCl_3$ to try to isolate a clean product of L^3 , it was found that diethylether was the best solvent for washing the brown crude to isolate a white precipitate. The procedure to synthesis this ligand is illustrated in Scheme 1. L^3 is thought to be much more interesting than the bithiourea ligand L^2 in terms of binding small oxyanions due to the C_{3v} symmetrical structure of L^3 , the extra H-bonding arm may make this ligand more efficient for binding tetrahedral anions. The binding of an anion may be supported by the presence of three intramolecular hydrogen bonds occurring between C=O of the benzoyl and N-H of thiourea and that will make the other NH point towards the cavity. This particular ligand, L^3 , is similar but significantly different to the complex published by Anslyn and coworkers (Fig. 4).⁷ Anslyn's host can accommodate an anion which may also be binding to the metal centre. L^3 will have the anion more remote to the metal centre.

Chapter 4: Co-ordination Behaviour of a Novel Tristhiourea Tripodal Ligand; Structural, Spectroscopic and Electrochemical properties of a series of Transition Metal Complexes



Scheme 1: Synthetic route to L^3

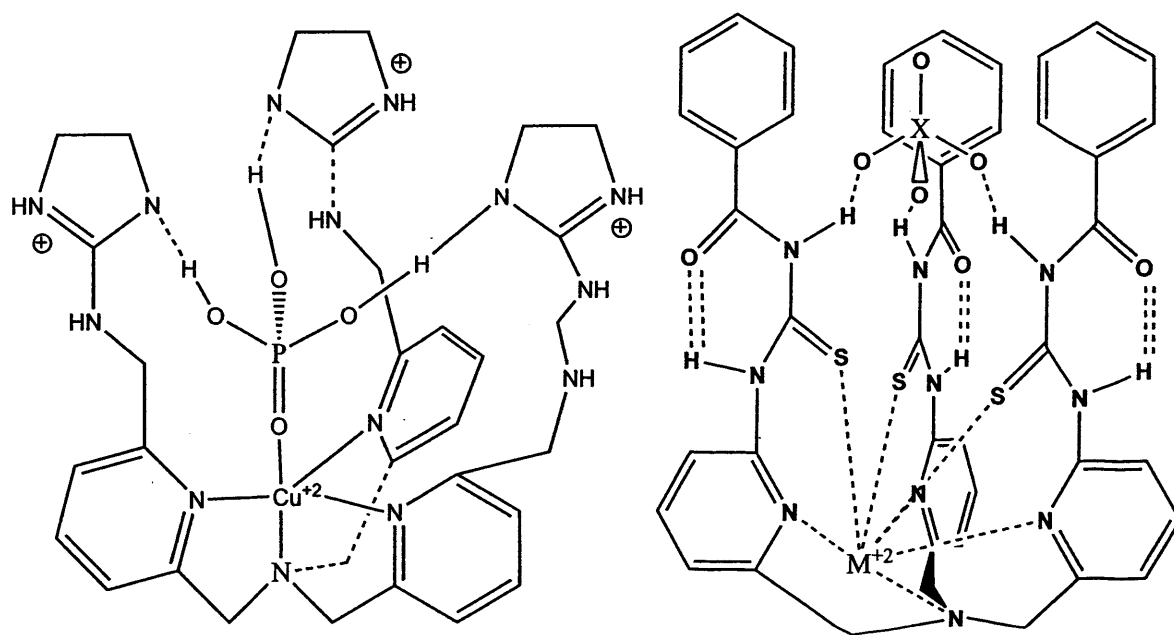


Figure 4: (Left) Ansyn structure; (right) ML³ in anion recognition.

Synthesis of Complexes

Ligand L³ (1 equivalent, typically 0.077 mmol) was dissolved in the minimum amount of CHCl₃ in the case of 4.6 or THF for all other compounds (typically 3 mL). The solutions were warmed to ca. 60°C to ensure that the ligand fully dissolved. To this stirring solution, the metal perchlorate salt (1 equivalent) dissolved in acetonitrile (ca. 2 mL) was added dropwise and left stirring for 2-3 hours with no precipitation occurred, colour change was observed for Mn²⁺ (yellow), Ni²⁺ (green). However, a colourless solution was obtained for Zn²⁺ and Cd²⁺. Recrystallisation of the compounds typically involved the diffusion of diethyl ether into mixture of acetonitrile and THF or CHCl₃ solutions which were first filtered through Celite. The yields from these reactions were moderate to high (24-69%). This crystalline material was then subsequently used for all spectroscopic measurements.

Spectroscopic Properties of Complexes

Vibrational Spectroscopy

The infra-red data observed for the complexes of L^3 are very similar to those observed for L^1 and L^2 . A very strong band at 1674 cm^{-1} , assigned to the $\nu(\text{C}=\text{O})$ vibration of L^3 (Table 1) is shifted in all complexes. A strong peak at 1331 cm^{-1} , assigned to the $\nu(\text{C}=\text{S})$ is also shifted to lower energy between $1261\text{--}1263\text{ cm}^{-1}$ typically, indicating the co-ordination of the sulfur groups to metal centres which reduces the bond order because of electrons donated by sulfur atom to metals and thus weakens the $\text{C}=\text{S}$ bond. The shift of pyridine ring vibration at around 1550 cm^{-1} and 1450 cm^{-1} in all complexes indicates coordination from the pyridine ring nitrogens. All compounds reveal two characteristic unsplit infrared active bands at $\sim 1,100\text{ cm}^{-1}$ and $\sim 622\text{ cm}^{-1}$ indicative of ionic perchlorate (T_d symmetry).^{33,34} All of these features are consistent with the X-ray diffraction data for the complexes.

Table 1: IR Stretching Frequencies of L^3 and complexes. IR spectra measured as KBr discs

Compound	$\nu(\text{C}=\text{O})$	$\nu(\text{C}=\text{S})$	$\nu(\text{O}-\text{H})$	$\nu(\text{C}=\text{N})$ and $\nu(\text{C}=\text{C})$	(C-H)	$\nu(\text{Cl}-\text{O})$
L^3	1674(s)	1331(s)	3414(br)	1598(s), 1454(s),	755(s)	-
4.1	1608(s)	1262(s)	3432(br)	1532(m), 1455(s)	706(s)	1086(s), 622(s)
4.2	1613(s)	1263(s)	3419(br)	1539(m), 1447(s)	710(s)	1087(s), 626(s)
4.3	1616(s)	1261(s)	3464(br)	1539(m), 1488(s)	707(s)	1082(s), 622(s)
4.4	1610(s)	1261(s)	3448(br)	1523(m), 1480(s)	709(s)	1088(s), 621(s)
4.5	1623(s)	1261(s)	3437(br)	1522(s), 1447(s)	711(s)	1094(s), 622(s)
4.6	1601(s)	1263(s)	3450(br)	1522(s), 1491(s)	706(m)	1107(s), 620(s)

^1H and ^{13}C NMR of Zn and Cd Complexes

Inspection of the ^1H -NMR of the Zn^{II} (4.5) and Cd^{II} (4.6) complexes, reveals that all protons have significantly deshielded compared to the free ligand. This effect is most likely caused by the presence of strong Lewis acidic Zn^{II} cation.

The ^{13}C NMR spectra of Zn^{II} complex of L^3 have been overlaid with the ^{13}C of the free ligand in (Fig. 5) which also shows the best possible ^{13}C spectra for Cd^{II} complex. It is not

Chapter 4: Co-ordination Behaviour of a Novel Tristhiourea Tripodal Ligand; Structural, Spectroscopic and Electrochemical properties of a series of Transition Metal Complexes

possible to compare these NMR due to the use of different solvents. However, it is useful to notice that the upfield signal in each case is much weaker on comparison to the other signals. Such quaternary carbons signals are often weak due to slow relaxation. Both ^{13}C NMR spectra reveal all of the expected twelve carbon atoms.

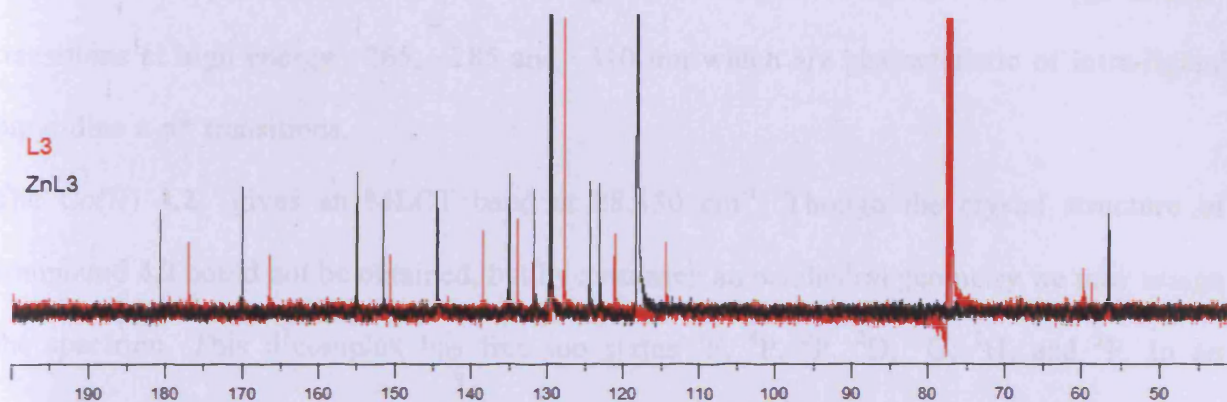


Figure 5: Superimposed ^{13}C NMR spectra of the free ligand L^3 (red), zinc complex (black).

Electronic Absorption Spectroscopy

The electronic spectra of L^3 and its complexes: Co^{2+} (4.2), Ni^{2+} (4.3) and Cu^{2+} (4.4) have been measured in solution and the significant absorption bands are presented in Table 2. The electronic absorption spectra for the free ligand L^3 and all complexes show typical $\pi-\pi^*$ transitions at high energy ~ 265 , ~ 285 and ~ 310 nm which are characteristic of intra-ligand bipyridine $\pi-\pi^*$ transitions.

The $Co(II)$ 4.2 gives an MLCT band at $28,430\text{ cm}^{-1}$. Though the crystal structure of compound 4.2 could not be obtained, but by assuming an octahedral geometry we may assign the spectrum. This d^7 complex has free ion states 4F , 4P , 2P , 2D , 2G , 2H , and 2F . In an octahedral electronic field the lowest energy free ion state, 4F , splits into two orbital triplets, $^4T_{1g}$ and $^4T_{2g}$, and an orbital singlet, $^4A_{2g}$, while the next lowest energy free ion state is 4P , remains unsplit ($^4T_{1g}$). Transitions from the ground state, $^4T_{1g}(F)$ to $^4T_{2g}(F)$, $^4A_{2g}(F)$ and $^4T_{1g}(P)$ lead to broad banded absorptions in the visible and near infrared spectral regions. Typically, the spectrum of cobalt(II) in an octahedral environment consists of a broad band in the near infrared $^4T_{1g}(F) \rightarrow ^4T_{2g}(F)$, a broad and less intense band in the visible $^4T_{1g}(F) \rightarrow ^4A_{2g}(F)$ and another broad band in the visible $^4T_{1g}(F) \rightarrow ^4T_{1g}(P)$. The band at $10,390\text{ cm}^{-1}$ is assigned to the $^4T_{1g}(F) \rightarrow ^4T_{2g}(F)$ transition and the broad absorption at $15,870\text{ cm}^{-1}$ is assigned to $^4T_{1g}(F) \rightarrow ^4A_{2g}(F)$ and the band located at $19,980\text{ cm}^{-1}$ is assigned as the $^4T_{1g}(F) \rightarrow ^4T_{1g}(P)$ transition. The octahedral cobalt compound $[Co(ntb)(OAc)](OAc)$ $ntb = \text{tris-(2-benzimidazolylmethyl)amine}$; published by Lah and Moon has shown only two d-d bands at 529 cm^{-1} and 590 cm^{-1} .³⁵

The nickel compound 4.3 gives a MLCT band at $25,200\text{ cm}^{-1}$ and four d-d transitions at $9,560\text{ cm}^{-1}$, $11,750\text{ cm}^{-1}$, $12,575\text{ cm}^{-1}$ and $17,850\text{ cm}^{-1}$ (Fig. 6). These transitions could be ascribed to $^3A_{2g} \rightarrow ^3T_{2g}$, $^3A_{2g} \rightarrow ^3T_{1g}(F)$, $^3A_{2g} \rightarrow ^1E_g(D)$ and $^3A_{2g} \rightarrow ^3T_{1g}(P)$ respectively. Using

these assignments yields $\Delta = 9,560 \text{ cm}^{-1}$; $B = 0.27$. The octahedral compound $[\{\text{Ni}(\text{terpy})(\text{NCS})_2\}_2]$ (terpy = 2,2': 6',2''-terpyridine) reported by Rojo *et. al.* exhibits the same environment of N5S around the nickel and shows three transitions at 10,600, 17,200 and 24,300 cm^{-1} , the bands have been assigned as ${}^3A_{2g} \rightarrow {}^3T_{2g}$, ${}^3A_{2g} \rightarrow {}^3T_{1g}(\text{F})$, ${}^3A_{2g} \rightarrow {}^3T_{1g}(\text{P})$ respectively.³⁶

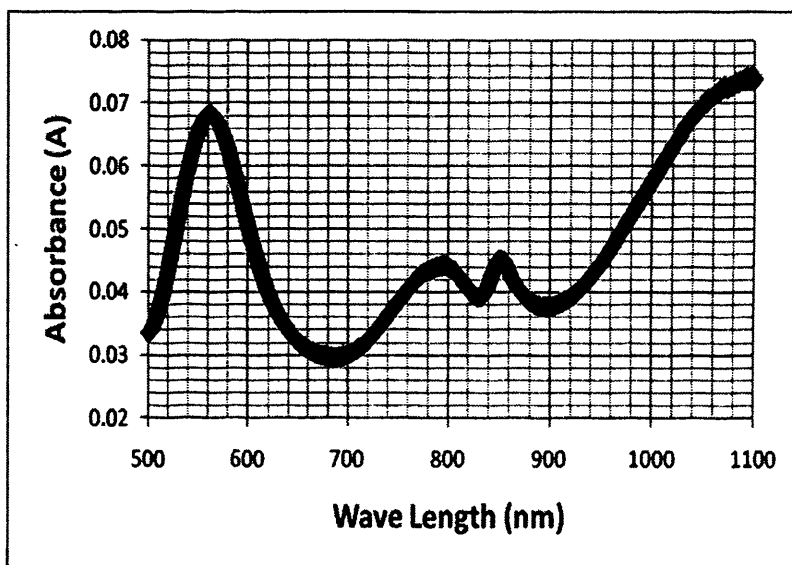


Figure 6: The electronic spectra of 4.3.

The electronic spectrum of Cu(II), 4.4, gives an electronic spectrum of a MLCT at 23,250 cm^{-1} . The electronic spectra contains a very broad asymmetric peak in the visible region which is very common for Jahn-Teller distorted Cu^{II} complexes. For all ions with a d^9 configuration. In an octahedral field, the lowest electron configuration is $t_{2g}^6 e_g^3$ leading to an 2E_g term ground state and a ${}^2T_{2g}$ term excited state. Due to the asymmetric filling of the anti-bonding e_g subset of orbitals a tetragonal distortion arises in an attempt to remove the orbital degeneracy. Consequently, the 2E_g term splits into ${}^2B_{1g}$ and ${}^2A_{1g}$, while the ${}^2T_{2g}$ term splits into ${}^2B_{2g}$ and 2E_g (Fig. 7). Thus three peaks should be observed. However, only two are observed for 4.4 at (16,100 cm^{-1} and 10,250 cm^{-1}) which are attributable to the transitions $\nu_1 = {}^2B_{2g} \leftarrow {}^2B_{1g}$, $\nu_2 = {}^2E_g \leftarrow {}^2B_{1g}$, in order of increasing energy. These transitions are tentatively

labelled as ($d_{xy} \rightarrow d_{x^2-y^2}$) and ($d_{xz/yz} \rightarrow d_{x^2-y^2}$) respectively.

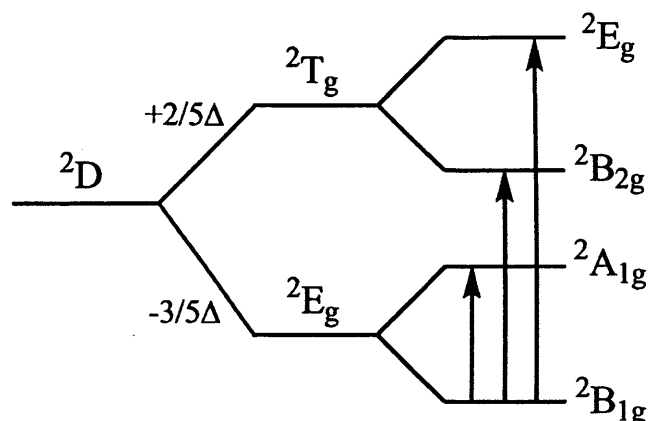


Figure 7: A splitting diagram revealing how the Jahn-Teller effect causes the 2T_g and 2E_g term symbols to split, leading to three separate transitions for the d^9 ion.

Alternatively, the compound may adapt a 5 co-ordinate trigonal bipyramidal structure similar to 3.4 which will not undergo a Jahn-Teller distortion, but will also give two peaks. Typically trigonal bipyramidal CuN_5 complexes have a band envelope of $10,500-14,600\text{ cm}^{-1}$ with a greater absorption intensity at lower energy, however this is not seen with complex 4.4.

Table 2: Electronic spectral assignments for L^3 and complexes

Compound ^a	$\pi-\pi^*$ transitions / λ (nm)	MLCT / λ (nm)	d-d transitions / λ (nm)	Δ (cm^{-1}) ^b	B (cm^{-1}) ^b	β
L^3	268(106600), 288(94200), 310(58100)	-	-	-	-	-
4.2	260(20500), 290(14300), 310(18000)	350(6600),	500(100), 630(50), 960(2)	-	-	-
4.3	260(43950), 280(36435), 320(265000)	395(2000), 560(15)	795(10), 850(10) 1046(16)	9560	285.4	0.27
4.4	242(35700), 262(40825), 287(31580), 311(27535)	430(900)	621(60), 975(10)	-	-	-

^aPerformed at room temperature (4.2, 4.3, 4.4) in CH_3CN solution, L^3 in THF solution; Numbers in parentheses indicate molar absorption coefficients ϵ ($M^{-1}cm^{-1}$). ^bvalues calculated by assuming an octahedral geometry.

Electrochemical Studies

The cyclic voltammetry experiments were carried out as mentioned in previous chapters.

Table 3: Electrochemical parameters for the redox processes exhibited by complexes 4.1, 4.2, 4.3 and 4.4 in acetonitrile solution (supporting electrolyte: $[\text{Bu}_4\text{N}][\text{PF}_6]$ (0.1 mol dm^{-3}); $T = 20 \text{ }^\circ\text{C}$). Measured at 0.1 Vs^{-1} .

Compound	E_p/V (ΔE , mV) ^{a,b}
4.1	-1.96, -1.30
4.2	-2.04
4.3	-1.83, -1.24, +0.753
4.4	-0.370 (675)

^aThe potentials at which reversible processes occur are calculated as the average of the oxidative and reductive peak potentials ($E_p^{\text{ox}} + E_p^{\text{red}}/2$). ^bFor irreversible processes, the anodic or cathodic peak potentials are given. Potentials are given in volts *versus* Ferrocenium/Ferrocene.

The cyclic voltammogram of the manganese compound, 4.1, reveals two irreversible reduction processes in the cathodic region at -1.96 V and -1.30 V referenced against ferrocenium/ferrocene (Fc^+/Fc) (Fig. 8). Discrete mononuclear complexes of manganese in a heptacoordinated environment are quite rare, thus only limited comparisons can be drawn. The seven co-ordinate manganese (II) complex of Mn-TPAA exhibits the same wave processes at +1.2 V and +1.7 V (*vs* SCE); 0.74 V and 1.24 V (*vs* Fc^+/Fc).³⁷ It seems difficult to ascribe unequivocally any of the waves to metal rather than to ligand-centered electron transfer. Such a behavior of Mn (II) complexes is not uncommon.³⁸ Interestingly, the voltammogram of compound 4.1 reveals no processes in the anodic region and thus no indication of the Mn (II/III) redox couple which is typically expected to be seen at about 0.34 V (*vs* Fc^+/Fc).

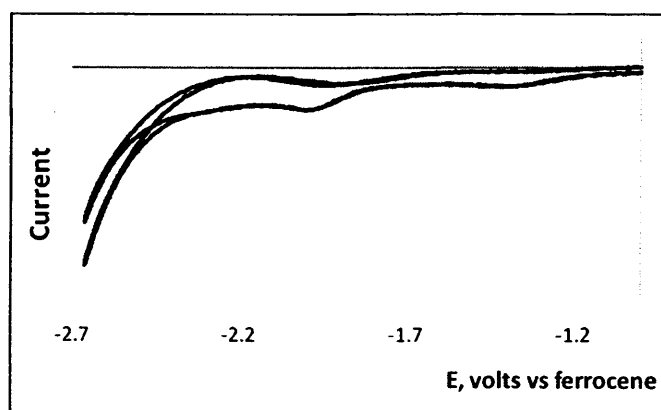


Figure 8: Cyclic voltammogram of 4.1

Chapter 4: Co-ordination Behaviour of a Novel Tristhiourea Tripodal Ligand; Structural, Spectroscopic and Electrochemical properties of a series of Transition Metal Complexes

The voltammogram of the Co^{II} complex, **4.2**, has quite similar electrochemical behaviour to the analogous Mn^{II} complex **4.1**. It shows a similar irreversible reduction at -2.04 V (vs Fc^+/Fc) (Fig. 9). By assuming an octahedral geometry for Co^{II} complex, the complex $[\text{Co}^{\text{II}}\text{H}_2\text{L}]\text{Cl}_2 \cdot 4\text{H}_2\text{O}$ ($\text{L} = \text{di-N-carboxymethylated tetraaza macrocycle}$) reported by Choi exhibits an irreversible one-electron reduction corresponding to $\text{Co}(\text{II})/\text{Co}(\text{I})$ at -0.19 V vs (Ag/AgCl); -0.69 V vs (Fc^+/Fc).³⁹ As with the Mn^{II} compound, **4.1**, without further investigation or perhaps crystalline material it is difficult to deduce the exact origins of this feature. However, the similarities of the voltammograms of **4.1** and **4.2**, does suggest that the observed processes are largely ligand based.

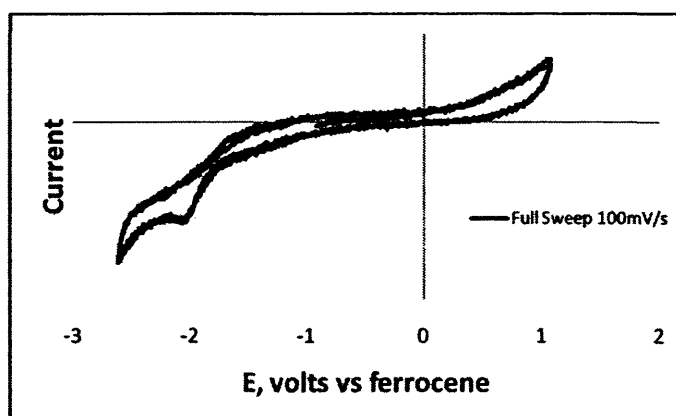


Figure 9: Cyclic voltammogram of **4.2**

The nickel complex, **4.3**, consists of a series of small and ill-defined waves in the anodic as well as in the cathodic regions suggesting rapid decomposition of the oxidized or reduced species formed (Fig. 10). The overall picture does not change upon variation of the scan rate from 100 to 500 mV/s .

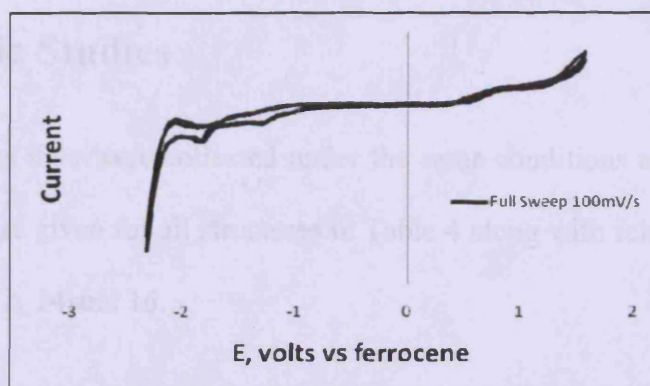


Figure 10: Cyclic voltammogram of 4.3

The voltammogram of the copper compound, 4.4, reveals a reversible redox process at -0.370 V which is typical of $\text{Cu}^{\text{II/I}}$ species (Fig. 11), a peak-to-peak separation of 675 mV, most likely attributable to the $\text{Cu}^{\text{II/I}}$ redox couple. This couple is representative of a quasi reversible behaviour.

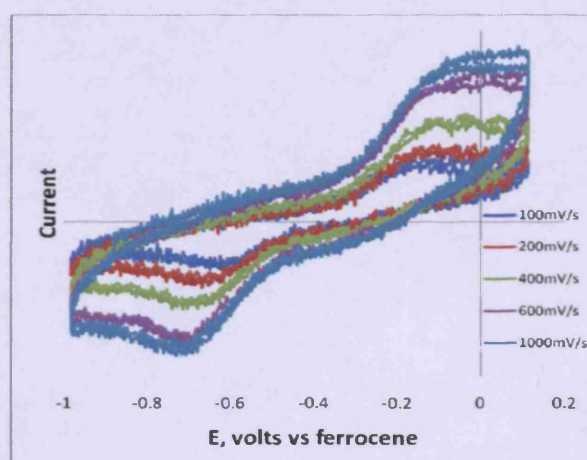


Figure 11: The reversibility of the $\text{Cu}^{\text{II/I}}$ redox couple in 4.4.

Crystallographic Studies

All single crystal X-ray data were collected under the same conditions as in previous chapters.

Relevant crystal data are given for all structures in Table 4 along with relevant bond lengths and angles in Tables 6, 9, 12, 14 and 16.

Table 4: Crystal Structure Data for 4.1, 4.3, 4.5, 4.5.1 and 4.6

compound	Chemical formula	Colour/shape	Geometry	Mw, g/mol	Crystal system	Space group	T(K)	a, Å	b, Å	c, Å	α , deg	β , deg	γ , deg	V, Å ³	Z	Observed Reflections	Unique Reflections	R_{int}	R_1 [$I > 2\sigma(I)$]	wR_2 (all data)
4.1	MnG ₄ H ₃₉ N ₁₁ O ₁₁ S ₃ Cl ₂	Colourless/plate	Capped octahedron	1119.88	Trigonal	R-3:h	293(2)	13.7370(4)	13.7370(13)	44.1110(15)	90	90	120	7208.8(8)	6	2027	1285	0.1438	0.0919	0.2051
4.3	NiC ₃₁ H _{50.3} N _{14.3} O _{11.3} Cl ₂ S ₃	Green/needle	Octahedron	1276.35	Triclinic	P-1	293(2)	13.8450(5)	14.6430(5)	15.8030(6)	107.831(2)	97.828(2)	94.342(2)	2997.95(19)	2	13501	6566	0.1043	0.0898	0.2437
4.5	ZnC ₄₃ H ₄₀ N ₁₁ O ₁₁ Cl ₅ S ₃	Colourless/needle	trigonal bipyramid	1249.68	Orthorhombic	Pccn	150(2)	30.5910(3)	19.7950(3)	17.5370(5)	90	90	90	10619.5(4)	8	7326	5489	0.0869	0.0834	0.2117
4.5.1	ZnC ₄₃ H _{41.3} N _{11.3} O _{11.3} Cl ₂ S ₃	Colourless/plate	Capped octahedron	1159.85	Triclinic	P-1	150(2)	13.7530(2)	13.9620(2)	16.3920(3)	69.2030(10)	71.1580(10)	61.9880(10)	2550.83(7)	2	11611	9541	0.0289	0.0884	0.2644
4.6	CdC ₄₂ H ₃₇ N ₁₀ O _{11.3} Cl ₂ S ₃	Colourless/plate	Capped octahedron	1145.30	Trigonal	R-3	150(2)	13.8780(17)	13.8780(17)	43.257(8)	90	90	120	7215.1(18)	6	1420	1008	0.1127	0.0856	0.2593

Crystal Structure of $[\text{Mn}^{\text{II}}(\text{L}^3)][\text{ClO}_4]_2 \cdot \text{CH}_3\text{CN}$ (4.1)

The manganese compound crystallises in the trigonal space group R-3:h and contains one complex within the asymmetric unit (asu) (Fig. 12). The Mn^{II} ion lies at the centre of a slightly distorted capped octahedron co-ordination geometry which is confirmed by Continuous Shape Mapping (CShM) (Fig. 13; Table 5). The Mn^{II} ion is surrounded by two types of donor atoms. There are four nitrogen donors (N1, N2, N5 and N8) and three sulfur donors (S1, S2 and S3). The co-ordinative bond lengths range from 2.280(15) Å to 2.618(2) Å. This is the first example of a complex where the Mn^{II} cation is surrounded by this particular donor set. The co-ordinative bond lengths are given in Table 6. The bridge head nitrogen donor (N1) is shorter than expected when compared to the related octahedral compound $[\text{Mn}^{\text{II}}(\text{TPA})][\text{Cl}]_2$ reported by Ogo *et al.*, which comes at 2.388(2) Å whereas it is at 2.280 (15) Å for the manganese 4.1.⁴⁰ However, the other nitrogen donors N2, N2ⁱ and N2ⁱⁱ are longer in comparison to the same example and this due to the co-ordination of three sulphurs which make the length of Mn-N(pyridyl) a bit longer than expected for a typical TPA complex. When compared to other 7-coordinate manganese complexes involving similar TPA frameworks, the co-ordinative bond lengths and angles seem to be shorter. For example, the compound reported by Baldeau *et al.* exhibits co-ordinating N-pyridyl groups at 2.292(17) Å which is shorter than the nitrogen pyridyl for 4.1.⁴¹ Three hydrogens located on N4, N4ⁱⁱ, N4ⁱⁱⁱ are directed towards the cavity and interact with the tetrahedral perchlorate ion via three intra-hydrogen bonds (Fig. 14; Table 7). A similar behaviour for phosphate ion has been reported by Tobey and Anslyn.⁷ Another intra-molecular hydrogen bond between the NH of the amide and the carbonyl group of each arm is observed in Mn complex and all other analogues 4.5, 4.5.1 and 4.6 (Fig. 14).

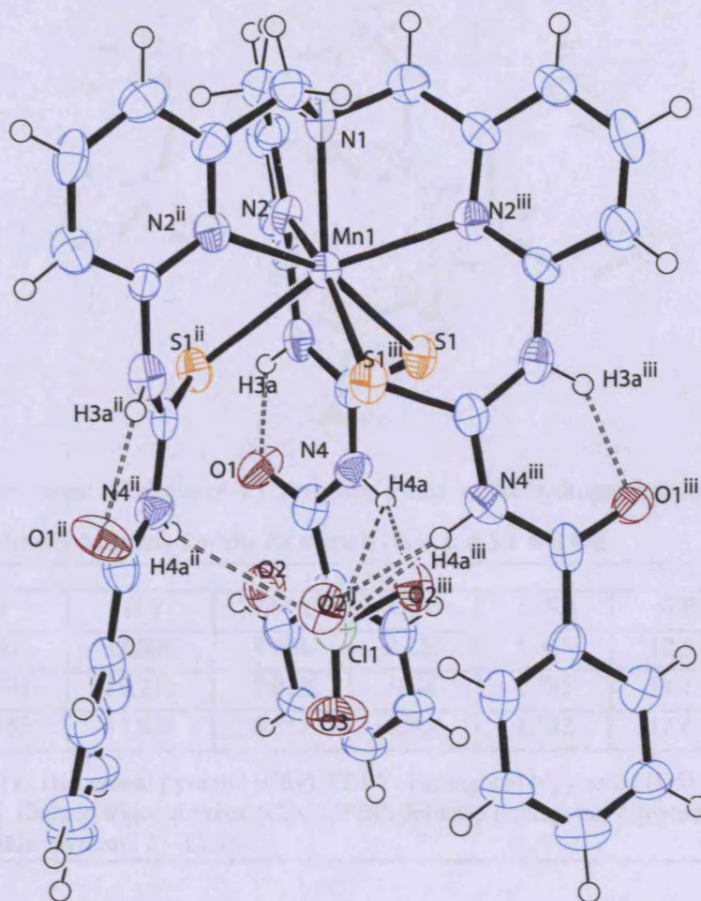


Figure 12: The asymmetric unit of 4.1. Displacement ellipsoids are shown at 50% probability. H atoms are of arbitrary size. H-bonds are represented by dashed lines.

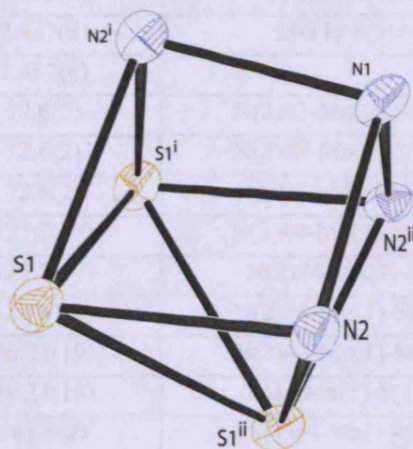


Figure 13: A view of the core geometry of 4.1 of covalent bond radius less than 3.

Chapter 4: Co-ordination Behaviour of a Novel Trithiourea Tripodal Ligand; Structural, Spectroscopic and Electrochemical properties of a series of Transition Metal Complexes

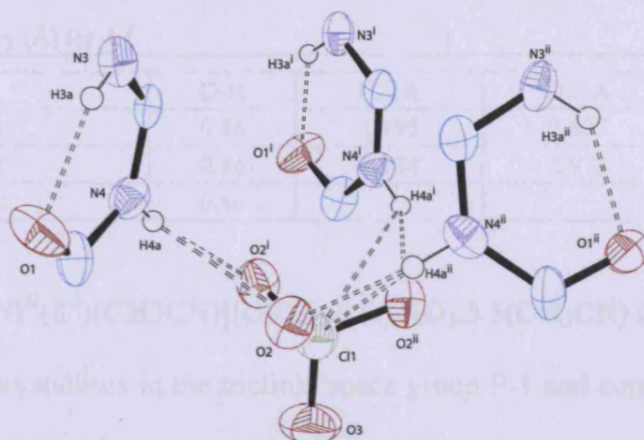


Figure 14: A fragment of the asu of **4.1**, revealing a view of the hydrogen bonding interactions.

Table 5: Continuous Symmetry Mapping Results for complexes **4.1**, **4.5.1** and **4.6**

Structure	HP	HPY	PBPY	OCF	TPRS	JPBP	(JETPY)
Mn (4.1)	37.401	18.305	8.251	0.256	1.648	12.515	20.799
Zn (4.5.1)	36.791	19.211	7.029	0.46	1.295	11.199	19.843
Cd (4.6)	37.652	17.858	8.353	0.304	1.722	12.639	20.967

HP: Heptagon (D7h), HPY: Hexagonal pyramid (C6v), PBPY: Pentagonal bipyramid (D5h), OCF: Capped octahedron (C3v), TPRS: Capped trigonal prism (C2v), JPBP: Johnson pentagonal bipyramid J13 (D5h), JETPY: Johnson elongated triangular pyramid J7 (C3v).

Table 6: Selected Bond lengths (Å) and Angles (°) for [MnL³]²⁺ **4.1**

Mn(1)-N(1)	2.280(15)	Mn(1)-S(1)	2.618(2)
Mn(1)-N(2)	2.438(8)	Mn(1)-S(1)#3	2.618(2)
Mn(1)-N(2)#3	2.437(8)	Mn(1)-S(1)#4	2.617(2)
Mn(1)-N(2)#4	2.437(8)		
N(1)-Mn(1)-N(2)	72.6(2)	N(2)#3-Mn(1)-S(1)#3	76.22(19)
N(1)-Mn(1)-N(2)#3	72.6(2)	N(2)#3-Mn(1)-S(1)#4	79.27(19)
N(1)-Mn(1)-N(2)#4	72.6(2)	N(2)#4-Mn(1)-N(2)	111.47(19)
N(1)-Mn(1)-S(1)	125.76(7)	N(2)#4-Mn(1)-N(2)#3	111.50(19)
N(1)-Mn(1)-S(1)#3	125.75(7)	N(2)#4-Mn(1)-S(1)	79.26(19)
N(1)-Mn(1)-S(1)#4	125.77(7)	N(2)#4-Mn(1)-S(1)#3	161.5(2)
N(2)-Mn(1)-S(1)	76.21(19)	N(2)#4-Mn(1)-S(1)#4	76.25(19)
N(2)-Mn(1)-S(1)#3	79.23(19)	S(1)-Mn(1)-S(1)#3	89.28(10)
N(2)-Mn(1)-S(1)#4	161.5(2)	S(1)#4-Mn(1)-S(1)	89.30(10)
N(2)#3-Mn(1)-N(2)	111.46(19)	S(1)#4-Mn(1)-S(1)#3	89.30(10)
N(2)#3-Mn(1)-S(1)	161.5(2)		

Symmetry transformations used to generate equivalent atoms:

#1 -y+1,x-y+1,z #2 -x+y,-x+1,z #3 -x+y+1,-x+1,z

#4 -y+1,x-y,z

Table 7: H-bonding geometry (Å) for 4.1

D-H...A	D-H	H...A	D...A	D-H...A
N3-H3A ...O1	0.86	1.935	2.627	136.55
N4-H4A ...O2	0.86	2.184	2.973	152.26
N4-H4A ...Cl2	0.86			

Crystal Structure of $[\text{Ni}^{\text{II}}(\text{L}^3)(\text{CH}_3\text{CN})][\text{ClO}_4]_2 \cdot 0.5(\text{H}_2\text{O}) \cdot 3.5(\text{CH}_3\text{CN})$ (4.3)

The nickel compound crystallises in the triclinic space group P-1 and contains a single complex within the asu (Fig. 15). The geometry of 4.3 was calculated by continuous shape mapping to be octahedron as shown in Table 8. The co-ordinative nitrogen bond lengths range from 2.054(4) Å to 2.262(4) Å (Fig. 16; Table 9). Interestingly, there are two Ni-N bond lengths which are markedly longer than the others [Ni-N(8) 2.262(4), Ni-N(5) 2.26(4) compared to the other Ni-N 2.054-2.074(4)]; the long Ni-N bonds correspond to the pyridyl donors containing the thiourea groups which do not co-ordinate to the metal centre. The related compound $[\text{Ni}(\text{terpy})(\text{NCS})_2]$; (terpy = 2,2': 6',2"-terpyridine) reported by Rojo *et al*, exhibits co-ordinative bond lengths ranging between 1.97(1) Å and 2.09(1) Å in a distorted octahedral environment. Clearly these bond lengths are similar to the shorter Ni-N bonds observed in 4.3. However, the Ni^{II}-S bond is longer in the $\text{Ni}(\text{terpy})(\text{NCS})_2$ (2.62(5) Å), as it is 2.344(14) Å in 4.3.³⁶ In the related complex, $[\text{Ni}^{\text{II}}(\text{TPA})(\text{NCS})_2]$, the bond lengths of the Ni-N are shorter in all pyridyl nitrogen but longer for the bridge head nitrogen.⁴² As in all structurally characterised complexes of L^3 , there is strong intramolecular hydrogen bonding between the amide and the carbonyl in each arm (Table 10). The structure is very similar to the Ni-bisthiourea tripodal complex in terms of bond length and angles as well as the geometry (chapter 3; page 101).

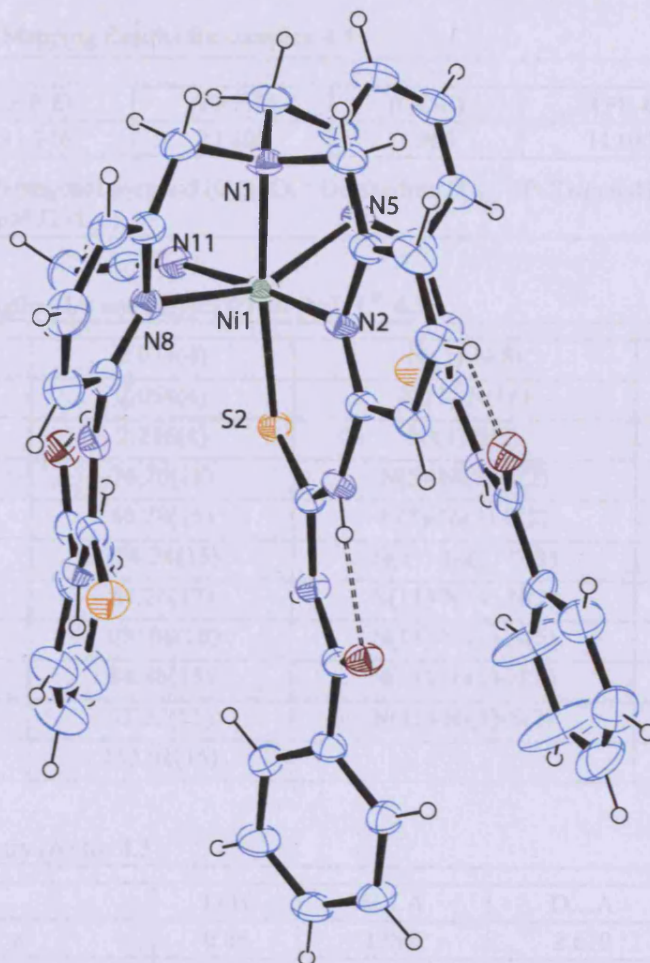


Figure 15: The asymmetric unit of 4.3. Displacement ellipsoids are shown at 50% probability. H atoms are of arbitrary size. H-bonds are represented by dashed lines.

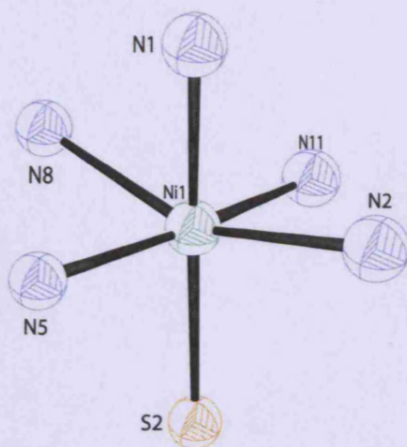


Figure 16: A view of the core geometry of 4.3 of covalent bond radius less than 3.

Chapter 4: Co-ordination Behaviour of a Novel Trithiourea Tripodal Ligand; Structural, Spectroscopic and Electrochemical properties of a series of Transition Metal Complexes

Table 8: Continuous Shape Mapping Results for complex 4.3

Structure	(HP-6)	(PPY-6)	(OC-6)	(TPR-6)	(JPPY-6)
4.3	31.376	23.400	1.969	11.013	27.458

HP: Hexagon (D_{6h}), PPY: Pentagonal pyramid (C_{5v}), OC: Octahedron (O_h), TP: Trigonal Pyramidal (D_{3h}), JPPY: Johnson's pentagonal pyramid J2 (C_{5v}).

Table 9: Selected Bond lengths (\AA) and Angles ($^\circ$) for $[\text{NiL}^3]^{2+}$ 4.3

Ni(1)-N(1)	2.074(4)	Ni(1)-N(8)	2.262(4)
Ni(1)-N(2)	2.054(4)	Ni(1)-N(11)	2.054(5)
Ni(1)-N(5)	2.216(4)	Ni(1)-S(2)	2.3441(14)
N(1)-Ni(1)-N(5)	76.70(16)	N(5)-Ni(1)-S(2)	99.06(12)
N(1)-Ni(1)-N(8)	80.28(16)	N(8)-Ni(1)-S(2)	104.36(11)
N(1)-Ni(1)-S(2)	174.24(13)	N(11)-Ni(1)-N(1)	97.44(18)
N(2)-Ni(1)-N(1)	84.26(17)	N(11)-Ni(1)-N(2)	173.35(16)
N(2)-Ni(1)-N(5)	100.08(16)	N(11)-Ni(1)-N(5)	86.57(17)
N(2)-Ni(1)-N(8)	84.46(15)	N(11)-Ni(1)-N(8)	89.48(17)
N(2)-Ni(1)-S(2)	92.72(11)	N(11)-Ni(1)-S(2)	86.11(13)
N(5)-Ni(1)-N(8)	155.91(16)		

Table 10: H-bonding geometry (\AA) for 4.3

D-H...A	D-H	H...A	D...A	D-H...A
N6-H6_a ...O1_a	0.86	1.906	2.610	138.11
N3-H3A_a ...O2_a	0.86	1.878	2.602	140.78
N9-H9_a...O3_a	0.86	1.876	2.608	142.11

Crystal Structure of $[\text{Zn}^{\text{II}}(\text{L}^3)][\text{ClO}_4]_2 \cdot \text{CH}_3\text{CN} \cdot \text{CHCl}_3$ (4.5)

The zinc compound crystallises in the orthorhombic space group Pccn and contains one complex within the asu (Fig. 17). The Zn^{II} cation lies at the centre of a slightly distorted trigonal bipyramid geometry (Fig. 18; Table 11) and reveals a completely different co-ordination environment to the related Mn^{II} and Ni^{II} complexes. There are three equatorial nitrogen donors (N2, N5 and N8) from the pyridyl groups, with the bridge-head nitrogen, and a sulfur donor occupying axial position. The equatorial co-ordinative bond lengths vary from 2.105(6) Å to 2.148(6) Å (Table 12) which is a slightly longer range in terms of M-N bonds of the pyridyl on comparison to the similar compound reported by Duboc *et al*, $[\text{Zn}^{\text{II}}(\text{TPA})\text{Cl}]\text{Cl}$ [2.062(2) Å-2.083(2) Å] whereas the bridge head nitrogen is longer in the given example at 2.264(2) Å in a trigonal bipyramidal environment and that is shorter than observed in 4.5 (2.346(2) Å).⁴³ Finally, a perchlorate counter ion is hydrogen bonded to the amide N3-H3A...O9 at 2.39 Å (Fig. 19; Table 19). Another structure for the same sample shows different geometry 4.5.1.

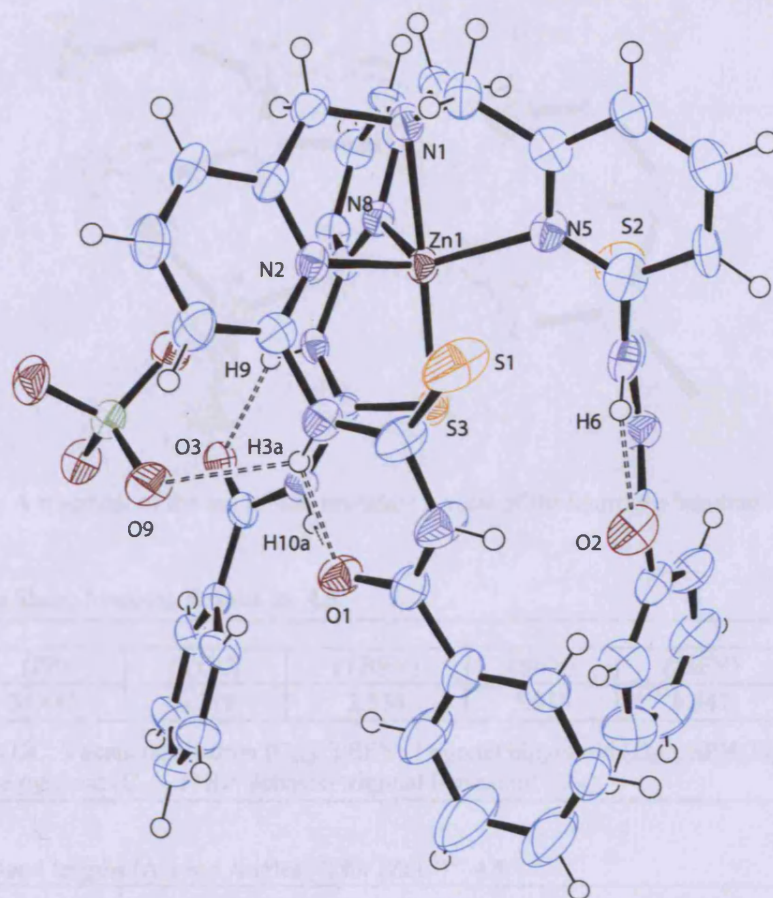


Figure 17: The asymmetric unit of **4.5**. Displacement ellipsoids are shown at 50% probability. H atoms are of arbitrary size. H-bonds are represented by dashed lines.

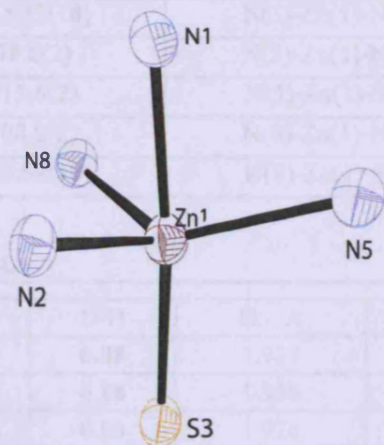


Figure 18: A view of the core geometry of **4.5** of covalent bond radius less than 3.

Chapter 4: Co-ordination Behaviour of a Novel Trithioureia Tripodal Ligand; Structural, Spectroscopic and Electrochemical properties of a series of Transition Metal Complexes

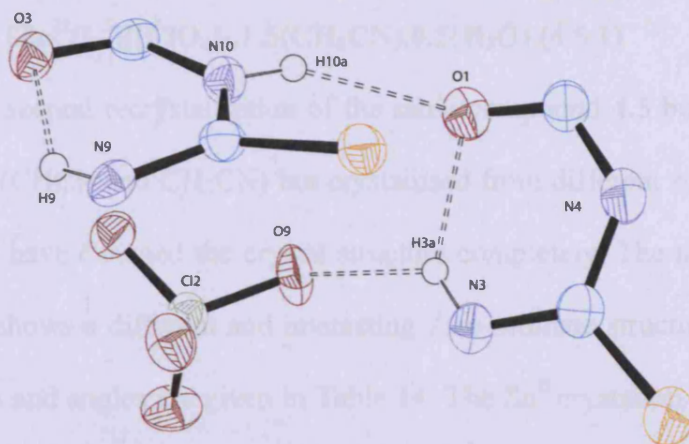


Figure 19: A fragment of the asu of **4.5**, revealing a view of the hydrogen bonding interactions

Table 11: Continuous Shape Mapping Results for **4.5**.

Structure	(PP)	(VOC)	(TBPY)	(SPY)	(JSPY)	(JTBP)
Zn (4.5)	34.445	6.547	2.554	5.013	6.547	4.134

PP: Pentagon (D_{5h}), VOC: Vacant octahedron (C_{4v}), TBPY: Trigonal bipyramid (D_{3h}), SPY: Square pyramid (C_{4v}), JSPY: Johnson square pyramid (C_{4v}), JTBP: Johnson trigonal bipyramid (D_{3h}).

Table 12: Selected Bond lengths ($^{\circ}$) and Angles ($^{\circ}$) for $[ZnL^{3-}]^{2+}$ **4.5**

Zn(1)-N(1)	2.162(6)	Zn(1)-N(8)	2.148(6)
Zn(1)-N(2)	2.105(6)	Zn(1)-S(3)	2.346(2)
Zn(1)-N(5)	2.107(6)		
N(1)-Zn(1)-S(3)	165.52(18)	N(5)-Zn(1)-N(1)	78.6(2)
N(2)-Zn(1)-N(1)	78.6(2)	N(5)-Zn(1)-N(8)	123.1(2)
N(2)-Zn(1)-N(5)	115.6(2)	N(5)-Zn(1)-S(3)	108.07(18)
N(2)-Zn(1)-N(8)	108.0(2)	N(8)-Zn(1)-N(1)	76.0(2)
N(2)-Zn(1)-S(3)	108.69(18)	N(8)-Zn(1)-S(3)	89.72(17)

Table 13: H-bonding geometry (\AA) for **4.5**

D-H...A	D-H	H...A	D...A	D-H...A
N3-H3A...O1	0.88	1.921	2.610	133.94
N6-H6...O2	0.88	1.930	2.608	132.59
N9-H9...O3	0.88	1.926	2.634	136.45
N3-H3A...O9	0.88	2.393	3.044	131.04
N10-H10A...O1	0.88	2.236	3.058	155.37

Crystal Structure of $[\text{Zn}^{\text{II}}(\text{L}^3)][\text{ClO}_4]_2 \cdot 1.5(\text{CH}_3\text{CN}) \cdot 0.5(\text{H}_2\text{O})$ (4.5.1)

This structure is of a second recrystallisation of the same compound 4.5 but the compound was not crystallised from (CHCl_3 and CH_3CN) but crystallised from different solvents, (CH_3CN and H_2O). These solvents have changed the crystal structure completely. The molecule is no longer five co-ordinate and shows a different and interesting 7 co-ordinate structure shown in Fig. 20. Selected bond lengths and angles are given in Table 14. The Zn^{II} crystallises in the triclinic space group P-1 and contains one complex within the asu. The geometry of the complex is best considered as a slightly distorted capped octahedron with the metal ion and four nitrogen atoms (N1, N2, N5 and N8) and three sulfurs (Fig. 21). It is of high similarity in co-ordination sphere, geometry and bond length and angles to the analogous Mn^{II} (4.1) and surprisingly Cd^{II} (4.6) (Table 5). It is also the first example of this particular donor set where the zinc is surrounded by N4S3 donor atoms. When compare it to the compound tris(4-tert-butyl-2-mercaptobenzyl)-1,4,7-triazacyclononane N3S3 set, the Zn-S bonds length are almost identical and vary from 2.564(4) Å to 2.583(4) Å although the Zn-N bond lengths are significantly shorter and range between 2.21(1) Å and 2.25 (1) Å.⁴⁴ It is similar to the analogues Mn^{II} and Cd^{II} where the perchlorate anion is held in the cavity by three intermolecular hydrogen bonds (Fig. 22; Table 15). This is a remarkable structure as the Zn-L bond lengths are in general much longer than those normally seen even for 7 co-ordinate Zn structures. Whether this is caused by the inclusion of the ClO_4^- into the host remains unclear, but clearly its inclusion will in some ways expand the ligand framework.

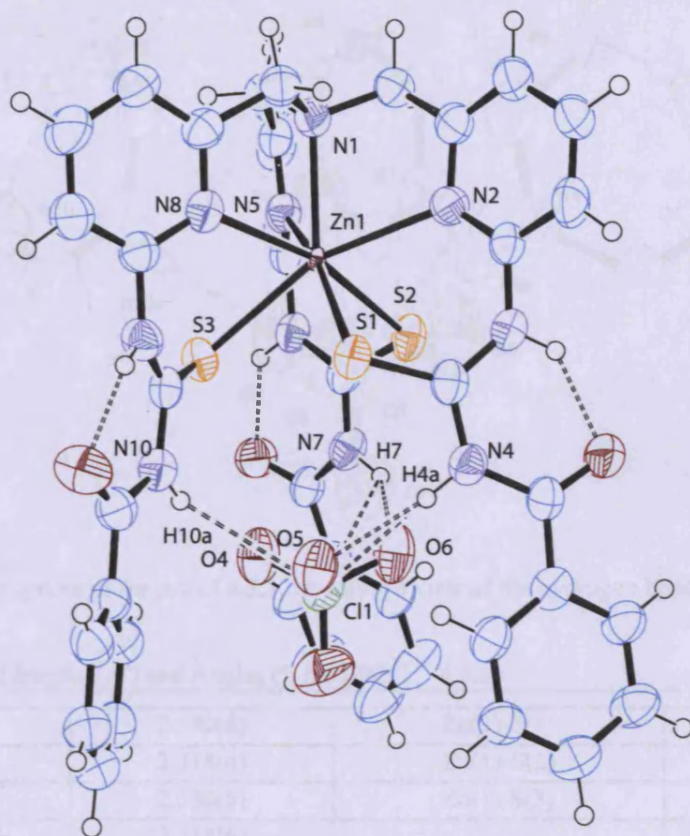


Figure 20: The asymmetric unit of 4.5.1. Displacement ellipsoids are shown at 50% probability. H atoms are of arbitrary size. H-bonds are represented by dashed lines.

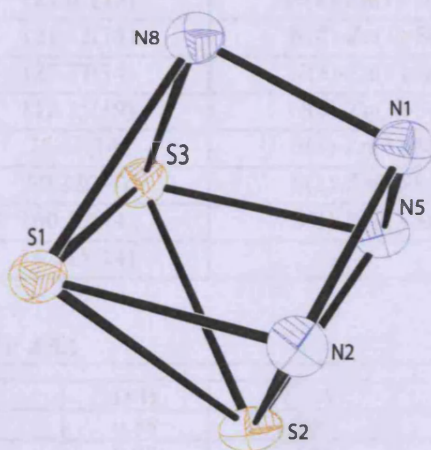


Figure 21: A view of the core geometry of 4.5.1 of covalent bond radius less than 3.

Chapter 4: Co-ordination Behaviour of a Novel Trithioureia Tripodal Ligand; Structural, Spectroscopic and Electrochemical properties of a series of Transition Metal Complexes

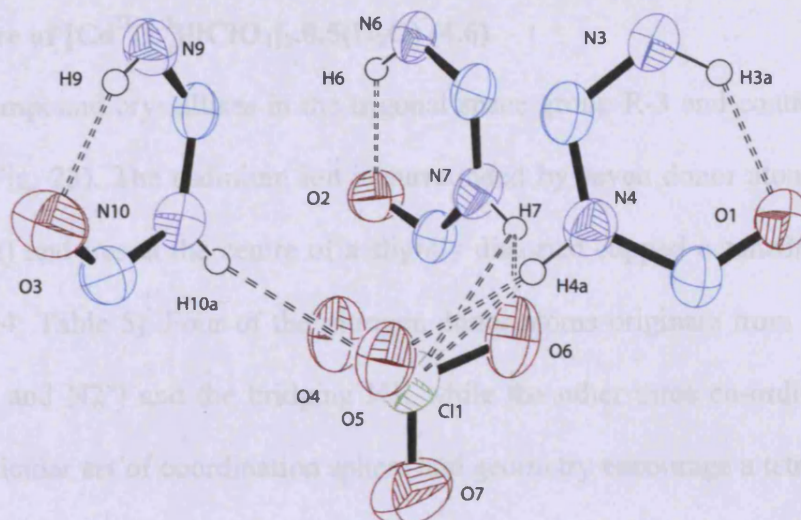


Figure 22: A fragment of the asu of 4.5.1, revealing a view of the hydrogen bonding interactions

Table 14: Selected Bond lengths (Å) and Angles (°) for $[ZnL^3]^{2+}$ 4.5.1

Zn(1)-N(1)	2.380(6)	Zn(1)-S(1)	2.6911(18)
Zn(1)-N(2)	2.518(6)	Zn(1)-S(2)	2.6602(17)
Zn(1)-N(5)	2.530(6)	Zn(1)-S(3)	2.6783(17)
Zn(1)-N(8)	2.514(6)		
N(1)-Zn(1)-N(2)	71.42(19)	N(5)-Zn(1)-S(2)	75.09(13)
N(1)-Zn(1)-N(5)	70.12(19)	N(5)-Zn(1)-S(3)	80.64(13)
N(1)-Zn(1)-N(8)	71.2(2)	N(8)-Zn(1)-N(2)	110.32(19)
N(1)-Zn(1)-S(1)	127.67(15)	N(8)-Zn(1)-N(5)	106.84(18)
N(1)-Zn(1)-S(2)	121.13(15)	N(8)-Zn(1)-S(1)	83.12(14)
N(1)-Zn(1)-S(3)	127.77(14)	N(8)-Zn(1)-S(2)	166.59(15)
N(2)-Zn(1)-N(5)	112.35(19)	N(8)-Zn(1)-S(3)	77.61(14)
N(2)-Zn(1)-S(1)	76.45(14)	S(2)-Zn(1)-S(1)	91.84(6)
N(2)-Zn(1)-S(2)	80.32(14)	S(2)-Zn(1)-S(3)	89.78(6)
N(2)-Zn(1)-S(3)	160.59(14)	S(3)-Zn(1)-S(1)	87.32(5)
N(5)-Zn(1)-S(1)	162.15(14)		

Table 15: H-bonding geometry (Å) for 4.5.1

D-H...A	D-H	H...A	D...A	D-H...A
N3-H3A ...O1	0.88	1.909	2.613	135.81
N3-H3A ...N11	0.88	2.480	3.147	133.06
N4-H4A ...O5	0.88	2.198	3.061	166.89
N4-H4A ...O6	0.88	2.567	3.022	113.03
N4-H4A ...Cl1	0.88	2.926	3.661	142.13
N6-H6...O2	0.88	1.928	2.620	134.29
N7-H7...O6	0.88	2.248	3.004	143.85
N9-H9...O3	0.88	1.849	2.573	138.26
N10-H10A...O4	0.88	2.195	3.057	166.25
N10-H10A...O5	0.88	2.597	3.085	115.97
N10-H10A...Cl1	0.88	2.924	3.676	144.56

Crystal Structure of [Cd^{II}(L³)](ClO₄)₂·0.5(H₂O) (4.6)

The cadmium compound crystallises in the trigonal space group R-3 and contains one complex within the asu (Fig. 23). The cadmium ion is surrounded by seven donor atoms (four N atoms and three S atom) and lies at the centre of a slightly distorted capped octahedron co-ordination geometry (Fig. 24; Table 5). Four of the nitrogen donor atoms originate from the three pyridyl groups (N2, N2ⁱ and N2ⁱⁱ) and the bridging N1, while the other three co-ordinating atoms are sulfurs. This particular set of coordination sphere and geometry encourage a tetrahedron anion to be bound in the cavity via three hydrogen bond interactions (Fig. 25), such behaviour is not only occurring for the cadmium complex, it is also noticed for the analogous Mn^{II}(4.1) and Zn^{II}(4.5.1). This is the first example of crystallographically characterised co-ordination spheres involving N4S3 around a cadmium centre. The bond lengths between the pyridyl N-donors and the central Cd^{II} cation lie within the expected ranges on comparison to similar complexes, particularly the compound [Cd(SMDTC)₃]·2NO₃ synthesised by Bera *et al.* which comprises a N3S3 co-ordination sphere around the cadmium centre.⁴⁵ This example has Cd^{II}-S bond lengths range between 2.609(7) Å and 2.723(7) Å. There is only one structure of Cd in TPA environment. It is surrounded by N4O3 donor set. The Cd-N pyridyl bond lengths of this example is shorter than those observed for 4.6 and vary between 2.30(1) Å- 2.35(1) Å.⁴⁶ Cd^{II} (4.6) is again of high similarity in co-ordination sphere, geometry, bond length and angles and in hosting the perchlorate to the analogous Mn^{II}(4.1), Zn^{II}(4.5.1).

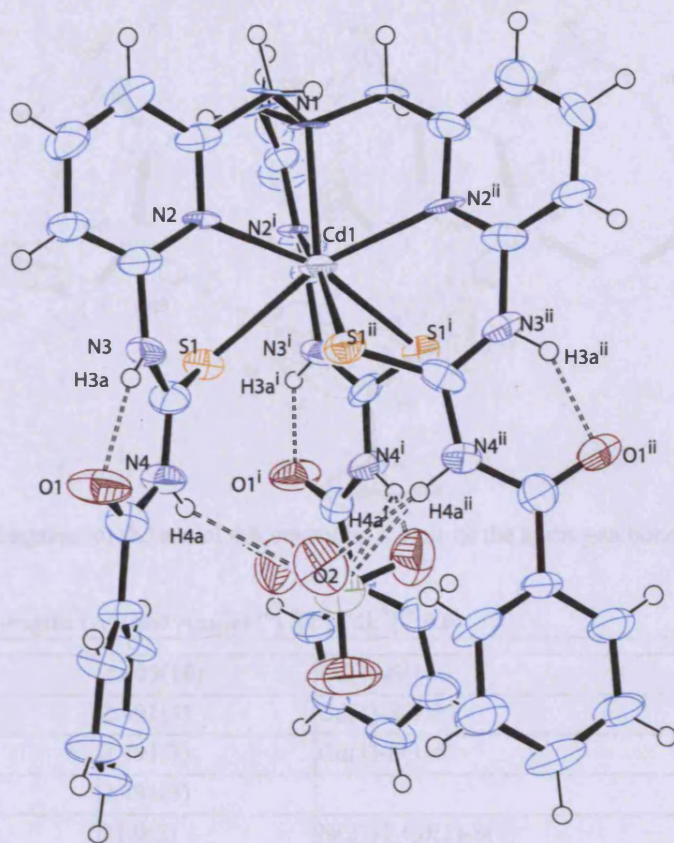


Figure 23: The asymmetric unit of 4.6. Displacement ellipsoids are shown at 50% probability. H atoms are of arbitrary size. H-bonds are represented by dashed lines.

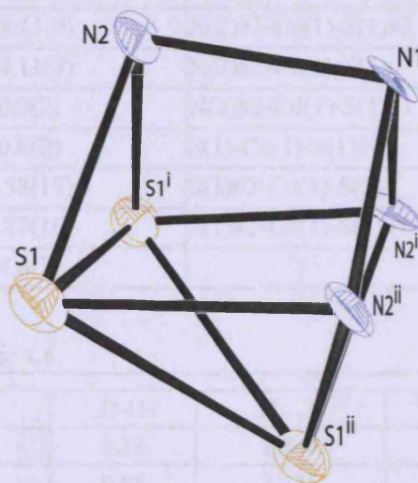


Figure 24: A view of the core geometry of 4.6 of covalent bond radius less than 3.

Chapter 4: Co-ordination Behaviour of a Novel Trithioureia Tripodal Ligand; Structural, Spectroscopic and Electrochemical properties of a series of Transition Metal Complexes

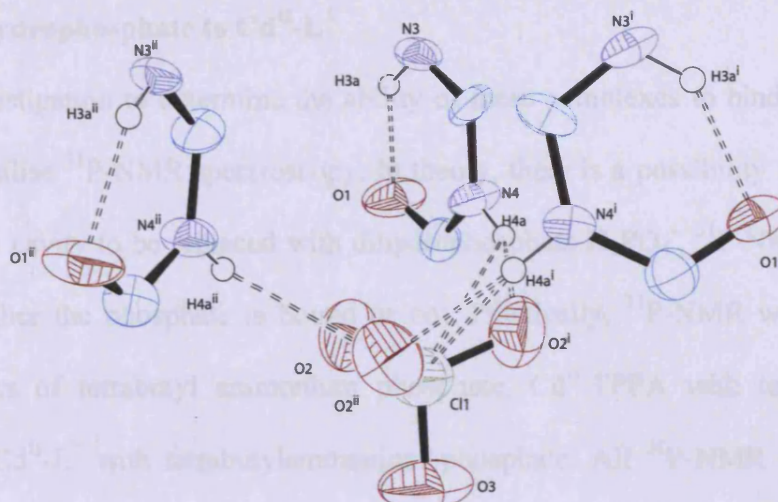


Figure 25: A fragment of the asu of **4.6**, revealing a view of the hydrogen bonding interactions

Table 16: Selected Bond lengths (Å) and Angles (°) for $[\text{CdL}^3]^{2+}$ **4.6**

Cd(1)-N(1)	2.405(10)	Cd(1)-S(1)	2.661(4)
Cd(1)-N(2)	2.491(3)	Cd(1)-S(1)#1	2.661(4)
Cd(1)-N(2)#1	2.491(3)	Cd(1)-S(1)#2	2.661(4)
Cd(1)-N(2)#2	2.491(3)		
N(1)-Cd(1)-N(2)	71.0(2)	N(2)#1-Cd(1)-S(1)	164.8(2)
N(1)-Cd(1)-N(2)#1	71.0(2)	N(2)#1-Cd(1)-S(1)#1	76.58(17)
N(1)-Cd(1)-N(2)#2	71.0(2)	N(2)#1-Cd(1)-S(1)#2	79.27(16)
N(1)-Cd(1)-S(1)	124.11(9)	N(2)#2-Cd(1)-N(2)#1	110.0(2)
N(1)-Cd(1)-S(1)#1	124.11(9)	N(2)#2-Cd(1)-S(1)#2	76.58(17)
N(1)-Cd(1)-S(1)#2	124.11(9)	N(2)#2-Cd(1)-S(1)	79.27(16)
N(2)-Cd(1)-N(2)#1	110.0(2)	N(2)#2-Cd(1)-S(1)#1	164.8(2)
N(2)-Cd(1)-N(2)#2	110.0(2)	S(1)-Cd(1)-S(1)#1	91.63(13)
N(2)-Cd(1)-S(1)	76.58(17)	S(1)#2-Cd(1)-S(1)	91.63(13)
N(2)-Cd(1)-S(1)#1	79.27(16)	S(1)#2-Cd(1)-S(1)#1	91.63(13)
N(2)-Cd(1)-S(1)#2	164.8(2)		

Table 17: H-bonding geometry (Å) for **4.6**

D-H...A	D-H	H...A	D...A	D-H...A
N3-H3A ...O1	0.88	1.848	2.575	138.61
N4-H4A ...O5	0.88	2.135	2.953	154.26
N4-H4A ...Cl2	0.88	2.954	3.575	129.07

Addition of dihydrophosphate to $\text{Cd}^{\text{II}}\text{-L}^3$

In an initial investigation to determine the ability of these complexes to bind the H_2PO_4^- anion we decided to utilise ^{31}P -NMR spectroscopy. In theory, there is a possibility for the perchlorate ion that is in the cavity to be replaced with dihydrophosphate H_2PO_4^- . ^{31}P -NMR is another way of proving whether the phosphate is bound or not. Practically, ^{31}P -NMR was taken for three different samples of tetrabutyl ammonium phosphate, Cd^{II} -TPPA with tetrabutylammonium phosphate and $\text{Cd}^{\text{II}}\text{-L}^3$ with tetrabutylammonium phosphate. All ^{31}P -NMR were taken in the presence of insert which consists of (tetrabutylammonium phosphate in water). As shown in (Fig. 26) a shift of 3.5 ppm is observed for the compound $\text{Cd}^{\text{II}}\text{-L}^3$ (4.6) with phosphate. This behaviour suggests a phosphate in $\text{Cd}^{\text{II}}\text{-L}^3$ (blue); being in different environment to the other two samples. No shift can be observed for the Cd^{II} (TPPA) complex which may be expected since there are three t-Butyl groups preventing phosphate from binding into the cavity.³⁰ Efforts have been spent in an attempt to grow crystals of the phosphate species but with no success. However, in this case, even with crystallographic data, it may be difficult to discriminate between ClO_4^- and H_2PO_4^- .

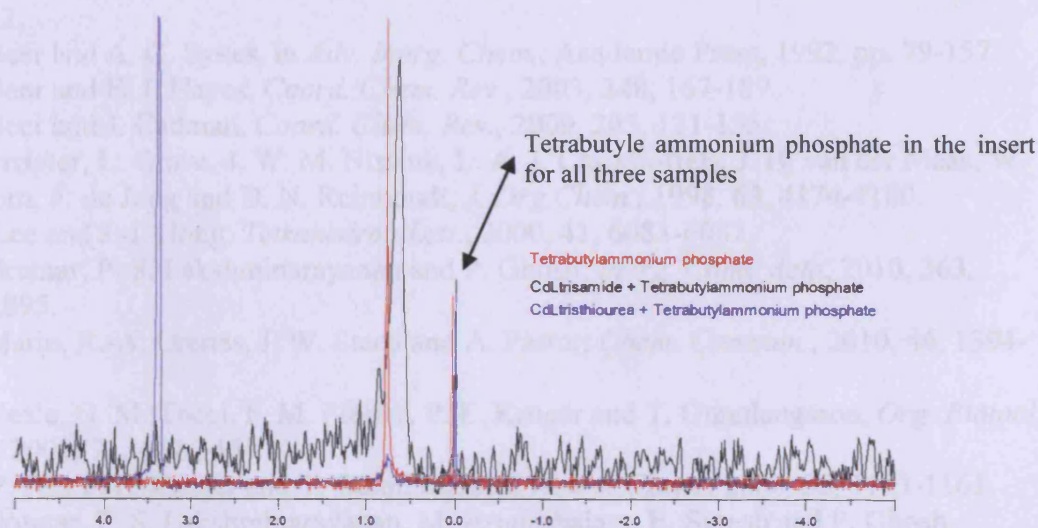


Figure 26: Superimposed ^{31}P NMR spectra of tetrabutylammonium phosphate (red), cadmium trisamide tetrabutylammonium phosphate (black) and cadmium tristhiourea tetrabutylammonium phosphate (blue) complexes. Insert of tetrabutylammonium phosphate in H_2O was used in all measurements. ^{31}P NMR was applied for reaction mixture which contains CH_3CN in all cases.

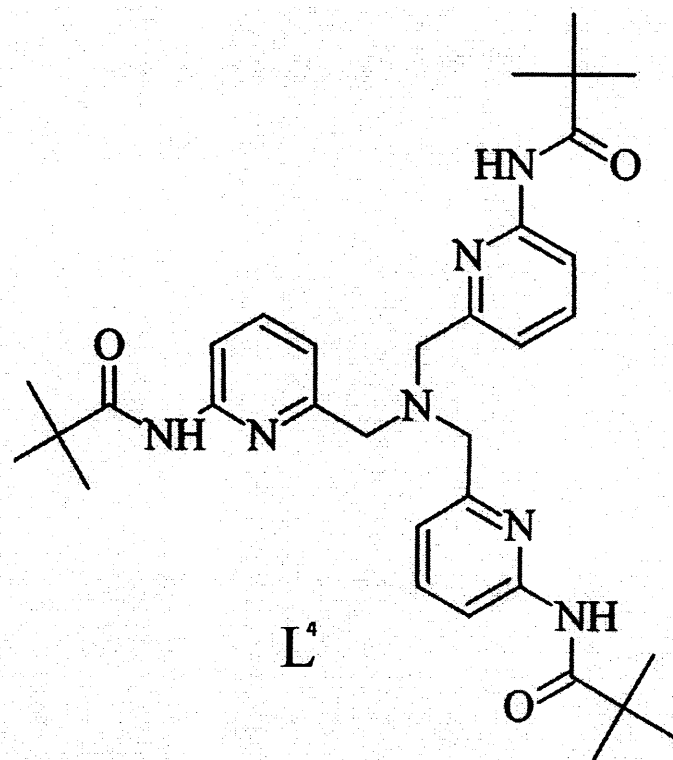
References

1. T. Gunnlaugsson, M. Glynn, G. M. Tocci, P. E. Kruger and F. M. Pfeffer, *Coord. Chem. Rev.*, 2006, **250**, 3094-3117.
2. M. H. Filby and J. W. Steed, *Coord. Chem. Rev.*, 2006, **250**, 3200-3218.
3. C. R. Bondy and S. J. Loeb, *Coord. Chem. Rev.*, 2003, **240**, 77-99.
4. E. J. O'Neil and B. D. Smith, *Coord. Chem. Rev.*, 2006, **250**, 3068-3080.
5. A. N. Khlobystov, A. J. Blake, N. R. Champness, D. A. Lemenovskii, A. G. Majouga, N. V. Zyk and M. Schröder, *Coord. Chem. Rev.*, 2001, **222**, 155-192.
6. H. M. Chawla and S. P. Singh, *Tetrahedron*, 2008, **64**, 741-748.
7. S. L. Tobey and E. V. Anslyn, *Org. Lett.*, 2003, **5**, 2029-2031.
8. D. Ramón Vilar, *Angew. Chem., Int. Ed.*, 2003, **42**, 1460-1477.
9. S. Devaraj, D. Saravanakumar and M. Kandaswamy, *Tetrahedron. Lett.*, 2007, **48**, 3077-3081.
10. E. J. Cho, B. J. Ryu, Y. J. Lee and K. C. Nam, *Org. Lett.*, 2005, **7**, 2607-2609.
11. F.-Y. Wu, X.-F. Tan, Y.-M. Wu and Y.-Q. Zhao, *Mol. Biomol. Spec.*, 2006, **65**, 925-929.
12. S. K. Kim, J. H. Bok, R. A. Bartsch, J. Y. Lee and J. S. Kim, *Org. Lett.*, 2005, **7**, 4839-4842.
13. P. A. Gale, *Chem. Commun.*, 2005, 3761-3772.
14. J. Cookson, M. S. Vickers, R. L. Paul, A. R. Cowley and P. D. Beer, *Inorg. Chim. Acta*, 2008, **361**, 1689-1698.
15. S. Camiolo, P. A. Gale, M. B. Hursthouse, M. E. Light and C. N. Warriner, *Tetrahedron Lett.*, 2003, **44**, 1367-1369.
16. E. Quinlan, S. E. Matthews and T. Gunnlaugsson, *J. Org. Chem.*, 2007, **72**, 7497-7503.
17. D. H. Lee, J. H. Im, J.-H. Lee and J.-I. Hong, *Tetrahedron Lett.*, 2002, **43**, 9637-9640.
18. D. A. Jose, D. K. Kumar, B. Ganguly and A. Das, *Tetrahedron Lett.*, 2005, **46**, 5343-5346.
19. P. A. Gale, Z. Chen, M. G. B. Drew, J. A. Heath and P. D. Beer, *Polyhedron*, 1998, **17**, 405-412.
20. P. D. Beer and A. G. Sykes, in *Adv. Inorg. Chem.*, Academic Press, 1992, pp. 79-157.
21. P. D. Beer and E. J. Hayes, *Coord. Chem. Rev.*, 2003, **240**, 167-189.
22. P. D. Beer and J. Cadman, *Coord. Chem. Rev.*, 2000, **205**, 131-155.
23. H. Boerrigter, L. Grave, J. W. M. Nissink, L. A. J. Chrisstoffels, J. H. van der Maas, W. Verboom, F. de Jong and D. N. Reinhoudt, *J. Org. Chem.*, 1998, **63**, 4174-4180.
24. K. H. Lee and J.-I. Hong, *Tetrahedron Lett.*, 2000, **41**, 6083-6087.
25. I. Ravikumar, P. S. Lakshminarayanan and P. Ghosh, *Inorg. Chim. Acta*, 2010, **363**, 2886-2895.
26. M. Alajarin, R.-A. Orenes, J. W. Steed and A. Pastor, *Chem. Commun.*, 2010, **46**, 1394-1403.
27. E. B. Veale, G. M. Tocci, F. M. Pfeffer, P. E. Kruger and T. Gunnlaugsson, *Org. Biomol. Chem.*, 2009, **7**, 3447-3454.
28. H. D. P. Ali, P. E. Kruger and T. Gunnlaugsson, *New J. Chem.*, 2008, **32**, 1153-1161.
29. I. Ravikumar, P. S. Lakshminarayanan, M. Arunachalam, E. Suresh and P. Ghosh, *Dalton Trans.*, 2009, 4160-4168.
30. M. Harata, K. Jitsukawa, H. Masuda and H. Einaga, *Chem. Lett.*, 1995, 61-62.
31. K. Jitsukawa, M. Harata, H. Arai, H. Sakurai and H. Masuda, *Inorg. Chim. Acta*, 2001, **324**, 108-116.

Chapter 4: Co-ordination Behaviour of a Novel Trithioureia Tripodal Ligand; Structural, Spectroscopic and Electrochemical properties of a series of Transition Metal Complexes

32. M. S. M. Yusof, S. K. C. Soh, N. Ngah and B. M. Yamin, *Acta Cryst.*, 2006, **E62**, 1446-1448.
33. M. G. B. Drew, J. Nelson, F. Esho, V. McKee and S. M. Nelson, *J. Chem. Soc., Dalton Trans.*, 1982, 1837 - 1843.
34. P. Dapporto, G. De Munno, A. Segal and C. Mealli, *Inorg. Chim. Acta*, 1984, **83**, 171-176.
35. M. S. Lah and M. Moon, *Bull. Korean Chem. Soc.*, 1997, **18**.
36. T. Rojo, R. Cortés, L. Lezama, M. I. Arriortua, K. Urtiaga and G. Villeneuve, *J. Chem. Soc., Dalton Trans.*, 1991, 1779 - 1783.
37. A. Deroche, I. Morgenstern-Badarau, M. Cesario, J. Guilhem, B. Keita, L. Nadjjo and C. Houee-Levin, *J. Am. Chem. Soc.*, 1996, **118**, 4567-4573.
38. Y. Nishida, N. Tanaka, A. Yamazaki, T. Tokii, N. Hashimoto, K. Ide and K. Iwasama, *Inorg. Chem.*, 1995, **34**, 3616-3620.
39. K.-Y. Choi, *Inorg. Chem. Commun.*, 2002, **5**, 220-222.
40. S. Ogo, Y. Watanabe and T. Funabiki, *Chem. Commun.*, 2003.
41. S. M. Baldeau, C. H. Slinn, B. Krebs and A. Rompel, *Inorg. Chim. Acta*, 2004, **357**, 3295-3303.
42. S. R. Randeniya and R. E. Norman, *Acta Cryst.*, 2009, **E65**, m771.
43. C. Duboc, T. Phoeung, D. Jouvenot, A. G. Blackman, L. F. McClintock, J. Pécaut, M.-N. Collomb and A. Deronzier, *Polyhedron*, 2007, **26**, 5243-5249.
44. T. Beissel, T. Glaser, F. Kesting, K. Wieghardt and B. Nuber, *Inorg. Chem.*, 1996, **35**, 3936-3947.
45. P. Bera, C.-H. Kim and S. I. Seok, *Polyhedron*, 2008, **27**, 3433-3438.
46. C. S. Allen, C.-L. Chuang, M. Cornebise and J. W. Canary, *Inorg. Chim. Acta*, 1995, **239**, 29-37.

Chapter 5: Co-ordinative properties of a Tripodal Trisamide Ligand with a Strong Capped Octahedral preference; Structural, Spectroscopic and Electrochemical properties of a series of Transition Metal Complexes



Introduction

The tripodal tetraamine ligand, tris(2-pyridylmethyl)amine (TPA), was first synthesised in 1967 by Anderegg and Wenk,¹ and its co-ordination chemistry has since been extensively studied.²⁻⁶

The TPA framework is sterically suited to co-ordinating via a trigonal pyramidal arrangement of donor atoms, and usually other ligands approach axially to form a trigonal bipyramidal arrangement of five donor atoms around the metal cation. However, there are several exceptions to this. For example, co-ordination to Pt^{II} and Pd^{II}, which each prefer a square planar environment, has been shown to cause the ligand to bind in a hypodentate manner in which one pyridine does not co-ordinate. This leads to square planar complexes of the form [Pt(TPA)Cl]⁺ and [Pd(TPA)Cl]⁺.^{7, 8} Similar tridentate co-ordination modes have also been observed upon co-ordination to ruthenium(II)⁹ and iron(II).¹⁰ Furthermore, there are also other exceptions in which seven and eight-coordinate TPA complexes have been reported. For example, [Fe(TPA)₂](BPh₄)₂¹⁰ and [Mn(TPA)₂](ClO₄)₂,¹¹ each contain two tetradentate TPA groups per metal ion.

There have been many reports of derivatives of TPA in which the pyridyl groups are substituted with various functionalities.^{5, 12, 13} The nature of these substituents and the position on the pyridyl rings has been shown to have a significant effect on the structural and physical properties of their metal complexes.¹⁴⁻¹⁶ Most commonly, derivatives of TPA are generated by alkyl substitution at the 6-position of the pyridyl groups. This simple modification can produce unfavourable steric interactions which influence the ligands ability to bind to the metal, in some instances causing the spin-state of the complex to change from low to high-spin. For example, [Fe(TPA)(CH₃CN)₂][ClO₄]₂, is reportedly low-spin, while the methylated derivatives [Fe(Me₂TPA)(CH₃CN)₂][ClO₄]₂ and [Fe(Me₃TPA)(CH₃CN)₂][ClO₄]₂, are both high spin iron(II) complexes.

Chapter 5: Co-ordinative properties of a Tripodal Trisamide Ligand with a Strong Capped Octahedral preference; Structural, Spectroscopic and Electrochemical properties of a series of Transition Metal Complexes

There are a few reported examples of TPA in which substituents at the 6-position on each of the pyridyl groups have been shown to block further co-ordination entirely. For example, some TPA derivatives containing methyl^{15, 16} and phenyl¹⁷ functionalities have been reported which, upon complexation to Cu^I cations, lead to four-coordinate Cu^I complexes. Though some structural data of the complexes of TPPA and TAPA ligands (Fig. 1) has been reported, the data available was largely limited to the complexes of copper. With this in mind, we decided to investigate the general co-ordination chemistry of TPPA with the first row transition metals. The nature of the formed complexes would be of interest as previous studies show how the differing substituent may give the possibility of hydrogen bonding with guest molecules.

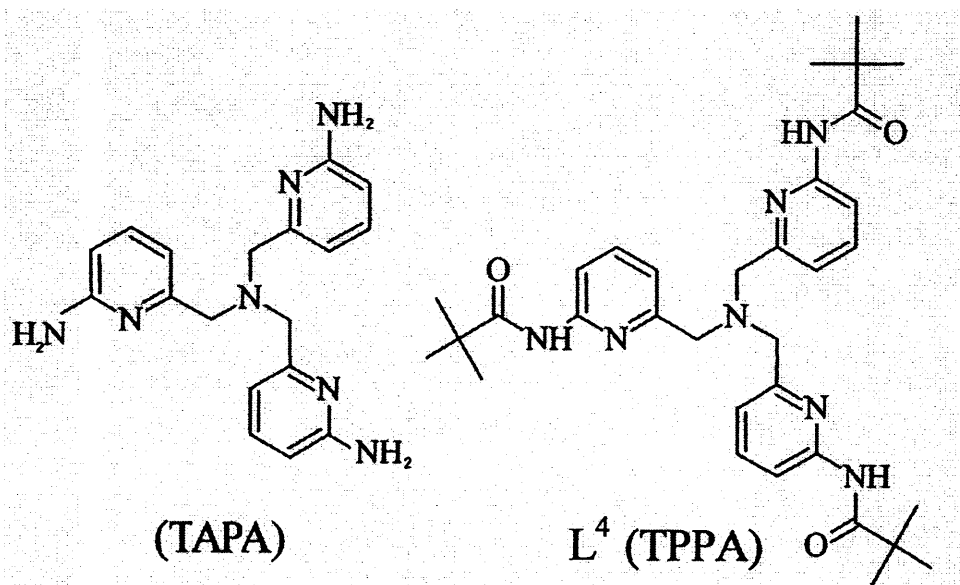


Figure 1: The ligand under investigation, L⁴ (right), alongside TPA (left).

Previous studies show this effect on small molecules such as chloride¹⁸ and peroxide.¹⁹ Zinc was chosen as it is diamagnetic, allowing for detection of binding via NMR spectroscopy.²⁰ Complexes are also known with some of the ligands tested.^{18,20,21,22} Copper was chosen as it has well studied Cu(I)/Cu(II) electrochemistry and therefore looks promising for anion detection using cyclic voltammetry. It has also been previously investigated with some of the ligands of interest, with promising results (Fig. 2).¹⁸

Chapter 5: Co-ordinative properties of a Tripodal Trisamide Ligand with a Strong Capped Octahedral preference; Structural, Spectroscopic and Electrochemical properties of a series of Transition Metal Complexes

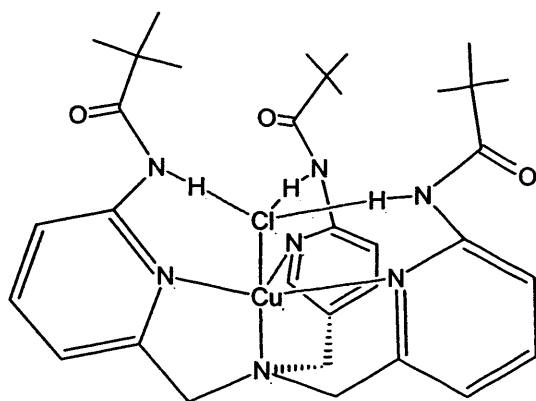


Figure 2: Copper complex of L⁴ as investigated by Rivas and co-workers.

Cobalt also has 2+/3+ oxidation states, which could also be used in electrochemical studies. By looking to the literature there are no crystallographic reports of TPPA, with the exception of copper. The ligand TPPA is a hepta dentate ligand, though one might expect that the three amide donors will be weak donors due to both their electronic properties and their spatial orientation. An investigation of the co-ordination chemistry of this ligand is expected to yield either 5 or 7 co-ordinate complexes and it seems appropriate that a brief introduction to the seven co-ordinate geometry should be included in this chapter.

Seven co-ordinate geometry

Seven co-ordinates geometry is one of the less common geometries, because of steric as well as electronic penalties incurred in the construction of complexes of high co-ordination number. A constructive generation of the idealized seven-coordinate structures is the addition of a vertex (ligand) to the regular octahedron, a formal process analogous to the initial phase of an associative substitution reaction of a six-coordinate complex. Vertex addition along an octahedral edge, 1, accompanied by a minor motion of four vertices coplanar with the new vertex, generates the D_{5h} pentagonal bipyramid 2. Face attack may generate either the C_{3v} capped octahedron 3 or the C_{2v} capped trigonal prism 4 (Fig. 3).²³

Chapter 5: Co-ordinative properties of a Tripodal Trisamide Ligand with a Strong Capped Octahedral preference; Structural, Spectroscopic and Electrochemical properties of a series of Transition Metal Complexes

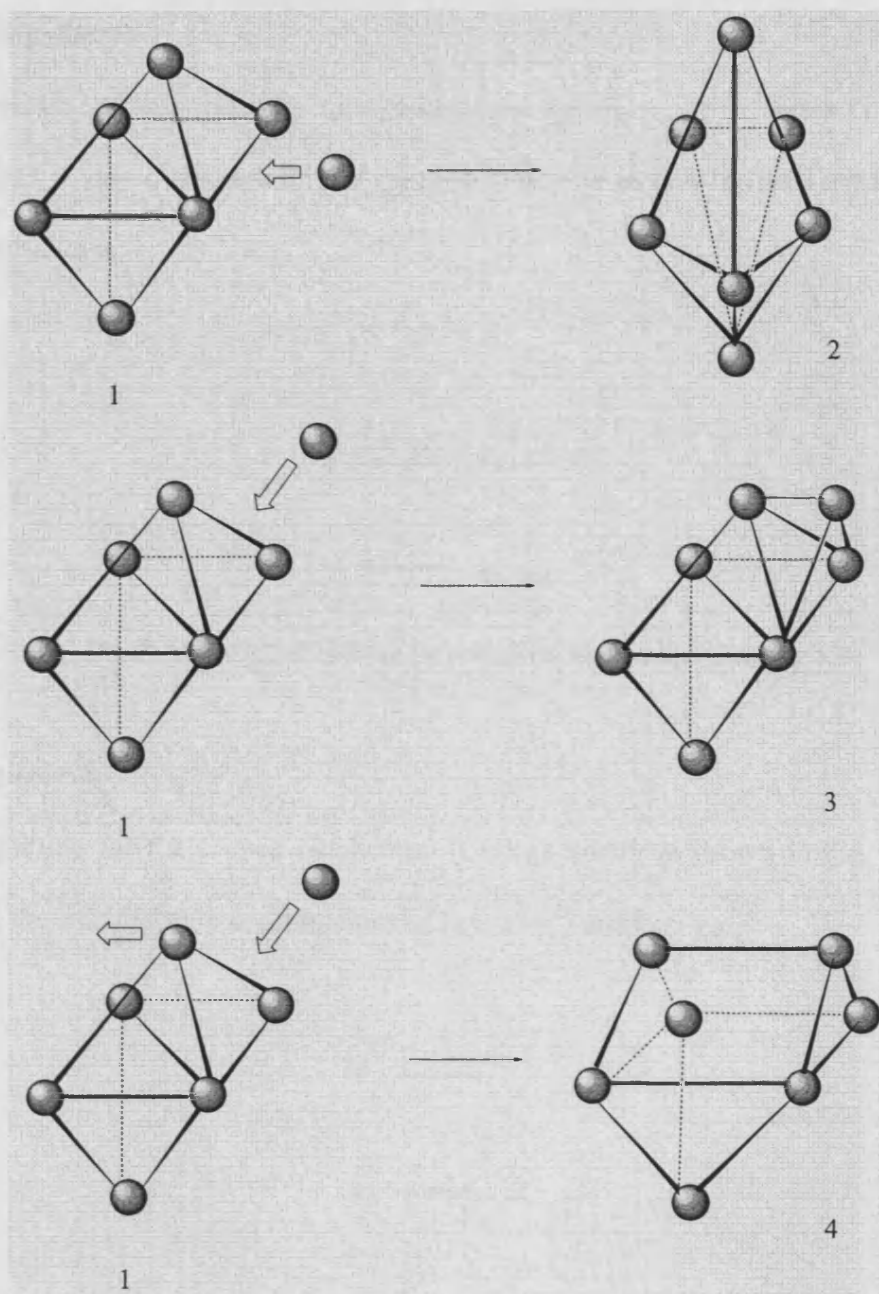


Figure 3: Pentagonal bipyramid (2), mono capped octahedron (3) and capped trigonal prism (4) generated from octahedral geometry (1).

Chapter 5: Co-ordinative properties of a Tripodal Trisamide Ligand with a Strong Capped Octahedral preference; Structural, Spectroscopic and Electrochemical properties of a series of Transition Metal Complexes

Pentagonal Bipyramid

The orbital splitting of this relatively rare geometry is shown in Fig. 4. While e_1'' is largely non bonding, e_2' and a_1' are σ^* in nature. The splitting is similar to that in five co-ordinates trigonal bipyramidal structures.

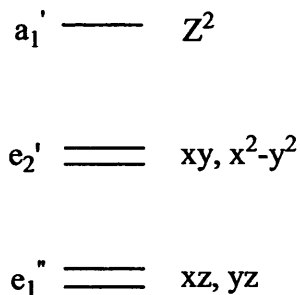


Figure 4: The orbital splitting for pentagonal bipyramidal geometry

Capped Octahedron

The orbital splitting for the capped octahedron (CO) geometry is shown in Fig. 5. While a_1 is nearly all dz^2 , the e orbitals are combinations of (xy, x^2-y^2) and (xz, yz) .

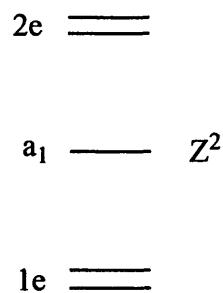


Figure 5: The orbital splitting for capped octahedron geometry

Chapter 5: Co-ordinative properties of a Tripodal Trisamide Ligand with a Strong Capped Octahedral preference; Structural, Spectroscopic and Electrochemical properties of a series of Transition Metal Complexes

The geometry of the CO complex may be described by two angles (Fig. 6).

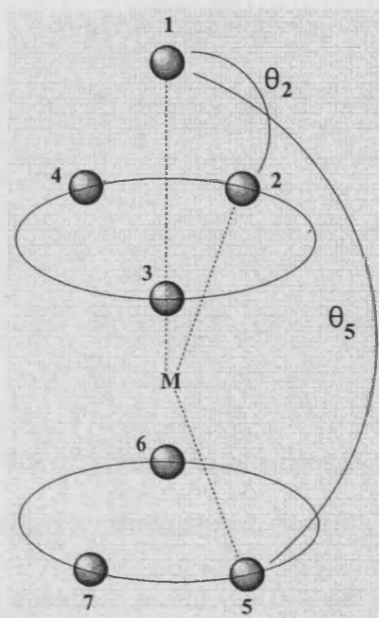


Figure 5: Angles between capped octahedron atoms.

The capped regular octahedron has $\theta_2 = 54.7^\circ$ ($=\theta_3 = \theta_4$) and $\theta_5 = 125.3^\circ$, and is clearly sterically congested. Calculations by Hoffman set for seven anions on a sphere (L_7^{-7}) yield the values $\theta_2 = 75^\circ$ and $\theta_5 = 138^\circ$.²³ Inserting a metal gave varying results depending on the d^n configuration. (d^0 $\theta_2 = 84^\circ$, $\theta_5 = 138^\circ$; d^2 $\theta_2 = 80^\circ$, $\theta_5 = 130^\circ$ and d^4 $\theta_2 = 70^\circ$, $\theta_5 = 130^\circ$). Unfortunately, the situation is typically further complicated as typically most CO structures are of the nature $ML_3 L_3'$ not ML_7 .

Capped Trigonal Prism

Two structures are possible: either by the capping of a triangular face or by capping a tetragonal face. The capping of the tetragonal face (C_{2v} symmetry) is the more commonly encounter of the two, presumably due to the lower congestion about the capping ligand. The orbital splitting of the C_{2v} case is shown in Fig. 7.

Chapter 5: Co-ordinative properties of a Tripodal Trisamide Ligand with a Strong Capped Octahedral preference; Structural, Spectroscopic and Electrochemical properties of a series of Transition Metal Complexes

a_2 ——— xy

a_1 ——— z^2

b_1 ——— xz

b_2 ——— yz

a_1 ——— x^2-y^2

Figure 7: The orbital splitting for capped trigonal prism.

The geometry of CTP may be defined by three angles $\theta_2 = (\theta_{3,4,5})$, \square_2 (making no assumption of a square face) and $\theta_6 (= \theta_7)$. Again calculations for d^0 ($\theta_2 = 68^\circ$, $\square_2 = 52^\circ$, $\theta_6 = 118^\circ$); d^2 ($\theta_2 = 80^\circ$, $\square_2 = 54^\circ$, $\theta_6 = 122^\circ$) and d^4 ($\theta_2 = 82^\circ$, $\square_2 = 46^\circ$, $\theta_6 = 148^\circ$) have been carried out. These values vary considerably when compared to the treatment as points in a sphere ($\theta_2 = 80.8^\circ$, $\square_2 = 49^\circ$, $\theta_6 = 144.2^\circ$) (Fig. 8).

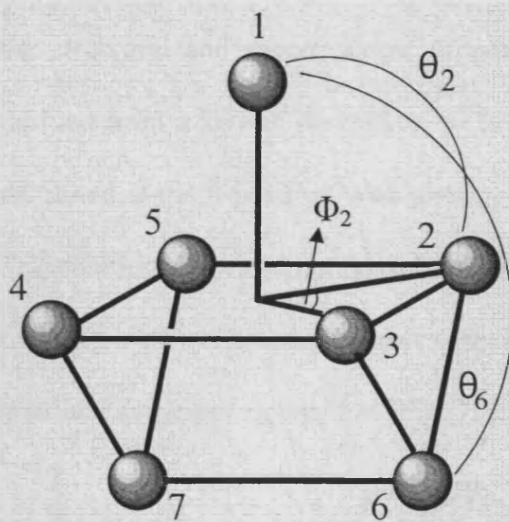


Figure 8: Angles between capped trigonal prism atoms.

Trigonal base – Tetragonal base

Finally, another type of seven co-ordination geometry that is theoretically possible is the trigonal base - tetragonal base structure where a metal is sandwiched by a square planar of donors and a trigonal plane of donors (Fig. 9).

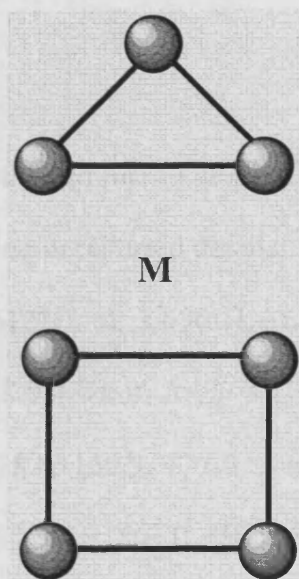


Figure 9: Metal is surrounded by square and trigonal donors.

In this chapter, we report the structural and spectroscopic properties of a series of first row transition metal complexes derived from a known derivative of TPA in which each of the three pyridyl groups have been substituted at the 6-position with pivaloylamino substituents. This C_{3v} symmetric ligand, tris(6-pivaloylamino-2-pyridylmethyl)amine (TPPA; L^4), prefers to adopt seven co-ordinate metal complexes with series of first row transition metals, resulting in co-ordination geometries best described as capped octahedral (Fig. 10).

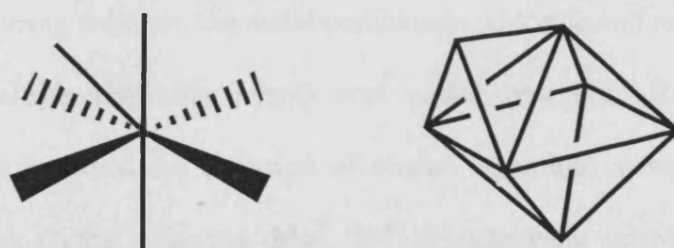


Figure 10: An ideal monocapped octahedral geometry.

Experimental

General

The details regarding the collection of experimental data are the same as those reported in the preceding chapters.

Synthesis of (L⁴)

Tris(6-pivalylamido-2-pyridylmethyl)amine (TPPA) L⁴ was synthesised as published by Harata *et al.*²¹ but with the following unreported details:

¹H NMR (250 MHz; CDCl₃): 1.25(27H, s); 3.69(6H, s); 7.20(3H, d, Ar, J=7.4Hz); 7.60(3H, t, Ar, J=7.8Hz); 7.94(3H, s, NH); 8.04(3H, d, Ar, J=8.1Hz). ¹³C δ_C (62.5 MHz; CDCl₃): 27.4, 39.7, 59.6, 112.1, 118.5, 138.8, 138.8, 150.9, 177.0. Accurate ESMS (*m/z*): 610.3505 (100), [L+Na]⁺ [calculated 610.3481], 588.3676 (80) [L+H]⁺ [calculated 588.3676]. IR KBr/cm⁻¹: ν = 3429m, 1691s. UV/Vis [λ_{max}, nm (εM, M⁻¹cm⁻¹)] in CH₃CN: 320.5(1811), 284.5(17915), 243.5(21865). The controlled dropwise addition of aqueous HBr to L⁴ dissolved in a 2-propanol, resulted in the precipitation of [HL⁴][Br]. ¹H NMR (400 MHz; CDCl₃): 1.29(27H, s); 4.43(6H, s); 7.61(3H,d, Ar, J=7.4); 8.68(3H, d, Ar, br); 7.89-8.15(6H, m, Ar).

General Procedure for the synthesis of metal complexes

The ligand (1 equivalent, typically 0.85 mmol) was dissolved in the minimum amount of acetonitrile (typically 3ml). The solutions were warmed to ca. 60°C to ensure that the ligand fully dissolved. To this stirring solution, the metal perchlorate, chloride and iodide salt (1 equivalent) dissolved in acetonitrile (typically ~2ml) was added dropwise. Recrystallisation of the compounds typically involved the diffusion of diethyl ether into acetonitrile solutions which were filtered through Celite. Whereas, Mn^{II}, Fe^{II} crystals were grown by slow evaporation

Chapter 5: Co-ordinative properties of a Tripodal Trisamide Ligand with a Strong Capped Octahedral preference; Structural, Spectroscopic and Electrochemical properties of a series of Transition Metal Complexes

method. Nothing important needs to be mentioned here as all complexations of metals into L^4 were typical as no precipitation were present.

[Mn^{II}(L⁴)] [ClO₄] [Br].CH₃CN (5.1): Cream-coloured plate crystals (46% yield); Accurate ESMS (*m/z*): 641.2864 (10) [Mn(L⁴)-H]⁺ [calculated 641.2886]; MnC₃₅H₄₈N₈O₃BrClO₄ (Found: C, 48.84; H, 5.72; N, 13.21 % requires C, 48.76; H, 5.61; N, 13.00%); IR KBr/cm⁻¹: $\nu = 3447\text{br}, 1617\text{s}, 1520\text{s}, 1424\text{s}, 1091\text{s}, 801\text{s}, 622\text{s}$.

[Fe^{II}(L⁴)] [ClO₄] [Br].CH₃CN (5.2): Yellow needle crystals (66% yield); Accurate ESMS (*m/z*): 642.2855 (20) [Fe(L⁴)-H]⁺ [calculated 642.2854]; FeC₃₅H₄₈N₈O₃BrClO₄ (Found: C, 48.92; H, 5.54; N, 13.12 % requires C, 48.71; H, 5.61; N, 12.99%); IR KBr/cm⁻¹: $\nu = 3445\text{br}, 1616\text{s}, 1533\text{s}, 1458\text{s}, 1443\text{s}, 1160\text{s}, 1086\text{s}, 622\text{s}$; UV/Vis [λ_{max} , nm ($\epsilon\text{M}, \text{M}^{-1}\text{cm}^{-1}$)] in CH₃CN: 321(1180), 285(20380), 237(30170), 366(315), 427(220), 628(3), 1087(3).

[Co^{II}(L⁴)] [Br]₂.0.5(H₂O).2(CH₃CN) (5.3): Pink plate crystals (29% yield); Accurate ESMS (*m/z*): 745.2412 (15) [Co(L⁴)+ClO₄] [calculated 745.2400] ,645.2801 (10) [Co(L⁴)-H]⁺ [calculated 645.2837]; CoC₃₇H₅₂N₉O_{3.50}Br₂ (Found: C, 49.66; H, 5.93; N, 14.23 % requires C, 49.50; H, 5.83; N, 14.04%); IR KBr/cm⁻¹: $\nu = 3372\text{s}, 1618\text{s}, 1525\text{s}, 1420\text{s}, 1160\text{s}, 1097\text{s}, 622\text{m}$; UV/Vis [λ_{max} , nm ($\epsilon\text{M}, \text{M}^{-1}\text{cm}^{-1}$)] in CH₃CN: 236.2(46100), 285.3(27500), 501.5(50), 618.4(160), 685.5(340).

[Ni^{II}(L⁴)] [ClO₄]_{1.67} [Br]_{0.33}.0.67(H₂O) (5.4): Yellow plate crystals (63% yield); Accurate ESMS (*m/z*): 644.2885 (60) [Ni(L⁴)-H]⁺ [calculated 644.2859]; NiC₃₃H_{46.33}Cl_{1.67}Br_{0.33}N₇O_{10.33}; IR KBr/cm⁻¹: $\nu = 3354\text{m}, 1618\text{s}, 1531\text{s}, 1459\text{s}, 1422\text{s}, 1106\text{s}, 622\text{s}$; UV/Vis [λ_{max} , nm ($\epsilon\text{M}, \text{M}^{-1}\text{cm}^{-1}$)] in CH₃CN: 232(26390), 285(15235), 440(30), 613(8), 748(7), 803(8), 1092(15).

[Zn^{II}(L⁴)] [ClO₄]₂.2(CH₃CN) (5.5): Colourless prism crystals (89% yied); ¹H-NMR δ_{H} (400 MHz; CD₃CN): 1.14 (27H, s); 4.09 (6H, s); 7.12 (3H, d, Ar, J=7.1Hz); 7.21 (3H, d, Ar,

Chapter 5: Co-ordinative properties of a Tripodal Trisamide Ligand with a Strong Capped Octahedral preference; Structural, Spectroscopic and Electrochemical properties of a series of Transition Metal Complexes

$J=7.8\text{Hz}$); 7.87 (3H, t, Ar, $J=7.8\text{Hz}$); 8.98 (3H, s, NH); ^{13}C δ_{C} (62.5 MHz; CD_3CN): 27.0, 41.2, 55.8, 114.7, 119.9, 141.9, 153.0, 153.3, 181.3; Accurate ESMS (m/z): 650.2823 (10) $[\text{Zn}(\text{L}^4)\text{-H}]^+$ [calculated 650.2797]; $\text{ZnC}_{33}\text{H}_{45}\text{N}_7\text{O}_3(\text{CH}_3\text{CN})_2(\text{ClO}_4)_2$ (Found: C, 46.93; H, 5.51; N, 13.51 requires C, 47.67; H, 5.51; N, 13.53%); IR $\text{KBr}/\text{cm}^{-1}$: $\nu=3401\text{br}, 1617\text{s}, 1530\text{s}, 1464\text{s}, 1421\text{s}, 1120\text{s}, 1091\text{s}, 622\text{s}$.

$[\text{Zn}^{\text{II}}(\text{L}^4)(\text{Cl}_2)]$ (5.6): colourless block crystals (80% yield). Colourless block crystals (80% yield); ^1H -NMR δ_{H} (250 MHz; DMSO): 1.34 (27H, s); 4.12 (6H, s); 7.18 (3H, d, Ar, $J=7.1\text{Hz}$); 7.49-8.31 (6H, m, Ar); 9.59 (3H, s, NH); ^{13}C -NMR δ_{C} (62.5 MHz; DMSO): 26.9, 54.9, 55.6, 114.8, 119.7, 140.6, 150.7, 151.0, 176.7; Accurate ESMS (m/z): 650.2786 (40) $[\text{Zn}(\text{L}^4)\text{-H}]^+$ [calculated 650.2797]; $\text{ZnC}_{33}\text{H}_{45}\text{N}_7\text{O}_3(\text{Cl})_2$ (Found: C, 54.54; H, 6.27; N, 13.32 % requires C, 54.90; H, 6.28; N, 13.59%). IR $\text{KBr}/\text{cm}^{-1}$: $\nu=3426\text{m}, 1683\text{s}, 1608\text{s}, 1517\text{s}, 1455\text{s}, 1152\text{s}$.

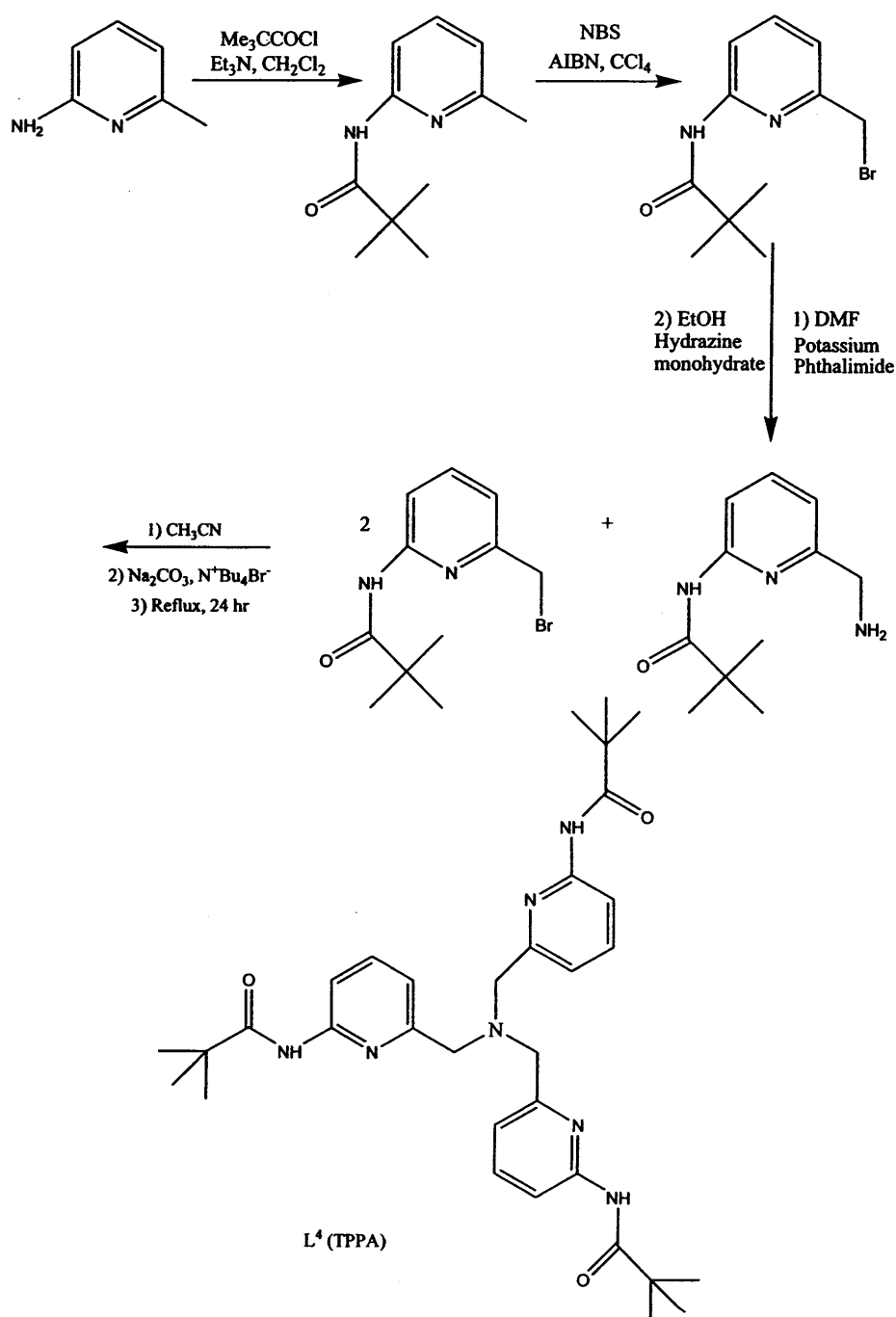
$[\text{Zn}^{\text{II}}(\text{L}^4)][\text{ZnI}_4]_{0.5}[\text{I}]$ (5.7): White plate crystals (63% yield); ^1H -NMR δ_{H} (250 MHz; DMSO): 1.16 (27H, s); 4.16 (6H, s); 7.24 (3H, d, Ar, $J=7.2\text{Hz}$); 7.49 (3H, d, Ar, $J=7.5\text{Hz}$); 8.07 (3H, t, Ar, $J=8.0\text{Hz}$); 10.44 (3H, s, NH); ^{13}C -NMR δ_{C} (62.5 MHz; DMSO): 26.5, 54.9, 55.0, 113.8, 119.0, 141.1, 151.8, 152.3, 179.9; Accurate ESMS (m/z): 778.1943 (10) $[\text{Zn}(\text{L}^4)+\text{I}]^+$ [calculated 778.1920]; $\text{ZnC}_{66}\text{H}_{90}\text{N}_{14}\text{O}_6(\text{ZnI}_4)\text{I}$; IR $\text{KBr}/\text{cm}^{-1}$: $\nu=3260\text{m}, 1615\text{s}, 1528\text{s}, 1456\text{s}, 1434\text{s}, 1417\text{s}, 1155\text{s}, 801\text{s}$.

$[\text{Cd}^{\text{II}}(\text{L}^4)][\text{ClO}_4]_2\cdot\text{Na}(\text{ClO}_4)\cdot\text{H}_2\text{O}$ (5.8): Colourless plate crystals (96 % yield); ^1H -NMR δ_{H} (250 MHz; CDCl_3): 0.96(27H, s); 3.76 (6H, s); 6.89(3H, d, Ar, $J=7.5\text{Hz}$); 6.98(3H, d, Ar, $J=8.2\text{Hz}$); 7.61(3H, d, Ar, $J=8.0\text{Hz}$); 8.62(3H, s, NH); ^{13}C -NMR δ_{C} : (62.5 MHz; CD_3CN): 27.4, 41.7, 56.7, 116.6, 121.4, 142.3, 153.5, 154.0, 183.1; Accurate ESMS (m/z): 700.2570 (70), $[\text{Cd}(\text{L}^4)\text{-H}]^+$ [calculated 700.2539]; IR $\text{KBr}/\text{cm}^{-1}$: $\nu=3370\text{br}, 1615\text{s}, 1533\text{s}, 1454\text{s}, 1419\text{s}, 1100\text{m}, 800\text{s}, 622\text{s}$.

Results and Discussion

Ligand Synthesis (L^4)

Tris(6-pivaloylamino-2-pyridylmethyl)amine (TPPA) was synthesised according to known literature procedures.²¹ (Scheme 1).



Scheme 1: Synthetic route to L^4 .

Synthesis of Ligand and Complexes

The ligand was synthesised according to the method of Harata and co-workers.²¹ Initial attempts to obtain crystals complexes of L^4 were only successful for $Zn(ClO_4)_2$ and $Cd(ClO_4)_2$. However, on using the protonated ligand $[HL^4][Br]$ we were able to obtain single crystals for Mn^{II} , Fe^{II} , Co^{II} and Ni^{II} complexes. Further investigations were then carried out for the Zn^{II} species by using different starting materials, $ZnCl_2$ and ZnI_2 . The complexation involved the use of either ligand L^4 or HL^4 (1 eq, typically 0.85 mmol) which was dissolved in the minimum amount of acetonitrile (typically 3ml). The solutions was warmed to ca. 60°C to insure that the ligand fully dissolved. To this stirring solution, the metal perchlorate, chloride or iodide salt (1 equivalent) dissolved in acetonitrile (typically ~2ml) was added dropwise. Crystallisation of the compounds typically involved the diffusion of diethyl ether into the acetonitrile reaction mixtures which had been filtered through Celite. On some occasions (Mn^{II} , Fe^{II}) slow evaporation was used to obtain crystals. The yields from these reactions were moderate (25-97%). The crystalline material was subsequently used for all spectroscopic measurements.

Spectroscopic Properties of Complexes

Vibrational Spectroscopy

The free ligand reveals a very strong single band at 1691 cm^{-1} , assigned to the $\nu(C=O)$ vibration of the three equivalent amide carbonyl groups (Table 1). This signal is observed at lower energy in all complexes upon co-ordination to the metal. Interestingly, for compound 5.6, two carbonyl stretches at 1608, 1683 cm^{-1} corresponding to co-ordinated and unco-ordinated carbonyl arms respectively. A typical O-H band is observed at around 3400 cm^{-1} indicating the presence of water in all complexes. Compounds 5.1-5.5 and 5.8 reveal two

Chapter 5: Co-ordinative properties of a Tripodal Trisamide Ligand with a Strong Capped Octahedral preference; Structural, Spectroscopic and Electrochemical properties of a series of Transition Metal Complexes

characteristic unsplit infrared active bands at $\sim 1,100\text{ cm}^{-1}$ and 622 cm^{-1} indicative of ionic perchlorate (T_d symmetry).^{24,25} All of these features are confirmed by X-ray diffraction studies.

Table 1: IR stretching frequencies of L^4 . IR spectra measured as KBr discs.

Compound	$\nu(\text{C}=\text{O})$	$\nu(\text{O}-\text{H})$	$\nu(\text{Cl}-\text{O})$
L^4	1691(s)	3429(m)	-
5.1	1617(s)	3447(br)	1091(m), 622(s)
5.2	1616(s)	3445(br)	1086(m), 622(s)
5.3	1618(s)	3372(s)	1097(s), 622(m)
5.4	1618(s)	3354(m)	1106(m), 622(s)
5.5	1617(s)	3401(br)	1091(s), 622(s)
5.6	1673(s)	3426(m)	-
5.7	1615(s)	3260(m)	-
5.8	1615(s)	3370(m)	1100(m), 622(s)

^1H and ^{13}C NMR of Zn and Cd Complexes

The ^1H NMR of the Zn^{II} and Cd^{II} complexes, 5.5, 5.6 and 5.7, are relatively simple due to the presence of C_3 symmetry in the complex. All signals shift to higher ppm on co-ordination to the metal centre due to the removal of electron density from the ligand to the metal.

While complex 5.6 is not as symmetrical as 5.5, 5.7 and 5.8 in solid state, the ^1H NMR and the ^{13}C NMR suggest that in solution all arms of the tripod are equivalent. This suggests either the chlorides dissociate in solution to give the symmetrical species, or the complex is fluxional, with each arm rapidly co-ordinating and then dissociating from the metal. Fig. 11 shows the ^{13}C NMR spectra of the free ligand (black), zinc (5.5) (red) and cadmium (blue) complexes of L^4 . The similarity of Zn and Cd L^4 species can clearly be seen.

Chapter 5: Co-ordinative properties of a Tripodal Trisamide Ligand with a Strong Capped Octahedral preference; Structural, Spectroscopic and Electrochemical properties of a series of Transition Metal Complexes

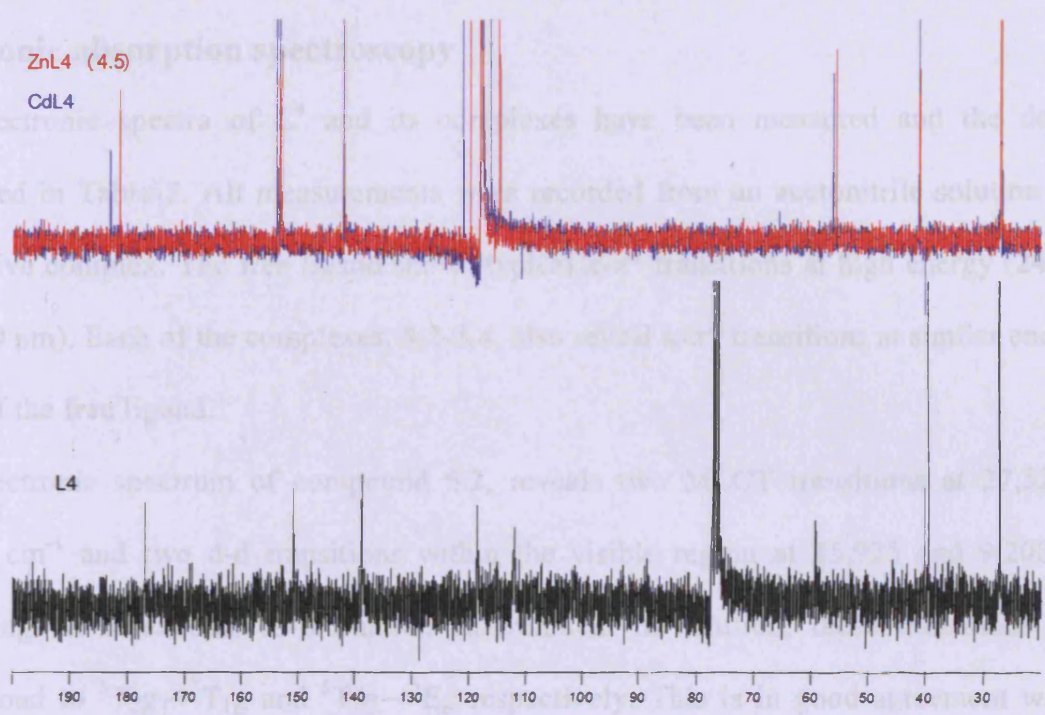


Figure 11: Superimposed ^{13}C NMR spectra of the free ligand (black), zinc (4.5) (red) and cadmium (blue) complexes of L^4 .

Electronic absorption spectroscopy

The electronic spectra of L⁴ and its complexes have been measured and the data are presented in Table 2. All measurements were recorded from an acetonitrile solution of the respective complex. The free ligand shows typical π - π^* transitions at high energy (243, 284 and 320 nm). Each of the complexes, 5.2-5.4, also reveal π - π^* transitions at similar energy to those of the free ligand.

The electronic spectrum of compound 5.2, reveals two MLCT transitions at 27,325 and 23,420 cm⁻¹ and two d-d transitions within the visible region at 15,925 and 9,200 cm⁻¹. Assuming an octahedral co-ordination environment in solution, these transitions would correspond to $^5T_{2g} \rightarrow ^3T_{1g}$ and $^5T_{2g} \rightarrow ^5E_g$ respectively. This is in good agreement with the related complex, [Fe(medpa)₂][ClO₄]₂ (medpa= bis(2-pyridylmethyl)methylamine) which also reveals transitions at 10,860 and 9,770 cm⁻¹.²⁶

The Co^{II} complex 5.3, has been shown crystallographically to contain a seven-coordinate environment around the metal centre. Thus, according to Tanabe-Sugano diagram of d⁷ there should be three transitions [$^4T_{1g}(F) \rightarrow ^4T_{1g}(P)$, $^4T_{1g} \rightarrow ^4A_{2g}$ and $^4T_{1g} \rightarrow ^4T_{2g}$] within the electronic spectrum. Those transitions have been observed at 19940, 16170 and 14590 cm⁻¹ which are most likely attributable to transitions $^4T_{1g}(F) \rightarrow ^4T_{1g}(P)$, $^4T_{1g} \rightarrow ^4A_{2g}$, respectively. The related compound [Co₂(bomp)(MeCO₂)₂]BPH₄ reported by Sakiyama *et al.* which contains a seven co-ordinate high spin cobalt(II) reveals three transitions at 21000, 19000 and 8000 cm⁻¹ (bomp= 2,6- bis[bis(2-methoxyethyl)aminomethyl]-4-methylphenol).²⁷

The UV-Vis spectrum of Ni^{II}, 5.4, reveals two LMCT bands observed at 22,730 and 16,300 cm⁻¹. In the solid state, the Ni^{II} cation lies at the centre of an N₄O₃ coordination environment within a mono capped octahedral geometry. Interestingly, its absorption pattern is more indicative of a six-coordinate geometry in solution. Three transitions are observed at

Chapter 5: Co-ordinative properties of a Tripodal Trisamide Ligand with a Strong Capped Octahedral preference; Structural, Spectroscopic and Electrochemical properties of a series of Transition Metal Complexes

13,370, 12,450 and 9,160 cm^{-1} (Fig. 12) corresponding to ${}^3\text{T}_{1g}(\text{P})$, ${}^3\text{T}_{1g}(\text{F})$ and ${}^3\text{T}_{2g}$ respectively. Further calculation shows ($B= 327.1 \text{ cm}^{-1}$; $\beta= 0.31$).

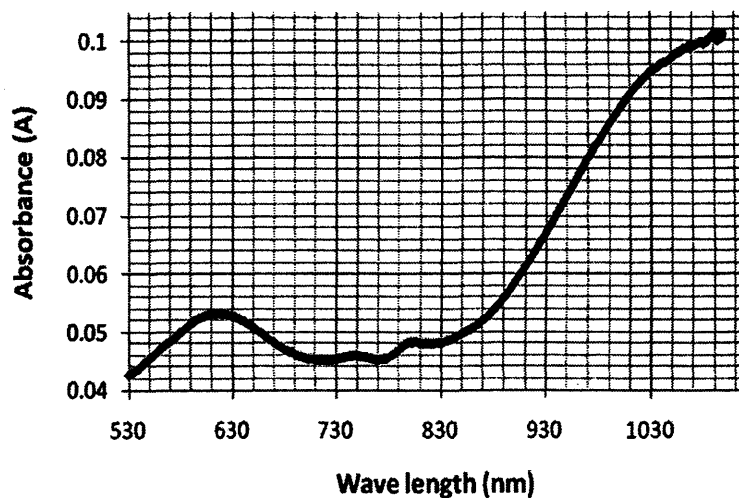


Figure 12: The electronic spectra of 5.4.

Table 2: Electronic spectral assignments for the ligand and complexes^a

Compound	$\pi-\pi^*$ λ (nm)	MLCT λ (nm)	d-d λ (nm)	Δ (cm^{-1}) ^b	B (cm^{-1}) ^b	β
L^4	243(21,870) 284(17,920) 320(1,810)	-	-	-	-	-
5.2	237(30,170) 285(20,380) 321(1,180)	366(315) 427(220)	628(3) 1087(3)	-	-	-
5.3	236.2(46100) 285.3(27500)	-	501.5(50), 618.4(160), 685.5(340)	-	-	-
5.4	232(26,390) 285(15,235)	440(30) 613(8)	748(7) 803(8) 1092(15)	9160	327.1	0.31

^aperformed in CH_3CN solution at room temperature; Numbers in parentheses indicate molar absorption coefficients ϵ ($\text{M}^{-1}\text{cm}^{-1}$). ^bvalues calculated by assuming an octahedral geometry.

Electrochemical Studies

General procedures for measuring the electrochemistry for L⁴ complexes are the same as explained in previous chapters.

The cyclic voltammogram of the manganese compound, **5.1**, reveals three irreversible oxidations within the anodic region at +0.420, +0.708 and +1.17 V referenced against ferrocenium/ferrocene (Fc⁺/Fc). Discrete mononuclear complexes of manganese in a heptacoordinated environment are rare, thus only limited comparisons can be made. The seven co-ordinate manganese(II) complex of N,N,N'-tris(2-pyridylmethyl)-N'-(2-salicylideneethyl)ethane-1,2 diamine and Mn^{II}(pyrdoxTPA)₂ reveal anodic wave processes at +0.56 V and +0.64 V (*vs* SCE) that is +0.16 V and +0.24 V (*vs* Fc⁺/Fc) respectively.^{28,29,30} In each case, these features have been attributed to the Mn(II/III) redox couple. Interestingly, the voltammogram of **5.1** does not reveal a reversible couple corresponding to this process. This is most likely due to a chemical reaction following oxidation of the Mn^{II} ion.

Table 3: Electrochemical parameters for the redox processes exhibited by complexes **5.1**, **5.2**, **5.3** and **5.4** in acetonitrile solution (supporting electrolyte: [Bu₄N][PF₆] (0.1 mol dm⁻³); T = 20 °C). Measured at 0.1 Vs⁻¹.

Compound	E_p/V (ΔE , mV) ^{a,b}
5.1	0.420, 0.708, 1.17
5.2	+0.253(140)
5.3	0.354, 0.588(65)
5.4	-2.14

^aThe potentials at which reversible processes occur are calculated as the average of the oxidative and reductive peak potentials ($E_p^{ox} + E_p^{red}$)/2. ^bFor irreversible processes, the anodic or cathodic peak potentials are given. Potentials are given in volts *versus* Ferrocenium/Ferrocene.

The cyclic voltammogram of **5.2**, exhibits a quasi-reversible wave at +0.253 V (*vs* Fc⁺/Fc) which has been ascribed to the Fe^{II/III} redox couple. The separation between the anodic and cathodic peaks, $E_p^c - E_p^a$, is 140 mV which is significantly higher than the 59 mV theoretically expected for a one-electron Nerstian process. The compound [Fe(*k*⁷N-L)](ClO₄)₂ L = N,N,N',N'-tetrakis(2-pyridylmethyl)-2,6-bis(aminomethyl)pyridine also exhibits a seven-coordinate environment around an Fe^{II} ion and reveals a quasi-reversible Fe(II)/Fe(III)

Chapter 5: Co-ordinative properties of a Tripodal Trisamide Ligand with a Strong Capped Octahedral preference; Structural, Spectroscopic and Electrochemical properties of a series of Transition Metal Complexes

couple at the higher potential of +0.51 V vs Fc⁺/Fc.³¹

The cyclic voltammogram of cobalt(II) complex, **5.3**, reveals a quasi-reversible redox process in the anodic region at +0.588V (65) which has been assigned to the Co(II)/Co(III) couple. There is also a further irreversible oxidation at +0.354V.

The cyclic voltammogram of the nickel compound **5.4**, reveals one irreversible reduction in the cathodic region at -2.14V referenced against Fc⁺/Fc. Without further investigation it is difficult to assign the exact origins of this feature.

Chapter 5: Co-ordinative properties of a Tripodal Trisamide Ligand with a Strong Capped Octahedral preference; Structural, Spectroscopic and Electrochemical properties of a series of Transition Metal Complexes

Crystallographic Studies

All single crystal X-ray data was collected as explained in previous chapters. Unfortunately, only poor quality crystals could be obtained for $[\text{Ni}^{\text{II}}(\text{L}^4)][\text{ClO}_4]_{1.67}[\text{Br}]_{0.33} \cdot 0.67(\text{H}_2\text{O})$, despite numerous attempts to grow better crystals. Selected bond lengths and angles of all complexes can be found in Table 5.

Table 4: Crystal structure data for complexes 5.1-5.8

Compound	5.1	5.2	5.3	5.4	5.5	5.6	5.7	5.8
Chemical Formula	$\text{MnC}_{35}\text{H}_{48}\text{N}_8\text{O}_7$ BrCl	$\text{FeC}_{35}\text{H}_{48}\text{N}_8\text{O}_7$ BrCl	$\text{CoC}_{37}\text{H}_{52}\text{N}_9\text{O}_{3.50}$ Br ₂	$\text{NiC}_{33}\text{H}_{46.33}\text{Br}_{0.33}\text{N}_7$ Cl _{1.67} O _{10.33}	$\text{ZnC}_{37}\text{H}_{51}\text{N}_9\text{O}_{11}$ Cl ₂	$\text{ZnC}_{33}\text{H}_{45}\text{N}_7\text{O}_3$ Cl ₂	$\text{Zn}_3\text{C}_{66}\text{H}_{90}\text{N}_{14}\text{O}_6$ I ₆	$\text{CdC}_{33}\text{H}_{47}\text{N}_7\text{O}_{16}$ NaCl ₃
Mr, g mol ⁻¹	863.11	864.02	897.63	850.87	934.14	724.03	2133.03	1039.52
Crystal System	Monoclinic	Monoclinic	Monoclinic	Hexagonal	Monoclinic	Monoclinic	Trigonal	Trigonal
Space group	P2 ₁ /m	P2 ₁ /m	C2/c	P6 ₃ /m	C2/c	C2/c	P-3c1	R32
T(K)	150(2)	150(2)	150(2)	396(2)	150(2)	140(2)	150(2)	150(2)
a, Å	10.8160(2)	10.730(5)	11.1532(3)	11.1018(7)	37.4589(10)	35.4990(4)	11.2190(2)	16.2800(5)
b, Å	40.8620(8)	40.995(5)	19.6165(5)	11.1018(7)	11.2206(3)	9.1250(7)	11.2190(10)	16.3070(5)
c, Å	11.1620(2)	11.101(5)	37.6128(12)	58.814(4)	21.1473(8)	24.5700(12)	38.5920(4)	28.8420(13)
α, deg	90	90	90	90	90	90	90	90
β, deg	116.9550(10)	117.050(5)	90.6930(10)	90	93.2280(10)	119.271(2)	90	90
γ, deg	90	90	90	120	90	90	120	120
Z	4	4	8	6	8	8	2	6
Dc, Mg/m ³	1.304	1.320	1.449	1.375	1.398	1.385	1.684	1.562
μ(Mo Kα), mm ⁻¹	1.320	1.378	2.407	0.875	0.740	0.906	3.102	0.760
Observed Reflections	4188	3638	6698	1987	4847	3956	2821	2421
Unique Reflections	5409	4787	8546	2176	10145	4983	3226	2726
R _{int}	0.0422	0.0380	0.0366	0.0735	0.1050	0.0599	0.0736	0.0809
R ₁ [<i>I</i> > 2σ(<i>I</i>)]	0.0783	0.0875	0.0486	0.2730	0.0831	0.0701	0.0462	0.1026
wR ₂ (all data)	0.2094	0.2294	0.1070	0.6453	0.2489	0.1914	0.1280	0.2877

Chapter 5: Co-ordinative properties of a Tripodal Trisamide Ligand with a Strong Capped Octahedral preference; Structural, Spectroscopic and Electrochemical properties of a series of Transition Metal Complexes

Table 5: Crystal structure data for complexes 5.1-5.7

	[MnL ⁴⁺] ²⁺ 5.1	[FeL ⁴⁺] ²⁺ 5.2	[CoL ⁴⁺] ²⁺ 5.3	[NiL ⁴⁺] ²⁺ 5.4	[ZnL ⁴⁺] ²⁺ 5.5	[ZnL ⁴⁺] ²⁺ 5.7	[CdL ⁴⁺] ²⁺ 5.8
M(1)-N(1)	2.264(7)	2.226(9)	2.185(3)	2.53(2)	2.223(4)	2.183(6)	2.349(12)
M(1)-N(2)	2.306(7)	2.252(8)	2.218(3)	2.264(7)	2.253(5)	2.234(4)	2.363(5)
M(1)-N(4)	2.319(7)	2.250(8)	2.239(3)	2.264(7)	2.179(4)	2.234(4)	2.366(5)
M(1)-N(6)	2.310(7)	2.259(9)	2.208(3)	2.264(7)	2.202(4)	2.234(4)	2.363(5)
M(1)-O(1)	2.173(6)	2.133(7)	2.141(2)	2.033(11)	2.146(4)	2.129(3)	2.255(9)
M(1)-O(2)	2.162(6)	2.155(7)	2.119(3)	2.033(11)	2.150(3)	2.129(3)	2.253(9)
M(1)-O(3)	2.181(6)	2.129(7)	2.115(2)	2.033(11)	2.139(3)	2.129(3)	2.252(9)
N(1)-M(1)-N(2)	73.2(2)	73.3(3)	73.71(10)	70.3(2)	73.73(19)	73.98(9)	71.89(11)
N(1)-M(1)-N(4)	71.8(2)	73.0(3)	73.03(10)	70.3(2)	74.57(15)	73.98(9)	71.92(11)
N(1)-M(1)-N(6)	72.1(2)	73.1(3)	74.40(10)	70.3(2)	73.47(17)	73.98(9)	71.89(11)
N(2)-M(1)-N(4)	111.5(2)	113.5(3)	112.51(10)	109.3(2)	110.22(16)	112.69(8)	110.84(11)
N(2)-M(1)-N(6)	113.2(2)	112.5(3)	111.52(10)	109.3(2)	113.38(16)	112.69(8)	110.72(11)
N(6)-M(1)-N(4)	109.1(2)	109.9(3)	113.33(10)	109.3(2)	114.29(16)	112.69(8)	110.86(11)
O(1)-M(1)-N(1)	130.4(2)	131.7(3)	130.45(10)	128.2(4)	132.22(16)	129.47(9)	126.5(3)
O(1)-M(1)-N(2)	76.7(2)	78.9(3)	79.01(9)	81.9(4)	78.74(17)	78.33(13)	73.2(4)
O(1)-M(1)-N(4)	157.5(2)	83.2(3)	156.52(10)	79.0(4)	79.52(15)	79.11(13)	160.1(4)
O(1)-M(1)-N(6)	85.1(2)	155.2(3)	78.45(10)	161.8(5)	154.28(15)	156.55(13)	84.4(5)
O(1)-M(1)-O(3)	85.2(2)	83.5(3)	85.19(9)	86.4(6)	81.49(14)	83.91(13)	88.2(4)
O(2)-M(1)-O(1)	84.7(2)	82.6(3)	83.22(10)	86.4(6)	83.57(14)	83.91(13)	88.2(4)
O(2)-M(1)-N(1)	126.2(2)	130.4(3)	129.94(10)	128.2(4)	128.93(17)	129.47(9)	126.6(3)
O(2)-M(1)-N(2)	79.8(2)	156.3(3)	80.12(10)	161.8(5)	157.33(16)	156.55(13)	84.6(5)
O(2)-M(1)-N(4)	76.5(2)	78.5(3)	79.01(10)	81.9(4)	79.98(14)	78.33(13)	73.2(4)
O(2)-M(1)-O(3)	86.1(2)	85.0(3)	84.48(10)	86.4(6)	85.06(13)	83.91(13)	88.1(4)
O(2)-M(1)-N(6)	161.1(2)	79.8(3)	155.65(10)	79.0(4)	78.07(14)	79.11(13)	160.1(4)
O(3)-M(1)-N(1)	128.9(2)	126.8(3)	127.23(10)	128.2(4)	128.33(15)	129.47(9)	126.6(3)
O(3)-M(1)-N(2)	157.9(2)	78.4(3)	159.06(10)	79.0(4)	78.44(15)	79.11(13)	160.1(4)
O(3)-M(1)-N(4)	81.2(2)	160.0(3)	77.98(9)	161.8(5)	156.97(15)	156.55(13)	84.5(5)
O(3)-M(1)-N(6)	77.2(2)	77.8(3)	78.18(10)	81.9(4)	79.14(15)	78.33(13)	73.3(4)

For convenience, the following labels table should be replaced with those indicated for the corresponding metal complexes:

For Ni(5.4), Zn(5.7) and Cd(5.8): N(4) = N(2)#1, N(6) = N(2)#2, O(2) = O(1)#1, O(3) = O(1)#2. For Zn (5): N(4) = N(3), N(6) = N(4). Symmetry operations represented by #1 and #2 are unique for each complex.

Crystal Structure of $[\text{Mn}^{\text{II}}(\text{L}^4)][\text{ClO}_4][\text{Br}]\cdot\text{CH}_3\text{CN}$ (5.1)

The manganese compound crystallises in the monoclinic space group P21/m and contains one complex within the asymmetric unit (asu) (Fig. 13). The Mn^{II} ion lies at the centre of a slightly distorted capped octahedron co-ordination geometry which has been confirmed by CShM (Table 6). The Mn^{II} ion is surrounded by two types of donor atoms. There are four N-donors N1, N2, N4 and N6 and three oxygen donors O1, O2 and O3 (Fig. 14). The co-ordinative bond lengths range from 2.162(6) Å to 2.319(7) Å. The co-ordinative bond lengths of nitrogen donors N1, N2, N4 and N6 (Table 5) are similar to those of the eight coordinate compound $[\text{Mn}^{\text{II}}(\text{TPA})][\text{NO}_3]_2$ reported by Barrios *et al.* which range from 2.2616(16) Å and 2.3889(16) Å.³² When compared to other 7-coordinate manganese complexes involving similar TPA frameworks, the co-ordinative bond lengths and angles are also very similar. For example, the compound reported by Baldeau, *et al.* exhibits co-ordinating pyridine groups ranging between 2.440(7) Å and 2.269(4) Å.³³

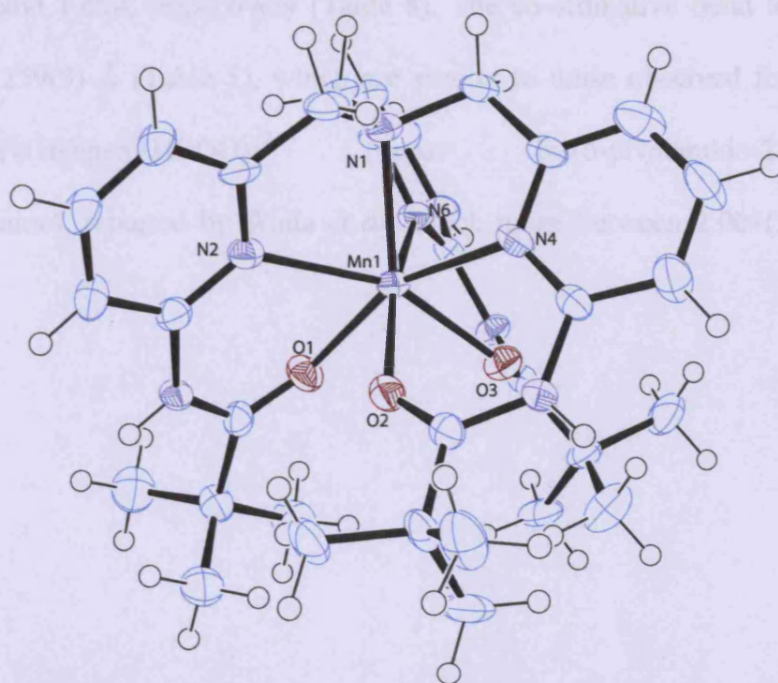


Figure 13: The asymmetric unit of 5.1. Displacement ellipsoids are shown at 50% probability. H atoms are of arbitrary size.

Chapter 5: Co-ordinative properties of a Tripodal Trisamide Ligand with a Strong Capped Octahedral preference; Structural, Spectroscopic and Electrochemical properties of a series of Transition Metal Complexes

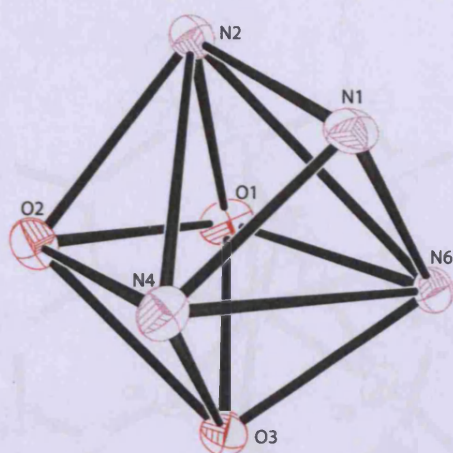


Figure 14: A view of the core geometry of **5.1** of covalent bond radius less than 3 Å. The metal has been removed to help illustrate the geometry.

Crystal Structure of $[\text{Fe}^{\text{II}}(\text{L}^4)][\text{ClO}_4][\text{Br}]\cdot\text{CH}_3\text{CN}$ (**5.2**)

The iron compound crystallises in the monoclinic space group P21/m and contains one complex within the asu (Fig. 15). The Fe^{II} is co-ordinated via four N-donors and three oxygen donors (Fig. 16). The core geometry is best described as capped octahedron, with $S(\text{OCF})$ and $S(\text{TPRS})$ values of 0.335 and 1.498, respectively (Table 8). The co-ordinative bond lengths range from 2.129(7) Å to 2.259(9) Å (Table 5), which are similar to those observed for the 7-coordinate complex, $[\text{Fe}(\text{H}_2\text{bppa})(\text{HCOO})]^{2+}$ (bppa= bis(6-pivalamido-2-pyridylmethyl)(2-pyridylmethyl)amine), reported by Wada *et al.* which range between 2.004(3) Å and 2.226(3) Å.³⁴

Chapter 5: Co-ordinative properties of a Tripodal Trisamide Ligand with a Strong Capped Octahedral preference; Structural, Spectroscopic and Electrochemical properties of a series of Transition Metal Complexes

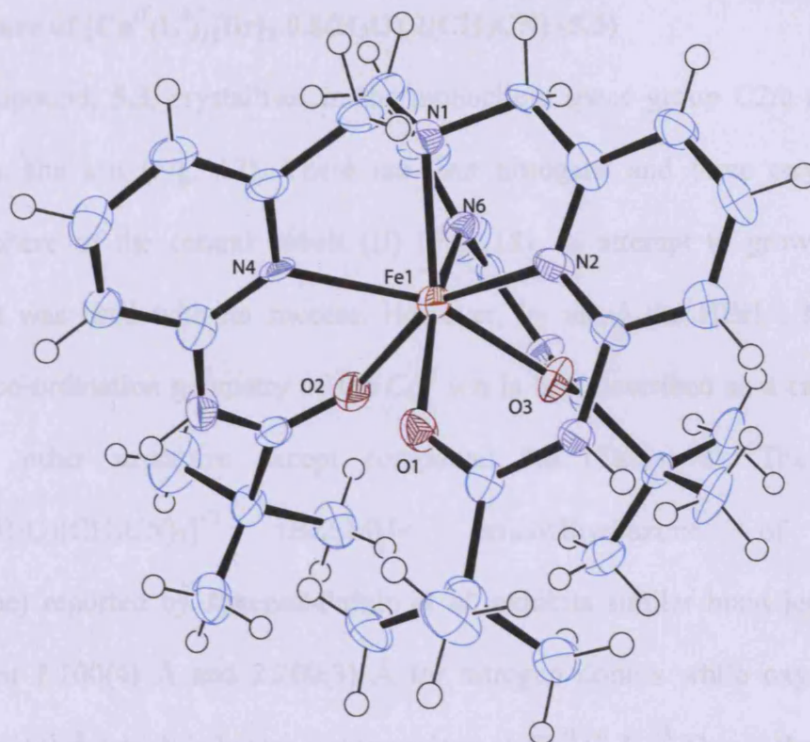


Figure 15: The asymmetric unit of **5.2**. Displacement ellipsoids are shown at 50% probability. H atoms are of arbitrary size.

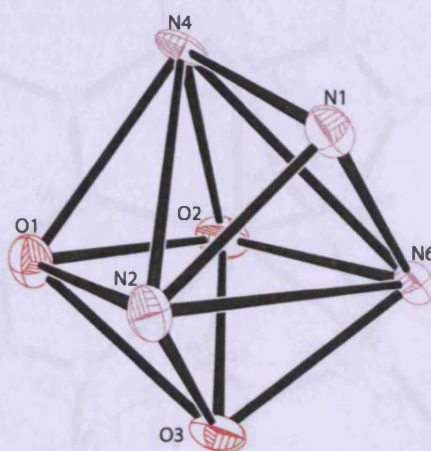


Figure 16: A view of the core geometry of **5.2** of covalent bond radius less than 3Å. The metal has been removed to help illustrate the geometry.

Crystal Structure of $[\text{Co}^{\text{II}}(\text{L}^4)][\text{Br}]_2 \cdot 0.5(\text{H}_2\text{O}) \cdot 2(\text{CH}_3\text{CN})$ (5.3)

The cobalt compound, **5.3**, crystallises in the monoclinic space group $C2/c$ and contains one complex within the asu (Fig. 17). There are four nitrogens and three oxygens within the coordinative sphere of the central cobalt (II) (Fig. 18). In attempt to grow crystals of **5.3**, perchlorate salt was used with no success. However, by using the HBrL^4 , the crystals were obtained. The co-ordination geometry of the Co^{II} ion is best described as a capped octahedron similar to all other structures except compound **5.6** (Table. 8). The compound the $[\text{Co}(\text{BZLMH})(\text{H}_2\text{O})(\text{CH}_3\text{CN})_2]^{+2}$ (BZLMH= benzoylhydrazone of 6-acetyl-1,3,7-trimethylumazine) reported by Jimenez-Pulido *et al.* exhibits similar bond lengths and angles ranging between 2.100(4) Å and 2.200(3) Å for nitrogen donors while oxygen donors vary 2.149(3) Å 2.364(3) Å which is longer in comparison to Co^{II} (**5.3**).³⁵ This is the first example of Co^{II} being seven coordinate in TPA based ligand.

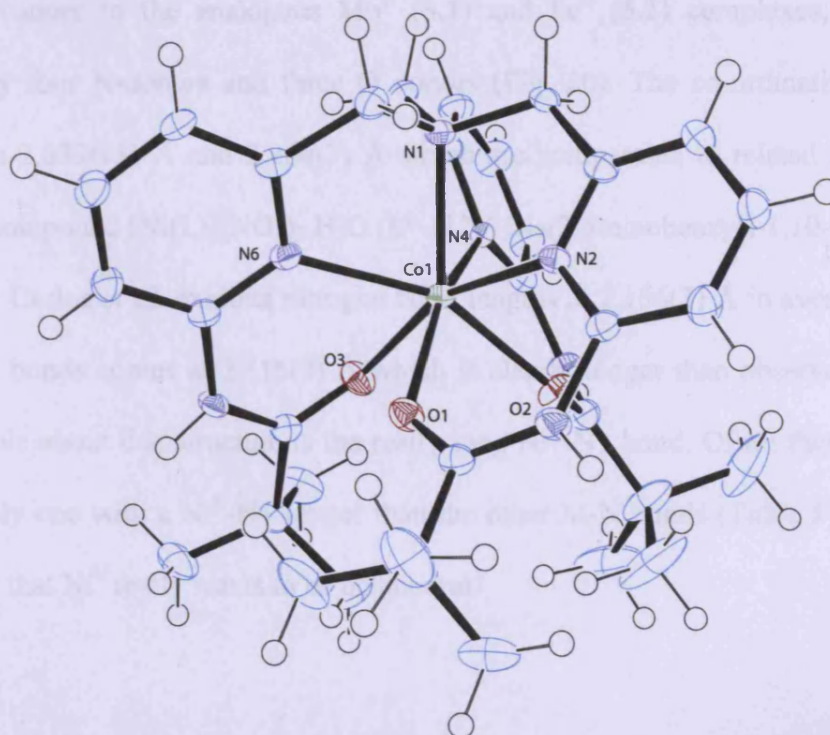


Figure 17: The asymmetric unit of **5.3**. Displacement ellipsoids are shown at 50% probability. H atoms are of arbitrary size.

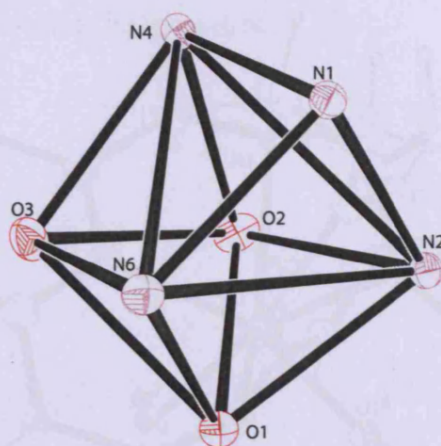


Figure 18: A view of the core geometry of **5.3** of covalent bond radius less than 3 Å. The metal has been removed to help illustrate the geometry.

Crystal Structure of $[\text{Ni}^{\text{II}}(\text{L}^4)][\text{ClO}_4]_{1.67}[\text{Br}]_{0.33} \cdot 0.67(\text{H}_2\text{O})$ (**5.4**)

The nickel compound crystallises in the hexagonal space group P63/m and contains two unique complexes within the asu one of them is very disordered while the other one is NiL^4 (Fig. 19). In an identical manner to the analogous Mn^{II} (**5.1**) and Fe^{II} (**5.2**) complexes, the Ni^{II} ion is coordinated by four N-donors and three O donors (Fig. 20). The co-ordinative bond lengths range between 2.033(11) Å and 2.264(7) Å which are comparable to related compounds. For example, the compound $[\text{Ni}(\text{L})](\text{NO}_3)_2 \cdot \text{H}_2\text{O}$ (L= N,N'-Bis(2-aminobenzyl)-1,10-diaza-15-crown-5) reported by Carlos *et al.* exhibits nitrogen bond lengths at 2.166(3) Å in average whereas the nickel oxygen bonds comes at 2.316(3) Å which is clearly longer than observed for **5.4**.³⁶ The really noticeable about this structure is the really long $\text{Ni}^{\text{II}}\text{-N1}$ bond. Of all these structures Ni^{II} (**5.4**) is the only one with a $\text{Ni}^{\text{II}}\text{-N1}$ longer than the other M-N bonds (Table 5), which perhaps reflect the fact that Ni^{II} really wants to be octahedral.

Chapter 5: Co-ordinative properties of a Tripodal Trisamide Ligand with a Strong Capped Octahedral preference; Structural, Spectroscopic and Electrochemical properties of a series of Transition Metal Complexes

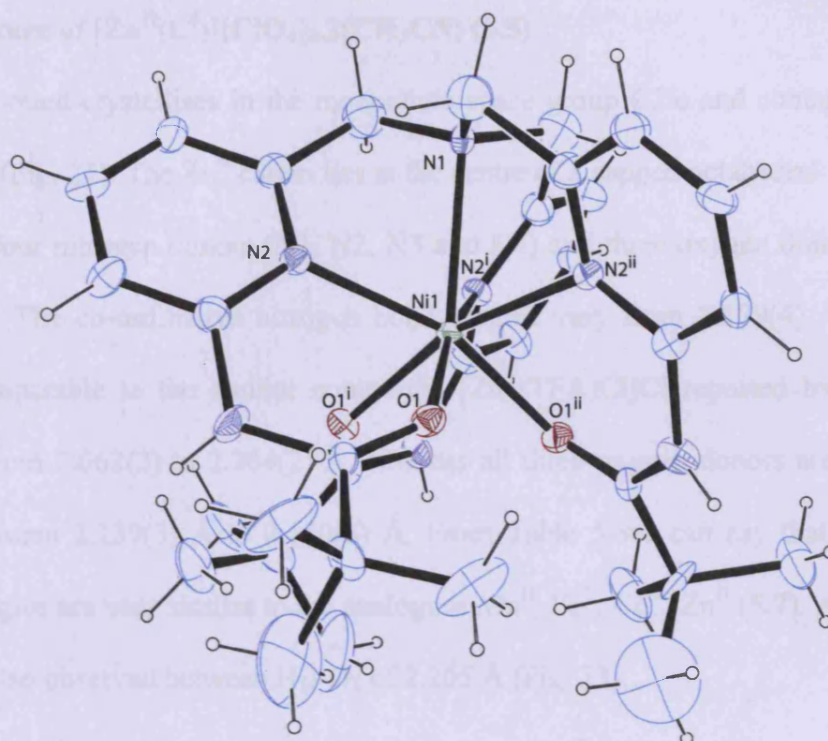


Figure 19: The asymmetric unit of **5.4**. Displacement ellipsoids are shown at 10% probability. H atoms are of arbitrary size.

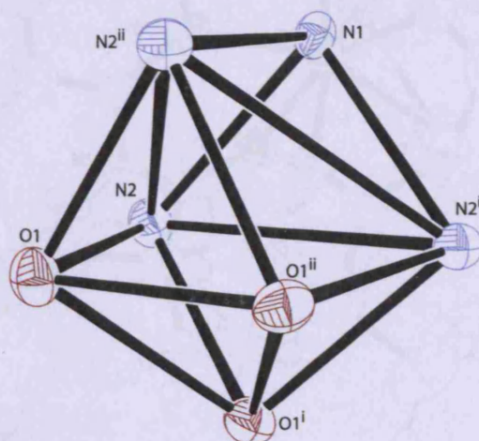


Figure 20: A view of the core geometry of **5.4** of covalent bond radius less than 3 Å. The metal has been removed to help illustrate the geometry.

Crystal Structure of $[\text{Zn}^{\text{II}}(\text{L}^4)][\text{ClO}_4]_2 \cdot 2(\text{CH}_3\text{CN})$ (5.5)

The zinc compound crystallises in the monoclinic space group $C2/c$ and contains one complex within the asu (Fig. 21). The Zn^{II} cation lies at the centre of a capped octahedral geometry (Table 8). There are four nitrogen donors (N1, N2, N3 and N4) and three oxygen donors (O1, O2 and O3) (Fig. 22). The co-ordinative nitrogen bond lengths vary from 2.179(4) Å to 2.253(5) Å which are comparable to the similar compound $[\text{Zn}^{\text{II}}(\text{TPA})\text{Cl}]\text{Cl}$ reported by Duboc *et al.*³⁷ which range from 2.062(2) to 2.264(2) Å, whereas all three oxygen donors are slightly shorter and range between 2.139(3) Å to 2.150(3) Å. From Table 5 we can say that Zn^{II} (5.5) bond lengths and angles are very similar to the analogues Mn^{II} , Fe^{II} , Co^{II} , Zn^{II} (5.7). A hydrogen bond interaction is also observed between $\text{H}_{5a}-\text{O}_5$ of 2.205 Å (Fig. 23).

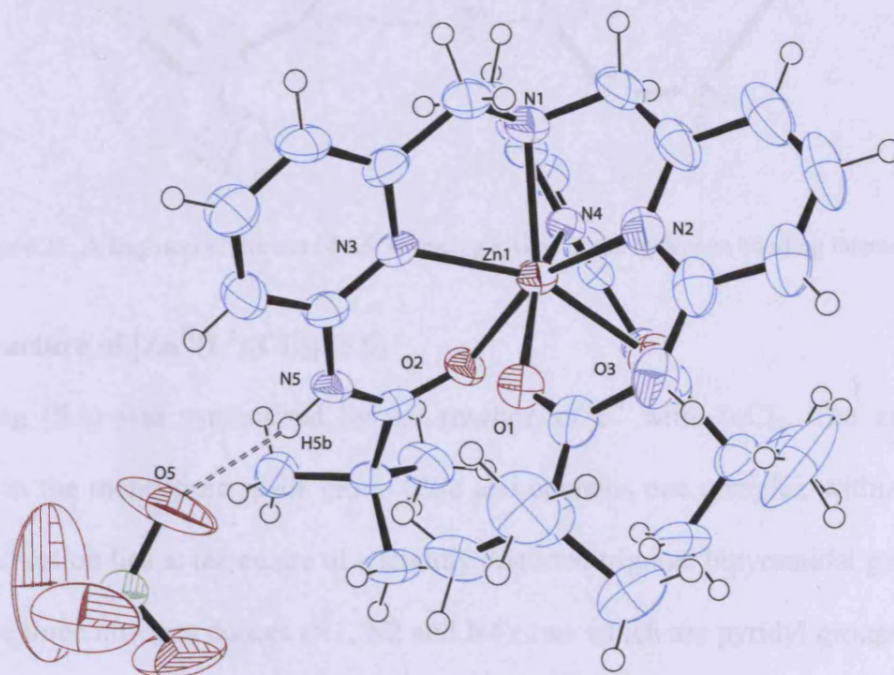


Figure 21: The asymmetric unit of 5.5. Displacement ellipsoids are shown at 50% probability. H atoms are of arbitrary size.

Chapter 5: Co-ordinative properties of a Tripodal Trisamide Ligand with a Strong Capped Octahedral preference; Structural, Spectroscopic and Electrochemical properties of a series of Transition Metal Complexes

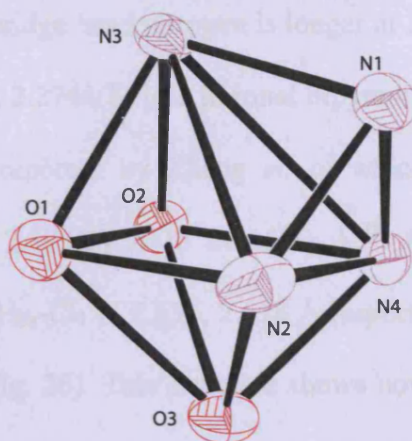


Figure 22: A view of the core geometry of **5.5** of covalent bond radius less than 3 Å. The metal has been removed to help illustrate the geometry.

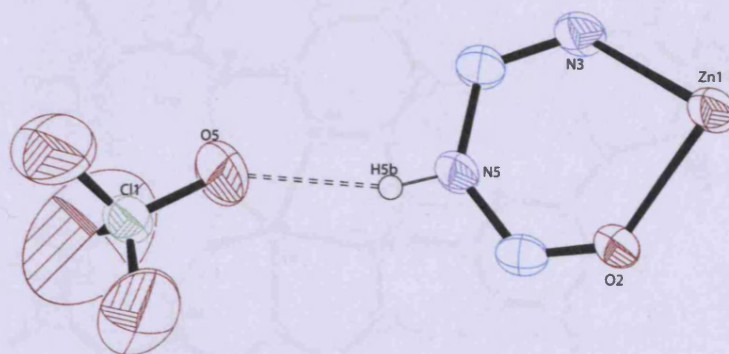


Figure 23: A fragment of the asu of **5.5**, revealing a view of the hydrogen bonding interactions.

Crystal Structure of $[\text{Zn}^{\text{II}}(\text{L}^4)(\text{Cl})_2]$ (**5.6**)

The resulting (**5.6**) was synthesised by the reaction of L^4 with ZnCl_2 . The zinc compound crystallises in the monoclinic space group $C2/c$ and contains one complex within the asu (Fig. 24). The Zn^{II} cation lies at the centre of a slightly distorted trigonal bipyramidal geometry (Table 6). There are three nitrogen donors (N1, N2 and N4), two which are pyridyl groups and with one bridge-head N1. In addition, there are two chloride donors taking the equatorial positions and the third position is occupied by the bridge head nitrogen N1 which cause one arm of TPPA not to co-ordinate to the metal centre (Fig. 25). The co-ordinative bond lengths are typical for nitrogen donors and vary from 2.139(5) Å to 2.233(5) Å (Table 7) and this is similar to the compound $[\text{Zn}^{\text{II}}(\text{TPA})\text{Cl}]\text{Cl}$ reported by Duboc *et al.*³⁷ which range from 2.062(2) Å to 2.083(2) Å for

Chapter 5: Co-ordinative properties of a Tripodal Trisamide Ligand with a Strong Capped Octahedral preference; Structural, Spectroscopic and Electrochemical properties of a series of Transition Metal Complexes

pyridyl nitrogens whereas the bridge head nitrogen is longer at 2.264(2), the chloride however is shorter in the given example at 2.2744(8) in a trigonal bipyramidal environment. However, it is very similar to the complex reported by Zhang *et. al* which has similar environment and geometry, which range from 2.309(2) Å to 2.116(3) Å.³⁸ A hydrogen bond interaction is observed between H_{3a}-Cl₁ and H_{5a}-Cl₁ of 2.637, 2.618 Å respectively. A weaker one is observed between H_{3a}-Cl₂ of 3.208 Å (Fig. 26). This structure shows how strongly the chloride acts as a ligand in comparison to iodide and bromide which do not co-ordinate to the metal centre.

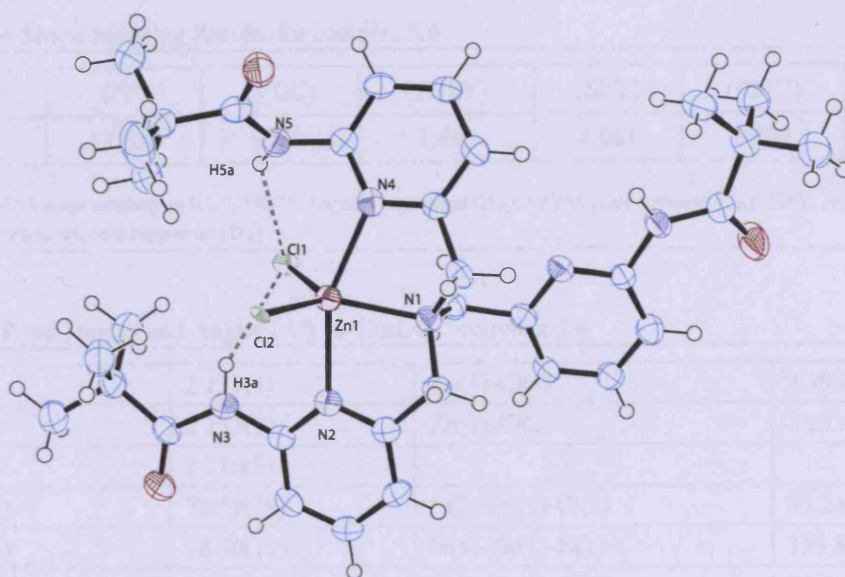


Figure 24: The asymmetric unit of **5.6**. Displacement ellipsoids are shown at 50% probability. H atoms are of arbitrary size.

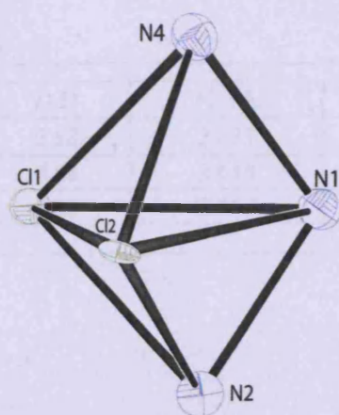


Figure 25: A view of the core geometry of **5.6** of covalent bond radius less than 3 Å. The metal has been removed to help illustrate the geometry.

Chapter 5: Co-ordinative properties of a Tripodal Trisamide Ligand with a Strong Capped Octahedral preference; Structural, Spectroscopic and Electrochemical properties of a series of Transition Metal Complexes

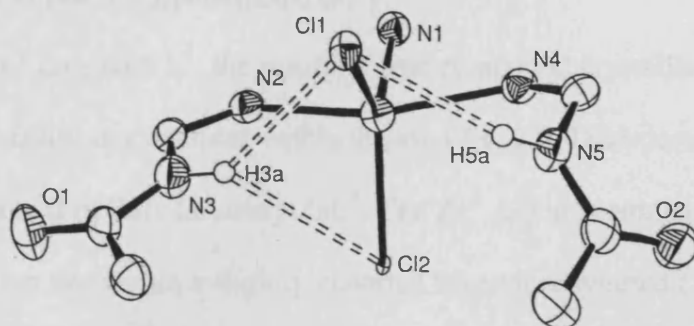


Figure 26: A fragment of the asu of 5.6, revealing a view of the hydrogen bonding interactions.

Table 6: Continuous Shape Mapping Results for complex 5.6.

Structure	(PP)	(VOC)	(TBPY)	(SPY)	(JSPY)	(JTBP)
L ¹ _Zn (5.6)	33.350	6.694	1.465	4.061	6.694	4.969

PP: Pentagon (D_{5h}), VOC: Vacant octahedron (C_{4v}), TBPY: Trigonal bipyramid (D_{3h}), SPY: Square pyramid (C_{4v}), JSPY: Johnson square pyramid (C_{4v}), JTBP: Johnson trigonal bipyramid (D_{3h}).

Table 7: Relevant Bond lengths and Angles ($^{\circ}$) for $[ZnL4]^{+2}$ complex 5.6

Zn(1)-N(1)	2.139(5)	Zn(1)-Cl(1)	2.3055(16)
Zn(1)-N(2)	2.233(5)	Zn(1)-Cl(2)	2.3330(14)
Zn(1)-N(4)	2.210(5)		
N(1)-Zn(1)-N(2)	78.52(19)	N(2)-Zn(1)-Cl(2)	93.24(14)
N(1)-Zn(1)-N(4)	78.30(19)	N(4)-Zn(1)-N(2)	156.81(19)
N(1)-Zn(1)-Cl(1)	116.74(15)	N(4)-Zn(1)-Cl(1)	94.50(14)
N(1)-Zn(1)-Cl(2)	123.84(14)	N(4)-Zn(1)-Cl(2)	99.09(14)
N(2)-Zn(1)-Cl(1)	96.45(14)	Cl(1)-Zn(1)-Cl(2)	119.38(6)

Table 8: H-bonding geometry (\AA , $^{\circ}$) for 5.6

D-H...A	D-H	H...A	D...A	D-H...A
N3-H3A...Cl1	0.88	2.637	3.376	142.24
N5-H5A...Cl1	0.88	2.618	3.319	137.35
N7-H7...O2	0.88	2.595	3.190	125.77

Crystal Structure of $[\text{Zn}^{\text{II}}(\text{L}^4)]_{0.5}[\text{ZnL}_4]_{0.5}[\text{I}]$ (5.7)

From the reaction of ZnL_2 with L^4 , the resulting zinc compound crystallises in the trigonal space group P-3c1 and contains one complex within the asu (Fig. 27). Disordered counter ion is present which consists of a half of ZnL_4 for every ZnL^4 . The Zn^{II} cation is similar to the zinc compound, 5.7, and the metal ion lies within a slightly distorted trigonal bipyramid (Table 9) surrounded by four nitrogen donors and three oxygens (Fig. 28). Comparison between complexes 5.5 and 5.7 shows very similar bond lengths and angles.

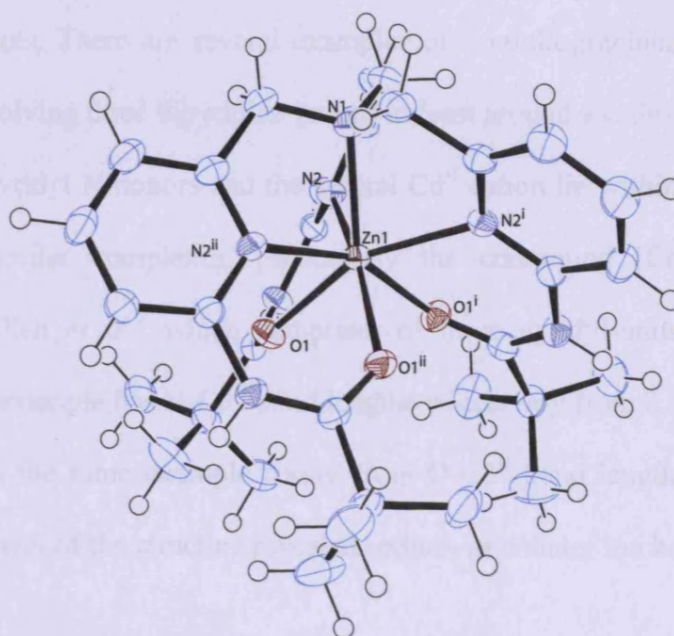


Figure 27: The asymmetric unit of 5.7. Displacement ellipsoids are shown at 50% probability. H atoms are of arbitrary size.

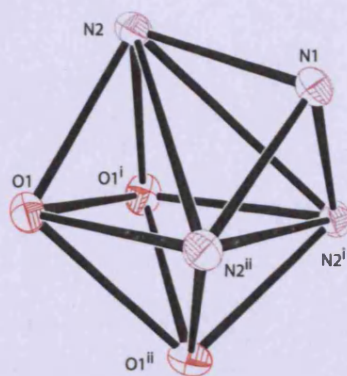


Figure 28: A view of the core geometry of 5.7 of covalent bond radius less than 3 Å. The metal has been removed to help illustrate the geometry.

Crystal Structure of $[\text{Cd}^{\text{II}}(\text{L}^4)][\text{ClO}_4]_2 \cdot \text{Na}(\text{ClO}_4)$ (5.8)

The cadmium compound crystallises in the trigonal space group R32 and contains one complex within the asu (Fig. 29). The cadmium ion lies at the centre of the molecule surrounded by seven donor atoms (four N atoms and three O atoms) in a slightly distorted capped octahedron coordination geometry (Fig. 30; Table 9). Three of the nitrogen donor atoms (N2, N2ⁱ and N2ⁱⁱ) originate from the three pyridyl groups and the bridging N1, while the other three co-ordinating atoms are oxygen and reveal a similar co-ordination environment to the analogous Mn^{II}, Fe^{II}, Ni^{II}, and Zn^{II} complexes. There are several examples of crystallographically characterised co-ordination spheres involving three bipyridine groups at least around a cadmium centre. The bond lengths between the pyridyl N-donors and the central Cd^{II} cation lie within the expected ranges on comparison to similar complexes, particularly the compound $[\text{Cd}^{\text{II}}(\text{TPA})(\text{NO}_3)(\text{H}_2\text{O})]$ NO₃ synthesised by Allen *et al.*³ which comprises of three pyridyl-units arranged around a cadmium centre. This example has N-Cd^{II} bond lengths which vary from 2.30(1) Å to 2.44(1) Å. A further similarity in the same example comes from O-Cd^{II} bond lengths of 2.431(9) Å and 2.40(1) Å. The refinement of the structure revealed sodium as counter ion however, the source of it is not known.

Chapter 5: Co-ordinative properties of a Tripodal Trisamide Ligand with a Strong Capped Octahedral preference; Structural, Spectroscopic and Electrochemical properties of a series of Transition Metal Complexes

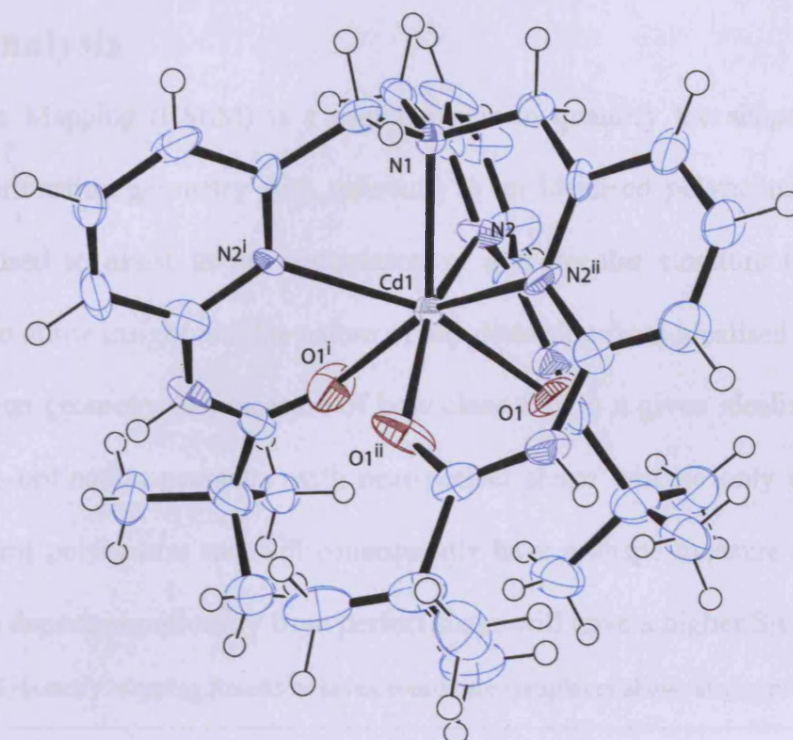


Figure 29: The asymmetric unit of **5.8**. Displacement ellipsoids are shown at 50% probability. H atoms are of arbitrary size.

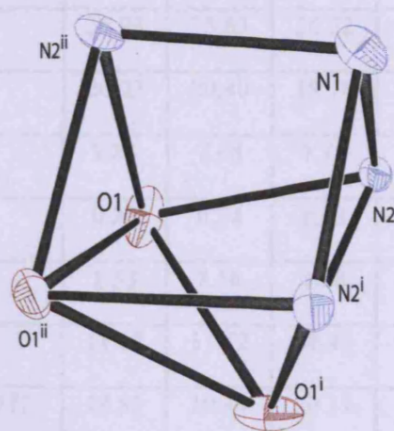


Figure 30: A view of the core geometry of **5.8** of covalent bond radius less than 3 Å. The metal has been removed to help illustrate the geometry.

Structural Analysis

Continuous Shape Mapping (CShM) is a useful means to quantify the shape (or symmetry) content of a co-ordination geometry with reference to an idealised polyhedron. The program SHAPE can be used to assist in the comparison of a molecular structure to a given ideal polyhedron, and so allow insight into the nature of any distortion from idealised geometries. The S values for a given geometry is a measure of how close it is to a given idealised geometry. A metal complex co-ordination geometry with near-perfect shape will lie only a small distance away from the ideal polyhedron and will consequently have a shape measure close to zero. A polyhedron which departs significantly from perfect shape will have a higher S value.

Table 9: Continuous Symmetry Mapping Results of seven coordinate complexes shows strong preferences of mono capped octahedron.

Geometry	Complex						
	5.1	5.2	5.3	5.4	5.5	5.7	5.8
Heptagon	35.93	35.63	36.22	36.52	35.78	36.64	36.53
Hexagonal pyramid	20.02	20.40	19.78	19.60	20.18	19.79	19.29
Pentagonal bipyramid	7.84	7.68	7.75	8.75	7.79	8.28	8.53
Capped octahedron	0.33	0.34	0.23	0.53	0.29	0.24	0.48
Capped trigonal prism	1.53	1.50	1.48	2.02	1.25	1.64	1.89
Johnson pentagonal bipyramid J13	11.67	11.42	11.49	12.08	11.37	12.05	12.40
Johnson elongated triangular pyramid J7	18.85	19.44	20.31	18.05	19.69	20.19	17.31

Without exceptions, all structures are best described as having a capped octahedral metal centre, though these numbers show how closely related the MCO and MCTP geometries are.

Table 10 shows the angles of θ_2 and θ_5 for all mono capped octahedron structures in relation to the ideal and Hoffman ideal angles.

Chapter 5: Co-ordinative properties of a Tripodal Trisamide Ligand with a Strong Capped Octahedral preference; Structural, Spectroscopic and Electrochemical properties of a series of Transition Metal Complexes

Table 10: A comparison between θ_2 and θ_5 averaged angles for $M^{II}L^4$ structures and their relation to Hoffman's angles:

	ideal	Hoffman ideal	Mn ^{II} (5.1)	Fe ^{II} (5.2)	Co ^{II} (5.3)	Ni ^{II} (5.4)	Zn ^{II} (5.5)	Zn ^{II} (5.7)	Cd ^{II} (5.8)
θ_2	54.7°	75°	72.4°	73.1°	73.7°	70.3°	73.9°	73.9°	71.9°
θ_5	125.3°	138°	128.5.4°	129.6°	129.2°	128.2°	129.8°	129.5°	126.6°

It is clearly from table 10 that all ML^4 structures are sterically congested and all angles lay between the ideal CO and Hoffman ideal angles. In addition, due to the long bond for Ni-N1 in comparison to all other M-N1 bonds we can see that θ_2 of N1-Ni-N2, N1-Ni-N4, N1-Ni-N6 is quite acute and not as obtuse as other N1-M-N2, N1-M-N4, N1-M-N6 where M-N1 is shorter than Ni-N1 (Diagram 1).

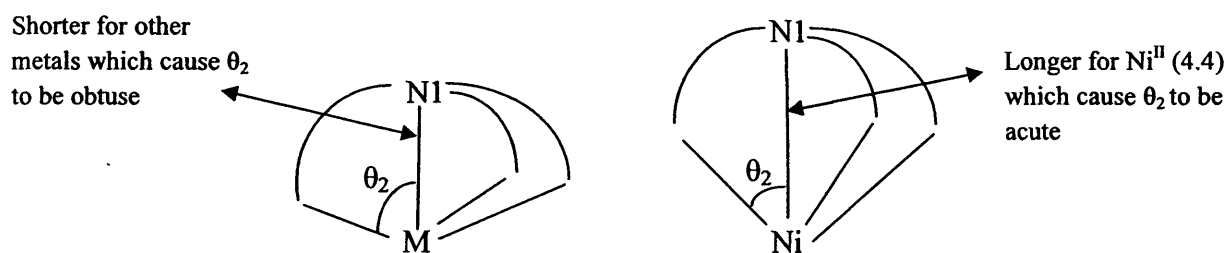


Diagram 1: A comparison between Ni^{II} (5.4) structure and other metal structures.

Conclusion

A series of transition metal complexes with a trisamide ligand based on a TPA framework have been synthesised and structurally characterised. This ligand seems to favour a seven co-ordinate capped octahedral coordination environment, except in the case of 5.6 in which a five coordinate trigonal bipyramidal geometry is preferred. The resulting co-ordination environment seems to be dependent on the identity of the counter ion. For example, chloride is able to occupy equatorial positions around the metal centre, whereas similar co-ordination of the larger iodide and perchlorate counter ions would lead to unfavourably close interactions. A CCDC database on June 2011 shows how rare is this coordination number for coordination compounds. For example, among all manganese structures only 3.79% are seven coordinate, iron 0.67%, cobalt 0.73%, nickel 0.25%, zinc 0.40%, cadmium 7.2%. This tripodal ligand heavily favours the formation of seven co-ordinate capped octahedral complexes. Such geometries are extremely rare and more typically seen in complexes of the larger cations, such as Mn(II) and Cd(II). It is particularly unusual to observe seven co-ordinate structures of Ni(II) and Zn(II). The crystallographic data highlights how the pre-organisation of the ligand enforces what may typical be regarded as an unfavourable geometry on all the transition metal ions.

Chapter 5: Co-ordinative properties of a Tripodal Trisamide Ligand with a Strong Capped Octahedral preference; Structural, Spectroscopic and Electrochemical properties of a series of Transition Metal Complexes

References

1. G. Anderegg and F. Wenk, *Helv. Chim. Acta*, 1967, **50**, 2330.
2. A. Hazell, K. B. Jensen, C. J. McKenzie and H. Toftlund, *Inorg. Chem.*, 1994, **33**, 3127.
3. C. S. Allen, C.-L. Chuang, M. Cornebise and J. W. Canary, *Inorg. Chim. Acta*, 1995, **239**, 29-37.
4. B. G. Gafford and R. A. Holwerda, *Inorg. Chem.*, 1989, **28**, 60.
5. C. X. Zhang, S. Kaderli, M. Costas, E. Kim, Y.-M. Neuhold, K. D. Karlin and A. D. Zuberbühler, *Inorg. Chem.*, 2003, **42**, 1807.
6. A. Diebold and K. S. Hagen, *Inorg. Chem.*, 1998, **37**, 215.
7. D. G. Lonnon, D. C. Craig and S. B. Colbran, *Dalton Trans.*, 2006, 3785.
8. Z. H. Zhang, X. H. Bu, Z. A. Zhu and Y. T. Chen, *Polyhedron*, 1996, **15**, 2787.
9. J. Bjernemose, A. Hazell, C. J. McKenzie, M. F. Mahon, L. P. Nielsen, P. R. Raithby, O. Simonsen, H. Toftlund and J. A. Wolny, *Polyhedron*, 2003, **22**, 875.
10. A. Diebold and K. S. Hagen, *Inorg. Chem.*, 1998, **37**, 215.
11. Y. Gultneh, A. Farooq, K. D. Karlin, S. Liu and J. Zubieta, *Inorg. Chim. Acta*, 1993, **211**, 171.
12. Z. He, D. C. Craig and S. B. Colbran, *Dalton Trans.*, 2002.
13. Z. He, P. J. Chaimungkalanont, D. C. Craig and S. B. Colbran, *Dalton Trans.*, 2000, 1419.
14. Y. Zang, J. Kim, Y. H. Dong, E. C. Wilkinson, E. H. Appelman and L. Que, *J. Am. Chem. Soc.*, 1997, **119**, 4197.
15. H. Hayashi, S. Fujinami, S. Nagatomo, S. Ogo, M. Suzuki, A. Uehara, Y. Watanabe and T. Kitagawa, *J. Am. Chem. Soc.*, 2000, **122**, 2124.
16. H. Hayashi, K. Uozumi, S. Fujinami, S. Nagatomo, K. Shiren, H. Furutachi, M. Suzuki, A. Uehara and T. Kitagawa, *Chem. Lett.*, 2002, 416.
17. C.-I. Chuang, K. Lim, Q. Chen, J. Zubieta and J. W. Canary, *Inorg. Chem.*, 1995, **34**, 2562.
18. J.C.M.Rivas, S.L.Hinchley, L.Metteau and S.Parsons, *Dalton Trans.*, 2006, 2316.
19. S. Yamaguchi, A. Wada, S. Nagatomo, Y. T. Kitagawa, Y. K. Jitsukawa and H. Masuda, *The Chem. Soc. Japan*, 2004, 1556.
20. S. Yamaguchi, T. Takahashi, A. Wada, Y. Funahashi, T. Ozawa, K. Jitsukawa and H. Masudall, *Chem. Lett.*, 2007, **36**, 842-843.
21. M. Harata, K. Jitsukawa, H. Masuda and H. Fujinaga, *Chem. Lett.*, 1995, 61-62.
22. A. Wada, Y. Honda, S. Yamaguchi, S. Nagatomo, T. Kitagawa, K. Jitsukawa and H. Masuda, *Inorg. Chem.*, 2004, **43**, 5725-5735.
23. R. Hoffmann, B. F. Beier, E. L. Muetterties and A. R. Rossi, *Inorganic Chemistry*, 1977, **16**, 511-522.
24. M. G. B. Drew, J. Nelson, F. Esho, V. McKee and S. M. Nelson, *J. Chem. Soc., Dalton Trans.*, 1982, 1837 - 1843.
25. P. Dapporto, G. De Munno, A. Sega and C. Mealli, *Inorg. Chim. Acta*, 1984, **83**, 171-176.
26. A. Hazell, C. J. McKenzie and L. P. Nielsen, *Polyhedron*, 2000, **19**, 1333-1338.
27. H. Sakiyama, Y. Watanabe, R. Ito and Y. Nishida, *Inorg. Chim. Acta*, 2004, **357**, 4309-4312.
28. O. Horner, J.-J. Girerd, C. Philouze and L. Tchertanov, *Inorg. Chim. Acta*, 1999, **290**, 139-144.

Chapter 5: Co-ordinative properties of a Tripodal Trisamide Ligand with a Strong Capped Octahedral preference; Structural, Spectroscopic and Electrochemical properties of a series of Transition Metal Complexes

29. P. Gili, M. G. Martín Reyes, P. Martín Zarza, M. F. C. Guedes da Silva, Y. Y. Tong and A. J. L. Pombeiro, *Inorg. Chim. Acta*, 1997, **255**, 279-288.
30. N. G. Connelly and W. E. Geiger, *Chem. Rev.*, 1996, **96**, 877-910.
31. D. G. Lonnon, G. E. Ball, I. Taylor, D. C. Craig and S. B. Colbran, *Inorg. Chem.*, 2009, **48**, 4863-4872.
32. S. M. Baldeau, C. H. Slinn, B. Krebs and A. Rompel, *Inorg. Chim. Acta*, 2004, **357**, 3295-3303.
33. G. Guisado-Barrios, Y. Li, A. M. Z. Slawin, D. T. Richens, I. A. Gass, P. R. Murray, L. J. Yellowlees and E. K. Brechin, *Dalton Trans.*, 2008, 551-558.
34. A. Wada, S. Ogo, S. Nagatomo, T. Kitagawa, Y. Watanabe, K. Jitsukawa and H. Masuda, *Inorg. Chem.*, 2002, **41**, 616-618.
35. S. B. Jiménez-Pulido, F. M. Linares-Ordóñez, J. M. Martínez-Martos, M. N. Moreno-Carretero, M. Quirós-Olozábal and M. J. Ramírez-Expósito, *J. Inorg. Biochem.*, 2008, **102**, 1677-1683.
36. C. Platas-Iglesias, L. Vaiana, D. Esteban-Gomez, F. Avecilla, J. A. Real, A. de Blas and T. Rodriguez-Blas, *Inorg. Chem.*, 2005, **44**, 9704-9713.
37. C. Duboc, T. Phoeung, D. Jouvenot, A. G. Blackman, L. F. McClintock, J. Pécaut, M.-N. Collomb and A. Deronzier, *Polyhedron*, 2007, **26**, 5243-5249.
38. L. Zhang, R. J. Clark and L. Zhu, *J. Eur. Chem.*, 2008, 2894-2903.

Appendix 1: Attempted Work

Introduction

It is impossible for the researcher to get positive results all the time and more often than not, researchers spend much of the time not achieving what they expect. This does not necessarily mean that the time spent was worthless! Such work will help to have a better understanding and appreciation of what they have been doing and better ideas might come from it.

During this work many experiments have been carried out. Some results are promising but need further investigation, while some were without real success. In this appendix, such work is presented thus; perhaps researchers in the future can avoid doing those experiments or may be improve the experimental conditions.

To make it easier and more understandable for readers, the style of this chapter will not be as same as previous chapters; graphs, figures, tables and equations will be utilised, making it much easier to convey the information. Moreover, numbering the attempted experiments would show the invaluable effort that has been done. The main themes of attempted work include: synthesis and attempts at growing crystals.

Experiments and discussion

1- Cleaving of L²

As illustrated in Fig. 1 (2.364g, 3.658 mmol) of L² was dissolved in 50 mL of (1M) NaOH and refluxed for 2 hours to yield yellowish suspension of desired product (0.871g, 54%).¹⁻³ However, the ¹H NMR suggests the presence of the product with lots of impurities. Recrystallising the product from methanol, ethanol and acetone was unsuccessful. An alternative attempt to purify the product was to synthesise the zinc complex and to try to grow crystals using the slow diffusion method. However, this work led to a crystal with a very small unit cell, identical to those of pure sulphur. In addition, column chromatography would not be suitable in this case because of the polar nature of the product and the strong interaction between the silica and the ligand.

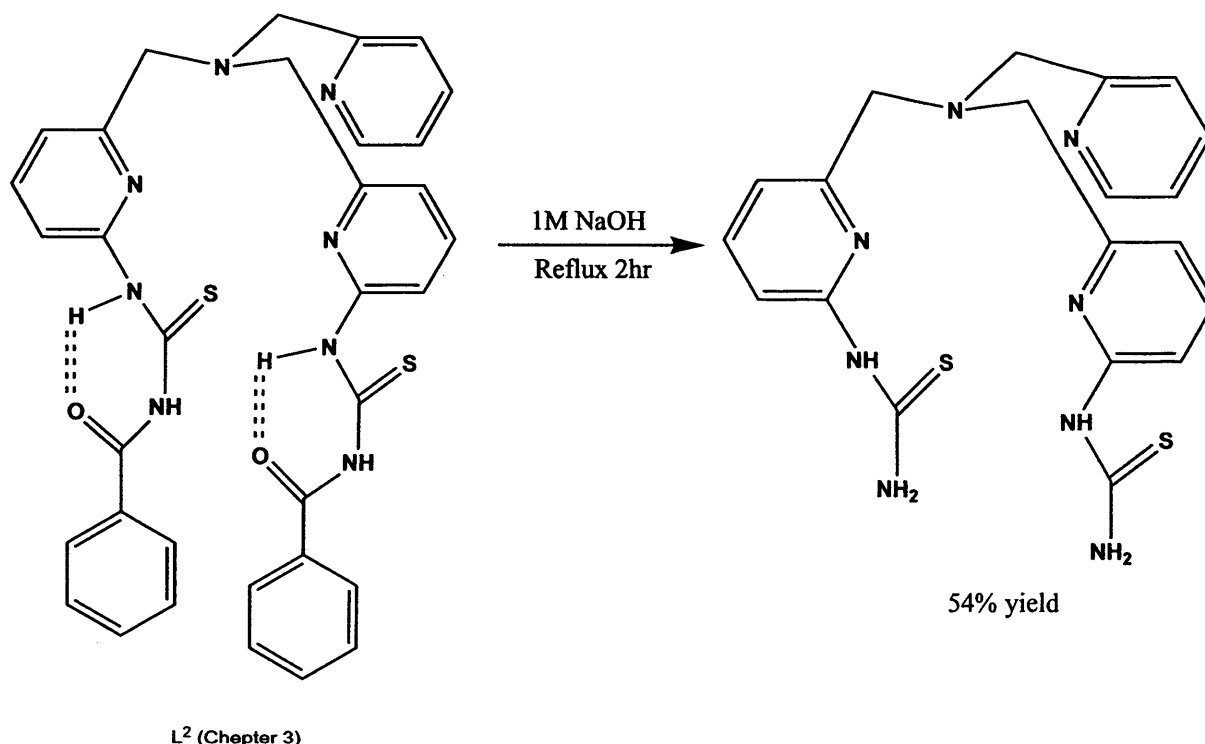


Figure 1: Cleaving of L²

2- Bromination of methyl groups

Researchers who have been working on making tripodal ligands (TPA) frame work have been following the literature procedures in making the tripod. This method was published by Harata *et al.*¹ which involves the protection of amino group following with bromination on the methyl using NBS in carbon tetrachloride (Fig. 2).

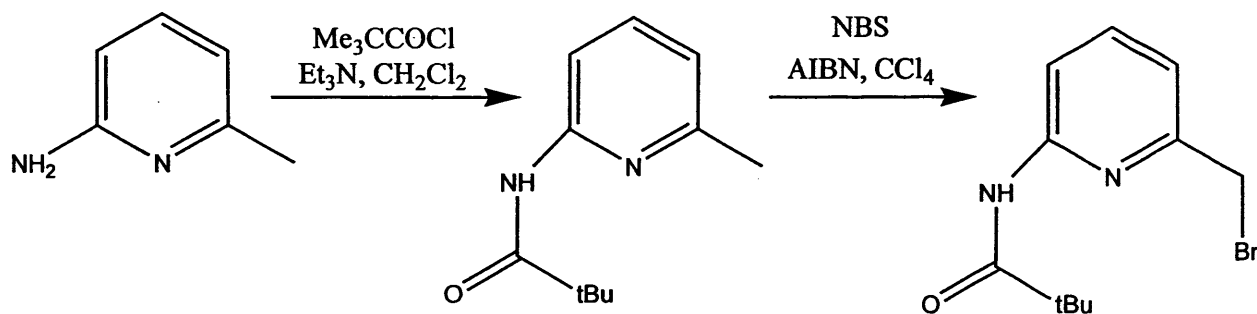


Figure 2: Literature procedure for the synthesis of the bromo compound N -(6-(bromomethyl)pyridin-2-yl)pivalamide

Unfortunately, we were not successful in trying to develop an alternative method of synthesis the bromo compounds in a direct manner (Fig. 3). The ^1H NMR indicated that the reaction was unsuccessful. Particularly telling was the complete absence of any alkyl protons. Compound (1) and (2) were prepared according to literature procedures.⁴⁻⁶

Appendix 1: Attempted Work

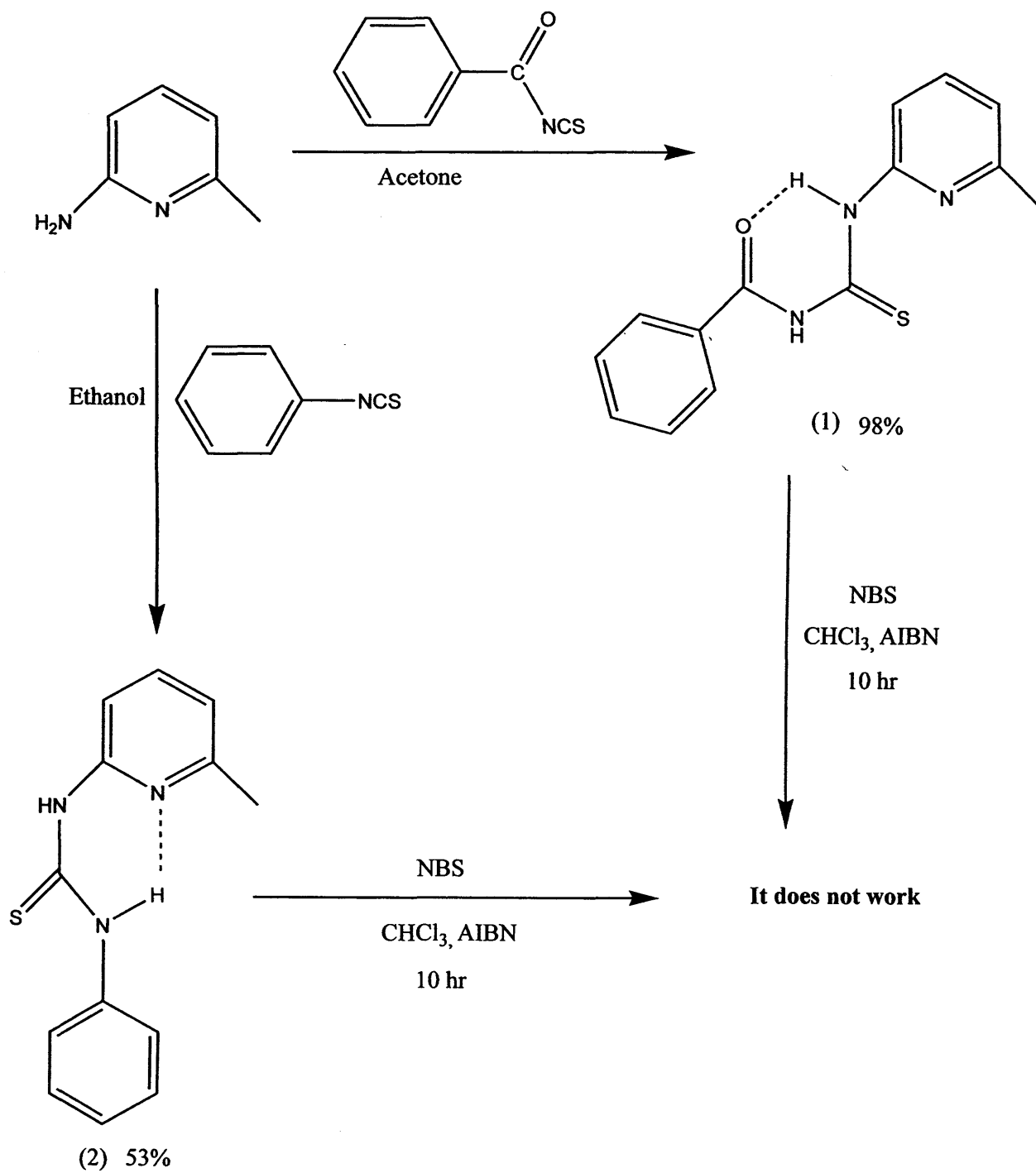


Figure 3: Literature procedures of synthesising the bromo compounds

Appendix 1: Attempted Work

3- Growing metal complex crystals of L^1 , L^2 and L^3

There are lots of recrystallizing methods and techniques. In this work mostly solvent diffusion and slow evaporation methods have been used to grow high quality crystals from different solvent mixtures. However, the material is often precipitated very rapidly resulting in microcrystalline or virtually amorphous products that are useless for conventional single crystal work. Some attempted work is summarised in Table 1.

In addition to attempts to grow crystals of simple metal complexes, there were numerous attempts to obtain guest-host structures of these complexes with hosts such as, phosphate, amino acids, di and tri carboxylic acids, halides and even oxone.

Appendix 1: Attempted Work

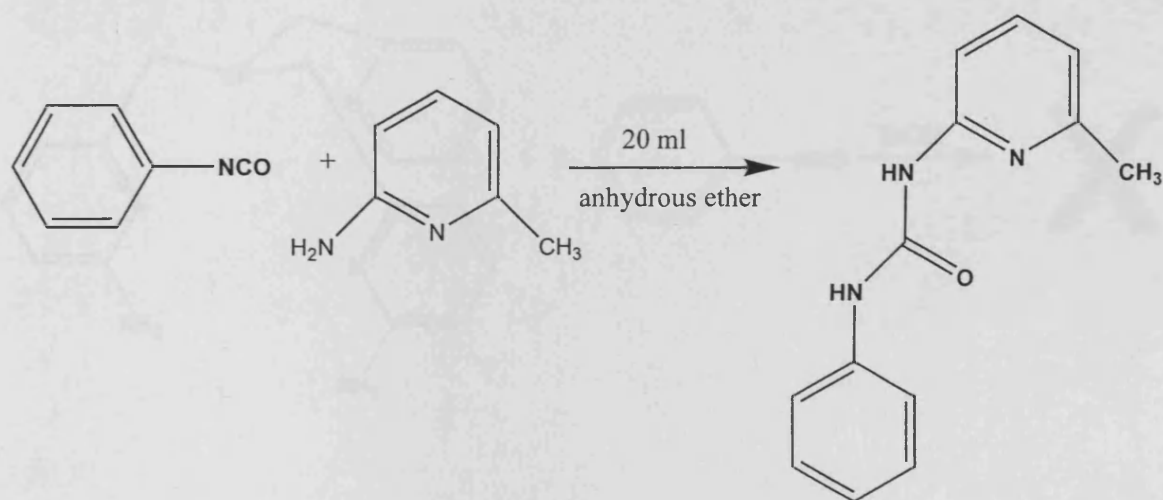
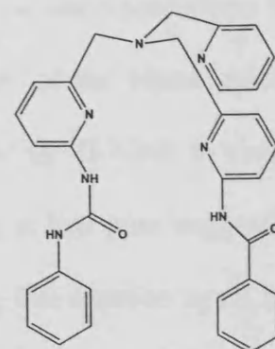
Table 1: summary of attempted work towards growing crystals

No.	Host	Guest	Solvent		Observation
			Host	Guest	
1	L ¹	Co(ClO ₄) ₂ .6H ₂ O	CH ₃ CN	CH ₃ CN	dark brown
2	L ¹	Co(ClO ₄) ₂ .6H ₂ O	EtOH	EtOH	dark brown
3	L ¹	Ni(ClO ₄) ₂ .6H ₂ O	CH ₃ CN	CH ₃ CN	pale brown
4	L ¹	Ni(ClO ₄) ₂ .6H ₂ O	EtOH	EtOH	pale green
5	L ¹	Zn(ClO ₄) ₂ .6H ₂ O	CH ₃ CN	CH ₃ CN	Colourless
6	L ¹	Zn(ClO ₄) ₂ .6H ₂ O	EtOH	EtOH	Colourless
7	L ¹	Mn(ClO ₄) ₂ .6H ₂ O	CH ₃ CN	CH ₃ CN	dark yellow
8	L ¹	Mn(ClO ₄) ₂ .6H ₂ O	EtOH	EtOH	dark yellow
9	L ²	ZnF ₂	Acetone	H ₂ O	white ppt
10	L ²	ZnCl ₂	Acetone	CH ₃ CN	White
11	L ²	ZnBr ₂	Acetone	Acetone	white ppt
12	L ²	ZnBr ₂	Acetone	MeOH	white ppt
13	L ²	ZnI ₂	Acetone	MeOH	white ppt
14	L ²	CdCO ₃	CH ₃ CN	H ₂ O	pale yellow
15	L ²	CdSO ₄	CH ₃ CN	H ₂ O	pale yellow
16	L ²	CdCl ₂	CH ₃ CN	H ₂ O	pale yellow
17	L ²	Hg(ClO ₄) ₂ .6H ₂ O	CH ₃ CN/Acetone	CH ₃ CN	cloudy yellow
18	L ²	Fe(ClO ₄) ₂ .6H ₂ O	CH ₃ CN/Acetone	CH ₃ CN	dark black
19	L ²	Fe(ClO ₄) ₂ .6H ₂ O	Acetone	MeOH	dark black
20	L ²	Oxalic acid	CH ₃ CN/Acetone	CH ₃ CN	yellow ppt
21	L ²	Malonic acid	CH ₃ CN/Acetone	CH ₃ CN	yellow sloution + white ppt
22	L ²	Bu ₄ NF.3H ₂ O	CH ₃ CN/Acetone	CH ₃ CN	yellow sloution + white ppt
23	L ²	Cu[(CH ₃ CN) ₄]BF ₄	Acetone	Acetone	dark green Cu ⁺²
24	L ²	Na ₃ (NO ₂) ₆ Co	Acetone	H ₂ O	dark red, 1H NMR is bad
25	L ²	Oxalic acid	CH ₃ CN	CH ₃ CN	Ppt
26	L ²	Malonic acid	CH ₃ CN	CH ₃ CN	Ppt
27	L ²	Succenic acid	Acetone	MeOH	No reaction
28	L ²	Glycine	Acetone	H ₂ O	Nothing change
29	L ²	Aspartic acid	Acetone	H ₂ O/CH ₃ CN	Ppt
30	L ²	Glutamic acid	Acetone	H ₂ O/CH ₃ CN	Ppt
31	L ²	1,3,5-Benzene Tricarboxilic acid	Acetone	MeOH	No reaction
32	L ²	Isophthalic acid	THF	THF	No reaction
33	ZnL ²	Bu ₄ NF.3H ₂ O	CH ₃ CN	CH ₃ CN	No reaction
34	MnL ²	Oxone	CH ₃ CN	CH ₃ CN	yellow solution + white ppt
35	CdL ²	Oxone	CH ₃ CN	H ₂ O	pale yellow
36	L ³	ZnCl ₂	THF	H ₂ O	white ppt
37	L ³	CdCl ₂	EtOH/H ₂ O	THF	No reaction
38	L ³	Hg(ClO ₄) ₂ .6H ₂ O	DMF	EtOH	oily brown
39	L ³	Cu(ClO ₄) ₂ .6H ₂ O	CHCl ₃	CH ₃ CN	dark green
40	L ³	Cu(ClO ₄) ₂ .6H ₂ O	DMF	EtOH	dark green
41	L ³	Cu(ClO ₄) ₂ .6H ₂ O	DCM	CH ₃ CN	dark green
42	L ³	CuCl ₂	CHCl ₃	CH ₃ CN	Green
43	L ³	Cu(NO ₃) ₂ .XH ₂ O	CHCl ₃	CH ₃ CN	Green
44	L ³	Co(ClO ₄) ₂ .6H ₂ O	THF	THF	dark brown
45	L ³	Co(ClO ₄) ₂ .6H ₂ O	CHCl ₃	EtOH	dark brown
46	L ³	CoCl ₂	CHCl ₃	CH ₃ CN	dark brown
47	L ³	1,3,5-Benzene Tricarboxilic acid	DMSO	DMSO	No reaction
48	L ³	1,3,5-Benzene Tricarboxilic acid	THF	THF	No reaction
49	MnL ³	Tetra butyl amonium phosphate	THF	CH ₃ CN	from yellow to colourless
50	MnL ³	Tetra butyl amonium phosphate	CH ₃ CN	CH ₃ CN	from yellow to colourless
51	CdL ³	Tetra butyl amonium phosphate	THF	CH ₃ CN	No reaction
52	CdL ³	Tetra butyl amonium phosphate	CH ₃ CN	CH ₃ CN	pale yellow/ Cd(NO ₃) ₂ source
53	CdL ³	Tetra butyl amonium phosphate	CH ₃ CN	CH ₃ CN	No reaction/ Cd(PF ₆) ₂ source
54	CdL ³	Tetra butyl amonium phosphate	CH ₃ CN	CH ₃ CN	No reaction/ CdCl ₂ source

4- Preparation of bis phenyl urea tripodal ligand

To test the possibility of this ligand to be synthesised, making the one arm urea species (1,3-pyridylphenylureas) was investigated as follows

(Fig. 4).⁷



90% White ppt in 20 sec.

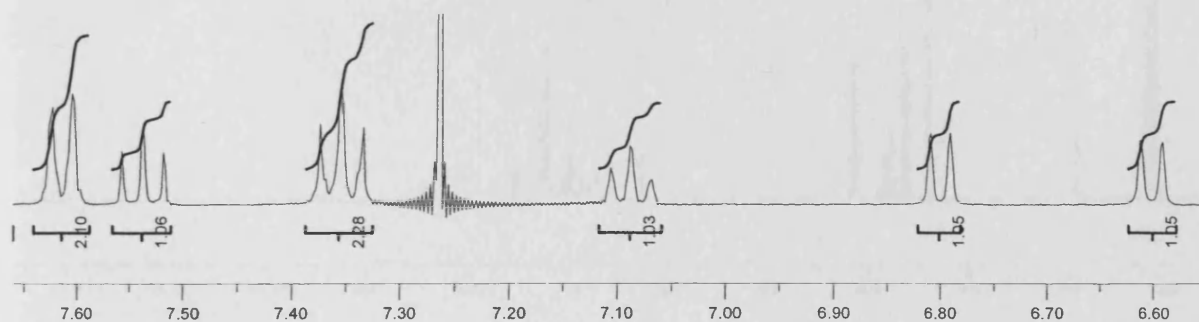


Figure 4: synthesis and ¹H NMR spectrum of (1,3-pyridylphenylureas)

Appendix 1: Attempted Work

This positive result led us to try to synthesis this tripodal ligand using the same procedures but changing the solvent to be EtOH rather than ether due to the solubility of the tripod starting material. The reaction was heated up to 40°C for 24 hours and monitored by ^1H NMR to yield a crude brown oil. Interestingly, the ^1H NMR showed numerous signals at low ppm suggesting some reaction between the reagents and ethanol (Fig. 4). Perhaps doing this reaction again in a different solvent, such as DMF, might lead to the requested ligand.

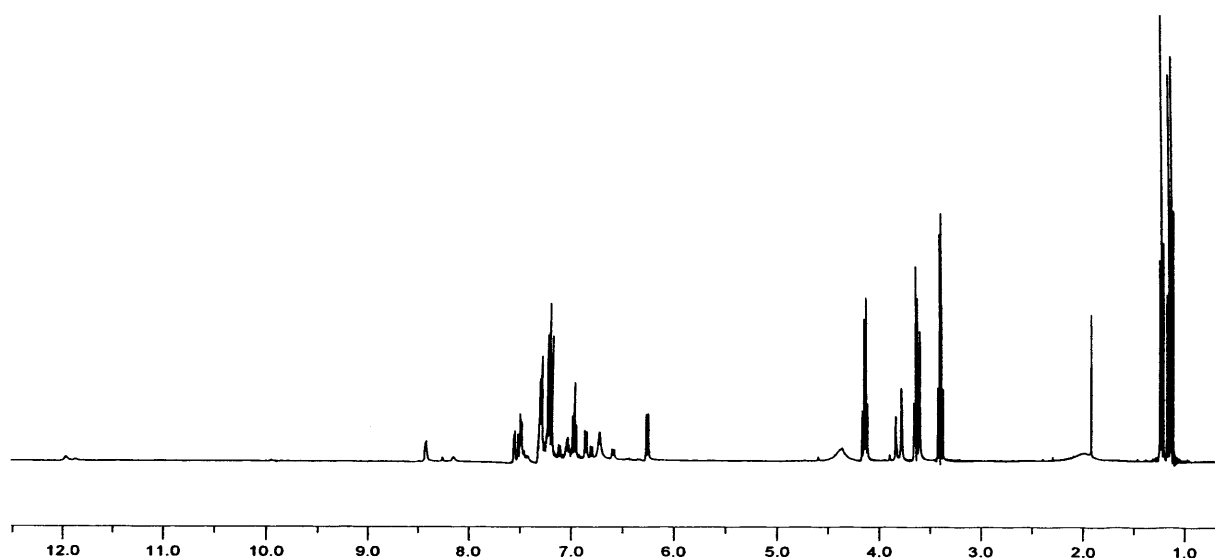
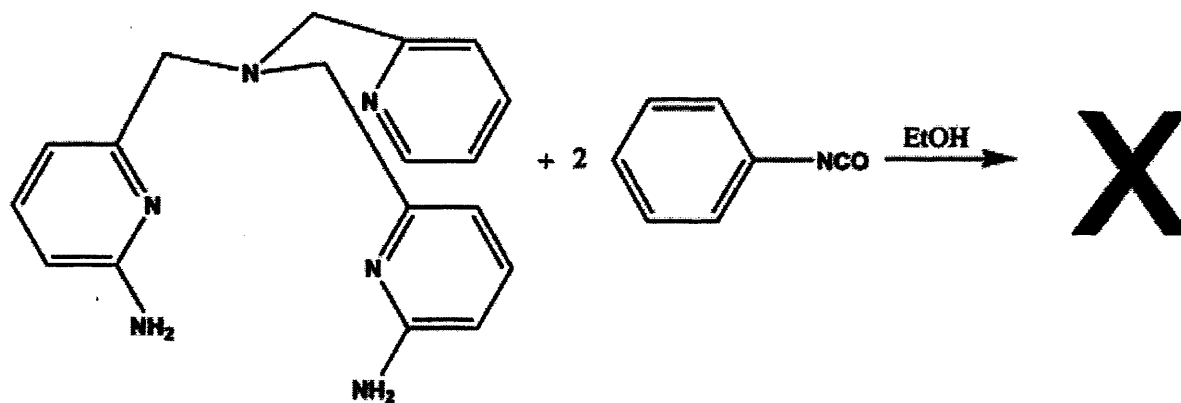


Figure 5: synthesis and ^1H NMR spectrum of tris phenyl urea tripodal ligand

5- Preparation of tris benzoyl urea tripodal ligand

Similar to above, 1-Benzoyl-3-(4-methylpyridin-2-yl) urea has been made for the first time following similar work by Sukeri and Yesilkaynak.^{6, 8} The idea behind this reaction (Fig. 6) is to investigate the possibility of making the tripod analogue.

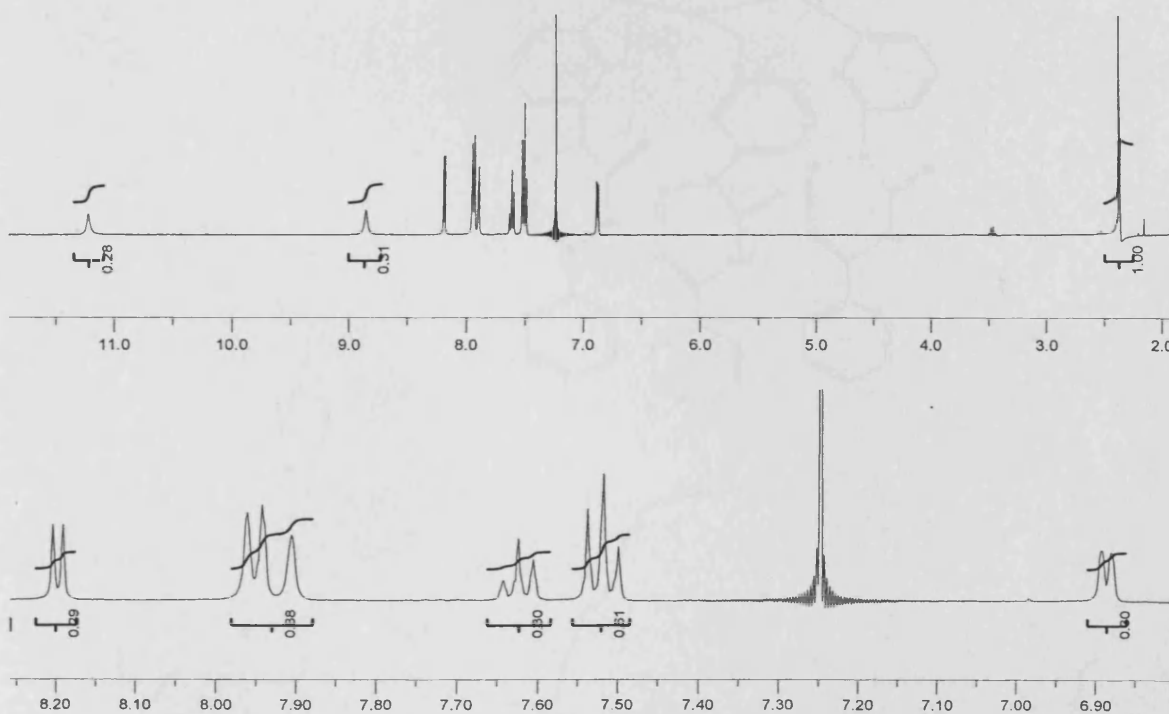
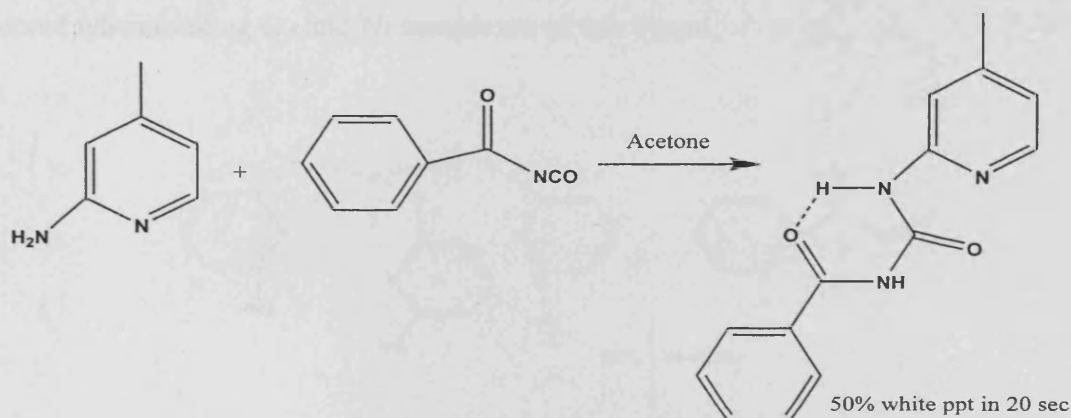
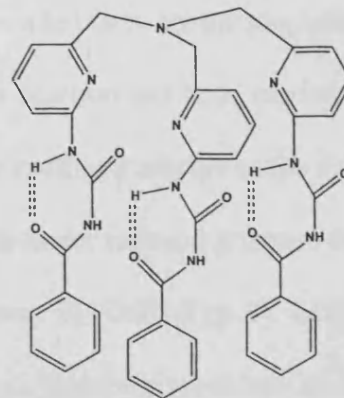


Figure 6: synthesis and ¹H NMR spectrum of 1-Benzoyl-3-(4-methylpyridin-2-yl)

Appendix 1: Attempted Work

The success in synthesising 1-Benzoyl-3-(4-methylpyridin-2-yl) urea led us to try the preparation of the tris benzoyl urea tripodal ligand starting from TAPA. This reaction has been carried out twice, the first time was in EtOH which appeared to react with the starting materials as the EtOH peaks were observed in ^1H NMR even after removing the solvents under reduced pressure for 6 hours. The second time was done in DMF which showed a better ^1H NMR (Fig. 7). Making metal complex of this ligand is a useful way of purifying the ligand. However, no colour change is observed when making Cu and Ni complexes of this ligand.

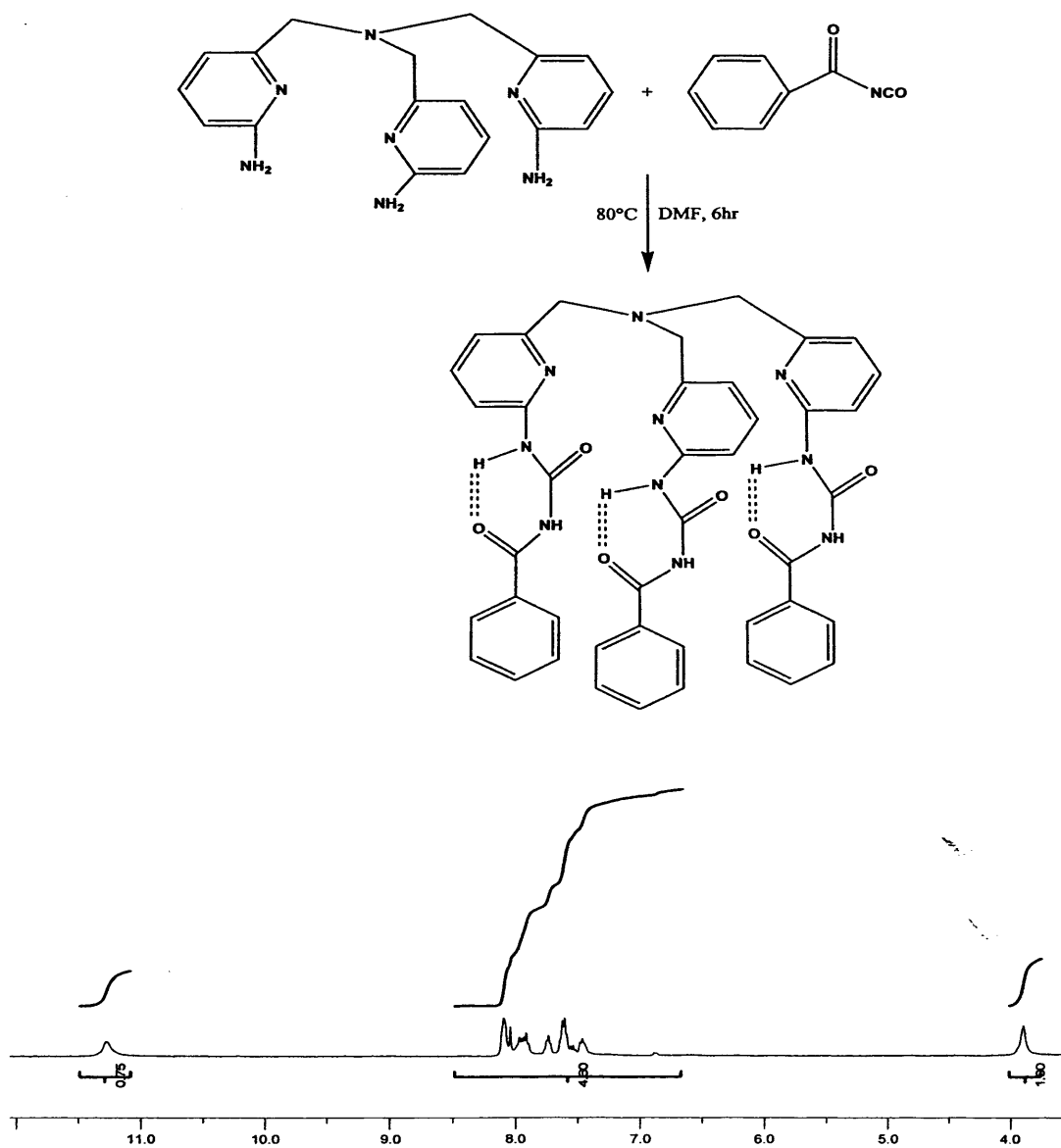
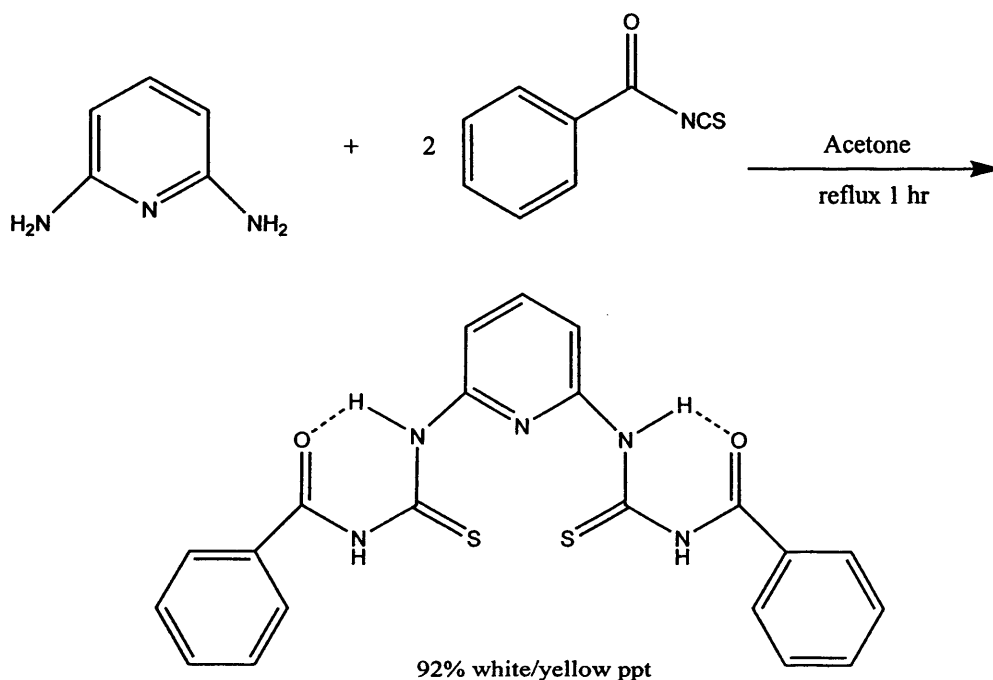


Figure 7: synthesis and ^1H NMR spectrum of tris benzoyl urea tripodal ligand

Appendix 1: Attempted Work

6- Preparation of 2,6-(di benzoylthiourea) pyridine

This ligand has been prepared to complex it with 2:1 ratio with some first row transition metals so when the metal is surrounded by two ligand species there would be a chance of the N-H groups being available to bind anions. The ^1H NMR is a little unusual but is consistent with the proposed product. There are seven signals, with two broad resonances at ~ 13 and 12 ppm being assigned to the N-H protons. Four further resonances occur between 7-8ppm. These sharp resonances account for 11 protons. Curiously the final 2Hs in the structure appear as a broad, featureless peak at ~ 8.5 ppm. The ^{13}C NMR is also consistent with the proposed structure in (Fig. 8). No colour change was observed in reacting this ligand with Ni^{II} , Mn^{II} , Co^{II} , Cu^{II} , Zn^{II} and Cd^{II} as the perchlorate salts. Thus, it would appear no co-ordination is occurring.



Appendix 1: Attempted Work

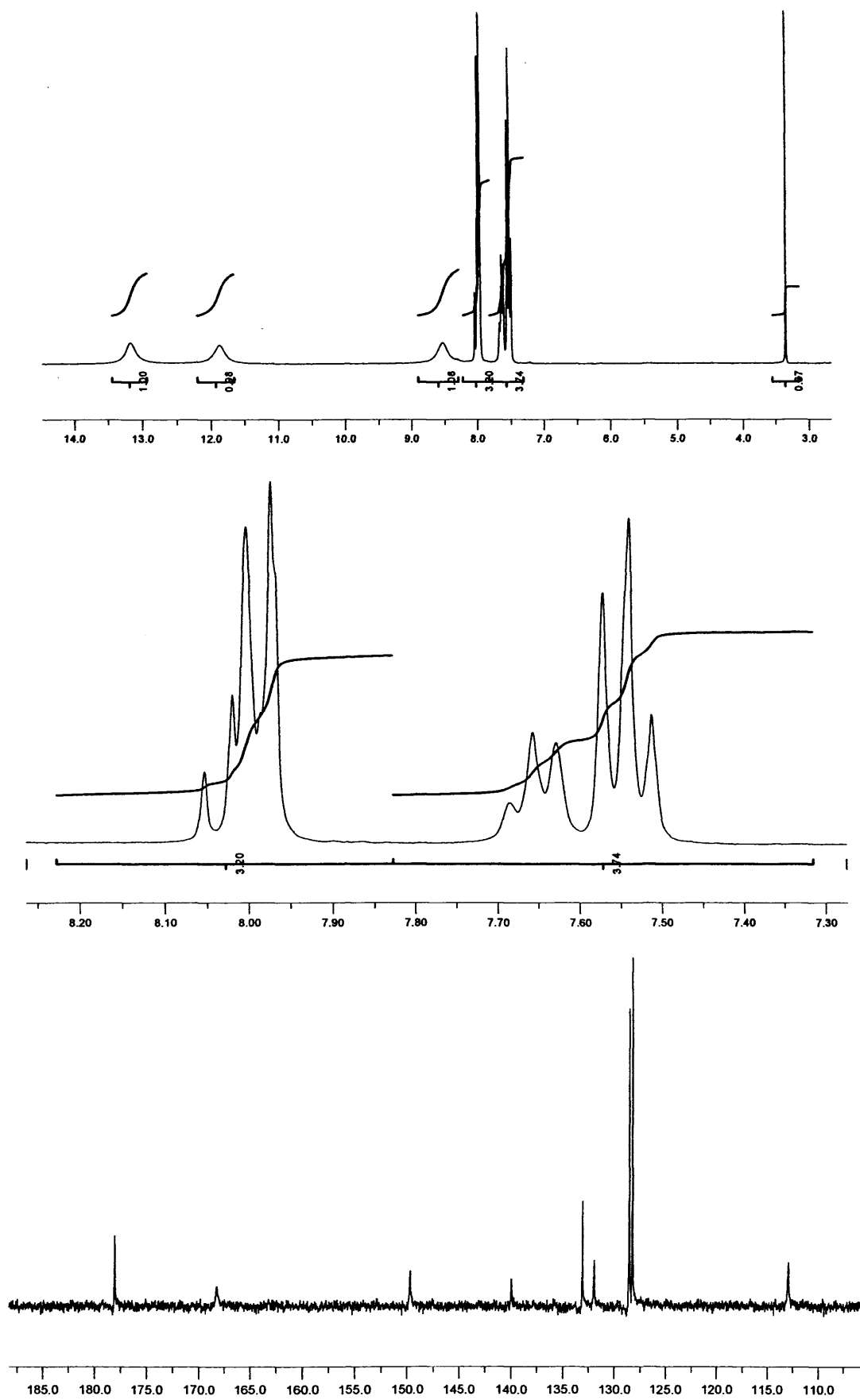
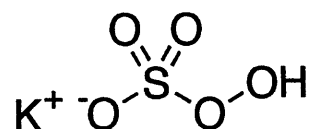


Figure 8: synthesis and ^1H and ^{13}C NMR spectrum of 1,3-(di benzoylthiourea) pyridine ligand.

7- Converting bistiourea tripodal ligand into urea using oxone



This work was carried out after observing crystals of ZnL^1 and MnL^2 being converted into ureas instead of thioureas (page 65 and 113). Using oxidising agents such as oxone, O_3 , O_2 , halides, H_2O_2 , MnO_4^{-2} might result in converting the thiourea species into a urea compound (Fig. 9).⁹

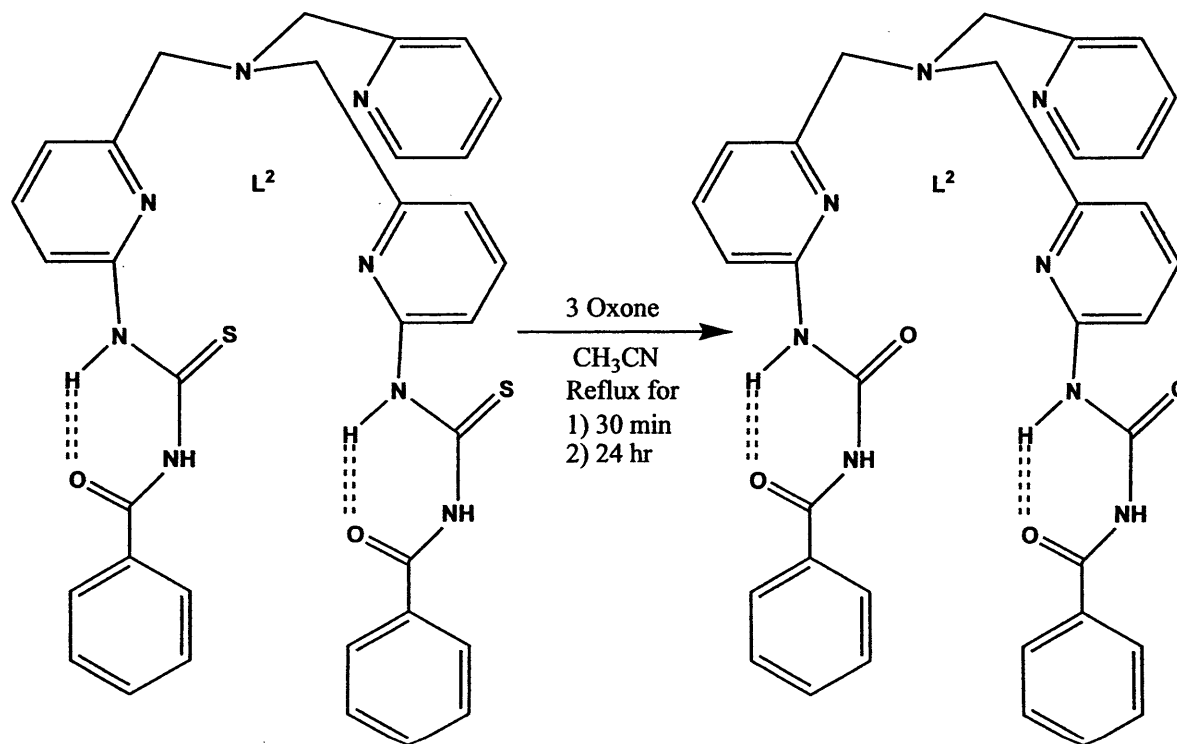


Figure 9: Converting thiourea into urea using oxone

The reaction with oxone was carried out twice, the first time it was refluxed for only 30 minutes resulting in a shift of 0.6 ppm for methylene groups in the 1H NMR in comparison to the spectra of the original ligand. However, mass spectrometry and Infra red spectra indicated the presence of only L^2 . When the reaction was left refluxing for 24 hours, the three methylene groups of the thiourea tripod were completely lost! By doing this reaction again for metal complex it is thought to get better results e.g. crystals of the new urea species or the oxone being coordinating to the metal or perhaps hydrogen bonded in the cavity. The same reaction has been repeated twice for MnL^2 (Fig. 10), refluxing this reaction for 3 hours was worthless as no significant change was observed. However, by leaving the reaction refluxing for 6 hours an interesting colour change

Appendix 1: Attempted Work

was observed from yellow into a green mixture which suggests that Mn^{+2} is no longer in the solution. The presence of MnL urea species was confirmed by mass spectrometer analysis ESMS (m/z): 667.1614 (100), $[Mn(L^{bisurea})-2H]^+$, [calculated 667.1627]. All attempts in growing crystal of this green mixture failed. Further investigations are needed to be considered in the future.

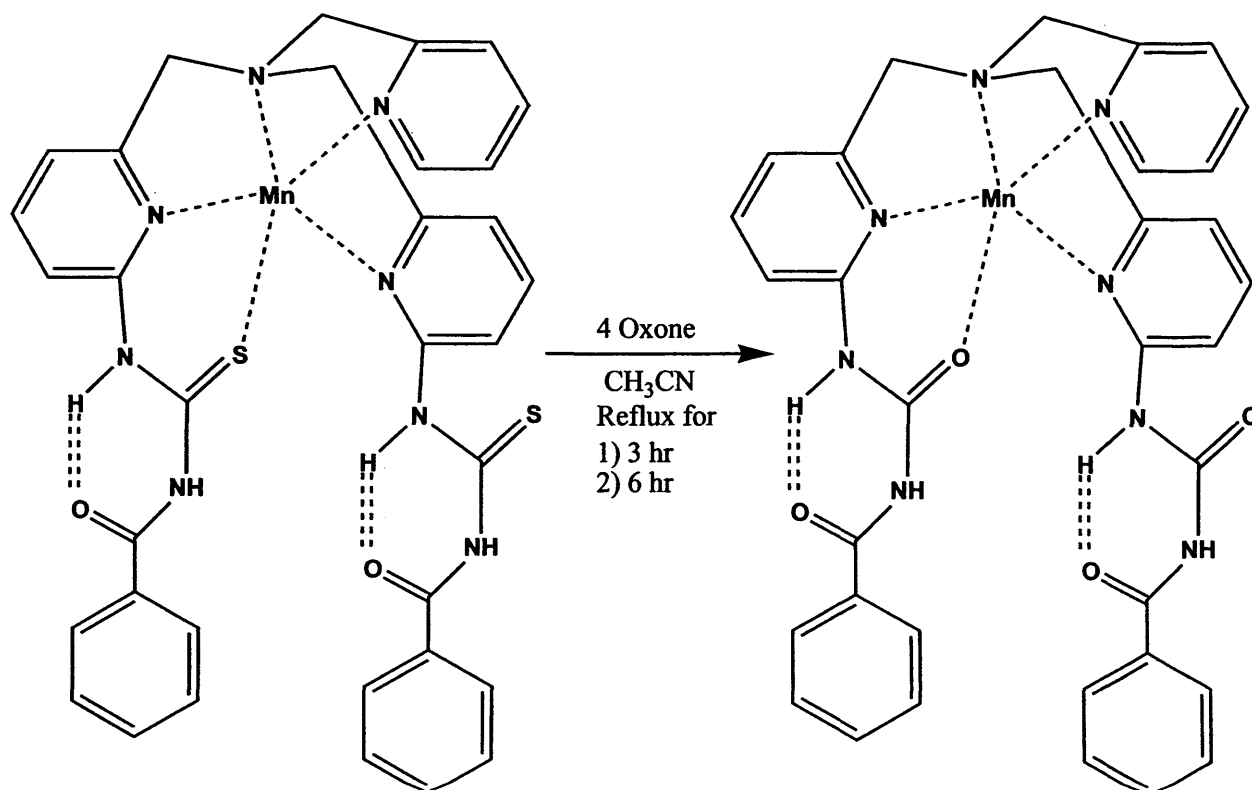


Figure 10: Converting thiourea into urea using oxone

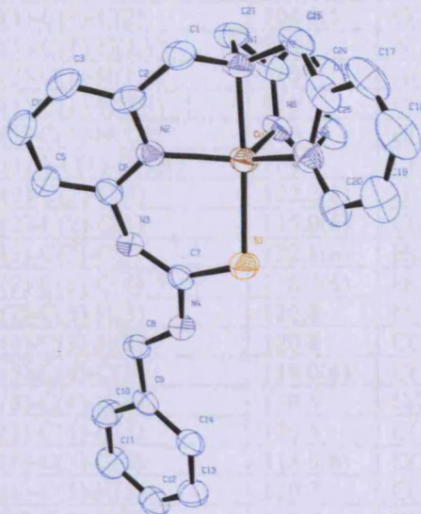
References

1. M. Harata, K. Jitsukawa, H. Masuda and H. Einaga, *Chem. Lett.*, 1995, 61-62.
2. M. Harata, K. Hasegawa, K. Jitsukawa, H. Masuda and H. Einaga, *Bull. Chem. Soc. Jpn.*, 1998, **71**, 1031.
3. A. Wada, Y. Honda, S. Yamaguchi, S. Nagatomo, T. Kitagawa, K. Jitsukawa and H. Masuda, *Inorg. Chem.*, 2004, **43**, 5725-5735.
4. J. Valdés-Martínez, S. Hernández-Ortega, G. Espinosa-Pérez, C. A. Presto, A. K. Hermetet, K. D. Haslow, L. J. Ackerman, L. F. Szczepura, K. I. Goldberg, W. Kaminsky and D. X. West, *J. Mol. Struct.*, 2002, **608**, 77-87.
5. D. X. West, A. K. Hermeter, L. J. V. Martinez and Hernandez-Ortega, *Acta Cryst.*, 1999, **C55**, 811.
6. M. S. M. Yusof, S. K. C. Soh, N. Ngah and B. M. Yamin, *Acta Cryst.*, 2006, **E62**, 1446-1448.
7. G. N. Vassilev and N. N. Nicolov, *Biologie Biochimie*, 1980, **33**, 1127-1130.
8. a. U. Tuncay Yesilkaynak, Flõrke,b* Nevzat Kũlcu'a and and H. Arslana, *Acta Cryst.*, 2006, **E62**, o3934–o3935.
9. Mohammadpoor-Baltork, M. M. Sadeghi and K. Esmayilpour, *Phosphorus, Sulfur and Silicon*, 2003, **178**, 61-65.

Appendix 2: Publications

- 1- F. A. Saad, A. J. Amoroso and B. M. Kariuki, *Dalton Trans.*, 2011, in preparation. (Chapter 2).
- 2- F. A. Saad, A. J. Amoroso, J. C. Knight and B. M. Kariuki, *Inorg. Chem.*, 2011, submitted. (Chapter 3).
- 3- F. A. Saad, A. J. Amoroso and B. M. Kariuki, *Dalton Trans.*, 2011, in preparation. (Chapter 4).
- 4- F. A. Saad, A. J. Amoroso and B. M. Kariuki, *Dalton Trans.*, 2011, in preparation. (Chapter 5).
- 5- F. A. Saad, in *SIC04*, Manchester, 2010. (Winner for the 2nd best paper in the conference).
- 6- J. C. Knight, F. A. Saad, B. M. Kariuki, A. J. Amoroso and S. J. Coles, *Acta Cryst.*, 2009, **E56**, o647.

Tables of Bond Distances and Angles

**Table A.1:** Crystal data and structure refinement for $[\text{Cu}^{\text{II}}\text{L}^1] \cdot 2[\text{ClO}_4] \cdot \text{CH}_3\text{CN} \cdot \text{H}_2\text{O}$. **2.1**

Identification code	aja0951b	
Empirical formula	$\text{C}_{28} \text{H}_{29} \text{Cl}_2 \text{Cu} \text{N}_7 \text{O}_{10} \text{S}$	
Formula weight	790.08	
Temperature	150(2) K	
Wavelength	0.71073 Å	
Crystal system	Triclinic	
Space group	P-1	
Unit cell dimensions	$a = 10.0397(9) \text{ \AA}$	$\alpha = 96.995(5)^\circ$
	$b = 12.7362(9) \text{ \AA}$	$\beta = 90.820(4)^\circ$
	$c = 13.7012(10) \text{ \AA}$	$\gamma = 110.356(4)^\circ$
Volume	$1627.3(2) \text{ \AA}^3$	
Z	2	
Density (calculated)	1.612 Mg/m^3	
Absorption coefficient	0.967 mm^{-1}	
F(000)	810	
Crystal size	$0.35 \times 0.30 \times 0.05 \text{ mm}^3$	
Theta range for data collection	2.64 to 27.48°	
Index ranges	$-12 \leq h \leq 13$, $-16 \leq k \leq 16$, $-17 \leq l \leq 17$	
Reflections collected	10714	
Independent reflections	7349 [R(int) = 0.0469]	
Completeness to $\theta = 27.48^\circ$	98.6 %	
Max. and min. transmission	0.9532 and 0.7283	
Refinement method	Full-matrix least-squares on F^2	
Data / restraints / parameters	7349 / 224 / 489	
Goodness-of-fit on F^2	1.086	
Final R indices [$I > 2\sigma(I)$]	R1 = 0.0879, wR2 = 0.2013	
R indices (all data)	R1 = 0.1432, wR2 = 0.2300	
Largest diff. peak and hole	0.700 and $-0.584 \text{ e. \AA}^{-3}$	

Appendix 3: Crystals data

Table A.2: Bond lengths [Å] and angles [°] for $[\text{Cu}^{\text{II}}\text{L}^1]_2[\text{ClO}_4] \cdot \text{CH}_3\text{CN} \cdot \text{H}_2\text{O} \cdot 2.1$

C(1)-N(1)	1.488(8)	N(1)-C(1)-C(2)	108.3(5)	C(24)-C(25)-H(25)	120.6
C(1)-C(2)	1.510(9)	N(1)-C(1)-H(1A)	110	N(6)-C(26)-C(25)	122.7(6)
C(1)-H(1A)	0.99	C(2)-C(1)-H(1A)	110	N(6)-C(26)-H(26)	118.7
C(1)-H(1B)	0.99	N(1)-C(1)-H(1B)	110	C(25)-C(26)-H(26)	118.7
C(2)-N(2)	1.355(7)	C(2)-C(1)-H(1B)	110	C(28)-C(27)-H(27A)	109.5
C(2)-C(3)	1.378(9)	H(1A)-C(1)-H(1B)	108.4	C(28)-C(27)-H(27B)	109.5
C(3)-C(4)	1.402(10)	N(2)-C(2)-C(3)	122.2(6)	H(27A)-C(27)-H(27B)	109.5
C(3)-H(3)	0.95	N(2)-C(2)-C(1)	115.0(6)	C(28)-C(27)-H(27C)	109.5
C(4)-C(5)	1.377(9)	C(3)-C(2)-C(1)	122.8(6)	H(27A)-C(27)-H(27C)	109.5
C(4)-H(4)	0.95	C(2)-C(3)-C(4)	118.4(6)	H(27B)-C(27)-H(27C)	109.5
C(5)-C(6)	1.364(9)	C(2)-C(3)-H(3)	120.8	N(7)-C(28)-C(27)	175(2)
C(5)-H(5)	0.95	C(4)-C(3)-H(3)	120.8	C(15)-N(1)-C(21)	111.1(5)
C(6)-N(2)	1.332(8)	C(5)-C(4)-C(3)	119.0(6)	C(15)-N(1)-C(1)	111.6(5)
C(6)-N(3)	1.417(8)	C(5)-C(4)-H(4)	120.5	C(21)-N(1)-C(1)	111.8(5)
C(7)-N(3)	1.328(8)	C(3)-C(4)-H(4)	120.5	C(15)-N(1)-Cu(1)	109.0(4)
C(7)-N(4)	1.363(7)	C(6)-C(5)-C(4)	118.6(6)	C(21)-N(1)-Cu(1)	107.9(4)
C(7)-S(1)	1.692(6)	C(6)-C(5)-H(5)	120.7	C(1)-N(1)-Cu(1)	105.3(4)
C(8)-O(1)	1.225(7)	C(4)-C(5)-H(5)	120.7	C(6)-N(2)-C(2)	117.8(5)
C(8)-N(4)	1.393(8)	N(2)-C(6)-C(5)	123.9(6)	C(6)-N(2)-Cu(1)	129.7(4)
C(8)-C(9)	1.480(9)	N(2)-C(6)-N(3)	119.4(5)	C(2)-N(2)-Cu(1)	112.4(4)
C(9)-C(10)	1.391(9)	C(5)-C(6)-N(3)	116.7(5)	C(7)-N(3)-C(6)	132.8(5)
C(9)-C(14)	1.405(9)	N(3)-C(7)-N(4)	116.6(5)	C(7)-N(3)-H(3A)	113.6
C(10)-C(11)	1.374(10)	N(3)-C(7)-S(1)	127.3(4)	C(6)-N(3)-H(3A)	113.6
C(10)-H(10)	0.95	N(4)-C(7)-S(1)	116.0(4)	C(7)-N(4)-C(8)	127.0(5)
C(11)-C(12)	1.386(11)	O(1)-C(8)-N(4)	120.7(6)	C(7)-N(4)-H(4A)	116.5
C(11)-H(11)	0.95	O(1)-C(8)-C(9)	120.7(6)	C(8)-N(4)-H(4A)	116.5
C(12)-C(13)	1.372(10)	N(4)-C(8)-C(9)	118.5(5)	C(20)-N(5)-C(16)	119.5(6)
C(12)-H(12)	0.95	C(10)-C(9)-C(14)	119.4(6)	C(20)-N(5)-Cu(1)	127.8(4)
C(13)-C(14)	1.395(9)	C(10)-C(9)-C(8)	117.1(6)	C(16)-N(5)-Cu(1)	112.6(5)
C(13)-H(13)	0.95	C(14)-C(9)-C(8)	123.5(6)	C(26)-N(6)-C(22)	118.3(5)
C(14)-H(14)	0.95	C(11)-C(10)-C(9)	120.1(7)	C(26)-N(6)-Cu(1)	128.8(4)
C(15)-N(1)	1.484(9)	C(11)-C(10)-H(10)	119.9	C(22)-N(6)-Cu(1)	112.6(4)
C(15)-C(16)	1.486(11)	C(9)-C(10)-H(10)	119.9	C(7)-S(1)-Cu(1)	103.7(2)
C(15)-H(15A)	0.99	C(10)-C(11)-C(12)	120.7(7)	N(2)-Cu(1)-N(1)	82.4(2)
C(15)-H(15B)	0.99	C(10)-C(11)-H(11)	119.6	N(2)-Cu(1)-N(5)	129.3(2)
C(16)-N(5)	1.347(8)	C(12)-C(11)-H(11)	119.6	N(1)-Cu(1)-N(5)	82.8(2)
C(16)-C(17)	1.400(10)	C(13)-C(12)-C(11)	119.8(6)	N(2)-Cu(1)-N(6)	110.8(2)
C(17)-C(18)	1.395(13)	C(13)-C(12)-H(12)	120.1	N(1)-Cu(1)-N(6)	81.8(2)
C(17)-H(17)	0.95	C(11)-C(12)-H(12)	120.1	N(5)-Cu(1)-N(6)	114.6(2)
C(18)-C(19)	1.362(12)	C(12)-C(13)-C(14)	120.7(7)	N(2)-Cu(1)-S(1)	94.20(14)
C(18)-H(18)	0.95	C(12)-C(13)-H(13)	119.7	N(1)-Cu(1)-S(1)	174.95(16)
C(19)-C(20)	1.367(10)	C(14)-C(13)-H(13)	119.7	N(5)-Cu(1)-S(1)	96.52(16)
C(19)-H(19)	0.95	C(13)-C(14)-C(9)	119.3(6)	N(6)-Cu(1)-S(1)	102.95(14)
C(20)-N(5)	1.345(9)	C(13)-C(14)-H(14)	120.4	O(3)-Cl(1)-O(4)	109.8(7)
C(20)-H(20)	0.95	C(9)-C(14)-H(14)	120.4	O(3)-Cl(1)-O(5)	107.1(5)
C(21)-N(1)	1.484(9)	N(1)-C(15)-C(16)	110.2(5)	O(4)-Cl(1)-O(5)	105.9(6)
C(21)-C(22)	1.507(9)	N(1)-C(15)-H(15A)	109.6	O(3)-Cl(1)-O(2)	113.9(5)
C(21)-H(21A)	0.99	C(16)-C(15)-H(15A)	109.6	O(4)-Cl(1)-O(2)	107.0(4)
C(21)-H(21B)	0.99	N(1)-C(15)-H(15B)	109.6	O(5)-Cl(1)-O(2)	112.9(4)
C(22)-N(6)	1.348(8)	C(16)-C(15)-H(15B)	109.6	O(9)-Cl(2)-O(8)	101.2(10)
C(22)-C(23)	1.373(9)	H(15A)-C(15)-H(15B)	108.1	O(9)-Cl(2)-O(7)	102.2(9)
C(23)-C(24)	1.367(11)	N(5)-C(16)-C(17)	121.0(8)	O(8)-Cl(2)-O(7)	109.7(9)
C(23)-H(23)	0.95	N(5)-C(16)-C(15)	116.9(6)	O(9)-Cl(2)-O(6)	126.2(11)
C(24)-C(25)	1.377(12)	C(17)-C(16)-C(15)	122.0(7)	O(8)-Cl(2)-O(6)	107.3(9)
C(24)-H(24)	0.95	C(18)-C(17)-C(16)	118.6(7)	O(7)-Cl(2)-O(6)	109.4(9)
C(25)-C(26)	1.365(10)	C(18)-C(17)-H(17)	120.7	O(8A)-Cl(2A)-O(9A)	103.3(12)
C(25)-H(25)	0.95	C(16)-C(17)-H(17)	120.7	O(8A)-Cl(2A)-O(7A)	114.5(10)

Appendix 3: Crystals data

C(26)-N(6)	1.346(8)	C(19)-C(18)-C(17)	118.8(7)	O(9A)-Cl(2A)-O(7A)	103.5(10)
C(26)-H(26)	0.95	C(19)-C(18)-H(18)	120.6	O(8A)-Cl(2A)-O(6A)	108.3(10)
C(27)-C(28)	1.4203(11)	C(17)-C(18)-H(18)	120.6	O(9A)-Cl(2A)-O(6A)	118.9(12)
C(27)-H(27A)	0.98	C(18)-C(19)-C(20)	120.7(8)	O(7A)-Cl(2A)-O(6A)	108.5(10)
C(27)-H(27B)	0.98	C(18)-C(19)-H(19)	119.7		
C(27)-H(27C)	0.98	C(20)-C(19)-H(19)	119.7		
C(28)-N(7)	1.2005(11)	N(5)-C(20)-C(19)	121.4(7)		
N(1)-Cu(1)	2.015(5)	N(5)-C(20)-H(20)	119.3		
N(2)-Cu(1)	2.006(5)	C(19)-C(20)-H(20)	119.3		
N(3)-H(3A)	0.88	N(1)-C(21)-C(22)	109.7(6)		
N(4)-H(4A)	0.88	N(1)-C(21)-H(21A)	109.7		
N(5)-Cu(1)	2.036(5)	C(22)-C(21)-H(21A)	109.7		
N(6)-Cu(1)	2.086(5)	N(1)-C(21)-H(21B)	109.7		
S(1)-Cu(1)	2.2612(17)	C(22)-C(21)-H(21B)	109.7		
O(2)-Cl(1)	1.434(6)	H(21A)-C(21)-H(21B)	108.2		
O(3)-Cl(1)	1.386(6)	N(6)-C(22)-C(23)	121.2(6)		
O(4)-Cl(1)	1.393(7)	N(6)-C(22)-C(21)	114.3(5)		
O(5)-Cl(1)	1.401(5)	C(23)-C(22)-C(21)	124.4(6)		
O(6)-Cl(2)	1.418(9)	C(24)-C(23)-C(22)	120.0(7)		
O(7)-Cl(2)	1.406(9)	C(24)-C(23)-H(23)	120		
O(8)-Cl(2)	1.404(10)	C(22)-C(23)-H(23)	120		
O(9)-Cl(2)	1.397(8)	C(23)-C(24)-C(25)	119.0(7)		
O(6A)-Cl(2A)	1.439(10)	C(23)-C(24)-H(24)	120.5		
O(7A)-Cl(2A)	1.402(9)	C(25)-C(24)-H(24)	120.5		
O(8A)-Cl(2A)	1.378(10)	C(26)-C(25)-C(24)	118.8(7)		
O(9A)-Cl(2A)	1.394(8)	C(26)-C(25)-H(25)	120.6		

Appendix 3: Crystals data

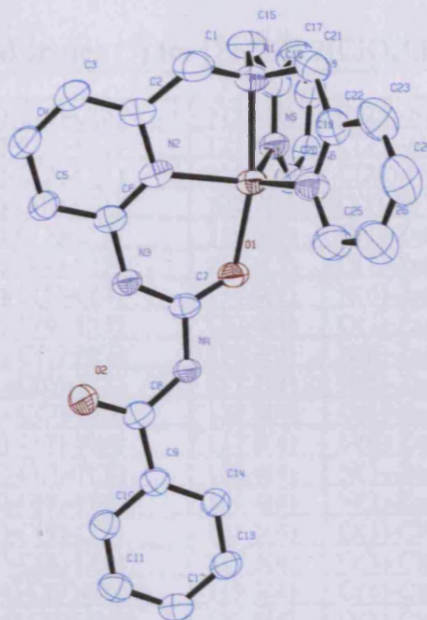


Table B.1: Crystal data and structure refinement for $[\text{Zn}^{\text{II}}\text{L}^*].2[\text{ClO}_4].\text{H}_2\text{O}$. 2.2.1

Identification code	aja1002	
Empirical formula	$\text{C}_{26}\text{H}_{26}\text{Cl}_2\text{N}_6\text{O}_{11}\text{Zn}$	
Formula weight	734.80	
Temperature	150(2) K	
Wavelength	0.71073 Å	
Crystal system	Monoclinic	
Space group	P21/c	
Unit cell dimensions	$a = 18.9883(10)$ Å	$\alpha = 90^\circ$.
	$b = 9.7711(6)$ Å	$\beta = 118.765(3)^\circ$.
	$c = 18.2005(11)$ Å	$\gamma = 90^\circ$.
Volume	$2960.2(3)$ Å ³	
Z	4	
Density (calculated)	1.649 Mg/m ³	
Absorption coefficient	1.082 mm ⁻¹	
F(000)	1504	
Crystal size	0.30 x 0.30 x 0.15 mm ³	
Theta range for data collection	2.99 to 27.51°.	
Index ranges	-22 ≤ h ≤ 23, -9 ≤ k ≤ 12, -23 ≤ l ≤ 23	
Reflections collected	9006	
Independent reflections	6166 [R(int) = 0.0398]	
Completeness to theta = 27.51°	90.5 %	
Max. and min. transmission	0.8545 and 0.7373	
Refinement method	Full-matrix least-squares on F ²	
Data / restraints / parameters	6166 / 225 / 467	
Goodness-of-fit on F ²	1.030	
Final R indices [I > 2σ(I)]	R1 = 0.0684, wR2 = 0.1411	
R indices (all data)	R1 = 0.1161, wR2 = 0.1632	
Largest diff. peak and hole	0.723 and -0.455 e.Å ⁻³	

Appendix 3: Crystals data

Table B.2: Bond lengths [Å] and angles [°] for $[\text{Zn}^{\text{II}}\text{L}^{\text{I}}]_2[\text{ClO}_4] \cdot \text{H}_2\text{O}$. 2.2.1

C(1)-N(1)	1.474(7)	N(1)-C(1)-C(2)	112.9(4)	C(25)-N(6)-C(22)	118.8(5)
C(1)-C(2)	1.507(7)	N(2)-C(2)-C(3)	121.5(5)	C(25)-N(6)-Zn(1)	126.3(4)
C(2)-N(2)	1.368(6)	N(2)-C(2)-C(1)	115.3(4)	C(22)-N(6)-Zn(1)	114.9(4)
C(2)-C(3)	1.373(7)	C(3)-C(2)-C(1)	122.7(5)	C(7)-O(1)-Zn(1)	128.8(3)
C(3)-C(4)	1.367(7)	C(4)-C(3)-C(2)	119.6(5)	O(1)-Zn(1)-N(6)	105.15(15)
C(4)-C(5)	1.389(7)	C(3)-C(4)-C(5)	119.4(5)	O(1)-Zn(1)-N(5)	101.77(15)
C(5)-C(6)	1.383(7)	C(6)-C(5)-C(4)	118.4(5)	N(6)-Zn(1)-N(5)	125.05(17)
C(6)-N(2)	1.333(6)	N(2)-C(6)-C(5)	122.6(4)	O(1)-Zn(1)-N(2)	87.87(14)
C(6)-N(3)	1.401(6)	N(2)-C(6)-N(3)	120.3(4)	N(6)-Zn(1)-N(2)	111.34(16)
C(7)-O(1)	1.230(5)	C(5)-C(6)-N(3)	117.1(4)	N(5)-Zn(1)-N(2)	116.69(16)
C(7)-N(3)	1.347(6)	O(1)-C(7)-N(3)	125.8(4)	O(1)-Zn(1)-N(1)	168.86(15)
C(7)-N(4)	1.378(5)	O(1)-C(7)-N(4)	117.8(4)	N(6)-Zn(1)-N(1)	81.69(16)
C(8)-O(2)	1.237(5)	N(3)-C(7)-N(4)	116.4(4)	N(5)-Zn(1)-N(1)	80.66(15)
C(8)-N(4)	1.377(6)	O(2)-C(8)-N(4)	121.4(4)	N(2)-Zn(1)-N(1)	81.39(15)
C(8)-C(9)	1.484(6)	O(2)-C(8)-C(9)	121.3(4)	O(3)-Cl(1)-O(6)	108.6(3)
C(9)-C(14)	1.378(7)	N(4)-C(8)-C(9)	117.3(4)	O(3)-Cl(1)-O(5)	107.4(4)
C(9)-C(10)	1.398(7)	C(14)-C(9)-C(10)	119.3(4)	O(6)-Cl(1)-O(5)	111.7(4)
C(10)-C(11)	1.381(7)	C(14)-C(9)-C(8)	123.8(4)	O(3)-Cl(1)-O(4)	109.6(3)
C(11)-C(12)	1.387(7)	C(10)-C(9)-C(8)	116.9(4)	O(6)-Cl(1)-O(4)	109.7(3)
C(12)-C(13)	1.389(7)	C(11)-C(10)-C(9)	120.6(5)	O(5)-Cl(1)-O(4)	109.8(2)
C(13)-C(14)	1.386(7)	C(10)-C(11)-C(12)	120.0(5)	O(9)-Cl(2)-O(8)	108.6(10)
C(15)-N(1)	1.478(7)	C(11)-C(12)-C(13)	119.3(5)	O(9)-Cl(2)-O(10)	109.0(10)
C(15)-C(16)	1.519(7)	C(14)-C(13)-C(12)	120.6(5)	O(8)-Cl(2)-O(10)	110.5(7)
C(16)-N(5)	1.344(6)	C(9)-C(14)-C(13)	120.2(5)	O(9)-Cl(2)-O(7)	110.4(10)
C(16)-C(17)	1.388(7)	N(1)-C(15)-C(16)	111.5(4)	O(8)-Cl(2)-O(7)	109.8(9)
C(17)-C(18)	1.371(8)	N(5)-C(16)-C(17)	121.5(5)	O(10)-Cl(2)-O(7)	108.4(9)
C(18)-C(19)	1.367(8)	N(5)-C(16)-C(15)	116.6(4)	O(10A)-Cl(2A)-O(9A)	110.2(16)
C(19)-C(20)	1.357(7)	C(17)-C(16)-C(15)	121.8(5)	O(10A)-Cl(2A)-O(8A)	111.0(16)
C(20)-N(5)	1.351(6)	C(18)-C(17)-C(16)	119.3(5)	O(9A)-Cl(2A)-O(8A)	109.6(14)
C(21)-N(1)	1.451(7)	C(19)-C(18)-C(17)	119.0(5)	O(10A)-Cl(2A)-O(7A)	108.1(13)
C(21)-C(22)	1.536(8)	C(20)-C(19)-C(18)	119.4(5)	O(9A)-Cl(2A)-O(7A)	108.7(11)
C(22)-N(6)	1.338(7)	N(5)-C(20)-C(19)	122.9(5)	O(8A)-Cl(2A)-O(7A)	109.1(13)
C(22)-C(23)	1.379(8)	N(1)-C(21)-C(22)	111.6(4)		
C(23)-C(24)	1.383(9)	N(6)-C(22)-C(23)	121.9(6)		
C(24)-C(26)	1.361(9)	N(6)-C(22)-C(21)	116.4(5)		
C(25)-N(6)	1.328(7)	C(23)-C(22)-C(21)	121.5(5)		
C(25)-C(26)	1.364(8)	C(22)-C(23)-C(24)	118.2(6)		
N(1)-Zn(1)	2.181(4)	C(26)-C(24)-C(23)	119.5(6)		
N(2)-Zn(1)	2.070(4)	N(6)-C(25)-C(26)	122.5(6)		
N(5)-Zn(1)	2.048(4)	C(24)-C(26)-C(25)	119.1(6)		
N(6)-Zn(1)	2.014(4)	C(21)-N(1)-C(1)	113.4(5)		
O(1)-Zn(1)	2.013(3)	C(21)-N(1)-C(15)	113.3(4)		
Cl(1)-O(3)	1.403(4)	C(1)-N(1)-C(15)	111.0(4)		
Cl(1)-O(6)	1.411(5)	C(21)-N(1)-Zn(1)	104.6(3)		
Cl(1)-O(5)	1.425(4)	C(1)-N(1)-Zn(1)	106.2(3)		
Cl(1)-O(4)	1.427(4)	C(15)-N(1)-Zn(1)	107.6(3)		
Cl(2)-O(9)	1.402(10)	C(6)-N(2)-C(2)	118.3(4)		
Cl(2)-O(8)	1.410(9)	C(6)-N(2)-Zn(1)	126.9(3)		
Cl(2)-O(10)	1.431(10)	C(2)-N(2)-Zn(1)	114.5(3)		
Cl(2)-O(7)	1.442(10)	C(7)-N(3)-C(6)	129.1(4)		
Cl(2A)-O(10A)	1.391(14)	C(8)-N(4)-C(7)	128.0(4)		
Cl(2A)-O(9A)	1.413(13)	C(16)-N(5)-C(20)	117.7(4)		
Cl(2A)-O(8A)	1.418(14)	C(16)-N(5)-Zn(1)	116.2(3)		
Cl(2A)-O(7A)	1.476(11)	C(20)-N(5)-Zn(1)	126.1(3)		

Appendix 3: Crystals data

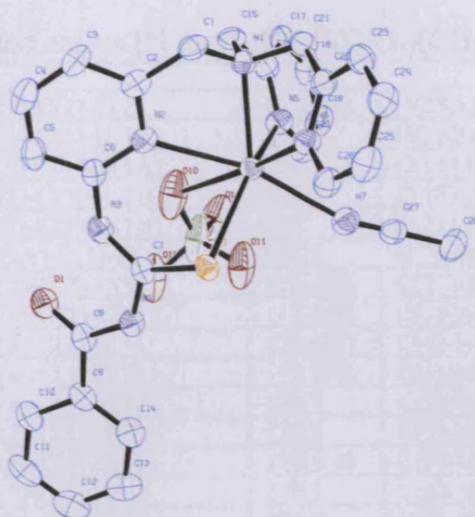


Table C.1: Crystal data and structure refinement for $[\text{Cd}^{\text{II}}(\text{L}^1)(\text{ClO}_4)(\text{CH}_3\text{CN})][\text{ClO}_4]$. 2.3

Identification code	aja0937	
Empirical formula	C ₂₈ H ₂₇ Cd Cl ₂ N ₇ O ₉ S	
Formula weight	820.93	
Temperature	150(2) K	
Wavelength	0.71073 Å	
Crystal system	Monoclinic	
Space group	C2/c	
Unit cell dimensions	a = 32.3620(5) Å b = 13.3540(2) Å c = 15.8960(3) Å	$\alpha = 90^\circ$ $\beta = 113.2920(10)^\circ$ $\gamma = 90^\circ$
Volume	6309.78(18) Å ³	
Z	8	
Density (calculated)	1.728 Mg/m ³	
Absorption coefficient	0.994 mm ⁻¹	
F(000)	3312	
Crystal size	0.30 x 0.30 x 0.20 mm ³	
Theta range for data collection	2.56 to 27.50°.	
Index ranges	-41 ≤ h ≤ 42, -17 ≤ k ≤ 16, -20 ≤ l ≤ 20	
Reflections collected	12201	
Independent reflections	7212 [R(int) = 0.0350]	
Completeness to theta = 27.50°	99.4 %	
Max. and min. transmission	0.8260 and 0.7548	
Refinement method	Full-matrix least-squares on F ²	
Data / restraints / parameters	7212 / 86 / 490	
Goodness-of-fit on F ²	1.040	
Final R indices [I > 2σ(I)]	R1 = 0.0482, wR2 = 0.1099	
R indices (all data)	R1 = 0.0759, wR2 = 0.1228	
Largest diff. peak and hole	0.715 and -0.880 e.Å ⁻³	

Appendix 3: Crystals data

Table C.2: Bond lengths [Å] and angles [°] for [Cd^{II}(L¹)(ClO₄)(CH₃CN)][ClO₄]. 2.3

C(1)-N(1)	1.473(5)	N(1)-C(1)-C(2)	113.0(3)	H(28A)-C(28)-H(28C)	109.5
C(1)-C(2)	1.499(6)	N(1)-C(1)-H(1A)	109	H(28B)-C(28)-H(28C)	109.5
C(1)-H(1A)	0.99	C(2)-C(1)-H(1A)	109	C(15)-N(1)-C(21)	111.7(3)
C(1)-H(1B)	0.99	N(1)-C(1)-H(1B)	109	C(15)-N(1)-C(1)	111.2(3)
C(2)-N(2)	1.360(5)	C(2)-C(1)-H(1B)	109	C(21)-N(1)-C(1)	111.6(3)
C(2)-C(3)	1.387(6)	H(1A)-C(1)-H(1B)	107.8	C(15)-N(1)-Cd(1)	106.4(2)
C(3)-C(4)	1.376(7)	N(2)-C(2)-C(3)	121.4(4)	C(21)-N(1)-Cd(1)	104.9(2)
C(3)-H(3)	0.95	N(2)-C(2)-C(1)	117.8(3)	C(1)-N(1)-Cd(1)	110.7(2)
C(4)-C(5)	1.373(7)	C(3)-C(2)-C(1)	120.6(4)	C(6)-N(2)-C(2)	117.7(3)
C(4)-H(4)	0.95	C(4)-C(3)-C(2)	119.6(4)	C(6)-N(2)-Cd(1)	127.3(3)
C(5)-C(6)	1.390(6)	C(4)-C(3)-H(3)	120.2	C(2)-N(2)-Cd(1)	115.0(3)
C(5)-H(5)	0.95	C(2)-C(3)-H(3)	120.2	C(7)-N(3)-C(6)	129.7(3)
C(6)-N(2)	1.333(5)	C(5)-C(4)-C(3)	119.5(4)	C(7)-N(3)-H(3A)	115.1
C(6)-N(3)	1.407(5)	C(5)-C(4)-H(4)	120.2	C(6)-N(3)-H(3A)	115.1
C(7)-N(3)	1.329(5)	C(3)-C(4)-H(4)	120.2	C(7)-N(4)-C(8)	128.2(4)
C(7)-N(4)	1.375(5)	C(4)-C(5)-C(6)	118.0(4)	C(7)-N(4)-H(4A)	115.9
C(7)-S(1)	1.691(4)	C(4)-C(5)-H(5)	121	C(8)-N(4)-H(4A)	115.9
C(8)-O(1)	1.225(5)	C(6)-C(5)-H(5)	121	C(16)-N(5)-C(20)	118.9(4)
C(8)-N(4)	1.400(5)	N(2)-C(6)-C(5)	123.8(4)	C(16)-N(5)-Cd(1)	117.8(3)
C(8)-C(9)	1.480(6)	N(2)-C(6)-N(3)	119.7(3)	C(20)-N(5)-Cd(1)	123.3(3)
C(9)-C(14)	1.390(6)	C(5)-C(6)-N(3)	116.6(4)	C(22)-N(6)-C(26)	118.9(4)
C(9)-C(10)	1.393(6)	N(3)-C(7)-N(4)	115.9(3)	C(22)-N(6)-Cd(1)	116.6(3)
C(10)-C(11)	1.389(7)	N(3)-C(7)-S(1)	128.6(3)	C(26)-N(6)-Cd(1)	124.5(3)
C(10)-H(10)	0.95	N(4)-C(7)-S(1)	115.4(3)	C(27)-N(7)-Cd(1)	163.2(4)
C(11)-C(12)	1.380(8)	O(1)-C(8)-N(4)	121.4(4)	C(7)-S(1)-Cd(1)	100.56(14)
C(11)-H(11)	0.95	O(1)-C(8)-C(9)	122.8(4)	N(5)-Cd(1)-N(6)	114.79(12)
C(12)-C(13)	1.369(7)	N(4)-C(8)-C(9)	115.8(4)	N(5)-Cd(1)-N(1)	71.93(12)
C(12)-H(12)	0.95	C(14)-C(9)-C(10)	118.8(4)	N(6)-Cd(1)-N(1)	69.80(11)
C(13)-C(14)	1.391(6)	C(14)-C(9)-C(8)	124.8(4)	N(5)-Cd(1)-N(7)	82.57(12)
C(13)-H(13)	0.95	C(10)-C(9)-C(8)	116.3(4)	N(6)-Cd(1)-N(7)	78.09(12)
C(14)-H(14)	0.95	C(11)-C(10)-C(9)	119.7(5)	N(1)-Cd(1)-N(7)	124.24(12)
C(15)-N(1)	1.467(5)	C(11)-C(10)-H(10)	120.1	N(5)-Cd(1)-N(2)	110.30(11)
C(15)-C(16)	1.510(6)	C(9)-C(10)-H(10)	120.1	N(6)-Cd(1)-N(2)	102.71(11)
C(15)-H(15A)	0.99	C(12)-C(11)-C(10)	121.0(5)	N(1)-Cd(1)-N(2)	69.28(11)
C(15)-H(15B)	0.99	C(12)-C(11)-H(11)	119.5	N(7)-Cd(1)-N(2)	164.68(11)
C(16)-N(5)	1.338(5)	C(10)-C(11)-H(11)	119.5	N(5)-Cd(1)-S(1)	145.18(9)
C(16)-C(17)	1.387(6)	C(13)-C(12)-C(11)	119.5(5)	N(6)-Cd(1)-S(1)	95.29(9)
C(17)-C(18)	1.381(7)	C(13)-C(12)-H(12)	120.3	N(1)-Cd(1)-S(1)	138.66(9)
C(17)-H(17)	0.95	C(11)-C(12)-H(12)	120.3	N(7)-Cd(1)-S(1)	87.24(9)
C(18)-C(19)	1.379(7)	C(12)-C(13)-C(14)	120.5(5)	N(2)-Cd(1)-S(1)	77.44(8)
C(18)-H(18)	0.95	C(12)-C(13)-H(13)	119.8	O(4)-Cl(1)-O(3)	112.0(6)
C(19)-C(20)	1.385(6)	C(14)-C(13)-H(13)	119.8	O(4)-Cl(1)-O(5)	109.1(7)
C(19)-H(19)	0.95	C(9)-C(14)-C(13)	120.5(4)	O(3)-Cl(1)-O(5)	109.3(5)
C(20)-N(5)	1.341(5)	C(9)-C(14)-H(14)	119.8	O(4)-Cl(1)-O(2)	108.1(5)
C(20)-H(20)	0.95	C(13)-C(14)-H(14)	119.8	O(3)-Cl(1)-O(2)	110.3(5)
C(21)-N(1)	1.467(5)	N(1)-C(15)-C(16)	112.4(3)	O(5)-Cl(1)-O(2)	108.0(5)
C(21)-C(22)	1.511(6)	N(1)-C(15)-H(15A)	109.1	O(5A)-Cl(1)-O(2)	112.9(7)
C(21)-H(21A)	0.99	C(16)-C(15)-H(15A)	109.1	O(2A)-Cl(1)-O(2)	69.9(7)
C(21)-H(21B)	0.99	N(1)-C(15)-H(15B)	109.1	O(5A)-Cl(1)-O(3A)	110.5(4)
C(22)-N(6)	1.336(5)	C(16)-C(15)-H(15B)	109.1	O(2A)-Cl(1)-O(3A)	110.2(4)
C(22)-C(23)	1.390(6)	H(15A)-C(15)-H(15B)	107.8	O(5A)-Cl(1)-O(4A)	108.8(4)
C(23)-C(24)	1.366(6)	N(5)-C(16)-C(17)	121.5(4)	O(2A)-Cl(1)-O(4A)	108.2(4)
C(23)-H(23)	0.95	N(5)-C(16)-C(15)	117.2(3)	O(3A)-Cl(1)-O(4A)	107.6(4)
C(24)-C(25)	1.375(6)	C(17)-C(16)-C(15)	121.1(4)	O(9)-Cl(2)-O(9)#1	62.6(7)
C(24)-H(24)	0.95	C(18)-C(17)-C(16)	119.3(4)	O(9)-Cl(2)-O(7)#1	99.7(8)
C(25)-C(26)	1.384(6)	C(18)-C(17)-H(17)	120.3	O(9)#1-Cl(2)-O(7)#1	115.2(4)
C(25)-H(25)	0.95	C(16)-C(17)-H(17)	120.3	O(9)-Cl(2)-O(7)	115.2(4)

Appendix 3: Crystals data

C(26)-N(6)	1.353(5)	C(19)-C(18)-C(17)	119.3(4)	O(9)#1-Cl(2)-O(7)	99.7(8)
C(26)-H(26)	0.95	C(19)-C(18)-H(18)	120.4	O(7)#1-Cl(2)-O(7)	139.3(10)
C(27)-N(7)	1.136(5)	C(17)-C(18)-H(18)	120.4	O(9)-Cl(2)-O(8)#1	145.7(6)
C(27)-C(28)	1.458(6)	C(18)-C(19)-C(20)	118.4(5)	O(9)#1-Cl(2)-O(8)#1	112.0(4)
C(28)-H(28A)	0.98	C(18)-C(19)-H(19)	120.8	O(7)#1-Cl(2)-O(8)#1	112.0(4)
C(28)-H(28B)	0.98	C(20)-C(19)-H(19)	120.8	O(7)-Cl(2)-O(8)#1	30.5(6)
C(28)-H(28C)	0.98	N(5)-C(20)-C(19)	122.6(4)	O(9)-Cl(2)-O(8)	112.0(4)
N(1)-Cd(1)	2.431(3)	N(5)-C(20)-H(20)	118.7	O(9)#1-Cl(2)-O(8)	145.7(6)
N(2)-Cd(1)	2.499(3)	C(19)-C(20)-H(20)	118.7	O(7)#1-Cl(2)-O(8)	30.5(6)
N(3)-H(3A)	0.88	N(1)-C(21)-C(22)	110.5(3)	O(7)-Cl(2)-O(8)	112.0(4)
N(4)-H(4A)	0.88	N(1)-C(21)-H(21A)	109.5	O(8)#1-Cl(2)-O(8)	90.8(10)
N(5)-Cd(1)	2.293(3)	C(22)-C(21)-H(21A)	109.5	O(9)-Cl(2)-O(6)	106.8(4)
N(6)-Cd(1)	2.357(3)	N(1)-C(21)-H(21B)	109.5	O(9)#1-Cl(2)-O(6)	52.6(5)
N(7)-Cd(1)	2.483(4)	C(22)-C(21)-H(21B)	109.5	O(7)#1-Cl(2)-O(6)	81.5(4)
O(2)-Cl(1)	1.435(6)	H(21A)-C(21)-H(21B)	108.1	O(7)-Cl(2)-O(6)	106.1(4)
O(2A)-Cl(1)	1.428(4)	N(6)-C(22)-C(23)	121.6(4)	O(8)#1-Cl(2)-O(6)	91.3(4)
O(3)-Cl(1)	1.385(6)	N(6)-C(22)-C(21)	116.2(3)	O(8)-Cl(2)-O(6)	103.9(3)
O(3A)-Cl(1)	1.439(4)	C(23)-C(22)-C(21)	122.2(4)	O(9)-Cl(2)-O(6)#1	52.6(5)
O(4)-Cl(1)	1.366(6)	C(24)-C(23)-C(22)	119.3(4)	O(9)#1-Cl(2)-O(6)#1	106.8(4)
O(4A)-Cl(1)	1.457(4)	C(24)-C(23)-H(23)	120.3	O(7)#1-Cl(2)-O(6)#1	106.1(4)
O(5)-Cl(1)	1.385(6)	C(22)-C(23)-H(23)	120.3	O(7)-Cl(2)-O(6)#1	81.5(4)
O(5A)-Cl(1)	1.418(4)	C(23)-C(24)-C(25)	119.6(4)	O(8)#1-Cl(2)-O(6)#1	103.9(3)
O(7)-Cl(2)	1.404(4)	C(23)-C(24)-H(24)	120.2	O(8)-Cl(2)-O(6)#1	91.3(4)
O(6)-Cl(2)	1.508(4)	C(25)-C(24)-H(24)	120.2	O(6)-Cl(2)-O(6)#1	158.5(5)
O(9)-Cl(2)	1.404(4)	C(24)-C(25)-C(26)	118.8(4)	O(11)-Cl(3)-O(11)#1	110.3(3)
O(8)-Cl(2)	1.434(4)	C(24)-C(25)-H(25)	120.6	O(11)-Cl(3)-O(10)	109.7(3)
O(10)-Cl(3)	1.432(4)	C(26)-C(25)-H(25)	120.6	O(11)#1-Cl(3)-O(10)	109.1(3)
O(11)-Cl(3)	1.430(3)	N(6)-C(26)-C(25)	121.8(4)	O(11)-Cl(3)-O(10)#1	109.1(3)
S(1)-Cd(1)	2.5962(10)	N(6)-C(26)-H(26)	119.1	O(11)#1-Cl(3)-O(10)#1	109.7(3)
Cl(2)-O(9)#1	1.404(4)	C(25)-C(26)-H(26)	119.1	O(10)-Cl(3)-O(10)#1	108.9(4)
Cl(2)-O(7)#1	1.404(4)	N(7)-C(27)-C(28)	179.4(5)		
Cl(2)-O(8)#1	1.434(4)	C(27)-C(28)-H(28A)	109.5		
Cl(2)-O(6)#1	1.508(4)	C(27)-C(28)-H(28B)	109.5		
Cl(3)-O(11)#1	1.430(3)	H(28A)-C(28)-H(28B)	109.5		
Cl(3)-O(10)#1	1.432(4)	C(27)-C(28)-H(28C)	109.5		

Symmetry transformations used to generate equivalent atoms:

#1 -x+2,y,-z+3/2

Appendix 3: Crystals data

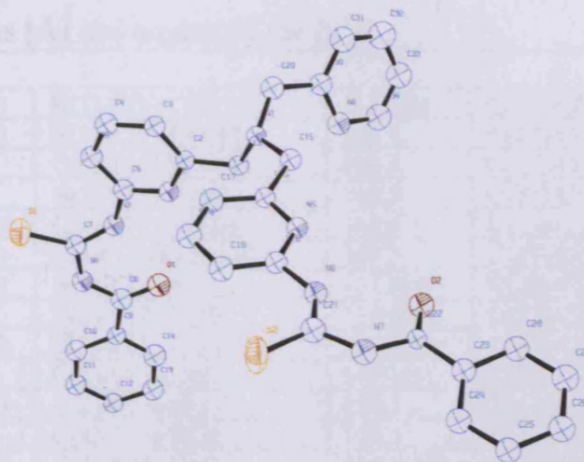


Table D.1: Crystal data and structure refinement for [L²].

Identification code	aja0832	
Empirical formula	C ₃₄ H ₃₀ N ₈ O ₂ S ₂	
Formula weight	646.78	
Temperature	150(2) K	
Wavelength	0.71073 Å	
Crystal system	Triclinic	
Space group	P-1	
Unit cell dimensions	a = 5.7870(10) Å	α = 97.285(5)°.
	b = 15.603(2) Å	β = 96.425(6)°.
	c = 17.042(4) Å	γ = 91.148(7)°.
Volume	1515.9(5) Å ³	
Z	2	
Density (calculated)	1.417 Mg/m ³	
Absorption coefficient	0.224 mm ⁻¹	
F(000)	676	
Crystal size	0.16 x 0.10 x 0.06 mm ³	
Theta range for data collection	3.64 to 19.76°.	
Index ranges	-5 ≤ h ≤ 5, -14 ≤ k ≤ 14, -16 ≤ l ≤ 16	
Reflections collected	4216	
Independent reflections	2516 [R(int) = 0.1388]	
Completeness to theta = 19.76°	91.6 %	
Max. and min. transmission	0.9867 and 0.9651	
Refinement method	Full-matrix least-squares on F ²	
Data / restraints / parameters	2516 / 0 / 195	
Goodness-of-fit on F ²	1.012	
Final R indices [I > 2σ(I)]	R ₁ = 0.0916, wR ₂ = 0.1638	
R indices (all data)	R ₁ = 0.1731, wR ₂ = 0.1978	
Largest diff. peak and hole	0.311 and -0.261 e.Å ⁻³	

Appendix 3: Crystals data

Table D.2: Bond lengths [Å] and angles [°] for [L²].

C(1)-N(1)	1.469(11)	N(1)-C(1)-C(2)	113.9(8)	C(24)-C(25)-H(25)	120.2
C(1)-C(2)	1.499(12)	N(1)-C(1)-H(1A)	108.8	C(27)-C(26)-C(25)	120.6(10)
C(1)-H(1A)	0.99	C(2)-C(1)-H(1A)	108.8	C(27)-C(26)-H(26)	119.7
C(1)-H(1B)	0.99	N(1)-C(1)-H(1B)	108.8	C(25)-C(26)-H(26)	119.7
C(2)-N(2)	1.330(11)	C(2)-C(1)-H(1B)	108.8	C(26)-C(27)-C(28)	120.5(9)
C(2)-C(3)	1.374(12)	H(1A)-C(1)-H(1B)	107.7	C(26)-C(27)-H(27)	119.8
C(3)-C(4)	1.392(12)	N(2)-C(2)-C(3)	121.9(9)	C(28)-C(27)-H(27)	119.8
C(3)-H(3)	0.95	N(2)-C(2)-C(1)	113.9(8)	C(27)-C(28)-C(23)	119.0(9)
C(4)-C(5)	1.378(13)	C(3)-C(2)-C(1)	124.1(8)	C(27)-C(28)-H(28)	120.5
C(4)-H(4)	0.95	C(2)-C(3)-C(4)	119.1(9)	C(23)-C(28)-H(28)	120.5
C(5)-C(6)	1.368(13)	C(2)-C(3)-H(3)	120.5	N(1)-C(29)-C(30)	118.7(8)
C(5)-H(5)	0.95	C(4)-C(3)-H(3)	120.5	N(1)-C(29)-H(29A)	107.6
C(6)-N(2)	1.336(11)	C(5)-C(4)-C(3)	118.8(10)	C(30)-C(29)-H(29A)	107.6
C(6)-N(3)	1.433(11)	C(5)-C(4)-H(4)	120.6	N(1)-C(29)-H(29B)	107.6
C(7)-N(3)	1.308(11)	C(3)-C(4)-H(4)	120.6	C(30)-C(29)-H(29B)	107.6
C(7)-N(4)	1.378(12)	C(6)-C(5)-C(4)	118.1(10)	H(29A)-C(29)-H(29B)	107.1
C(7)-S(1)	1.675(10)	C(6)-C(5)-H(5)	120.9	N(8)-C(30)-C(31)	123.1(9)
C(8)-O(1)	1.241(11)	C(4)-C(5)-H(5)	120.9	N(8)-C(30)-C(29)	117.7(8)
C(8)-N(4)	1.379(12)	N(2)-C(6)-C(5)	123.4(9)	C(31)-C(30)-C(29)	119.1(9)
C(8)-C(9)	1.488(14)	N(2)-C(6)-N(3)	110.8(9)	C(32)-C(31)-C(30)	120.4(11)
C(9)-C(10)	1.386(13)	C(5)-C(6)-N(3)	125.8(9)	C(32)-C(31)-H(31)	119.8
C(9)-C(14)	1.395(13)	N(3)-C(7)-N(4)	114.6(9)	C(30)-C(31)-H(31)	119.8
C(10)-C(11)	1.389(13)	N(3)-C(7)-S(1)	128.4(8)	C(33)-C(32)-C(31)	117.6(11)
C(10)-H(10)	0.95	N(4)-C(7)-S(1)	116.9(7)	C(33)-C(32)-H(32)	121.2
C(11)-C(12)	1.353(13)	O(1)-C(8)-N(4)	120.9(9)	C(31)-C(32)-H(32)	121.2
C(11)-H(11)	0.95	O(1)-C(8)-C(9)	121.7(10)	C(34)-C(33)-C(32)	119.1(11)
C(12)-C(13)	1.389(13)	N(4)-C(8)-C(9)	117.3(9)	C(34)-C(33)-H(33)	120.5
C(12)-H(12)	0.95	C(10)-C(9)-C(14)	119.7(9)	C(32)-C(33)-H(33)	120.5
C(13)-C(14)	1.405(13)	C(10)-C(9)-C(8)	124.2(9)	C(33)-C(34)-N(8)	124.6(11)
C(13)-H(13)	0.95	C(14)-C(9)-C(8)	116.1(9)	C(33)-C(34)-H(34)	117.7
C(14)-H(14)	0.95	C(9)-C(10)-C(11)	119.5(10)	N(8)-C(34)-H(34)	117.7
C(15)-N(1)	1.455(11)	C(9)-C(10)-H(10)	120.3	C(29)-N(1)-C(15)	114.4(7)
C(15)-C(16)	1.501(12)	C(11)-C(10)-H(10)	120.3	C(29)-N(1)-C(1)	112.6(8)
C(15)-H(15A)	0.99	C(12)-C(11)-C(10)	120.5(10)	C(15)-N(1)-C(1)	116.4(7)
C(15)-H(15B)	0.99	C(12)-C(11)-H(11)	119.7	C(2)-N(2)-C(6)	118.5(8)
C(16)-N(5)	1.329(11)	C(10)-C(11)-H(11)	119.7	C(7)-N(3)-C(6)	133.2(9)
C(16)-C(17)	1.382(12)	C(11)-C(12)-C(13)	122.2(9)	C(7)-N(3)-H(3A)	113.4
C(17)-C(18)	1.370(13)	C(11)-C(12)-H(12)	118.9	C(6)-N(3)-H(3A)	113.4
C(17)-H(17)	0.95	C(13)-C(12)-H(12)	118.9	C(7)-N(4)-C(8)	130.9(8)
C(18)-C(19)	1.367(13)	C(12)-C(13)-C(14)	117.5(10)	C(7)-N(4)-H(4A)	114.5
C(18)-H(18)	0.95	C(12)-C(13)-H(13)	121.2	C(8)-N(4)-H(4A)	114.5
C(19)-C(20)	1.390(12)	C(14)-C(13)-H(13)	121.2	C(16)-N(5)-C(20)	117.1(8)
C(19)-H(19)	0.95	C(9)-C(14)-C(13)	120.7(10)	C(21)-N(6)-C(20)	131.8(8)
C(20)-N(5)	1.334(11)	C(9)-C(14)-H(14)	119.7	C(21)-N(6)-H(6)	114.1
C(20)-N(6)	1.418(11)	C(13)-C(14)-H(14)	119.7	C(20)-N(6)-H(6)	114.1
C(21)-N(6)	1.322(11)	N(1)-C(15)-C(16)	113.5(7)	C(22)-N(7)-C(21)	131.7(9)
C(21)-N(7)	1.394(12)	N(1)-C(15)-H(15A)	108.9	C(22)-N(7)-H(7)	114.2
C(21)-S(2)	1.670(10)	C(16)-C(15)-H(15A)	108.9	C(21)-N(7)-H(7)	114.2
C(22)-O(2)	1.232(10)	N(1)-C(15)-H(15B)	108.9	C(30)-N(8)-C(34)	115.0(8)
C(22)-N(7)	1.388(11)	C(16)-C(15)-H(15B)	108.9		
C(22)-C(23)	1.470(13)	H(15A)-C(15)-H(15B)	107.7		
C(23)-C(24)	1.376(12)	N(5)-C(16)-C(17)	122.3(8)		
C(23)-C(28)	1.397(12)	N(5)-C(16)-C(15)	114.7(8)		
C(24)-C(25)	1.388(13)	C(17)-C(16)-C(15)	123.0(9)		
C(24)-H(24)	0.95	C(18)-C(17)-C(16)	119.6(10)		
C(25)-C(26)	1.382(12)	C(18)-C(17)-H(17)	120.2		
C(25)-H(25)	0.95	C(16)-C(17)-H(17)	120.2		

Appendix 3: Crystals data

C(26)-C(27)	1.363(13)	C(19)-C(18)-C(17)	119.5(10)		
C(26)-H(26)	0.95	C(19)-C(18)-H(18)	120.2		
C(27)-C(28)	1.393(13)	C(17)-C(18)-H(18)	120.2		
C(27)-H(27)	0.95	C(18)-C(19)-C(20)	117.1(10)		
C(28)-H(28)	0.95	C(18)-C(19)-H(19)	121.5		
C(29)-N(1)	1.448(11)	C(20)-C(19)-H(19)	121.5		
C(29)-C(30)	1.541(13)	N(5)-C(20)-C(19)	124.4(9)		
C(29)-H(29A)	0.99	N(5)-C(20)-N(6)	111.5(8)		
C(29)-H(29B)	0.99	C(19)-C(20)-N(6)	124.1(9)		
C(30)-N(8)	1.325(12)	N(6)-C(21)-N(7)	114.8(8)		
C(30)-C(31)	1.376(13)	N(6)-C(21)-S(2)	128.6(8)		
C(31)-C(32)	1.373(14)	N(7)-C(21)-S(2)	116.6(8)		
C(31)-H(31)	0.95	O(2)-C(22)-N(7)	118.7(9)		
C(32)-C(33)	1.365(15)	O(2)-C(22)-C(23)	124.6(8)		
C(32)-H(32)	0.95	N(7)-C(22)-C(23)	116.6(8)		
C(33)-C(34)	1.351(13)	C(24)-C(23)-C(28)	120.0(9)		
C(33)-H(33)	0.95	C(24)-C(23)-C(22)	124.5(8)		
C(34)-N(8)	1.372(12)	C(28)-C(23)-C(22)	115.5(8)		
C(34)-H(34)	0.95	C(23)-C(24)-C(25)	120.2(9)		
N(3)-H(3A)	0.88	C(23)-C(24)-H(24)	119.9		
N(4)-H(4A)	0.88	C(25)-C(24)-H(24)	119.9		
N(6)-H(6)	0.88	C(26)-C(25)-C(24)	119.6(9)		
N(7)-H(7)	0.88	C(26)-C(25)-H(25)	120.2		

Appendix 3: Crystals data

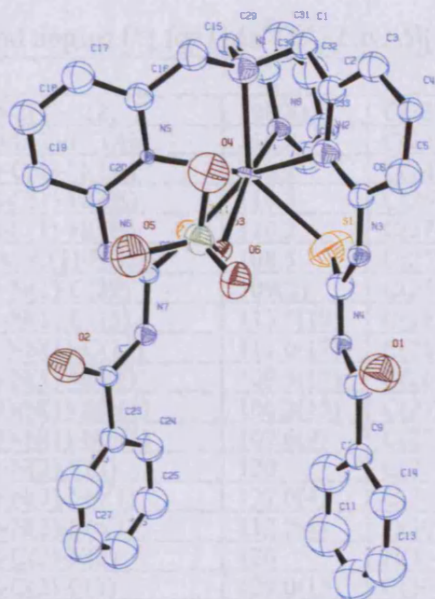


Table E.1: Crystal data and structure refinement for $[\text{Mn}^{\text{II}}(\text{L}^2)(\text{ClO}_4)][\text{ClO}_4].2(\text{H}_2\text{O})$. 3.1

Identification code	aja0942	
Empirical formula	$\text{C}_{34} \text{H}_{34} \text{Cl}_2 \text{Mn} \text{N}_8 \text{O}_{12} \text{S}_2$	
Formula weight	936.65	
Temperature	150(2) K	
Wavelength	0.71073 Å	
Crystal system	Monoclinic	
Space group	P21/n	
Unit cell dimensions	$a = 14.846(3) \text{ \AA}$ $b = 11.049(3) \text{ \AA}$ $c = 23.882(6) \text{ \AA}$	$\alpha = 90^\circ$ $\beta = 97.313(9)^\circ$ $\gamma = 90^\circ$
Volume	$3885.6(16) \text{ \AA}^3$	
Z	4	
Density (calculated)	1.601 Mg/m^3	
Absorption coefficient	0.659 mm^{-1}	
F(000)	1924	
Crystal size	$0.15 \times 0.10 \times 0.10 \text{ mm}^3$	
Theta range for data collection	2.98 to 19.30°	
Index ranges	$-13 \leq h \leq 13$, $-9 \leq k \leq 10$, $-21 \leq l \leq 21$	
Reflections collected	4391	
Independent reflections	2818 [R(int) = 0.0838]	
Completeness to theta = 19.30°	85.8 %	
Max. and min. transmission	0.9371 and 0.9076	
Refinement method	Full-matrix least-squares on F^2	
Data / restraints / parameters	2818 / 94 / 232	
Goodness-of-fit on F^2	1.239	
Final R indices [$I > 2\sigma(I)$]	R1 = 0.2481, wR2 = 0.5043	
R indices (all data)	R1 = 0.2603, wR2 = 0.5138	
Largest diff. peak and hole	1.081 and $-0.961 \text{ e.\AA}^{-3}$	

Appendix 3: Crystals data

Table E.2: Bond lengths [Å] and angles [°] for $[\text{Mn}^{\text{II}}(\text{L}^2)(\text{ClO}_4)][\text{ClO}_4] \cdot 2(\text{H}_2\text{O})$. 3.1

C(1)-N(1)	1.45(4)	N(1)-C(1)-C(2)	108(3)	C(23)-C(24)-H(24)	120
C(1)-C(2)	1.51(4)	N(1)-C(1)-H(1A)	110.2	C(24)-C(25)-C(26)	120
C(1)-H(1A)	0.99	C(2)-C(1)-H(1A)	110.2	C(24)-C(25)-H(25)	120
C(1)-H(1B)	0.99	N(1)-C(1)-H(1B)	110.2	C(26)-C(25)-H(25)	120
N(1)-C(29)	1.50(4)	C(2)-C(1)-H(1B)	110.2	C(27)-C(26)-C(25)	120
N(1)-C(15)	1.50(2)	H(1A)-C(1)-H(1B)	108.5	C(27)-C(26)-H(26)	120
N(1)-Mn(1)	2.335(15)	C(1)-N(1)-C(29)	109(2)	C(25)-C(26)-H(26)	120
N(2)-C(6)	1.3888	C(1)-N(1)-C(15)	113.5(19)	C(28)-C(27)-C(26)	120
N(2)-C(2)	1.3889	C(29)-N(1)-C(15)	111.0(17)	C(28)-C(27)-H(27)	120
N(2)-Mn(1)	2.262(15)	C(1)-N(1)-Mn(1)	109.5(17)	C(26)-C(27)-H(27)	120
C(2)-C(3)	1.3883	C(29)-N(1)-Mn(1)	106.2(15)	C(27)-C(28)-C(23)	120
C(3)-C(4)	1.3888	C(15)-N(1)-Mn(1)	107.6(9)	C(27)-C(28)-H(28)	120
C(3)-H(3)	0.95	C(6)-N(2)-C(2)	120	C(23)-C(28)-H(28)	120
C(4)-C(5)	1.3889	C(6)-N(2)-Mn(1)	127.0(4)	C(30)-C(29)-N(1)	111(2)
C(4)-H(4)	0.95	C(2)-N(2)-Mn(1)	112.2(4)	C(30)-C(29)-H(29A)	109.5
C(5)-C(6)	1.3883	C(3)-C(2)-N(2)	120	N(1)-C(29)-H(29A)	109.5
C(5)-H(5)	0.95	C(3)-C(2)-C(1)	120.0(15)	C(30)-C(29)-H(29B)	109.5
C(6)-N(3)	1.28(3)	N(2)-C(2)-C(1)	119.0(15)	N(1)-C(29)-H(29B)	109.5
C(7)-N(4)	1.27(4)	C(2)-C(3)-C(4)	120	H(29A)-C(29)-H(29B)	108
C(7)-N(3)	1.40(4)	C(2)-C(3)-H(3)	120	C(20)-N(6)-C(21)	131(3)
C(7)-S(1)	1.598(10)	C(4)-C(3)-H(3)	120	C(20)-N(6)-H(6)	114.4
C(8)-O(1)	1.23(4)	C(3)-C(4)-C(5)	120	C(21)-N(6)-H(6)	114.4
C(8)-N(4)	1.36(4)	C(3)-C(4)-H(4)	120	C(22)-N(7)-C(21)	132.5(17)
C(8)-C(9)	1.57(4)	C(5)-C(4)-H(4)	120	C(22)-N(7)-H(7)	113.8
N(3)-H(3A)	0.88	C(6)-C(5)-C(4)	120	C(21)-N(7)-H(7)	113.8
N(4)-H(4A)	0.88	C(6)-C(5)-H(5)	120	C(34)-N(8)-C(30)	120
C(9)-C(10)	1.3884	C(4)-C(5)-H(5)	120	C(34)-N(8)-Mn(1)	123.1(4)
C(9)-C(14)	1.3889	N(3)-C(6)-C(5)	118.2(14)	C(30)-N(8)-Mn(1)	116.9(4)
C(10)-C(11)	1.3889	N(3)-C(6)-N(2)	121.7(14)	N(8)-C(30)-C(31)	120
C(10)-H(10)	0.95	C(5)-C(6)-N(2)	120	N(8)-C(30)-C(29)	114.5(16)
C(11)-C(12)	1.3889	N(4)-C(7)-N(3)	122(2)	C(31)-C(30)-C(29)	125.0(15)
C(11)-H(11)	0.95	N(4)-C(7)-S(1)	116(2)	C(32)-C(31)-C(30)	120
C(12)-C(13)	1.3884	N(3)-C(7)-S(1)	121(3)	C(32)-C(31)-H(31)	120
C(12)-H(12)	0.95	O(1)-C(8)-N(4)	127(4)	C(30)-C(31)-H(31)	120
C(13)-C(14)	1.3889	O(1)-C(8)-C(9)	115(3)	C(31)-C(32)-C(33)	120
C(13)-H(13)	0.95	N(4)-C(8)-C(9)	119(3)	C(31)-C(32)-H(32)	120
C(14)-H(14)	0.95	C(6)-N(3)-C(7)	131(3)	C(33)-C(32)-H(32)	120
C(15)-C(16)	1.4598	C(6)-N(3)-H(3A)	114.4	C(32)-C(33)-C(34)	120
C(15)-H(15A)	0.99	C(7)-N(3)-H(3A)	114.4	C(32)-C(33)-H(33)	120
C(15)-H(15B)	0.99	C(7)-N(4)-C(8)	124(2)	C(34)-C(33)-H(33)	120
N(5)-C(20)	1.3887	C(7)-N(4)-H(4A)	117.8	N(8)-C(34)-C(33)	120
N(5)-C(16)	1.3888	C(8)-N(4)-H(4A)	117.8	N(8)-C(34)-H(34)	120
N(5)-Mn(1)	2.298(16)	C(10)-C(9)-C(14)	120	C(33)-C(34)-H(34)	120
C(16)-C(17)	1.3887	C(10)-C(9)-C(8)	118.5(16)	Cl(1)-O(3)-Mn(1)	128.2(10)
C(17)-C(18)	1.3886	C(14)-C(9)-C(8)	121.5(16)	C(7)-S(1)-Mn(1)	100.7(16)
C(17)-H(17)	0.95	C(9)-C(10)-C(11)	120	C(21)-S(2)-Mn(1)	98.9(13)
C(18)-C(19)	1.3888	C(9)-C(10)-H(10)	120	N(2)-Mn(1)-N(8)	104.2(5)
C(18)-H(18)	0.95	C(11)-C(10)-H(10)	120	N(2)-Mn(1)-N(5)	117.7(6)
C(19)-C(20)	1.3886	C(12)-C(11)-C(10)	120	N(8)-Mn(1)-N(5)	116.5(6)
C(19)-H(19)	0.95	C(12)-C(11)-H(11)	120	N(2)-Mn(1)-N(1)	74.9(5)
C(20)-N(6)	1.31(3)	C(10)-C(11)-H(11)	120	N(8)-Mn(1)-N(1)	72.3(6)
C(21)-N(6)	1.33(4)	C(13)-C(12)-C(11)	120	N(5)-Mn(1)-N(1)	75.2(5)
C(21)-N(7)	1.38(3)	C(13)-C(12)-H(12)	120	N(2)-Mn(1)-O(3)	79.6(6)
C(21)-S(2)	1.600(10)	C(11)-C(12)-H(12)	120	N(8)-Mn(1)-O(3)	166.3(6)
C(22)-O(2)	1.18(3)	C(12)-C(13)-C(14)	120	N(5)-Mn(1)-O(3)	71.7(5)
C(22)-N(7)	1.34(2)	C(12)-C(13)-H(13)	120	N(1)-Mn(1)-O(3)	121.3(5)
C(22)-C(23)	1.5576	C(14)-C(13)-H(13)	120	N(2)-Mn(1)-S(1)	75.8(5)

Appendix 3: Crystals data

C(23)-C(24)	1.3889	C(9)-C(14)-C(13)	120	N(8)-Mn(1)-S(1)	83.8(6)
C(23)-C(28)	1.3892	C(9)-C(14)-H(14)	120	N(5)-Mn(1)-S(1)	148.7(6)
C(24)-C(25)	1.3889	C(13)-C(14)-H(14)	120	N(1)-Mn(1)-S(1)	135.8(6)
C(24)-H(24)	0.95	C(16)-C(15)-N(1)	111.8(8)	O(3)-Mn(1)-S(1)	84.4(5)
C(25)-C(26)	1.3892	C(16)-C(15)-H(15A)	109.3	N(2)-Mn(1)-S(2)	155.9(5)
C(25)-H(25)	0.95	N(1)-C(15)-H(15A)	109.3	N(8)-Mn(1)-S(2)	79.9(5)
C(26)-C(27)	1.3889	C(16)-C(15)-H(15B)	109.3	N(5)-Mn(1)-S(2)	79.5(5)
C(26)-H(26)	0.95	N(1)-C(15)-H(15B)	109.3	N(1)-Mn(1)-S(2)	128.0(5)
C(27)-C(28)	1.3889	H(15A)-C(15)-H(15B)	107.9	O(3)-Mn(1)-S(2)	91.4(5)
C(27)-H(27)	0.95	C(20)-N(5)-C(16)	120	S(1)-Mn(1)-S(2)	81.2(5)
C(28)-H(28)	0.95	C(20)-N(5)-Mn(1)	128.1(4)	O(4)-Cl(1)-O(5)	109.8(8)
C(29)-C(30)	1.46(4)	C(16)-N(5)-Mn(1)	111.9(4)	O(4)-Cl(1)-O(6)	109.6(8)
C(29)-H(29A)	0.99	C(17)-C(16)-N(5)	120	O(5)-Cl(1)-O(6)	109.5(8)
C(29)-H(29B)	0.99	C(17)-C(16)-C(15)	118.5	O(4)-Cl(1)-O(3)	109.7(8)
N(6)-H(6)	0.88	N(5)-C(16)-C(15)	121.4	O(5)-Cl(1)-O(3)	109.2(8)
N(7)-H(7)	0.88	C(18)-C(17)-C(16)	120	O(6)-Cl(1)-O(3)	109.1(7)
N(8)-C(34)	1.3888	C(18)-C(17)-H(17)	120	O(9)-Cl(2)-O(7)	109.7(8)
N(8)-C(30)	1.389	C(16)-C(17)-H(17)	120	O(9)-Cl(2)-O(8)	109.6(8)
N(8)-Mn(1)	2.269(16)	C(17)-C(18)-C(19)	120	O(7)-Cl(2)-O(8)	109.5(8)
C(30)-C(31)	1.3892	C(17)-C(18)-H(18)	120	O(9)-Cl(2)-O(10)	109.4(8)
C(31)-C(32)	1.3888	C(19)-C(18)-H(18)	120	O(7)-Cl(2)-O(10)	109.4(8)
C(31)-H(31)	0.95	C(20)-C(19)-C(18)	120	O(8)-Cl(2)-O(10)	109.3(8)
C(32)-C(33)	1.389	C(20)-C(19)-H(19)	120		
C(32)-H(32)	0.95	C(18)-C(19)-H(19)	120		
C(33)-C(34)	1.3892	N(6)-C(20)-C(19)	121.1(14)		
C(33)-H(33)	0.95	N(6)-C(20)-N(5)	118.7(13)		
C(34)-H(34)	0.95	C(19)-C(20)-N(5)	120		
O(3)-Cl(1)	1.442(8)	N(6)-C(21)-N(7)	112.1(17)		
O(3)-Mn(1)	2.508(17)	N(6)-C(21)-S(2)	127(3)		
O(4)-Cl(1)	1.433(8)	N(7)-C(21)-S(2)	121(2)		
O(5)-Cl(1)	1.436(8)	O(2)-C(22)-N(7)	122(2)		
O(6)-Cl(1)	1.438(8)	O(2)-C(22)-C(23)	121.5(17)		
O(7)-Cl(2)	1.436(9)	N(7)-C(22)-C(23)	115.9(11)		
O(8)-Cl(2)	1.437(9)	C(24)-C(23)-C(28)	120		
O(9)-Cl(2)	1.435(9)	C(24)-C(23)-C(22)	122.6		
O(10)-Cl(2)	1.439(9)	C(28)-C(23)-C(22)	117.4		
S(1)-Mn(1)	2.527(16)	C(25)-C(24)-C(23)	120		
S(2)-Mn(1)	2.560(12)	C(25)-C(24)-H(24)	120		

Appendix 3: Crystals data

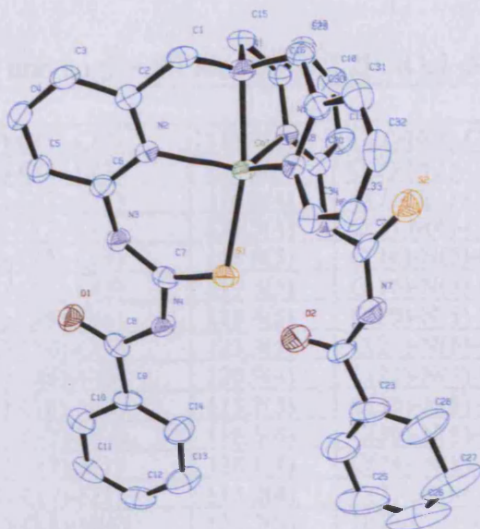


Table G.1: Crystal data and structure refinement for $[\text{Co}^{\text{II}}\text{L}^2] \cdot 2[\text{ClO}_4] \cdot 3.2$

Identification code	aja0820t	
Empirical formula	C ₃₄ H ₃₀ Cl ₂ Co N ₈ O ₁₀ S ₂	
Formula weight	904.61	
Temperature	150(2) K	
Wavelength	0.71073 Å	
Crystal system	Monoclinic	
Space group	P2 ₁ /n	
Unit cell dimensions	a = 14.0690(6) Å	α = 90°.
	b = 11.8060(4) Å	β = 90.400(10)°.
	c = 22.1260(9) Å	γ = 90°.
Volume	3675.0(2) Å ³	
Z	4	
Density (calculated)	1.635 Mg/m ³	
Absorption coefficient	0.797 mm ⁻¹	
F(000)	1852	
Crystal size	0.40 x 0.30 x 0.10 mm ³	
Theta range for data collection	2.90 to 27.54°.	
Index ranges	-18 ≤ h ≤ 18, -15 ≤ k ≤ 14, -28 ≤ l ≤ 28	
Reflections collected	23933	
Independent reflections	7889 [R(int) = 0.1589]	
Completeness to theta = 27.54°	93.1 %	
Max. and min. transmission	0.9246 and 0.7411	
Refinement method	Full-matrix least-squares on F ²	
Data / restraints / parameters	7889 / 0 / 514	
Goodness-of-fit on F ²	1.019	
Final R indices [I > 2σ(I)]	R1 = 0.0782, wR2 = 0.1604	
R indices (all data)	R1 = 0.1564, wR2 = 0.1912	
Largest diff. peak and hole	0.485 and -0.651 e.Å ⁻³	

Appendix 3: Crystals data

Table G.2: Bond lengths [Å] and angles [°] for [Co^{II}L²].2[ClO₄]. 3.2

C(1)-N(1)	1.470(6)	N(1)-C(1)-C(2)	110.0(4)	C(6)-N(2)-Co(1)	128.2(3)
C(1)-C(2)	1.510(7)	N(2)-C(2)-C(3)	122.6(5)	C(2)-N(2)-Co(1)	114.3(3)
C(2)-N(2)	1.344(6)	N(2)-C(2)-C(1)	116.0(4)	C(7)-N(3)-C(6)	130.9(4)
C(2)-C(3)	1.375(7)	C(3)-C(2)-C(1)	121.3(4)	C(7)-N(4)-C(8)	129.0(4)
C(3)-C(4)	1.388(7)	C(2)-C(3)-C(4)	118.8(5)	C(16)-N(5)-C(20)	117.1(4)
C(4)-C(5)	1.359(7)	C(5)-C(4)-C(3)	119.3(5)	C(16)-N(5)-Co(1)	116.0(3)
C(5)-C(6)	1.391(7)	C(4)-C(5)-C(6)	118.4(5)	C(20)-N(5)-Co(1)	126.9(3)
C(6)-N(2)	1.332(6)	N(2)-C(6)-C(5)	123.3(5)	C(21)-N(6)-C(20)	121.3(4)
C(6)-N(3)	1.403(6)	N(2)-C(6)-N(3)	120.9(4)	C(22)-N(7)-C(21)	129.3(5)
C(7)-N(3)	1.319(6)	C(5)-C(6)-N(3)	115.7(5)	C(30)-N(8)-C(34)	117.6(5)
C(7)-N(4)	1.364(6)	N(3)-C(7)-N(4)	116.5(4)	C(30)-N(8)-Co(1)	117.2(4)
C(7)-S(1)	1.693(5)	N(3)-C(7)-S(1)	128.1(4)	C(34)-N(8)-Co(1)	125.0(4)
C(8)-O(1)	1.212(6)	N(4)-C(7)-S(1)	115.2(4)	C(7)-S(1)-Co(1)	102.14(18)
C(8)-N(4)	1.395(6)	O(1)-C(8)-N(4)	120.7(5)	N(8)-Co(1)-N(5)	116.53(16)
C(8)-C(9)	1.472(7)	O(1)-C(8)-C(9)	123.7(5)	N(8)-Co(1)-N(2)	118.88(16)
C(9)-C(14)	1.382(7)	N(4)-C(8)-C(9)	115.6(5)	N(5)-Co(1)-N(2)	112.89(15)
C(9)-C(10)	1.409(7)	C(14)-C(9)-C(10)	119.2(5)	N(8)-Co(1)-N(1)	78.33(16)
C(10)-C(11)	1.377(8)	C(14)-C(9)-C(8)	124.5(5)	N(5)-Co(1)-N(1)	78.39(15)
C(11)-C(12)	1.373(8)	C(10)-C(9)-C(8)	116.3(5)	N(2)-Co(1)-N(1)	78.67(15)
C(12)-C(13)	1.354(8)	C(11)-C(10)-C(9)	119.6(6)	N(8)-Co(1)-S(1)	99.42(12)
C(13)-C(14)	1.392(8)	C(12)-C(11)-C(10)	120.2(6)	N(5)-Co(1)-S(1)	114.08(12)
C(15)-N(1)	1.474(6)	C(13)-C(12)-C(11)	120.8(6)	N(2)-Co(1)-S(1)	91.04(12)
C(15)-C(16)	1.489(7)	C(12)-C(13)-C(14)	120.5(6)	N(1)-Co(1)-S(1)	166.45(11)
C(16)-N(5)	1.343(6)	C(9)-C(14)-C(13)	119.7(6)	O(6)-Cl(1)-O(3)	107.4(3)
C(16)-C(17)	1.388(7)	N(1)-C(15)-C(16)	110.8(4)	O(6)-Cl(1)-O(5)	111.2(3)
C(17)-C(18)	1.386(7)	N(5)-C(16)-C(17)	122.3(4)	O(3)-Cl(1)-O(5)	110.1(3)
C(18)-C(19)	1.385(8)	N(5)-C(16)-C(15)	115.6(4)	O(6)-Cl(1)-O(4)	109.0(3)
C(19)-C(20)	1.371(7)	C(17)-C(16)-C(15)	122.0(5)	O(3)-Cl(1)-O(4)	109.3(3)
C(20)-N(5)	1.349(6)	C(18)-C(17)-C(16)	119.4(5)	O(5)-Cl(1)-O(4)	109.8(3)
C(20)-N(6)	1.415(6)	C(19)-C(18)-C(17)	118.8(5)	O(10)-Cl(2)-O(9)	111.1(3)
C(21)-N(6)	1.364(7)	C(20)-C(19)-C(18)	118.1(5)	O(10)-Cl(2)-O(7)	109.3(3)
C(21)-N(7)	1.392(7)	N(5)-C(20)-C(19)	124.3(5)	O(9)-Cl(2)-O(7)	108.2(3)
C(21)-S(2)	1.627(6)	N(5)-C(20)-N(6)	116.2(4)	O(10)-Cl(2)-O(8)	109.4(3)
C(22)-O(2)	1.230(7)	C(19)-C(20)-N(6)	119.5(5)	O(9)-Cl(2)-O(8)	107.9(3)
C(22)-N(7)	1.374(7)	N(6)-C(21)-N(7)	114.1(5)	O(7)-Cl(2)-O(8)	111.0(3)
C(22)-C(23)	1.478(8)	N(6)-C(21)-S(2)	125.0(4)		
C(23)-C(24)	1.372(9)	N(7)-C(21)-S(2)	120.9(4)		
C(23)-C(28)	1.384(10)	O(2)-C(22)-N(7)	122.1(5)		
C(24)-C(25)	1.375(10)	O(2)-C(22)-C(23)	121.2(6)		
C(25)-C(26)	1.396(14)	N(7)-C(22)-C(23)	116.7(6)		
C(26)-C(27)	1.382(13)	C(24)-C(23)-C(28)	120.9(7)		
C(27)-C(28)	1.399(10)	C(24)-C(23)-C(22)	115.9(7)		
C(29)-N(1)	1.474(6)	C(28)-C(23)-C(22)	123.1(7)		
C(29)-C(30)	1.500(7)	C(23)-C(24)-C(25)	121.5(9)		
C(30)-N(8)	1.340(6)	C(24)-C(25)-C(26)	117.1(10)		
C(30)-C(31)	1.363(7)	C(27)-C(26)-C(25)	123.1(8)		
C(31)-C(32)	1.378(8)	C(26)-C(27)-C(28)	118.0(9)		
C(32)-C(33)	1.370(8)	C(23)-C(28)-C(27)	119.5(9)		
C(33)-C(34)	1.389(7)	N(1)-C(29)-C(30)	110.9(4)		
C(34)-N(8)	1.343(6)	N(8)-C(30)-C(31)	123.0(5)		
N(1)-Co(1)	2.147(4)	N(8)-C(30)-C(29)	114.5(5)		
N(2)-Co(1)	2.086(4)	C(31)-C(30)-C(29)	122.4(5)		
N(5)-Co(1)	2.065(4)	C(30)-C(31)-C(32)	119.0(5)		
N(8)-Co(1)	2.051(4)	C(33)-C(32)-C(31)	119.5(5)		
O(3)-Cl(1)	1.429(4)	C(32)-C(33)-C(34)	118.3(5)		
O(4)-Cl(1)	1.442(4)	N(8)-C(34)-C(33)	122.6(5)		

Appendix 3: Crystals data

O(5)-Cl(1)	1.432(4)	C(1)-N(1)-C(15)	112.1(4)		
O(6)-Cl(1)	1.422(4)	C(1)-N(1)-C(29)	112.0(4)		
O(7)-Cl(2)	1.435(4)	C(15)-N(1)-C(29)	112.6(4)		
O(8)-Cl(2)	1.439(4)	C(1)-N(1)-Co(1)	106.0(3)		
O(9)-Cl(2)	1.419(4)	C(15)-N(1)-Co(1)	106.9(3)		
O(10)-Cl(2)	1.417(4)	C(29)-N(1)-Co(1)	106.8(3)		
S(1)-Co(1)	2.3170(14)	C(6)-N(2)-C(2)	117.5(4)		

Appendix 3: Crystals data

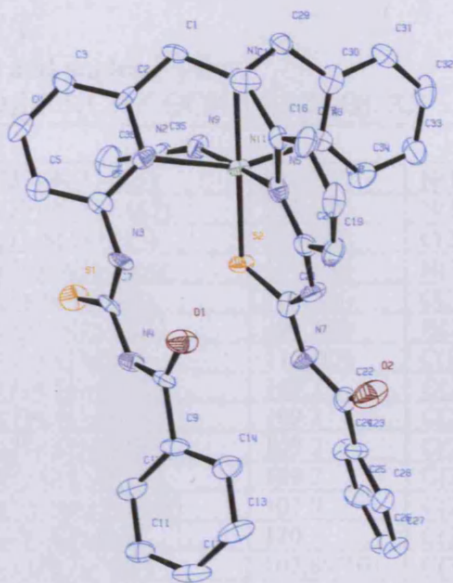


Table H.1: Crystal data and structure refinement for $[\text{Ni}^{\text{II}}(\text{L}^2)(\text{ClO}_4)(\text{CH}_3\text{CN})][\text{ClO}_4] \cdot 0.5(\text{CH}_3\text{COCH}_3) \cdot 0.5(\text{H}_2\text{O})$. **3.3**

Identification code	aja0815b	
Empirical formula	C _{37.50} H ₃₇ Cl ₂ N ₉ Ni O ₁₁ S ₂	
Formula weight	983.49	
Temperature	150(2) K	
Wavelength	0.71073 Å	
Crystal system	Monoclinic	
Space group	P2 ₁ /n	
Unit cell dimensions	a = 12.6653(6) Å	α = 90°.
	b = 18.0877(9) Å	β = 96.484(3)°.
	c = 18.8600(10) Å	γ = 90°.
Volume	4292.9(4) Å ³	
Z	4	
Density (calculated)	1.522 Mg/m ³	
Absorption coefficient	0.743 mm ⁻¹	
F(000)	2028	
Crystal size	0.42 x 0.03 x 0.02 mm ³	
Theta range for data collection	2.45 to 20.81°.	
Index ranges	-12 ≤ h ≤ 12, -18 ≤ k ≤ 17, -18 ≤ l ≤ 18	
Reflections collected	8397	
Independent reflections	4431 [R(int) = 0.0624]	
Completeness to theta = 20.81°	98.9 %	
Max. and min. transmission	0.9853 and 0.7454	
Refinement method	Full-matrix least-squares on F ²	
Data / restraints / parameters	4431 / 18 / 497	
Goodness-of-fit on F ²	1.252	
Final R indices [I > 2σ(I)]	R ₁ = 0.0939, wR ₂ = 0.1774	
R indices (all data)	R ₁ = 0.1185, wR ₂ = 0.1861	
Largest diff. peak and hole	0.882 and -0.388 e.Å ⁻³	

Appendix 3: Crystals data

Table H.2: Bond lengths [Å] and angles [°] for
 $[\text{Ni}^{\text{II}}(\text{L}^2)(\text{ClO}_4)(\text{CH}_3\text{CN})][\text{ClO}_4] \cdot 0.5(\text{CH}_3\text{COCH}_3) \cdot 0.5(\text{H}_2\text{O}) \cdot 3.3$

N(1)-C(29)	1.455(12)	C(29)-N(1)-C(1)	110.2(7)	N(1)-C(29)-C(30)	114.1(7)
N(1)-C(1)	1.479(8)	C(29)-N(1)-C(15)	112.6(8)	N(1)-C(29)-H(29A)	108.7
N(1)-C(15)	1.483(12)	C(1)-N(1)-C(15)	108.8(7)	C(30)-C(29)-H(29A)	108.7
N(1)-Ni(1)	2.072(8)	C(29)-N(1)-Ni(1)	110.3(6)	N(1)-C(29)-H(29B)	108.7
C(1)-C(2)	1.4616	C(1)-N(1)-Ni(1)	109.5(5)	C(30)-C(29)-H(29B)	108.7
C(1)-H(1A)	0.99	C(15)-N(1)-Ni(1)	105.3(6)	H(29A)-C(29)-H(29B)	107.6
C(1)-H(1B)	0.99	C(2)-C(1)-N(1)	112.2(3)	C(21)-N(6)-C(20)	133.8(8)
N(2)-C(2)	1.39	C(2)-C(1)-H(1A)	109.2	C(21)-N(6)-H(6)	113.1
N(2)-C(6)	1.39	N(1)-C(1)-H(1A)	109.2	C(20)-N(6)-H(6)	113.1
N(2)-Ni(1)	2.237(4)	C(2)-C(1)-H(1B)	109.2	C(21)-N(7)-C(22)	128.3(5)
C(2)-C(3)	1.39	N(1)-C(1)-H(1B)	109.2	C(21)-N(7)-H(7)	115.9
C(3)-C(4)	1.39	H(1A)-C(1)-H(1B)	107.9	C(22)-N(7)-H(7)	115.9
C(3)-H(3)	0.95	C(2)-N(2)-C(6)	120	C(30)-N(8)-C(34)	120
C(4)-C(5)	1.39	C(2)-N(2)-Ni(1)	107.89(10)	C(30)-N(8)-Ni(1)	113.01(11)
C(4)-H(4)	0.95	C(6)-N(2)-Ni(1)	127.55(11)	C(34)-N(8)-Ni(1)	126.96(11)
C(5)-C(6)	1.39	N(2)-C(2)-C(3)	120	N(8)-C(30)-C(31)	120
C(5)-H(5)	0.95	N(2)-C(2)-C(1)	116.6	N(8)-C(30)-C(29)	115.7(4)
C(6)-N(3)	1.373(9)	C(3)-C(2)-C(1)	123.4	C(31)-C(30)-C(29)	124.2(4)
C(7)-N(3)	1.339(12)	C(4)-C(3)-C(2)	120	C(32)-C(31)-C(30)	120
C(7)-N(4)	1.392(11)	C(4)-C(3)-H(3)	120	C(32)-C(31)-H(31)	120
C(7)-S(1)	1.636(11)	C(2)-C(3)-H(3)	120	C(30)-C(31)-H(31)	120
C(8)-O(1)	1.233(8)	C(3)-C(4)-C(5)	120	C(31)-C(32)-C(33)	120
C(8)-N(4)	1.378(6)	C(3)-C(4)-H(4)	120	C(31)-C(32)-H(32)	120
C(8)-C(9)	1.4821	C(5)-C(4)-H(4)	120	C(33)-C(32)-H(32)	120
C(9)-C(10)	1.39	C(6)-C(5)-C(4)	120	C(34)-C(33)-C(32)	120
C(9)-C(14)	1.39	C(6)-C(5)-H(5)	120	C(34)-C(33)-H(33)	120
C(10)-C(11)	1.39	C(4)-C(5)-H(5)	120	C(32)-C(33)-H(33)	120
C(10)-H(10)	0.95	N(3)-C(6)-C(5)	122.9(4)	C(33)-C(34)-N(8)	120
C(11)-C(12)	1.39	N(3)-C(6)-N(2)	117.0(4)	C(33)-C(34)-H(34)	120
C(11)-H(11)	0.95	C(5)-C(6)-N(2)	120	N(8)-C(34)-H(34)	120
C(12)-C(13)	1.39	N(3)-C(7)-N(4)	113.9(8)	N(9)-C(35)-C(36)	176.1(12)
C(12)-H(12)	0.95	N(3)-C(7)-S(1)	126.2(8)	C(35)-C(36)-H(36A)	109.5
C(13)-C(14)	1.39	N(4)-C(7)-S(1)	119.9(7)	C(35)-C(36)-H(36B)	109.5
C(13)-H(13)	0.95	O(1)-C(8)-N(4)	121.6(5)	H(36A)-C(36)-H(36B)	109.5
C(14)-H(14)	0.95	O(1)-C(8)-C(9)	121.8(4)	C(35)-C(36)-H(36C)	109.5
C(15)-C(16)	1.471(11)	N(4)-C(8)-C(9)	116.6(2)	H(36A)-C(36)-H(36C)	109.5
C(15)-H(15A)	0.99	C(10)-C(9)-C(14)	120	H(36B)-C(36)-H(36C)	109.5
C(15)-H(15B)	0.99	C(10)-C(9)-C(8)	121.4	C(38)-C(37)-H(37A)	109.5
N(3)-H(3A)	0.88	C(14)-C(9)-C(8)	118.3	C(38)-C(37)-H(37B)	109.5
N(4)-H(4A)	0.88	C(11)-C(10)-C(9)	120	H(37A)-C(37)-H(37B)	109.5
N(5)-C(16)	1.39	C(11)-C(10)-H(10)	120	C(38)-C(37)-H(37C)	109.5
N(5)-C(20)	1.39	C(9)-C(10)-H(10)	120	H(37A)-C(37)-H(37C)	109.5
N(5)-Ni(1)	2.050(4)	C(10)-C(11)-C(12)	120	H(37B)-C(37)-H(37C)	109.5
C(16)-C(17)	1.39	C(10)-C(11)-H(11)	120	O(12)-C(38)-C(37)	124.7(8)
C(17)-C(18)	1.39	C(12)-C(11)-H(11)	120	O(12)-C(38)-C(39)	122.5(8)
C(17)-H(17)	0.95	C(13)-C(12)-C(11)	120	C(37)-C(38)-C(39)	112.8(7)
C(18)-C(19)	1.39	C(13)-C(12)-H(12)	120	C(38)-C(39)-H(39A)	109.5
C(18)-H(18)	0.95	C(11)-C(12)-H(12)	120	C(38)-C(39)-H(39B)	109.5
C(19)-C(20)	1.39	C(14)-C(13)-C(12)	120	H(39A)-C(39)-H(39B)	109.5
C(19)-H(19)	0.95	C(14)-C(13)-H(13)	120	C(38)-C(39)-H(39C)	109.5
C(20)-N(6)	1.388(8)	C(12)-C(13)-H(13)	120	H(39A)-C(39)-H(39C)	109.5
C(21)-N(6)	1.347(12)	C(13)-C(14)-C(9)	120	H(39B)-C(39)-H(39C)	109.5
C(21)-N(7)	1.362(10)	C(13)-C(14)-H(14)	120	N(5)-Ni(1)-N(1)	85.9(3)
C(21)-S(2)	1.676(11)	C(9)-C(14)-H(14)	120	N(5)-Ni(1)-N(8)	88.44(15)

Appendix 3: Crystals data

C(22)-O(2)	1.236(9)	C(16)-C(15)-N(1)	116.5(7)	N(1)-Ni(1)-N(8)	82.1(2)
C(22)-N(7)	1.403(6)	C(16)-C(15)-H(15A)	108.2	N(5)-Ni(1)-N(9)	177.6(3)
C(22)-C(23)	1.4802	N(1)-C(15)-H(15A)	108.2	N(1)-Ni(1)-N(9)	94.4(3)
C(23)-C(24)	1.39	C(16)-C(15)-H(15B)	108.2	N(8)-Ni(1)-N(9)	94.0(3)
C(23)-C(28)	1.39	N(1)-C(15)-H(15B)	108.2	N(5)-Ni(1)-N(2)	95.07(14)
C(24)-C(25)	1.39	H(15A)-C(15)-H(15B)	107.3	N(1)-Ni(1)-N(2)	75.9(2)
C(24)-H(24)	0.95	C(7)-N(3)-C(6)	121.9(8)	N(8)-Ni(1)-N(2)	157.47(16)
C(25)-C(26)	1.39	C(7)-N(3)-H(3A)	119	N(9)-Ni(1)-N(2)	82.7(3)
C(25)-H(25)	0.95	C(6)-N(3)-H(3A)	119	N(5)-Ni(1)-S(2)	94.15(13)
C(26)-C(27)	1.39	C(8)-N(4)-C(7)	129.5(5)	N(1)-Ni(1)-S(2)	179.8(3)
C(26)-H(26)	0.95	C(8)-N(4)-H(4A)	115.2	N(8)-Ni(1)-S(2)	98.01(13)
C(27)-C(28)	1.39	C(7)-N(4)-H(4A)	115.2	N(9)-Ni(1)-S(2)	85.6(2)
C(27)-H(27)	0.95	C(16)-N(5)-C(20)	120	N(2)-Ni(1)-S(2)	103.90(13)
C(28)-H(28)	0.95	C(16)-N(5)-Ni(1)	110.38(11)	C(35)-N(9)-Ni(1)	148.0(9)
C(29)-C(30)	1.496(10)	C(20)-N(5)-Ni(1)	129.61(11)	C(21)-S(2)-Ni(1)	108.1(4)
C(29)-H(29A)	0.99	N(5)-C(16)-C(17)	120	O(3)-Cl(1)-O(4)	110.0(6)
C(29)-H(29B)	0.99	N(5)-C(16)-C(15)	117.3(4)	O(3)-Cl(1)-O(6)	108.9(6)
N(6)-H(6)	0.88	C(17)-C(16)-C(15)	122.6(4)	O(4)-Cl(1)-O(6)	109.6(6)
N(7)-H(7)	0.88	C(16)-C(17)-C(18)	120	O(3)-Cl(1)-O(5)	109.1(7)
N(8)-C(30)	1.39	C(16)-C(17)-H(17)	120	O(4)-Cl(1)-O(5)	109.6(6)
N(8)-C(34)	1.39	C(18)-C(17)-H(17)	120	O(6)-Cl(1)-O(5)	109.6(7)
N(8)-Ni(1)	2.086(4)	C(19)-C(18)-C(17)	120	O(7)-Cl(2)-O(8)	109.8(5)
C(30)-C(31)	1.39	C(19)-C(18)-H(18)	120	O(7)-Cl(2)-O(10)	108.5(5)
C(31)-C(32)	1.39	C(17)-C(18)-H(18)	120	O(8)-Cl(2)-O(10)	108.9(5)
C(31)-H(31)	0.95	C(18)-C(19)-C(20)	120	O(7)-Cl(2)-O(9)	109.8(5)
C(32)-C(33)	1.39	C(18)-C(19)-H(19)	120	O(8)-Cl(2)-O(9)	110.0(5)
C(32)-H(32)	0.95	C(20)-C(19)-H(19)	120	O(10)-Cl(2)-O(9)	109.9(6)
C(33)-C(34)	1.39	N(6)-C(20)-C(19)	117.3(4)		
C(33)-H(33)	0.95	N(6)-C(20)-N(5)	122.1(4)		
C(34)-H(34)	0.95	C(19)-C(20)-N(5)	120		
C(35)-N(9)	1.153(13)	N(6)-C(21)-N(7)	114.7(8)		
C(35)-C(36)	1.454(17)	N(6)-C(21)-S(2)	128.3(8)		
C(36)-H(36A)	0.98	N(7)-C(21)-S(2)	117.0(7)		
C(36)-H(36B)	0.98	O(2)-C(22)-N(7)	120.6(5)		
C(36)-H(36C)	0.98	O(2)-C(22)-C(23)	121.5(4)		
C(37)-C(38)	1.523(8)	N(7)-C(22)-C(23)	117.9(2)		
C(37)-H(37A)	0.98	C(24)-C(23)-C(28)	120		
C(37)-H(37B)	0.98	C(24)-C(23)-C(22)	123.1		
C(37)-H(37C)	0.98	C(28)-C(23)-C(22)	116.8		
C(38)-O(12)	1.227(8)	C(23)-C(24)-C(25)	120		
C(38)-C(39)	1.544(8)	C(23)-C(24)-H(24)	120		
C(39)-H(39A)	0.98	C(25)-C(24)-H(24)	120		
C(39)-H(39B)	0.98	C(26)-C(25)-C(24)	120		
C(39)-H(39C)	0.98	C(26)-C(25)-H(25)	120		
O(3)-Cl(1)	1.426(8)	C(24)-C(25)-H(25)	120		
O(4)-Cl(1)	1.431(9)	C(27)-C(26)-C(25)	120		
O(5)-Cl(1)	1.456(10)	C(27)-C(26)-H(26)	120		
O(6)-Cl(1)	1.444(9)	C(25)-C(26)-H(26)	120		
O(7)-Cl(2)	1.424(7)	C(26)-C(27)-C(28)	120		
O(8)-Cl(2)	1.429(7)	C(26)-C(27)-H(27)	120		
O(9)-Cl(2)	1.434(8)	C(28)-C(27)-H(27)	120		
O(10)-Cl(2)	1.430(7)	C(23)-C(28)-C(27)	120		
Ni(1)-N(9)	2.090(10)	C(23)-C(28)-H(28)	120		
Ni(1)-S(2)	2.345(3)	C(27)-C(28)-H(28)	120		

Appendix 3: Crystals data

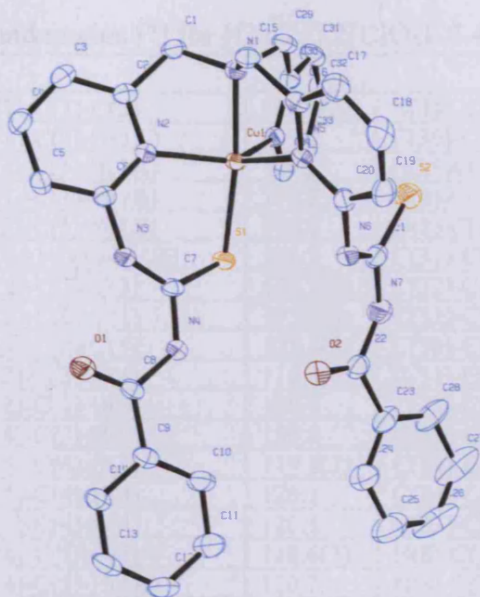


Table I.1: Crystal data and structure refinement for $[\text{Cu}^{\text{II}}\text{L}^2] \cdot 2[\text{ClO}_4] \cdot 3.4$

Identification code	aja0816	
Empirical formula	$\text{C}_{34} \text{H}_{30} \text{Cl}_2 \text{Cu} \text{N}_8 \text{O}_{10} \text{S}_2$	
Formula weight	909.22	
Temperature	150(2) K	
Wavelength	0.71073 Å	
Crystal system	Monoclinic	
Space group	$P2_1/n$	
Unit cell dimensions	$a = 13.9290(3)$ Å $b = 11.8320(2)$ Å $c = 22.3070(5)$ Å	$\alpha = 90^\circ$ $\beta = 91.2240(10)^\circ$ $\gamma = 90^\circ$
Volume	$3675.53(13)$ Å ³	
Z	4	
Density (calculated)	1.643 Mg/m^3	
Absorption coefficient	0.924 mm^{-1}	
F(000)	1860	
Crystal size	$0.20 \times 0.12 \times 0.10 \text{ mm}^3$	
Theta range for data collection	2.92 to 27.45°	
Index ranges	$-18 \leq h \leq 16$, $-15 \leq k \leq 15$, $-28 \leq l \leq 27$	
Reflections collected	29591	
Independent reflections	8371 [R(int) = 0.1136]	
Completeness to theta = 27.45°	99.6 %	
Max. and min. transmission	0.9133 and 0.8367	
Refinement method	Full-matrix least-squares on F^2	
Data / restraints / parameters	8371 / 0 / 514	
Goodness-of-fit on F^2	1.032	
Final R indices [I > 2σ(I)]	$R_1 = 0.0539$, $wR_2 = 0.1147$	
R indices (all data)	$R_1 = 0.0875$, $wR_2 = 0.1280$	
Largest diff. peak and hole	0.555 and -0.698 e.Å^{-3}	

Appendix 3: Crystals data

Table I.2: Bond lengths [Å] and angles [°] for [Cu^{II}L²].2[ClO₄]. 3.4

C(1)-N(1)	1.481(4)	N(1)-C(1)-C(2)	109.2(2)	N(1)-C(29)-H(29B)	109.5
C(1)-C(2)	1.507(4)	N(1)-C(1)-H(1A)	109.8	C(30)-C(29)-H(29B)	109.5
C(1)-H(1A)	0.99	C(2)-C(1)-H(1A)	109.8	H(29A)-C(29)-H(29B)	108.1
C(1)-H(1B)	0.99	N(1)-C(1)-H(1B)	109.8	N(8)-C(30)-C(31)	121.4(3)
C(2)-N(2)	1.350(4)	C(2)-C(1)-H(1B)	109.8	N(8)-C(30)-C(29)	115.6(3)
C(2)-C(3)	1.374(5)	H(1A)-C(1)-H(1B)	108.3	C(31)-C(30)-C(29)	122.8(3)
C(3)-C(4)	1.386(5)	N(2)-C(2)-C(3)	122.7(3)	C(32)-C(31)-C(30)	119.5(3)
C(3)-H(3)	0.95	N(2)-C(2)-C(1)	115.0(3)	C(32)-C(31)-H(31)	120.2
C(4)-C(5)	1.373(5)	C(3)-C(2)-C(1)	122.4(3)	C(30)-C(31)-H(31)	120.2
C(4)-H(4)	0.95	C(2)-C(3)-C(4)	118.4(3)	C(31)-C(32)-C(33)	119.1(3)
C(5)-C(6)	1.389(4)	C(2)-C(3)-H(3)	120.8	C(31)-C(32)-H(32)	120.5
C(5)-H(5A)	0.95	C(4)-C(3)-H(3)	120.8	C(33)-C(32)-H(32)	120.5
C(6)-N(2)	1.343(4)	C(5)-C(4)-C(3)	119.8(3)	C(34)-C(33)-C(32)	118.9(3)
C(6)-N(3)	1.400(4)	C(5)-C(4)-H(4)	120.1	C(34)-C(33)-H(33)	120.5
C(7)-N(3)	1.328(4)	C(3)-C(4)-H(4)	120.1	C(32)-C(33)-H(33)	120.5
C(7)-N(4)	1.373(4)	C(4)-C(5)-C(6)	118.6(3)	N(8)-C(34)-C(33)	122.3(3)
C(7)-S(1)	1.691(3)	C(4)-C(5)-H(5A)	120.7	N(8)-C(34)-H(34)	118.8
C(8)-O(1)	1.216(4)	C(6)-C(5)-H(5A)	120.7	C(33)-C(34)-H(34)	118.8
C(8)-N(4)	1.403(4)	N(2)-C(6)-C(5)	122.1(3)	C(1)-N(1)-C(15)	111.3(3)
C(8)-C(9)	1.479(4)	N(2)-C(6)-N(3)	120.3(3)	C(1)-N(1)-C(29)	112.2(2)
C(9)-C(10)	1.384(5)	C(5)-C(6)-N(3)	117.5(3)	C(15)-N(1)-C(29)	111.6(3)
C(9)-C(14)	1.398(5)	N(3)-C(7)-N(4)	116.7(3)	C(1)-N(1)-Cu(1)	105.33(19)
C(10)-C(11)	1.386(5)	N(3)-C(7)-S(1)	128.1(2)	C(15)-N(1)-Cu(1)	107.98(19)
C(10)-H(10)	0.95	N(4)-C(7)-S(1)	115.1(2)	C(29)-N(1)-Cu(1)	108.04(19)
C(11)-C(12)	1.377(5)	O(1)-C(8)-N(4)	120.9(3)	C(6)-N(2)-C(2)	118.4(3)
C(11)-H(11)	0.95	O(1)-C(8)-C(9)	123.0(3)	C(6)-N(2)-Cu(1)	129.4(2)
C(12)-C(13)	1.385(5)	N(4)-C(8)-C(9)	116.0(3)	C(2)-N(2)-Cu(1)	112.2(2)
C(12)-H(12)	0.95	C(10)-C(9)-C(14)	118.7(3)	C(7)-N(3)-C(6)	130.4(3)
C(13)-C(14)	1.375(5)	C(10)-C(9)-C(8)	124.4(3)	C(7)-N(3)-H(3A)	114.8
C(13)-H(13)	0.95	C(14)-C(9)-C(8)	116.9(3)	C(6)-N(3)-H(3A)	114.8
C(14)-H(14)	0.95	C(9)-C(10)-C(11)	120.6(3)	C(7)-N(4)-C(8)	127.7(3)
C(15)-N(1)	1.483(4)	C(9)-C(10)-H(10)	119.7	C(7)-N(4)-H(4A)	116.2
C(15)-C(16)	1.496(4)	C(11)-C(10)-H(10)	119.7	C(8)-N(4)-H(4A)	116.2
C(15)-H(15A)	0.99	C(12)-C(11)-C(10)	120.4(4)	C(20)-N(5)-C(16)	118.0(3)
C(15)-H(15B)	0.99	C(12)-C(11)-H(11)	119.8	C(20)-N(5)-Cu(1)	130.9(2)
C(16)-N(5)	1.348(4)	C(10)-C(11)-H(11)	119.8	C(16)-N(5)-Cu(1)	111.0(2)
C(16)-C(17)	1.385(5)	C(11)-C(12)-C(13)	119.3(3)	C(21)-N(6)-C(20)	121.7(3)
C(17)-C(18)	1.379(5)	C(11)-C(12)-H(12)	120.4	C(21)-N(6)-H(6)	119.1
C(17)-H(17)	0.95	C(13)-C(12)-H(12)	120.4	C(20)-N(6)-H(6)	119.1
C(18)-C(19)	1.382(5)	C(14)-C(13)-C(12)	120.7(3)	C(22)-N(7)-C(21)	128.8(3)
C(18)-H(18)	0.95	C(14)-C(13)-H(13)	119.6	C(22)-N(7)-H(7)	115.6
C(19)-C(20)	1.376(5)	C(12)-C(13)-H(13)	119.6	C(21)-N(7)-H(7)	115.6
C(19)-H(19)	0.95	C(13)-C(14)-C(9)	120.3(3)	C(34)-N(8)-C(30)	118.8(3)
C(20)-N(5)	1.331(4)	C(13)-C(14)-H(14)	119.9	C(34)-N(8)-Cu(1)	128.2(2)
C(20)-N(6)	1.413(4)	C(9)-C(14)-H(14)	119.9	C(30)-N(8)-Cu(1)	113.0(2)
C(21)-N(6)	1.350(4)	N(1)-C(15)-C(16)	110.7(3)	C(7)-S(1)-Cu(1)	103.75(11)
C(21)-N(7)	1.383(4)	N(1)-C(15)-H(15A)	109.5	N(1)-Cu(1)-N(2)	81.55(10)
C(21)-S(2)	1.663(4)	C(16)-C(15)-H(15A)	109.5	N(1)-Cu(1)-N(8)	83.17(11)
C(22)-O(2)	1.230(4)	N(1)-C(15)-H(15B)	109.5	N(2)-Cu(1)-N(8)	129.04(10)
C(22)-N(7)	1.376(5)	C(16)-C(15)-H(15B)	109.5	N(1)-Cu(1)-N(5)	80.11(10)
C(22)-C(23)	1.488(5)	H(15A)-C(15)-H(15B)	108.1	N(2)-Cu(1)-N(5)	113.57(10)
C(23)-C(28)	1.394(6)	N(5)-C(16)-C(17)	122.3(3)	N(8)-Cu(1)-N(5)	111.11(10)
C(23)-C(24)	1.400(6)	N(5)-C(16)-C(15)	115.9(3)	N(1)-Cu(1)-S(1)	172.88(8)
C(24)-C(25)	1.393(6)	C(17)-C(16)-C(15)	121.8(3)	N(2)-Cu(1)-S(1)	92.79(8)
C(24)-H(24)	0.95	C(18)-C(17)-C(16)	118.9(3)	N(8)-Cu(1)-S(1)	97.24(8)
C(25)-C(26)	1.359(8)	C(18)-C(17)-H(17)	120.6	N(5)-Cu(1)-S(1)	106.23(7)
C(25)-H(25)	0.95	C(16)-C(17)-H(17)	120.6	O(6)-Cl(1)-O(4)	110.1(2)

Appendix 3: Crystals data

C(26)-C(27)	1.378(8)	C(17)-C(18)-C(19)	118.9(3)	O(6)-Cl(1)-O(3)	109.62(19)
C(26)-H(26)	0.95	C(17)-C(18)-H(18)	120.5	O(4)-Cl(1)-O(3)	107.85(18)
C(27)-C(28)	1.393(6)	C(19)-C(18)-H(18)	120.5	O(6)-Cl(1)-O(5)	109.81(18)
C(27)-H(27)	0.95	C(20)-C(19)-C(18)	118.8(3)	O(4)-Cl(1)-O(5)	111.5(3)
C(28)-H(28)	0.95	C(20)-C(19)-H(19)	120.6	O(3)-Cl(1)-O(5)	107.96(19)
C(29)-N(1)	1.487(4)	C(18)-C(19)-H(19)	120.6	O(10)-Cl(2)-O(9)	109.5(2)
C(29)-C(30)	1.503(5)	N(5)-C(20)-C(19)	123.1(3)	O(10)-Cl(2)-O(7)	107.47(18)
C(29)-H(29A)	0.99	N(5)-C(20)-N(6)	117.1(3)	O(9)-Cl(2)-O(7)	110.9(2)
C(29)-H(29B)	0.99	C(19)-C(20)-N(6)	119.8(3)	O(10)-Cl(2)-O(8)	109.55(18)
C(30)-N(8)	1.352(4)	N(6)-C(21)-N(7)	116.1(3)	O(9)-Cl(2)-O(8)	109.47(17)
C(30)-C(31)	1.380(5)	N(6)-C(21)-S(2)	124.3(3)	O(7)-Cl(2)-O(8)	109.90(17)
C(31)-C(32)	1.374(5)	N(7)-C(21)-S(2)	119.6(3)		
C(31)-H(31)	0.95	O(2)-C(22)-N(7)	122.0(3)		
C(32)-C(33)	1.382(5)	O(2)-C(22)-C(23)	121.5(3)		
C(32)-H(32)	0.95	N(7)-C(22)-C(23)	116.4(3)		
C(33)-C(34)	1.378(5)	C(28)-C(23)-C(24)	119.2(4)		
C(33)-H(33)	0.95	C(28)-C(23)-C(22)	124.1(4)		
C(34)-N(8)	1.337(4)	C(24)-C(23)-C(22)	116.7(4)		
C(34)-H(34)	0.95	C(25)-C(24)-C(23)	120.1(5)		
N(1)-Cu(1)	2.018(3)	C(25)-C(24)-H(24)	120		
N(2)-Cu(1)	2.030(2)	C(23)-C(24)-H(24)	120		
N(3)-H(3A)	0.88	C(26)-C(25)-C(24)	119.9(5)		
N(4)-H(4A)	0.88	C(26)-C(25)-H(25)	120.1		
N(5)-Cu(1)	2.148(3)	C(24)-C(25)-H(25)	120.1		
N(6)-H(6)	0.88	C(25)-C(26)-C(27)	121.2(4)		
N(7)-H(7)	0.88	C(25)-C(26)-H(26)	119.4		
N(8)-Cu(1)	2.034(3)	C(27)-C(26)-H(26)	119.4		
S(1)-Cu(1)	2.2605(9)	C(26)-C(27)-C(28)	120.0(5)		
O(3)-Cl(1)	1.428(3)	C(26)-C(27)-H(27)	120		
O(4)-Cl(1)	1.424(3)	C(28)-C(27)-H(27)	120		
O(5)-Cl(1)	1.434(3)	C(27)-C(28)-C(23)	119.6(5)		
O(6)-Cl(1)	1.423(3)	C(27)-C(28)-H(28)	120.2		
O(7)-Cl(2)	1.429(3)	C(23)-C(28)-H(28)	120.2		
O(8)-Cl(2)	1.438(2)	N(1)-C(29)-C(30)	110.6(3)		
O(9)-Cl(2)	1.425(3)	N(1)-C(29)-H(29A)	109.5		
O(10)-Cl(2)	1.423(3)	C(30)-C(29)-H(29A)	109.5		

Appendix 3: Crystals data

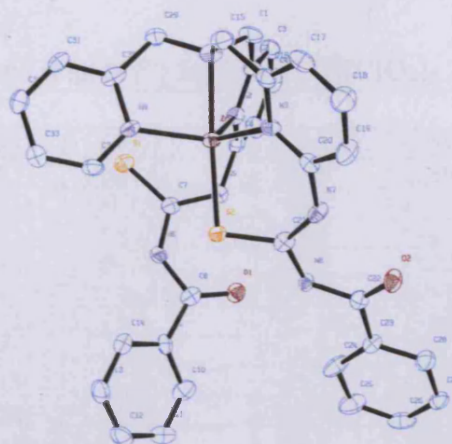


Table J.1: Crystal data and structure refinement for $[\text{Zn}^{\text{II}}(\text{L}^2)][\text{ClO}_4]_2 \cdot 2(\text{CH}_3\text{CN})$. **3.5**

Identification code	aja0804	
Empirical formula	$\text{C}_{70} \text{H}_{63} \text{Cl}_4 \text{N}_{17} \text{O}_{20} \text{S}_4 \text{Zn}_2$	
Formula weight	1863.23	
Temperature	150(2) K	
Wavelength	0.71073 Å	
Crystal system	Monoclinic	
Space group	P21/c	
Unit cell dimensions	$a = 10.46660(10)$ Å	$\alpha = 90^\circ$.
	$b = 42.1309(4)$ Å	$\beta = 91.2101(4)^\circ$.
	$c = 17.5050(2)$ Å	$\gamma = 90^\circ$.
Volume	$7717.41(14)$ Å ³	
Z	4	
Density (calculated)	1.604 Mg/m ³	
Absorption coefficient	0.953 mm ⁻¹	
F(000)	3816	
Crystal size	0.45 x 0.4 x 0.15 mm ³	
Theta range for data collection	2.96 to 27.48°.	
Index ranges	$-13 \leq h \leq 13, -54 \leq k \leq 54, -21 \leq l \leq 22$	
Reflections collected	37445	
Independent reflections	14469 [R(int) = 0.1463]	
Completeness to theta = 27.48°	99.7 %	
Absorption correction	None	
Refinement method	Full-matrix least-squares on F ²	
Data / restraints / parameters	17709 / 0 / 1055	
Goodness-of-fit on F ²	1.055	
Final R indices [I > 2σ(I)]	R1 = 0.0800, wR2 = 0.2002	
R indices (all data)	R1 = 0.1262, wR2 = 0.2425	
Largest diff. peak and hole	1.016 and -0.818 e.Å ⁻³	

Appendix 3: Crystals data

Table J.2: Bond lengths [Å] and angles [°] for $[\text{Zn}^{\text{II}}(\text{L}^2)][\text{ClO}_4]_2 \cdot 2(\text{CH}_3\text{CN}) \cdot 3.5$

C(1)-N(1)	1.454(8)	N(1)-C(1)-C(2)	111.8(5)	C(58)-C(59)-H(59)	119.8
C(1)-C(2)	1.525(9)	N(1)-C(1)-H(1A)	109.3	C(59)-C(60)-C(61)	120.1(7)
C(1)-H(1A)	0.99	C(2)-C(1)-H(1A)	109.3	C(59)-C(60)-H(60)	119.9
C(1)-H(1B)	0.99	N(1)-C(1)-H(1B)	109.3	C(61)-C(60)-H(60)	119.9
C(2)-N(2)	1.330(8)	C(2)-C(1)-H(1B)	109.3	C(62)-C(61)-C(60)	120.3(6)
C(2)-C(3)	1.381(9)	H(1A)-C(1)-H(1B)	107.9	C(62)-C(61)-H(61)	119.8
C(3)-C(4)	1.374(10)	N(2)-C(2)-C(3)	122.3(6)	C(60)-C(61)-H(61)	119.8
C(3)-H(3)	0.95	N(2)-C(2)-C(1)	116.5(6)	C(61)-C(62)-C(57)	119.5(6)
C(4)-C(5)	1.383(10)	C(3)-C(2)-C(1)	121.1(6)	C(61)-C(62)-H(62)	120.2
C(4)-H(4)	0.95	C(4)-C(3)-C(2)	118.8(6)	C(57)-C(62)-H(62)	120.2
C(5)-C(6)	1.372(9)	C(4)-C(3)-H(3)	120.6	N(9)-C(63)-C(64)	110.8(5)
C(5)-H(5)	0.95	C(2)-C(3)-H(3)	120.6	N(9)-C(63)-H(63A)	109.5
C(6)-N(2)	1.342(8)	C(3)-C(4)-C(5)	119.8(6)	C(64)-C(63)-H(63A)	109.5
C(6)-N(5)	1.425(8)	C(3)-C(4)-H(4)	120.1	N(9)-C(63)-H(63B)	109.5
C(7)-N(5)	1.342(8)	C(5)-C(4)-H(4)	120.1	C(64)-C(63)-H(63B)	109.5
C(7)-N(6)	1.364(8)	C(6)-C(5)-C(4)	117.4(7)	H(63A)-C(63)-H(63B)	108.1
C(7)-S(1)	1.670(6)	C(6)-C(5)-H(5)	121.3	N(12)-C(64)-C(65)	120.7(7)
C(8)-O(1)	1.222(7)	C(4)-C(5)-H(5)	121.3	N(12)-C(64)-C(63)	116.0(6)
C(8)-N(6)	1.400(7)	N(2)-C(6)-C(5)	123.7(6)	C(65)-C(64)-C(63)	123.1(6)
C(8)-C(9)	1.487(9)	N(2)-C(6)-N(5)	116.5(5)	C(64)-C(65)-C(66)	121.1(7)
C(9)-C(14)	1.386(8)	C(5)-C(6)-N(5)	119.7(6)	C(64)-C(65)-H(65)	119.4
C(9)-C(10)	1.406(8)	N(5)-C(7)-N(6)	116.8(5)	C(66)-C(65)-H(65)	119.4
C(10)-C(11)	1.368(9)	N(5)-C(7)-S(1)	123.5(5)	C(67)-C(66)-C(65)	117.7(7)
C(10)-H(10)	0.95	N(6)-C(7)-S(1)	119.7(5)	C(67)-C(66)-H(66)	121.1
C(11)-C(12)	1.374(10)	O(1)-C(8)-N(6)	121.1(6)	C(65)-C(66)-H(66)	121.1
C(11)-H(11)	0.95	O(1)-C(8)-C(9)	123.4(5)	C(66)-C(67)-C(68)	118.8(7)
C(12)-C(13)	1.375(9)	N(6)-C(8)-C(9)	115.4(5)	C(66)-C(67)-H(67)	120.6
C(12)-H(12)	0.95	C(14)-C(9)-C(10)	120.1(6)	C(68)-C(67)-H(67)	120.6
C(13)-C(14)	1.389(9)	C(14)-C(9)-C(8)	121.1(5)	N(12)-C(68)-C(67)	123.4(7)
C(13)-H(13)	0.95	C(10)-C(9)-C(8)	118.7(5)	N(12)-C(68)-H(68)	118.3
C(14)-H(14)	0.95	C(11)-C(10)-C(9)	119.4(6)	C(67)-C(68)-H(68)	118.3
C(15)-N(1)	1.454(8)	C(11)-C(10)-H(10)	120.3	C(70)-C(69)-H(69A)	109.5
C(15)-C(16)	1.498(9)	C(9)-C(10)-H(10)	120.3	C(70)-C(69)-H(69B)	109.5
C(15)-H(15A)	0.99	C(10)-C(11)-C(12)	120.0(6)	H(69A)-C(69)-H(69B)	109.5
C(15)-H(15B)	0.99	C(10)-C(11)-H(11)	120	C(70)-C(69)-H(69C)	109.5
C(16)-N(3)	1.346(7)	C(12)-C(11)-H(11)	120	H(69A)-C(69)-H(69C)	109.5
C(16)-C(17)	1.401(9)	C(13)-C(12)-C(11)	121.5(6)	H(69B)-C(69)-H(69C)	109.5
C(17)-C(18)	1.370(10)	C(13)-C(12)-H(12)	119.3	N(17)-C(70)-C(69)	177.7(10)
C(17)-H(17)	0.95	C(11)-C(12)-H(12)	119.3	C(1)-N(1)-C(15)	114.4(5)
C(18)-C(19)	1.377(9)	C(12)-C(13)-C(14)	119.3(6)	C(1)-N(1)-C(29)	112.3(5)
C(18)-H(18)	0.95	C(12)-C(13)-H(13)	120.3	C(15)-N(1)-C(29)	112.3(5)
C(19)-C(20)	1.388(8)	C(14)-C(13)-H(13)	120.3	C(1)-N(1)-Zn(1)	105.4(3)
C(19)-H(19)	0.95	C(9)-C(14)-C(13)	119.6(6)	C(15)-N(1)-Zn(1)	106.4(4)
C(20)-N(3)	1.343(8)	C(9)-C(14)-H(14)	120.2	C(29)-N(1)-Zn(1)	105.2(4)
C(20)-N(7)	1.420(7)	C(13)-C(14)-H(14)	120.2	C(2)-N(2)-C(6)	117.9(5)
C(21)-N(7)	1.342(8)	N(1)-C(15)-C(16)	111.2(5)	C(2)-N(2)-Zn(1)	114.7(4)
C(21)-N(8)	1.359(7)	N(1)-C(15)-H(15A)	109.4	C(6)-N(2)-Zn(1)	127.3(4)
C(21)-S(2)	1.689(6)	C(16)-C(15)-H(15A)	109.4	C(20)-N(3)-C(16)	117.8(5)
C(22)-O(2)	1.223(7)	N(1)-C(15)-H(15B)	109.4	C(20)-N(3)-Zn(1)	128.3(4)
C(22)-N(8)	1.398(7)	C(16)-C(15)-H(15B)	109.4	C(16)-N(3)-Zn(1)	113.8(4)
C(22)-C(23)	1.508(8)	H(15A)-C(15)-H(15B)	108	C(34)-N(4)-C(30)	119.4(5)
C(23)-C(24)	1.398(9)	N(3)-C(16)-C(17)	122.3(6)	C(34)-N(4)-Zn(1)	126.3(4)
C(23)-C(28)	1.410(9)	N(3)-C(16)-C(15)	116.6(6)	C(30)-N(4)-Zn(1)	114.2(4)
C(24)-C(25)	1.381(9)	C(17)-C(16)-C(15)	121.1(6)	C(7)-N(5)-C(6)	122.7(5)
C(24)-H(24)	0.95	C(18)-C(17)-C(16)	118.5(6)	C(7)-N(5)-H(5A)	118.6
C(25)-C(26)	1.382(10)	C(18)-C(17)-H(17)	120.7	C(6)-N(5)-H(5A)	118.6

Appendix 3: Crystals data

C(25)-H(25)	0.95	C(16)-C(17)-H(17)	120.7	C(7)-N(6)-C(8)	129.7(5)
C(26)-C(27)	1.385(10)	C(17)-C(18)-C(19)	119.9(7)	C(7)-N(6)-H(6)	115.2
C(26)-H(26)	0.95	C(17)-C(18)-H(18)	120.1	C(8)-N(6)-H(6)	115.2
C(27)-C(28)	1.409(9)	C(19)-C(18)-H(18)	120.1	C(21)-N(7)-C(20)	130.9(5)
C(27)-H(27)	0.95	C(18)-C(19)-C(20)	118.4(6)	C(21)-N(7)-H(7)	114.5
C(28)-H(28)	0.95	C(18)-C(19)-H(19)	120.8	C(20)-N(7)-H(7)	114.5
C(29)-N(1)	1.485(8)	C(20)-C(19)-H(19)	120.8	C(21)-N(8)-C(22)	127.5(5)
C(29)-C(30)	1.506(9)	N(3)-C(20)-C(19)	123.0(5)	C(21)-N(8)-H(8)	116.3
C(29)-H(29A)	0.99	N(3)-C(20)-N(7)	120.4(5)	C(22)-N(8)-H(8)	116.3
C(29)-H(29B)	0.99	C(19)-C(20)-N(7)	116.5(5)	C(63)-N(9)-C(35)	112.0(5)
C(30)-N(4)	1.365(7)	N(7)-C(21)-N(8)	116.0(5)	C(63)-N(9)-C(49)	113.2(5)
C(30)-C(31)	1.384(8)	N(7)-C(21)-S(2)	126.3(4)	C(35)-N(9)-C(49)	111.7(5)
C(31)-C(32)	1.378(9)	N(8)-C(21)-S(2)	117.7(5)	C(63)-N(9)-Zn(2)	107.9(4)
C(31)-H(31)	0.95	O(2)-C(22)-N(8)	121.6(5)	C(35)-N(9)-Zn(2)	106.1(4)
C(32)-C(33)	1.394(9)	O(2)-C(22)-C(23)	121.7(5)	C(49)-N(9)-Zn(2)	105.4(4)
C(32)-H(32)	0.95	N(8)-C(22)-C(23)	116.7(5)	C(36)-N(10)-C(40)	118.6(5)
C(33)-C(34)	1.394(9)	C(24)-C(23)-C(28)	121.0(6)	C(36)-N(10)-Zn(2)	113.4(4)
C(33)-H(33)	0.95	C(24)-C(23)-C(22)	123.7(5)	C(40)-N(10)-Zn(2)	127.4(4)
C(34)-N(4)	1.333(8)	C(28)-C(23)-C(22)	115.3(6)	C(54)-N(11)-C(50)	118.2(6)
C(34)-H(34)	0.95	C(25)-C(24)-C(23)	118.5(6)	C(54)-N(11)-Zn(2)	127.5(4)
C(35)-N(9)	1.487(9)	C(25)-C(24)-H(24)	120.7	C(50)-N(11)-Zn(2)	114.2(4)
C(35)-C(36)	1.499(9)	C(23)-C(24)-H(24)	120.7	C(64)-N(12)-C(68)	118.2(6)
C(35)-H(35A)	0.99	C(24)-C(25)-C(26)	121.9(7)	C(64)-N(12)-Zn(2)	116.3(4)
C(35)-H(35B)	0.99	C(24)-C(25)-H(25)	119	C(68)-N(12)-Zn(2)	125.4(5)
C(36)-N(10)	1.337(8)	C(26)-C(25)-H(25)	119	C(41)-N(13)-C(40)	130.7(6)
C(36)-C(37)	1.382(9)	C(25)-C(26)-C(27)	119.8(6)	C(41)-N(13)-H(13A)	114.7
C(37)-C(38)	1.384(9)	C(25)-C(26)-H(26)	120.1	C(40)-N(13)-H(13A)	114.7
C(37)-H(37)	0.95	C(27)-C(26)-H(26)	120.1	C(41)-N(14)-C(42)	127.9(6)
C(38)-C(39)	1.381(9)	C(26)-C(27)-C(28)	120.4(6)	C(41)-N(14)-H(14A)	116
C(38)-H(38)	0.95	C(26)-C(27)-H(27)	119.8	C(42)-N(14)-H(14A)	116
C(39)-C(40)	1.379(9)	C(28)-C(27)-H(27)	119.8	C(55)-N(15)-C(54)	120.5(5)
C(39)-H(39)	0.95	C(27)-C(28)-C(23)	118.4(7)	C(55)-N(15)-H(15)	119.7
C(40)-N(10)	1.353(8)	C(27)-C(28)-H(28)	120.8	C(54)-N(15)-H(15)	119.7
C(40)-N(13)	1.397(8)	C(23)-C(28)-H(28)	120.8	C(56)-N(16)-C(55)	127.9(5)
C(41)-N(13)	1.338(8)	N(1)-C(29)-C(30)	110.9(5)	C(56)-N(16)-H(16)	116.1
C(41)-N(14)	1.367(8)	N(1)-C(29)-H(29A)	109.5	C(55)-N(16)-H(16)	116.1
C(41)-S(3)	1.689(7)	C(30)-C(29)-H(29A)	109.5	C(21)-S(2)-Zn(1)	101.1(2)
C(42)-O(3)	1.221(8)	N(1)-C(29)-H(29B)	109.5	C(41)-S(3)-Zn(2)	100.5(2)
C(42)-N(14)	1.390(8)	C(30)-C(29)-H(29B)	109.5	O(5)-Cl(1)-O(8)	109.7(4)
C(42)-C(43)	1.480(9)	H(29A)-C(29)-H(29B)	108.1	O(5)-Cl(1)-O(7)	110.1(4)
C(43)-C(44)	1.376(9)	N(4)-C(30)-C(31)	120.8(6)	O(8)-Cl(1)-O(7)	109.6(3)
C(43)-C(48)	1.409(10)	N(4)-C(30)-C(29)	116.9(5)	O(5)-Cl(1)-O(6)	108.5(3)
C(44)-C(45)	1.389(10)	C(31)-C(30)-C(29)	122.1(5)	O(8)-Cl(1)-O(6)	110.3(3)
C(44)-H(44)	0.95	C(32)-C(31)-C(30)	120.0(6)	O(7)-Cl(1)-O(6)	108.7(3)
C(45)-C(46)	1.365(12)	C(32)-C(31)-H(31)	120	O(10)-Cl(2)-O(9)	112.0(6)
C(45)-H(45)	0.95	C(30)-C(31)-H(31)	120	O(10)-Cl(2)-O(12)	111.0(5)
C(46)-C(47)	1.383(12)	C(31)-C(32)-C(33)	119.0(6)	O(9)-Cl(2)-O(12)	110.4(5)
C(46)-H(46)	0.95	C(31)-C(32)-H(32)	120.5	O(10)-Cl(2)-O(11)	106.2(6)
C(47)-C(48)	1.384(10)	C(33)-C(32)-H(32)	120.5	O(9)-Cl(2)-O(11)	107.2(5)
C(47)-H(47)	0.95	C(32)-C(33)-C(34)	118.4(6)	O(12)-Cl(2)-O(11)	109.9(4)
C(48)-H(48)	0.95	C(32)-C(33)-H(33)	120.8	O(13)-Cl(3)-O(16)	109.8(3)
C(49)-N(9)	1.489(8)	C(34)-C(33)-H(33)	120.8	O(13)-Cl(3)-O(15)	111.1(3)
C(49)-C(50)	1.523(10)	N(4)-C(34)-C(33)	122.2(6)	O(16)-Cl(3)-O(15)	108.5(3)
C(49)-H(49A)	0.99	N(4)-C(34)-H(34)	118.9	O(13)-Cl(3)-O(14)	110.2(3)
C(49)-H(49B)	0.99	C(33)-C(34)-H(34)	118.9	O(16)-Cl(3)-O(14)	108.6(3)
C(50)-N(11)	1.359(8)	N(9)-C(35)-C(36)	111.2(5)	O(15)-Cl(3)-O(14)	108.6(3)
C(50)-C(51)	1.387(9)	N(9)-C(35)-H(35A)	109.4	O(18)-Cl(4)-O(17)	110.6(4)
C(51)-C(52)	1.385(11)	C(36)-C(35)-H(35A)	109.4	O(18)-Cl(4)-O(20)	111.0(4)
C(51)-H(51)	0.95	N(9)-C(35)-H(35B)	109.4	O(17)-Cl(4)-O(20)	109.2(3)

Appendix 3: Crystals data

C(52)-C(53)	1.367(11)	C(36)-C(35)-H(35B)	109.4	O(18)-Cl(4)-O(19)	109.3(4)
C(52)-H(52)	0.95	H(35A)-C(35)-H(35B)	108	O(17)-Cl(4)-O(19)	108.6(4)
C(53)-C(54)	1.383(9)	N(10)-C(36)-C(37)	122.7(6)	O(20)-Cl(4)-O(19)	108.1(4)
C(53)-H(53)	0.95	N(10)-C(36)-C(35)	117.4(6)	N(4)-Zn(1)-N(2)	113.8(2)
C(54)-N(11)	1.346(8)	C(37)-C(36)-C(35)	119.8(6)	N(4)-Zn(1)-N(3)	121.05(19)
C(54)-N(15)	1.412(8)	C(36)-C(37)-C(38)	118.3(6)	N(2)-Zn(1)-N(3)	114.5(2)
C(55)-N(15)	1.342(8)	C(36)-C(37)-H(37)	120.8	N(4)-Zn(1)-N(1)	80.6(2)
C(55)-N(16)	1.393(8)	C(38)-C(37)-H(37)	120.8	N(2)-Zn(1)-N(1)	79.3(2)
C(55)-S(4)	1.652(7)	C(39)-C(38)-C(37)	119.6(6)	N(3)-Zn(1)-N(1)	77.16(19)
C(56)-O(4)	1.224(7)	C(39)-C(38)-H(38)	120.2	N(4)-Zn(1)-S(2)	99.70(14)
C(56)-N(16)	1.390(8)	C(37)-C(38)-H(38)	120.2	N(2)-Zn(1)-S(2)	114.35(14)
C(56)-C(57)	1.485(9)	C(40)-C(39)-C(38)	118.9(7)	N(3)-Zn(1)-S(2)	89.42(13)
C(57)-C(58)	1.391(9)	C(40)-C(39)-H(39)	120.6	N(1)-Zn(1)-S(2)	164.19(15)
C(57)-C(62)	1.396(8)	C(38)-C(39)-H(39)	120.6	N(12)-Zn(2)-N(11)	111.5(2)
C(58)-C(59)	1.397(9)	N(10)-C(40)-C(39)	121.9(6)	N(12)-Zn(2)-N(10)	122.8(2)
C(58)-H(58)	0.95	N(10)-C(40)-N(13)	119.0(6)	N(11)-Zn(2)-N(10)	115.0(2)
C(59)-C(60)	1.378(10)	C(39)-C(40)-N(13)	118.7(6)	N(12)-Zn(2)-N(9)	79.3(2)
C(59)-H(59)	0.95	N(13)-C(41)-N(14)	115.9(6)	N(11)-Zn(2)-N(9)	79.8(2)
C(60)-C(61)	1.393(10)	N(13)-C(41)-S(3)	126.6(5)	N(10)-Zn(2)-N(9)	78.1(2)
C(60)-H(60)	0.95	N(14)-C(41)-S(3)	117.5(5)	N(12)-Zn(2)-S(3)	99.24(16)
C(61)-C(62)	1.375(10)	O(3)-C(42)-N(14)	122.2(6)	N(11)-Zn(2)-S(3)	115.22(15)
C(61)-H(61)	0.95	O(3)-C(42)-C(43)	122.8(6)	N(10)-Zn(2)-S(3)	89.58(15)
C(62)-H(62)	0.95	N(14)-C(42)-C(43)	115.1(6)	N(9)-Zn(2)-S(3)	163.92(15)
C(63)-N(9)	1.463(8)	C(44)-C(43)-C(48)	118.6(6)		
C(63)-C(64)	1.513(10)	C(44)-C(43)-C(42)	118.2(6)		
C(63)-H(63A)	0.99	C(48)-C(43)-C(42)	123.1(6)		
C(63)-H(63B)	0.99	C(43)-C(44)-C(45)	121.2(7)		
C(64)-N(12)	1.344(8)	C(43)-C(44)-H(44)	119.4		
C(64)-C(65)	1.384(10)	C(45)-C(44)-H(44)	119.4		
C(65)-C(66)	1.390(11)	C(46)-C(45)-C(44)	119.6(7)		
C(65)-H(65)	0.95	C(46)-C(45)-H(45)	120.2		
C(66)-C(67)	1.375(11)	C(44)-C(45)-H(45)	120.2		
C(66)-H(66)	0.95	C(45)-C(46)-C(47)	120.7(7)		
C(67)-C(68)	1.384(10)	C(45)-C(46)-H(46)	119.6		
C(67)-H(67)	0.95	C(47)-C(46)-H(46)	119.6		
C(68)-N(12)	1.349(9)	C(46)-C(47)-C(48)	120.0(8)		
C(68)-H(68)	0.95	C(46)-C(47)-H(47)	120		
C(69)-C(70)	1.439(16)	C(48)-C(47)-H(47)	120		
C(69)-H(69A)	0.98	C(47)-C(48)-C(43)	119.8(8)		
C(69)-H(69B)	0.98	C(47)-C(48)-H(48)	120.1		
C(69)-H(69C)	0.98	C(43)-C(48)-H(48)	120.1		
C(70)-N(17)	1.105(13)	N(9)-C(49)-C(50)	108.7(5)		
N(1)-Zn(1)	2.181(5)	N(9)-C(49)-H(49A)	110		
N(2)-Zn(1)	2.078(5)	C(50)-C(49)-H(49A)	110		
N(3)-Zn(1)	2.131(5)	N(9)-C(49)-H(49B)	110		
N(4)-Zn(1)	2.058(5)	C(50)-C(49)-H(49B)	110		
N(5)-H(5A)	0.88	H(49A)-C(49)-H(49B)	108.3		
N(6)-H(6)	0.88	N(11)-C(50)-C(51)	121.5(7)		
N(7)-H(7)	0.88	N(11)-C(50)-C(49)	116.5(6)		
N(8)-H(8)	0.88	C(51)-C(50)-C(49)	122.0(6)		
N(9)-Zn(2)	2.163(5)	C(52)-C(51)-C(50)	119.0(7)		
N(10)-Zn(2)	2.134(5)	C(52)-C(51)-H(51)	120.5		
N(11)-Zn(2)	2.066(5)	C(50)-C(51)-H(51)	120.5		
N(12)-Zn(2)	2.054(5)	C(53)-C(52)-C(51)	119.7(7)		
N(13)-H(13A)	0.88	C(53)-C(52)-H(52)	120.1		
N(14)-H(14A)	0.88	C(51)-C(52)-H(52)	120.1		
N(15)-H(15)	0.88	C(52)-C(53)-C(54)	118.8(7)		
N(16)-H(16)	0.88	C(52)-C(53)-H(53)	120.6		
O(5)-Cl(1)	1.412(5)	C(54)-C(53)-H(53)	120.6		

Appendix 3: Crystals data

O(6)-Cl(1)	1.441(5)	N(11)-C(54)-C(53)	122.7(6)	
O(7)-Cl(1)	1.425(5)	N(11)-C(54)-N(15)	116.5(5)	
O(8)-Cl(1)	1.420(5)	C(53)-C(54)-N(15)	120.9(6)	
O(9)-Cl(2)	1.408(6)	N(15)-C(55)-N(16)	115.8(6)	
O(10)-Cl(2)	1.356(7)	N(15)-C(55)-S(4)	123.3(5)	
O(11)-Cl(2)	1.446(7)	N(16)-C(55)-S(4)	120.8(5)	
O(12)-Cl(2)	1.413(6)	O(4)-C(56)-N(16)	122.0(6)	
O(13)-Cl(3)	1.430(5)	O(4)-C(56)-C(57)	122.3(6)	
O(14)-Cl(3)	1.446(5)	N(16)-C(56)-C(57)	115.7(5)	
O(15)-Cl(3)	1.436(5)	C(58)-C(57)-C(62)	120.8(6)	
O(16)-Cl(3)	1.432(5)	C(58)-C(57)-C(56)	121.9(5)	
O(17)-Cl(4)	1.424(5)	C(62)-C(57)-C(56)	117.1(5)	
O(18)-Cl(4)	1.407(6)	C(57)-C(58)-C(59)	118.8(6)	
O(19)-Cl(4)	1.443(5)	C(57)-C(58)-H(58)	120.6	
O(20)-Cl(4)	1.437(5)	C(59)-C(58)-H(58)	120.6	
S(2)-Zn(1)	2.3716(15)	C(60)-C(59)-C(58)	120.4(6)	
S(3)-Zn(2)	2.3653(17)	C(60)-C(59)-H(59)	119.8	

Appendix 3: Crystals data

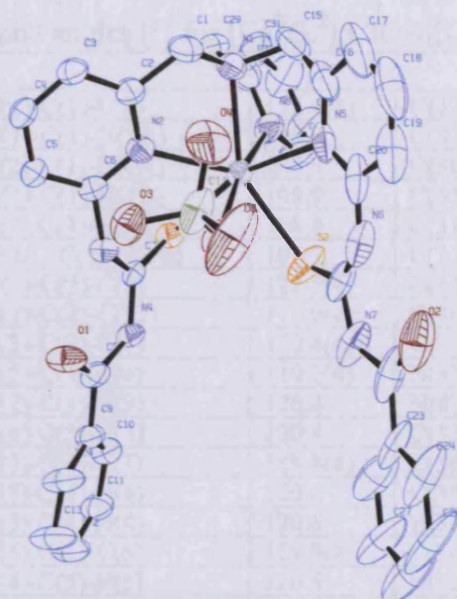


Table K.1: Crystal data and structure refinement for $[\text{Cd}^{\text{II}}(\text{L}^2)(\text{ClO}_4)][\text{ClO}_4] \cdot \text{CH}_3\text{CN}$. 3.6

Identification code	aja0817	
Empirical formula	C ₃₆ H ₃₃ Cd Cl ₂ N ₉ O ₁₀ S ₂	
Formula weight	999.13	
Temperature	293(2) K	
Wavelength	0.71073 Å	
Crystal system	Monoclinic	
Space group	P2 ₁ /n	
Unit cell dimensions	a = 16.4240(3) Å	α = 90°.
	b = 10.8230(2) Å	β = 97.7600(10)°.
	c = 22.9750(6) Å	γ = 90°.
Volume	4046.57(15) Å ³	
Z	4	
Density (calculated)	1.640 Mg/m ³	
Absorption coefficient	0.844 mm ⁻¹	
F(000)	2024	
Crystal size	0.20 x 0.20 x 0.20 mm ³	
Theta range for data collection	2.99 to 27.48°.	
Index ranges	-21 ≤ h ≤ 21, -9 ≤ k ≤ 14, -29 ≤ l ≤ 29	
Reflections collected	32603	
Independent reflections	9235 [R(int) = 0.1183]	
Completeness to theta = 27.48°	99.6 %	
Absorption correction	Empirical	
Max. and min. transmission	0.8494 and 0.8494	
Refinement method	Full-matrix least-squares on F ²	
Data / restraints / parameters	9235 / 0 / 543	
Goodness-of-fit on F ²	0.994	
Final R indices [I > 2σ(I)]	R1 = 0.0598, wR2 = 0.1186	
R indices (all data)	R1 = 0.1457, wR2 = 0.1465	
Extinction coefficient	0.0010(2)	
Largest diff. peak and hole	0.823 and -0.735 e.Å ⁻³	

Appendix 3: Crystals data

Table K.2: Bond lengths [Å] and angles [°] for [Cd^{II}(L²)(ClO₄)](ClO₄).CH₃CN. 3.6

C(1)-N(1)	1.470(6)	N(1)-C(1)-C(2)	113.4(4)	C(32)-C(31)-C(30)	120.6(6)
C(1)-C(2)	1.513(7)	N(1)-C(1)-H(1A)	108.9	C(32)-C(31)-H(31)	119.7
C(1)-H(1A)	0.97	C(2)-C(1)-H(1A)	108.9	C(30)-C(31)-H(31)	119.7
C(1)-H(1B)	0.97	N(1)-C(1)-H(1B)	108.9	C(31)-C(32)-C(33)	118.7(7)
C(2)-N(2)	1.349(6)	C(2)-C(1)-H(1B)	108.9	C(31)-C(32)-H(32)	120.6
C(2)-C(3)	1.378(6)	H(1A)-C(1)-H(1B)	107.7	C(33)-C(32)-H(32)	120.6
C(3)-C(4)	1.380(6)	N(2)-C(2)-C(3)	122.5(4)	C(34)-C(33)-C(32)	118.5(6)
C(3)-H(3)	0.93	N(2)-C(2)-C(1)	117.0(4)	C(34)-C(33)-H(33)	120.8
C(4)-C(5)	1.370(6)	C(3)-C(2)-C(1)	120.4(4)	C(32)-C(33)-H(33)	120.8
C(4)-H(4)	0.93	C(2)-C(3)-C(4)	119.2(4)	N(8)-C(34)-C(33)	123.3(6)
C(5)-C(6)	1.372(6)	C(2)-C(3)-H(3)	120.4	N(8)-C(34)-H(34)	118.4
C(5)-H(5)	0.93	C(4)-C(3)-H(3)	120.4	C(33)-C(34)-H(34)	118.4
C(6)-N(2)	1.338(6)	C(5)-C(4)-C(3)	118.8(4)	C(36)-C(35)-H(35A)	109.5
C(6)-N(3)	1.417(5)	C(5)-C(4)-H(4)	120.6	C(36)-C(35)-H(35B)	109.5
C(7)-N(3)	1.325(5)	C(3)-C(4)-H(4)	120.6	H(35A)-C(35)-H(35B)	109.5
C(7)-N(4)	1.392(5)	C(4)-C(5)-C(6)	118.9(4)	C(36)-C(35)-H(35C)	109.5
C(7)-S(1)	1.681(5)	C(4)-C(5)-H(5)	120.5	H(35A)-C(35)-H(35C)	109.5
C(8)-O(1)	1.231(5)	C(6)-C(5)-H(5)	120.5	H(35B)-C(35)-H(35C)	109.5
C(8)-N(4)	1.385(6)	N(2)-C(6)-C(5)	123.6(4)	N(9)-C(36)-C(35)	170.9(9)
C(8)-C(9)	1.485(7)	N(2)-C(6)-N(3)	118.6(4)	C(1)-N(1)-C(29)	110.9(5)
C(9)-C(10)	1.378(6)	C(5)-C(6)-N(3)	117.6(4)	C(1)-N(1)-C(15)	110.8(4)
C(9)-C(14)	1.395(7)	N(3)-C(7)-N(4)	115.1(4)	C(29)-N(1)-C(15)	112.5(5)
C(10)-C(11)	1.388(7)	N(3)-C(7)-S(1)	126.1(4)	C(1)-N(1)-Cd(1)	110.2(3)
C(10)-H(10)	0.93	N(4)-C(7)-S(1)	118.7(3)	C(29)-N(1)-Cd(1)	106.3(3)
C(11)-C(12)	1.370(8)	O(1)-C(8)-N(4)	121.5(4)	C(15)-N(1)-Cd(1)	106.0(3)
C(11)-H(11)	0.93	O(1)-C(8)-C(9)	121.3(5)	C(6)-N(2)-C(2)	117.0(4)
C(12)-C(13)	1.387(8)	N(4)-C(8)-C(9)	117.2(4)	C(6)-N(2)-Cd(1)	125.8(3)
C(12)-H(12)	0.93	C(10)-C(9)-C(14)	119.5(5)	C(2)-N(2)-Cd(1)	117.1(3)
C(13)-C(14)	1.383(7)	C(10)-C(9)-C(8)	124.4(5)	C(7)-N(3)-C(6)	130.7(4)
C(13)-H(13)	0.93	C(14)-C(9)-C(8)	116.1(4)	C(7)-N(3)-H(3A)	114.7
C(14)-H(14)	0.93	C(9)-C(10)-C(11)	120.0(5)	C(6)-N(3)-H(3A)	114.7
C(15)-N(1)	1.482(7)	C(9)-C(10)-H(10)	120	C(8)-N(4)-C(7)	126.8(4)
C(15)-C(16)	1.494(9)	C(11)-C(10)-H(10)	120	C(8)-N(4)-H(4A)	116.6
C(15)-H(15A)	0.97	C(12)-C(11)-C(10)	120.5(5)	C(7)-N(4)-H(4A)	116.6
C(15)-H(15B)	0.97	C(12)-C(11)-H(11)	119.8	C(16)-N(5)-C(20)	119.1(5)
C(16)-N(5)	1.334(7)	C(10)-C(11)-H(11)	119.8	C(16)-N(5)-Cd(1)	111.2(4)
C(16)-C(17)	1.399(9)	C(11)-C(12)-C(13)	120.2(5)	C(20)-N(5)-Cd(1)	126.5(4)
C(17)-C(18)	1.388(12)	C(11)-C(12)-H(12)	119.9	C(21)-N(6)-C(20)	134.0(5)
C(17)-H(17)	0.93	C(13)-C(12)-H(12)	119.9	C(21)-N(6)-H(6)	113
C(18)-C(19)	1.355(11)	C(14)-C(13)-C(12)	119.6(6)	C(20)-N(6)-H(6)	113
C(18)-H(18)	0.93	C(14)-C(13)-H(13)	120.2	C(22)-N(7)-C(21)	129.8(6)
C(19)-C(20)	1.400(8)	C(12)-C(13)-H(13)	120.2	C(22)-N(7)-H(7)	115.1
C(19)-H(19)	0.93	C(13)-C(14)-C(9)	120.3(5)	C(21)-N(7)-H(7)	115.1
C(20)-N(5)	1.351(8)	C(13)-C(14)-H(14)	119.8	C(34)-N(8)-C(30)	117.8(5)
C(20)-N(6)	1.396(8)	C(9)-C(14)-H(14)	119.8	C(34)-N(8)-Cd(1)	126.6(4)
C(21)-N(6)	1.320(7)	N(1)-C(15)-C(16)	113.0(5)	C(30)-N(8)-Cd(1)	115.1(4)
C(21)-N(7)	1.403(7)	N(1)-C(15)-H(15A)	109	C(7)-S(1)-Cd(1)	93.75(14)
C(21)-S(2)	1.663(5)	C(16)-C(15)-H(15A)	109	C(21)-S(2)-Cd(1)	106.7(2)
C(22)-O(2)	1.242(8)	N(1)-C(15)-H(15B)	109	N(2)-Cd(1)-N(8)	117.83(15)
C(22)-N(7)	1.385(7)	C(16)-C(15)-H(15B)	109	N(2)-Cd(1)-N(1)	71.50(13)
C(22)-C(23)	1.511(10)	H(15A)-C(15)-H(15B)	107.8	N(8)-Cd(1)-N(1)	70.20(16)
C(23)-C(28)	1.359(10)	N(5)-C(16)-C(17)	122.8(7)	N(2)-Cd(1)-N(5)	114.63(14)
C(23)-C(24)	1.416(8)	N(5)-C(16)-C(15)	118.0(5)	N(8)-Cd(1)-N(5)	99.55(16)
C(24)-C(25)	1.395(12)	C(17)-C(16)-C(15)	119.1(7)	N(1)-Cd(1)-N(5)	74.29(17)
C(24)-H(24)	0.93	C(18)-C(17)-C(16)	117.2(8)	N(2)-Cd(1)-S(2)	138.58(11)
C(25)-C(26)	1.352(14)	C(18)-C(17)-H(17)	121.4	N(8)-Cd(1)-S(2)	94.97(12)
C(25)-H(25)	0.93	C(16)-C(17)-H(17)	121.4	N(1)-Cd(1)-S(2)	148.19(10)

Appendix 3: Crystals data

C(26)-C(27)	1.365(10)	C(19)-C(18)-C(17)	120.5(7)	N(5)-Cd(1)-S(2)	81.03(13)
C(26)-H(26)	0.93	C(19)-C(18)-H(18)	119.8	N(2)-Cd(1)-S(1)	78.59(9)
C(27)-C(28)	1.394(10)	C(17)-C(18)-H(18)	119.8	N(8)-Cd(1)-S(1)	83.04(11)
C(27)-H(27)	0.93	C(18)-C(19)-C(20)	119.5(8)	N(1)-Cd(1)-S(1)	122.53(12)
C(28)-H(28)	0.93	C(18)-C(19)-H(19)	120.2	N(5)-Cd(1)-S(1)	162.33(13)
C(29)-N(1)	1.472(7)	C(20)-C(19)-H(19)	120.2	S(2)-Cd(1)-S(1)	81.33(4)
C(29)-C(30)	1.496(8)	N(5)-C(20)-N(6)	122.8(5)	O(6)-Cl(1)-O(3)	109.9(3)
C(29)-H(29A)	0.97	N(5)-C(20)-C(19)	120.8(7)	O(6)-Cl(1)-O(4)	109.2(3)
C(29)-H(29B)	0.97	N(6)-C(20)-C(19)	116.4(7)	O(3)-Cl(1)-O(4)	110.3(3)
C(30)-N(8)	1.353(7)	N(6)-C(21)-N(7)	114.5(5)	O(6)-Cl(1)-O(5)	109.5(2)
C(30)-C(31)	1.375(8)	N(6)-C(21)-S(2)	130.2(5)	O(3)-Cl(1)-O(5)	108.7(2)
C(31)-C(32)	1.364(9)	N(7)-C(21)-S(2)	115.3(4)	O(4)-Cl(1)-O(5)	109.2(3)
C(31)-H(31)	0.93	O(2)-C(22)-N(7)	118.3(8)	O(8)-Cl(2)-O(7)	108.5(3)
C(32)-C(33)	1.380(9)	O(2)-C(22)-C(23)	124.0(6)	O(8)-Cl(2)-O(10)	110.2(3)
C(32)-H(32)	0.93	N(7)-C(22)-C(23)	117.6(7)	O(7)-Cl(2)-O(10)	110.1(3)
C(33)-C(34)	1.370(9)	C(28)-C(23)-C(24)	122.5(8)	O(8)-Cl(2)-O(9)	109.2(2)
C(33)-H(33)	0.93	C(28)-C(23)-C(22)	123.7(6)	O(7)-Cl(2)-O(9)	109.3(2)
C(34)-N(8)	1.344(7)	C(24)-C(23)-C(22)	113.8(8)	O(10)-Cl(2)-O(9)	109.6(3)
C(34)-H(34)	0.93	C(25)-C(24)-C(23)	117.4(9)		
C(35)-C(36)	1.480(10)	C(25)-C(24)-H(24)	121.3		
C(35)-H(35A)	0.96	C(23)-C(24)-H(24)	121.3		
C(35)-H(35B)	0.96	C(26)-C(25)-C(24)	120.1(8)		
C(35)-H(35C)	0.96	C(26)-C(25)-H(25)	120		
C(36)-N(9)	1.100(8)	C(24)-C(25)-H(25)	119.9		
N(1)-Cd(1)	2.386(4)	C(25)-C(26)-C(27)	121.5(11)		
N(2)-Cd(1)	2.365(4)	C(25)-C(26)-H(26)	119.3		
N(3)-H(3A)	0.86	C(27)-C(26)-H(26)	119.3		
N(4)-H(4A)	0.86	C(26)-C(27)-C(28)	121.0(10)		
N(5)-Cd(1)	2.409(4)	C(26)-C(27)-H(27)	119.5		
N(6)-H(6)	0.86	C(28)-C(27)-H(27)	119.5		
N(7)-H(7)	0.86	C(23)-C(28)-C(27)	117.5(7)		
N(8)-Cd(1)	2.378(5)	C(23)-C(28)-H(28)	121.3		
S(1)-Cd(1)	2.7130(12)	C(27)-C(28)-H(28)	121.3		
S(2)-Cd(1)	2.5746(14)	N(1)-C(29)-C(30)	112.9(5)		
O(3)-Cl(1)	1.431(4)	N(1)-C(29)-H(29A)	109		
O(4)-Cl(1)	1.444(4)	C(30)-C(29)-H(29A)	109		
O(5)-Cl(1)	1.450(3)	N(1)-C(29)-H(29B)	109		
O(6)-Cl(1)	1.410(4)	C(30)-C(29)-H(29B)	109		
O(7)-Cl(2)	1.429(4)	H(29A)-C(29)-H(29B)	107.8		
O(8)-Cl(2)	1.429(4)	N(8)-C(30)-C(31)	121.1(6)		
O(9)-Cl(2)	1.448(4)	N(8)-C(30)-C(29)	116.2(5)		
O(10)-Cl(2)	1.435(4)	C(31)-C(30)-C(29)	122.7(6)		

Appendix 3: Crystals data

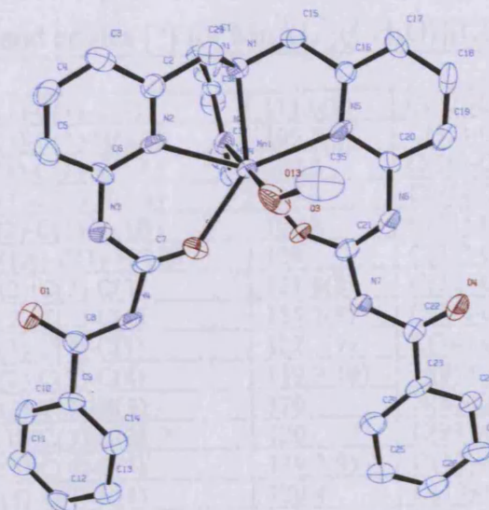


Table F.1: Crystal data and structure refinement for $\text{Mn}^{\text{II}}(\text{L}^*)(\text{CH}_3\text{O})[\text{ClO}_4]_2$. **3.7**

Identification code	aja0830	
Empirical formula	C ₃₅ H ₃₃ Cl ₂ Mn N ₈ O ₁₃	
Formula weight	899.53	
Temperature	150(2) K	
Wavelength	0.71073 Å	
Crystal system	Monoclinic	
Space group	P21	
Unit cell dimensions	a = 10.3840(5) Å	$\alpha = 90^\circ$.
	b = 18.6250(12) Å	$\beta = 113.785(3)^\circ$.
	c = 10.5820(7) Å	$\gamma = 90^\circ$.
Volume	1872.8(2) Å ³	
Z	2	
Density (calculated)	1.595 Mg/m ³	
Absorption coefficient	0.574 mm ⁻¹	
F(000)	924	
Crystal size	0.20 x 0.18 x 0.05 mm ³	
Theta range for data collection	2.14 to 24.43°.	
Index ranges	-12 ≤ h ≤ 12, -20 ≤ k ≤ 21, -12 ≤ l ≤ 12	
Reflections collected	5390	
Independent reflections	5390 [R(int) = 0.0000]	
Completeness to theta = 24.43°	99.4 %	
Max. and min. transmission	0.9718 and 0.8938	
Refinement method	Full-matrix least-squares on F ²	
Data / restraints / parameters	5390 / 1 / 533	
Goodness-of-fit on F ²	1.099	
Final R indices [I > 2σ(I)]	R1 = 0.0874, wR2 = 0.1444	
R indices (all data)	R1 = 0.1286, wR2 = 0.1594	
Absolute structure parameter	-0.02(4)	
Largest diff. peak and hole	0.534 and -0.374 e.Å ⁻³	

Appendix 3: Crystals data

Table F.2: Bond lengths [Å] and angles [°] for Mn^{II}(L^{*})(CH₃O)[ClO₄]₂. 3.7

C(1)-N(1)	1.471(12)	N(1)-C(1)-C(2)	111.6(8)	C(32)-C(31)-C(30)	121.0(9)
C(1)-C(2)	1.489(12)	N(1)-C(1)-H(1A)	109.3	C(32)-C(31)-H(31)	119.5
C(1)-H(1A)	0.99	C(2)-C(1)-H(1A)	109.3	C(30)-C(31)-H(31)	119.5
C(1)-H(1B)	0.99	N(1)-C(1)-H(1B)	109.3	C(31)-C(32)-C(33)	119.3(10)
C(2)-N(2)	1.365(11)	C(2)-C(1)-H(1B)	109.3	C(31)-C(32)-H(32)	120.3
C(2)-C(3)	1.382(13)	H(1A)-C(1)-H(1B)	108	C(33)-C(32)-H(32)	120.3
C(3)-C(4)	1.383(14)	N(2)-C(2)-C(3)	121.6(8)	C(32)-C(33)-C(34)	119.2(9)
C(3)-H(3)	0.95	N(2)-C(2)-C(1)	115.7(8)	C(32)-C(33)-H(33)	120.4
C(4)-C(5)	1.371(14)	C(3)-C(2)-C(1)	122.7(9)	C(34)-C(33)-H(33)	120.4
C(4)-H(4)	0.95	C(2)-C(3)-C(4)	119.9(10)	N(8)-C(34)-C(33)	122.0(9)
C(5)-C(6)	1.397(12)	C(2)-C(3)-H(3)	120	N(8)-C(34)-H(34)	119
C(5)-H(5)	0.95	C(4)-C(3)-H(3)	120	C(33)-C(34)-H(34)	119
C(6)-N(2)	1.326(11)	C(5)-C(4)-C(3)	119.2(9)	O(13)-C(35)-H(35A)	109.5
C(6)-N(3)	1.401(11)	C(5)-C(4)-H(4)	120.4	O(13)-C(35)-H(35B)	109.5
C(7)-O(2)	1.213(11)	C(3)-C(4)-H(4)	120.4	H(35A)-C(35)-H(35B)	109.5
C(7)-N(3)	1.359(11)	C(4)-C(5)-C(6)	117.7(9)	O(13)-C(35)-H(35C)	109.5
C(7)-N(4)	1.401(11)	C(4)-C(5)-H(5)	121.1	H(35A)-C(35)-H(35C)	109.5
C(8)-O(1)	1.229(10)	C(6)-C(5)-H(5)	121.1	H(35B)-C(35)-H(35C)	109.5
C(8)-N(4)	1.361(11)	N(2)-C(6)-C(5)	124.4(9)	C(15)-N(1)-C(1)	111.2(7)
C(8)-C(9)	1.514(13)	N(2)-C(6)-N(3)	119.9(8)	C(15)-N(1)-C(29)	109.5(7)
C(9)-C(10)	1.357(12)	C(5)-C(6)-N(3)	115.6(8)	C(1)-N(1)-C(29)	111.8(7)
C(9)-C(14)	1.398(13)	O(2)-C(7)-N(3)	126.4(9)	C(15)-N(1)-Mn(1)	112.2(5)
C(10)-C(11)	1.377(13)	O(2)-C(7)-N(4)	119.2(8)	C(1)-N(1)-Mn(1)	104.8(5)
C(10)-H(10)	0.95	N(3)-C(7)-N(4)	114.3(8)	C(29)-N(1)-Mn(1)	107.3(5)
C(11)-C(12)	1.369(14)	O(1)-C(8)-N(4)	122.6(9)	C(6)-N(2)-C(2)	117.2(8)
C(11)-H(11)	0.95	O(1)-C(8)-C(9)	120.7(8)	C(6)-N(2)-Mn(1)	131.1(6)
C(12)-C(13)	1.375(15)	N(4)-C(8)-C(9)	116.7(8)	C(2)-N(2)-Mn(1)	111.5(6)
C(12)-H(12)	0.95	C(10)-C(9)-C(14)	120.7(9)	C(7)-N(3)-C(6)	127.8(8)
C(13)-C(14)	1.379(14)	C(10)-C(9)-C(8)	117.4(8)	C(7)-N(3)-H(3A)	116.1
C(13)-H(13)	0.95	C(14)-C(9)-C(8)	121.9(9)	C(6)-N(3)-H(3A)	116.1
C(14)-H(14)	0.95	C(9)-C(10)-C(11)	120.5(9)	C(8)-N(4)-C(7)	127.8(8)
C(15)-N(1)	1.469(11)	C(9)-C(10)-H(10)	119.7	C(8)-N(4)-H(4A)	116.1
C(15)-C(16)	1.514(12)	C(11)-C(10)-H(10)	119.7	C(7)-N(4)-H(4A)	116.1
C(15)-H(15A)	0.99	C(12)-C(11)-C(10)	120.1(10)	C(20)-N(5)-C(16)	116.6(8)
C(15)-H(15B)	0.99	C(12)-C(11)-H(11)	119.9	C(20)-N(5)-Mn(1)	125.7(6)
C(16)-N(5)	1.368(11)	C(10)-C(11)-H(11)	119.9	C(16)-N(5)-Mn(1)	115.5(5)
C(16)-C(17)	1.379(12)	C(11)-C(12)-C(13)	119.2(10)	C(21)-N(6)-C(20)	126.7(7)
C(17)-C(18)	1.386(13)	C(11)-C(12)-H(12)	120.4	C(21)-N(6)-H(6A)	116.7
C(17)-H(17)	0.95	C(13)-C(12)-H(12)	120.4	C(20)-N(6)-H(6A)	116.7
C(18)-C(19)	1.360(13)	C(12)-C(13)-C(14)	121.8(11)	C(22)-N(7)-C(21)	127.1(8)
C(18)-H(18)	0.95	C(12)-C(13)-H(13)	119.1	C(22)-N(7)-H(7)	116.4
C(19)-C(20)	1.393(13)	C(14)-C(13)-H(13)	119.1	C(21)-N(7)-H(7)	116.4
C(19)-H(19)	0.95	C(13)-C(14)-C(9)	117.6(10)	C(34)-N(8)-C(30)	118.4(8)
C(20)-N(5)	1.335(10)	C(13)-C(14)-H(14)	121.2	C(34)-N(8)-Mn(1)	124.9(6)
C(20)-N(6)	1.402(11)	C(9)-C(14)-H(14)	121.2	C(30)-N(8)-Mn(1)	115.8(6)
C(21)-O(3)	1.203(10)	N(1)-C(15)-C(16)	114.3(7)	O(12)-Cl(1)-O(11)	108.2(4)
C(21)-N(6)	1.329(12)	N(1)-C(15)-H(15A)	108.7	O(12)-Cl(1)-O(9)	108.8(5)
C(21)-N(7)	1.420(12)	C(16)-C(15)-H(15A)	108.7	O(11)-Cl(1)-O(9)	112.3(5)
C(22)-O(4)	1.230(11)	N(1)-C(15)-H(15B)	108.7	O(12)-Cl(1)-O(10)	109.9(5)
C(22)-N(7)	1.390(11)	C(16)-C(15)-H(15B)	108.7	O(11)-Cl(1)-O(10)	108.3(5)
C(22)-C(23)	1.496(13)	H(15A)-C(15)-H(15B)	107.6	O(9)-Cl(1)-O(10)	109.3(4)
C(23)-C(28)	1.381(12)	N(5)-C(16)-C(17)	123.7(8)	O(8)-Cl(2)-O(5)	113.8(6)
C(23)-C(24)	1.402(13)	N(5)-C(16)-C(15)	114.2(7)	O(8)-Cl(2)-O(6)	109.5(7)
C(24)-C(25)	1.366(13)	C(17)-C(16)-C(15)	121.7(8)	O(5)-Cl(2)-O(6)	107.6(6)
C(24)-H(24)	0.95	C(16)-C(17)-C(18)	117.8(9)	O(8)-Cl(2)-O(7)	110.7(5)
C(25)-C(26)	1.399(14)	C(16)-C(17)-H(17)	121.1	O(5)-Cl(2)-O(7)	108.6(5)
C(25)-H(25)	0.95	C(18)-C(17)-H(17)	121.1	O(6)-Cl(2)-O(7)	106.3(5)

Appendix 3: Crystals data

C(26)-C(27)	1.378(14)	C(19)-C(18)-C(17)	119.3(9)	C(7)-O(2)-Mn(1)	139.4(6)
C(26)-H(26)	0.95	C(19)-C(18)-H(18)	120.4	C(21)-O(3)-Mn(1)	128.1(6)
C(27)-C(28)	1.370(13)	C(17)-C(18)-H(18)	120.4	C(35)-O(13)-Mn(1)	135.5(7)
C(27)-H(27)	0.95	C(18)-C(19)-C(20)	119.9(9)	O(2)-Mn(1)-O(13)	82.8(2)
C(28)-H(28)	0.95	C(18)-C(19)-H(19)	120	O(2)-Mn(1)-O(3)	75.2(2)
C(29)-C(30)	1.475(14)	C(20)-C(19)-H(19)	120	O(13)-Mn(1)-O(3)	92.5(3)
C(29)-N(1)	1.478(11)	N(5)-C(20)-C(19)	122.4(8)	O(2)-Mn(1)-N(8)	96.8(3)
C(29)-H(29A)	0.99	N(5)-C(20)-N(6)	120.6(8)	O(13)-Mn(1)-N(8)	177.5(3)
C(29)-H(29B)	0.99	C(19)-C(20)-N(6)	117.0(8)	O(3)-Mn(1)-N(8)	85.0(2)
C(30)-N(8)	1.370(10)	O(3)-C(21)-N(6)	127.3(9)	O(2)-Mn(1)-N(1)	141.6(2)
C(30)-C(31)	1.401(13)	O(3)-C(21)-N(7)	117.6(9)	O(13)-Mn(1)-N(1)	107.4(3)
C(31)-C(32)	1.335(14)	N(6)-C(21)-N(7)	115.1(8)	O(3)-Mn(1)-N(1)	138.7(2)
C(31)-H(31)	0.95	O(4)-C(22)-N(7)	122.0(9)	N(8)-Mn(1)-N(1)	74.4(3)
C(32)-C(33)	1.375(14)	O(4)-C(22)-C(23)	121.4(8)	O(2)-Mn(1)-N(5)	144.3(2)
C(32)-H(32)	0.95	N(7)-C(22)-C(23)	116.6(9)	O(13)-Mn(1)-N(5)	79.3(2)
C(33)-C(34)	1.392(14)	C(28)-C(23)-C(24)	119.6(9)	O(3)-Mn(1)-N(5)	75.0(2)
C(33)-H(33)	0.95	C(28)-C(23)-C(22)	116.3(9)	N(8)-Mn(1)-N(5)	99.8(2)
C(34)-N(8)	1.339(11)	C(24)-C(23)-C(22)	124.0(9)	N(1)-Mn(1)-N(5)	73.8(2)
C(34)-H(34)	0.95	C(25)-C(24)-C(23)	119.9(10)	O(2)-Mn(1)-N(2)	73.8(2)
C(35)-O(13)	1.373(15)	C(25)-C(24)-H(24)	120.1	O(13)-Mn(1)-N(2)	83.6(3)
C(35)-H(35A)	0.98	C(23)-C(24)-H(24)	120.1	O(3)-Mn(1)-N(2)	149.0(2)
C(35)-H(35B)	0.98	C(24)-C(25)-C(26)	119.9(10)	N(8)-Mn(1)-N(2)	98.6(2)
C(35)-H(35C)	0.98	C(24)-C(25)-H(25)	120	N(1)-Mn(1)-N(2)	70.8(2)
N(1)-Mn(1)	2.333(7)	C(26)-C(25)-H(25)	120	N(5)-Mn(1)-N(2)	133.5(3)
N(2)-Mn(1)	2.454(7)	C(27)-C(26)-C(25)	120.0(10)		
N(3)-H(3A)	0.88	C(27)-C(26)-H(26)	120		
N(4)-H(4A)	0.88	C(25)-C(26)-H(26)	120		
N(5)-Mn(1)	2.340(7)	C(28)-C(27)-C(26)	120.0(11)		
N(6)-H(6A)	0.88	C(28)-C(27)-H(27)	120		
N(7)-H(7)	0.88	C(26)-C(27)-H(27)	120		
N(8)-Mn(1)	2.247(7)	C(27)-C(28)-C(23)	120.5(10)		
Cl(1)-O(12)	1.419(7)	C(27)-C(28)-H(28)	119.7		
Cl(1)-O(11)	1.420(7)	C(23)-C(28)-H(28)	119.7		
Cl(1)-O(9)	1.425(7)	C(30)-C(29)-N(1)	111.7(7)		
Cl(1)-O(10)	1.452(7)	C(30)-C(29)-H(29A)	109.3		
Cl(2)-O(8)	1.366(9)	N(1)-C(29)-H(29A)	109.3		
Cl(2)-O(5)	1.404(7)	C(30)-C(29)-H(29B)	109.3		
Cl(2)-O(6)	1.421(9)	N(1)-C(29)-H(29B)	109.3		
Cl(2)-O(7)	1.437(7)	H(29A)-C(29)-H(29B)	107.9		
O(2)-Mn(1)	2.184(6)	N(8)-C(30)-C(31)	120.0(9)		
O(3)-Mn(1)	2.228(6)	N(8)-C(30)-C(29)	116.1(8)		
O(13)-Mn(1)	2.212(7)	C(31)-C(30)-C(29)	123.6(8)		

Appendix 3: Crystals data

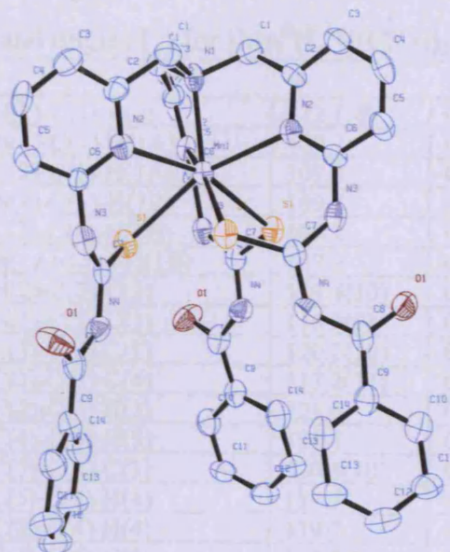


Table L.1: Crystal data and structure refinement for $[\text{Mn}^{\text{II}}(\text{L}^3)][\text{ClO}_4]_2 \cdot \text{CH}_3\text{CN}$. 4.1

Identification code	aja0907	
Empirical formula	C ₄₄ H ₃₉ Cl ₂ Mn N ₁₁ O ₁₁ S ₃	
Formula weight	1119.88	
Temperature	293(2) K	
Wavelength	0.71073 Å	
Crystal system	Trigonal	
Space group	R-3:h	
Unit cell dimensions	a = 13.7370(4) Å	$\alpha = 90^\circ$.
	b = 13.7370(13) Å	$\beta = 90^\circ$.
	c = 44.1110(15) Å	$\gamma = 120^\circ$.
Volume	7208.8(8) Å ³	
Z	6	
Density (calculated)	1.548 Mg/m ³	
Absorption coefficient	0.589 mm ⁻¹	
F(000)	3450	
Crystal size	0.20 x 0.20 x 0.02 mm ³	
Theta range for data collection	2.52 to 22.24°.	
Index ranges	-13 ≤ h ≤ 14, -14 ≤ k ≤ 14, -41 ≤ l ≤ 46	
Reflections collected	6951	
Independent reflections	2027 [R(int) = 0.1438]	
Completeness to theta = 22.24°	99.2 %	
Absorption correction	Empirical	
Max. and min. transmission	0.9883 and 0.8913	
Refinement method	Full-matrix least-squares on F ²	
Data / restraints / parameters	2027 / 3 / 217	
Goodness-of-fit on F ²	1.052	
Final R indices [I > 2σ(I)]	R1 = 0.0919, wR2 = 0.1808	
R indices (all data)	R1 = 0.1477, wR2 = 0.2051	
Largest diff. peak and hole	1.116 and -0.999 e.Å ⁻³	

Appendix 3: Crystals data

Table L.2: Bond lengths [Å] and angles [°] for $[\text{Mn}^{\text{II}}(\text{L}^3)][\text{ClO}_4]_2 \cdot \text{CH}_3\text{CN}$. 4.1

C(1)-N(1)	1.486(11)	N(1)-C(1)-C(2)	112.1(8)	C(1)#4-N(1)-C(1)	109.0(7)
C(1)-C(2)	1.503(14)	N(1)-C(1)-H(1A)	109.2	C(1)#3-N(1)-Mn(1)	109.9(7)
C(1)-H(1A)	0.97	C(2)-C(1)-H(1A)	109.2	C(1)#4-N(1)-Mn(1)	109.9(7)
C(1)-H(1B)	0.97	N(1)-C(1)-H(1B)	109.2	C(1)-N(1)-Mn(1)	109.9(7)
C(2)-N(2)	1.342(12)	C(2)-C(1)-H(1B)	109.2	C(2)-N(2)-C(6)	116.8(8)
C(2)-C(3)	1.378(14)	H(1A)-C(1)-H(1B)	107.9	C(2)-N(2)-Mn(1)	113.0(6)
C(3)-C(4)	1.406(15)	N(2)-C(2)-C(3)	123.4(10)	C(6)-N(2)-Mn(1)	129.8(7)
C(3)-H(3)	0.93	N(2)-C(2)-C(1)	116.3(9)	C(7)-N(3)-C(6)	130.4(9)
C(4)-C(5)	1.365(15)	C(3)-C(2)-C(1)	120.2(10)	C(7)-N(3)-H(3A)	114.8
C(4)-H(4)	0.93	C(2)-C(3)-C(4)	117.2(11)	C(6)-N(3)-H(3A)	114.8
C(5)-C(6)	1.369(13)	C(2)-C(3)-H(3)	121.4	C(7)-N(4)-C(8)	128.6(9)
C(5)-H(5)	0.93	C(4)-C(3)-H(3)	121.4	C(7)-N(4)-H(4A)	115.7
C(6)-N(2)	1.346(12)	C(5)-C(4)-C(3)	120.6(10)	C(8)-N(4)-H(4A)	115.7
C(6)-N(3)	1.408(13)	C(5)-C(4)-H(4)	119.7	C(15)-N(5)-C(15)#1	79(2)
C(7)-N(3)	1.327(12)	C(3)-C(4)-H(4)	119.7	C(15)-N(5)-C(15)#2	79(2)
C(7)-N(4)	1.358(13)	C(4)-C(5)-C(6)	117.3(10)	C(15)#1-N(5)-C(15)#2	79(2)
C(7)-S(1)	1.666(10)	C(4)-C(5)-H(5)	121.4	C(7)-S(1)-Mn(1)	104.1(3)
C(8)-O(1)	1.237(12)	C(6)-C(5)-H(5)	121.4	N(1)-Mn(1)-N(2)#4	72.6(2)
C(8)-N(4)	1.398(13)	N(2)-C(6)-C(5)	124.7(10)	N(1)-Mn(1)-N(2)#3	72.6(2)
C(8)-C(9)	1.476(16)	N(2)-C(6)-N(3)	118.5(8)	N(2)#4-Mn(1)-N(2)#3	111.50(19)
C(9)-C(14)	1.380(14)	C(5)-C(6)-N(3)	116.8(9)	N(1)-Mn(1)-N(2)	72.6(2)
C(9)-C(10)	1.389(14)	N(3)-C(7)-N(4)	118.6(9)	N(2)#4-Mn(1)-N(2)	111.47(19)
C(10)-C(11)	1.362(16)	N(3)-C(7)-S(1)	123.5(9)	N(2)#3-Mn(1)-N(2)	111.46(19)
C(10)-H(10)	0.93	N(4)-C(7)-S(1)	117.9(8)	N(1)-Mn(1)-S(1)#4	125.77(7)
C(11)-C(12)	1.379(15)	O(1)-C(8)-N(4)	119.1(11)	N(2)#4-Mn(1)-S(1)#4	76.25(19)
C(11)-H(11)	0.93	O(1)-C(8)-C(9)	123.5(10)	N(2)#3-Mn(1)-S(1)#4	79.27(19)
C(12)-C(13)	1.379(15)	N(4)-C(8)-C(9)	117.4(9)	N(2)-Mn(1)-S(1)#4	161.5(2)
C(12)-H(12)	0.93	C(14)-C(9)-C(10)	119.0(11)	N(1)-Mn(1)-S(1)	125.76(7)
C(13)-C(14)	1.377(16)	C(14)-C(9)-C(8)	123.7(10)	N(2)#4-Mn(1)-S(1)	79.26(19)
C(13)-H(13)	0.93	C(10)-C(9)-C(8)	117.2(10)	N(2)#3-Mn(1)-S(1)	161.5(2)
C(14)-H(14)	0.93	C(11)-C(10)-C(9)	120.6(11)	N(2)-Mn(1)-S(1)	76.21(19)
C(15)-N(5)	1.0108(11)	C(11)-C(10)-H(10)	119.7	S(1)#4-Mn(1)-S(1)	89.30(10)
C(15)-C(15)#1	1.29(3)	C(9)-C(10)-H(10)	119.7	N(1)-Mn(1)-S(1)#3	125.75(7)
C(15)-C(15)#2	1.29(3)	C(10)-C(11)-C(12)	120.3(11)	N(2)#4-Mn(1)-S(1)#3	161.5(2)
C(15)-C(16)	1.5023(11)	C(10)-C(11)-H(11)	119.8	N(2)#3-Mn(1)-S(1)#3	76.22(19)
C(16)-H(16A)	0.96	C(12)-C(11)-H(11)	119.8	N(2)-Mn(1)-S(1)#3	79.23(19)
C(16)-H(16B)	0.96	C(13)-C(12)-C(11)	119.6(12)	S(1)#4-Mn(1)-S(1)#3	89.30(10)
C(16)-H(16C)	0.96	C(13)-C(12)-H(12)	120.2	S(1)-Mn(1)-S(1)#3	89.28(10)
N(1)-C(1)#3	1.484(11)	C(11)-C(12)-H(12)	120.2	O(3)-Cl(1)-O(2)#3	111.0(4)
N(1)-C(1)#4	1.485(11)	C(14)-C(13)-C(12)	120.1(11)	O(3)-Cl(1)-O(2)#4	111.0(4)
N(1)-Mn(1)	2.280(15)	C(14)-C(13)-H(13)	119.9	O(2)#3-Cl(1)-O(2)#4	107.9(4)
N(2)-Mn(1)	2.438(8)	C(12)-C(13)-H(13)	119.9	O(3)-Cl(1)-O(2)	111.0(4)
N(3)-H(3A)	0.86	C(13)-C(14)-C(9)	120.3(11)	O(2)#3-Cl(1)-O(2)	107.9(4)
N(4)-H(4A)	0.86	C(13)-C(14)-H(14)	119.9	O(2)#4-Cl(1)-O(2)	107.9(4)
N(5)-C(15)#1	1.0108(11)	C(9)-C(14)-H(14)	119.9	O(4)-Cl(2)-O(5)	107.9(6)
N(5)-C(15)#2	1.0108(11)	N(5)-C(15)-C(15)#1	50.3(12)	O(4)-Cl(2)-O(5)#2	107.9(6)
S(1)-Mn(1)	2.618(2)	N(5)-C(15)-C(15)#2	50.3(12)	O(5)-Cl(2)-O(5)#2	111.0(5)
O(2)-Cl(1)	1.459(7)	C(15)#1-C(15)-C(15)#2	60.000(17)	O(4)-Cl(2)-O(5)#1	107.9(6)
O(3)-Cl(1)	1.389(15)	N(5)-C(15)-C(16)	173.6(16)	O(5)-Cl(2)-O(5)#1	111.0(5)
O(4)-Cl(2)	1.33(2)	C(15)#1-C(15)-C(16)	125(6)	O(5)#2-Cl(2)-O(5)#1	111.0(5)
O(5)-Cl(2)	1.414(9)	C(15)#2-C(15)-C(16)	124(6)		
Mn(1)-N(2)#4	2.437(8)	C(15)-C(16)-H(16A)	109.5		
Mn(1)-N(2)#3	2.437(8)	C(15)-C(16)-H(16B)	109.5		
Mn(1)-S(1)#4	2.617(2)	H(16A)-C(16)-H(16B)	109.5		
Mn(1)-S(1)#3	2.618(2)	C(15)-C(16)-H(16C)	109.5		
Cl(1)-O(2)#3	1.458(7)	H(16A)-C(16)-H(16C)	109.5		
Cl(1)-O(2)#4	1.458(7)	H(16B)-C(16)-H(16C)	109.5		

Appendix 3: Crystals data

Cl(2)-O(5)#2	1.414(9)	C(1)#3-N(1)-C(1)#4	109.1(7)		
Cl(2)-O(5)#1	1.414(9)	C(1)#3-N(1)-C(1)	109.0(7)		

Symmetry transformations used to generate equivalent atoms:

#1 -y+1,x-y+1,z #2 -x+y,-x+1,z #3 -x+y+1,-x+1,z

#4 -y+1,x-y,z

Appendix 3: Crystals data

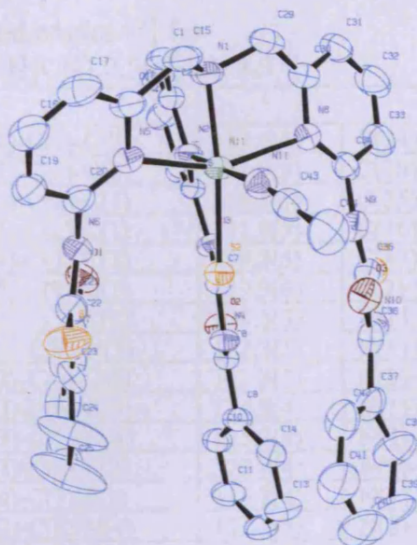


Table M.1: Crystal data and structure refinement for $[\text{Ni}^{\text{II}}(\text{L}^3)(\text{CH}_3\text{CN})][\text{ClO}_4]_2 \cdot 3.5(\text{CH}_3\text{CN}) \cdot 0.5(\text{H}_2\text{O})$. **4.3**

Identification code	aja0821	
Empirical formula	C51 H50.50 Cl2 N14.50 Ni O11.50 S3	
Formula weight	1276.35	
Temperature	293(2) K	
Wavelength	0.71073 Å	
Crystal system	Triclinic	
Space group	P-1	
Unit cell dimensions	$a = 13.8450(5)$ Å	$\alpha = 107.831(2)^\circ$
	$b = 14.6430(5)$ Å	$\beta = 97.828(2)^\circ$
	$c = 15.8030(6)$ Å	$\gamma = 94.342(2)^\circ$
Volume	$2997.95(19)$ Å ³	
Z	2	
Density (calculated)	1.414 Mg/m ³	
Absorption coefficient	0.587 mm ⁻¹	
F(000)	1320	
Crystal size	0.25 x 0.15 x 0.10 mm ³	
Theta range for data collection	2.92 to 27.57°	
Index ranges	-18 ≤ h ≤ 17, -18 ≤ k ≤ 18, -20 ≤ l ≤ 20	
Reflections collected	25225	
Independent reflections	13501 [R(int) = 0.1043]	
Completeness to theta = 27.57°	97.5 %	
Absorption correction	Empirical	
Max. and min. transmission	0.9436 and 0.8671	
Refinement method	Full-matrix least-squares on F ²	
Data / restraints / parameters	13501 / 186 / 836	
Goodness-of-fit on F ²	1.027	
Final R indices [I > 2σ(I)]	R1 = 0.0898, wR2 = 0.1973	
R indices (all data)	R1 = 0.1911, wR2 = 0.2437	
Largest diff. peak and hole	0.586 and -0.477 e.Å ⁻³	

Appendix 3: Crystals data

Table M.2: Bond lengths [Å] and angles [°] for
 $[\text{Ni}^{\text{II}}(\text{L}^3)(\text{CH}_3\text{CN})][\text{ClO}_4]_2 \cdot 3.5(\text{CH}_3\text{CN}) \cdot 0.5(\text{H}_2\text{O}) \cdot 4.3$

C(1)-N(1)	1.483(7)	N(1)-C(1)-C(2)	112.5(4)	C(34)-N(8)-Ni(1)	129.4(3)
C(1)-C(2)	1.495(7)	N(2)-C(2)-C(3)	121.9(5)	C(30)-N(8)-Ni(1)	107.1(3)
C(2)-N(2)	1.367(6)	N(2)-C(2)-C(1)	116.1(5)	C(35)-N(9)-C(34)	129.7(5)
C(2)-C(3)	1.382(8)	C(3)-C(2)-C(1)	121.9(5)	C(36)-N(10)-C(35)	127.9(4)
C(3)-C(4)	1.372(8)	C(4)-C(3)-C(2)	119.3(5)	C(43)-N(11)-Ni(1)	165.7(4)
C(4)-C(5)	1.359(8)	C(5)-C(4)-C(3)	119.9(6)	C(7)-S(2)-Ni(1)	107.28(18)
C(5)-C(6)	1.410(7)	C(4)-C(5)-C(6)	118.4(5)	N(11)-Ni(1)-N(2)	173.35(16)
C(6)-N(2)	1.325(6)	N(2)-C(6)-N(3)	122.3(5)	N(11)-Ni(1)-N(1)	97.44(18)
C(6)-N(3)	1.391(6)	N(2)-C(6)-C(5)	122.8(5)	N(2)-Ni(1)-N(1)	84.26(17)
C(7)-N(3)	1.327(6)	N(3)-C(6)-C(5)	114.9(4)	N(11)-Ni(1)-N(5)	86.57(17)
C(7)-N(4)	1.400(6)	N(3)-C(7)-N(4)	115.2(4)	N(2)-Ni(1)-N(5)	100.08(16)
C(7)-S(2)	1.672(5)	N(3)-C(7)-S(2)	129.0(4)	N(1)-Ni(1)-N(5)	76.70(16)
C(8)-O(2)	1.219(6)	N(4)-C(7)-S(2)	115.8(4)	N(11)-Ni(1)-N(8)	89.48(17)
C(8)-N(4)	1.392(6)	O(2)-C(8)-N(4)	121.8(5)	N(2)-Ni(1)-N(8)	84.46(15)
C(8)-C(9)	1.481(7)	O(2)-C(8)-C(9)	122.7(5)	N(1)-Ni(1)-N(8)	80.28(16)
C(9)-C(14)	1.390(8)	N(4)-C(8)-C(9)	115.5(5)	N(5)-Ni(1)-N(8)	155.91(16)
C(9)-C(10)	1.408(7)	C(14)-C(9)-C(10)	118.6(5)	N(11)-Ni(1)-S(2)	86.11(13)
C(10)-C(11)	1.364(7)	C(14)-C(9)-C(8)	124.1(5)	N(2)-Ni(1)-S(2)	92.72(11)
C(11)-C(12)	1.372(9)	C(10)-C(9)-C(8)	117.0(5)	N(1)-Ni(1)-S(2)	174.24(13)
C(12)-C(13)	1.378(8)	C(11)-C(10)-C(9)	120.2(6)	N(5)-Ni(1)-S(2)	99.06(12)
C(13)-C(14)	1.378(8)	C(10)-C(11)-C(12)	120.4(5)	N(8)-Ni(1)-S(2)	104.36(11)
C(15)-N(1)	1.469(7)	C(11)-C(12)-C(13)	120.7(6)	N(12)-C(45)-C(46)	178.8(8)
C(15)-C(16)	1.515(8)	C(12)-C(13)-C(14)	119.6(6)	N(13)-C(47)-C(48)	177.7(9)
C(16)-N(5)	1.353(6)	C(13)-C(14)-C(9)	120.5(5)	N(14)-C(49)-C(50)	162.7(18)
C(16)-C(17)	1.373(7)	N(1)-C(15)-C(16)	109.6(4)	N(15)-C(51)-C(52)	176(2)
C(17)-C(18)	1.362(8)	N(5)-C(16)-C(17)	122.1(5)	N(15)-C(51)-C(52)#1	148.1(17)
C(18)-C(19)	1.382(8)	N(5)-C(16)-C(15)	116.5(4)	C(52)-C(51)-C(52)#1	29.7(14)
C(19)-C(20)	1.364(7)	C(17)-C(16)-C(15)	121.5(5)	N(16)-C(53)-C(54)	166(3)
C(20)-N(5)	1.350(6)	C(18)-C(17)-C(16)	120.1(5)	O(5)-Cl(1)-O(7)	112.5(4)
C(20)-N(6)	1.414(6)	C(17)-C(18)-C(19)	118.4(5)	O(5)-Cl(1)-O(4)	110.0(3)
C(21)-N(6)	1.338(7)	C(20)-C(19)-C(18)	119.4(5)	O(7)-Cl(1)-O(4)	109.0(3)
C(21)-N(7)	1.386(7)	N(5)-C(20)-C(19)	122.7(5)	O(5)-Cl(1)-O(6)	108.4(4)
C(21)-S(1)	1.659(6)	N(5)-C(20)-N(6)	115.5(4)	O(7)-Cl(1)-O(6)	107.6(3)
C(22)-O(1)	1.228(6)	C(19)-C(20)-N(6)	121.7(5)	O(4)-Cl(1)-O(6)	109.3(3)
C(22)-N(7)	1.388(7)	N(6)-C(21)-N(7)	115.4(5)	O(10)-Cl(2)-O(8)	125.4(11)
C(22)-C(23)	1.511(8)	N(6)-C(21)-S(1)	126.2(4)	O(10)-Cl(2)-O(9)	108.7(10)
C(23)-C(24)	1.319(11)	N(7)-C(21)-S(1)	118.4(4)	O(8)-Cl(2)-O(9)	95.5(10)
C(23)-C(28)	1.353(9)	O(1)-C(22)-N(7)	122.4(5)	O(10)-Cl(2)-O(11)	114.7(11)
C(24)-C(25)	1.388(11)	O(1)-C(22)-C(23)	121.8(5)	O(8)-Cl(2)-O(11)	103.5(12)
C(25)-C(26)	1.268(13)	N(7)-C(22)-C(23)	115.8(5)	O(9)-Cl(2)-O(11)	106.2(9)
C(26)-C(27)	1.329(13)	C(24)-C(23)-C(28)	117.7(6)		
C(27)-C(28)	1.425(11)	C(24)-C(23)-C(22)	124.9(6)		
C(29)-C(30)	1.476(7)	C(28)-C(23)-C(22)	117.4(6)		
C(29)-N(1)	1.482(7)	C(23)-C(24)-C(25)	122.8(9)		
C(30)-N(8)	1.367(7)	C(26)-C(25)-C(24)	120.1(11)		
C(30)-C(31)	1.374(8)	C(25)-C(26)-C(27)	120.6(9)		
C(31)-C(32)	1.377(8)	C(26)-C(27)-C(28)	120.4(9)		
C(32)-C(33)	1.379(9)	C(23)-C(28)-C(27)	118.2(8)		
C(33)-C(34)	1.384(8)	C(30)-C(29)-N(1)	111.6(4)		
C(34)-N(8)	1.316(6)	N(8)-C(30)-C(31)	121.5(5)		
C(34)-N(9)	1.410(7)	N(8)-C(30)-C(29)	115.3(5)		
C(35)-N(9)	1.343(6)	C(31)-C(30)-C(29)	122.9(5)		
C(35)-N(10)	1.405(7)	C(30)-C(31)-C(32)	118.7(6)		
C(35)-S(3)	1.651(5)	C(31)-C(32)-C(33)	120.1(6)		
C(36)-O(3)	1.231(6)	C(32)-C(33)-C(34)	117.7(6)		
C(36)-N(10)	1.397(7)	N(8)-C(34)-C(33)	123.4(5)		

Appendix 3: Crystals data

C(36)-C(37)	1.479(8)	N(8)-C(34)-N(9)	113.8(4)		
C(37)-C(38)	1.370(8)	C(33)-C(34)-N(9)	122.4(5)		
C(37)-C(42)	1.385(8)	N(9)-C(35)-N(10)	114.0(4)		
C(38)-C(39)	1.391(9)	N(9)-C(35)-S(3)	126.7(5)		
C(39)-C(40)	1.382(10)	N(10)-C(35)-S(3)	119.2(4)		
C(40)-C(41)	1.373(10)	O(3)-C(36)-N(10)	122.0(5)		
C(41)-C(42)	1.358(10)	O(3)-C(36)-C(37)	121.6(5)		
C(43)-N(11)	1.137(7)	N(10)-C(36)-C(37)	116.4(5)		
C(43)-C(44)	1.447(9)	C(38)-C(37)-C(42)	119.1(6)		
N(1)-Ni(1)	2.074(4)	C(38)-C(37)-C(36)	123.8(5)		
N(2)-Ni(1)	2.054(4)	C(42)-C(37)-C(36)	117.1(5)		
N(5)-Ni(1)	2.216(4)	C(37)-C(38)-C(39)	120.8(6)		
N(8)-Ni(1)	2.262(4)	C(40)-C(39)-C(38)	118.9(7)		
N(11)-Ni(1)	2.054(5)	C(41)-C(40)-C(39)	120.1(7)		
S(2)-Ni(1)	2.3441(14)	C(42)-C(41)-C(40)	120.6(7)		
C(45)-N(12)	1.102(6)	C(41)-C(42)-C(37)	120.6(7)		
C(45)-C(46)	1.447(8)	N(11)-C(43)-C(44)	179.8(9)		
C(47)-N(13)	1.110(9)	C(15)-N(1)-C(29)	110.2(4)		
C(47)-C(48)	1.459(10)	C(15)-N(1)-C(1)	112.3(4)		
C(49)-N(14)	1.112(14)	C(29)-N(1)-C(1)	111.5(4)		
C(49)-C(50)	1.382(16)	C(15)-N(1)-Ni(1)	106.9(3)		
C(51)-N(15)	1.095(9)	C(29)-N(1)-Ni(1)	110.6(3)		
C(51)-C(52)	1.444(12)	C(1)-N(1)-Ni(1)	105.1(3)		
C(51)-C(52)#1	1.62(3)	C(6)-N(2)-C(2)	117.7(5)		
C(53)-N(16)	1.100(10)	C(6)-N(2)-Ni(1)	130.2(4)		
C(53)-C(54)	1.446(11)	C(2)-N(2)-Ni(1)	111.2(3)		
Cl(1)-O(5)	1.390(5)	C(7)-N(3)-C(6)	133.4(4)		
Cl(1)-O(7)	1.419(4)	C(8)-N(4)-C(7)	127.5(4)		
Cl(1)-O(4)	1.437(5)	C(20)-N(5)-C(16)	117.2(4)		
Cl(1)-O(6)	1.448(5)	C(20)-N(5)-Ni(1)	133.0(3)		
Cl(2)-O(10)	1.374(12)	C(16)-N(5)-Ni(1)	109.2(3)		
Cl(2)-O(8)	1.405(18)	C(21)-N(6)-C(20)	125.4(5)		
Cl(2)-O(9)	1.418(9)	C(21)-N(7)-C(22)	127.6(5)		
Cl(2)-O(11)	1.440(11)	C(34)-N(8)-C(30)	118.5(5)		

Symmetry transformations used to generate equivalent atoms:

#1 -x,-y+1,-z+1

Appendix 3: Crystals data

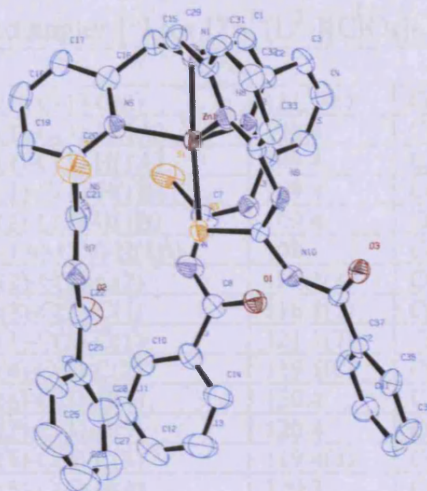


Table N.1: Crystal data and structure refinement for $[Zn^{II}(L^3)][ClO_4]_2 \cdot CH_3CN \cdot CHCl_3$. 4.5

Identification code	aja0909	
Empirical formula	C ₄₅ H ₄₀ Cl ₁₅ N ₁₁ O ₁₁ S ₃ Zn	
Formula weight	1249.68	
Temperature	150(2) K	
Wavelength	0.71073 Å	
Crystal system	Orthorhombic	
Space group	Pccn	
Unit cell dimensions	a = 30.5910(3) Å	α = 90°.
	b = 19.7950(3) Å	β = 90°.
	c = 17.5370(5) Å	γ = 90°.
Volume	10619.5(4) Å ³	
Z	8	
Density (calculated)	1.563 Mg/m ³	
Absorption coefficient	0.901 mm ⁻¹	
F(000)	5104	
Crystal size	0.50 x 0.10 x 0.02 mm ³	
Theta range for data collection	2.45 to 24.02°.	
Index ranges	-32 ≤ h ≤ 32, -20 ≤ k ≤ 21, -19 ≤ l ≤ 17	
Reflections collected	35686	
Independent reflections	7326 [R(int) = 0.0869]	
Completeness to theta = 24.02°	87.5 %	
Max. and min. transmission	0.9822 and 0.6615	
Refinement method	Full-matrix least-squares on F ²	
Data / restraints / parameters	7326 / 102 / 719	
Goodness-of-fit on F ²	1.049	
Final R indices [I > 2σ(I)]	R1 = 0.0834, wR2 = 0.1942	
R indices (all data)	R1 = 0.1178, wR2 = 0.2117	
Largest diff. peak and hole	1.662 and -1.089 e.Å ⁻³	

Appendix 3: Crystals data

Table N.2: Bond lengths [Å] and angles [°] for $[\text{Zn}^{\text{II}}(\text{L}^3)][\text{ClO}_4]_2 \cdot \text{CH}_3\text{CN} \cdot \text{CHCl}_3 \cdot 4.5$

C(1)-N(1)	1.478(10)	N(1)-C(1)-C(2)	111.1(6)	C(29)-N(1)-C(15)	113.8(6)
C(1)-C(2)	1.500(11)	N(1)-C(1)-H(1A)	109.4	C(29)-N(1)-C(1)	113.1(6)
C(1)-H(1A)	0.99	C(2)-C(1)-H(1A)	109.4	C(15)-N(1)-C(1)	111.2(6)
C(1)-H(1B)	0.99	N(1)-C(1)-H(1B)	109.4	C(29)-N(1)-Zn(1)	105.3(5)
C(2)-N(2)	1.339(9)	C(2)-C(1)-H(1B)	109.4	C(15)-N(1)-Zn(1)	106.6(5)
C(2)-C(3)	1.383(11)	H(1A)-C(1)-H(1B)	108	C(1)-N(1)-Zn(1)	106.2(4)
C(3)-C(4)	1.372(12)	N(2)-C(2)-C(3)	122.1(8)	C(2)-N(2)-C(6)	117.5(7)
C(3)-H(3)	0.95	N(2)-C(2)-C(1)	116.8(7)	C(2)-N(2)-Zn(1)	114.3(5)
C(4)-C(5)	1.369(12)	C(3)-C(2)-C(1)	121.1(7)	C(6)-N(2)-Zn(1)	128.1(5)
C(4)-H(4)	0.95	C(4)-C(3)-C(2)	119.1(8)	C(7)-N(3)-C(6)	121.9(7)
C(5)-C(6)	1.373(11)	C(4)-C(3)-H(3)	120.4	C(7)-N(3)-H(3A)	119.1
C(5)-H(5)	0.95	C(2)-C(3)-H(3)	120.4	C(6)-N(3)-H(3A)	119.1
C(6)-N(2)	1.341(10)	C(5)-C(4)-C(3)	119.4(8)	C(8)-N(4)-C(7)	128.5(7)
C(6)-N(3)	1.428(10)	C(5)-C(4)-H(4)	120.3	C(8)-N(4)-H(4A)	115.7
C(7)-N(3)	1.324(10)	C(3)-C(4)-H(4)	120.3	C(7)-N(4)-H(4A)	115.7
C(7)-N(4)	1.400(11)	C(4)-C(5)-C(6)	118.4(8)	C(16)-N(5)-C(20)	118.0(7)
C(7)-S(1)	1.654(9)	C(4)-C(5)-H(5)	120.8	C(16)-N(5)-Zn(1)	113.7(5)
C(8)-O(1)	1.230(9)	C(6)-C(5)-H(5)	120.8	C(20)-N(5)-Zn(1)	128.3(6)
C(8)-N(4)	1.349(11)	N(2)-C(6)-C(5)	123.4(7)	C(21)-N(6)-C(20)	120.2(7)
C(8)-C(9)	1.482(12)	N(2)-C(6)-N(3)	116.6(7)	C(21)-N(6)-H(6)	119.9
C(9)-C(14)	1.365(13)	C(5)-C(6)-N(3)	119.9(7)	C(20)-N(6)-H(6)	119.9
C(9)-C(10)	1.401(12)	N(3)-C(7)-N(4)	115.7(7)	C(21)-N(7)-C(22)	127.2(7)
C(10)-C(11)	1.388(12)	N(3)-C(7)-S(1)	124.2(7)	C(21)-N(7)-H(7)	116.4
C(10)-H(10)	0.95	N(4)-C(7)-S(1)	120.1(6)	C(22)-N(7)-H(7)	116.4
C(11)-C(12)	1.363(15)	O(1)-C(8)-N(4)	121.9(8)	C(34)-N(8)-C(30)	117.6(7)
C(11)-H(11)	0.95	O(1)-C(8)-C(9)	120.5(8)	C(34)-N(8)-Zn(1)	128.3(5)
C(12)-C(13)	1.402(16)	N(4)-C(8)-C(9)	117.6(8)	C(30)-N(8)-Zn(1)	113.5(5)
C(12)-H(12)	0.95	C(14)-C(9)-C(10)	119.5(9)	C(35)-N(9)-C(34)	129.5(6)
C(13)-C(14)	1.390(15)	C(14)-C(9)-C(8)	116.7(8)	C(35)-N(9)-H(9)	115.3
C(13)-H(13)	0.95	C(10)-C(9)-C(8)	123.8(8)	C(34)-N(9)-H(9)	115.3
C(14)-H(14)	0.95	C(11)-C(10)-C(9)	119.6(9)	C(35)-N(10)-C(36)	129.1(6)
C(15)-N(1)	1.464(10)	C(11)-C(10)-H(10)	120.2	C(35)-N(10)-H(10A)	115.5
C(15)-C(16)	1.511(11)	C(9)-C(10)-H(10)	120.2	C(36)-N(10)-H(10A)	115.5
C(15)-H(15A)	0.99	C(12)-C(11)-C(10)	120.6(9)	C(35)-S(3)-Zn(1)	101.3(3)
C(15)-H(15B)	0.99	C(12)-C(11)-H(11)	119.7	N(2)-Zn(1)-N(5)	115.6(2)
C(16)-N(5)	1.340(10)	C(10)-C(11)-H(11)	119.7	N(2)-Zn(1)-N(8)	108.0(2)
C(16)-C(17)	1.377(11)	C(11)-C(12)-C(13)	120.1(10)	N(5)-Zn(1)-N(8)	123.1(2)
C(17)-C(18)	1.372(12)	C(11)-C(12)-H(12)	119.9	N(2)-Zn(1)-N(1)	78.6(2)
C(17)-H(17)	0.95	C(13)-C(12)-H(12)	119.9	N(5)-Zn(1)-N(1)	78.6(2)
C(18)-C(19)	1.377(12)	C(14)-C(13)-C(12)	119.0(11)	N(8)-Zn(1)-N(1)	76.0(2)
C(18)-H(18)	0.95	C(14)-C(13)-H(13)	120.5	N(2)-Zn(1)-S(3)	108.69(18)
C(19)-C(20)	1.388(12)	C(12)-C(13)-H(13)	120.5	N(5)-Zn(1)-S(3)	108.07(18)
C(19)-H(19)	0.95	C(9)-C(14)-C(13)	121.1(10)	N(8)-Zn(1)-S(3)	89.72(17)
C(20)-N(5)	1.346(10)	C(9)-C(14)-H(14)	119.5	N(1)-Zn(1)-S(3)	165.52(18)
C(20)-N(6)	1.427(11)	C(13)-C(14)-H(14)	119.5	O(6)-Cl(1)-O(5)	107.9(4)
C(21)-N(6)	1.344(10)	N(1)-C(15)-C(16)	110.3(6)	O(6)-Cl(1)-O(4)	109.7(5)
C(21)-N(7)	1.386(10)	N(1)-C(15)-H(15A)	109.6	O(5)-Cl(1)-O(4)	109.2(4)
C(21)-S(2)	1.664(9)	C(16)-C(15)-H(15A)	109.6	O(6)-Cl(1)-O(7)	110.3(4)
C(22)-O(2)	1.233(10)	N(1)-C(15)-H(15B)	109.6	O(5)-Cl(1)-O(7)	110.2(4)
C(22)-N(7)	1.387(11)	C(16)-C(15)-H(15B)	109.6	O(4)-Cl(1)-O(7)	109.5(4)
C(22)-C(23)	1.490(12)	H(15A)-C(15)-H(15B)	108.1	O(8)#1-Cl(2)-O(8)	109.8(5)
C(23)-C(24)	1.377(13)	N(5)-C(16)-C(17)	122.5(8)	O(8)#1-Cl(2)-O(9)#1	109.5(3)
C(23)-C(28)	1.390(13)	N(5)-C(16)-C(15)	117.2(7)	O(8)-Cl(2)-O(9)#1	109.3(3)
C(24)-C(25)	1.399(14)	C(17)-C(16)-C(15)	120.3(7)	O(8)#1-Cl(2)-O(9)	109.3(3)
C(24)-H(24)	0.95	C(18)-C(17)-C(16)	119.0(8)	O(8)-Cl(2)-O(9)	109.5(3)
C(25)-C(26)	1.370(16)	C(18)-C(17)-H(17)	120.5	O(9)#1-Cl(2)-O(9)	109.5(5)
C(25)-H(25)	0.95	C(16)-C(17)-H(17)	120.5	Cl(4)-C(43)-Cl(3)	116.1(7)

Appendix 3: Crystals data

C(26)-C(27)	1.374(16)	C(17)-C(18)-C(19)	119.6(8)	Cl(4)-C(43)-Cl(5)	106.4(10)
C(26)-H(26)	0.95	C(17)-C(18)-H(18)	120.2	Cl(3)-C(43)-Cl(5)	105.1(10)
C(27)-C(28)	1.371(14)	C(19)-C(18)-H(18)	120.2	Cl(4)-C(43)-H(43)	109.7
C(27)-H(27)	0.95	C(18)-C(19)-C(20)	118.3(8)	Cl(3)-C(43)-H(43)	109.7
C(28)-H(28)	0.95	C(18)-C(19)-H(19)	120.9	Cl(5)-C(43)-H(43)	109.7
C(29)-N(1)	1.462(10)	C(20)-C(19)-H(19)	120.9	Cl(6)#2-O(10)-Cl(6)	26.9(4)
C(29)-C(30)	1.516(11)	N(5)-C(20)-C(19)	122.4(8)	Cl(6)-O(11)-Cl(6)#2	26.6(4)
C(29)-H(29A)	0.99	N(5)-C(20)-N(6)	118.2(7)	Cl(6)-O(12)-Cl(6)#2	3.6(6)
C(29)-H(29B)	0.99	C(19)-C(20)-N(6)	119.4(8)	Cl(6)#2-Cl(6)-O(10)#2	88.2(14)
C(30)-N(8)	1.346(9)	N(6)-C(21)-N(7)	116.4(7)	Cl(6)#2-Cl(6)-O(11)	76.72(18)
C(30)-C(31)	1.369(11)	N(6)-C(21)-S(2)	124.9(7)	O(10)#2-Cl(6)-O(11)	118.4(9)
C(31)-C(32)	1.379(11)	N(7)-C(21)-S(2)	118.8(6)	Cl(6)#2-Cl(6)-O(10)	64.8(13)
C(31)-H(31)	0.95	O(2)-C(22)-N(7)	121.9(8)	O(10)#2-Cl(6)-O(10)	116.5(11)
C(32)-C(33)	1.396(11)	O(2)-C(22)-C(23)	120.9(8)	O(11)-Cl(6)-O(10)	109.8(6)
C(32)-H(32)	0.95	N(7)-C(22)-C(23)	117.2(8)	Cl(6)#2-Cl(6)-O(12)	168.1(19)
C(33)-C(34)	1.371(10)	C(24)-C(23)-C(28)	119.7(9)	O(10)#2-Cl(6)-O(12)	102.5(7)
C(33)-H(33)	0.95	C(24)-C(23)-C(22)	123.0(9)	O(11)-Cl(6)-O(12)	102.1(5)
C(34)-N(8)	1.337(10)	C(28)-C(23)-C(22)	117.3(8)	O(10)-Cl(6)-O(12)	105.1(7)
C(34)-N(9)	1.425(9)	C(23)-C(24)-C(25)	119.6(10)	Cl(6)#2-Cl(6)-O(12)#2	8.3(13)
C(35)-N(9)	1.322(9)	C(23)-C(24)-H(24)	120.2	O(10)#2-Cl(6)-O(12)#2	81.4(5)
C(35)-N(10)	1.383(9)	C(25)-C(24)-H(24)	120.2	O(11)-Cl(6)-O(12)#2	76.3(4)
C(35)-S(3)	1.693(7)	C(26)-C(25)-C(24)	119.1(10)	O(10)-Cl(6)-O(12)#2	72.4(5)
C(36)-O(3)	1.237(9)	C(26)-C(25)-H(25)	120.4	O(12)-Cl(6)-O(12)#2	176.1(7)
C(36)-N(10)	1.389(9)	C(24)-C(25)-H(25)	120.4	N(11)-C(44)-C(45)	175.5(15)
C(36)-C(37)	1.480(10)	C(25)-C(26)-C(27)	121.7(11)	N(11A)-C(44A)-C(45A)	177(3)
C(37)-C(42)	1.374(11)	C(25)-C(26)-H(26)	119.1	C(44A)-C(45A)-H(45D)	109.5
C(37)-C(38)	1.397(10)	C(27)-C(26)-H(26)	119.1	C(44A)-C(45A)-H(45E)	109.5
C(38)-C(39)	1.377(11)	C(28)-C(27)-C(26)	118.9(11)	H(45D)-C(45A)-H(45E)	109.5
C(38)-H(38)	0.95	C(28)-C(27)-H(27)	120.5	C(44A)-C(45A)-H(45F)	109.5
C(39)-C(40)	1.385(12)	C(26)-C(27)-H(27)	120.5	H(45D)-C(45A)-H(45F)	109.5
C(39)-H(39)	0.95	C(27)-C(28)-C(23)	120.8(10)	H(45E)-C(45A)-H(45F)	109.5
C(40)-C(41)	1.380(12)	C(27)-C(28)-H(28)	119.6		
C(40)-H(40)	0.95	C(23)-C(28)-H(28)	119.6		
C(41)-C(42)	1.376(11)	N(1)-C(29)-C(30)	110.4(6)		
C(41)-H(41)	0.95	N(1)-C(29)-H(29A)	109.6		
C(42)-H(42)	0.95	C(30)-C(29)-H(29A)	109.6		
N(1)-Zn(1)	2.162(6)	N(1)-C(29)-H(29B)	109.6		
N(2)-Zn(1)	2.105(6)	C(30)-C(29)-H(29B)	109.6		
N(3)-H(3A)	0.88	H(29A)-C(29)-H(29B)	108.1		
N(4)-H(4A)	0.88	N(8)-C(30)-C(31)	122.8(7)		
N(5)-Zn(1)	2.107(6)	N(8)-C(30)-C(29)	114.7(7)		
N(6)-H(6)	0.88	C(31)-C(30)-C(29)	122.5(7)		
N(7)-H(7)	0.88	C(30)-C(31)-C(32)	118.8(7)		
N(8)-Zn(1)	2.148(6)	C(30)-C(31)-H(31)	120.6		
N(9)-H(9)	0.88	C(32)-C(31)-H(31)	120.6		
N(10)-H(10A)	0.88	C(31)-C(32)-C(33)	119.4(7)		
S(3)-Zn(1)	2.346(2)	C(31)-C(32)-H(32)	120.3		
O(4)-Cl(1)	1.439(6)	C(33)-C(32)-H(32)	120.3		
O(5)-Cl(1)	1.430(6)	C(34)-C(33)-C(32)	117.5(7)		
O(6)-Cl(1)	1.426(7)	C(34)-C(33)-H(33)	121.2		
O(7)-Cl(1)	1.440(6)	C(32)-C(33)-H(33)	121.2		
O(8)-Cl(2)	1.439(5)	N(8)-C(34)-C(33)	123.9(7)		
O(9)-Cl(2)	1.442(5)	N(8)-C(34)-N(9)	119.3(7)		
Cl(2)-O(8)#1	1.439(5)	C(33)-C(34)-N(9)	116.6(7)		
Cl(2)-O(9)#1	1.442(5)	N(9)-C(35)-N(10)	116.0(6)		
C(43)-Cl(4)	1.683(14)	N(9)-C(35)-S(3)	128.1(5)		
C(43)-Cl(3)	1.706(13)	N(10)-C(35)-S(3)	115.7(5)		
C(43)-Cl(5)	1.87(2)	O(3)-C(36)-N(10)	120.0(6)		
C(43)-H(43)	1	O(3)-C(36)-C(37)	124.5(7)		

Appendix 3: Crystals data

O(10)-Cl(6)#2	1.306(12)	N(10)-C(36)-C(37)	115.4(7)		
O(10)-Cl(6)	1.442(8)	C(42)-C(37)-C(38)	119.3(7)		
O(11)-Cl(6)	1.424(7)	C(42)-C(37)-C(36)	123.1(7)		
O(11)-Cl(6)#2	1.424(7)	C(38)-C(37)-C(36)	117.6(7)		
O(12)-Cl(6)	1.482(8)	C(39)-C(38)-C(37)	119.9(7)		
O(12)-Cl(6)#2	2.126(9)	C(39)-C(38)-H(38)	120.1		
Cl(6)-Cl(6)#2	0.654(8)	C(37)-C(38)-H(38)	120.1		
Cl(6)-O(10)#2	1.306(12)	C(38)-C(39)-C(40)	120.5(8)		
Cl(6)-O(12)#2	2.126(9)	C(38)-C(39)-H(39)	119.8		
C(44)-N(11)	1.1010(10)	C(40)-C(39)-H(39)	119.8		
C(44)-C(45)	1.4205(9)	C(41)-C(40)-C(39)	119.2(8)		
C(45)-H(45A)	0.98	C(41)-C(40)-H(40)	120.4		
C(45)-H(45B)	0.98	C(39)-C(40)-H(40)	120.4		
C(45)-H(45C)	0.98	C(42)-C(41)-C(40)	120.6(8)		
C(44A)-N(11A)	1.1003(10)	C(42)-C(41)-H(41)	119.7		
C(44A)-C(45A)	1.4202(10)	C(40)-C(41)-H(41)	119.7		
C(45A)-H(45D)	0.98	C(37)-C(42)-C(41)	120.5(8)		
C(45A)-H(45E)	0.98	C(37)-C(42)-H(42)	119.7		
C(45A)-H(45F)	0.98	C(41)-C(42)-H(42)	119.7		

Symmetry transformations used to generate equivalent atoms:

#1 $-x+3/2, -y+1/2, z$ #2 $-x+3/2, -y+3/2, z$

Appendix 3: Crystals data

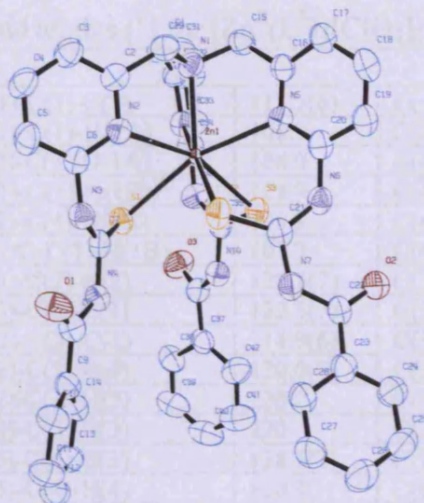


Table O.1: Crystal data and structure refinement for $[Zn^{II}(L^3)][ClO_4]_2 \cdot 1.5(CH_3CN) \cdot 0.5(H_2O)$.
4.5.1

Identification code	aja0945	
Empirical formula	C ₄₅ H _{41.50} Cl ₂ N _{11.50} O _{11.50} S ₃ Zn	
Formula weight	1159.85	
Temperature	150(2) K	
Wavelength	0.71073 Å	
Crystal system	Triclinic	
Space group	P-1	
Unit cell dimensions	a = 13.7530(2) Å	α = 69.2030(10)°.
	b = 13.9620(2) Å	β = 71.1580(10)°.
	c = 16.3920(3) Å	γ = 61.9880(10)°.
Volume	2550.83(7) Å ³	
Z	2	
Density (calculated)	1.510 Mg/m ³	
Absorption coefficient	0.780 mm ⁻¹	
F(000)	1192	
Crystal size	0.40 x 0.30 x 0.10 mm ³	
Theta range for data collection	1.70 to 27.62°.	
Index ranges	-17 ≤ h ≤ 16, -18 ≤ k ≤ 14, -21 ≤ l ≤ 21	
Reflections collected	16596	
Independent reflections	11611 [R(int) = 0.0289]	
Completeness to theta = 27.62°	98.0 %	
Absorption correction	Empirical	
Max. and min. transmission	0.9260 and 0.7454	
Refinement method	Full-matrix least-squares on F ²	
Data / restraints / parameters	11611 / 137 / 725	
Goodness-of-fit on F ²	1.058	
Final R indices [I > 2σ(I)]	R1 = 0.0884, wR2 = 0.2644	
R indices (all data)	R1 = 0.1054, wR2 = 0.2852	
Extinction coefficient	0.066(4)	
Largest diff. peak and hole	4.898 and -1.139 e.Å ⁻³	

Appendix 3: Crystals data

Table O.2: Bond lengths [Å] and angles [°] for $[\text{Zn}^{\text{II}}(\text{L}^3)][\text{ClO}_4]_2 \cdot 1.5(\text{CH}_3\text{CN}) \cdot 0.5(\text{H}_2\text{O})$. 4.5.1

C(1)-N(1)	1.483(9)	N(1)-C(1)-C(2)	113.5(6)	C(41)-C(40)-H(40)	119.7
C(1)-C(2)	1.496(10)	N(1)-C(1)-H(1A)	108.9	C(42)-C(41)-C(40)	120.2(10)
C(1)-H(1A)	0.99	C(2)-C(1)-H(1A)	108.9	C(42)-C(41)-H(41)	119.9
C(1)-H(1B)	0.99	N(1)-C(1)-H(1B)	108.9	C(40)-C(41)-H(41)	119.9
C(2)-C(3)	1.353(10)	C(2)-C(1)-H(1B)	108.9	C(41)-C(42)-C(37)	118.3(9)
C(2)-N(2)	1.369(9)	H(1A)-C(1)-H(1B)	107.7	C(41)-C(42)-H(42)	120.8
C(3)-C(4)	1.389(11)	C(3)-C(2)-N(2)	122.5(7)	C(37)-C(42)-H(42)	120.8
C(3)-H(3)	0.95	C(3)-C(2)-C(1)	122.5(7)	C(15)-N(1)-C(29)	109.3(5)
C(4)-C(5)	1.384(12)	N(2)-C(2)-C(1)	114.9(6)	C(15)-N(1)-C(1)	110.7(6)
C(4)-H(4)	0.95	C(2)-C(3)-C(4)	120.0(7)	C(29)-N(1)-C(1)	108.5(5)
C(5)-C(6)	1.396(10)	C(2)-C(3)-H(3)	120	C(15)-N(1)-Zn(1)	111.3(4)
C(5)-H(5)	0.95	C(4)-C(3)-H(3)	120	C(29)-N(1)-Zn(1)	108.4(4)
C(6)-N(2)	1.335(9)	C(5)-C(4)-C(3)	118.5(7)	C(1)-N(1)-Zn(1)	108.6(4)
C(6)-N(3)	1.404(9)	C(5)-C(4)-H(4)	120.8	C(6)-N(2)-C(2)	117.7(6)
C(7)-N(3)	1.329(9)	C(3)-C(4)-H(4)	120.8	C(6)-N(2)-Zn(1)	127.7(5)
C(7)-N(4)	1.386(9)	C(4)-C(5)-C(6)	118.7(7)	C(2)-N(2)-Zn(1)	112.5(4)
C(7)-S(1)	1.694(7)	C(4)-C(5)-H(5)	120.7	C(7)-N(3)-C(6)	127.7(6)
C(8)-O(1)	1.227(9)	C(6)-C(5)-H(5)	120.7	C(7)-N(3)-H(3A)	116.1
C(8)-N(4)	1.391(9)	N(2)-C(6)-C(5)	122.7(7)	C(6)-N(3)-H(3A)	116.1
C(8)-C(9)	1.482(10)	N(2)-C(6)-N(3)	118.8(6)	C(7)-N(4)-C(8)	126.8(6)
C(9)-C(10)	1.394(10)	C(5)-C(6)-N(3)	118.3(6)	C(7)-N(4)-H(4A)	116.6
C(9)-C(14)	1.401(10)	N(3)-C(7)-N(4)	117.4(6)	C(8)-N(4)-H(4A)	116.6
C(10)-C(11)	1.372(11)	N(3)-C(7)-S(1)	125.5(6)	C(16)-N(5)-C(20)	117.5(6)
C(10)-H(10)	0.95	N(4)-C(7)-S(1)	117.1(5)	C(16)-N(5)-Zn(1)	113.8(4)
C(11)-C(12)	1.400(12)	O(1)-C(8)-N(4)	120.9(7)	C(20)-N(5)-Zn(1)	127.6(5)
C(11)-H(11)	0.95	O(1)-C(8)-C(9)	121.6(6)	C(21)-N(6)-C(20)	126.2(6)
C(12)-C(13)	1.404(12)	N(4)-C(8)-C(9)	117.5(6)	C(21)-N(6)-H(6)	116.9
C(12)-H(12)	0.95	C(10)-C(9)-C(14)	119.4(7)	C(20)-N(6)-H(6)	116.9
C(13)-C(14)	1.369(11)	C(10)-C(9)-C(8)	117.0(7)	C(22)-N(7)-C(21)	127.9(6)
C(13)-H(13)	0.95	C(14)-C(9)-C(8)	123.5(6)	C(22)-N(7)-H(7)	116
C(14)-H(14)	0.95	C(11)-C(10)-C(9)	120.3(7)	C(21)-N(7)-H(7)	116
C(15)-N(1)	1.466(9)	C(11)-C(10)-H(10)	119.9	C(34)-N(8)-C(30)	116.6(6)
C(15)-C(16)	1.503(10)	C(9)-C(10)-H(10)	119.9	C(34)-N(8)-Zn(1)	129.3(5)
C(15)-H(15A)	0.99	C(10)-C(11)-C(12)	120.4(8)	C(30)-N(8)-Zn(1)	113.0(4)
C(15)-H(15B)	0.99	C(10)-C(11)-H(11)	119.8	C(35)-N(9)-C(34)	130.4(6)
C(16)-N(5)	1.338(9)	C(12)-C(11)-H(11)	119.8	C(35)-N(9)-H(9)	114.8
C(16)-C(17)	1.383(10)	C(11)-C(12)-C(13)	119.3(8)	C(34)-N(9)-H(9)	114.8
C(17)-C(18)	1.413(11)	C(11)-C(12)-H(12)	120.4	C(35)-N(10)-C(36)	127.1(6)
C(17)-H(17)	0.95	C(13)-C(12)-H(12)	120.4	C(35)-N(10)-H(10A)	116.5
C(18)-C(19)	1.376(12)	C(14)-C(13)-C(12)	120.1(8)	C(36)-N(10)-H(10A)	116.5
C(18)-H(18)	0.95	C(14)-C(13)-H(13)	120	C(7)-S(1)-Zn(1)	100.8(2)
C(19)-C(20)	1.380(10)	C(12)-C(13)-H(13)	120	C(21)-S(2)-Zn(1)	100.2(2)
C(19)-H(19)	0.95	C(13)-C(14)-C(9)	120.5(7)	C(35)-S(3)-Zn(1)	101.3(2)
C(20)-N(5)	1.342(9)	C(13)-C(14)-H(14)	119.7	N(1)-Zn(1)-N(8)	71.2(2)
C(20)-N(6)	1.416(9)	C(9)-C(14)-H(14)	119.7	N(1)-Zn(1)-N(2)	71.42(19)
C(21)-N(6)	1.352(9)	N(1)-C(15)-C(16)	113.2(5)	N(8)-Zn(1)-N(2)	110.32(19)
C(21)-N(7)	1.387(10)	N(1)-C(15)-H(15A)	108.9	N(1)-Zn(1)-N(5)	70.12(19)
C(21)-S(2)	1.678(7)	C(16)-C(15)-H(15A)	108.9	N(8)-Zn(1)-N(5)	106.84(18)
C(22)-O(2)	1.215(8)	N(1)-C(15)-H(15B)	108.9	N(2)-Zn(1)-N(5)	112.35(19)
C(22)-N(7)	1.386(9)	C(16)-C(15)-H(15B)	108.9	N(1)-Zn(1)-S(2)	121.13(15)
C(22)-C(23)	1.482(10)	H(15A)-C(15)-H(15B)	107.8	N(8)-Zn(1)-S(2)	166.59(15)
C(23)-C(24)	1.362(11)	N(5)-C(16)-C(17)	123.0(7)	N(2)-Zn(1)-S(2)	80.32(14)
C(23)-C(28)	1.405(11)	N(5)-C(16)-C(15)	116.3(6)	N(5)-Zn(1)-S(2)	75.09(13)
C(24)-C(25)	1.379(13)	C(17)-C(16)-C(15)	120.6(7)	N(1)-Zn(1)-S(3)	127.77(14)
C(24)-H(24)	0.95	C(16)-C(17)-C(18)	118.4(7)	N(8)-Zn(1)-S(3)	77.61(14)
C(25)-C(26)	1.396(15)	C(16)-C(17)-H(17)	120.8	N(2)-Zn(1)-S(3)	160.59(14)
C(25)-H(25)	0.95	C(18)-C(17)-H(17)	120.8	N(5)-Zn(1)-S(3)	80.64(13)

Appendix 3: Crystals data

C(26)-C(27)	1.392(14)	C(19)-C(18)-C(17)	118.5(7)	S(2)-Zn(1)-S(3)	89.78(6)
C(26)-H(26)	0.95	C(19)-C(18)-H(18)	120.7	N(1)-Zn(1)-S(1)	127.67(15)
C(27)-C(28)	1.385(12)	C(17)-C(18)-H(18)	120.7	N(8)-Zn(1)-S(1)	83.12(14)
C(27)-H(27)	0.95	C(18)-C(19)-C(20)	118.6(7)	N(2)-Zn(1)-S(1)	76.45(14)
C(28)-H(28)	0.95	C(18)-C(19)-H(19)	120.7	N(5)-Zn(1)-S(1)	162.15(14)
C(29)-N(1)	1.473(9)	C(20)-C(19)-H(19)	120.7	S(2)-Zn(1)-S(1)	91.84(6)
C(29)-C(30)	1.520(10)	N(5)-C(20)-C(19)	123.8(7)	S(3)-Zn(1)-S(1)	87.32(5)
C(29)-H(29A)	0.99	N(5)-C(20)-N(6)	118.2(6)	O(7)-Cl(1)-O(4)	110.7(5)
C(29)-H(29B)	0.99	C(19)-C(20)-N(6)	117.9(6)	O(7)-Cl(1)-O(5)	109.4(5)
C(30)-N(8)	1.350(9)	N(6)-C(21)-N(7)	116.1(6)	O(4)-Cl(1)-O(5)	108.6(4)
C(30)-C(31)	1.362(10)	N(6)-C(21)-S(2)	126.3(6)	O(7)-Cl(1)-O(6)	111.1(5)
C(31)-C(32)	1.396(12)	N(7)-C(21)-S(2)	117.5(5)	O(4)-Cl(1)-O(6)	109.3(4)
C(31)-H(31)	0.95	O(2)-C(22)-N(7)	121.3(7)	O(5)-Cl(1)-O(6)	107.7(4)
C(32)-C(33)	1.382(13)	O(2)-C(22)-C(23)	121.7(6)	O(11)-Cl(2)-O(8A)	65.2(17)
C(32)-H(32)	0.95	N(7)-C(22)-C(23)	117.0(6)	O(11)-Cl(2)-O(9)	110.0(8)
C(33)-C(34)	1.352(11)	C(24)-C(23)-C(28)	119.0(8)	O(8A)-Cl(2)-O(9)	95(2)
C(33)-H(33)	0.95	C(24)-C(23)-C(22)	117.8(7)	O(11)-Cl(2)-O(11A)	44.1(17)
C(34)-N(8)	1.338(9)	C(28)-C(23)-C(22)	122.9(7)	O(8A)-Cl(2)-O(11A)	108.6(5)
C(34)-N(9)	1.418(9)	C(23)-C(24)-C(25)	121.2(8)	O(9)-Cl(2)-O(11A)	115(2)
C(35)-N(9)	1.330(9)	C(23)-C(24)-H(24)	119.4	O(11)-Cl(2)-O(9A)	117.8(19)
C(35)-N(10)	1.378(9)	C(25)-C(24)-H(24)	119.4	O(8A)-Cl(2)-O(9A)	111.3(5)
C(35)-S(3)	1.678(7)	C(24)-C(25)-C(26)	121.0(9)	O(9)-Cl(2)-O(9A)	17(2)
C(36)-O(3)	1.218(9)	C(24)-C(25)-H(25)	119.5	O(11A)-Cl(2)-O(9A)	109.2(5)
C(36)-N(10)	1.395(9)	C(26)-C(25)-H(25)	119.5	O(11)-Cl(2)-O(10A)	131.2(19)
C(36)-C(37)	1.479(10)	C(27)-C(26)-C(25)	117.8(9)	O(8A)-Cl(2)-O(10A)	110.0(5)
C(37)-C(38)	1.394(11)	C(27)-C(26)-H(26)	121.1	O(9)-Cl(2)-O(10A)	118.7(19)
C(37)-C(42)	1.400(12)	C(25)-C(26)-H(26)	121.1	O(11A)-Cl(2)-O(10A)	108.7(5)
C(38)-C(39)	1.360(12)	C(28)-C(27)-C(26)	121.0(9)	O(9A)-Cl(2)-O(10A)	109.1(4)
C(38)-H(38)	0.95	C(28)-C(27)-H(27)	119.5	O(11)-Cl(2)-O(10)	109.4(8)
C(39)-C(40)	1.375(15)	C(26)-C(27)-H(27)	119.5	O(8A)-Cl(2)-O(10)	154.9(19)
C(39)-H(39)	0.95	C(27)-C(28)-C(23)	119.8(8)	O(9)-Cl(2)-O(10)	109.6(8)
C(40)-C(41)	1.385(16)	C(27)-C(28)-H(28)	120.1	O(11A)-Cl(2)-O(10)	66.7(18)
C(40)-H(40)	0.95	C(23)-C(28)-H(28)	120.1	O(9A)-Cl(2)-O(10)	93(2)
C(41)-C(42)	1.384(13)	N(1)-C(29)-C(30)	112.9(5)	O(10A)-Cl(2)-O(10)	53.5(17)
C(41)-H(41)	0.95	N(1)-C(29)-H(29A)	109	O(11)-Cl(2)-O(8)	109.4(8)
C(42)-H(42)	0.95	C(30)-C(29)-H(29A)	109	O(8A)-Cl(2)-O(8)	55.5(17)
N(1)-Zn(1)	2.380(6)	N(1)-C(29)-H(29B)	109	O(9)-Cl(2)-O(8)	109.6(8)
N(2)-Zn(1)	2.518(6)	C(30)-C(29)-H(29B)	109	O(11A)-Cl(2)-O(8)	134.1(19)
N(3)-H(3A)	0.88	H(29A)-C(29)-H(29B)	107.8	O(9A)-Cl(2)-O(8)	117(2)
N(4)-H(4A)	0.88	N(8)-C(30)-C(31)	123.4(7)	O(10A)-Cl(2)-O(8)	55.8(17)
N(5)-Zn(1)	2.530(6)	N(8)-C(30)-C(29)	115.3(6)	O(10)-Cl(2)-O(8)	108.8(8)
N(6)-H(6)	0.88	C(31)-C(30)-C(29)	121.3(7)	C(44)-C(43)-H(43A)	109.5
N(7)-H(7)	0.88	C(30)-C(31)-C(32)	118.5(8)	C(44)-C(43)-H(43B)	109.5
N(8)-Zn(1)	2.514(6)	C(30)-C(31)-H(31)	120.8	H(43A)-C(43)-H(43B)	109.5
N(9)-H(9)	0.88	C(32)-C(31)-H(31)	120.8	C(44)-C(43)-H(43C)	109.5
N(10)-H(10A)	0.88	C(33)-C(32)-C(31)	118.2(8)	H(43A)-C(43)-H(43C)	109.5
O(4)-Cl(1)	1.420(6)	C(33)-C(32)-H(32)	120.9	H(43B)-C(43)-H(43C)	109.5
O(5)-Cl(1)	1.439(6)	C(31)-C(32)-H(32)	120.9	N(11)-C(44)-C(43)	179.2(10)
O(6)-Cl(1)	1.447(6)	C(34)-C(33)-C(32)	119.2(8)	C(46)-C(45)-H(45A)	109.5
O(7)-Cl(1)	1.410(8)	C(34)-C(33)-H(33)	120.4	C(46)-C(45)-H(45B)	109.5
O(8)-Cl(2)	1.420(7)	C(32)-C(33)-H(33)	120.4	H(45A)-C(45)-H(45B)	109.5
O(9)-Cl(2)	1.414(6)	N(8)-C(34)-C(33)	123.9(7)	C(46)-C(45)-H(45C)	109.5
O(10)-Cl(2)	1.418(7)	N(8)-C(34)-N(9)	118.0(6)	H(45A)-C(45)-H(45C)	109.5
O(11)-Cl(2)	1.414(6)	C(33)-C(34)-N(9)	117.8(7)	H(45B)-C(45)-H(45C)	109.5
O(8A)-Cl(2)	1.414(5)	N(9)-C(35)-N(10)	115.4(6)	N(12)-C(46)-C(45)	170(2)
O(9A)-Cl(2)	1.415(5)	N(9)-C(35)-S(3)	127.1(6)		
O(10A)-Cl(2)	1.417(5)	N(10)-C(35)-S(3)	117.4(5)		
O(11A)-Cl(2)	1.414(5)	O(3)-C(36)-N(10)	121.1(7)		
S(1)-Zn(1)	2.6911(18)	O(3)-C(36)-C(37)	121.8(7)		

Appendix 3: Crystals data

S(2)-Zn(1)	2.6602(17)	N(10)-C(36)-C(37)	117.1(7)		
S(3)-Zn(1)	2.6783(17)	C(38)-C(37)-C(42)	120.7(8)		
C(43)-C(44)	1.433(10)	C(38)-C(37)-C(36)	116.1(7)		
C(43)-H(43A)	0.98	C(42)-C(37)-C(36)	123.1(7)		
C(43)-H(43B)	0.98	C(39)-C(38)-C(37)	119.6(9)		
C(43)-H(43C)	0.98	C(39)-C(38)-H(38)	120.2		
C(44)-N(11)	1.134(9)	C(37)-C(38)-H(38)	120.2		
C(45)-C(46)	1.434(11)	C(38)-C(39)-C(40)	120.4(10)		
C(45)-H(45A)	0.98	C(38)-C(39)-H(39)	119.8		
C(45)-H(45B)	0.98	C(40)-C(39)-H(39)	119.8		
C(45)-H(45C)	0.98	C(39)-C(40)-C(41)	120.6(9)		
C(46)-N(12)	1.136(10)	C(39)-C(40)-H(40)	119.7		

Appendix 3: Crystals data

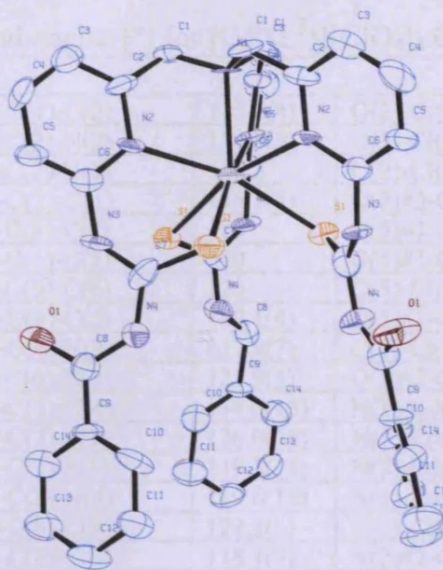


Table P.1: Crystal data and structure refinement for $[\text{Cd}^{\text{II}}(\text{L}^3)][\text{ClO}_4]_2 \cdot 0.5(\text{H}_2\text{O})$. 4.6

Identification code	ala0838	
Empirical formula	C ₄₂ H ₃₇ Cd Cl ₂ N ₁₀ O _{11.50} S ₃	
Formula weight	1145.30	
Temperature	150(2) K	
Wavelength	0.71073 Å	
Crystal system	Trigonal	
Space group	R-3	
Unit cell dimensions	a = 13.8780(17) Å	α = 90°.
	b = 13.8780(17) Å	β = 90°.
	c = 43.257(8) Å	γ = 120°.
Volume	7215.1(18) Å ³	
Z	6	
Density (calculated)	1.582 Mg/m ³	
Absorption coefficient	0.766 mm ⁻¹	
F(000)	3486	
Crystal size	0.20 x 0.04 x 0.02 mm ³	
Theta range for data collection	2.90 to 27.52°.	
Index ranges	-9 ≤ h ≤ 16, -13 ≤ k ≤ 13, -55 ≤ l ≤ 30	
Reflections collected	2571	
Independent reflections	1420 [R(int) = 0.1127]	
Completeness to theta = 27.52°	38.5 %	
Max. and min. transmission	0.9848 and 0.8619	
Refinement method	Full-matrix least-squares on F ²	
Data / restraints / parameters	1420 / 12 / 174	
Goodness-of-fit on F ²	1.067	
Final R indices [I > 2σ(I)]	R ₁ = 0.0856, wR ₂ = 0.2231	
R indices (all data)	R ₁ = 0.1229, wR ₂ = 0.2593	
Largest diff. peak and hole	0.776 and -0.906 e.Å ⁻³	

Appendix 3: Crystals data

Table P.2: Bond lengths [Å] and angles [°] for [Cd^{II}(L³)](ClO₄)₂·0.5(H₂O). 4.6

C(1)-N(1)	1.439(7)	N(1)-C(1)-C(2)	115.2(4)	O(2)-Cl(1)-O(2)#3	110.5(6)
C(1)-C(2)	1.4853	C(3)-C(2)-N(2)	119.8(3)	O(3)-Cl(1)-O(2)#4	108.4(6)
C(2)-C(3)	1.39	C(3)-C(2)-C(1)	124.2	O(2)-Cl(1)-O(2)#4	110.5(6)
C(2)-N(2)	1.394(11)	N(2)-C(2)-C(1)	115.7(3)	O(2)#3-Cl(1)-O(2)#4	110.5(6)
C(3)-C(4)	1.39	C(4)-C(3)-C(2)	120	O(5)#1-Cl(2)-O(5)	109.7(7)
C(4)-C(5)	1.39	C(3)-C(4)-C(5)	120	O(5)#1-Cl(2)-O(5)#2	109.7(7)
C(5)-C(6)	1.39	C(4)-C(5)-C(6)	120	O(5)-Cl(2)-O(5)#2	109.7(7)
C(6)-N(2)	1.385(8)	N(2)-C(6)-C(5)	120.1(4)	O(5)#1-Cl(2)-O(4)	109.3(7)
C(6)-N(3)	1.419(13)	N(2)-C(6)-N(3)	117.8(7)	O(5)-Cl(2)-O(4)	109.3(7)
C(7)-N(3)	1.319(18)	C(5)-C(6)-N(3)	121.9(5)	O(5)#2-Cl(2)-O(4)	109.3(7)
C(7)-N(4)	1.374(19)	N(3)-C(7)-N(4)	114.8(15)	N(1)-Cd(1)-N(2)	71.0(2)
C(7)-S(1)	1.652(17)	N(3)-C(7)-S(1)	126.0(16)	N(1)-Cd(1)-N(2)#2	71.0(2)
C(8)-O(1)	1.268(12)	N(4)-C(7)-S(1)	119.2(11)	N(2)-Cd(1)-N(2)#2	110.0(2)
C(8)-N(4)	1.357(14)	O(1)-C(8)-N(4)	119.6(10)	N(1)-Cd(1)-N(2)#1	71.0(2)
C(8)-C(9)	1.4525	O(1)-C(8)-C(9)	122.3(6)	N(2)-Cd(1)-N(2)#1	110.0(2)
C(9)-C(10)	1.39	N(4)-C(8)-C(9)	118.1(7)	N(2)#2-Cd(1)-N(2)#1	110.0(2)
C(9)-C(14)	1.39	C(10)-C(9)-C(14)	120	N(1)-Cd(1)-S(1)#2	124.11(9)
C(10)-C(11)	1.39	C(10)-C(9)-C(8)	121.8	N(2)-Cd(1)-S(1)#2	164.8(2)
C(11)-C(12)	1.39	C(14)-C(9)-C(8)	118.2	N(2)#2-Cd(1)-S(1)#2	76.58(17)
C(12)-C(13)	1.39	C(11)-C(10)-C(9)	120	N(2)#1-Cd(1)-S(1)#2	79.27(16)
C(13)-C(14)	1.39	C(10)-C(11)-C(12)	120	N(1)-Cd(1)-S(1)	124.11(9)
N(1)-C(1)#1	1.439(7)	C(13)-C(12)-C(11)	120	N(2)-Cd(1)-S(1)	76.58(17)
N(1)-C(1)#2	1.439(7)	C(12)-C(13)-C(14)	120	N(2)#2-Cd(1)-S(1)	79.27(16)
N(1)-Cd(1)	2.405(10)	C(13)-C(14)-C(9)	120	N(2)#1-Cd(1)-S(1)	164.8(2)
N(2)-Cd(1)	2.491(3)	C(1)#1-N(1)-C(1)	110.8(4)	S(1)#2-Cd(1)-S(1)	91.63(13)
O(2)-Cl(1)	1.413(12)	C(1)#1-N(1)-C(1)#2	110.8(4)	N(1)-Cd(1)-S(1)#1	124.11(9)
O(3)-Cl(1)	1.40(2)	C(1)-N(1)-C(1)#2	110.8(4)	N(2)-Cd(1)-S(1)#1	79.27(16)
O(4)-Cl(2)	1.58(3)	C(1)#1-N(1)-Cd(1)	108.1(4)	N(2)#2-Cd(1)-S(1)#1	164.8(2)
O(5)-Cl(2)	1.423(12)	C(1)-N(1)-Cd(1)	108.1(4)	N(2)#1-Cd(1)-S(1)#1	76.58(17)
S(1)-Cd(1)	2.661(4)	C(1)#2-N(1)-Cd(1)	108.1(4)	S(1)#2-Cd(1)-S(1)#1	91.63(13)
Cl(1)-O(2)#3	1.413(12)	C(6)-N(2)-C(2)	120.1(5)	S(1)-Cd(1)-S(1)#1	91.63(13)
Cl(1)-O(2)#4	1.413(12)	C(6)-N(2)-Cd(1)	127.1(6)		
Cl(2)-O(5)#1	1.423(12)	C(2)-N(2)-Cd(1)	112.6(4)		
Cl(2)-O(5)#2	1.423(12)	C(7)-N(3)-C(6)	130.0(13)		
Cd(1)-N(2)#2	2.491(3)	C(8)-N(4)-C(7)	129.8(12)		
Cd(1)-N(2)#1	2.491(3)	C(7)-S(1)-Cd(1)	101.2(6)		
Cd(1)-S(1)#2	2.661(4)	O(3)-Cl(1)-O(2)	108.4(6)		
Cd(1)-S(1)#1	2.661(4)	O(3)-Cl(1)-O(2)#3	108.4(6)		

Symmetry transformations used to generate equivalent atoms:

#1 -x+y,-x,z #2 -y,x-y,z #3 -x+y,-x+1,z #4 -y+1,x-y+1,z

Appendix 3: Crystals data

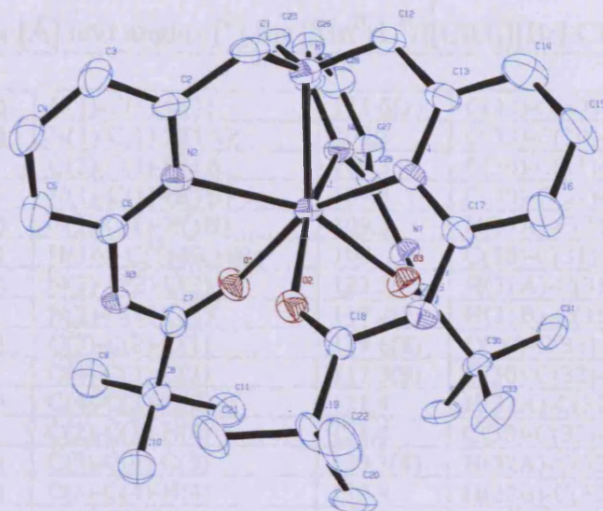


Table Q.1: Crystal data and structure refinement for $[\text{Mn}^{\text{II}}(\text{L}^4)][\text{ClO}_4][\text{Br}]\cdot\text{CH}_3\text{CN} \cdot 5.1$

Identification code	aja0901	
Empirical formula	C ₃₅ H ₄₈ Br Cl Mn N ₈ O ₇	
Formula weight	863.11	
Temperature	150(2) K	
Wavelength	0.71073 Å	
Crystal system	Monoclinic	
Space group	P2 ₁ /m	
Unit cell dimensions	a = 10.8160(2) Å	α = 90°.
	b = 40.8620(8) Å	β = 116.9550(10)°.
	c = 11.1620(2) Å	γ = 90°.
Volume	4397.27(14) Å ³	
Z	4	
Density (calculated)	1.304 Mg/m ³	
Absorption coefficient	1.320 mm ⁻¹	
F(000)	1788	
Crystal size	0.25 x 0.20 x 0.15 mm ³	
Theta range for data collection	2.95 to 23.89°.	
Index ranges	-11 ≤ h ≤ 10, -45 ≤ k ≤ 39, -12 ≤ l ≤ 12	
Reflections collected	9447	
Independent reflections	5409 [R(int) = 0.0422]	
Completeness to theta = 23.89°	78.1 %	
Max. and min. transmission	0.8265 and 0.7337	
Refinement method	Full-matrix least-squares on F ²	
Data / restraints / parameters	5409 / 47 / 516	
Goodness-of-fit on F ²	1.059	
Final R indices [I > 2σ(I)]	R ₁ = 0.0783, wR ₂ = 0.1964	
R indices (all data)	R ₁ = 0.1007, wR ₂ = 0.2094	
Largest diff. peak and hole	1.660 and -1.207 e.Å ⁻³	

Appendix 3: Crystals data

Table Q.2: Bond lengths [Å] and angles [°] for $[\text{Mn}^{\text{II}}(\text{L}^4)][\text{ClO}_4][\text{Br}]\cdot\text{CH}_3\text{CN}\cdot 5.1$

C(1)-N(1)	1.487(11)	N(1)-C(1)-C(2)	111.6(7)	C(32)-C(30)-C(29)	110.4(7)
C(1)-C(2)	1.512(12)	N(1)-C(1)-H(1A)	109.3	C(33)-C(30)-C(29)	107.9(7)
C(1)-H(1A)	0.99	C(2)-C(1)-H(1A)	109.3	C(30)-C(31)-H(31A)	109.5
C(1)-H(1B)	0.99	N(1)-C(1)-H(1B)	109.3	C(30)-C(31)-H(31B)	109.5
C(2)-N(2)	1.345(10)	C(2)-C(1)-H(1B)	109.3	H(31A)-C(31)-H(31B)	109.5
C(2)-C(3)	1.389(12)	H(1A)-C(1)-H(1B)	108	C(30)-C(31)-H(31C)	109.5
C(3)-C(4)	1.373(13)	N(2)-C(2)-C(3)	123.2(8)	H(31A)-C(31)-H(31C)	109.5
C(3)-H(3)	0.95	N(2)-C(2)-C(1)	117.2(7)	H(31B)-C(31)-H(31C)	109.5
C(4)-C(5)	1.372(13)	C(3)-C(2)-C(1)	119.6(8)	C(30)-C(32)-H(32A)	109.5
C(4)-H(4)	0.95	C(4)-C(3)-C(2)	117.3(9)	C(30)-C(32)-H(32B)	109.5
C(5)-C(6)	1.384(12)	C(4)-C(3)-H(3)	121.4	H(32A)-C(32)-H(32B)	109.5
C(5)-H(5)	0.95	C(2)-C(3)-H(3)	121.4	C(30)-C(32)-H(32C)	109.5
C(6)-N(2)	1.335(11)	C(5)-C(4)-C(3)	120.3(8)	H(32A)-C(32)-H(32C)	109.5
C(6)-N(3)	1.406(10)	C(5)-C(4)-H(4)	119.9	H(32B)-C(32)-H(32C)	109.5
C(7)-O(1)	1.222(10)	C(3)-C(4)-H(4)	119.9	C(30)-C(33)-H(33A)	109.5
C(7)-N(3)	1.368(10)	C(4)-C(5)-C(6)	119.0(9)	C(30)-C(33)-H(33B)	109.5
C(7)-C(8)	1.524(12)	C(4)-C(5)-H(5)	120.5	H(33A)-C(33)-H(33B)	109.5
C(8)-C(11)	1.526(12)	C(6)-C(5)-H(5)	120.5	C(30)-C(33)-H(33C)	109.5
C(8)-C(10)	1.529(13)	N(2)-C(6)-C(5)	122.0(8)	H(33A)-C(33)-H(33C)	109.5
C(8)-C(9)	1.543(13)	N(2)-C(6)-N(3)	120.2(7)	H(33B)-C(33)-H(33C)	109.5
C(9)-H(9A)	0.98	C(5)-C(6)-N(3)	117.7(8)	C(12)-N(1)-C(23)	110.0(7)
C(9)-H(9B)	0.98	O(1)-C(7)-N(3)	122.1(8)	C(12)-N(1)-C(1)	111.1(7)
C(9)-H(9C)	0.98	O(1)-C(7)-C(8)	121.8(8)	C(23)-N(1)-C(1)	110.7(7)
C(10)-H(10A)	0.98	N(3)-C(7)-C(8)	116.2(7)	C(12)-N(1)-Mn(1)	109.9(5)
C(10)-H(10B)	0.98	C(7)-C(8)-C(11)	107.6(7)	C(23)-N(1)-Mn(1)	107.2(5)
C(10)-H(10C)	0.98	C(7)-C(8)-C(10)	110.7(7)	C(1)-N(1)-Mn(1)	107.8(5)
C(11)-H(11A)	0.98	C(11)-C(8)-C(10)	109.2(8)	C(6)-N(2)-C(2)	118.1(7)
C(11)-H(11B)	0.98	C(7)-C(8)-C(9)	110.5(7)	C(6)-N(2)-Mn(1)	126.6(6)
C(11)-H(11C)	0.98	C(11)-C(8)-C(9)	109.0(8)	C(2)-N(2)-Mn(1)	113.4(5)
C(12)-N(1)	1.475(10)	C(10)-C(8)-C(9)	109.7(7)	C(7)-N(3)-C(6)	129.6(7)
C(12)-C(13)	1.524(12)	C(8)-C(9)-H(9A)	109.5	C(7)-N(3)-H(3A)	115.2
C(12)-H(12A)	0.99	C(8)-C(9)-H(9B)	109.5	C(6)-N(3)-H(3A)	115.2
C(12)-H(12B)	0.99	H(9A)-C(9)-H(9B)	109.5	C(17)-N(4)-C(13)	118.5(7)
C(13)-N(4)	1.348(10)	C(8)-C(9)-H(9C)	109.5	C(17)-N(4)-Mn(1)	124.6(6)
C(13)-C(14)	1.377(12)	H(9A)-C(9)-H(9C)	109.5	C(13)-N(4)-Mn(1)	112.7(5)
C(14)-C(15)	1.375(14)	H(9B)-C(9)-H(9C)	109.5	C(18)-N(5)-C(17)	127.9(7)
C(14)-H(14)	0.95	C(8)-C(10)-H(10A)	109.5	C(18)-N(5)-H(5A)	116.1
C(15)-C(16)	1.378(13)	C(8)-C(10)-H(10B)	109.5	C(17)-N(5)-H(5A)	116.1
C(15)-H(15)	0.95	H(10A)-C(10)-H(10B)	109.5	C(28)-N(6)-C(24)	117.5(7)
C(16)-C(17)	1.402(12)	C(8)-C(10)-H(10C)	109.5	C(28)-N(6)-Mn(1)	128.6(6)
C(16)-H(16)	0.95	H(10A)-C(10)-H(10C)	109.5	C(24)-N(6)-Mn(1)	113.1(5)
C(17)-N(4)	1.332(11)	H(10B)-C(10)-H(10C)	109.5	C(29)-N(7)-C(28)	130.1(7)
C(17)-N(5)	1.402(10)	C(8)-C(11)-H(11A)	109.5	C(29)-N(7)-H(7)	115
C(18)-O(2)	1.229(10)	C(8)-C(11)-H(11B)	109.5	C(28)-N(7)-H(7)	115
C(18)-N(5)	1.361(10)	H(11A)-C(11)-H(11B)	109.5	O(2)-Mn(1)-O(1)	84.7(2)
C(18)-C(19)	1.532(12)	C(8)-C(11)-H(11C)	109.5	O(2)-Mn(1)-O(3)	86.1(2)
C(19)-C(20)	1.514(13)	H(11A)-C(11)-H(11C)	109.5	O(1)-Mn(1)-O(3)	85.2(2)
C(19)-C(21)	1.519(12)	H(11B)-C(11)-H(11C)	109.5	O(2)-Mn(1)-N(1)	126.2(2)
C(19)-C(22)	1.532(13)	N(1)-C(12)-C(13)	111.5(7)	O(1)-Mn(1)-N(1)	130.4(2)
C(20)-H(20A)	0.98	N(1)-C(12)-H(12A)	109.3	O(3)-Mn(1)-N(1)	128.9(2)
C(20)-H(20B)	0.98	C(13)-C(12)-H(12A)	109.3	O(2)-Mn(1)-N(2)	79.8(2)
C(20)-H(20C)	0.98	N(1)-C(12)-H(12B)	109.3	O(1)-Mn(1)-N(2)	76.7(2)
C(21)-H(21A)	0.98	C(13)-C(12)-H(12B)	109.3	O(3)-Mn(1)-N(2)	157.9(2)
C(21)-H(21B)	0.98	H(12A)-C(12)-H(12B)	108	N(1)-Mn(1)-N(2)	73.2(2)
C(21)-H(21C)	0.98	N(4)-C(13)-C(14)	122.8(8)	O(2)-Mn(1)-N(6)	161.1(2)
C(22)-H(22A)	0.98	N(4)-C(13)-C(12)	116.8(7)	O(1)-Mn(1)-N(6)	85.1(2)
C(22)-H(22B)	0.98	C(14)-C(13)-C(12)	120.5(8)	O(3)-Mn(1)-N(6)	77.2(2)

Appendix 3: Crystals data

C(22)-H(22C)	0.98	C(15)-C(14)-C(13)	118.7(9)	N(1)-Mn(1)-N(6)	72.1(2)
C(23)-N(1)	1.475(11)	C(15)-C(14)-H(14)	120.7	N(2)-Mn(1)-N(6)	113.2(2)
C(23)-C(24)	1.494(12)	C(13)-C(14)-H(14)	120.7	O(2)-Mn(1)-N(4)	76.5(2)
C(23)-H(23A)	0.99	C(14)-C(15)-C(16)	119.4(9)	O(1)-Mn(1)-N(4)	157.5(2)
C(23)-H(23B)	0.99	C(14)-C(15)-H(15)	120.3	O(3)-Mn(1)-N(4)	81.2(2)
C(24)-N(6)	1.356(11)	C(16)-C(15)-H(15)	120.3	N(1)-Mn(1)-N(4)	71.8(2)
C(24)-C(25)	1.374(12)	C(15)-C(16)-C(17)	118.8(9)	N(2)-Mn(1)-N(4)	111.5(2)
C(25)-C(26)	1.374(13)	C(15)-C(16)-H(16)	120.6	N(6)-Mn(1)-N(4)	109.1(2)
C(25)-H(25)	0.95	C(17)-C(16)-H(16)	120.6	C(7)-O(1)-Mn(1)	132.0(6)
C(26)-C(27)	1.377(12)	N(4)-C(17)-N(5)	120.5(7)	C(18)-O(2)-Mn(1)	134.5(5)
C(26)-H(26)	0.95	N(4)-C(17)-C(16)	121.7(8)	C(29)-O(3)-Mn(1)	134.1(5)
C(27)-C(28)	1.380(12)	N(5)-C(17)-C(16)	117.8(8)	O(6)#1-Cl(1)-O(6)	110.8(5)
C(27)-H(27)	0.95	O(2)-C(18)-N(5)	123.6(8)	O(6)#1-Cl(1)-O(4)	109.9(5)
C(28)-N(6)	1.351(11)	O(2)-C(18)-C(19)	119.9(7)	O(6)-Cl(1)-O(4)	109.9(5)
C(28)-N(7)	1.409(10)	N(5)-C(18)-C(19)	116.4(7)	O(6)#1-Cl(1)-O(5)	108.9(5)
C(29)-O(3)	1.240(10)	C(20)-C(19)-C(21)	110.6(8)	O(6)-Cl(1)-O(5)	108.9(5)
C(29)-N(7)	1.365(11)	C(20)-C(19)-C(22)	110.3(8)	O(4)-Cl(1)-O(5)	108.6(6)
C(29)-C(30)	1.539(11)	C(21)-C(19)-C(22)	108.8(7)	O(8)-Cl(2)-O(8)#1	48.5(10)
C(30)-C(31)	1.527(13)	C(20)-C(19)-C(18)	106.7(7)	O(8)-Cl(2)-O(10)#1	125.8(5)
C(30)-C(32)	1.531(13)	C(21)-C(19)-C(18)	107.7(7)	O(8)#1-Cl(2)-O(10)#1	111.9(4)
C(30)-C(33)	1.531(13)	C(22)-C(19)-C(18)	112.7(8)	O(8)-Cl(2)-O(10)	111.9(4)
C(31)-H(31A)	0.98	C(19)-C(20)-H(20A)	109.5	O(8)#1-Cl(2)-O(10)	125.8(5)
C(31)-H(31B)	0.98	C(19)-C(20)-H(20B)	109.5	O(10)#1-Cl(2)-O(10)	29.9(8)
C(31)-H(31C)	0.98	H(20A)-C(20)-H(20B)	109.5	O(8)-Cl(2)-O(7)	111.7(4)
C(32)-H(32A)	0.98	C(19)-C(20)-H(20C)	109.5	O(8)#1-Cl(2)-O(7)	122.4(5)
C(32)-H(32B)	0.98	H(20A)-C(20)-H(20C)	109.5	O(10)#1-Cl(2)-O(7)	118.4(4)
C(32)-H(32C)	0.98	H(20B)-C(20)-H(20C)	109.5	O(10)-Cl(2)-O(7)	111.8(4)
C(33)-H(33A)	0.98	C(19)-C(21)-H(21A)	109.5	O(8)-Cl(2)-O(7)#1	122.4(5)
C(33)-H(33B)	0.98	C(19)-C(21)-H(21B)	109.5	O(8)#1-Cl(2)-O(7)#1	111.7(4)
C(33)-H(33C)	0.98	H(21A)-C(21)-H(21B)	109.5	O(10)#1-Cl(2)-O(7)#1	111.8(4)
N(1)-Mn(1)	2.264(7)	C(19)-C(21)-H(21C)	109.5	O(10)-Cl(2)-O(7)#1	118.4(4)
N(2)-Mn(1)	2.306(7)	H(21A)-C(21)-H(21C)	109.5	O(7)-Cl(2)-O(7)#1	23.4(8)
N(3)-H(3A)	0.88	H(21B)-C(21)-H(21C)	109.5	O(8)-Cl(2)-O(9)	107.1(4)
N(4)-Mn(1)	2.319(7)	C(19)-C(22)-H(22A)	109.5	O(8)#1-Cl(2)-O(9)	58.7(9)
N(5)-H(5A)	0.88	C(19)-C(22)-H(22B)	109.5	O(10)#1-Cl(2)-O(9)	77.1(8)
N(6)-Mn(1)	2.310(7)	H(22A)-C(22)-H(22B)	109.5	O(10)-Cl(2)-O(9)	106.8(4)
N(7)-H(7)	0.88	C(19)-C(22)-H(22C)	109.5	O(7)-Cl(2)-O(9)	107.2(4)
Mn(1)-O(2)	2.162(6)	H(22A)-C(22)-H(22C)	109.5	O(7)#1-Cl(2)-O(9)	83.9(8)
Mn(1)-O(1)	2.173(6)	H(22B)-C(22)-H(22C)	109.5	O(8)-Cl(2)-O(9)#1	58.7(9)
Mn(1)-O(3)	2.181(6)	N(1)-C(23)-C(24)	111.3(7)	O(8)#1-Cl(2)-O(9)#1	107.1(4)
Cl(1)-O(6)#1	1.445(4)	N(1)-C(23)-H(23A)	109.4	O(10)#1-Cl(2)-O(9)#1	106.8(4)
Cl(1)-O(6)	1.445(4)	C(24)-C(23)-H(23A)	109.4	O(10)-Cl(2)-O(9)#1	77.1(8)
Cl(1)-O(4)	1.448(9)	N(1)-C(23)-H(23B)	109.4	O(7)-Cl(2)-O(9)#1	83.9(8)
Cl(1)-O(5)	1.469(9)	C(24)-C(23)-H(23B)	109.4	O(7)#1-Cl(2)-O(9)#1	107.2(4)
Cl(2)-O(8)	1.438(4)	H(23A)-C(23)-H(23B)	108	O(9)-Cl(2)-O(9)#1	165.1(10)
Cl(2)-O(8)#1	1.438(4)	N(6)-C(24)-C(25)	122.4(8)	O(7)#1-O(7)-Cl(2)	78.3(4)
Cl(2)-O(10)#1	1.439(4)	N(6)-C(24)-C(23)	116.4(7)	O(8)#1-O(8)-Cl(2)	65.8(5)
Cl(2)-O(10)	1.439(4)	C(25)-C(24)-C(23)	121.1(8)	O(8)#1-O(8)-O(9)#1	128.4(3)
Cl(2)-O(7)	1.441(4)	C(24)-C(25)-C(26)	119.3(9)	Cl(2)-O(8)-O(9)#1	62.7(5)
Cl(2)-O(7)#1	1.441(4)	C(24)-C(25)-H(25)	120.4	O(8)#1-O(9)-Cl(2)	58.6(5)
Cl(2)-O(9)	1.497(4)	C(26)-C(25)-H(25)	120.4	O(10)#1-O(10)-Cl(2)	75.0(4)
Cl(2)-O(9)#1	1.497(4)	C(25)-C(26)-C(27)	119.3(9)	N(8)-C(34)-C(35)	179(3)
O(7)-O(7)#1	0.58(2)	C(25)-C(26)-H(26)	120.4	C(34)-C(35)-H(35A)	109.5
O(8)-O(8)#1	1.18(2)	C(27)-C(26)-H(26)	120.4	C(34)-C(35)-H(35B)	109.5
O(8)-O(9)#1	1.44(2)	C(26)-C(27)-C(28)	118.9(9)	H(35A)-C(35)-H(35B)	109.5
O(9)-O(8)#1	1.44(2)	C(26)-C(27)-H(27)	120.5	C(34)-C(35)-H(35C)	109.5
O(10)-O(10)#1	0.74(2)	C(28)-C(27)-H(27)	120.5	H(35A)-C(35)-H(35C)	109.5
N(8)-C(34)	1.09(2)	N(6)-C(28)-C(27)	122.5(8)	H(35B)-C(35)-H(35C)	109.5
C(34)-C(35)	1.51(3)	N(6)-C(28)-N(7)	119.3(7)	N(9)-C(36)-C(37)	164(3)

Appendix 3: Crystals data

C(35)-H(35A)	0.98	C(27)-C(28)-N(7)	118.2(8)	C(36)-C(37)-H(37A)	109.5
C(35)-H(35B)	0.98	O(3)-C(29)-N(7)	122.7(8)	C(36)-C(37)-H(37B)	109.5
C(35)-H(35C)	0.98	O(3)-C(29)-C(30)	120.7(7)	H(37A)-C(37)-H(37B)	109.5
N(9)-C(36)	1.10(2)	N(7)-C(29)-C(30)	116.5(8)	C(36)-C(37)-H(37C)	109.5
C(36)-C(37)	1.52(3)	C(31)-C(30)-C(32)	110.2(8)	H(37A)-C(37)-H(37C)	109.5
C(37)-H(37A)	0.98	C(31)-C(30)-C(33)	110.3(8)	H(37B)-C(37)-H(37C)	109.5
C(37)-H(37B)	0.98	C(32)-C(30)-C(33)	109.6(8)		
C(37)-H(37C)	0.98	C(31)-C(30)-C(29)	108.5(7)		

Symmetry transformations used to generate equivalent atoms:

#1 $x, -y+1/2, z$

Appendix 3: Crystals data

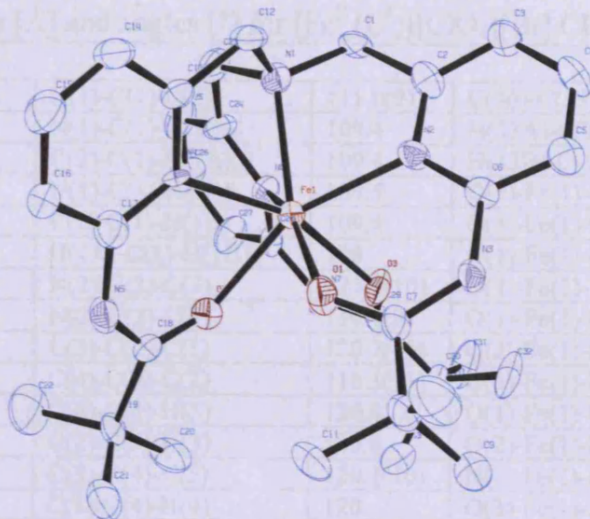


Table R.1: Crystal data and structure refinement for $[\text{Fe}^{\text{II}}(\text{L}^4)][\text{ClO}_4][\text{Br}]\cdot\text{CH}_3\text{CN}$. 5.2

Identification code	aja0918	
Empirical formula	C ₃₅ H ₄₈ Br Cl Fe N ₈ O ₇	
Formula weight	864.02	
Temperature	150(2) K	
Wavelength	0.71073 Å	
Crystal system	Monoclinic	
Space group	P2 ₁ /m	
Unit cell dimensions	a = 10.730(5) Å	α = 90°.
	b = 40.995(5) Å	β = 117.050(5)°.
	c = 11.101(5) Å	γ = 90°.
Volume	4349(3) Å ³	
Z	4	
Density (calculated)	1.320 Mg/m ³	
Absorption coefficient	1.378 mm ⁻¹	
F(000)	1792	
Crystal size	0.40 x 0.30 x 0.04 mm ³	
Theta range for data collection	3.31 to 23.32°.	
Index ranges	-11 ≤ h ≤ 11, -42 ≤ k ≤ 42, -11 ≤ l ≤ 11	
Reflections collected	7296	
Independent reflections	4787 [R(int) = 0.0380]	
Completeness to theta = 23.32°	74.8 %	
Max. and min. transmission	0.9469 and 0.6086	
Refinement method	Full-matrix least-squares on F ²	
Data / restraints / parameters	4787 / 315 / 545	
Goodness-of-fit on F ²	1.068	
Final R indices [I > 2σ(I)]	R1 = 0.0875, wR2 = 0.2140	
R indices (all data)	R1 = 0.1162, wR2 = 0.2294	
Largest diff. peak and hole	1.539 and -1.402 e.Å ⁻³	

Appendix 3: Crystals data

Table R.2: Bond lengths [Å] and angles [°] for [Fe^{II}(L⁴)](ClO₄)[Br].CH₃CN. 5.2

C(1)-N(1)	1.481(12)	N(1)-C(1)-C(2)	111.0(9)	C(30)-C(33)-H(33C)	109.5
C(1)-C(2)	1.497(15)	N(1)-C(1)-H(1A)	109.4	H(33A)-C(33)-H(33C)	109.5
C(1)-H(1A)	0.99	C(2)-C(1)-H(1A)	109.4	H(33B)-C(33)-H(33C)	109.5
C(1)-H(1B)	0.99	N(1)-C(1)-H(1B)	109.4	O(3)-Fe(1)-O(1)	83.5(3)
C(2)-N(2)	1.352(14)	C(2)-C(1)-H(1B)	109.4	O(3)-Fe(1)-O(2)	85.0(3)
C(2)-C(3)	1.382(14)	H(1A)-C(1)-H(1B)	108	O(1)-Fe(1)-O(2)	82.6(3)
C(3)-C(4)	1.362(15)	N(2)-C(2)-C(3)	123.1(10)	O(3)-Fe(1)-N(1)	126.8(3)
C(3)-H(3)	0.95	N(2)-C(2)-C(1)	116.1(9)	O(1)-Fe(1)-N(1)	131.7(3)
C(4)-C(5)	1.367(16)	C(3)-C(2)-C(1)	120.7(11)	O(2)-Fe(1)-N(1)	130.4(3)
C(4)-H(4)	0.95	C(4)-C(3)-C(2)	118.3(11)	O(3)-Fe(1)-N(4)	160.0(3)
C(5)-C(6)	1.399(14)	C(4)-C(3)-H(3)	120.8	O(1)-Fe(1)-N(4)	83.2(3)
C(5)-H(5)	0.95	C(2)-C(3)-H(3)	120.8	O(2)-Fe(1)-N(4)	78.5(3)
C(6)-N(2)	1.336(13)	C(3)-C(4)-C(5)	120.1(10)	N(1)-Fe(1)-N(4)	73.0(3)
C(6)-N(3)	1.400(13)	C(3)-C(4)-H(4)	120	O(3)-Fe(1)-N(2)	78.4(3)
C(7)-O(1)	1.249(11)	C(5)-C(4)-H(4)	120	O(1)-Fe(1)-N(2)	78.9(3)
C(7)-N(3)	1.363(12)	C(4)-C(5)-C(6)	118.8(10)	O(2)-Fe(1)-N(2)	156.3(3)
C(7)-C(8)	1.513(16)	C(4)-C(5)-H(5)	120.6	N(1)-Fe(1)-N(2)	73.3(3)
C(8)-C(10)	1.509(17)	C(6)-C(5)-H(5)	120.6	N(4)-Fe(1)-N(2)	113.5(3)
C(8)-C(11)	1.534(14)	N(2)-C(6)-C(5)	122.1(10)	O(3)-Fe(1)-N(6)	77.8(3)
C(8)-C(9)	1.551(17)	N(2)-C(6)-N(3)	119.9(8)	O(1)-Fe(1)-N(6)	155.2(3)
C(9)-H(9A)	0.98	C(5)-C(6)-N(3)	117.9(9)	O(2)-Fe(1)-N(6)	79.8(3)
C(9)-H(9B)	0.98	O(1)-C(7)-N(3)	121.9(10)	N(1)-Fe(1)-N(6)	73.1(3)
C(9)-H(9C)	0.98	O(1)-C(7)-C(8)	120.3(9)	N(4)-Fe(1)-N(6)	109.9(3)
C(10)-H(10A)	0.98	N(3)-C(7)-C(8)	117.7(8)	N(2)-Fe(1)-N(6)	112.5(3)
C(10)-H(10B)	0.98	C(10)-C(8)-C(7)	111.1(10)	C(12)-N(1)-C(1)	110.2(8)
C(10)-H(10C)	0.98	C(10)-C(8)-C(11)	109.5(10)	C(12)-N(1)-C(23)	110.2(8)
C(11)-H(11A)	0.98	C(7)-C(8)-C(11)	108.9(9)	C(1)-N(1)-C(23)	110.5(8)
C(11)-H(11B)	0.98	C(10)-C(8)-C(9)	110.4(10)	C(12)-N(1)-Fe(1)	108.5(7)
C(11)-H(11C)	0.98	C(7)-C(8)-C(9)	109.2(9)	C(1)-N(1)-Fe(1)	108.2(6)
C(12)-N(1)	1.469(14)	C(11)-C(8)-C(9)	107.6(10)	C(23)-N(1)-Fe(1)	109.2(7)
C(12)-C(13)	1.518(15)	C(8)-C(9)-H(9A)	109.5	C(6)-N(2)-C(2)	117.4(8)
C(12)-H(12A)	0.99	C(8)-C(9)-H(9B)	109.5	C(6)-N(2)-Fe(1)	127.0(7)
C(12)-H(12B)	0.99	H(9A)-C(9)-H(9B)	109.5	C(2)-N(2)-Fe(1)	114.2(6)
C(13)-N(4)	1.335(14)	C(8)-C(9)-H(9C)	109.5	C(7)-N(3)-C(6)	130.2(9)
C(13)-C(14)	1.418(15)	H(9A)-C(9)-H(9C)	109.5	C(7)-N(3)-H(3A)	114.9
C(14)-C(15)	1.388(16)	H(9B)-C(9)-H(9C)	109.5	C(6)-N(3)-H(3A)	114.9
C(14)-H(14)	0.95	C(8)-C(10)-H(10A)	109.5	C(13)-N(4)-C(17)	117.8(10)
C(15)-C(16)	1.356(16)	C(8)-C(10)-H(10B)	109.5	C(13)-N(4)-Fe(1)	113.4(6)
C(15)-H(15)	0.95	H(10A)-C(10)-H(10B)	109.5	C(17)-N(4)-Fe(1)	128.2(8)
C(16)-C(17)	1.394(16)	C(8)-C(10)-H(10C)	109.5	C(18)-N(5)-C(17)	129.0(9)
C(16)-H(16)	0.95	H(10A)-C(10)-H(10C)	109.5	C(18)-N(5)-H(5A)	115.5
C(17)-N(4)	1.339(14)	H(10B)-C(10)-H(10C)	109.5	C(17)-N(5)-H(5A)	115.5
C(17)-N(5)	1.409(15)	C(8)-C(11)-H(11A)	109.5	C(28)-N(6)-C(24)	118.1(9)
C(18)-O(2)	1.236(12)	C(8)-C(11)-H(11B)	109.5	C(28)-N(6)-Fe(1)	125.5(7)
C(18)-N(5)	1.346(14)	H(11A)-C(11)-H(11B)	109.5	C(24)-N(6)-Fe(1)	113.0(7)
C(18)-C(19)	1.543(15)	C(8)-C(11)-H(11C)	109.5	C(29)-N(7)-C(28)	128.1(10)
C(19)-C(20)	1.528(15)	H(11A)-C(11)-H(11C)	109.5	C(29)-N(7)-H(7)	116
C(19)-C(21)	1.534(17)	H(11B)-C(11)-H(11C)	109.5	C(28)-N(7)-H(7)	116
C(19)-C(22)	1.551(15)	N(1)-C(12)-C(13)	108.7(9)	C(7)-O(1)-Fe(1)	131.2(7)
C(20)-H(20A)	0.98	N(1)-C(12)-H(12A)	110	C(18)-O(2)-Fe(1)	132.9(8)
C(20)-H(20B)	0.98	C(13)-C(12)-H(12A)	110	C(29)-O(3)-Fe(1)	134.2(6)
C(20)-H(20C)	0.98	N(1)-C(12)-H(12B)	110	O(4)#1-Cl(1)-O(4)	109.55(10)
C(21)-H(21A)	0.98	C(13)-C(12)-H(12B)	110	O(4)#1-Cl(1)-O(4A)	157.1(4)
C(21)-H(21B)	0.98	H(12A)-C(12)-H(12B)	108.3	O(4)-Cl(1)-O(4A)	65.6(2)

Appendix 3: Crystals data

C(21)-H(21C)	0.98	N(4)-C(13)-C(14)	124.2(10)	O(4)#1-Cl(1)-O(4A)#1	65.6(2)
C(22)-H(22A)	0.98	N(4)-C(13)-C(12)	117.6(10)	O(4)-Cl(1)-O(4A)#1	157.1(4)
C(22)-H(22B)	0.98	C(14)-C(13)-C(12)	118.2(11)	O(4A)-Cl(1)-O(4A)#1	109.51(10)
C(22)-H(22C)	0.98	C(15)-C(14)-C(13)	115.3(12)	O(4)#1-Cl(1)-O(5)	109.51(7)
C(23)-N(1)	1.488(13)	C(15)-C(14)-H(14)	122.4	O(4)-Cl(1)-O(5)	109.51(7)
C(23)-C(24)	1.498(16)	C(13)-C(14)-H(14)	122.4	O(4A)-Cl(1)-O(5)	56.02(15)
C(23)-H(23A)	0.99	C(16)-C(15)-C(14)	121.4(11)	O(4A)#1-Cl(1)-O(5)	56.02(15)
C(23)-H(23B)	0.99	C(16)-C(15)-H(15)	119.3	O(4)#1-Cl(1)-O(5A)	56.05(15)
C(24)-N(6)	1.363(13)	C(14)-C(15)-H(15)	119.3	O(4)-Cl(1)-O(5A)	56.05(15)
C(24)-C(25)	1.385(16)	C(15)-C(16)-C(17)	119.1(11)	O(4A)-Cl(1)-O(5A)	109.47(7)
C(25)-C(26)	1.388(17)	C(15)-C(16)-H(16)	120.5	O(4A)#1-Cl(1)-O(5A)	109.47(7)
C(25)-H(25)	0.95	C(17)-C(16)-H(16)	120.5	O(5)-Cl(1)-O(5A)	110.9(8)
C(26)-C(27)	1.385(16)	N(4)-C(17)-C(16)	122.1(12)	O(4)#1-Cl(1)-O(6A)	92.9(5)
C(26)-H(26)	0.95	N(4)-C(17)-N(5)	120.4(10)	O(4)-Cl(1)-O(6A)	92.9(5)
C(27)-C(28)	1.387(15)	C(16)-C(17)-N(5)	117.5(10)	O(4A)-Cl(1)-O(6A)	109.47(7)
C(27)-H(27)	0.95	O(2)-C(18)-N(5)	123.6(11)	O(4A)#1-Cl(1)-O(6A)	109.47(7)
C(28)-N(6)	1.328(13)	O(2)-C(18)-C(19)	119.5(10)	O(5)-Cl(1)-O(6A)	139.7(8)
C(28)-N(7)	1.405(13)	N(5)-C(18)-C(19)	116.7(9)	O(5A)-Cl(1)-O(6A)	109.43(10)
C(29)-O(3)	1.221(13)	C(20)-C(19)-C(21)	109.4(10)	O(4)#1-Cl(1)-O(6)	109.43(7)
C(29)-N(7)	1.376(14)	C(20)-C(19)-C(18)	109.2(9)	O(4)-Cl(1)-O(6)	109.43(7)
C(29)-C(30)	1.540(14)	C(21)-C(19)-C(18)	110.2(9)	O(4A)-Cl(1)-O(6)	92.9(5)
C(30)-C(33)	1.524(16)	C(20)-C(19)-C(22)	110.2(10)	O(4A)#1-Cl(1)-O(6)	92.9(5)
C(30)-C(31)	1.524(16)	C(21)-C(19)-C(22)	110.0(9)	O(5)-Cl(1)-O(6)	109.40(10)
C(30)-C(32)	1.544(15)	C(18)-C(19)-C(22)	107.9(9)	O(5A)-Cl(1)-O(6)	139.7(8)
C(31)-H(31A)	0.98	C(19)-C(20)-H(20A)	109.5	O(6A)-Cl(1)-O(6)	30.3(8)
C(31)-H(31B)	0.98	C(19)-C(20)-H(20B)	109.5	O(5A)-O(4)-Cl(1)	62.01(9)
C(31)-H(31C)	0.98	H(20A)-C(20)-H(20B)	109.5	O(5A)-O(4)-O(4A)	107.5(4)
C(32)-H(32A)	0.98	C(19)-C(20)-H(20C)	109.5	Cl(1)-O(4)-O(4A)	57.20(11)
C(32)-H(32B)	0.98	H(20A)-C(20)-H(20C)	109.5	O(4A)-O(5)-O(4A)#1	120.8(5)
C(32)-H(32C)	0.98	H(20B)-C(20)-H(20C)	109.5	O(4A)-O(5)-Cl(1)	61.97(9)
C(33)-H(33A)	0.98	C(19)-C(21)-H(21A)	109.5	O(4A)#1-O(5)-Cl(1)	61.97(9)
C(33)-H(33B)	0.98	C(19)-C(21)-H(21B)	109.5	O(6A)-O(6)-Cl(1)	74.8(4)
C(33)-H(33C)	0.98	H(21A)-C(21)-H(21B)	109.5	O(7)#1-Cl(2)-O(7)	109.53(10)
Fe(1)-O(3)	2.129(7)	C(19)-C(21)-H(21C)	109.5	O(7)#1-Cl(2)-O(9)	109.49(7)
Fe(1)-O(1)	2.133(7)	H(21A)-C(21)-H(21C)	109.5	O(7)-Cl(2)-O(9)	109.49(7)
Fe(1)-O(2)	2.155(7)	H(21B)-C(21)-H(21C)	109.5	O(7)#1-Cl(2)-O(7A)	141.02(11)
Fe(1)-N(1)	2.226(9)	C(19)-C(22)-H(22A)	109.5	O(7)-Cl(2)-O(7A)	56.20(10)
Fe(1)-N(4)	2.250(8)	C(19)-C(22)-H(22B)	109.5	O(9)-Cl(2)-O(7A)	109.49(7)
Fe(1)-N(2)	2.252(8)	H(22A)-C(22)-H(22B)	109.5	O(7)#1-Cl(2)-O(7A)#1	56.20(10)
Fe(1)-N(6)	2.259(9)	C(19)-C(22)-H(22C)	109.5	O(7)-Cl(2)-O(7A)#1	141.02(11)
N(3)-H(3A)	0.88	H(22A)-C(22)-H(22C)	109.5	O(9)-Cl(2)-O(7A)#1	109.49(7)
N(5)-H(5A)	0.88	H(22B)-C(22)-H(22C)	109.5	O(7A)-Cl(2)-O(7A)#1	109.47(10)
N(7)-H(7)	0.88	N(1)-C(23)-C(24)	111.8(9)	O(7)#1-Cl(2)-O(8A)	56.29(6)
Cl(1)-O(4)#1	1.4387(8)	N(1)-C(23)-H(23A)	109.3	O(7)-Cl(2)-O(8A)	56.29(6)
Cl(1)-O(4)	1.4387(8)	C(24)-C(23)-H(23A)	109.3	O(9)-Cl(2)-O(8A)	109.47(10)
Cl(1)-O(4A)	1.4389(8)	N(1)-C(23)-H(23B)	109.3	O(7A)-Cl(2)-O(8A)	109.46(7)
Cl(1)-O(4A)#1	1.4389(8)	C(24)-C(23)-H(23B)	109.3	O(7A)#1-Cl(2)-O(8A)	109.46(7)
Cl(1)-O(5)	1.4394(12)	H(23A)-C(23)-H(23B)	107.9	O(7)#1-Cl(2)-O(8)	109.44(7)
Cl(1)-O(5A)	1.4396(12)	N(6)-C(24)-C(25)	122.4(11)	O(7)-Cl(2)-O(8)	109.44(7)
Cl(1)-O(6A)	1.4396(12)	N(6)-C(24)-C(23)	116.3(10)	O(9)-Cl(2)-O(8)	109.44(10)
Cl(1)-O(6)	1.4400(11)	C(25)-C(24)-C(23)	121.2(10)	O(7A)-Cl(2)-O(8)	56.26(6)
O(4)-O(5A)	1.352(3)	C(24)-C(25)-C(26)	118.6(11)	O(7A)#1-Cl(2)-O(8)	56.26(6)
O(4)-O(4A)	1.559(4)	C(24)-C(25)-H(25)	120.7	O(8A)-Cl(2)-O(8)	141.09(15)
O(5)-O(4A)	1.352(3)	C(26)-C(25)-H(25)	120.7	O(7A)-O(7)-O(8A)	120.04(9)
O(5)-O(4A)#1	1.352(3)	C(27)-C(26)-C(25)	118.9(11)	O(7A)-O(7)-Cl(2)	61.92(6)
O(6)-O(6A)	0.752(19)	C(27)-C(26)-H(26)	120.6	O(8A)-O(7)-Cl(2)	61.88(5)

Appendix 3: Crystals data

Cl(2)-O(7)#1	1.4388(8)	C(25)-C(26)-H(26)	120.6	O(7A)#1-O(8)-O(7A)	119.92(17)
Cl(2)-O(7)	1.4388(8)	C(26)-C(27)-C(28)	119.2(12)	O(7A)#1-O(8)-Cl(2)	61.85(7)
Cl(2)-O(9)	1.4391(11)	C(26)-C(27)-H(27)	120.4	O(7A)-O(8)-Cl(2)	61.85(7)
Cl(2)-O(7A)	1.4392(8)	C(28)-C(27)-H(27)	120.4	N(8)-C(35)-C(34)	176.969(1)
Cl(2)-O(7A)#1	1.4392(8)	N(6)-C(28)-C(27)	122.6(10)	C(35)-C(34)-H(34A)	109.5
Cl(2)-O(8A)	1.4395(12)	N(6)-C(28)-N(7)	119.7(9)	C(35)-C(34)-H(34B)	109.5
Cl(2)-O(8)	1.4399(11)	C(27)-C(28)-N(7)	117.7(10)	H(34A)-C(34)-H(34B)	109.5
O(7)-O(7A)	1.356(3)	O(3)-C(29)-N(7)	122.6(9)	C(35)-C(34)-H(34C)	109.5
O(7)-O(8A)	1.3577(14)	O(3)-C(29)-C(30)	122.2(10)	H(34A)-C(34)-H(34C)	109.5
O(8)-O(7A)#1	1.3574(14)	N(7)-C(29)-C(30)	115.1(10)	H(34B)-C(34)-H(34C)	109.5
O(8)-O(7A)	1.3574(14)	C(33)-C(30)-C(31)	111.8(10)	C(37)-C(36)-H(36A)	109.5
N(8)-C(35)	1.1082(3)	C(33)-C(30)-C(29)	106.9(8)	C(37)-C(36)-H(36B)	109.5
C(35)-C(34)	1.5060(4)	C(31)-C(30)-C(29)	113.2(10)	H(36A)-C(36)-H(36B)	109.5
C(34)-H(34A)	0.98	C(33)-C(30)-C(32)	109.5(10)	C(37)-C(36)-H(36C)	109.5
C(34)-H(34B)	0.98	C(31)-C(30)-C(32)	109.4(9)	H(36A)-C(36)-H(36C)	109.5
C(34)-H(34C)	0.98	C(29)-C(30)-C(32)	105.9(9)	H(36B)-C(36)-H(36C)	109.5
N(9)-C(37)	1.18(4)	C(30)-C(31)-H(31A)	109.5	N(9)-C(37)-C(36)	178(3)
C(36)-C(37)	1.43(4)	C(30)-C(31)-H(31B)	109.5	O(4)-O(5A)-O(4)#1	120.7(5)
C(36)-H(36A)	0.98	H(31A)-C(31)-H(31B)	109.5	O(4)-O(5A)-Cl(1)	61.94(9)
C(36)-H(36B)	0.98	C(30)-C(31)-H(31C)	109.5	O(4)#1-O(5A)-Cl(1)	61.94(9)
C(36)-H(36C)	0.98	H(31A)-C(31)-H(31C)	109.5	O(5)-O(4A)-Cl(1)	62.01(8)
O(5A)-O(4)#1	1.352(3)	H(31B)-C(31)-H(31C)	109.5	O(5)-O(4A)-O(4)	107.5(4)
O(8A)-O(7)#1	1.3577(13)	C(30)-C(32)-H(32A)	109.5	Cl(1)-O(4A)-O(4)	57.19(11)
		C(30)-C(32)-H(32B)	109.5	O(6)-O(6A)-Cl(1)	74.9(4)
		H(32A)-C(32)-H(32B)	109.5	O(7)-O(7A)-O(8)	120.05(9)
		C(30)-C(32)-H(32C)	109.5	O(7)-O(7A)-Cl(2)	61.89(6)
		H(32A)-C(32)-H(32C)	109.5	O(8)-O(7A)-Cl(2)	61.89(4)
		H(32B)-C(32)-H(32C)	109.5	O(7)-O(8A)-O(7)#1	119.90(17)
		C(30)-C(33)-H(33A)	109.5	O(7)-O(8A)-Cl(2)	61.83(7)
		C(30)-C(33)-H(33B)	109.5	O(7)#1-O(8A)-Cl(2)	61.83(7)
		H(33A)-C(33)-H(33B)	109.5		

Symmetry transformations used to generate equivalent atoms:

#1 x,-y+1/2,z

Appendix 3: Crystals data

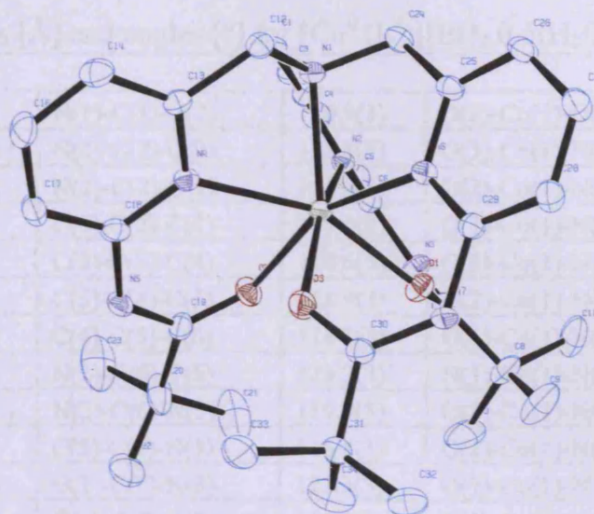


Table S.1: Crystal data and structure refinement for $[\text{Co}^{\text{II}}(\text{L}^4)][\text{Br}]_2 \cdot 0.5(\text{H}_2\text{O}) \cdot 2(\text{CH}_3\text{CN})$. **5.3**

Identification code	aja1001b	
Empirical formula	C ₃₇ H ₅₂ Br ₂ Co N ₉ O _{3.50}	
Formula weight	897.63	
Temperature	150(2) K	
Wavelength	0.71073 Å	
Crystal system	Monoclinic	
Space group	C2/c	
Unit cell dimensions	a = 11.1532(3) Å	α = 90°.
	b = 19.6165(5) Å	β = 90.6930(10)°.
	c = 37.6128(12) Å	γ = 90°.
Volume	8228.6(4) Å ³	
Z	8	
Density (calculated)	1.449 Mg/m ³	
Absorption coefficient	2.407 mm ⁻¹	
F(000)	3696	
Crystal size	0.40 x 0.40 x 0.40 mm ³	
Theta range for data collection	2.67 to 27.42°.	
Index ranges	-14 ≤ h ≤ 14, -25 ≤ k ≤ 18, -48 ≤ l ≤ 48	
Reflections collected	13096	
Independent reflections	8546 [R(int) = 0.0366]	
Completeness to theta = 27.42°	90.9 %	
Max. and min. transmission	0.4460 and 0.4460	
Refinement method	Full-matrix least-squares on F ²	
Data / restraints / parameters	8546 / 0 / 482	
Goodness-of-fit on F ²	1.045	
Final R indices [I > 2σ(I)]	R1 = 0.0486, wR2 = 0.0973	
R indices (all data)	R1 = 0.0709, wR2 = 0.1070	
Largest diff. peak and hole	0.793 and -0.600 e.Å ⁻³	

Appendix 3: Crystals data

Table S.2: Bond lengths [Å] and angles [°] for [Co^{II}(L⁴)]Br₂·0.5(H₂O)·2(CH₃CN). 5.3

C(1)-N(1)	1.472(4)	N(1)-C(1)-C(2)	110.9(3)	O(2)-Co(1)-O(1)	83.22(10)
C(1)-C(2)	1.506(5)	N(2)-C(2)-C(3)	123.3(3)	O(3)-Co(1)-N(1)	127.23(10)
C(2)-N(2)	1.350(4)	N(2)-C(2)-C(1)	115.6(3)	O(2)-Co(1)-N(1)	129.94(10)
C(2)-C(3)	1.381(5)	C(3)-C(2)-C(1)	121.0(3)	O(1)-Co(1)-N(1)	130.45(10)
C(3)-C(4)	1.388(5)	C(2)-C(3)-C(4)	118.6(3)	O(3)-Co(1)-N(6)	78.18(10)
C(4)-C(5)	1.383(5)	C(5)-C(4)-C(3)	118.9(3)	O(2)-Co(1)-N(6)	155.65(10)
C(5)-C(6)	1.391(5)	C(4)-C(5)-C(6)	118.7(3)	O(1)-Co(1)-N(6)	78.45(10)
C(6)-N(2)	1.337(4)	N(2)-C(6)-C(5)	123.2(3)	N(1)-Co(1)-N(6)	74.40(10)
C(6)-N(3)	1.409(4)	N(2)-C(6)-N(3)	119.9(3)	O(3)-Co(1)-N(2)	159.06(10)
C(7)-O(1)	1.230(4)	C(5)-C(6)-N(3)	116.8(3)	O(2)-Co(1)-N(2)	80.12(10)
C(7)-N(3)	1.365(4)	O(1)-C(7)-N(3)	123.3(3)	O(1)-Co(1)-N(2)	79.01(9)
C(7)-C(8)	1.535(4)	O(1)-C(7)-C(8)	121.0(3)	N(1)-Co(1)-N(2)	73.71(10)
C(8)-C(10)	1.522(6)	N(3)-C(7)-C(8)	115.7(3)	N(6)-Co(1)-N(2)	111.52(10)
C(8)-C(9)	1.526(6)	C(10)-C(8)-C(9)	110.0(4)	O(3)-Co(1)-N(4)	77.98(9)
C(8)-C(11)	1.534(5)	C(10)-C(8)-C(11)	110.4(4)	O(2)-Co(1)-N(4)	79.01(10)
C(12)-N(1)	1.473(4)	C(9)-C(8)-C(11)	108.9(3)	O(1)-Co(1)-N(4)	156.52(10)
C(12)-C(13)	1.507(5)	C(10)-C(8)-C(7)	108.7(3)	N(1)-Co(1)-N(4)	73.03(10)
C(13)-N(4)	1.347(4)	C(9)-C(8)-C(7)	108.5(3)	N(6)-Co(1)-N(4)	113.33(10)
C(13)-C(14)	1.382(5)	C(11)-C(8)-C(7)	110.4(3)	N(2)-Co(1)-N(4)	112.51(10)
C(14)-C(16)	1.379(5)	N(1)-C(12)-C(13)	109.3(3)	C(1)-N(1)-C(12)	110.4(3)
C(16)-C(17)	1.378(5)	N(4)-C(13)-C(14)	123.5(3)	C(1)-N(1)-C(24)	112.4(2)
C(17)-C(18)	1.386(5)	N(4)-C(13)-C(12)	115.3(3)	C(12)-N(1)-C(24)	110.3(3)
C(18)-N(4)	1.344(4)	C(14)-C(13)-C(12)	121.2(3)	C(1)-N(1)-Co(1)	107.6(2)
C(18)-N(5)	1.400(4)	C(16)-C(14)-C(13)	118.4(3)	C(12)-N(1)-Co(1)	108.79(19)
C(19)-O(2)	1.234(4)	C(17)-C(16)-C(14)	119.1(3)	C(24)-N(1)-Co(1)	107.26(19)
C(19)-N(5)	1.360(4)	C(16)-C(17)-C(18)	119.2(3)	C(6)-N(2)-C(2)	117.2(3)
C(19)-C(20)	1.520(5)	N(4)-C(18)-C(17)	122.4(3)	C(6)-N(2)-Co(1)	127.6(2)
C(20)-C(23)	1.523(7)	N(4)-C(18)-N(5)	120.0(3)	C(2)-N(2)-Co(1)	112.4(2)
C(20)-C(22)	1.530(7)	C(17)-C(18)-N(5)	117.6(3)	C(7)-N(3)-C(6)	128.5(3)
C(20)-C(21)	1.539(6)	O(2)-C(19)-N(5)	123.1(3)	C(18)-N(4)-C(13)	117.3(3)
C(24)-N(1)	1.476(4)	O(2)-C(19)-C(20)	121.1(3)	C(18)-N(4)-Co(1)	127.9(2)
C(24)-C(25)	1.500(5)	N(5)-C(19)-C(20)	115.9(3)	C(13)-N(4)-Co(1)	114.3(2)
C(25)-N(6)	1.354(4)	C(19)-C(20)-C(23)	107.8(4)	C(19)-N(5)-C(18)	128.8(3)
C(25)-C(26)	1.376(5)	C(19)-C(20)-C(22)	111.4(4)	C(29)-N(6)-C(25)	117.7(3)
C(26)-C(27)	1.396(5)	C(23)-C(20)-C(22)	110.3(4)	C(29)-N(6)-Co(1)	127.3(2)
C(27)-C(28)	1.369(5)	C(19)-C(20)-C(21)	108.2(3)	C(25)-N(6)-Co(1)	114.9(2)
C(28)-C(29)	1.392(5)	C(23)-C(20)-C(21)	110.4(4)	C(30)-N(7)-C(29)	126.8(3)
C(29)-N(6)	1.344(4)	C(22)-C(20)-C(21)	108.7(4)	C(7)-O(1)-Co(1)	133.9(2)
C(29)-N(7)	1.412(4)	N(1)-C(24)-C(25)	109.7(3)	C(19)-O(2)-Co(1)	133.5(2)
C(30)-O(3)	1.235(4)	N(6)-C(25)-C(26)	122.8(3)	C(30)-O(3)-Co(1)	128.2(2)
C(30)-N(7)	1.355(4)	N(6)-C(25)-C(24)	114.6(3)	N(8)-C(36)-C(35)	179.2(6)
C(30)-C(31)	1.534(4)	C(26)-C(25)-C(24)	122.6(3)	N(9)-C(38)-C(37)	176.2(11)
C(31)-C(32)	1.515(5)	C(25)-C(26)-C(27)	118.6(3)	N(9)-C(38)-C(37)#1	177.6(10)
C(31)-C(34)	1.528(6)	C(28)-C(27)-C(26)	119.2(3)	C(37)-C(38)-C(37)#1	6.1(8)
C(31)-C(33)	1.534(5)	C(27)-C(28)-C(29)	118.9(3)	N(10)-C(40)-C(39)	178.8(14)

Appendix 3: Crystals data

Co(1)-O(3)	2.115(2)	N(6)-C(29)-C(28)	122.6(3)		
Co(1)-O(2)	2.119(3)	N(6)-C(29)-N(7)	119.6(3)		
Co(1)-O(1)	2.141(2)	C(28)-C(29)-N(7)	117.7(3)		
Co(1)-N(1)	2.185(3)	O(3)-C(30)-N(7)	122.6(3)		
Co(1)-N(6)	2.208(3)	O(3)-C(30)-C(31)	118.2(3)		
Co(1)-N(2)	2.218(3)	N(7)-C(30)-C(31)	119.2(3)		
Co(1)-N(4)	2.239(3)	C(32)-C(31)-C(34)	109.4(3)		
C(35)-C(36)	1.460(7)	C(32)-C(31)-C(33)	109.7(3)		
C(36)-N(8)	1.132(6)	C(34)-C(31)-C(33)	109.9(3)		
C(37)-C(38)	1.368(15)	C(32)-C(31)-C(30)	114.3(3)		
C(38)-N(9)	1.144(12)	C(34)-C(31)-C(30)	107.0(3)		
C(38)-C(37)#1	1.554(16)	C(33)-C(31)-C(30)	106.4(3)		
C(39)-C(40)	1.493(14)	O(3)-Co(1)-O(2)	84.48(10)		
C(40)-N(10)	1.073(13)	O(3)-Co(1)-O(1)	85.19(9)		

Symmetry transformations used to generate equivalent atoms:

#1 -x,y,-z+1/2

Appendix 3: Crystals data

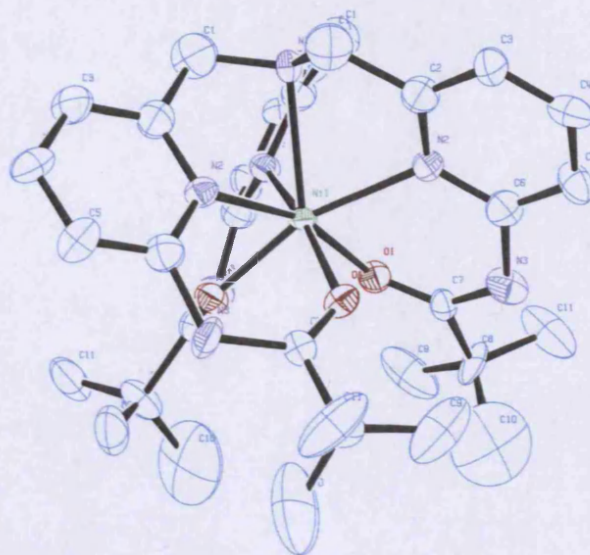


Table T.1: Crystal data and structure refinement for $[\text{Ni}^{\text{II}}(\text{L}^4)[\text{ClO}_4]_{1.67}[\text{Br}]_{0.33} \cdot 0.67(\text{H}_2\text{O})$. 5.4

Identification code	aja0913t	
Empirical formula	C33 H46.33 Cl1.67 I0.33 N7 Ni O10.33	
Formula weight	866.53	
Temperature	396(2) K	
Wavelength	0.71073 Å	
Crystal system	Hexagonal	
Space group	P63/m	
Unit cell dimensions	a = 11.1018(7) Å	$\alpha = 90^\circ$.
	b = 11.1018(7) Å	$\beta = 90^\circ$.
	c = 58.814(4) Å	$\gamma = 120^\circ$.
Volume	6277.7(7) Å ³	
Z	6	
Density (calculated)	1.375 Mg/m ³	
Absorption coefficient	0.875 mm ⁻¹	
F(000)	2700	
Crystal size	0.40 x 0.40 x 0.08 mm ³	
Theta range for data collection	2.97 to 20.95°.	
Index ranges	-10 ≤ h ≤ 11, -11 ≤ k ≤ 11, -54 ≤ l ≤ 58	
Reflections collected	7894	
Independent reflections	2176 [R(int) = 0.0735]	
Completeness to theta = 20.95°	95.6 %	
Absorption correction	Empirical	
Max. and min. transmission	0.9333 and 0.7209	
Refinement method	Full-matrix least-squares on F ²	
Data / restraints / parameters	2176 / 463 / 276	
Goodness-of-fit on F ²	3.409	
Final R indices [I > 2σ(I)]	R1 = 0.2540, wR2 = 0.6398	
R indices (all data)	R1 = 0.2607, wR2 = 0.6430	
Largest diff. peak and hole	1.365 and -1.764 e.Å ⁻³	

Appendix 3: Crystals data

Table T.2: Bond lengths [Å] and angles [°] for $[\text{Ni}^{\text{II}}(\text{L}^4)[\text{ClO}_4]_{1.67}[\text{Br}]_{0.33} \cdot 0.67(\text{H}_2\text{O}) \cdot 5.4$

Ni(1)-O(1)	2.033(11)	N(2)#2-Ni(1)-N(2)	109.3(2)	Ni(2)#3-Ni(2)-C(18)#5	104.3(8)
Ni(1)-O(1)#1	2.033(11)	O(1)-Ni(1)-N(1)	128.2(4)	O(2)#4-Ni(2)-C(18)#5	142.4(7)
Ni(1)-O(1)#2	2.033(11)	O(1)#1-Ni(1)-N(1)	128.2(4)	O(2)#3-Ni(2)-C(18)#5	95.0(7)
Ni(1)-N(2)#1	2.264(7)	O(1)#2-Ni(1)-N(1)	128.2(4)	O(2)#5-Ni(2)-C(18)#5	28.5(8)
Ni(1)-N(2)#2	2.264(7)	N(2)#1-Ni(1)-N(1)	70.3(2)	O(2)-Ni(2)-C(18)#5	95.7(9)
Ni(1)-N(2)	2.264(7)	N(2)#2-Ni(1)-N(1)	70.3(2)	O(2)#6-Ni(2)-C(18)#5	145.1(7)
Ni(1)-N(1)	2.53(2)	N(2)-Ni(1)-N(1)	70.3(2)	O(2)#7-Ni(2)-C(18)#5	64.8(11)
O(1)-C(7)	1.224(8)	C(7)-O(1)-Ni(1)	130.8(10)	N(5)#7-Ni(2)-C(18)#5	89.4(9)
N(1)-C(1)#1	1.511(7)	C(1)#1-N(1)-C(1)#2	115.9(6)	N(5)#6-Ni(2)-C(18)#5	132.5(5)
N(1)-C(1)#2	1.511(7)	C(1)#1-N(1)-C(1)	115.9(6)	N(5)-Ni(2)-C(18)#5	24.9(6)
N(1)-C(1)	1.511(7)	C(1)#2-N(1)-C(1)	115.9(6)	Ni(2)#3-Ni(2)-N(4)	180
C(1)-C(2)	1.6158	C(1)#1-N(1)-Ni(1)	101.0(9)	O(2)#4-Ni(2)-N(4)	91.5(9)
N(2)-C(6)	1.3869	C(1)#2-N(1)-Ni(1)	101.0(9)	O(2)#3-Ni(2)-N(4)	91.5(9)
N(2)-C(2)	1.3904	C(1)-N(1)-Ni(1)	101.0(9)	O(2)#5-Ni(2)-N(4)	91.5(9)
C(2)-C(3)	1.3878	N(1)-C(1)-C(2)	103.4(6)	O(2)-Ni(2)-N(4)	130.5(7)
C(3)-C(4)	1.3872	C(6)-N(2)-C(2)	120	O(2)#6-Ni(2)-N(4)	130.5(7)
C(4)-C(5)	1.3904	C(6)-N(2)-Ni(1)	123.9(2)	O(2)#7-Ni(2)-N(4)	130.5(7)
C(5)-C(6)	1.3878	C(2)-N(2)-Ni(1)	112.2(2)	N(5)#7-Ni(2)-N(4)	71.4(3)
C(6)-N(3)	1.460(8)	C(3)-C(2)-N(2)	120.1	N(5)#6-Ni(2)-N(4)	71.4(3)
C(7)-N(3)	1.456(9)	C(3)-C(2)-C(1)	119.4	N(5)-Ni(2)-N(4)	71.4(3)
C(7)-C(8)	1.525(5)	N(2)-C(2)-C(1)	120.4	C(18)#5-Ni(2)-N(4)	76.4(8)
C(8)-C(9)	1.523(5)	C(4)-C(3)-C(2)	119.9	N(5)#4-O(2)-C(18)	52.2(12)
C(8)-C(11)	1.524(5)	C(3)-C(4)-C(5)	120	N(5)#4-O(2)-Ni(2)#3	130(3)
C(8)-C(10)	1.525(5)	C(6)-C(5)-C(4)	120.1	C(18)-O(2)-Ni(2)#3	115(2)
Ni(2)-Ni(2)#3	1.361(17)	N(2)-C(6)-C(5)	119.9	N(5)#4-O(2)-C(17)#4	54.2(14)
Ni(2)-O(2)#4	1.52(2)	N(2)-C(6)-N(3)	120.5(6)	C(18)-O(2)-C(17)#4	70.6(18)
Ni(2)-O(2)#3	1.52(2)	C(5)-C(6)-N(3)	119.2(6)	Ni(2)#3-O(2)-C(17)#4	174.0(19)
Ni(2)-O(2)#5	1.52(2)	O(1)-C(7)-N(3)	126.8(10)	N(5)#4-O(2)-Ni(2)	172(3)
Ni(2)-O(2)	2.036(12)	O(1)-C(7)-C(8)	121.3(8)	C(18)-O(2)-Ni(2)	129.3(12)
Ni(2)-O(2)#6	2.036(12)	N(3)-C(7)-C(8)	111.8(7)	Ni(2)#3-O(2)-Ni(2)	41.9(7)
Ni(2)-O(2)#7	2.036(12)	C(9)-C(8)-C(11)	109.7(7)	C(17)#4-O(2)-Ni(2)	133.9(18)
Ni(2)-N(5)#7	2.263(8)	C(9)-C(8)-C(10)	109.8(6)	C(12)-N(4)-C(12)#7	117.3(8)
Ni(2)-N(5)#6	2.263(8)	C(11)-C(8)-C(10)	109.4(7)	C(12)-N(4)-C(12)#6	117.3(8)
Ni(2)-N(5)	2.263(8)	C(9)-C(8)-C(7)	109.3(6)	C(12)#7-N(4)-C(12)#6	117.3(8)
Ni(2)-C(18)#5	2.32(2)	C(11)-C(8)-C(7)	109.3(6)	C(12)-N(4)-Ni(2)	103.4(9)
Ni(2)-N(4)	2.52(2)	C(10)-C(8)-C(7)	109.4(6)	C(12)#7-N(4)-Ni(2)	103.4(9)
O(2)-N(5)#4	0.967(19)	C(7)-N(3)-C(6)	122.6(11)	C(12)#6-N(4)-Ni(2)	103.4(9)
O(2)-C(18)	1.226(10)	Ni(2)#3-Ni(2)-O(2)#4	89.9(10)	N(4)-C(12)-C(13)	105.3(9)
O(2)-Ni(2)#3	1.52(2)	Ni(2)#3-Ni(2)-O(2)#3	89.9(10)	O(2)#5-N(5)-C(17)	91(2)
O(2)-C(17)#4	1.71(3)	O(2)#4-Ni(2)-O(2)#3	119.999(17)	O(2)#5-N(5)-C(13)	137(2)
N(4)-C(12)	1.516(9)	Ni(2)#3-Ni(2)-O(2)#5	89.9(10)	C(17)-N(5)-C(13)	120.1
N(4)-C(12)#7	1.516(9)	O(2)#4-Ni(2)-O(2)#5	119.999(16)	O(2)#5-N(5)-Ni(2)	31(2)
N(4)-C(12)#6	1.516(9)	O(2)#3-Ni(2)-O(2)#5	119.999(15)	C(17)-N(5)-Ni(2)	122.3(3)
C(12)-C(13)	1.5772	Ni(2)#3-Ni(2)-O(2)	48.2(9)	C(13)-N(5)-Ni(2)	112.7(4)
N(5)-O(2)#5	0.967(19)	O(2)#4-Ni(2)-O(2)	68.0(10)	C(14)-C(13)-N(5)	120
N(5)-C(17)	1.3894	O(2)#3-Ni(2)-O(2)	138.1(7)	C(14)-C(13)-C(12)	114.8
N(5)-C(13)	1.39	O(2)#5-Ni(2)-O(2)	68.0(10)	N(5)-C(13)-C(12)	124.1
C(13)-C(14)	1.388	Ni(2)#3-Ni(2)-O(2)#6	48.2(9)	C(13)-C(14)-C(15)	119.9
C(14)-C(15)	1.3898	O(2)#4-Ni(2)-O(2)#6	68.0(10)	C(13)-C(14)-C(20)#5	57.2(13)
C(14)-C(20)#5	1.93(3)	O(2)#3-Ni(2)-O(2)#6	68.0(10)	C(15)-C(14)-C(20)#5	84.5(19)
C(15)-C(16)	1.3895	O(2)#5-Ni(2)-O(2)#6	138.1(7)	C(16)-C(15)-C(14)	120.1
C(16)-C(17)	1.3881	O(2)-Ni(2)-O(2)#6	80.4(14)	C(17)-C(16)-C(15)	120
C(17)-N(6)	1.459(9)	Ni(2)#3-Ni(2)-O(2)#7	48.2(9)	C(16)-C(17)-N(5)	119.9
C(18)-N(6)	1.458(10)	O(2)#4-Ni(2)-O(2)#7	138.1(7)	C(16)-C(17)-N(6)	118.8(7)
C(18)-C(19)	1.524(6)	O(2)#3-Ni(2)-O(2)#7	68.0(10)	N(5)-C(17)-N(6)	120.3(8)
C(18)-Ni(2)#3	2.32(2)	O(2)#5-Ni(2)-O(2)#7	68.0(10)	O(2)-C(18)-N(6)	125.6(12)
C(19)-C(20)	1.522(7)	O(2)-Ni(2)-O(2)#7	80.4(14)	O(2)-C(18)-C(19)	121.8(11)
C(19)-C(22)	1.525(7)	O(2)#6-Ni(2)-O(2)#7	80.4(14)	N(6)-C(18)-C(19)	111.4(9)

Appendix 3: Crystals data

C(19)-C(21)	1.525(7)	Ni(2)#3-Ni(2)-N(5)#7	109.0(3)	O(2)-C(18)-Ni(2)#3	36.2(14)
C(20)-C(14)#4	1.93(3)	O(2)#4-Ni(2)-N(5)#7	119.0(7)	N(6)-C(18)-Ni(2)#3	106.4(13)
Cl(2)-O(4)	1.440(3)	O(2)#3-Ni(2)-N(5)#7	19.2(11)	C(19)-C(18)-Ni(2)#3	136.3(13)
Cl(2)-O(3)	1.440(3)	O(2)#5-Ni(2)-N(5)#7	117.5(9)	C(20)-C(19)-C(18)	109.5(9)
Cl(2)-O(3)#8	1.440(3)	O(2)-Ni(2)-N(5)#7	157.2(11)	C(20)-C(19)-C(22)	109.7(9)
Cl(2)-O(5)	1.440(3)	O(2)#6-Ni(2)-N(5)#7	82.7(8)	C(18)-C(19)-C(22)	109.1(9)
Cl(3)-O(7)	1.440(3)	O(2)#7-Ni(2)-N(5)#7	81.8(5)	C(20)-C(19)-C(21)	109.9(9)
Cl(3)-O(6)#2	1.440(3)	Ni(2)#3-Ni(2)-N(5)#6	109.0(3)	C(18)-C(19)-C(21)	109.3(9)
Cl(3)-O(6)	1.440(3)	O(2)#4-Ni(2)-N(5)#6	19.2(11)	C(22)-C(19)-C(21)	109.2(9)
Cl(3)-O(6)#1	1.440(3)	O(2)#3-Ni(2)-N(5)#6	117.5(9)	C(19)-C(20)-C(14)#4	26.5(8)
O(1)-Ni(1)-O(1)#1	86.4(6)	O(2)#5-Ni(2)-N(5)#6	119.0(7)	C(18)-N(6)-C(17)	122.3(13)
O(1)-Ni(1)-O(1)#2	86.4(6)	O(2)-Ni(2)-N(5)#6	82.7(8)	O(4)-Cl(2)-O(3)	109.5(6)
O(1)#1-Ni(1)-O(1)#2	86.4(6)	O(2)#6-Ni(2)-N(5)#6	81.8(5)	O(4)-Cl(2)-O(3)#8	109.5(6)
O(1)-Ni(1)-N(2)#1	79.0(4)	O(2)#7-Ni(2)-N(5)#6	157.2(11)	O(3)-Cl(2)-O(3)#8	109.4(7)
O(1)#1-Ni(1)-N(2)#1	81.9(4)	N(5)#7-Ni(2)-N(5)#6	109.9(3)	O(4)-Cl(2)-O(5)	109.5(7)
O(1)#2-Ni(1)-N(2)#1	161.8(5)	Ni(2)#3-Ni(2)-N(5)	109.0(3)	O(3)-Cl(2)-O(5)	109.4(6)
O(1)-Ni(1)-N(2)#2	161.8(5)	O(2)#4-Ni(2)-N(5)	117.5(9)	O(3)#8-Cl(2)-O(5)	109.4(6)
O(1)#1-Ni(1)-N(2)#2	79.0(4)	O(2)#3-Ni(2)-N(5)	119.0(7)	O(7)-Cl(3)-O(6)#2	109.6(4)
O(1)#2-Ni(1)-N(2)#2	81.9(4)	O(2)#5-Ni(2)-N(5)	19.2(11)	O(7)-Cl(3)-O(6)	109.6(4)
N(2)#1-Ni(1)-N(2)#2	109.3(2)	O(2)-Ni(2)-N(5)	81.8(5)	O(6)#2-Cl(3)-O(6)	109.4(4)
O(1)-Ni(1)-N(2)	81.9(4)	O(2)#6-Ni(2)-N(5)	157.2(11)	O(7)-Cl(3)-O(6)#1	109.6(4)
O(1)#1-Ni(1)-N(2)	161.8(5)	O(2)#7-Ni(2)-N(5)	82.7(8)	O(6)#2-Cl(3)-O(6)#1	109.4(4)
O(1)#2-Ni(1)-N(2)	79.0(4)	N(5)#7-Ni(2)-N(5)	109.9(3)	O(6)-Cl(3)-O(6)#1	109.4(4)
N(2)#1-Ni(1)-N(2)	109.3(2)	N(5)#6-Ni(2)-N(5)	109.9(3)		

Symmetry transformations used to generate equivalent atoms:

#1 -x+y+1,-x,z #2 -y,x-y-1,z #3 -x,-y,-z

#4 x-y,x,-z #5 y,-x+y,-z #6 -y,x-y,z #7 -x+y,-x,z

#8 x,y,-z-1/2

Appendix 3: Crystals data

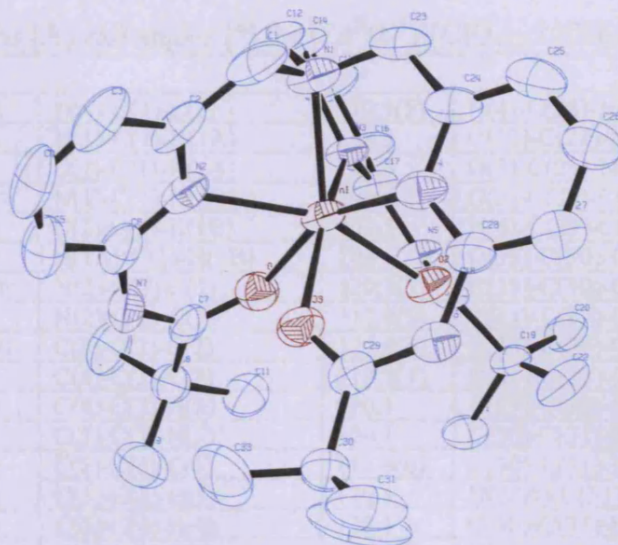


Table U.1: Crystal data and structure refinement for $[\text{Zn}^{\text{II}}(\text{L}^4)][\text{ClO}_4]_2 \cdot 2(\text{CH}_3\text{CN})$. 5.5

Identification code	aja0726	
Empirical formula	C ₃₇ H ₅₁ Cl ₂ N ₉ O ₁₁ Zn	
Formula weight	934.14	
Temperature	150(2) K	
Wavelength	0.71073 Å	
Crystal system	Monoclinic	
Space group	C 2/c	
Unit cell dimensions	a = 37.4589(10) Å	α = 90°.
	b = 11.2206(3) Å	β = 93.2280(10)°.
	c = 21.1473(8) Å	γ = 90°.
Volume	8874.3(5) Å ³	
Z	8	
Density (calculated)	1.398 Mg/m ³	
Absorption coefficient	0.740 mm ⁻¹	
F(000)	3904	
Crystal size	0.35 x 0.32 x 0.32 mm ³	
Theta range for data collection	2.99 to 27.52°.	
Index ranges	-48 ≤ h ≤ 48, -12 ≤ k ≤ 14, -27 ≤ l ≤ 27	
Reflections collected	29824	
Independent reflections	10144 [R(int) = 0.1050]	
Completeness to theta = 27.52°	99.1 %	
Absorption correction	Empirical	
Max. and min. transmission	0.7977 and 0.7818	
Refinement method	Full-matrix least-squares on F ²	
Data / restraints / parameters	10144 / 0 / 552	
Goodness-of-fit on F ²	1.037	
Final R indices [I > 2σ(I)]	R1 = 0.0832, wR2 = 0.2037	
R indices (all data)	R1 = 0.1813, wR2 = 0.2482	
Largest diff. peak and hole	0.868 and -0.628 e.Å ⁻³	

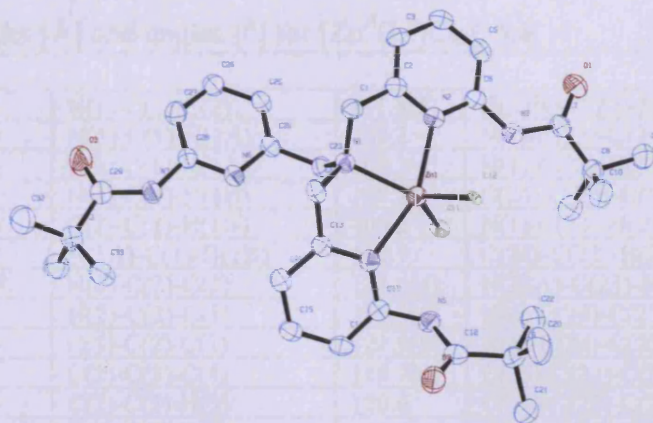
Appendix 3: Crystals data

Table U.2: Bond lengths [Å] and angles [°] for $[\text{Zn}^{\text{II}}(\text{L}^4)][\text{ClO}_4]_2 \cdot 2(\text{CH}_3\text{CN})$. 5.5

C(1)-N(1)	1.466(7)	N(1)-C(1)-C(2)	110.9(5)	N(4)-C(28)-N(6)	119.1(5)
C(1)-C(2)	1.503(9)	N(1)-C(1)-H(1A)	109.5	C(27)-C(28)-N(6)	117.9(5)
C(1)-H(1A)	0.99	C(2)-C(1)-H(1A)	109.5	O(3)-C(29)-N(6)	122.5(5)
C(1)-H(1B)	0.99	N(1)-C(1)-H(1B)	109.5	O(3)-C(29)-C(30)	119.9(5)
C(2)-N(2)	1.360(7)	C(2)-C(1)-H(1B)	109.5	N(6)-C(29)-C(30)	117.6(5)
C(2)-C(3)	1.391(8)	H(1A)-C(1)-H(1B)	108	C(33)-C(30)-C(31)	108.4(6)
C(3)-C(4)	1.342(10)	N(2)-C(2)-C(3)	120.3(7)	C(33)-C(30)-C(29)	108.4(5)
C(3)-H(3)	0.95	N(2)-C(2)-C(1)	117.8(5)	C(31)-C(30)-C(29)	114.0(5)
C(4)-C(5)	1.362(10)	C(3)-C(2)-C(1)	121.8(6)	C(33)-C(30)-C(32)	110.8(8)
C(4)-H(4)	0.95	C(4)-C(3)-C(2)	119.8(7)	C(31)-C(30)-C(32)	109.5(6)
C(5)-C(6)	1.390(8)	C(4)-C(3)-H(3)	120.1	C(29)-C(30)-C(32)	105.7(5)
C(5)-H(5)	0.95	C(2)-C(3)-H(3)	120.1	C(30)-C(31)-H(34A)	109.5
C(6)-N(2)	1.314(7)	C(3)-C(4)-C(5)	119.9(6)	C(30)-C(31)-H(34B)	109.5
C(6)-N(7)	1.422(8)	C(3)-C(4)-H(4)	120.1	H(34A)-C(31)-H(34B)	109.5
C(7)-O(1)	1.238(6)	C(5)-C(4)-H(4)	120.1	C(30)-C(31)-H(34C)	109.5
C(7)-N(7)	1.337(7)	C(4)-C(5)-C(6)	118.9(7)	H(34A)-C(31)-H(34C)	109.5
C(7)-C(8)	1.534(8)	C(4)-C(5)-H(5)	120.6	H(34B)-C(31)-H(34C)	109.5
C(8)-C(11)	1.527(8)	C(6)-C(5)-H(5)	120.6	C(30)-C(32)-H(35A)	109.5
C(8)-C(10)	1.535(8)	N(2)-C(6)-C(5)	122.0(6)	C(30)-C(32)-H(35B)	109.5
C(8)-C(9)	1.542(8)	N(2)-C(6)-N(7)	119.4(5)	H(35A)-C(32)-H(35B)	109.5
C(9)-H(10A)	0.98	C(5)-C(6)-N(7)	118.5(6)	C(30)-C(32)-H(35C)	109.5
C(9)-H(10B)	0.98	O(1)-C(7)-N(7)	122.7(5)	H(35A)-C(32)-H(35C)	109.5
C(9)-H(10C)	0.98	O(1)-C(7)-C(8)	120.0(5)	H(35B)-C(32)-H(35C)	109.5
C(10)-H(11A)	0.98	N(7)-C(7)-C(8)	117.3(5)	C(30)-C(33)-H(36A)	109.5
C(10)-H(11B)	0.98	C(11)-C(8)-C(7)	108.5(5)	C(30)-C(33)-H(36B)	109.5
C(10)-H(11C)	0.98	C(11)-C(8)-C(10)	110.3(5)	H(36A)-C(33)-H(36B)	109.5
C(11)-H(12A)	0.98	C(7)-C(8)-C(10)	108.6(5)	C(30)-C(33)-H(36C)	109.5
C(11)-H(12B)	0.98	C(11)-C(8)-C(9)	109.9(5)	H(36A)-C(33)-H(36C)	109.5
C(11)-H(12C)	0.98	C(7)-C(8)-C(9)	109.8(5)	H(36B)-C(33)-H(36C)	109.5
C(12)-N(1)	1.475(7)	C(10)-C(8)-C(9)	109.8(5)	C(35)-C(34)-H(37A)	109.5
C(12)-C(13)	1.495(7)	C(8)-C(9)-H(10A)	109.5	C(35)-C(34)-H(37B)	109.5
C(12)-H(13A)	0.99	C(8)-C(9)-H(10B)	109.5	H(37A)-C(34)-H(37B)	109.5
C(12)-H(13B)	0.99	H(10A)-C(9)-H(10B)	109.5	C(35)-C(34)-H(37C)	109.5
C(13)-N(3)	1.355(6)	C(8)-C(9)-H(10C)	109.5	H(37A)-C(34)-H(37C)	109.5
C(13)-C(14)	1.376(7)	H(10A)-C(9)-H(10C)	109.5	H(37B)-C(34)-H(37C)	109.5
C(14)-C(15)	1.361(8)	H(10B)-C(9)-H(10C)	109.5	N(8)-C(35)-C(34)	177.7(12)
C(14)-H(15)	0.95	C(8)-C(10)-H(11A)	109.5	C(37)-C(36)-H(39A)	109.5
C(15)-C(16)	1.388(8)	C(8)-C(10)-H(11B)	109.5	C(37)-C(36)-H(39B)	109.5
C(15)-H(16)	0.95	H(11A)-C(10)-H(11B)	109.5	H(39A)-C(36)-H(39B)	109.5
C(16)-C(17)	1.360(7)	C(8)-C(10)-H(11C)	109.5	C(37)-C(36)-H(39C)	109.5
C(16)-H(17)	0.95	H(11A)-C(10)-H(11C)	109.5	H(39A)-C(36)-H(39C)	109.5
C(17)-N(3)	1.353(6)	H(11B)-C(10)-H(11C)	109.5	H(39B)-C(36)-H(39C)	109.5
C(17)-N(5)	1.402(6)	C(8)-C(11)-H(12A)	109.5	N(9)-C(37)-C(36)	177.5(14)
C(18)-O(2)	1.235(6)	C(8)-C(11)-H(12B)	109.5	C(23)-N(1)-C(1)	110.7(5)
C(18)-N(5)	1.358(6)	H(12A)-C(11)-H(12B)	109.5	C(23)-N(1)-C(12)	112.5(5)
C(18)-C(19)	1.522(7)	C(8)-C(11)-H(12C)	109.5	C(1)-N(1)-C(12)	112.0(5)
C(19)-C(21)	1.518(7)	H(12A)-C(11)-H(12C)	109.5	C(23)-N(1)-Zn(1)	107.4(3)
C(19)-C(20)	1.533(7)	H(12B)-C(11)-H(12C)	109.5	C(1)-N(1)-Zn(1)	107.1(3)
C(19)-C(22)	1.535(7)	N(1)-C(12)-C(13)	110.9(4)	C(12)-N(1)-Zn(1)	106.9(3)
C(20)-H(22A)	0.98	N(1)-C(12)-H(13A)	109.5	C(6)-N(2)-C(2)	119.1(5)
C(20)-H(22B)	0.98	C(13)-C(12)-H(13A)	109.5	C(6)-N(2)-Zn(1)	126.4(4)
C(20)-H(22C)	0.98	N(1)-C(12)-H(13B)	109.5	C(2)-N(2)-Zn(1)	110.1(4)
C(21)-H(23A)	0.98	C(13)-C(12)-H(13B)	109.5	C(17)-N(3)-C(13)	117.8(4)
C(21)-H(23B)	0.98	H(13A)-C(12)-H(13B)	108	C(17)-N(3)-Zn(1)	126.9(3)
C(21)-H(23C)	0.98	N(3)-C(13)-C(14)	122.4(5)	C(13)-N(3)-Zn(1)	113.7(3)
C(22)-H(24A)	0.98	N(3)-C(13)-C(12)	116.7(4)	C(28)-N(4)-C(24)	117.4(5)
C(22)-H(24B)	0.98	C(14)-C(13)-C(12)	120.9(5)	C(28)-N(4)-Zn(1)	126.3(3)

Appendix 3: Crystals data

C(22)-H(24C)	0.98	C(15)-C(14)-C(13)	118.8(5)	C(24)-N(4)-Zn(1)	113.7(3)
C(23)-N(1)	1.457(8)	C(15)-C(14)-H(15)	120.6	C(18)-N(5)-C(17)	129.6(4)
C(23)-C(24)	1.490(8)	C(13)-C(14)-H(15)	120.6	C(18)-N(5)-H(5B)	115.2
C(23)-H(25A)	0.99	C(14)-C(15)-C(16)	119.5(5)	C(17)-N(5)-H(5B)	115.2
C(23)-H(25B)	0.99	C(14)-C(15)-H(16)	120.2	C(29)-N(6)-C(28)	129.5(5)
C(24)-N(4)	1.353(6)	C(16)-C(15)-H(16)	120.2	C(29)-N(6)-H(6)	115.2
C(24)-C(25)	1.388(8)	C(17)-C(16)-C(15)	119.3(5)	C(28)-N(6)-H(6)	115.2
C(25)-C(26)	1.388(8)	C(17)-C(16)-H(17)	120.4	C(7)-N(7)-C(6)	130.3(5)
C(25)-H(27)	0.95	C(15)-C(16)-H(17)	120.4	C(7)-N(7)-H(7)	114.8
C(26)-C(27)	1.368(8)	N(3)-C(17)-C(16)	122.1(5)	C(6)-N(7)-H(7)	114.8
C(26)-H(28)	0.95	N(3)-C(17)-N(5)	119.3(4)	C(7)-O(1)-Zn(1)	133.8(4)
C(27)-C(28)	1.395(8)	C(16)-C(17)-N(5)	118.6(5)	C(18)-O(2)-Zn(1)	131.2(3)
C(27)-H(29)	0.95	O(2)-C(18)-N(5)	122.7(5)	C(29)-O(3)-Zn(1)	131.2(4)
C(28)-N(4)	1.347(7)	O(2)-C(18)-C(19)	120.2(4)	O(6)-Cl(1)-O(4)	108.1(7)
C(28)-N(6)	1.405(6)	N(5)-C(18)-C(19)	117.0(4)	O(6)-Cl(1)-O(5)	107.9(8)
C(29)-O(3)	1.234(6)	C(21)-C(19)-C(18)	108.6(4)	O(4)-Cl(1)-O(5)	110.0(4)
C(29)-N(6)	1.359(7)	C(21)-C(19)-C(20)	110.5(4)	O(6)-Cl(1)-O(7)	102.1(5)
C(29)-C(30)	1.511(7)	C(18)-C(19)-C(20)	112.3(4)	O(4)-Cl(1)-O(7)	116.0(4)
C(30)-C(33)	1.489(10)	C(21)-C(19)-C(22)	109.0(4)	O(5)-Cl(1)-O(7)	112.2(4)
C(30)-C(31)	1.505(8)	C(18)-C(19)-C(22)	107.9(4)	O(11)-Cl(2)-O(8)	112.9(7)
C(30)-C(32)	1.514(9)	C(20)-C(19)-C(22)	108.4(5)	O(11)-Cl(2)-O(9)	108.0(3)
C(31)-H(34A)	0.98	C(19)-C(20)-H(22A)	109.5	O(8)-Cl(2)-O(9)	110.5(5)
C(31)-H(34B)	0.98	C(19)-C(20)-H(22B)	109.5	O(11)-Cl(2)-O(10)	112.0(5)
C(31)-H(34C)	0.98	H(22A)-C(20)-H(22B)	109.5	O(8)-Cl(2)-O(10)	100.8(5)
C(32)-H(35A)	0.98	C(19)-C(20)-H(22C)	109.5	O(9)-Cl(2)-O(10)	112.6(4)
C(32)-H(35B)	0.98	H(22A)-C(20)-H(22C)	109.5	O(3)-Zn(1)-O(1)	81.49(14)
C(32)-H(35C)	0.98	H(22B)-C(20)-H(22C)	109.5	O(3)-Zn(1)-O(2)	85.06(13)
C(33)-H(36A)	0.98	C(19)-C(21)-H(23A)	109.5	O(1)-Zn(1)-O(2)	83.57(14)
C(33)-H(36B)	0.98	C(19)-C(21)-H(23B)	109.5	O(3)-Zn(1)-N(3)	156.97(15)
C(33)-H(36C)	0.98	H(23A)-C(21)-H(23B)	109.5	O(1)-Zn(1)-N(3)	79.52(15)
C(34)-C(35)	1.332(10)	C(19)-C(21)-H(23C)	109.5	O(2)-Zn(1)-N(3)	79.98(14)
C(34)-H(37A)	0.98	H(23A)-C(21)-H(23C)	109.5	O(3)-Zn(1)-N(4)	79.14(15)
C(34)-H(37B)	0.98	H(23B)-C(21)-H(23C)	109.5	O(1)-Zn(1)-N(4)	154.28(15)
C(34)-H(37C)	0.98	C(19)-C(22)-H(24A)	109.5	O(2)-Zn(1)-N(4)	78.07(14)
C(35)-N(8)	1.061(8)	C(19)-C(22)-H(24B)	109.5	N(3)-Zn(1)-N(4)	114.29(16)
C(36)-C(37)	1.422(13)	H(24A)-C(22)-H(24B)	109.5	O(3)-Zn(1)-N(1)	128.33(15)
C(36)-H(39A)	0.98	C(19)-C(22)-H(24C)	109.5	O(1)-Zn(1)-N(1)	132.22(16)
C(36)-H(39B)	0.98	H(24A)-C(22)-H(24C)	109.5	O(2)-Zn(1)-N(1)	128.93(17)
C(36)-H(39C)	0.98	H(24B)-C(22)-H(24C)	109.5	N(3)-Zn(1)-N(1)	74.57(15)
C(37)-N(9)	1.098(13)	N(1)-C(23)-C(24)	111.4(5)	N(4)-Zn(1)-N(1)	73.47(17)
N(1)-Zn(1)	2.223(4)	N(1)-C(23)-H(25A)	109.3	O(3)-Zn(1)-N(2)	78.44(15)
N(2)-Zn(1)	2.253(5)	C(24)-C(23)-H(25A)	109.3	O(1)-Zn(1)-N(2)	78.74(17)
N(3)-Zn(1)	2.179(4)	N(1)-C(23)-H(25B)	109.3	O(2)-Zn(1)-N(2)	157.33(16)
N(4)-Zn(1)	2.202(4)	C(24)-C(23)-H(25B)	109.3	N(3)-Zn(1)-N(2)	110.22(16)
N(5)-H(5B)	0.88	H(25A)-C(23)-H(25B)	108	N(4)-Zn(1)-N(2)	113.38(16)
N(6)-H(6)	0.88	N(4)-C(24)-C(25)	122.7(5)	N(1)-Zn(1)-N(2)	73.73(19)
N(7)-H(7)	0.88	N(4)-C(24)-C(23)	115.9(5)		
O(1)-Zn(1)	2.146(4)	C(25)-C(24)-C(23)	121.4(5)		
O(2)-Zn(1)	2.150(3)	C(26)-C(25)-C(24)	118.6(5)		
O(3)-Zn(1)	2.139(3)	C(26)-C(25)-H(27)	120.7		
O(4)-Cl(1)	1.355(5)	C(24)-C(25)-H(27)	120.7		
O(5)-Cl(1)	1.359(5)	C(27)-C(26)-C(25)	119.6(6)		
O(6)-Cl(1)	1.279(7)	C(27)-C(26)-H(28)	120.2		
O(7)-Cl(1)	1.397(5)	C(25)-C(26)-H(28)	120.2		
O(8)-Cl(2)	1.351(6)	C(26)-C(27)-C(28)	118.6(6)		
O(9)-Cl(2)	1.390(5)	C(26)-C(27)-H(29)	120.7		
O(10)-Cl(2)	1.409(5)	C(28)-C(27)-H(29)	120.7		
O(11)-Cl(2)	1.312(5)	N(4)-C(28)-C(27)	123.0(5)		

**Table V.1:** Crystal data and structure refinement for $[\text{Zn}^{\text{II}}(\text{L}^4)\text{Cl}_2]$. 5.6

Identification code	aja0919b	
Empirical formula	C ₃₃ H ₄₅ Cl ₂ N ₇ O ₃ Zn	
Formula weight	724.03	
Temperature	140(2) K	
Wavelength	0.71073 Å	
Crystal system	Monoclinic	
Space group	C2/c	
Unit cell dimensions	a = 35.4990(4) Å	$\alpha = 90^\circ$.
	b = 9.1250(7) Å	$\beta = 119.271(2)^\circ$.
	c = 24.5700(12) Å	$\gamma = 90^\circ$.
Volume	6942.7(6) Å ³	
Z	8	
Density (calculated)	1.385 Mg/m ³	
Absorption coefficient	0.906 mm ⁻¹	
F(000)	3040	
Crystal size	0.30 x 0.20 x 0.20 mm ³	
Theta range for data collection	1.70 to 23.36°.	
Index ranges	-39 ≤ h ≤ 39, -10 ≤ k ≤ 10, -26 ≤ l ≤ 27	
Reflections collected	13709	
Independent reflections	4983 [R(int) = 0.0599]	
Completeness to theta = 23.36°	98.8 %	
Max. and min. transmission	0.8397 and 0.7729	
Refinement method	Full-matrix least-squares on F ²	
Data / restraints / parameters	4983 / 0 / 424	
Goodness-of-fit on F ²	1.075	
Final R indices [I > 2σ(I)]	R1 = 0.0701, wR2 = 0.1785	
R indices (all data)	R1 = 0.0929, wR2 = 0.1912	
Largest diff. peak and hole	1.754 and -0.752 e.Å ⁻³	

Appendix 3: Crystals data

Table V.2: Bond lengths [Å] and angles [°] for [Zn^{II}(L⁴)Cl₂]. 5.6

C(1)-N(1)	1.486(8)	N(1)-C(1)-C(2)	111.8(5)	H(22B)-C(22)-H(22C)	109.5
C(1)-C(2)	1.511(9)	N(1)-C(1)-H(1A)	109.2	N(1)-C(23)-C(24)	115.0(5)
C(1)-H(1A)	0.99	C(2)-C(1)-H(1A)	109.2	N(1)-C(23)-H(23A)	108.5
C(1)-H(1B)	0.99	N(1)-C(1)-H(1B)	109.2	C(24)-C(23)-H(23A)	108.5
C(2)-N(2)	1.351(8)	C(2)-C(1)-H(1B)	109.2	N(1)-C(23)-H(23B)	108.5
C(2)-C(3)	1.380(9)	H(1A)-C(1)-H(1B)	107.9	C(24)-C(23)-H(23B)	108.5
C(3)-C(4)	1.383(10)	N(2)-C(2)-C(3)	121.6(6)	H(23A)-C(23)-H(23B)	107.5
C(3)-H(3)	0.95	N(2)-C(2)-C(1)	116.3(6)	N(6)-C(24)-C(25)	122.7(6)
C(4)-C(5)	1.377(9)	C(3)-C(2)-C(1)	121.9(6)	N(6)-C(24)-C(23)	114.8(6)
C(4)-H(4)	0.95	C(2)-C(3)-C(4)	118.7(6)	C(25)-C(24)-C(23)	122.4(6)
C(5)-C(6)	1.397(9)	C(2)-C(3)-H(3)	120.6	C(24)-C(25)-C(26)	118.4(6)
C(5)-H(5)	0.95	C(4)-C(3)-H(3)	120.6	C(24)-C(25)-H(25)	120.8
C(6)-N(2)	1.341(8)	C(5)-C(4)-C(3)	120.5(6)	C(26)-C(25)-H(25)	120.8
C(6)-N(3)	1.396(8)	C(5)-C(4)-H(4)	119.8	C(27)-C(26)-C(25)	119.9(7)
C(7)-O(1)	1.207(8)	C(3)-C(4)-H(4)	119.8	C(27)-C(26)-H(26)	120.1
C(7)-N(3)	1.381(9)	C(4)-C(5)-C(6)	117.8(6)	C(25)-C(26)-H(26)	120.1
C(7)-C(8)	1.538(10)	C(4)-C(5)-H(5)	121.1	C(26)-C(27)-C(28)	117.9(7)
C(8)-C(9)	1.527(10)	C(6)-C(5)-H(5)	121.1	C(26)-C(27)-H(27)	121
C(8)-C(11)	1.533(11)	N(2)-C(6)-N(3)	114.5(6)	C(28)-C(27)-H(27)	121
C(8)-C(10)	1.553(10)	N(2)-C(6)-C(5)	122.2(6)	N(6)-C(28)-C(27)	123.3(6)
C(9)-H(9A)	0.98	N(3)-C(6)-C(5)	123.3(6)	N(6)-C(28)-N(7)	112.1(6)
C(9)-H(9B)	0.98	O(1)-C(7)-N(3)	121.7(6)	C(27)-C(28)-N(7)	124.6(6)
C(9)-H(9C)	0.98	O(1)-C(7)-C(8)	122.9(6)	O(3)-C(29)-N(7)	121.8(7)
C(10)-H(10A)	0.98	N(3)-C(7)-C(8)	115.4(6)	O(3)-C(29)-C(30)	121.5(7)
C(10)-H(10B)	0.98	C(9)-C(8)-C(11)	109.2(6)	N(7)-C(29)-C(30)	116.5(6)
C(10)-H(10C)	0.98	C(9)-C(8)-C(7)	108.6(6)	C(31)-C(30)-C(33)	109.2(6)
C(11)-H(11A)	0.98	C(11)-C(8)-C(7)	110.8(6)	C(31)-C(30)-C(29)	106.9(6)
C(11)-H(11B)	0.98	C(9)-C(8)-C(10)	108.5(6)	C(33)-C(30)-C(29)	114.5(6)
C(11)-H(11C)	0.98	C(11)-C(8)-C(10)	111.3(6)	C(31)-C(30)-C(32)	109.1(6)
C(12)-C(13)	1.489(9)	C(7)-C(8)-C(10)	108.5(6)	C(33)-C(30)-C(32)	109.8(6)
C(12)-N(1)	1.502(8)	C(8)-C(9)-H(9A)	109.5	C(29)-C(30)-C(32)	107.2(6)
C(12)-H(12A)	0.99	C(8)-C(9)-H(9B)	109.5	C(30)-C(31)-H(31A)	109.5
C(12)-H(12B)	0.99	H(9A)-C(9)-H(9B)	109.5	C(30)-C(31)-H(31B)	109.5
C(13)-N(4)	1.353(8)	C(8)-C(9)-H(9C)	109.5	H(31A)-C(31)-H(31B)	109.5
C(13)-C(14)	1.391(9)	H(9A)-C(9)-H(9C)	109.5	C(30)-C(31)-H(31C)	109.5
C(14)-C(15)	1.399(9)	H(9B)-C(9)-H(9C)	109.5	H(31A)-C(31)-H(31C)	109.5
C(14)-H(14)	0.95	C(8)-C(10)-H(10A)	109.5	H(31B)-C(31)-H(31C)	109.5
C(15)-C(16)	1.395(10)	C(8)-C(10)-H(10B)	109.5	C(30)-C(32)-H(32A)	109.5
C(15)-H(15)	0.95	H(10A)-C(10)-H(10B)	109.5	C(30)-C(32)-H(32B)	109.5
C(16)-C(17)	1.368(9)	C(8)-C(10)-H(10C)	109.5	H(32A)-C(32)-H(32B)	109.5
C(16)-H(16)	0.95	H(10A)-C(10)-H(10C)	109.5	C(30)-C(32)-H(32C)	109.5
C(17)-N(4)	1.359(8)	H(10B)-C(10)-H(10C)	109.5	H(32A)-C(32)-H(32C)	109.5
C(17)-N(5)	1.403(8)	C(8)-C(11)-H(11A)	109.5	H(32B)-C(32)-H(32C)	109.5
C(18)-O(2)	1.225(8)	C(8)-C(11)-H(11B)	109.5	C(30)-C(33)-H(33A)	109.5
C(18)-N(5)	1.373(9)	H(11A)-C(11)-H(11B)	109.5	C(30)-C(33)-H(33B)	109.5
C(18)-C(19)	1.528(10)	C(8)-C(11)-H(11C)	109.5	H(33A)-C(33)-H(33B)	109.5
C(19)-C(22)	1.517(11)	H(11A)-C(11)-H(11C)	109.5	C(30)-C(33)-H(33C)	109.5
C(19)-C(21)	1.537(10)	H(11B)-C(11)-H(11C)	109.5	H(33A)-C(33)-H(33C)	109.5
C(19)-C(20)	1.537(11)	C(13)-C(12)-N(1)	108.6(5)	H(33B)-C(33)-H(33C)	109.5
C(20)-H(20A)	0.98	C(13)-C(12)-H(12A)	110	C(1)-N(1)-C(23)	111.3(5)
C(20)-H(20B)	0.98	N(1)-C(12)-H(12A)	110	C(1)-N(1)-C(12)	111.4(5)
C(20)-H(20C)	0.98	C(13)-C(12)-H(12B)	110	C(23)-N(1)-C(12)	111.1(5)
C(21)-H(21A)	0.98	N(1)-C(12)-H(12B)	110	C(1)-N(1)-Zn(1)	106.7(4)
C(21)-H(21B)	0.98	H(12A)-C(12)-H(12B)	108.4	C(23)-N(1)-Zn(1)	111.8(4)
C(21)-H(21C)	0.98	N(4)-C(13)-C(14)	121.9(6)	C(12)-N(1)-Zn(1)	104.4(4)
C(22)-H(22A)	0.98	N(4)-C(13)-C(12)	114.1(5)	C(6)-N(2)-C(2)	119.2(6)
C(22)-H(22B)	0.98	C(14)-C(13)-C(12)	124.0(6)	C(6)-N(2)-Zn(1)	129.2(4)

Appendix 3: Crystals data

C(22)-H(22C)	0.98	C(13)-C(14)-C(15)	118.7(6)	C(2)-N(2)-Zn(1)	111.5(4)
C(23)-N(1)	1.496(8)	C(13)-C(14)-H(14)	120.6	C(7)-N(3)-C(6)	128.6(6)
C(23)-C(24)	1.514(9)	C(15)-C(14)-H(14)	120.6	C(7)-N(3)-H(3A)	115.7
C(23)-H(23A)	0.99	C(16)-C(15)-C(14)	119.1(6)	C(6)-N(3)-H(3A)	115.7
C(23)-H(23B)	0.99	C(16)-C(15)-H(15)	120.4	C(13)-N(4)-C(17)	118.4(5)
C(24)-N(6)	1.360(8)	C(14)-C(15)-H(15)	120.4	C(13)-N(4)-Zn(1)	111.4(4)
C(24)-C(25)	1.369(9)	C(17)-C(16)-C(15)	118.8(6)	C(17)-N(4)-Zn(1)	128.6(4)
C(25)-C(26)	1.390(9)	C(17)-C(16)-H(16)	120.6	C(18)-N(5)-C(17)	121.3(6)
C(25)-H(25)	0.95	C(15)-C(16)-H(16)	120.6	C(18)-N(5)-H(5A)	119.4
C(26)-C(27)	1.383(10)	N(4)-C(17)-C(16)	122.9(6)	C(17)-N(5)-H(5A)	119.4
C(26)-H(26)	0.95	N(4)-C(17)-N(5)	114.2(6)	C(28)-N(6)-C(24)	117.7(6)
C(27)-C(28)	1.383(9)	C(16)-C(17)-N(5)	122.9(6)	C(29)-N(7)-C(28)	128.5(6)
C(27)-H(27)	0.95	O(2)-C(18)-N(5)	120.6(7)	C(29)-N(7)-H(7)	115.7
C(28)-N(6)	1.339(8)	O(2)-C(18)-C(19)	121.7(6)	C(28)-N(7)-H(7)	115.7
C(28)-N(7)	1.401(8)	N(5)-C(18)-C(19)	117.7(6)	N(1)-Zn(1)-N(4)	78.30(19)
C(29)-O(3)	1.208(9)	C(22)-C(19)-C(18)	114.2(6)	N(1)-Zn(1)-N(2)	78.52(19)
C(29)-N(7)	1.374(9)	C(22)-C(19)-C(21)	109.9(7)	N(4)-Zn(1)-N(2)	156.81(19)
C(29)-C(30)	1.534(10)	C(18)-C(19)-C(21)	107.0(6)	N(1)-Zn(1)-Cl(1)	116.74(15)
C(30)-C(31)	1.528(10)	C(22)-C(19)-C(20)	109.7(7)	N(4)-Zn(1)-Cl(1)	94.50(14)
C(30)-C(33)	1.531(10)	C(18)-C(19)-C(20)	105.8(6)	N(2)-Zn(1)-Cl(1)	96.45(14)
C(30)-C(32)	1.546(10)	C(21)-C(19)-C(20)	110.1(7)	N(1)-Zn(1)-Cl(2)	123.84(14)
C(31)-H(31A)	0.98	C(19)-C(20)-H(20A)	109.5	N(4)-Zn(1)-Cl(2)	99.09(14)
C(31)-H(31B)	0.98	C(19)-C(20)-H(20B)	109.5	N(2)-Zn(1)-Cl(2)	93.24(14)
C(31)-H(31C)	0.98	H(20A)-C(20)-H(20B)	109.5	Cl(1)-Zn(1)-Cl(2)	119.38(6)
C(32)-H(32A)	0.98	C(19)-C(20)-H(20C)	109.5		
C(32)-H(32B)	0.98	H(20A)-C(20)-H(20C)	109.5		
C(32)-H(32C)	0.98	H(20B)-C(20)-H(20C)	109.5		
C(33)-H(33A)	0.98	C(19)-C(21)-H(21A)	109.5		
C(33)-H(33B)	0.98	C(19)-C(21)-H(21B)	109.5		
C(33)-H(33C)	0.98	H(21A)-C(21)-H(21B)	109.5		
N(1)-Zn(1)	2.139(5)	C(19)-C(21)-H(21C)	109.5		
N(2)-Zn(1)	2.233(5)	H(21A)-C(21)-H(21C)	109.5		
N(3)-H(3A)	0.88	H(21B)-C(21)-H(21C)	109.5		
N(4)-Zn(1)	2.210(5)	C(19)-C(22)-H(22A)	109.5		
N(5)-H(5A)	0.88	C(19)-C(22)-H(22B)	109.5		
N(7)-H(7)	0.88	H(22A)-C(22)-H(22B)	109.5		
Zn(1)-Cl(1)	2.3055(16)	C(19)-C(22)-H(22C)	109.5		
Zn(1)-Cl(2)	2.3330(14)	H(22A)-C(22)-H(22C)	109.5		

Appendix 3: Crystals data

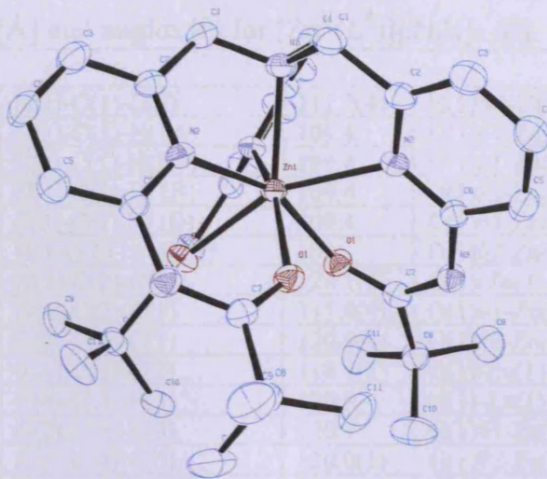


Table W.1: Crystal data and structure refinement for $[\text{Zn}^{\text{II}}(\text{L}^4)][\text{ZnI}_4]_{0.5}[\text{I}]$ **5.7**

Identification code	aja0925	
Empirical formula	C ₆₆ H ₉₀ I ₆ N ₁₄ O ₆ Zn ₃	
Formula weight	2133.03	
Temperature	150(2) K	
Wavelength	0.71073 Å	
Crystal system	Trigonal	
Space group	P-3c1	
Unit cell dimensions	a = 11.2190(2) Å	α = 90°.
	b = 11.2190(10) Å	β = 90°.
	c = 38.5920(4) Å	γ = 120°.
Volume	4206.65(9) Å ³	
Z	2	
Density (calculated)	1.684 Mg/m ³	
Absorption coefficient	3.102 mm ⁻¹	
F(000)	2080	
Crystal size	0.40 x 0.20 x 0.04 mm ³	
Theta range for data collection	2.35 to 27.49°.	
Index ranges	-13 ≤ h ≤ 14, -14 ≤ k ≤ 14, -40 ≤ l ≤ 50	
Reflections collected	23030	
Independent reflections	3226 [R(int) = 0.0736]	
Completeness to theta = 27.49°	99.4 %	
Max. and min. transmission	0.8860 and 0.3701	
Refinement method	Full-matrix least-squares on F ²	
Data / restraints / parameters	3226 / 0 / 151	
Goodness-of-fit on F ²	1.118	
Final R indices [I > 2σ(I)]	R1 = 0.0462, wR2 = 0.1203	
R indices (all data)	R1 = 0.0562, wR2 = 0.1280	
Extinction coefficient	0.0019(2)	
Largest diff. peak and hole	1.875 and -2.018 e.Å ⁻³	

Appendix 3: Crystals data

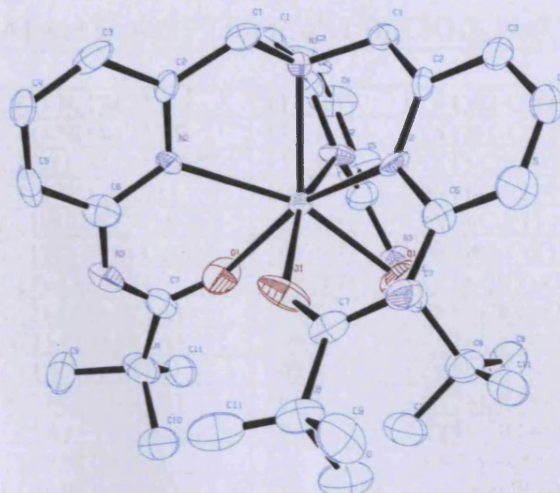
Table W.2: Bond lengths [Å] and angles [°] for $[\text{Zn}^{\text{II}}(\text{L}^4)][\text{ZnI}_4]_{0.5}[\text{I}] \cdot 5.7$

C(1)-N(1)	1.470(5)	N(1)-C(1)-C(2)	111.2(4)	H(11B)-C(11)-H(11C)	109.5
C(1)-C(2)	1.515(7)	N(1)-C(1)-H(1A)	109.4	O(1)#1-Zn(1)-O(1)#2	83.91(13)
C(1)-H(1A)	0.99	C(2)-C(1)-H(1A)	109.4	O(1)#1-Zn(1)-O(1)	83.91(13)
C(1)-H(1B)	0.99	N(1)-C(1)-H(1B)	109.4	O(1)#2-Zn(1)-O(1)	83.91(13)
C(2)-N(2)	1.345(6)	C(2)-C(1)-H(1B)	109.4	O(1)#1-Zn(1)-N(1)	129.47(9)
C(2)-C(3)	1.384(7)	H(1A)-C(1)-H(1B)	108	O(1)#2-Zn(1)-N(1)	129.47(9)
C(3)-C(4)	1.375(8)	N(2)-C(2)-C(3)	123.1(4)	O(1)-Zn(1)-N(1)	129.47(9)
C(3)-H(3)	0.95	N(2)-C(2)-C(1)	115.9(4)	O(1)#1-Zn(1)-N(2)#1	78.33(13)
C(4)-C(5)	1.385(7)	C(3)-C(2)-C(1)	120.9(4)	O(1)#2-Zn(1)-N(2)#1	156.55(13)
C(4)-H(4)	0.95	C(4)-C(3)-C(2)	118.1(5)	O(1)-Zn(1)-N(2)#1	79.11(13)
C(5)-C(6)	1.389(7)	C(4)-C(3)-H(3)	120.9	N(1)-Zn(1)-N(2)#1	73.98(9)
C(5)-H(5)	0.95	C(2)-C(3)-H(3)	120.9	O(1)#1-Zn(1)-N(2)#2	79.11(13)
C(6)-N(2)	1.339(6)	C(3)-C(4)-C(5)	120.0(5)	O(1)#2-Zn(1)-N(2)#2	78.33(13)
C(6)-N(3)	1.411(6)	C(3)-C(4)-H(4)	120	O(1)-Zn(1)-N(2)#2	156.55(13)
C(7)-O(1)	1.225(5)	C(5)-C(4)-H(4)	120	N(1)-Zn(1)-N(2)#2	73.98(9)
C(7)-N(3)	1.358(6)	C(4)-C(5)-C(6)	118.1(5)	N(2)#1-Zn(1)-N(2)#2	112.69(8)
C(7)-C(8)	1.533(6)	C(4)-C(5)-H(5)	121	O(1)#1-Zn(1)-N(2)	156.55(13)
C(8)-C(11)	1.526(7)	C(6)-C(5)-H(5)	121	O(1)#2-Zn(1)-N(2)	79.11(13)
C(8)-C(9)	1.532(7)	N(2)-C(6)-C(5)	122.8(4)	O(1)-Zn(1)-N(2)	78.33(13)
C(8)-C(10)	1.535(7)	N(2)-C(6)-N(3)	119.6(4)	N(1)-Zn(1)-N(2)	73.98(9)
C(9)-H(9A)	0.98	C(5)-C(6)-N(3)	117.6(4)	N(2)#1-Zn(1)-N(2)	112.69(8)
C(9)-H(9B)	0.98	O(1)-C(7)-N(3)	123.5(4)	N(2)#2-Zn(1)-N(2)	112.69(8)
C(9)-H(9C)	0.98	O(1)-C(7)-C(8)	120.1(4)	Zn(2)#3-Zn(2)-I(3)	180
C(10)-H(10A)	0.98	N(3)-C(7)-C(8)	116.4(4)	Zn(2)#3-Zn(2)-I(2)#3	67.22(4)
C(10)-H(10B)	0.98	C(11)-C(8)-C(9)	109.0(5)	I(3)-Zn(2)-I(2)#3	112.78(4)
C(10)-H(10C)	0.98	C(11)-C(8)-C(7)	107.5(4)	Zn(2)#3-Zn(2)-I(2)#4	67.22(4)
C(11)-H(11A)	0.98	C(9)-C(8)-C(7)	110.5(4)	I(3)-Zn(2)-I(2)#4	112.78(4)
C(11)-H(11B)	0.98	C(11)-C(8)-C(10)	110.5(5)	I(2)#3-Zn(2)-I(2)#4	105.97(4)
C(11)-H(11C)	0.98	C(9)-C(8)-C(10)	110.8(5)	Zn(2)#3-Zn(2)-I(2)	67.22(4)
Zn(1)-O(1)#1	2.129(3)	C(7)-C(8)-C(10)	108.4(4)	I(3)-Zn(2)-I(2)	112.78(4)
Zn(1)-O(1)#2	2.129(3)	C(8)-C(9)-H(9A)	109.5	I(2)#3-Zn(2)-I(2)	105.97(4)
Zn(1)-O(1)	2.129(3)	C(8)-C(9)-H(9B)	109.5	I(2)#4-Zn(2)-I(2)	105.97(4)
Zn(1)-N(1)	2.183(6)	H(9A)-C(9)-H(9B)	109.5	Zn(2)#3-I(2)-Zn(2)	45.55(8)
Zn(1)-N(2)#1	2.234(4)	C(8)-C(9)-H(9C)	109.5	C(1)#2-N(1)-C(1)#1	110.6(3)
Zn(1)-N(2)#2	2.234(4)	H(9A)-C(9)-H(9C)	109.5	C(1)#2-N(1)-C(1)	110.6(3)
Zn(1)-N(2)	2.234(4)	H(9B)-C(9)-H(9C)	109.5	C(1)#1-N(1)-C(1)	110.6(3)
Zn(2)-Zn(2)#3	2.047(4)	C(8)-C(10)-H(10A)	109.5	C(1)#2-N(1)-Zn(1)	108.3(3)
Zn(2)-I(3)	2.575(2)	C(8)-C(10)-H(10B)	109.5	C(1)#1-N(1)-Zn(1)	108.3(3)
Zn(2)-I(2)#3	2.6442(9)	H(10A)-C(10)-H(10B)	109.5	C(1)-N(1)-Zn(1)	108.3(3)
Zn(2)-I(2)#4	2.6442(9)	C(8)-C(10)-H(10C)	109.5	C(6)-N(2)-C(2)	117.8(4)
Zn(2)-I(2)	2.6442(9)	H(10A)-C(10)-H(10C)	109.5	C(6)-N(2)-Zn(1)	126.1(3)
I(2)-Zn(2)#3	2.6442(9)	H(10B)-C(10)-H(10C)	109.5	C(2)-N(2)-Zn(1)	112.3(3)
N(1)-C(1)#2	1.470(5)	C(8)-C(11)-H(11A)	109.5	C(7)-N(3)-C(6)	128.4(4)
N(1)-C(1)#1	1.470(5)	C(8)-C(11)-H(11B)	109.5	C(7)-N(3)-H(3A)	115.8
N(3)-H(3A)	0.88	H(11A)-C(11)-H(11B)	109.5	C(6)-N(3)-H(3A)	115.8
		C(8)-C(11)-H(11C)	109.5	C(7)-O(1)-Zn(1)	132.9(3)
		H(11A)-C(11)-H(11C)	109.5		

Symmetry transformations used to generate equivalent atoms:

#1 -y+1,x-y+1,z #2 -x+y,-x+1,z #3 y,x,-z+1/2

#4 -y,x-y,z

**Table X.1:** Crystal data and structure refinement for $[\text{Cd}^{\text{II}}(\text{L}^4)][\text{ClO}_4]_2 \cdot \text{Na}(\text{ClO}_4) \cdot \text{H}_2\text{O}$. 5.8

Identification code	aja0834	
Empirical formula	C33 H47 Cd Cl3 N7 Na O16	
Formula weight	1039.52	
Temperature	150(2) K	
Wavelength	0.71073 Å	
Crystal system	Trigonal	
Space group	R32	
Unit cell dimensions	$a = 16.2800(5)$ Å	$\alpha = 90^\circ$.
	$b = 16.3070(5)$ Å	$\beta = 90^\circ$.
	$c = 28.8420(13)$ Å	$\gamma = 120^\circ$.
Volume	$6631.1(4)$ Å ³	
Z	6	
Density (calculated)	1.562 Mg/m ³	
Absorption coefficient	0.760 mm ⁻¹	
F(000)	3192	
Crystal size	0.23 x 0.22 x 0.10 mm ³	
Theta range for data collection	1.61 to 27.50°.	
Index ranges	-21 ≤ h ≤ 15, -18 ≤ k ≤ 18, -37 ≤ l ≤ 29	
Reflections collected	5243	
Independent reflections	2726 [R(int) = 0.0809]	
Completeness to theta = 27.50°	88.8 %	
Max. and min. transmission	0.9279 and 0.8447	
Refinement method	Full-matrix least-squares on F ²	
Data / restraints / parameters	2726 / 110 / 220	
Goodness-of-fit on F ²	1.137	
Final R indices [I > 2σ(I)]	R1 = 0.1026, wR2 = 0.2779	
R indices (all data)	R1 = 0.1136, wR2 = 0.2877	
Absolute structure parameter	0.43(14)	
Extinction coefficient	0.0025(5)	
Largest diff. peak and hole	1.228 and -1.410 e.Å ⁻³	

Appendix 3: Crystals data

Table X.2: Bond lengths [Å] and angles [°] for [Cd^{II}(L⁴)](ClO₄)₂.Na(ClO₄).H₂O. 5.8

N(1)-C(1)	1.509(6)	C(1)-N(1)-C(1)#1	111.4(4)	O(1)#2-Cd(1)-N(2)#1	84.5(5)
N(1)-C(1)#1	1.510(6)	C(1)-N(1)-C(1)#2	111.4(4)	O(1)#1-Cd(1)-N(2)#1	73.2(4)
N(1)-C(1)#2	1.511(6)	C(1)#1-N(1)-C(1)#2	111.5(4)	O(1)-Cd(1)-N(2)#1	160.1(4)
N(1)-Cd(1)	2.349(12)	C(1)-N(1)-Cd(1)	107.5(5)	N(1)-Cd(1)-N(2)#1	71.92(11)
C(1)-C(2)	1.4938	C(1)#1-N(1)-Cd(1)	107.4(5)	N(2)-Cd(1)-N(2)#1	110.84(11)
C(1)-H(1A)	0.99	C(1)#2-N(1)-Cd(1)	107.4(5)	N(2)#2-Cd(1)-N(2)#1	110.86(11)
C(1)-H(1B)	0.99	C(2)-C(1)-N(1)	109.3(4)	O(5)-Cl(1)-O(2)	109.8(4)
N(2)-C(6)	1.3907	C(2)-C(1)-H(1A)	109.8	O(5)-Cl(1)-O(4)	109.6(4)
N(2)-C(2)	1.3914	N(1)-C(1)-H(1A)	109.8	O(2)-Cl(1)-O(4)	109.3(4)
N(2)-Cd(1)	2.363(5)	C(2)-C(1)-H(1B)	109.8	O(5)-Cl(1)-O(3)	109.5(4)
C(2)-C(3)	1.3905	N(1)-C(1)-H(1B)	109.8	O(2)-Cl(1)-O(3)	109.3(4)
C(3)-C(4)	1.3906	H(1A)-C(1)-H(1B)	108.3	O(4)-Cl(1)-O(3)	109.3(4)
C(3)-H(3)	0.95	C(6)-N(2)-C(2)	120	Cl(1A)-O(3A)-Na(1)	130.5(13)
C(4)-C(5)	1.3914	C(6)-N(2)-Cd(1)	126.39(12)	O(2A)-Cl(1A)-O(4A)	109.7(4)
C(4)-H(4)	0.95	C(2)-N(2)-Cd(1)	111.29(13)	O(2A)-Cl(1A)-O(5A)	109.4(4)
C(5)-C(6)	1.3904	C(3)-C(2)-N(2)	120	O(4A)-Cl(1A)-O(5A)	109.5(4)
C(5)-H(5)	0.95	C(3)-C(2)-C(1)	119.2	O(2A)-Cl(1A)-O(3A)	109.5(4)
C(6)-N(3)	1.362(13)	N(2)-C(2)-C(1)	120.4	O(4A)-Cl(1A)-O(3A)	109.3(4)
N(3)-C(7)	1.33(2)	C(2)-C(3)-C(4)	120	O(5A)-Cl(1A)-O(3A)	109.4(4)
N(3)-H(3A)	0.88	C(2)-C(3)-H(3)	120	O(6)#3-Na(1)-O(6)#4	78.9(13)
C(7)-O(1)	1.18(2)	C(4)-C(3)-H(3)	120	O(6)#3-Na(1)-O(6)	79.0(13)
C(7)-C(8)	1.56(2)	C(3)-C(4)-C(5)	120	O(6)#4-Na(1)-O(6)	79.1(12)
C(8)-C(11)	1.30(3)	C(3)-C(4)-H(4)	120	O(6)#3-Na(1)-O(7)	94.6(12)
C(8)-C(9)	1.52(2)	C(5)-C(4)-H(4)	120	O(6)#4-Na(1)-O(7)	43.2(4)
C(8)-C(10)	1.61(2)	C(6)-C(5)-C(4)	120	O(6)-Na(1)-O(7)	43.1(4)
C(9)-H(9A)	0.98	C(6)-C(5)-H(5)	120	O(6)#3-Na(1)-O(7)#3	43.2(4)
C(9)-H(9B)	0.98	C(4)-C(5)-H(5)	120	O(6)#4-Na(1)-O(7)#3	94.6(12)
C(9)-H(9C)	0.98	N(3)-C(6)-C(5)	121.6(6)	O(6)-Na(1)-O(7)#3	43.1(4)
C(10)-H(10A)	0.98	N(3)-C(6)-N(2)	118.2(6)	O(7)-Na(1)-O(7)#3	79(2)
C(10)-H(10B)	0.98	C(5)-C(6)-N(2)	120	O(6)#3-Na(1)-O(7)#4	43.1(4)
C(10)-H(10C)	0.98	C(7)-N(3)-C(6)	131.9(11)	O(6)#4-Na(1)-O(7)#4	43.1(4)
C(11)-H(11A)	0.98	C(7)-N(3)-H(3A)	114.1	O(6)-Na(1)-O(7)#4	94.7(12)
C(11)-H(11B)	0.98	C(6)-N(3)-H(3A)	114.1	O(7)-Na(1)-O(7)#4	79(2)
C(11)-H(11C)	0.98	O(1)-C(7)-N(3)	122.8(14)	O(7)#3-Na(1)-O(7)#4	79(2)
O(1)-Cd(1)	2.255(9)	O(1)-C(7)-C(8)	118.5(15)	O(6)#3-Na(1)-O(3A)	79.3(9)
Cd(1)-O(1)#2	2.252(9)	N(3)-C(7)-C(8)	118.7(13)	O(6)#4-Na(1)-O(3A)	140.4(6)
Cd(1)-O(1)#1	2.253(9)	C(11)-C(8)-C(9)	111.6(18)	O(6)-Na(1)-O(3A)	128.0(5)
Cd(1)-N(2)#2	2.363(5)	C(11)-C(8)-C(7)	116.4(15)	O(7)-Na(1)-O(3A)	170.7(10)
Cd(1)-N(2)#1	2.366(5)	C(9)-C(8)-C(7)	112.3(15)	O(7)#3-Na(1)-O(3A)	91.7(12)
O(2)-Cl(1)	1.407(5)	C(11)-C(8)-C(10)	108.5(17)	O(7)#4-Na(1)-O(3A)	100.6(10)
O(3)-Cl(1)	1.409(5)	C(9)-C(8)-C(10)	104.6(15)	O(6)#3-Na(1)-O(3A)#3	127.9(5)
O(4)-Cl(1)	1.408(4)	C(7)-C(8)-C(10)	102.2(14)	O(6)#4-Na(1)-O(3A)#3	79.3(9)
O(5)-Cl(1)	1.404(5)	C(8)-C(9)-H(9A)	109.5	O(6)-Na(1)-O(3A)#3	140.5(6)
O(2A)-Cl(1A)	1.406(5)	C(8)-C(9)-H(9B)	109.5	O(7)-Na(1)-O(3A)#3	100.7(10)
O(3A)-Cl(1A)	1.408(5)	H(9A)-C(9)-H(9B)	109.5	O(7)#3-Na(1)-O(3A)#3	170.7(10)
O(3A)-Na(1)	2.407(19)	C(8)-C(9)-H(9C)	109.5	O(7)#4-Na(1)-O(3A)#3	91.6(12)
O(4A)-Cl(1A)	1.406(5)	H(9A)-C(9)-H(9C)	109.5	O(3A)-Na(1)-O(3A)#3	88.7(7)
O(5A)-Cl(1A)	1.407(5)	H(9B)-C(9)-H(9C)	109.5	O(6)#3-Na(1)-O(3A)#4	140.5(6)
Na(1)-O(6)#3	2.37(4)	C(8)-C(10)-H(10A)	109.5	O(6)#4-Na(1)-O(3A)#4	128.1(5)
Na(1)-O(6)#4	2.37(4)	C(8)-C(10)-H(10B)	109.5	O(6)-Na(1)-O(3A)#4	79.3(9)
Na(1)-O(6)	2.37(4)	H(10A)-C(10)-	109.5	O(7)-Na(1)-O(3A)#4	91.6(12)
Na(1)-O(7)	2.37(6)	C(8)-C(10)-H(10C)	109.5	O(7)#3-Na(1)-O(3A)#4	100.5(10)
Na(1)-O(7)#3	2.37(6)	H(10A)-C(10)-	109.5	O(7)#4-Na(1)-O(3A)#4	170.7(10)
Na(1)-O(7)#4	2.37(6)	H(10B)-C(10)-	109.5	O(3A)-Na(1)-O(3A)#4	88.7(7)
Na(1)-	2.41(2)	C(8)-C(11)-H(11A)	109.5	O(3A)#3-Na(1)-	88.8(7)
Na(1)-	2.409(19)	C(8)-C(11)-H(11B)	109.5	O(6)#3-Na(1)-Na(1)#5	47.2(8)
Na(1)-Na(1)#5	3.214(17)	H(11A)-C(11)-	109.5	O(6)#4-Na(1)-Na(1)#5	47.3(8)

Appendix 3: Crystals data

O(6)-O(7)#3	1.74(3)	C(8)-C(11)-H(11C)	109.5	O(6)-Na(1)-Na(1)#5	47.3(8)
O(6)-O(7)	1.74(4)	H(11A)-C(11)-	109.5	O(7)-Na(1)-Na(1)#5	47.3(14)
O(6)-Na(1)#5	2.37(4)	H(11B)-C(11)-	109.5	O(7)#3-Na(1)-Na(1)#5	47.4(14)
O(7)-O(6)#4	1.74(3)	C(7)-O(1)-Cd(1)	134.9(15)	O(7)#4-Na(1)-Na(1)#5	47.4(14)
O(7)-Na(1)#5	2.37(6)	O(1)#2-Cd(1)-O(1)#1	88.1(4)	O(3A)-Na(1)-Na(1)#5	126.2(5)
		O(1)#2-Cd(1)-O(1)	88.2(4)	O(3A)#3-Na(1)-Na(1)#5	126.2(5)
		O(1)#1-Cd(1)-O(1)	88.2(4)	O(3A)#4-Na(1)-Na(1)#5	126.1(5)
		O(1)#2-Cd(1)-N(1)	126.6(3)	O(7)#3-O(6)-O(7)	120(7)
		O(1)#1-Cd(1)-N(1)	126.6(3)	O(7)#3-O(6)-Na(1)#5	69(3)
		O(1)-Cd(1)-N(1)	126.5(3)	O(7)-O(6)-Na(1)#5	69(3)
		O(1)#2-Cd(1)-N(2)	160.1(4)	O(7)#3-O(6)-Na(1)	69(3)
		O(1)#1-Cd(1)-N(2)	84.6(5)	O(7)-O(6)-Na(1)	69(3)
		O(1)-Cd(1)-N(2)	73.2(4)	Na(1)#5-O(6)-Na(1)	85.4(16)
		N(1)-Cd(1)-N(2)	71.89(11)	O(6)-O(7)-O(6)#4	120(7)
		O(1)#2-Cd(1)-N(2)#2	73.3(4)	O(6)-O(7)-Na(1)#5	68(3)
		O(1)#1-Cd(1)-N(2)#2	160.1(4)	O(6)#4-O(7)-Na(1)#5	68(3)
		O(1)-Cd(1)-N(2)#2	84.4(5)	O(6)-O(7)-Na(1)	68(3)
		N(1)-Cd(1)-N(2)#2	71.89(11)	O(6)#4-O(7)-Na(1)	68(3)
		N(2)-Cd(1)-N(2)#2	110.72(11)	Na(1)#5-O(7)-Na(1)	85(3)

Symmetry transformations used to generate equivalent atoms:

#1 -x+y,-x,z #2 -y,x-y,z #3 -x+y+1,-x+1,z

#4 -y+1,x-y,z #5 x-y+1/3,-y+2/3,-z+2/3

